

Ultrastructural Modelling of the Matrix-Cilium-Golgi Continuum in Hyaline Chondrocytes

Michael John Jennings

A thesis submitted for the degree of
Doctor of Philosophy
of the University of Otago, Dunedin,
New Zealand

21st July, 2014

Abstract

Overlooked for decades as an evolutionary vestigial organelle, the primary cilium has recently become the focus of intensive investigations into understanding of the physical structure and processes of eukaryote cell function. The cilium is central to various signalling pathways and modalities for signalling, allowing centrosomal processing and regulation of cellular and organelle function. The enigmatic process of their nanoscale ciliogenesis and sensory function at present remain poorly understood. Dysfunction of their normal function or component proteins correlates with a wide spectrum of diseases, or ciliopathies, which express as developmental disorders and pathologies [1].

Normal connective tissue function requires their cells to sense and respond to mechanical and physiochemical changes in the extracellular environment, and matrix, in order to maintain their form and function. In hyaline cartilage, chondrocyte primary cilia are located at an intermediate position between the mechanically functional extracellular matrix (ECM) surrounding the cell, and the intracellular organelles responsible for producing, modifying, transporting and secreting extracellular matrix materials [26, 96]. While many cellular and physiological processes involving primary cilia are at present known, accurate *in situ* knowledge of their form and fine structure in connective tissue is lacking.

A three dimensional model has been created of an *in situ* chondrocyte primary cilium. This details the anatomical structure of the cilium and its relationship to other cellular organelles. Components were mapped and divided into groups containing: the Matrix, the Cilium, the Centrosome, the Golgi apparatus and the Nucleus. The extracellular matrix was found to consist of interconnected tethered proteoglycans and matrix granules, with the granules composed of aggregates of finer components. These are tethered to the ciliary membrane at localised binding points. The membrane itself was observed as a dynamic extension of the cell membrane, fitting neatly over the axoneme microtubule doublets and their transport cargoes, while responding to the bending and torsional forces induced by the ECM. The ciliary axoneme comprises a '9+0 structure' of microtubule doublets of various lengths and inclinations, associated linkage proteins, ciliary necklace proteins, and intraflagellar-transport particle 'rafts' of materials, contained within the ciliary membrane.

The basal body is composed of nine microtubule triplets, and is decorated with appendages of basal feet, for the attachment of radiant cytoplasmic microtubules (as the foci of the microtubule organising centre, MTOC), as well as alar sheets and transition fibres, which function to anchor the basal body to the cell and ciliary membrane. The basal body microtubule polarisation, curl and inclination have been determined, along with those of the subtending proximal centriole, together the constituent components of the centrosome. The nuclear double membrane, and nuclear pores, and their close co-relation with the centrosome are shown.

Golgi *cis*-, *medial*- and *trans*-compartments, with associated transport vesicles are described along with their polarization. Clathrin coated pits were found, indicating receptor-mediated endocytosis. The outcome of this study is the first high-resolution reconstruction of a primary cilium. The model will enable interpretation of the interactions and involvement of the many biochemical and biophysical pathways now known to be associated with the cilium, and will lead to new understandings of processes fundamental to the workings of the eukaryotic cell.

The model raises new questions about the visualisation of the structure and form of the primary cilium. A vast volume of literature exists upon many aspects of cell biology, however few studies have undertaken investigations of primary cilia to understand their structure, and attempt to translate it to function. This is the first study to attempt to probe the complex relationship between the extracellular matrix, the mechanosensitive primary cilium, the centrosome and the Golgi apparatus, which as a continuum are responsible for maintaining the cells microenvironment.

Acknowledgements

I am indebted to Associate Professors John and Jenny Leader for their kind support and guidance in making the completion of this manuscript possible. I would also like to thank Professor Rob Walker, and Dr Duane Harland and Mr Richard Walls of AgResearch Lincoln for their encouragement and invaluable assistance in gathering data during electron tomography visits to Ag-Research Lincoln, and with KAREN remote access sessions. Likewise, Associate Professor Tony Poole for many interactions, Mr Allan Mitchell, Mr Richard Easingwood and Ms Gillian Grayston for electron microscopy support, from specimen fixation, and electron microscopy techniques, to discussions and many coffees.

I would also like to thank Dr David Mastronarde of Boulder Colorado for his support with IMOD software packages, and many interesting discussions on removing bugs and glitches from the software during the many hours of reconstructions and final modelling processes. I am also indebted to Ms Megan Bailey, Ms Katrin Geist and Mr Chaz Forsyth for their patience in proof reading and kind support, as well to many others

And lastly, Mr Jean-Pierre Houdin, for sharing many interesting parallel discussions about the intricacies of designing and building specialist architectural structures from the inside that do not succumb to the rigors of time.

Table of Contents

Preliminaries	Page
Abstract	i
Acknowledgements	iii
Table of Contents	iv
List of Tables	ix
List of Figures	x
List of Abbreviations	xiii
1.0 Chapter One: The Matrix-Cilium-Golgi-Continuum	
1.01 Preamble	1
Section I – Previous Knowledge of the Structure of the Primary Cilium	
1.02 A Brief History of the Primary Cilium	3
1.03 Early Work: Optical and Electron Microscopy of Cilia	4
1.04 The Discovery of Chondrocyte Primary Cilia	5
1.05 The Ciliary Axoneme	5
1.06 Ciliary Ultrastructure	6
1.07 The Transition Zone ‘Compartment’	7
1.08 Basal Body Appendages - Proximal to Distal	8
1.09 The Basal Feet (Basal Appendages)	8
1.10 The Striated Rootlets	9
1.11 The Centriole: A Template for the Basal Body and Axoneme	10
1.20 The Matrix-Cilium-Golgi Continuum	11
1.21 The Microtubule Organising Centre (MTOC)	13
1.22 The Peri-Centriolar Matrix (PCM)	14
1.23 The Cytoskeleton	15
1.24 Microtubules	16
1.241 Tubulins	16
1.242 Microtubule Nucleation Complex	16
1.243 Polymerisation	16
1.244 Tubulin Post-Translational Modification	17
Section II – Functional Relations of the Cilium during the Cell Cycle	
1.30 The Cell-Centrosome-Cilium Cycle	19
1.31 Intra-Flagellar Transport (IFT)	20
1.311 Ciliary Transport	21
1.312 IFT co-ordination	21
1.32 Primary Cilium Biogenesis	21

1.33 Entry of Material to the Cilium	23
1.34 Ciliary Localisation Sequences	24
1.35 Dynamic Control of Ciliary Length	25
1.40 The Ciliary Membrane	25
1.41 The Cilium: Receptors and Luminal Components	27
1.42 The Cilium and the Extracellular Matrix	29
1.43 Signalling and Mechanotransduction	29
1.44 Purinergic Mechanotransduction	30
1.45 Ciliary Polymodal Sensory Function	31
1.50 The Centrosome: The Central Processing Unit	32
1.501 The Centrosome, the Cytoskeleton and Transport	32
1.502 The Kinesin Family	33
1.503 The Dynein Family	34
1.504 The Dynein Activator - Dynactin	34
1.51 The GTPase Family Members	36
1.511 Function of Rab Family Members	37
1.512 The Cilium, Rabs and GTPases	37
1.513 Rabs, Vesicular Processes and the Golgi	38
1.514 Golgi Derived Transport: Targeting of Materials from the Golgi	39
1.515 Transport and the Golgi Apparatus	41
1.60 Microtubule Roles During the Interphase	41
1.61 The Cilium, Centrosome and the Golgi	42
1.62 Centrosome Positioning	44
1.63 Intracellular Transport	44
1.64 Transport of Vesicles	44
1.65 Rabs and Microtubule Motors	44
1.66 Myosin Motors and Rabs	45
1.67 The Golgi Apparatus: Transport Motors	45
1.70 A Brief History of the Golgi Apparatus	47
1.71 Models of Transport Through The Golgi	48
1.72 The Golgi: Regulated Processing and Secretion	49
1.73 Planar Cell Polarity: The Centrosome and the Golgi	50
1.74 Planar Cell Polarity, Wnts and Cartilage	51
1.75 The Cilium to Golgi Continuum: Summary	51

Section III – A Biomechanical Connective Tissue: Cartilage

1.80 Introduction: Biomechanical Function of Connective Tissues	52
---	----

1.81 Overview: Connective Tissues	52
1.82 A Compressive Tissue Matrix: Hyaline Cartilage	53
1.83 The Chondron	54
1.84 Articular Cartilage Function	55
1.85 Cartilage Collagens	56
1.86 Cartilage Glycosaminoglycans (GAGs)	57
1.87 Cartilage Proteoglycan Core Proteins and Glycoproteins	57
1.88 Aggrecan	58
1.89 Synthesis of Extracellular Matrix: Proteoglycans, GAGs and Collagen	59
1.90 Binding the Matrix to the Cell Membrane	60
1.91 Chondrocyte Matrix-Coupled Receptors	61
1.92 Cartilage Biomechanics: The Chondrocyte Microenvironment	62
2.0 Chapter Two: Methods	
2.0 Overview	63
2.10 Introduction: Electron Tomography and Primary Cilia	63
2.11 Connective Tissue Models	63
2.12 Embryonic Chick Sternal Cartilage: A Model Tissue	64
2.13 Chick Embryo Cartilage Fixation: <i>in vivo</i>	64
2.14 Chondrocyte Cell Culture: <i>in vitro</i>	65
2.15 Fixation of Cultured Cells	65
2.20 Fixation, Osmification, Ruthenium Red (RHT) and Artefacts	66
2.21 Fixation with Ruthenium Complexes	66
2.22 Fixation of Extracellular Matrix Proteoglycans	67
2.30 Serial Sectioning and Detection of Primary Cilia	68
2.31 Semithick Sectioning of Sternal Cartilage	68
2.32 Tomography of Monolayer Cell Culture: Aligning Cilia With The Substrate	69
2.40 Investigative Electron Microscopy	70
2.41 Fiducial Marker Application	70
2.42 Imaging Microscope	71
2.43 Remote Tomography	71
2.44 Specimen Attrition	72
2.45 Collection and Analysis	72
2.46 Data Processing	73
2.47 Fiducial Tracking	73
2.50 Analysis and Modelling of the Tomogram	74
2.51 Model Display	75

2.6 A Virtual Cilium: SolidWorks	75
----------------------------------	----

Chapter Three: Results

3.0 Introduction	77
3.1 Mechanical Connective Tissues: Tendon	77
3.2-3.3 Mechanical Connective Tissues: Chondrocyte Cilia Morphology and Staining	77
3.4 The Chondrocyte Primary Cilium: <i>In Vitro</i>	78
3.5 The Chondrocyte Primary Cilium: <i>In Situ</i>	78
3.6 Tomography of Native Sternal Chondrocytes	79
3.7-3.9 A Single Axis Model	80
3.10 Tomographical Modelling of the Extracellular Matrix and Matrix Granules	80
3.11 Matrix Ciliary Membrane Interactions	80
3.12 Matrix to Ciliary Membrane to Microtubule Interactions	81
3.13-3.15 The Axoneme Microtubules	81
3.151 Localisation of Intra Ciliary Transport Materials	82
3.16 The Distal Axoneme	82
3.17 The Middle Axoneme	82
3.18 The Transition Zone – One	83
3.19 The Transition Zone – Two	83
3.20 The Basal Body Microtubule Triplets	84
3.21-3.22 Internal Structures, Luminal Disc, Fibres and Vesicle	84
3.23-3.24 Basal Appendage One	84
3.26-3.27 Basal Appendage Two (BA2)	85
3.28 A Review of Basal Appendages One and Two	86
3.29 The Cilium, Basal Body Materials and Orientation	86
3.30 The Proximal Centriole	87
3.31 Proximal Centriole Radial Components	87
3.32 The Centrosome (1) Ultrastructure and Modelling	88
3.33 The Centrosome (2) The Centrosomal Torus	88
3.34 The Centrosome (3) The Pericentriolar Environment	89
3.35 The Centrosome (4) Basal Body, Proximal Centriole within the MTOC	89
3.36-3.40 The Cytosolic Microtubules; Centrosome to Golgi Connectivity; The <i>Cis</i> -, <i>Medial</i> - and <i>Trans</i> -Golgi Compartments; Transport of Matrix from the Golgi	90
3.41-3.42 The Complete Model: The Matrix-Cilium-Golgi Continuum	90
3.43 The Continuum: The Cilium and Centrosome	91

Chapter Four: Discussion

4.0 Introduction and Overview	133
4.10 Limitations of Study	134
4.11 Ruthenium Interactions with Cells and Membrane Bound Structures	135
4.12 Occurrence and Morphology of Chondrocyte Primary Cilia	135
4.13 Chick Sternal Cartilage Tomogram Selection	136
4.14 Defining the Cilium and its Relation to the Golgi	136
4.20 Interpretation of the Model Structure	137
4.21 The Matrix of the Ciliary Pocket	137
4.22 The Periciliary Membrane and the Ciliary Pocket	139
4.23 The Ciliary Membrane	139
4.231 Linking Matrix to the Ciliary Membrane and Transduction	140
4.232 Cilia, ENac and Mechanotransduction	141
4.233 The Axoneme Membrane	142
4.234 Ciliary Membrane Forces	142
4.24 The 9+0 Microtubule Axoneme	143
4.241 The Flexural Rigidity of Primary Cilia	143
4.242 Distribution of Materials upon the Axoneme Doublets	144
4.243 Distribution of IFT-like Particles	145
4.25 The Transition Zone	147
4.251 Y-shaped Linker Structure	147
4.252 Sub-Distal Fibres: Filamentous Structures	148
4.253 The Alar-Sheets Structure	148
4.30 The Centrosome	150
4.31 The Basal Body	151
4.32 The Microtubule Triplet Structure	151
4.33 Luminal Vesicles	152
4.34 Basal Luminal Discs and Internal Structures	152
4.35 The Basal Appendages	153
4.36 The Proximal Centriole	154
4.40 Microtubule Populations	155
4.41 The Intermediate Filament Organisation Centre (IFOC)	156
4.42 Order in the Pericentriolar Matrix	157
4.43 The Centrosomal ‘Torus’	157
4.44 Nuclear Pores	158
4.50 The Golgi Apparatus	159
4.51 The trans-Golgi Network	159

4.52 Coated Pits and Caveoli	161
4.53 Are Primary Cilia Both Displacement Detectors and Pressure Sensors?	161
4.54 Matrix-Cilium-Golgi Continuum in Chondrocytes	162
4.60 Modelling the Primary Cilium	162
4.7 Future Work	163
References	165
Appendices Supplemental Information to Thesis	239
Appendix I: Receptors and Signalling in the Cilium and Centrosome	240
1.1 Membrane Receptors, Luminal Components and Signalling Pathways	240
1.2 Axoneme Associated Proteins	272
1.3 Centrosome Associated Proteins	283
1.4 Cell-Cycle Regulatory Kinases	299
1.5 Regulatory Components	304
Appendix II: Rab-GTPases - Ciliary and Golgi Function	309
Appendix III: Kinesin and Dynein Microtubule Motors	321
3.1 Kinesin Motor Proteins	322
3.2 Axonemal Dynein Proteins	333
3.3 Cytoplasmic Dynein Proteins	333
Appendix IV: Intra-Flagellar Transport Complexes	342
Appendix V: Kinesin and Dynein Motors Responsible for Organelle Processes and Transport	347
Appendix VI: A Select Review of Tomography and Modelling	360
Appendix VII: Animation List	370
Appendix VIII: Poster Presentations	372
List of Tables	
Table 3.1 Measurements of Chondrocyte Primary Cilia	79

List of Figures

Chapter One: The Matrix-Cilium-Golgi-Continuum

Figure 1.1 The 'Central Flagellum'	3
Figure 1.2 The Primary Cilium of a Chondrocyte	5
Figure 1.3 Diagrammatic Cross Sections of Axonemes	6
Figure 1.4 The Membrane, Axoneme and Basal Body of the Motile Cilium	7
Figure 1.5 The Basal Body and Transition Fibres (Alar Sheets)	8
Figure 1.6 Observations of the Range and Distribution of Basal Appendages	9
Figure 1.7 Striated Rootlets of the Diplosome	9
Figure 1.8 The Nine-Fold Symmetry of the Centriole	10
Figure 1.9 Illustration of the Matrix-Cilium-Golgi-Continuum	12
Figure 1.10 The Interphase Centrosome	13
Figure 1.11 The Centrosome	15
Figure 1.12 Microtubule Nucleation and Doublet Structure	17
Figure 1.13 The Cell Centrosome Cilium Cycle	20
Figure 1.14 Biogenesis of the Primary Cilium	23
Figure 1.15 Golgi Derived Materials for Ciliogenesis	24
Figure 1.16 The Primary Cilium	28
Figure 1.17 The PC1/PC2 Mechanotransduction Complex	30
Figure 1.18 Proposed Mechanism of Flow Induced Ciliary Ca^{2+} and cAMP Signalling Modalities	31
Figure 1.19 The Kinesin Motor	33
Figure 1.20 The Dynein Motor and Dynactin Complex	35
Figure 1.21: Regulated Golgi Transport and Signalling	40
Figure 1.22 Microtubules and Vesicle Transport	42
Figure 1.23 Polarisation of the Centrosome and Golgi in Cell Migration	43
Figure 1.24 The Golgi Intracellular Transport Pathways	48
Figure 1.25 Hyaline Articular Cartilage	54
Figure 1.26 The Chondron	55
Figure 1.27 Disaccharide components of hyaluronic acid, chondroitin-4, -6, and keratan sulphates.	57
Figure 1.28 Cartilage Proteoglycans	58
Figure 1.29 The Proteoglycan Aggrecan	59
Figure 1.30 The Golgi Apparatus	59
Figure 1.31 Synthesis and Formation of Collagen:	60
Figure 1.32 Chondrocyte Matrix Membrane Adhesion Receptors	61

Chapter Two: Methods

Figure 2.1 Imaging Resolution of Electron Tomography compared with Confocal Microscopy	63
Figure 2.2 Chick Embryo Cartilage	64
Figure 2.3 Cell Culture	65
Figure 2.4 Ruthenium Hexa-amine-Trichloride	67
Figure 2.5 Tomography of a Primary Cilium Aligned with the Substrate	70
Figure 2.6 Fiducial Markers	70
Figure 2.7 Remote Electron Tomography	71
Figure 2.8 The ‘Missing Wedge’ Problem	72
Figure 2.9 Data Acquisition	73
Figure 2.10 Fiducial Tracking in IMOD	74
Figure 2.11 The Modelling Process	75
Figure 2.12 The Virtual Cilium	76

Chapter Three: Results

Figure 3.1 Connective Tissue Primary Cilia Sectioning of Tendon	91
Figure 3.2 Serial Sectioning of Chick Sternal Cartilages	92
Figure 3.3 Projection Types of Chondrocyte Primary Cilia	93
Figure 3.4 Cilium-Centrosome Serial Sectioning of Cultured Chondrocytes	94
Figure 3.5 Selection of Tomograms and their Z-axis Optical Sections	95
Figure 3.6 A Semithick Section Containing a Primary Cilium	96
Figure 3.7 Alignment of Tomogram Dataset	96
Figure 3.8 Tomogram Z-Axis Stack	97
Figure 3.9 An Optical Section of the Cilium Axoneme	98
Figure 3.10 Tomographical Modelling of Extracellular Matrix and Matrix Granules	99
Figure 3.11 Matrix Ciliary Membrane Interactions	100
Figure 3.12 Matrix Ciliary Membrane Microtubule Interactions	101
Figure 3.13 Microtubule Doublet Nine-Fold Architecture	102
Figure 3.14 Localisation of Materials within the Axoneme	103
Figure 3.15 The Luminal Axoneme: Intra-Ciliary ‘Rafts’ and Microtubule-Microtubule Interactions	104
Figure 3.16 The Distal Axoneme (1)	105
Figure 3.17 The Middle Axoneme (2)	106
Figure 3.18 The Transition Zone (1) – Tapered Zone	107
Figure 3.19 The Transition Zone (2) – Alar Sheets / Transition Fibres	108
Figure 3.20 The Basal Body (1) Microtubule Triplets	109

Figure 3.21 The Basal Body (2) Luminal Discs, Deposits and Fibers	110
Figure 3.22 Basal Body (3) Internal Structures and Vesicle	111
Figure 3.23 Basal Appendage One: Optical Sectioning and Reconstruction	112
Figure 3.24 Basal Appendage One (1) Alignment of Basal Appendage Basement Structures	113
Figure 3.25 Basal Appendage One (2) Ultrastructure of Arm, Docking Station and Substrate	114
Figure 3.26 Basal Appendage Two (1) Ultrastructure and Modelling	115
Figure 3.27 Basal Appendage Two (2) Docking Complexes	116
Figure 3.28 Basal Body: Appendages Summary; Basement Structures, Basal Arm and Docking Complex	117
Figure 3.29 Basal Body And Cilium Radial Components	118
Figure 3.30 Proximal Centriole Ultrastructure, Deposits and Model	119
Figure 3.31 Proximal Centriole Radial Components and Proximity to Nuclear Pores	120
Figure 3.32 The Centrosome (1) Ultrastructure and Modelling	121
Figure 3.33 The Centrosome (2) The Centrosomal Torus	122
Figure 3.34 The Centrosome (3) The Pericentriolar Environment	123
Figure 3.35 The Centrosome (4) Basal Body, Proximal Centriole within the MTOC	124
Figure 3.36 The Cytosolic Microtubules	125
Figure 3.37 Centrosome to Golgi Connectivity	126
Figure 3.38 The <i>Cis</i> , <i>Medial</i> and <i>Trans</i> Golgi Compartments	127
Figure 3.49 Transport of Matrix from the Golgi	128
Figure 3.40 The Cilium, Coated Pits and Caveolae	129
Figure 3.41 The Matrix Cilium Golgi Continuum	130
Figure 3.42 Plan of Tomogram Features	131
Figure 3.43 The Cilium Centrosome Continuum	132

Chapter Four: Discussion

Figure 4.1 The Transition Zone ‘Compartment’	149
--	-----

List of Abbreviations

α	Alpha
β	Beta
γ	Gamma
δ	Delta
ζ	Zeta
ϵ	Epsilon
μ	micron 1×10^{-6}
\AA	Angstrom 1×10^{-10}
aDMEM	advanced Dulbecco's Modified Eagle Medium
AC	Adenylyl Cyclase
AKAP450	A-Kinase Anchoring Protein 450
ARF	ADP-Ribosylation Factor
ARHGAP21	Rho GTPase activating protein 21
Arp1	Actin Related Protein 1
ATP-2	ATP synthase
AP2	Cytosolic Adaptor Protein
ATP	Adenosine Tri-Phosphate
BA1	Basal Appendage 1
BA2	Basal Appendage 2
BBS	Bardet-Biedl Syndrome
BCL	B-cell lymphoma
BMP	Bone Metamorphic Protein
BP1	Binding Protein 1
BSA	Bovine Serum Albumen
CAM	Cell Adhesion Molecule
cAMP	cyclic-Adenosine Mono Phosphate
CDC42	Cell Division Control Protein 42
CC2D2A	Coil and C2 Domain Containing 2A
CDK	Cyclin Dependend Kinase
CEP	Centrosomal Protein
CFTR	Cystic Fibrosis Trans-membrane conductance Regulator
CLS / CTS	Ciliary Targeting Sequence / Ciliary Localisation Sequence
CLSM	Confocal Laser Scanning Microscopy
CNK2	Connector Enhancer Kinase 2
cnRNA	Centrosomal RNA
CLASP	Cytoplasmic Linker Associate Protein

COP1	Coat Protein One
CS	Chondroitin Sulphate
Da	Dalton
DAAM1	Dishevelled Associated Activator of Morphogenesis
DAG	Diacyl-Glycerol
DCTN1	Dynactin Subunit 1
DNA	Deoxyribo Nucleic Acid
DLIC-1	Dynein light intermediate chain-1
DYN	Dynein
EB1	End-Binding Protein 1
ECM	Extra Cellular Matrix
EGR	Epithelial Growth Factor
EGFR	Epidermal Growth Factor Receptor
ER	Endoplasmic Reticulum
ERGIC	Endoplasmic Reticulum Golgi Intermediate Compartment
ENaC	Epithelial Na ⁺ (Sodium) Transporter Channel
ET	Electron Tomography
FCS	Foetal Calf Serum
FGF	Fibroblast Growth Factor
γ -TuRC	γ -Tubulin Ring Complex
γ -TuSC	γ -Tubulin Small Complex
GAG	Glycoaminoglycan
G $\beta\gamma$	G beta gamma
GDP	Guanosine Di-Phosphatase
GCP	Gamma Complex Associated Protein
GERL	Golgi-Endoplasmic Reticulum-Lysosome
GM130	Golgi Matrix protein 130
GMAP210	Golgi-microtubule-associated protein of 210 kDa
GPC	Glypican
GPCR	G-Protein Coupled Receptor
GTP	Guanosine Tri-Phosphatase
GM130	Golgi Matrix Protein 130
GPC	Glypican
HA	Hyaluronic Acid
HF	Hydrofluoric Acid
HEK	Human Epithelial Kidney
HYLS1	Hydrolethalus syndrome protein 1

IFT	Intra-Flagellar Transport	
IGD	Interglobular Domain	
IGF	Insulin Like Growth Factor	
IGFR-1R	Insulin-Like Growth Factor-1 Receptor	
ImageJ	Freeware image analysis programme	
IMOD	An open-source suite for modelling electron microscopy data	
INPP5E	Inositol 1,4,5-trisphosphate (InsP3) 5-phosphatase	
IP3	Inositol Trisphosphate	
JBTS	Joubert Syndrome	
KAREN	Kiwi Advanced Research Network	
KIF	Kinesin Motor Protein	
KS	Keratan Sulphate	
l	litre	
Lis	Lissencephaly sequence	
LKB1	Liver Kinase B1	
LZTFL1	Leucine Zipper Transcription Factor-Like 1	
m	meter	
M	Mega	1×10^6
milli	milli	1×10^{-3}
ml	milli-litre	
μ	micro	1×10^{-6}
Osm	Osmolarity	
MARK	Microtubule Affinity Regulating Kinase	
MAP	Microtubule Associated Protein	
MAPK	Mitogen Activated Kinase	
MCH	Melanin Concentrating Hormone	
MDCK	Madin-Darby Canine Kidney	
MT	Microtubule	
MTOC	Microtubule Organising Centre	
n	Nano	1×10^{-9}
N	Newton	
NEDD1	Neural precursor cell Expressed, Developmentally Down-regulated 1	
NIH3T3	National Institute of Health 3T3	
NG2	Neural/Glial Antigen 2	
NKF-kB	Nuclear Factor Kappa Beta	
NPHP	Nephronophthisis (protein designator)	
NudE	Nuclear Distribution E	

Nup133	Nucleoporin 133
ODF	Outer Dense Fibre
ORP1L	Oxysterol-binding Protein-Related protein 1L
Pa	Pascal
Patched	HedgeHog Signalling Component
PC	Polycystin
PCM	Peri-Centriolar Matrix
PCM-1	Pericentriolar Material 1
PDB	Protein Data Bank
PDGF	Platelet-Derived Growth Factor
PG	Proteoglycan
pH	H ⁺ ion concentration
pico	Pico 1×10^{-12}
PIP3	Phosphoinositol-3
PI3K	Phosphoinositide 3-kinase
PKC	Protein Kinase C
PKD	Polycystic Kidney Disease
PSG	Penicillin Streptomycin Glutamine
p150 ^{Glued}	Dynactin Component
P2X	Purinergic ATP-gated ion channel
P2Y	G-coupled receptor
Rab	G Protein, member of the Ras family GTPases
RAC	Rho-GTPase subfamily member
RHT	Ruthenium Hexaamine Tri-Chloride
ROCK	Rho-GTPase effector
RP	Retinitis Pigmentosa
RPGRIP	Retinitis Pigmentosa GTPase Regulator Interacting Protein
RILP	Rab-Interacting Lysosomal Protein
RNA	Ribo Nucleic Acid
Shh	Sonic Hedgehog
Solidworks	Proprietary engineering software package
Smo	Smoothened
SuFu	Suppressor of Fused
SSTR	Somatostatin Receptor
STAT6	Signal Transducer and Activator of Transcription
SD/ σ	Standard Deviation
TMEM	Trans Membrane Protein

TRAP	Transport Protein Particle
TRP	Transient Receptor Protein
TGF- β	Transforming Growth Factor β
TRPV4	Transient Receptor Potential Vanilloid 4
TEM	Transmission Electron Microscopy
TGF- β	Tumour Growth Factor- β
Vangl2	Vang-like protein 2
VEGF	Vascular Endothelial Growth Factor
VxPx	Ciliary Targeting Motif
XMAP215	Xenopus Microtubule Associated Protein 215
Wnt	Wingless
ZW10	Zeste White 10
2D	Two dimensions
3D	Three dimensions

Pathways

Par3/Par6/aPKC	Polarity Pathway
PI3K/Akt/mTOR	Apoptosis Pathway
MEK/ERK	Mitogen Activated / Extracellular signal Regulated Kinases

NB: For proteins not listed here, see the Appendices.

Chapter One: The Matrix-Cilium-Golgi Continuum

1.01 Preamble

There has been an explosive growth of interest in the primary cilium since the realisation that its occurrence is almost universal in eukaryotic cells and its principal role is presumably to be sense features of the cellular environment significant to a particular cell type, allowing an appropriate response. Hence, the primary cilia of the renal epithelial cells detect flow, while the cilia of the rods of the retina are light detectors, the cells of the cochlea detect vibrations, and the cilium of the cartilaginous chondrocyte detects stress-induced deformation. The importance of this structure has been underlined by the discovery that about 2000 proteins¹ are involved in its construction and operation, with mutations in these being often lethal or imposing severe functional deficiencies, which have become known as ciliopathies [1]. This has focused attention on the relation between structure and function of this organelle. However, most of the primary cilium and its associated structures is at the limits of resolution of available imaging techniques.

The primary cilium is a singular centrosomal organelle present in almost all eukaryotic cells and is distinct from other kinds of motile cilia and flagella in its unique (9+0) microtubule structure. Few conventional electron microscopy based investigations have attempted to model the primary cilium. The main experimental objective of this study was to produce an anatomically accurate, ultrastructure based three-dimensional model of a connective tissue primary cilium using electron tomography. Previous connective tissue investigations of primary cilia used serial sectioning, and these were limited in their resolution by the ultrathin section thickness (90-120 nm). The technique of electron tomography is ideally suited for investigation of ultrastructure contained within thicker semithick (350 nm) sections that could contain a longitudinally aligned entire cilium. The application of tomography permits the construction of an interrogative model allowing investigation of the structural continuum between the biomechanically functional matrix, the mechanically sensitive primary cilium and the cytoplasmic organelles responsible for the secretion of the functionally effective extracellular matrix.

The principal aim of all biological investigation is to achieve a marriage between structure and function. Modern technological advances, including high voltage electron tomography, offer the potential to achieve a physical resolution near to atomic levels, and in three dimensions, albeit in a static form. Advances in the incorporation of function, on the other hand, have been less clear. There is an abundance of information, drawn from diverse sources, inferring presence of macromolecules, and intermolecular relationships, but at the present time there is little in the way of synthesis into a coherent picture. This work attempts to progress towards a unifying picture of the relation between structure and function of the primary cilium by introducing a valid, three dimensional representation of the primary cilium at high resolution upon which functional activity can be imposed as biochemical

¹ <http://www.ciliaproteome.org/>

knowledge advances. This introduction is intended to provide not only a summary of present knowledge of the ultrastructure of the primary cilium and its associated structures, but also a review of the proteins known or hypothesised to be involved with its regulation and functional role.

This study presents novel new research using the recently refined ultrastructural imaging technique of electron tomography. This advanced technology not only allows detailed investigation of structural relationships at extreme magnifications not previously possible, but also enables translation of this acquired data into an anatomically accurate, interactive, three-dimensional model of the ultrastructural continuum that exists between the matrix, the cilium and the Golgi apparatus in connective tissue cells. Hyaline cartilage chondrocytes from chick embryo sterna have previously used as a model of connective tissue to study primary cilia, and further study of this tissue forms the basis of this thesis.

Section I – Previous Knowledge of the Structure of the Primary Cilium

1.02 A Brief History of the Primary Cilium

The history of the investigation of primary cilia has been extensively reviewed by Bloodgood (2009) [2] and Wheatley (1982) [3]. Cilia are amongst the earliest known eukaryotic organelles, with the first observations of primary cilia likely unknowingly made around 1763 by Leeuwenhoek [2, 4] during his detailed observations of cells and other micro-organisms resulting from his invention of the optical microscope [5]. The descriptive term ‘cilium’ was first introduced by Muller in 1786 [6] meaning ‘eyelash’, while Dujardin [2] used the term ‘flagellum’ in 1841 to describe motile cilia [2]. In 1876 Langerhans [7] published sketches of epithelia, showing a singular cilium projecting from cells, with an intracellular component at its base. It is clear that many have observed both types of cilia, yet Zimmerman is credited with discovering the primary cilium in 1894 [8], which he termed the ‘central flagellum’ [9]. In 1898 Zimmerman [9] described motile cilia as being distinct from a singular ‘primary cilium’, which originated from a pair of centrioles (the diplosome), and he proposed a role for it as a sensory organelle (see Figure 1.1) [2]. Bernhard and deHarven, however, introduced the term ‘primary cilium’ in 1956 [3]. Cilia and flagella are unique microtubule based membrane bound organelles, where description in the common lexis, *flagella* pertain to the uni-cellular motile apparatus, *cilia* being used to describe both *motile*, and non-motile *primary cilia* alike [2, 10]. Importantly, a functional distinction should be clearly drawn between motile cilia, which act on the surrounding medium to generate motion, and the primary cilium, which not only has a unique and characteristic structure, but also is non-motile and functions as a sensory detector.

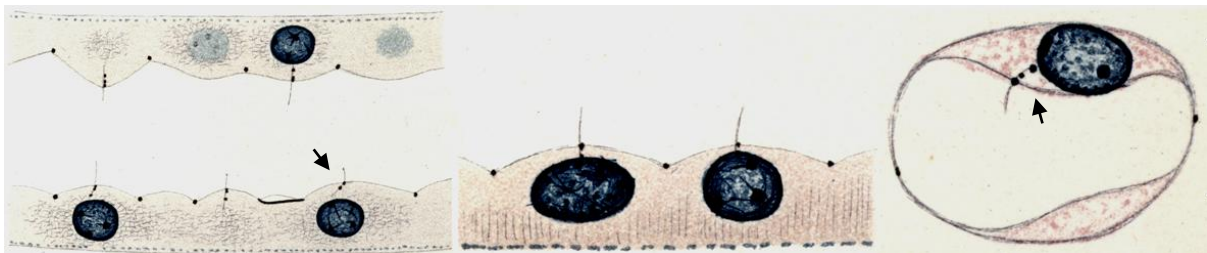


Figure 1.1 The ‘Central Flagellum’: A reproduction of images from Zimmerman’s original publication ‘*Beitrag zur Kenntniss einiger Drusen und Epithelien*’ [9] published in 1898, detailing observations of kidney tubule epithelium expressing a primary cilium from their centrosome (arrows). The centrosome consists of a ‘diplosome’ of two centrioles observed near the resolving limit of light microscopy. Reproduced from original scans published in Bloodgood (2009) [2], courtesy of Dr Bloodgood.

The discovery of the centrosome is attributed to Flemming, around 1875 [11, 12], while the common terms ‘centrosome’ and ‘centriole’ were introduced by Boveri in 1888 and 1895 respectively [13]. The *Henneguy-Lenhossek* hypothesis originated in 1898, defining the role of the centrosome in the formation of the spindle poles during cell division, the motile tail of spermatids in spermatogenesis, and generating the base of a primary cilium of a cell during interphase [3, 14]. Jennings (1899) [15] studied mechano-sensory reactions in unicellular organisms and described

behavioural responses to stimuli in the ciliate *Paramecium*, hinting at a sensory role for motile cilia [16], although a sensory function is now attributed to all cilia [17].

1.03 Early Work: Optical and Electron Microscopy of Cilia

A lot of the early 20th century work on cilia focussed on cilia of unicellular organisms or epithelial sheets contrasted against an optically transparent lumen. Unlike epithelial cells and unicellular organisms which often bear many cilia, most eukaryotic cells typically possess only a single primary cilium, whose small width of 200 nm and nominal length of 1-4 μm , places it near the limit of resolution of optical microscopes (about 200 nm) determined by Abbe (1873) [18, 19].

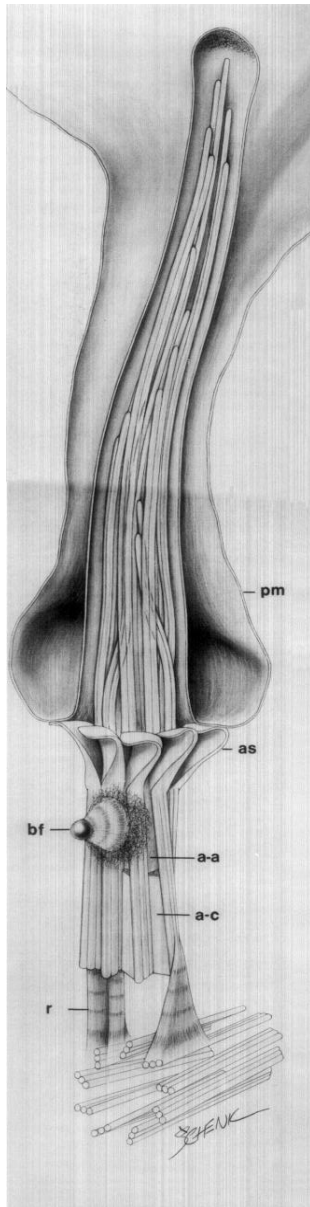
The invention of the transmission electron microscope (TEM) in 1931 by Max Knoll and Ernst Ruska [20] allowed far greater magnifications to be achieved. The use of osmium tetroxide [21] for fixation, combined with the embedding of biological materials into epoxy resins in the 1950's enabled the stabilisation of chemically fixed structures, and the use of heavy metal stains, such as lead or uranium, provided enhanced contrast [22]. With the development of diamond knives, reliable methods of ultra-thin sectioning emerged in the 1950's [2]. The main drawback with many of these early observations in electron microscopy was that inadequate fixation and processing techniques produced uncertain artefacts. During this period, different anatomical expressions of primary cilia were discovered to exist in many cell types and organisms ranging from protozoa to mammals [23]. For a review of historic publications on the primary cilium prior to 2005, see Wheatley (2005) [24]. Extensive ultrastructural analysis of primary cilia both *in vivo* [25-29] and *in vitro* [30, 31, 32] largely ignored their functional role within the eukaryotic cell until recently [33].

Studies by Praetorius et al., (2001, 2003) [34, 35] established that epithelial primary cilia could act as flow sensors in the renal collecting duct, and their bending resulted in the activation of intracellular calcium signalling. It has subsequently become apparent that primary cilia in vertebrates encompass a wide range of sensory modalities from the ocular rod and cone photoreceptors [36], including olfaction and audition, to tonicity and flow detection in renal primary cilia, which all play specialist roles in signal transduction. They also occur in numerous tissues and cell types (with a current list maintained at the Bowser Lab²), although red blood cells, oocytes and some lymphatic cells lack this structure. Signalling components and structural proteins involved with the cilium involve at least 2,000 genes, whose proteins are specific to, or associated with ciliary function or the Ciliome³ [37-41].

²<http://www.bowserlab.org/primarycilia/cilialist.html>

³ www.ciliome.com

1.04 The Discovery of Chondrocyte Primary Cilia



There are few anatomical examples of the basic structure of the primary cilium. One of these is from chondrocytes (Figure 1.2). Initially, these were thought to be non-ciliated. The first known recorded observations of primary cilia in chondrocytes were made by Scherft et al., (1967) [42] reviewing their occurrence in cartilage. Hart (1968) [43] undertook ultrastructural studies of the cilium, and this was followed by Federman et al., (1974) [44], and Wilsman [27, 28, 29]. Wilsman (1978) [27, 28] performed the first detailed studies of *in situ* chondrocyte primary cilia where their incidence and morphology were investigated by exhaustive serial sectioning. This allowed for the first artistic perspective of the three-dimensional anatomy of a chondrocyte primary cilium, which shares a strong similarity to the basal body described by Anderson in (1972) [45]. The axoneme is shown deflected, laying within an invagination. Not all microtubule doublets extend the full length of the axoneme, with many falling short, inclining lumenally inwards in their projection.

Figure 1.2 The Primary Cilium of a Chondrocyte: An artistic interpretation of a primary cilium invaginated within a 'ciliary pocket' of the cell membrane, generated by serial sectioning. The cilium consists of a distal tip, a ciliary axoneme and a basal body, with which the proximal centriole forms the centrosome. Detailed are the plasma membrane (**pm**), the alar sheets (**as**) / transition fibres, the basal foot (**bf**), basal body microtubule triplet linkers (**a-c**), the (**a-a**) connector and striated rootlets (**r**) linking to the proximal centriole. Modified and reproduced with permission from Wilsman (1978) [27].

1.05 The Ciliary Axoneme

The axoneme of all cilia shows distinct common zones: the *distal tip*, the *middle axoneme* and the *transition zone* adjacent to the *basal body* (see Figure 1.2). The *distal zone* contains the tapered end of the cilium, while the *middle axoneme* contains the bulk of the microtubule luminal components, and the *transition zone* marks the merging of the axoneme with the cell membrane and basal body [25]. The *distal tip* of the axoneme represents the terminus zone for bi-directional microtubule-dependent internal transport complexes (commonly referred to as intra-flagellar transport, IFT) [46] and represents a unique area for the assembly and maintenance of ciliary components [47-49]. It also contains a reduced number of microtubule doublets whose distal tips contain finer structures attached to the end caps of the microtubules [49, 50].

Investigation of ciliary membranes by freeze fracture techniques shows the presence of membrane embedded structures along the length of the axoneme, consisting of populations of longitudinal rows, rosettes, plaques and the ciliary necklace [51, 52]. These act as tethering points for fine filaments bridging between the ciliary membrane and the microtubule doublets of the axoneme [49, 51-53] (Figure 1.3).

1.06 *Ciliary Ultrastructure*

Electron microscopy studies of the more numerous motile cilia revealed much about the components of their mechanisms of motion and the axoneme ultrastructure, which they have common with primary cilia [28, 45, 49, 54-56]. Axonemes comprise a plasma membrane enclosing unique linear microtubule doublets extended from a centriole base, which when expressing a cilium is known as a 'basal body'. Centrioles possess a unique 'nine-fold' microtubule symmetry, which are shared with the microtubules of the axoneme projected from the basal body [3, 57]. While many authors have reviewed the ultrastructure of motile cilia [54], that of primary cilia is less well known due to their relative rarity, being first described ultrastructurally by Sotelo in 1958 [58]. Motile cilia and flagella usually contain a central doublet (9+2) architecture [37, 59] which was first described by Manton et al., (1952) [60] in the sperm flagellum, in which the axoneme contains a central pair of microtubules [54, 55] (Figure 1.3 A). The microtubule doublets extend most of the full length of the cilium, where the central microtubule pair defines the axis of flexion emanating from a base plate. In marked contrast, the (9+0) primary cilium lacks the central pair and base plate, as well as the microtubule doublet associated components of the dynein arms responsible for motion [3, 55, 49, 61, 62] (Figure 1.3 B).

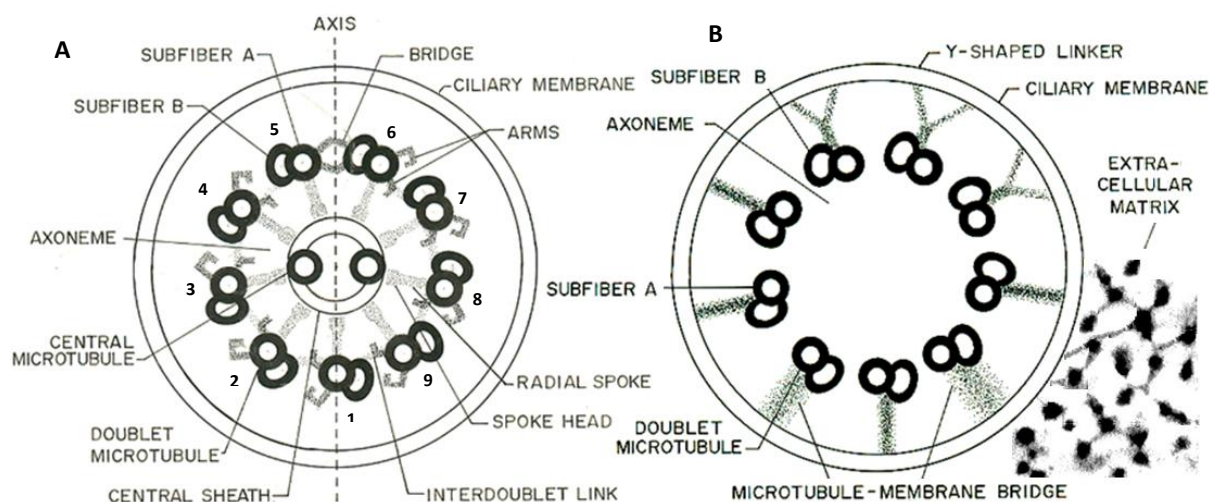


Figure 1.3 Diagrammatic Cross Sections of Axonemes: of [A] motile (9+2) and [B] primary (9+0) cilia viewed in the positive microtubule doublet direction from their respective basal bodies (into the page). Primary cilia are immotile, and lack the inner microtubule pair, the motive machinery of the outer dynein ciliary arms and radial spoke components of motile (9+2) cilia (see Lin et al., (2012) [56]). The (9+2) axoneme contains an axis of symmetry defined by the inner microtubule pair (see Gibbons (1961) [54]). Modified and reproduced courtesy of C.A. Poole.

In addition, primary cilia microtubule doublets commonly fall short of the tip of the axoneme and are commonly displaced inward. The primary cilium is uniquely defined by the presence of a subtending proximal centriole [28, 26, 63, 64]. All cilia contain extensive microtubule doublet-to-membrane linkages of filaments and y-shaped linkers (see Figure 1.3).

1.07 The Transition Zone ‘Compartment’

The *transition zone* separates the axoneme from the cytosol of the cell, demarcating the boundary between the ciliary membrane and its attachment to the cell membrane [49, 65]. Observed historically in both motile and primary cilia, the *transition zone* is a specialist membrane-bound area encompassing the proximal region of the axoneme, where it merges with the cell membrane. It comprises structures connecting microtubules to the membrane, made up of *y-shaped linkers*, *filaments* and *alar sheets* (see Figs 1.3-1.5) [54, 55]. These function as membrane-microtubule anchoring components and are highly conserved [65, 66] although their ultrastructure varies between species and cell types [49]). The transition-zone in primary cilia is proposed to be a regulatory zone, or ciliary gate analogous to a nuclear pore, organised for the orderly bi-directional transport of materials [66-70]. *Y-shaped linkers* commonly feature in the distal transition zone, where they comprise the principle components of the ‘ciliary necklace’, which encircles the shaft as a membrane microtubule complex [51, 55] (Figure 1.4). Investigation of ciliary structure by freeze fracture has relied heavily upon the study of motile cilia.

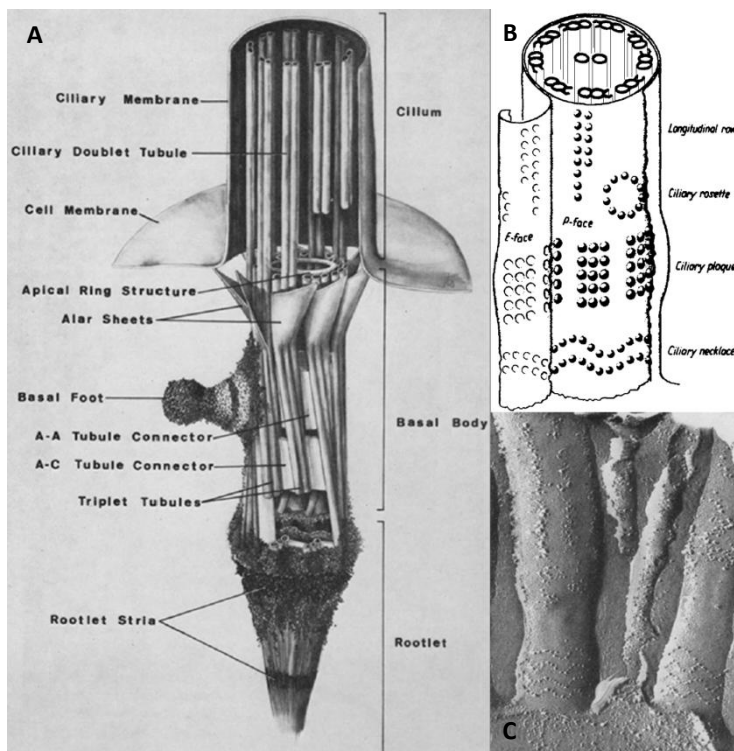


Figure 1.4 The Membrane, Axoneme and Basal Body of the Motile Cilium: **[A]** An artistic interpretation of the basal body of the motile cilium. Anatomical features detailed include the inclination of the basal body microtubule triplets (their connectivity to each other by linkages), their transition into the doublets of the axoneme, and where they are tethered to the plasma membrane by transition fibres (alar sheets). A single basal appendage (the ‘basal foot’) attaches to the microtubule triplet faces, while a striated rootlet binds to the distal end of the basal body. Reproduced and modified from Anderson [45]. **[B]** The axoneme membrane is decorated with distinct patterns of intra-membrane structures which make up such features as the ciliary necklace, plaques, rosettes, and longitudinal rows. These link the membrane to the microtubule doublets of the axoneme. Modified and reproduced from Bardele (1981) [52]. **[C]** A freeze fracture image of the ciliary membrane showing the protein linkages that make up the ciliary decorations described in **[B]**. Note presence of zones of ‘longitudinal rows’ of membrane bound materials within the axoneme membrane. Reproduced from Gilula et al., (1972) [51].

1.08 Basal Body Appendages - Proximal to Distal

There remains confusion in the literature about the naming convention for ciliary structures, especially of appendages observed upon basal bodies [71]. Anderson (1972) [45], using serial sectioning, investigated the structure of the basal body in motile cilia, and reconstructed a three dimensional model likeness defining the structural form of the microtubule triplet architecture, alar sheets and basal foot (Figure 1.5). Understanding of these structures is based largely upon studies of motile cilia. The basal body is delimited at the distal end by the presence of alar sheets or ‘transition fibres’, while conical shaped *basal feet* project from the mid-body (Figure 1.5). Subdistal appendages, as their name implies, are located in the ‘sub-distal zone’ between the *distal alar sheets*, and the *basal feet*.

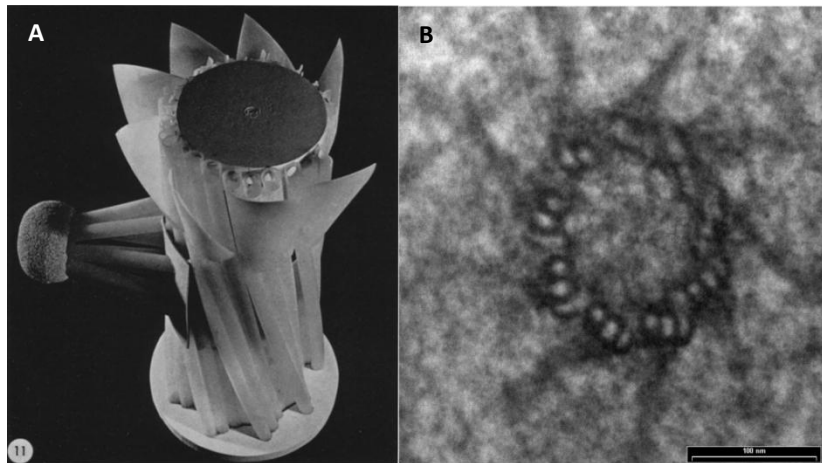


Figure 1.5 The Basal Body and Transition Fibres (Alar Sheets): [A] A scale model produced by Anderson (1972) [45] of a motile cilium from a cell in the ovary of a rhesus monkey, detailing the microtubule triplet architecture of the basal body, the single basal (foot) appendage and the alar sheets. Note the change of pitch angles and curl in the microtubule triplets in their distal projection along the axis of the basal body. The ‘alar sheets’ show as ‘cusps’ originating from the distal end of the triplets. [B] Comparison of a 100 nm thick ultrathin cross section of an ovine chondrocyte showing the transition fibres originating from the triplet faces, and tapering to a point of contact with the periciliary membrane in the adjacent section. Reproduced from Anderson [45].

1.09 The Basal Feet (Basal Appendages)

Primary cilia have been observed expressing up to five basal appendages [26, 25, 72] (Figure 1.6), yet regulation of their structure, packing density and role in centriole maturation remain unknown [73]. The basal appendages each consist of a conical structure, 174 nm long [45], which at its base spans a domain of at least three microtubule triplets of the basal body [74], and at its apex acts as a microtubule anchoring complex [26, 45]. In contrast, the ultrastructure of the motile cilium is defined by the presence of a single lateral basal foot, positioned perpendicular to the axis of the central microtubule pair, indicating the plane of motility and fluid flow [45, 54, 75]. Thus, the basal body of motile cilia exhibits a structural polarity [76], linking structure to the mechanism of planar cell polarity [77]. The possibility of a similar radial structural relationship with respect to polarisation of primary cilia remains unknown.

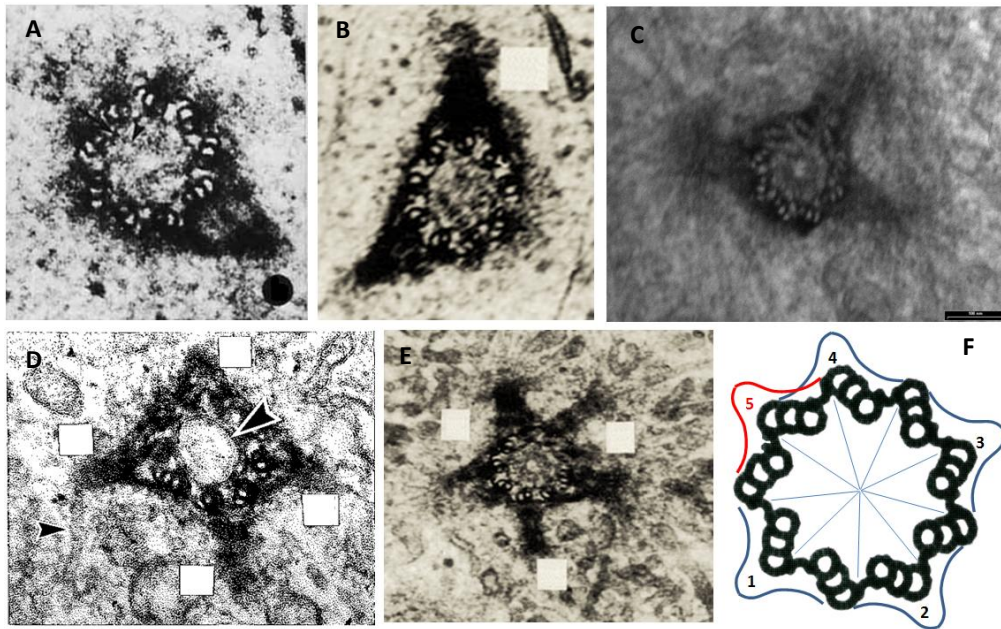
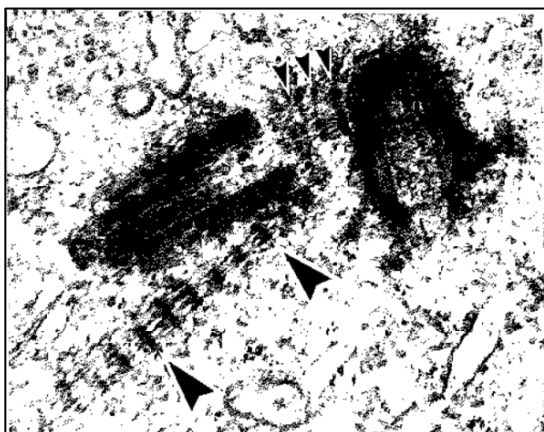


Figure 1.6 Observations of the Range and Distribution of Basal Appendages: The radial projections of basal feet upon basal bodies range from 1 to 5: [A] Wilsman (equine chondrocyte, *in situ*) [29], [B] from Alieva et al., (porcine kidney cells, *in vivo*) [72], [C] ovine, chondrocyte *in vitro*, [D] Poole et al., (1985) [26] unpublished image of chick embryo sternal cartilage and [E] Alieva (porcine kidney cells) [72]. [F] Centriole triplet nine-fold template reproduced and modified from Wheatley [3] reflecting images [A-E] where each basal appendage substrate covers at least three microtubule triplets evenly (blue), while occasionally an appendage ‘shares’ an adjacent triplet (red). Preferential order, orientation and assembly of basal appendages remain undetermined. Images reproduced with permission.

1.10 The Striated Rootlets

Striated rootlets commonly occur with motile cilia, where they form conical shaped, longitudinally aligned, filamentous periodic structures that frequently radiate from the proximal end of the basal body into the cytosol [45, 54, 78] (Figure 1.4). However, they are occasionally observed originating from the basal bodies of primary cilia (Figure 1.7), where they are proposed to be involved in ciliary stability [79] and may be crucial for basal body anchoring. Hagiwara et al., [78] revealed a conserved periodicity of striations in human oviduct epithelium of 68.5 ± 2.95 nm in the fibrillar part, and of shorter 63.9 ± 2.25 nm spacing in the conical zone. Variances in spacing exist between eukaryotes [80], indicating a possible link of their periodicity to specific functions [81]. The proximal ends of the basal body and the subtending proximal centriole are connected via inter-centriolar linker



fibres, which are sometimes striated [82], and which display a still shorter periodicity of about 55 nm [64, 83].

Figure 1.7 Striated Rootlets of the Diplosome: Inter-centriolar striated rootlets (small arrowheads) connect the basal body (right) with the proximal centriole (left), while a striated rootlet is seen radiating from the basal body (large arrowheads). Unpublished image, courtesy of C.A. Poole (circa 1985).

1.11 The Centriole: A Template for the Basal Body and Axoneme

As an ancient ‘inherited organelle’ from an ancestral eukaryote, the centriole is essential for the formation of microtubule based cilia and flagella [3, 59, 63, 84-87]. It has been widely speculated that its function is related to the unique nine-fold symmetry, whose structure is based upon microtubule triplet ‘vanes’ [3, 28, 63, 88]. These are inclined into a ‘barrel’ shaped structure with an inner 130 nm and outer 250 nm diameter of 400 nm length [28, 89, 90]. The microtubule triplet subfibres have a an inclination in the longitudinal axis forming an arc, between 10 to 15°, with each triplet having an average 40° ‘triplet angle’ with respect to the basal body [45, 63]. The inclination angle decreases distally along the axis of projection of the basal body, where the triplets are twisted with a left-handed ‘curl’. The first model of a basal body of a motile cilium interpreted by Anderson (1972) [45] (Figure 1.4 A), indicated that triplet angles and basal body diameter gradually decreased towards the transition zone from 40° to 15°. The first model of a primary cilium by Wilsman (1978) [27] (Figure 1.2) described an inclined taper in the microtubule projection towards the distal end from 51° to 28°, while Vorobjev et al., (1982) [63] observed their inclination varied from radially from proximal to distal by 55° to 85°. More recently Li et al., (2011) [89] tomographically confirmed this distally decreasing angle along the axis of the basal body.

Each microtubule triplet consists of a complete tubulin based A-subfibre (of 13 protofilaments), with the partial B and C-subfibres (each of 10 protofilaments) [88, 91, 92], shown in Figure 1.8 (for numbering conventions see Linck et al., (2007) [93]). The distal portion of the C-subfibre protofilaments progressively uncouple distally, forming a ‘hook’ [88, 94] (Figure 1.8) which terminates near the transition zone. The A and B-subfibres of the basal body extend to form the nine-microtubule doublets of the axoneme.

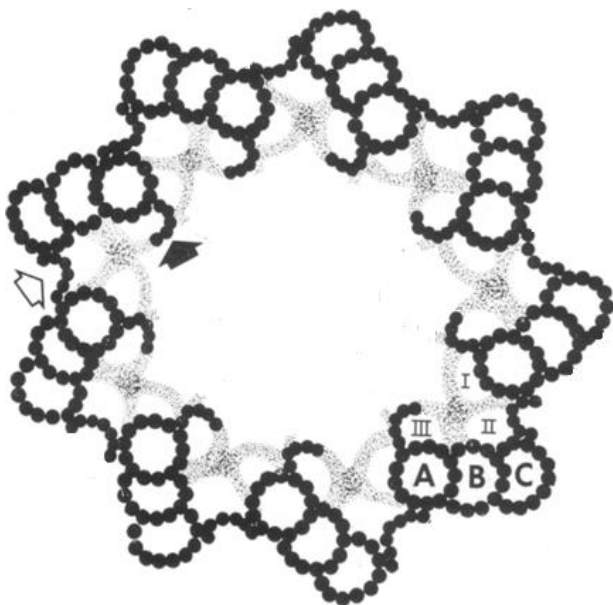


Figure 1.8 The Nine-Fold Symmetry of the Centriole: Detail of the tubulin based microtubule architecture of a centriole detailing symmetries, linkages and luminal spaces, from the aquatic fungus *Phlyctochytrium irregulare* (modified and reproduced from McNitt (1974) [91]). Each triplet consists of a central microtubule core (A) with subtending subfibres (B) and (C) composed of tubulin dimers. Protein linkages interconnect neighbouring triplets via A-C inter-triplet bridges providing structural support (white arrow, note uneven symmetry of A-C triplet linkers). A-subfibre ‘feet’ (black arrow) project luminally and are associated with the cartwheel complex during centriole biogenesis [57]. Luminal zones **I**, **II** and **III** encompass the faces of the A, B and C-subfibres, where fine filamentous materials have been observed. Studies by Li et al., (2010) [89] have confirmed the triplet tubulin arrangement of the A-subfibre having 13 protofilaments members (A1-A13), the B-subfibre (B1-B9) and the C-subfibre (C1-C9) following the Tilney-Linck convention [93], although no common standard yet exists. The nine-fold symmetry of the cartwheel (and basal body) arises from assembly of the SAS-6 homodimer [57]. Viewed in the positive microtubule direction, into the page, in the direction of the aligned thumb of the ‘left hand’, the fingers ‘curl’ in the orientation of the inclined triplets.

Linkers between adjacent triplet A and C-fibres occur along the proximal half of the basal body [28] where they are involved in inter-triplet stabilisation and structural integrity [45]. Often observed are A-subfibre ‘feet’ which link with the fine components of the cartwheel complex which are remnants of centriole assembly [3, 28, 91]. In comparison, ultrastructural details of proximal centrioles are less well known. Their triplets are reported to be inclined at 60° with respect to the longitudinal axis over the length of the centriole, and are devoid of any decorating appendages or association with the cell membrane [63]. Many studies show an absence of cartwheel-like structures in mature centrioles, and report the presence of luminal accumulations of proteinaceous materials and vesicles [25, 45, 63]. Due to their inherent difficulty for study, confusion has existed within the literature over the correct ‘handedness’ of centrosomal centrioles, particularly with regard to their polarisation and curl [63, 94].

1.20 The Matrix-Cilium-Golgi Continuum

The morphological relationship between the extracellular matrix, the primary cilium and the Golgi apparatus has been previously described in chondrocytes [25, 26, 28, 95-98] but structural and biochemical interactions between the matrix, the cilium and the Golgi have been neglected. Poole et al., (1985) [26] first proposed that the primary cilium was in fact a ‘cybernetic probe’ [99] capable of *detecting* extracellular information, *transducing* this information to the centrosome and microtubule network, which *responds* by polarising the Golgi secretory apparatus, leading to the regulated spatial and temporal secretion of connective tissue macromolecules. Furthermore, McGlashan et al., [100] identified the occurrence of $\alpha 2$, $\alpha 3$, $\alpha 5$, $\beta 1$ -integrins and NG2 receptors upon the primary cilium membrane, while the adhesion receptors of CD44 and Annexin-V were undetected, suggesting the chondrocyte ciliary membrane is only selective for certain matrix connections. Since these receptor proteins are known to physically link extracellular matrix components to the cellular membrane, it is hypothesised that the biomechanical signals from the matrix probably influence ciliary mechanotransduction.

Figure 1.9 shows an unpublished drawing of the ‘matrix-cilium-Golgi continuum’ derived from ultrastructural information (by Poole et al., [26]), hypothesising a putative signalling continuum between the mechanically functional extracellular matrix, the mechanically responsive primary cilium, the centrosome, and the secretory Golgi apparatus and the nucleus. Extracellular matrix is shown attached to the ciliary membrane via specific receptors, so that a pressure induced distortion can exert a bending moment on the axoneme. This distortion may be conveyed to the basal body, from which the cilium projects, and the centrosome could direct the microtubule network, which then coordinates Golgi assembly and polarisation for secretion. Thus, like an antenna, the primary cilium provides hypothetically the ability to detect extracellular signals and forces, and transduce these to the centrosome, which can then orchestrate and engender the appropriate cellular response. In addition, the primary cilium can potentially detect chemical changes in its environment. This is thought to be

achieved through bi-directional microtubule-dependent intra-flagellar transport (IFT) [101]. The lumen of the axoneme contains electron dense deposits of intra-ciliary transport ‘trains’, likely composed of cargo materials, their IFT-complexes powered by dynein [102] and kinesin family member (KIF) motors *in transit* within the axoneme [103].

Specific chemoreceptors and associated materials assemble in a regulated way within the centrosome and are conveyed into the ciliary membrane. The centrosome consists of two centrioles commonly called a ‘diplosome’, but when associated with a cilium, are referred to respectively as a basal body and the subtending proximal centriole. Centrosomal microtubules participate in the organisation, regulation and transport of cellular organelles, including the Golgi components. Primary cilia are frequently observed surrounded by a ciliary pocket generated by retraction of the centrosome within the cell. The presence of receptor-mediated endocytosis in proximity to the ciliary ‘pocket’ suggests materials are recycled to the Golgi cisternae through the endosomal-lysosomal system.

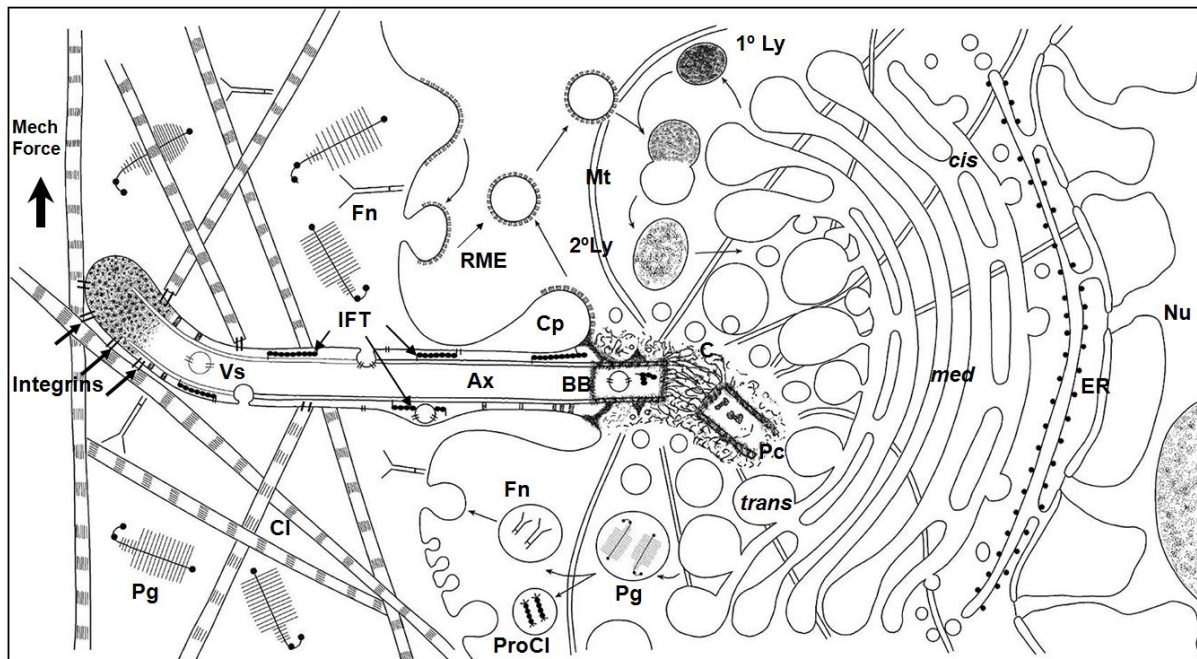


Figure 1.9 Illustration of the Matrix-Cilium-Golgi Continuum: The extracellular matrix consists of proteoglycans (**Pg**), fibronectin (**Fn**) and collagen fibres (**Cl**) which experience mechanical forces and are physically tethered to the membrane of the primary cilium by **integrins**. The basal body (**BB**) extends a microtubule based axoneme (**Ax**) into the extracellular domain. The axoneme contains components of intra-flagellar transport (**IFT**) particles, vesicles (**Vs**), fine internal linkages, and is partially invaginated into the cell within a ‘ciliary pocket’ (**Cp**). Orthogonally aligned to the basal body lies the proximal centriole (**Pc**), and these together form the structural core of the centrosome (**C**), which acts as the microtubule (**Mt**) organising centre of the cell. Located in a juxta-centrosome-nuclear position the Golgi apparatus occupies an intermediate position between the nucleus (**Nu**), the endoplasmic reticulum (**ER**), and the cell membrane. The Golgi consists of polarised stacks of *cis* (*cis*), *medial* (*med*) and *trans* (*trans*) cisternae, which modifies and secretes extracellular matrix (including pro-collagen **ProCl**) and forms the Golgi-endosomal-lysosome system. Receptor mediated endocytosis (**RME**) processes sequester materials within the lysosome system (primary **1° Ly** and secondary **2° Ly**). Note the attachment of collagen to the ciliary tip, and its capacity for deflection by mechanical force (**Mech Force**). Reproduced and modified courtesy of C.A. Poole (2003).

1.21 The Microtubule Organising Centre (MTOC)

The diplosome based centrosome (Figure 1.10) is a semi-conserved organelle which acts as the microtubule organising centre of the cell, regulating microtubule nucleation, organelle positioning, cellular transport, cell migration, cytokinesis as well as being intricately involved in aspects of the cell cycle [12, 104, 105]. The centrosome is also responsible for organising the bi-directional transport of vesicles, other materials and for positioning intracellular organelles of the endoplasmic reticulum (ER), the Golgi apparatus, the lysosomal system, mitochondria and the nucleus [106-108]. During interphase, the centrosome initiates ciliogenesis, and is responsible for cell polarisation, microtubule nucleation and maintaining the primary cilium [109]. The structural stability of the centrosome is dependent upon the centrioles [110], which are of greater resilience than cytoplasmic microtubules [111], and also participate in regulating centrosome size [112].

Conventional ultra-thin electron microscopy imaging, cut without reference to the plane of the interphase centrosome, usually reveals a cross-section of electron dense metal stain accumulation upon the microtubule structures of the axoneme, basal body, proximal centriole, the cytosolic microtubule network and amorphous surrounding materials (Figure 1.10).

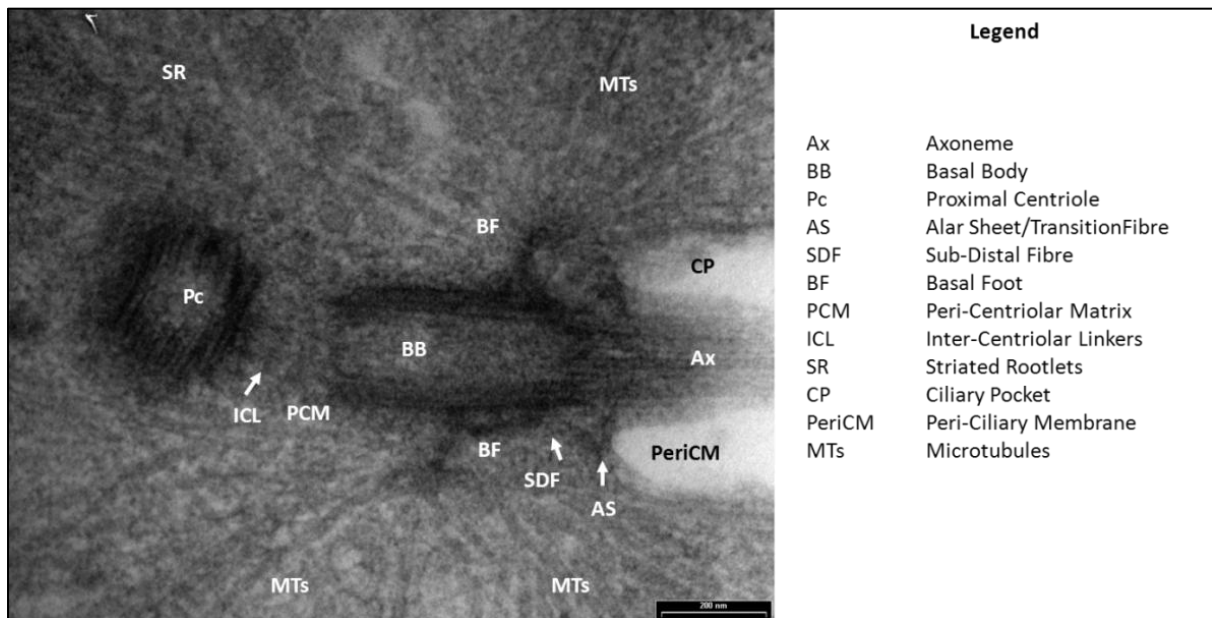


Figure 1.10 The Interphase Centrosome: An electron micrograph of a cross section of the centrosome of an ovine chondrocyte *in vitro*, section thickness 100 nm. The MTOC consists of a pair of ‘barrel shaped’ centrioles. The basal body extends the ciliary axoneme, and attaches to the periciliary membrane by alar sheets and sub-distal fibres, while its proximal end radiates a striated rootlet, and is also connected by inter-centriolar linkers to the subtending proximal centriole. Basal feet tether a number of cytosolic microtubules, which also radiate from the surrounding amorphous pericentriolar material. The obliquely sectioned subtending proximal centriole lacks appendages, and appears not to directly nucleate cytosolic microtubules. Scale bar 200 nm.

Alar sheets and finer sub-distal fibres link the distal end of the basal body to the periciliary cell membrane, while basal feet act as attachment points for arrays of cytosolic microtubules. Striated rootlets originate from the proximal end. Centrosomes may also contain varying numbers of densely

stained granular ‘satellite’ materials [113] that are involved in ciliogenesis [114] while the surrounding pericentriolar matrix acts as an amorphous MTOC.

The number of microtubules radiating from the centrosome has been estimated to vary between 20 and 100 [115], being divided between the pericentriolar matrix (PCM) ‘cloud’ and the globular heads of the basal appendages [116]. Aspects of their dynamics [117] and anchoring points [118] (Figure 1.11) and are believed to be cell type specific [119]. The PCM is a favourable site for microtubule nucleation and anchoring of microtubules [118]. Different anchors are believed to tether microtubules to the centrosome [120, 121], where some may be released into the cytosol [106, 118]. The ability of the proximal centriole to nucleate and anchor microtubules remains contentious [115, 118].

1.22 The Peri-Centriolar Matrix (PCM)

The pericentriolar matrix material is a dynamic, nebulous ‘cloud’ (1-2 μm^3) made up of a collection of fine fibres surrounding the ‘mother and daughter’ centrioles. Composed of both structural and regulatory proteins, these are thought to support higher order functions [3, 59, 63, 118, 120-125] and contribute to the complex processes of centrosome cohesion [126], centriole replication [127], cell regulation and ciliary control [62, 120]. Proteomic studies have revealed the presence of over 100 different proteins contained within the matrix [129-132] and its nebulous structure is observed to vary between cell types and during the cell cycle [127, 128, 133, 134]. Despite extensive studies of the centriole ultrastructure, investigation of the fine filamentous and nebulous nature of the pericentriolar matrix has remained elusive, and its functional makeup and regulation remain largely unknown [109, 124, 127, 128, 135, 136].

Recent confocal immuno-histochemistry visualisation of key pericentriolar matrix centrosomal proteins during interphase has revealed the detailed organisation of many protein species required for centrosomal function, which are confined in spatial layers surrounding the basal body [104, 123, 129]. The role of the matrix in support of basal body maturation, and of the protein machinery for ciliogenesis and maintaining the primary cilium is presently poorly known [62, 73, 128]. The centrosome is a dynamic structure, which occasionally ejects PCM flares [137]. Tomographic modelling of the centrosome has been undertaken by O’Toole et al., (2012) [138] and Moritz et al., (1995) [135] revealing that microtubule nucleation sites are distributed at a mean radial distance ~ 740 nm from the centre of the centrosome, and are excluded from near the centrioles [138]. Ultrastructurally, the matrix appears to support centriole and microtubule function by tethering microtubule anchoring complexes, and surrounding the basal appendages, whose anchoring head complexes are located some distance from the basal body surface (see Figure 1.11). The molecular composition and functional regulation of the pericentriolar components of the centrosome are yet to be determined [109], along with their intricate involvement in organelle positioning, especially with respect to the endoplasmic reticulum and the Golgi apparatus.

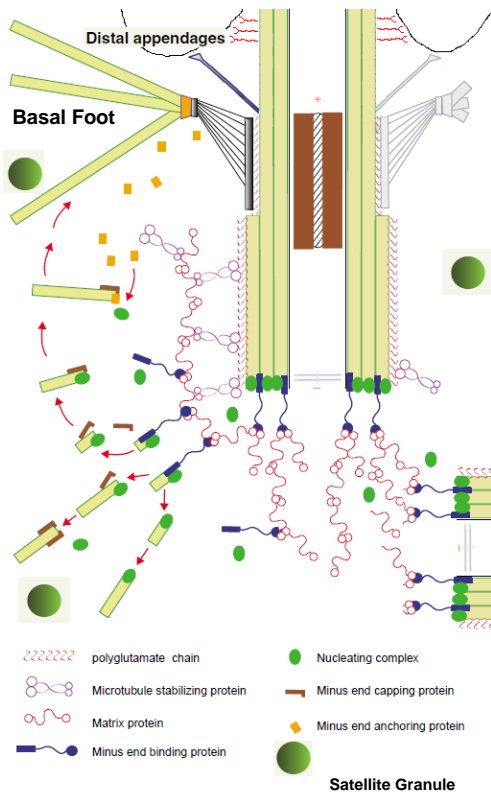


Figure 1.11 The Centrosome: An artistic interpretation of the microtubule based structure and organisation of the centrosome. Detailed are the microtubule structures of the orthogonal centrioles, and their surrounding pericentriolar matrix. Polyglutamylated of the microtubule triplet walls may be involved with binding the pericentriolar matrix and stabilising proteins. Microtubule binding proteins attach the γ -tubulin nucleation complexes to the pericentriolar matrix or to anchoring heads upon the basal feet, where their regulation is likely governed by components of the centrosome. Capped microtubules may be released, migrating into the cytoplasm. Many regulatory mechanisms remain poorly understood. Reproduced and modified with permission from Bornens (2002) [118] and Azimzadeh et al., (2007) [124].

1.23 The Cytoskeleton

The cytoskeleton is a three-dimensional protein network made up of actin filaments, microtubules (tubulin) and intermediate filaments (comprising the proteins desmin, cytokeratin and vimentin) [115, 139, 140, 141]. Beneath the cell membrane, a cortical layer of actin microfilament networks provides resistance to buckling from applied compressive forces [142, 143]. In interphase cells the centrosome acts as an MTOC extending a network of rigid microtubules throughout the cytoplasm [144, 145], which also assists in maintaining cellular shape under compressive loads [146]. Microtubules not only maintain cell shape, but also play a role in organelle positioning, directed cell migration and movement [147]. Intermediate filaments function as viscoelastic elements, with roles in maintaining cell architecture, plasticity control, stress absorption, and in signalling [115, 141, 148, 149] (for a review see Herrmann et al., (2009) [150]).

The centrosome functions as the primary organising and nucleating centre for both microtubules and intermediate filaments [115], which, in combination with actin, form a cytoskeletal tensegrity network of tensile and compressive elements that resist extracellular biomechanical forces [143, 151-155]. During interphase, the primary cilium is located at the structural focus of this network. Normal movements of the cell and the centrosome in positioning also likely contribute to a level of signal transduction upon the primary cilium [144]. The interphase microtubule ‘interactome’ is vital for the generation and maintenance of cell shape, polarity, vesicle and organelle transport and anchoring [156, 157, 158] that utilises microtubule’s different stability and physical properties [118, 121, 159, 160].

As the focus of the cytoplasm, the nucleus experiences forces transmitted through the cytoskeletal network. The viscoelastic properties of cell nuclei exceed those of the cytoplasm by three to four times [161, 162]. Application of an external force may therefore lead to alteration of nuclear shape. It has been proposed that such nuclear compression may alter gene expression, as cells such as chondrocytes change shape and volume under compression [163], resulting in increased matrix production [164].

1.24 Microtubules

Microtubules consist of 13 elements of tubulin α - β -dimers that polymerise into longitudinal protofilaments, which self-organise into polarised hollow cylinders [165-168] (Figure 1.12). With an inner and outer diameter of 15 nm and 25 nm respectively, microtubules may reversibly and dynamically polymerise into lengths of many microns, forming the more permanent complex structures of centrioles and the axoneme [166, 169].

1.241 Tubulins

The tubulin superfamily of globular proteins consists of six distinct known groups: α , β , γ , δ , ϵ , and ζ -tubulins with α , β and γ -tubulins being highly conserved in eukaryotes [92, 120, 170, 171].

α and β -tubulins, of which several isoforms of each member are known [172, 173], make up the majority of the content of microtubules [174] and these have been reported to be vital for ciliary function [175]. However, it is yet to be shown how these different isoforms affect microtubule structure [176], post-translational modification or influence interactions with microtubule associated proteins [177-179].

1.242 Microtubule Nucleation Complex

Tubulin nucleation has been reviewed by Wiese et al., (2006) [180], Kollman et al., (2011) [121], Teix et al., (2012) [181] and Prokop (2013) [182]. Microtubule formation typically occurs within the MTOC from a γ -tubulin template comprised of either small or larger ring complexes (γ -TuSC and γ -TuRC), which facilitate tubulin polymerisation, as well as forming an attachment site for tethering the nucleation complex [183]. The small γ -TuSC is comprised of γ -tubulin and the complex proteins GCP2 and GCP3, while the full γ -TuRC includes support proteins GCP4-6 [121, 184] (Figure 1.12). Each complex possesses separate attachment factor proteins, which may be substrate specific [120, 121] (see Figure 1.11).

1.243 Polymerisation

The ability of microtubules to direct translation of materials within the cell is depends upon their ability to be assemble and disassemble as required. For a review of microtubules, their assembly and regulation see Van Buren et al., (2005) [185] and Conde et al., (2009) [186]. Guanosine-

triphosphate (GTP) allows polymerisation of tubulins from their exposed β -ends into protofilaments [186], where hydrolysis to GDP allows inter-dimer linkage formation and microtubule assembly [187]. Dynamic instability arises during the assembly process at the β -end, where microtubules containing a non-hydrolysable GTP analogue are relatively stable [117, 182]. Discontinuities are observed in the microtubule structure arising from geometric constraints giving rise to a disjointed pattern known as ‘lattice seam’ [5, 188-191] (Figure 1.12), which may influence kinesin motor binding [192]. Limited information exists surrounding the process of initiation and assembly of the microtubule doublets of the axoneme through the extension of the A and B-subfibres of the centriole [93], where the B-subfibres do not always extend completely to the tip [193, 194]. Nicastro et al. (2011) [195] reported conserved features of the doublet architecture of *Chlamydomonas* flagellum, however, understanding of microtubule assembly, support molecules and their modification remains limited [196, 197].

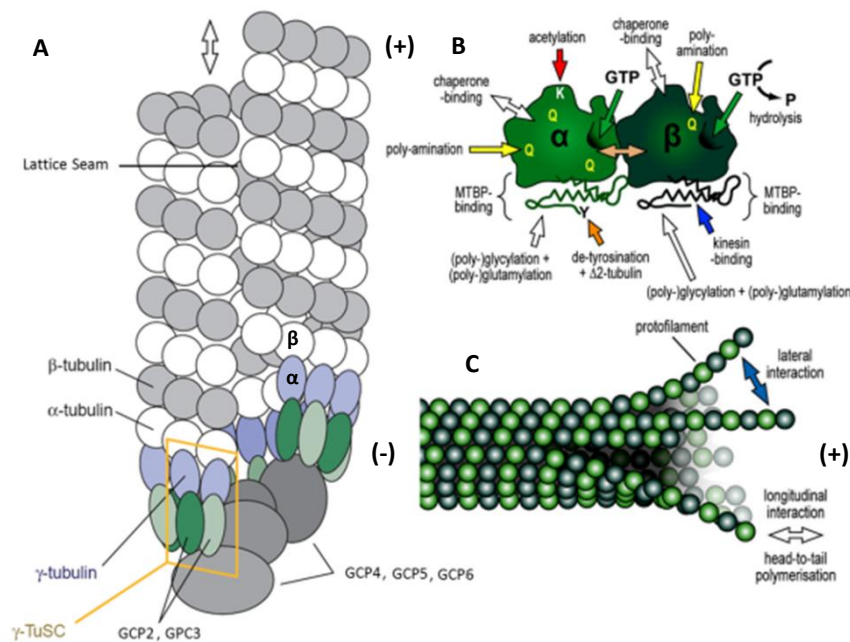


Figure 1.12 Microtubule Nucleation and Doublet Structure: **[A]** Microtubules normally consist of a ring of 13-tubulin protofilaments usually formed around a γ -tubulin nucleation base complex. Nucleation complexes consist of either ‘small complexes’ (yellow box, γ -TuSC, composed of γ -tubulin and complex proteins GCP2 and GCP3) or larger ‘ring complexes’ (grey, γ -TuRCs comprised of γ -TuSCs and proteins GCP4-6 [121]). Note the presence of the ‘lattice seam’. Reproduced and modified from Moritz et al., (2000) [189]. **[B]** The α - β dimers of tubulin incorporate into protofilaments, which then form the microtubule through hydrolysis of GTP, where the c-terminal tails are exposed to the outer surface. Post-translational modification of microtubules include acetylation, poly-amination, glycylation and glutaminylation [182], which influence protein structural and binding properties [199]. **[C]** Protofilament assembly, interactions and polymerisation required for microtubule assembly. Reproduced and modified with permission from Prokop (2013) [182].

1.244 Tubulin Post-Translational Modification

Post-translational modification of tubulin has been extensively reviewed (see Wloga et al., (2010) [200] and Westlake et al., (2003) [178]). Tubulin is subject to a range of specific post-translation modifications [199], including acetylation, de-acetylation [201, 202], palmitoylation [203], phosphorylation [120, 204], polyglutaminylation [205], polyglycylation [120, 206], tyrosination and

detyrosination [186, 199]). These result in specific microtubule properties, influencing stability, specificity, axonemal rigidity, signal transduction [180, 207], and the binding of proteins [208], chemicals and transient ionic species [209]. Post-translational modifying enzymes act upon microtubules, although tyrosine ligase is reported to act upon non-assembled tubulin [210]. Post-translational modifications have also been correlated with microtubule distribution and lifetime [186, 211], where it has been suggested they initiate important functions and contribute to the intrinsic properties of the cytoskeleton and axoneme [120, 194, 199, 212].

Variable levels of polyglutamylation exist on both axonemal microtubules and basal bodies [213], and a low level of glycation also occurs [214, 215] (although present upon longer length cilia [216]), implying that specific glycase and glutamylase enzymatic modifications are important to function and stability [216]. Most cytosolic microtubules are polyglutamylated to some extent [217], however, the role of such modifications, and control of their enzymes during the cell cycle and ciliogenesis remain presently unknown. Microtubule associated proteins are associated with tyrosination [218] and acetylation, where these modifications concur with increased flexural rigidity [219] and kinesin-1 motor binding [220] (see Figure 1.12). For example in *Chlamydomonas*, tubulin of both A and B-subfibres was found to be tyrosinated, while detyrosinated tubulin occurred mostly upon the B-subfibre [221]. Furthermore, many studies [222] have revealed that the microtubules of the centrioles and primary cilia are resistant to microtubule depolymerising drugs, suggesting a more stable structure than the cytoplasmic microtubules.

Poole et al., (2001) [97] utilised antibodies to locate acetylated α -tubulin and detyrosinated α -tubulin, demonstrating that the cilium and centrioles in chondrocytes, as well as parts of the microtubular cytoskeleton of the cell, consisted of both acetylated and detyrosinated α -tubulin, with a subset of acetylated α -tubulin microtubules being associated with the Golgi apparatus [96, 97]. Post-translational modifications of tubulin components determine microtubule stability and the ability to interact with associated proteins.

Section II – Functional Relations of the Cilium during the Cell Cycle

1.30 The Cell-Centrosome-Cilium Cycle

An enormous quantity of published literature reports attempts to probe the relation between the structure and function of the primary cilium and its environs. This basic structure, which appeared early in evolution, has subsequently remained basically constant in structure, yet has acquired new functionalities appropriate to particular specialised cells [3, 223-226]. Consequently, it is not surprising that the literature, which frequently reports on individual species ranging from algae to mammals, highlights variances in functional properties [223, 226]. Therefore, only generalities may be drawn at this stage in attempts to match structure with function.

The centrosome is an inherited structure that functions as the main MTOC of the cell. As a controller of the cell cycle, the centrosome and the cilium are required as necessary structural components for cycle progression, and to act as a physical substrate for numerous regulatory proteins [120, 124, 145, 227-230]. The centrosome is composed of a diplosome, made up of two polarised orthogonal centrioles (each cylinder consisting of nine microtubule triplets) sometimes termed the ‘mother’ and ‘daughter’, which once mature, become known as a basal body and proximal centriole of primary cilia [63, 105, 120, 230, 231]. Cell replication requires that the centrosome duplicates so that each new cell contains a diplosome. The evolutionary origins of eukaryotes, the centrosome and the cilium have been extensively reviewed [124, 222-234].

Basal body formation occurs at G1 (or G0) during ‘interphase’, when the mother centriole ‘matures’ with distal and subdistal appendages and associates with the cell membrane, where it starts assembling a primary cilium (Figure 1.13) [3, 62, 63, 95, 120, 235]. Piel et al., (2000) [236] has revealed the dynamics of the mother and daughter centrioles during G1-phase, with the ‘daughter’, or the proximal centriole, undertaking excursions within the cytoplasm. Centriole replication starts near the onset of the G1/S boundary with the formation of immature procentrioles [237, 238] on the basal body and proximal centriole, which elongate during the progression of the cell cycle, until the cell contains two pairs of centrioles [63, 94, 239].

At some point between the S-phase (DNA replication) and the G2/M transition [240], the cilium is resorbed (or severed [241]), freeing the diplosomes for the process of cell division [242], where each new cell inherits a centrosome [63, 105, 141, 243, 244]. Recently, Paridaen et al., (2013) [245] established that the cilium is not completely resorbed, but remains throughout mitosis, resulting in the ‘asymmetric’ inheritance of the centrosome. The cell-centrosome-cilium cycle concludes with entry of the newly divided cells into G1/G0-phase, with the formation of a new primary cilium upon the matured mother centriole [105, 240].

Cyclin dependent kinase-2 (CDK2) regulates control of the G1/S-phase transition, and is necessary for DNA replication as part of the progression of the cell cycle [110, 246-250]. Primary cilia have been ascribed a function as the ‘keeper of the key’ to cell division [235], since repression of

primary cilium formation leads to progression of the cell cycle [251]. The role of gene expression during the chondrocyte cell cycle has been reviewed by Schibler et al., (2009) [252], while the structure and duplication of the centrosome has been reviewed by Azimzadeh et al., (2010) [253] and Hinchcliffe et al., (2001) [254]. Cyclins and cyclin-dependent kinases, their interaction, localisation and cell cycle implications are tabulated within Appendix I.

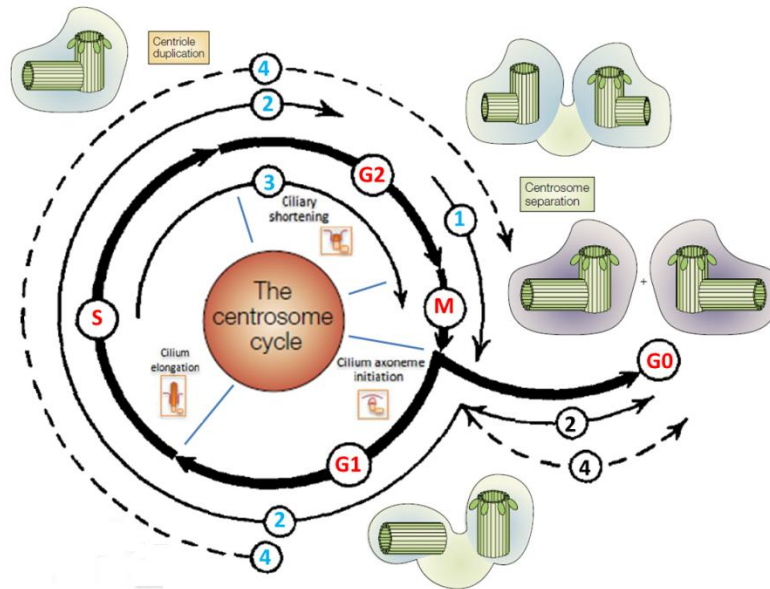


Figure 1.13 The Cell Centrosome Cilia Cycle: A composite demonstrating the cell and centrosome cycle through G1, S, G2, M and G0-phases [63]. Key events in the cell cycle include the formation of the mitotic spindle for mitosis (1), the presence of interphase microtubules (2), initiation of centriole replication through procentriole formation (3) and the formation and expression of a primary cilium (4). The exact details of specific aspects of the centrosome and the cilium cycle are still subject to debate [255, 256]. Modified from Nigg et al., (2002) [248], Vorobjev et al., (1982) [63] and Schibler et al., (2009) [252].

1.31 *Intra-Flagellar Transport (IFT)*

Intra-flagellar transport complex proteins are highly conserved across eukaryotes [257], and orchestrate the bi-directional microtubule transport of materials and macromolecules from the basal body to their required destinations within the cilium [23, 62, 101, 102]. IFT transport components [258] accumulate upon the basal body [259, 260] where they interact with the Bardet-Biedl Syndrome (BBS or BBsome) [46] family of proteins for the regulation of IFT assembly, ciliary protein targeting, re-cycling turnaround [261-264] and signalling [265], as well as for Golgi trafficking [66]. Comprising A and B-assemblies [62, 257] of at least 8 and 14 subunits respectively, the A-assembly is involved in retrograde transport, while the B-assembly participates in anterograde ciliary transport. Anterograde transport is known to utilise kinesin motor members KIF3A, KIF3B and KIF17, while cytoplasmic dyneins DYNC2H1 and DYNC2LI1 are utilised for retrograde transport [62, 257, 266]. IFT172 is reported to enable the dis-engagement of kinesin, and preferential activation of dynein motors [267, 268] (for a review of transport motors and IFT-components, see Ishikawa et al., (2011) [62], and Appendices III and IV. Electron microscopy of IFT particles reveals them as fine electron-dense granules located between the membrane and the microtubule doublets of the axoneme, which are commonly found concatenated into transport trains or 'rafts' [269].

1.311 Ciliary Transport

The mechanisms of IFT in ciliary function, regulation and signalling remain poorly understood [102, 258]. The exact roles of the kinesin and dynein motors involved within the cilium remain obscure, with KIF3C, KIF7, KIF19A and KIF24 members also having roles within the cilium (Appendices IV and V). KIF3 and KIF17 both serve as IFT-complex motors (joined by BBS7 and BBS8) [262, 270], with only KIF17 reportedly operating in the distal axoneme region [47, 270], where, in photoreceptors, it supports outer segment development [271]. KIF7 localises to the ciliary tips where it regulates Sonic Hedgehog (Shh) signalling, acting downstream of Smo and upstream of Gli [272, 273]. However, without its ligand, KIF7 is localised to the base of the cilium and only translocates to the distal tip upon activation [274], where it is suspected to play a role in Gli transport [275] and as a regulator of Gli transcription [272, 276]. KIF7 acts as a critical regulator in the Shh signalling cascade [272], restricting ‘suppressor of fused’ (SuFu), and promoting chondrocyte signalling in the growth plate [277].

The IFT-A complex with Tubby-Like protein TULP3 [278] promotes the trafficking of G-coupled protein receptors into the cilium [279], additionally requiring the BBSome [280], as well as components of the Shh signalling pathway [281]. IFT-B may be required for the transport of Gli2, SuFu and KIF7, while the absence of IFT-A results in the failure of the ADP-ribosylation factor (ARF) like GTPase ARL13B, Adenylate Cyclase-3 (AC3) and Smoothed (Smo) to localise to the ciliary tip [281] (see Appendix D). Protein LZTFL1 regulates the trafficking of Hedgehog signalling pathway member Smo and the BBSome [282, 283].

1.312 IFT co-ordination

Little is known about docking and arrangement of IFT particles upon the basal body, or their transport preference for certain axoneme microtubules. Buisson et al., (2012) [261] and Absalon et al., (2008) [284] established in *Trypanosoma brucei* that IFT particles travel upon distinct, or ‘restricted’, subsets of axonemal microtubules. Retrograde trafficking occurs at a higher velocity than anterograde transport, although IFT trains have been observed to travel at different speeds, and their recycling is dependent upon ciliary length and the number of IFT particles in transit [261]. However, not all IFT particles present at the basal body participate in transport [261, 285].

1.32 Primary Cilium Biogenesis

Sorokin (1962) [95] first described the process of genesis of the primary cilium from the diplosome, where he documented initiation through a Golgi derived vesicle docking at the distal tip of the mature basal body (Figure 1.14). Cilium formation requires the intricate combination of many proteins and pathways. At present, incomplete information exists about their role. Sonic Hedgehog signalling pathways are certainly involved in ciliogenesis [286] and interpretation of their mode of

action is still on-going [287]. It has been found that Patch1 regulates Smo activity in a late endosomal sorting pathway [288], which is important for placement of proteins.

Planar cell polarity effector Inturned, together with Dishevelled and Rho-GTPase act in the process of apical membrane docking [289], where Talpid3 is reported to influence actin localisation during docking of the basal body [73]. Wnt signalling also plays a role in ciliogenesis [289], involving shared components of the planar cell polarity pathway [290], since reduction of Wnt/ β -catenin signalling has been found to disrupt ciliogenesis. Proteins of the Par3/Par6/aPKC cassette are also involved with ciliogenesis through control of kinesin motors [291], although many of these intricate processes are not yet fully understood [292].

CEP164 is required for vesicle docking to the basal body [293, 294], and ciliary assembly is initiated by Rab11-GTPase, the transport protein particle two (TRAPII) and Rabin-8 in the centrosome [295]. Rab8 is required for ciliary formation through vesicle docking and fusion at the base of the cilium and at the ciliary pocket [296-298] and facilitates membrane ciliogenesis with the clathrin adaptor protein (AP-1) [295, 296, 299, 300]. Components of the Exocyst complex (sec10 [301]) and SNAREs are additionally required for ciliogenesis [302].

Centrosomal proteins CP110, CEP97 and CEP290 suppress primary cilium formation upon the mother centriole [303, 304]. CEP97 and CP110 are located at the distal end of the basal body and act to prevent maturation [305] where CP110 coordinates ciliary assembly [306]. For a review of regulation of vertebrate ciliogenesis see Santos et al., (2008) [223].

The transition fibres are required for physical adherence to the plasma membrane, but also act as docking sites for IFT particles involved in assembly and trafficking [307, 308]. Small GTPase ARL6/BBS3 regulates membrane protein transport into the cilium [283], functioning near the ciliary 'gate', where it also incidentally plays a role in modulating Wnt signalling [309]. Components of the Exocyst complex are required for ciliary function [301, 310], and are downstream effectors of Rab8 and Rab11 [311].

Extension of the axoneme requires co-ordinated active transport of material into the ciliary 'bud' using components derived from the cell membrane, and from transport vesicles. It is believed that materials are highly concentrated through intra-ciliary transport mechanisms, allowing for the elongation of the axoneme microtubules. Axoneme extension during initial ciliogenesis utilises MARK4 kinase [312] and requires microtubule associated protein EB1 [313]. Assemblage leads to formation of a 'transition zone' compartment, followed by the axoneme, and the distal tip, although the exact mechanisms are yet to be elucidated [62, 65, 244, 298, 302, 312].

Ciliary formation and assembly also requires various ancillary complexes to accumulate within the centrosome [55, 314]. These include many obscure proteins which form, regulate and maintain ciliary function [315] through regulation of IFT, microtubule processes of tubulin transport, specific poly-modifications [212, 316, 317], katanin mediated severing [318], and kinesin and dynein transport motors [319, 320]. Tubulin transport into the cilium has recently been reported to occur

through IFT74 and IFT81 [321, 322], which allows for the control of microtubule polymerisation and post-translation modifications [211, 321, 323], since IFT regulates turnover of the outer doublets [323], providing the structural substrate for transport and numerous regulatory processes [315]. The exact transport mechanisms, regulation and ciliary gating of materials required for ciliogenesis remain poorly understood.

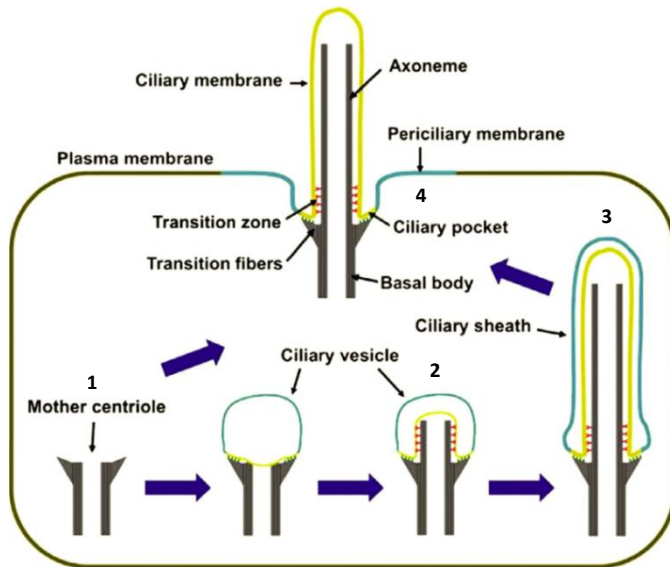


Figure 1.14 Biogenesis of the Primary Cilium: Ciliogenesis is believed to be initiated from the docking of a Golgi derived vesicle to the alar sheets at the distal end of the basal body, or from binding with the cell membrane (1). The 'ciliary bud' forms allowing growth of the transition zone enclosed by the ciliary membrane (2). Ciliary elongation continues where the cilium is surrounded by a peri-ciliary membrane 'ciliary sheath' (3), and subsequent fusion with the cell membrane allows externalisation of the primary cilium into the extracellular domain, and with displacement of the centrosome, sometimes forms the ciliary pocket (4). Reproduced and modified with permission from Garcia-Gonzalo et al., (2012) [302].

1.33 Entry of Material to the Cilium

Conventional notions of transport of Golgi-derived material to the cilium suggests that the centrosome directs vesicle transport and fusion with the periciliary membrane at the base of the cilium [324]. This allows for the active fusion and transport of membrane bound components, and/or diffusion of vesicle contents into the cilium [300, 307, 325] (see Figure 1.15). The transition fibres act as an entry barrier or 'ciliary gate' [326, 327] for the regulation and targeting of IFT-complexes and their cargoes into the cilium [325] (with the fibres acting as docking sites for IFT52 [308]). IFT54 interacts with Rab8 via the endocytosis regulator Rabaptin-5 [328]. Rab8 is also involved in promoting vesicle trafficking and ciliary assembly [298, 299]. IFT22 has a role in regulating the cellular pool size and number of ciliary IFT-particles [329], while IFT27 is associated with control of the cell cycle [330]. For a review of the function of IFT components, see Wood et al., (2012) [331].

As part of the IFT-B assembly, IFT20 plays a role in ciliogenesis, where it is also implicated in membrane protein transport from the Golgi [259, 328, 332], allowing for vesicle membrane transport and fusion at the base of the cilium [298, 307] (Figure 1.15). BBS proteins participate extensively in membrane trafficking and ciliogenesis [283, 307], IFT localisation of ciliary receptors [46, 48], membrane biogenesis [333], ciliary length control [334] and in cargo targeting to the centriolar region [335]. BBSome components influence and modulate Wnt signalling near the transition fibres [336, 337] and play a role in planar cell polarity [338].

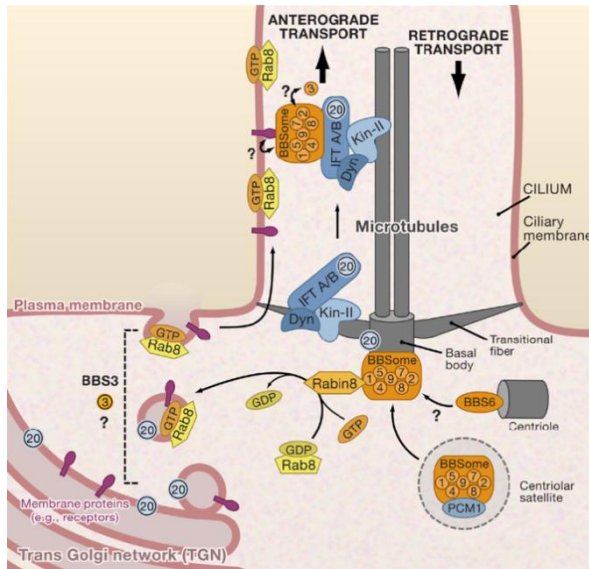


Figure 1.15 Golgi Derived Materials for Ciliogenesis: Ciliogenesis and ciliary maintenance require the regulated transport of specific cargoes and receptors to be delivered to the periciliary membrane. Components are sequestered from the Golgi apparatus through involvement of IFT20 and the BBSome in vesicular events, from where they are transported to the centrosome and made available for transport into the cilium by IFT-B (anterograde kinesin transport) and recycled via IFT-A (retrograde dynein transport). BBSome proteins BBS4 and BBS8 interact with the pericentriolar matrix protein PCM-1 surrounding the basal body. BBS1 cooperates with Rabin8 for Rab8-GTP bound mediated docking and fusion of vesicles at the membrane and ciliary pocket. Rab8 regulates ciliary protein trafficking, and is controlled by Rabin8, whose activity and localisation is controlled by the BBSome and Rab11 [300]. Reproduced with permission from LeCroux (2007) [307].

Receptors such as retinitis pigmentosa-2 (RP2) require importin- β 2 for ciliary entry [67], while KIF17 motor entry is governed by Ran-GTPase and importin- β 2 [339, 340]. Curiously, the KIF17 c-terminal tail domain possesses both ciliary and nuclear localisation sequences [67, 339], with inhibition of Ran-BP1 disrupting distal localisation of KIF17 [339, 341], since importin- β 2 controls ciliary entry [339]. Ran members and initiation processes are important for a host of cytosolic and nuclear functions [67, 342], where control of centrosome activity and ciliary entry is known to utilise β -arrestin [343].

1.34 Ciliary Localisation Sequences

Many key receptors and their adaptor molecules share complex interactions in which their localisation requires specialised signalling for their proper inclusion into ciliary processes [326, 344, 345]. This is believed to be achieved through ciliary targeting motifs that are required for the orderly transport of proteins and macromolecules from the Golgi to the cilium [297, 300, 325, 307, 346, 347]. Many details of the mechanisms of ciliary receptor transport, localisation, turnover, cell specificity, downstream signalling effects and their partners presently remain little known [348]. Ciliary receptors which are known to have localisation sequences include smoothed (Smo) [337], polycystin-1 (PC1/TRPP1) [349], polycystin-2 (PC2/TRPP2) [350], retinitis pigmentosa protein (RP2) [349], opsin [325], rhodopsin [351], fibrocystin [352], somatostatin (SSTR3) [325], serotonin (5HTR6) [353] and melanin concentrating hormone (MCH) [354].

Some ciliary proteins also reportedly contain nuclear localisation sequences, including transient receptor potential (TRP) vanilloid member OCR-2 [355], the KIF17 c-tail [67], the PC1 c-tail [356], Sonic Hedgehog Gli family members [357] and G-coupled receptor kinase GRK5 (which includes a DNA binding motif [358]).

Localisation of ciliary messengers to the nucleus is requirement for Notch signalling [359], for Dishevelled function in Wnt/beta-catenin signalling [360], in components of Hedgehog signalling, and for Gli transcriptional activity, regulated by cyclic-Adenosine Mono Phosphate (cAMP) [361]. Protein c-terminal residues are likely critical for recognition and localisation for ciliary targeting, where trafficking takes place by several molecular processes, which can vary between proteins of the same family [354]. The 'VxPx' targeting motif [354, 362] utilises GTPases, ARF4 and Rab11, the Rab11/ARF effector FIP3, and the ARF GTPase-activating protein ASAP1 [362]. At present, an incomplete picture exists of the mechanisms of targeting of many ciliary proteins.

1.35 Dynamic Control of Ciliary Length

The length of the primary cilium is influenced by external factors such as mechanical load, fluid shear, osmotic challenge and heat induced shortening [255, 363-365]. Cilia may lengthen following injury [366], or in response to certain soluble cations [363]. Wilsman [27-29] observed variation in microtubule doublet lengths within the axoneme, which may indicate that length regulation is a dynamic process, with each doublet being subject to individual control mechanisms.

Ciliary length is under the control of IFT, which balances the continuous turnover of the microtubule doublet tips [323, 363, 367]. It is not yet known how differences in microtubule doublet lengths occur, as the regulatory mechanisms of ciliary dynamics and cell cycle remain as yet unknown [284]. Kinases LF4 and CNK2 are reported to determine the length of cilia in *Chlamadymonas reinhardtii* by controlling the rate of assembly and disassembly [368] through increasing IFT traffic and halting anterograde cargo loading [369].

Other ciliary components involved in length regulation include Septins-2, 7 and 9 (with MAP4) [370], galectin Gal-7 [371] and ciliary associated kinesins KIF19A and KIF24. KIF19A is observed to reduce microtubule length through depolymerisation at the tip in mammals [372], whilst KIF24 contributes to microtubule remodelling and depolymerisation. It also interacts with centrosomal proteins CP110 and CEP97 in HEK cells in culture [305]. Interleukin-1 has been found to increase ciliary length in chondrocytes through a protein kinase pathway [366]. The Rer1p protein regulates ciliary length through recruiting γ -secretase and Foxj1 [373], and Rer1p is also reported to be necessary for endoplasmic reticulum protein retrieval, where it cycles between the Golgi [374].

1.40 The Ciliary Membrane

The ciliary membrane is a lipid bilayer structure of unique composition, enclosing the axoneme, enriched with lipid rafts of specific components, receptors and their luminal mediated processes, which vary in their abundance along the ciliary membrane [345, 375]. Differing from both the periciliary and plasma membranes, it is greatly enriched in sterols, glycolipids and sphingolipids relative to the plasma membrane [376, 377]. External to the membrane is a glycocalyx of glycoproteins, which are involved in adhesion and signalling, as well as interacting with fluids,

solutes, osmolytes, and signalling molecules [345, 378, 379]. They may also be influenced by compression induced electric fields in cartilage [380]. Regions of ciliary membranes may vary in their charge density [381], as ferritin labelling has revealed negatively charged sites located in association with fine filaments [49] and at ciliary necklace sites [49, 382]. The presence of ciliary necklace, plaques, rosettes and longitudinal rows indicates a higher order of complexity in the membrane, which is supported by the presence of membrane linkages aligned with the microtubules [52] (Figure 1.4). As yet, the spatial and functional interaction between ciliary receptors and the linkages remains obscure [383].

Receptors become localised to the membrane after ciliogenesis, and their proper function is dependent on correct sorting, trafficking and placement within the ciliary membrane [345, 383-385]. Localisation of receptors and their components within the cilium usually requires IFT [281], while Rab-effector related proteins Rilpl1 and Rilpl2 [386] regulate ciliary membrane content. Much remains unknown with regard to receptor entry, regulation, and sorting within the cilium [297].

In flagella, membrane localisation of specific proteins may occur on lipid 'rafts' [377], where some receptor clusters (such as epidermal growth factor receptor EGFR) are known to vary in size, and to be associated with cholesterol and sphingolipids [387]. Many membrane receptors occur in close proximity to the axoneme microtubules, and their organisation appears to regulate polycystin-2 (PC2) signalling [388], while the transient receptor potential vanilloid-4 (TRPV4) [389] channel is known to form complexes with regulatory kinases enabling roles in cytoskeletal interactions and microtubule depolymerisation [390].

Proteins within the cilium and its membrane undergo preferential turnover, influencing function [391, 392]. An extreme example is the photoreceptor cilium, which is estimated to contain 10^9 rhodopsin (GPCR) molecules in 10^3 photo-sensitive stacks [297]. In the murine photoreceptor, opsin is delivered to the base of the cilium, and transported along the 'connecting cilium' for forming new photoreceptor membranes at 2000 opsin units per minute [393], indicating that this cilium is a highly ordered and regulated structure capable of rapid molecular transport [394]. To maintain ciliary function, proteins must be actively transported from the Golgi to the centrosome, from where they are actively vectored into the cilium. The regulated transport of Golgi-derived receptors and structural proteins remains largely unknown, however many proteins possess 'ciliary targeting sequences' enabling active directed transport [297]. The Taurine transporter, for example, has a high expression in the primary cilia of NIH3T3 fibroblasts (Appendix I).

1.41 The Cilium: Receptors and Luminal Components

Primary cilia are ancient specialist compartments for the detection, amplification and transmission of a wide range of signals. For example, the murine photoreceptor sensory complex [132] is reported to contain over 2000 proteins⁴ specific to or involved with, ciliary function [38, 40]. Primary cilia utilise various membrane receptors, channels and signalling components whose transport and function is tightly controlled [17, 48, 297]. Figure 1.16 illustrates an abbreviated summary of known ciliary membrane receptors, and associated luminal and structural components, that are listed in further detail in Appendix I.

Depending upon its sensory requirements, the ciliary membrane and lumen may contain specialist receptors and downstream components for Notch [395], Wnt (Frizzled, Dishevelled, Chibby and Inversin) [396], Hedgehog (Smo, SuFu, Patched (Ptch) and Gli1-3) [69, 396, 398, 399, 400, 401] and platelet derived growth factor receptor (PDGFR α) [384] signalling pathways. Many other receptors allow for a wide range of physiological signals to be transduced [402], while structural and luminal associated proteins like the Nephrocystins (NPHP) and IFT-complexes influence the dynamic support of many receptors whose full function in the cilium remain to be determined. Appendix I details known receptors, interactions, signalling cascades, structural proteins and some of the diseases resulting from loss or mutation of known genes [1]. These represent only a small number of the proteins believed at present to be involved within the cilium, however not all of these receptor proteins have been shown to be present upon chondrocyte primary cilia.

⁴ <http://www.ciliaproteome.org/>

Signalling Pathways

Hedge-Hog (Sonic, Indian and Desert)
Smo,
SuFu,
Patched,
Gli1-3

Wnt Signalling
Frizzled,
Dishevelled,
Chibby,
Inv

Notch Signalling
Notch 1-2

Ca²⁺ signalling

Intra Ciliary Transport

IFT Components IFTA and IFTB

Extra Cellular Forces

Matrix,
Osmotic,
Electrostatic,
Fluid Shear,
Morphogens
Signalling peptides

The Basal Body - Centrosome

Structural Proteins

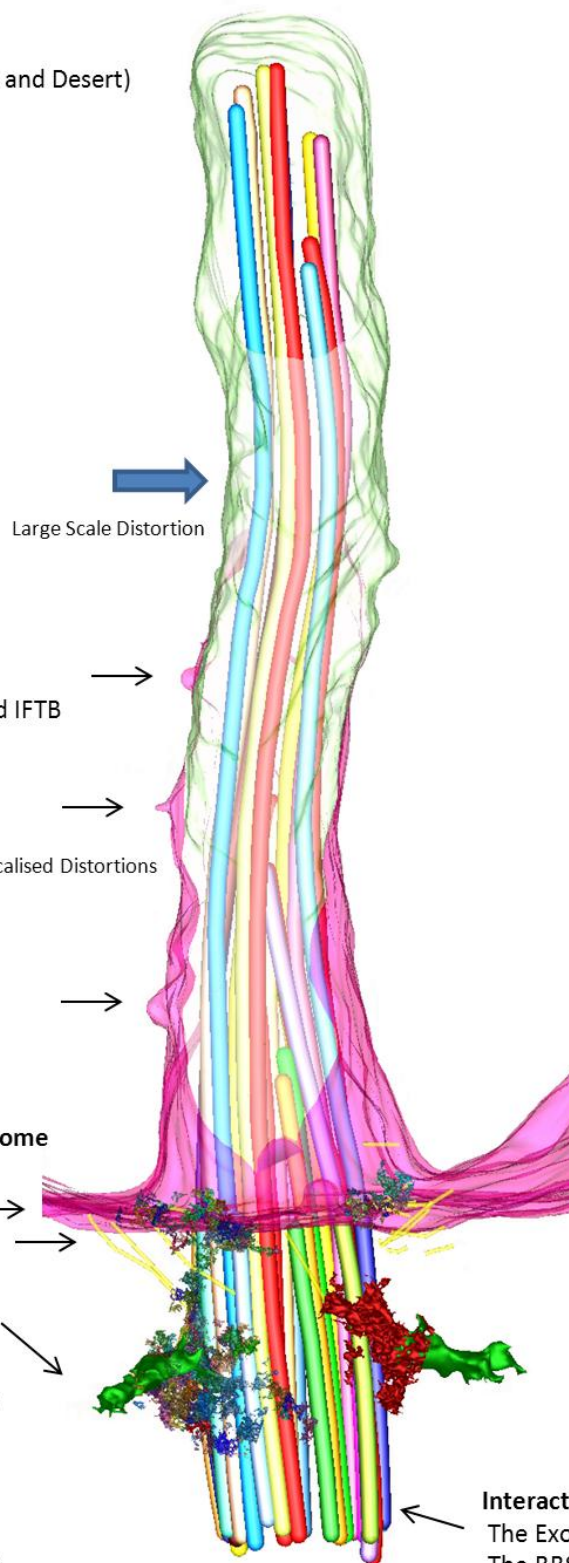
Alar Sheets
Sub-Distal Appendages
Basal Feet

Microtubules

α , β , γ , δ and ϵ -Tubulins

Peri-Centriolar Matrix

Centrosome Associated
Cell Cycle Regulation
Cell Function Regulation
Kinases, Ran and Rab-GTPases



Ciliary Components

α 2, α 3 and β 1-Integrins,
NG2,
Connexin-43, hemi-channels,
Cystin,
Napa,
Tie,
Serotonin,
Somatostatin,
Rhodopsin,
Channel TRPP, TRPC, TRPM,
TRPV and TRPA Families,
ENaC,
VEGF,
EGFR,
IGFR,
PDGFR- α ,
Mek,
LKB1,
P2X2/P2Y12 receptors,
 β -arrestins,
Collectrin,
Vasopressin,
Aquaporin,
Bromi,
Fibrocystin,
Adenylate Cyclase,
Galectins,
ARL13B,
INPP5E,
TMEM216,
Meckelins,
Nephrocystins,
AH1,
CRMP-2,
Sec6, 8, 10 and 15 (Exocyst),
FAP2,
Septins,
Tubby-Like Proteins

Microtubule Transport

Kinesin and Dynein Family
Motor Proteins
Dynactin Regulatory Complex

Interactive Complexes

The Exocyst
The BBSome

Figure 1.16 The Primary Cilium: The *distal*, *middle* and *transition zones* projected from the basal body. The ciliary membrane has been shown to contain numerous receptors and their associated components of several signalling pathways, although not all are present within every cilium. These are activated by a variety of extracellular signals and ligands, as well as from mechanotransductive forces acting upon the cilium. Small forces may result in the localised distortion of the ciliary membrane, while larger forces may translate into bending of the microtubule doublet based axoneme. Ciliary functionality is maintained by microtubule based anterograde and retrograde bi-directional intra-flagellar transport components, which are organised from the basal body. These transfer receptors, structural proteins and regulatory complexes are vital for maintaining ciliary homeostasis. Details of these components are tabulated within the Appendices.

1.42 The Cilium and the Extracellular Matrix

The primary cilium is known to interact with the extracellular environment, and convey information to the cell, for example, the membrane of the chondrocyte cilium has been observed to interact with collagen fibres and proteoglycans of the extracellular matrix [25, 26, 97]. Cartilage extracellular matrix has been found to contain matrix vesicles [403] and a variety of signalling molecules intrinsic to the roles of development and homeostasis of the chondron [404, 405]. The chondrocyte ciliary membrane is known to contain matrix receptors of $\alpha 2$, $\alpha 3$, $\beta 1$ -integrins and NG2, but not for of Annexin-V and CD44 (see Section 1.90), indicating that the ciliary membrane is only selective for certain matrix connections [25, 26, 97, 100]. $\beta 1$ -integrins on MDCK epithelial cell primary cilia are reported to detect fluid flow following deflection via fibronectin induced Ca^{2+} signalling in association with PC2 [34, 406, 407].

It is widely known that proteoglycans are important signalling components in many cell pathways [209, 408-410] with their role in the chondrocyte matrix being particularly important for differentiation [411]. The heparan sulphate proteoglycans [412] (syndecan, glypican and perlecan [410], see Section 1.86 - 1.89) are signalling components of the pericellular microenvironment [413]. Glypican-5 (GPC5) core proteins containing heparin sulphate and 2-O-sulpho-iduronic acid are reported to be involved with Sonic Hedgehog as co-receptors [414], assisting in binding of Hh to Patched1. GPC5 increases binding of Shh to Patched1, conversely GPC3 inhibits this interaction through competition for Shh [415, 416]. Li et al., (2011) [415] argue that Glypican-5 binds to primary cilia, and stabilises interactions between Shh and Patched1, facilitating signalling. The solubility and diffusion of Hedgehog ligands within the extracellular matrix may depend not only upon their modification, but also on their interactions with the matrix [417, 418], while Wnt protein concentration may be influenced by the concentration of matrix at the cell membrane [419]. Recently, TGF- β signalling is reported to occur through clathrin-dependent endocytosis at the ciliary pocket, where receptors localise to the ciliary tip and clathrin vesicles at the base of the cilium [420]. For a review of signalling in cartilage development, see Brochhausen et al., (2010) [404] and Kirn-Safran et al., (2004) [410].

1.43 Signalling and Mechanotransduction

The ciliary membrane provides a large surface area to volume ratio for detecting and amplifying external chemical stimuli. Electrical signals from patch clamped primary cilia have recently been measured, indicating the presence of conducting channels and secondary messengers [421], however the majority of studies on primary cilia have examined their role as flow sensors in epithelia, with few studies being concerned with mechanical loads experienced by the cilium within a cartilaginous matrix [422]. Many receptors have been identified localised to primary cilia, but in connective tissues, their full role in, for example, chondrocytes remains unknown [423]. Channels of the transient receptor potential (TRP) family members participate in a wide range of sensory

modalities [424], and each is specific to one of a number of stimuli; mechanical [407, 425], light detection [132], oxidative stress, tonicity changes [426, 427], pH, temperature and sensitivity to chemical species [428].

Praetorius and Spring (2001) [34] established that primary cilia acted as flow sensors in MDCK cells, for mechanical bending induced an increase in intracellular Ca^{2+} concentration, and this was communicated to adjacent cells. Nauli et al., (2003) [425] later found that Polycystin-1 (PC1) and Polycystin-2 (PC2) ion channels were responsible for mediation of mechanotransduction in renal primary cilia (Figure 1.17). PC1 and PC2 are well known to form a membrane bound mechano-molecular complex localised to the primary cilium [406, 429, 430] (Figure 1.17). PC1 contains a lengthy extracellular component responsible for mediating kidney cell mechanotransduction [425, 431]. PC1 is known to interact with PIP9 [432] and influences transcription factor Jade1 [433], for cleavage of the PC1 c-tail domain may control β -catenin and canonical Wnt signalling [429]. PC2 is responsible for angiotensin II-induced Ca^{2+} signalling [407, 434], and may include other binding partners EGFR, TRPC1, TRPC4 [434], and TRPV4 (which is mechano- and thermosensitive) [428, 429, 435], although many aspects of their ciliary roles remain unknown. In chondrocytes TRPV4 acts as an osmotically sensitive Ca^{2+} channel, and its loss results in osteoarthritic matrix changes [436]. It also plays a role in regulation of chondrogenic differentiation [437].

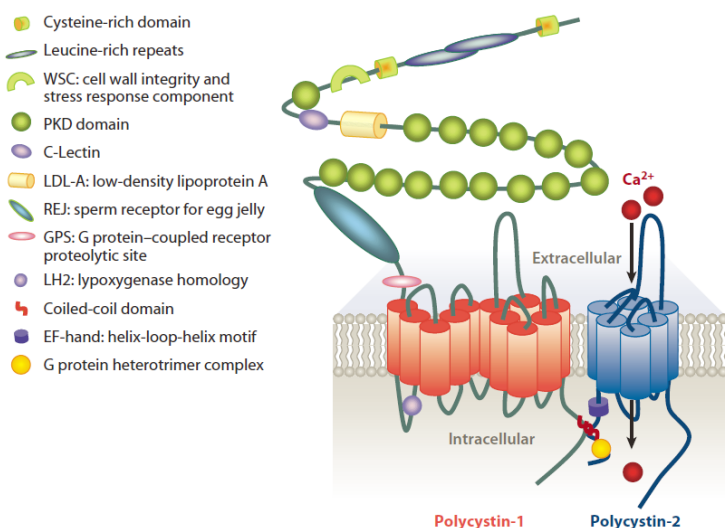


Figure 1.17 The PC1/PC2 Mechanotransduction Complex: The PC1/PC2 complex contains an extra-cellular PC1 (polycystin-1 or PKD1) domain, and the PC2 (polycystin-2, PKD2 or TRPP1) Ca^{2+} cation channel which are both defined by a shared complex *trans*-membrane loop, accompanied by extracellular and intracellular components which interact at their c-terminal domains. Extracellular stimulation of the PC1 protein is responsible for activating the PC2 channel, where PC1 c-terminal cleavage is controlled by PC2 expression. Reproduced and modified from Zhou et al., (2009) [429].

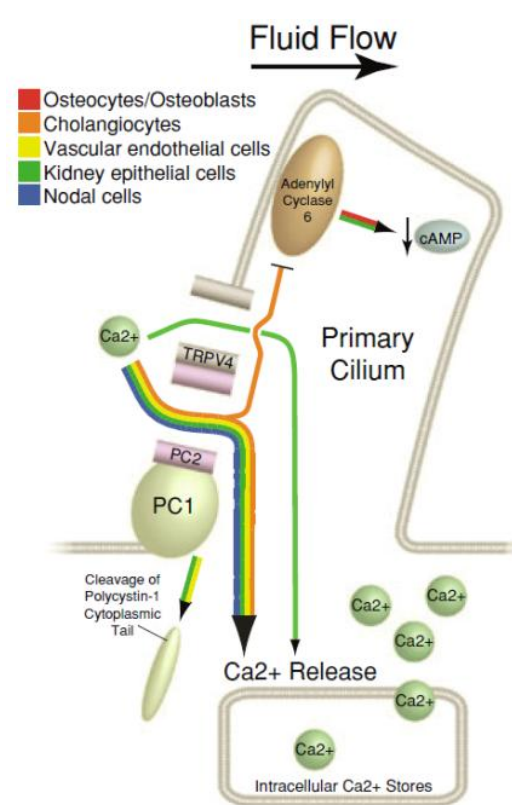
1.44 Purinergic Mechanotransduction

Purinergic family members are composed of two groups; P2X ATP-gated ion channels, and P2Y G-coupled receptors. P2Y1, P2Y2, P2X2, P2X4 and P2X7 have been identified upon chondrocyte membranes [438] (Appendix I). Purinergic mechanotransduction in chondrocyte cilia had been speculated upon [438, 439], since the cilia of cholangiocytes are known to utilise P2Y12 purinergic receptors as chemosensors [440]. It has been demonstrated that cilia of compressed chondrocytes mediate mechano-transduction through ATP-induced Ca^{2+} signalling [422, 441], but

they are not necessary for the initial stage of induced ATP release. They are however required for exogenous detection of ATP [422]. Connexin-43 hemichannels have also been located upon the ciliary membrane [438] and are believed to provide an avenue for release of ATP in response to mechanical loading in chondrocytes [422]. Mechano-transductive purinergic Ca^{2+} signalling may be regulated by PC1 in the chondrocyte cilium, which could also mediate control of ATP reception [422], since the proteolytically cleaved PC1 tail is known to translocate to the nucleus for STAT6 gene activation [442]. Activation of the G-coupled receptor Smo [443] results in the targeting of Gli, altering transcription and gene expression [398, 444] while Gpr161 negatively regulates the Shh pathway through cAMP signalling [445]. Such cAMP dependent processes are central to ciliary signalling.

1.45 Ciliary Polymodal Sensory Function

Ciliary mechanosensitive molecular pathways are believed to be shared, but also vary between cell types [446, 447], where some utilise the cAMP pathway instead of Ca^{2+} signalling. Adenylyl cyclases AC3, AC4, AC6 and AC8 have been identified within the cilium, and are required for the production of cAMP (Appendix I). Hoey et al., (2012) [448] indicated that ciliary biomechanical transduction in bone cells is distinct from that in the kidney distal epithelium. It is believed that osteocyte cilia transduce flow via AC6 and cAMP, independent of extracellular Ca^{2+} ,



resulting in protein kinase-A cascade signalling [447, 449]. Renal cilia are believed to transduce flow as a result of Ca^{2+} entry through the TRPV4/PC2 membrane domain as well as utilising PC1 cleavage for signalling [425, 428 447, 448] (Figure 1.18). It is reported that AC6/cAMP [449] signalling is preserved through the osteocyte lineage in mesenchymal cells [448, 450]. It is probable that similar signalling modalities may occur in chondrocyte primary cilia.

Figure 1.18 Proposed Mechanism of Flow Induced Ciliary Ca^{2+} and cAMP Signalling Modalities: Extracellular Ca^{2+} may enter the cilium through either the PC1/PC2 or from TRPV4 channels form a polymodal sensory channel complex [428]. Cell phenotype is believed to determine the signalling modality utilising PC1/PC2 and / or TRPV4 Ca^{2+} entry, adenylyl cyclase-6 initiating intracellular Ca^{2+} release. Cleavage of the luminal PC1 tail results in nuclear localisation via STAT6 and P100. Reproduced with permission from Kwon et al., (2011) [447].

PC2 ciliary Ca^{2+} entry modality occurs in nodal, osteocyte, cholangiocyte, vascular endothelial and kidney epithelial cells, while kidney and vascular cells also utilise PC1 c-tail cleavage

in signalling and nuclear localisation [356, 447], including transcription activation in T-cells [451]. Loss or altered functionality of ciliary polycystin is implicated in polycystic kidney disease [452] and the growth of renal cysts [453]. It has been shown that while fluid induced movement of the primary cilium results in PC2 activation, the transductive cellular response also requires feedback from combined components of the cell cytoskeleton and the extracellular matrix [454]. Fibrocystin/polyductin (PKHD1) serves as a bi-directional signalling molecule, which may undergo Notch-like cleavage of its extracellular domain [48, 455] (Appendix I).

In connective tissues, a network of mechanically interconnected collagen fibres and proteoglycans surrounds chondrocyte cilia, which if bound through integrin and NG2 matrix receptors may provide a physical link to the many possible receptors within the ciliary membrane [25, 100, 456, 457]. Integrins are also reported to potentiate fibronectin induced Ca^{2+} signalling in renal cilia [458], although it remains to be seen which other channels may play a role in mechanotransduction within connective tissues. It is not possible to discuss all known primary ciliary receptors in detail, or receptors that could be specific to the chondrocyte.

1.50 The Centrosome: The Central Processing Unit

The centrosome contains functional groups of proteins involved in microtubule nucleation, anchoring, duplication, cell cycle, and primary cilia regulation (reviewed by Alieva et al., (2008) [120]). The centrosome is an inherited structure [229, 459-461] and functions as the main microtubule organising centre of the cell [138, 145] as well as the controller of the cell cycle [124, 459, 461]. It is required for cell cycle transitions and as a substrate for numerous regulatory proteins [109, 461, 462]. Microtubules are polarised dynamic structures [463] which extend with a defined orientation originating from γ -tubulin ring complexes (γ -TuRC) [118, 135, 189, 198, 461], some of which attach to the basal appendage docking complexes, while others are anchored within the PCM lattice 'cloud' surrounding the diplosome [105, 464-466]. Numerous molecules are involved in microtubule tubulin polymerisation and depolymerisation, as well as severing.

1.501 The Centrosome, the Cytoskeleton and Transport

The centrosome is the main director of the primary cilium, and also contains functional groups of proteins involved in a wide range of cellular functions. Control of cell cycle, planar cell polarity, organelle transport and motility requires coordination of the cytoskeleton. The cytoskeleton consists of a dynamic interplay of actin microfilaments, intermediate filaments and microtubules. Microtubules are dynamic directional structural conduits involved in cell movement, polarisation, cell cycle, cytokinesis and pathogenesis. The physical ability of actin microfilaments and tubulin microtubules to dynamically assemble and disassemble as required permits their use in the physical transport of vesicles, organelles and for signalling. During interphase, intermediate filaments and

microtubules radiate from the organising centre of the centrosome, while actin microfilaments associate with the cell membrane [120, 141].

Cytoskeletal molecular transport motors are ATP-dependent nano-actuators consisting of three classes; kinesins, dyneins and myosins, which are responsible for driving directional movement for the transport of materials, vesicles, organelles and cytoskeletal dynamics within the cell [120, 188, 270, 467-472]. Myosins are microfilament transport motors, while dynein and kinesin family members facilitate the directed transport along microtubules. The Kinesin family of proteins are anterograde transport motors (except family 14B members [270]), while dynein family members facilitate retrograde transport [270, 473]. The majority of structural information concerning these motors comes from studies using crystallography and electron tomography [474]. X-ray crystallographic structures of various conformation states are known for members of kinesin [475], dynein [476] and myosin motors [474]. Motor complex components bind to different receptors [477, 478] along with the dynein interaction complex dynactin, which is a multi-unit protein that normally directs retrograde traffic [473].

The spatial regulation and ‘interactome’ of microtubules, their motor cargo interactions, transport specificity and signalling remain poorly understood [120, 146, 147, 158, 186, 477, 478]. These aspects include specific movement of cellular components of the cytosol, the nucleus, mitochondria, endoplasmic reticulum, centrosome, and the Golgi [479, 480]. Functional interactions of kinesin and dynein member motors are central to both ciliary and non-ciliary transport alike, where they are utilised in a host of cytoplasmic processes for signalling, regulation and organelle trafficking (tabulated in Appendices II, III and V). Ciliary processes are known to selectively utilise only cytoplasmic dynein DYNC2LI1, DYNC2H1 [492] and kinesin family members KIFs 3A, 3B, 3C, 7, 17, 19A and 24 (where IFT-complexes utilises KIFs 3A, 3B, and 17).

1.502 The Kinesin Family

The crystal structure of kinesin domains consists of two synchronous motor domains existing as a tetramer of two homodimers roughly $8 \times 5 \times 5$ nm in size [474, 481-483] (Figure 1.19). Each motor can generate a force up to 7 picoNewtons [484] (although ATP and Mg^{2+} concentration may influence kinesin performance [485]), involving steps of 8 nm, the corresponding length of the tubulin α - β dimer [474]. Kinesin contains many subfamily members that exhibit a variety of properties, sharing similar evolutionary structural properties to the myosin family [471, 472, 474]. Eukaryotic kinesins consist of a conserved ATPase core and many isoforms, alternative splicing and variable sub-assemblies allowing for a variety of cargoes to be transported [270, 471, 472].

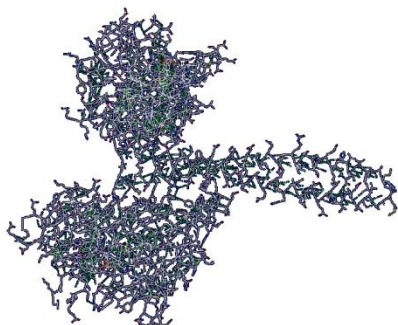


Figure 1.19 The Kinesin Motor: A molecular model of the crystal structure of kinesin member kinesin NCD (1N6M) [475] obtained from the PDB protein databank [486] viewed in the Swiss-PDB viewer [487].

1.503 The Dynein Family

Dynein consists of a diverse family of proteins whose components participate in a range of cellular functions [488, 489]. There are two classes of dyneins; axonemal and cytoplasmic [489, 490]. Cytoplasmic dynein complex naming nomenclature varies [491], since dynein is built around respective DYNC1H1 and DYNC2H1 units, and these have been reviewed [492] (Appendix III). Dynein generates forces of around 1.1 pN [493], and although the output is similar to kinesin motors, it is speculated that dynein output may be tuned for transport needs in response to load [473, 493]. Crystal structure studies of dynein motors [476, 494] have revealed them as high molecular weight homodimers of 1-2 MDa, consisting of a central head complex and a long tail [495], which contains significant residues involved in cargo binding [496]. Regulation of dynein properties is known to occur through three cofactors, the dynactin complex, lissecephaly-1 (Lis1), and nuclear distribution-E (NudE) proteins [496, 497], and these determine its motile properties [471]. Lis1, NudE, and Rab6A are involved with the centrosomal and nuclear localisation of dynein [473], in which the Lis1 enzyme is an initiation factor for dynein transport [498, 499], and Rab6A removes Lis1 from the idle dynein complex and promotes retrograde movement [500]. Lis1 is recruited to dynein by NudE, to regulate motor force production [501].

Cytoplasmic dynein isoforms-1 and 2 mediate vesicular transport, while dynein-2 has in addition ciliary and Golgi functions [502]. Dynein binds to centrosomal protein pericentrin (via DLIC-1) [471] and transport regulatory components such as the glucocorticoid receptor [503]. Dyneins may also have specific membrane functions within the cell for the transport of organelles and signalling [270, 504], as well as in maintaining the Golgi apparatus [492, 505], since dynein dysfunction disrupts intracellular vesicle trafficking [506]. Appendix III details the known roles of dynein family members.

1.504 The Dynein Activator - Dynactin

The dynactin transport complex [507] consists of a filament 37 nm in length and 10 nm wide (resembling F-actin) comprised of globular protein heads [508], and a molecular mass 1×10^6 Da [473]. It is responsible for bi-directional microtubule transport [509] (acting through dynein and kinesin motors), as well as a wide range of regulatory interactions [120, 473, 507, 510], and is also required for microtubule anchoring within the centrosome [511]. As a regulator of dynein and kinesin function [507], it is involved in vesicle transport [513], cell cycle and cell division [514, 515, 516]. Dynactin is a multi-protein complex involved in linking cargo [517, 518] and it consists of many subunits [507] (Figure 1.20). Dynein microtubule transport depends upon complex interactions between dynein, the dynactin regulatory complex, linkage proteins spectrin- β III, ZW10 [519] and syntaxin [520]. Arp1 vesicle binding occurs through spectrin- β , allowing binding to Golgi spectrin, as well as containing two microtubule-binding domains [5, 507, 521].

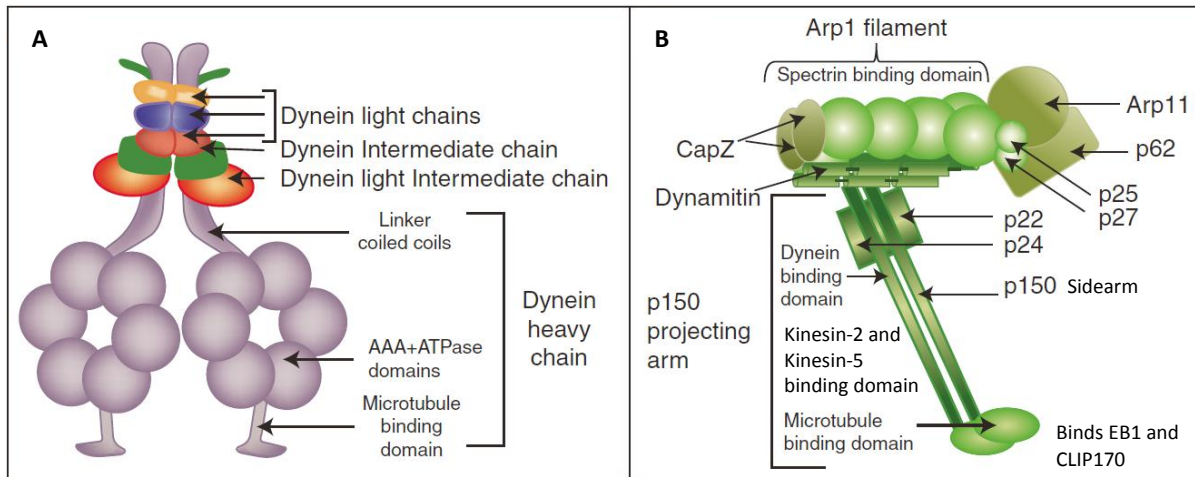


Figure 1.20 The Dynein Motor and Dynactin Complex: **[A]** The dynein motor complex consists of two hexameric ATPase modules and intermediate chains. **[B]** The dynactin complex consists of a p150 arm that binds with the dynein intermediate chain (also containing a microtubule binding domain) which is connected to Arp1 (and other components), allowing binding to spectrin upon membranes. Reproduced and modified with permission from Yadav et al., (2011) [518] and Kardon et al., (2009) [473].

During interphase, dynactin accumulates in the centrosome for a cell cycle specific role in which dynactin influences microtubule function and components of the PCM [511, 514]. It is found localised to endocytic organelles and vesicles in the Golgi region [522], while spectrin- β III regulates secretory protein and Golgi integrity [521]. Dynactin subunit p150^{Glued} is found localised to the maternal centriole [514], where it and other pericentrally located subunits provide as yet unknown regulatory roles related to the recruitment of materials, signalling, transport of organelles and the cell-cycle [120, 507, 515]. KIF3A interacts with p150^{Glued} for the organisation of basal feet [523]. Loss of p150^{Glued} from Arp1 results in microtubule disorganisation [507, 514]. The dynactin p50 sub-unit interacts with CEP135 in the centrosome, playing a role in assembly and maintenance of the MTOC [524].

Dynactin subunit-1 (DCTN1) interacts with BBS4, where it is involved in microtubule and cargo anchoring within the centrosome [335] (Appendix I). p50 and Golgi-Rab6 bind to bicaudin-D [473], while Rab6A [525] regulates the recruitment of the dynactin complex to membranes of the Golgi [526], where it is involved with intra-Golgi and Golgi-endoplasmic reticulum trafficking [525]. Rab7 is involved with p150 in the late endosome mediating fusion [473]. Interactions with spectrin- β III attachment via Arp1 are required for long-range vesicle transport [473, 510].

Dynactin regulates bi-directional transport of both dynein and kinesin [471], and dynein, kinesin-2 and kinesin-5 are known to interact with p150^{Glued} [473]. The dynactin adaptor complex links to dynein between the intermediate chains and p150^{Glued}, where it facilitates a diverse transport array, including vesicle transport of material from the endoplasmic reticulum to the Golgi [473, 517]. In this process, Rab6 acts as a membrane receptor, and also binds p50 to dynactin and bicaudin-D [473]. Rab6-bicaudin-D binding is important for Golgi function, where it is reported to inhibit Golgi fragmentation [527].

Most cellular dynein activity requires the dynactin complex [507, 509], disruption of which inhibits endoplasmic reticulum to Golgi transport and leads to re-arrangement of the Golgi and the endosomal/lysosome system [511, 528]. Independent vesicle transport from the Golgi to the ER-COP1 requires biclaudin-D for recruitment of the dynein-dynactin complex [525]. Cell division control protein CDC42, dynein and dynactin are reported to be involved with orientation of the MTOC and Golgi in migrating cells [529] (see Section 1.61). It is believed that dynactin regulates the presence of dynein at specific cytosolic locations, providing linkage to cargoes and adaptor molecules, although complete understanding of these processes is presently lacking. GTPase family members function at specific subcellular compartments [473], where they may provide a link between dynein and regulatory protein function [530].

1.51 The GTPase Family Members

The GTPase superfamily contain four well known subfamily members Arf, Rab, Ran and Ras and with their effectors and regulators are involved with most aspects of signal transduction, cell cycle, cell migration and intracellular function [531-536]. GTPases are involved in signal transduction at the intracellular domain of many *trans*-membrane receptor proteins, in cellular control, cell polarity, protein synthesis, cytoskeletal dynamics, transport, and vesicle targeting as well as membrane organisation [342, 537-539]. Switching is achieved through the hydrolysis of the GTP form to the inactive GDP state [534].

Members of the Ras family of GTPases are involved in cell division, differentiation, and cytoskeletal dynamics [540-543] as well as in apoptosis and cancer progression [543]. For example, B-cell lymphoma protein (BCL-2) and Ras-GTPase may determine regulation of cell fate [543]. Rho is a subset of the Ras family [532] whose members RAC1, CDC42 and RhoA are involved in gene expression and cell proliferation [544], as well as in regulation of cytoskeletal and cell division. RhoA-mediates cytoskeletal actin enrichment for ciliogenesis [545], with Meckelin and Nesprin proteins being required components for primary cilium formation [546, 547]. RhoA plays a role in cytoskeletal dependent functions in hematopoietic stem cells [548], with its centrosome associated kinase p160ROCK regulates centrosome position [549]. Rho-family members are involved with pathways of adhesion signalling between matrix and integrins [550], as well as cell shape and motility [551] in cell migration, requiring alteration of the centrosome, cytoskeleton and microtubules [543, 552]. Rho, Rac and CDC42-GTPases also regulate the formation of cell-matrix focal adhesion complexes, control polarity, adhesion during cell migration, as well as assisting with the reorganisation of the actin cytoskeleton in response to mechanical forces [550, 553, 554]

Ran is involved with ciliary entry [555], ciliogenesis [341], centrosome division [556], in nuclear entry [547] and is required for centrosome microtubule organising activity [558]. The ARL-GTPases regulate several different aspects of centrosome microtubule function and polymerisation [559, 560]. Zhang et al., (2013) [561] reviewed the role of the Arf-like GTPases ARL3, ARL6 and

ARL13 and their vital functional roles within the cilium. ARL3 is reported to be a negative regulator of ciliogenesis, but it is required for functionality of the IFT-B complex and interacts with NPHP3. ARL6 is required for signalling (where it functions within the BBSome) while ARL13 is required for both ciliogenesis and functional IFT-targeting of receptors (such as PC2 [562]). Furthermore, ARL13B, with CEP164 is reported to be involved with INPP5E for targeting to the cilium [347].

A full review of the GTPase members and their intrinsic cellular and ciliary roles is beyond this thesis; however, their importance in driving transport, vesicular processes and signalling is complex and fundamental to ciliary function. Cross-talk occurring between GTPase families has recently been reviewed by Derecic et al., (2013) [563] (for example Rabs and ARF-members for ciliary transport), where family members coordinate to control cell shape, motility and functionality of the Golgi [539].

1.511 Function of Rab Family Members

Rab-GTPases represent the largest branch of the Ras superfamily [564]. Intracellular vesicle trafficking is partially regulated by Rab-GTPases and their effector proteins, which determine temporal and spatial regulation of vesicle trafficking [565]. The role of Rabs as master regulators, their effectors, interactions and organelle specific roles has been extensively reviewed [535, 538, 566-568]. Rab family members participate in cytoskeletal transport motor processes [565, 569], as well as membrane based vesicle formation and fusion [538, 567]. These involve enzymes, elements of the cytoskeleton, and soluble N-ethylmaleimide-sensitive factor attachment protein receptors (SNAREs) [570] which control the specificity of docking and fusion processes [571]. Together with vesicle coat proteins they enable a wide range of cellular functions [572] which mediate the intracellular destination of vesicles [573], vesicle fusion and motility [535]. The Rab family of proteins and their effectors allow precise control over endo- and exocytotic processes [574], membrane bound vesicles (and their contents), providing a wide variety of cellular functions, including those within the cilium [566]. Aspects of Rab expression may vary between cell types [575] and within the cell cycle, where it is reported that differential regulation of Rab expression modulates cell maturation [576]. Rabs and their effectors are also essential for viral infections [577], such as hepatitis-c replication [578], and are associated with pathologies ranging from protein trafficking disorders [579] to cancer [580]. Various mechanisms are involved in prevention of Rab overlap and dysfunction [567]. Rabs function as master regulators of cellular membrane bound trafficking, sorting, and targeted fusion, however their temporal expression is still unknown [567, 576]. A select list of Rab members involved in ciliary and organelle function is contained in Appendices II and III.

1.512 The Cilium, Rabs and GTPases

As a specialist organelle the cilium represents a novel ‘compartment’ in which Rab5, Rab6, Rab8, Rab10, Rab11 Rab17 and Rab23 are selectively involved with ciliary genesis and function

[300, 538, 563, 581] (Appendix II). Of those Rabs involved in the cilium [300], some are involved in vesicle and membrane fusion, as well as serving secondary functions. While Rab-GTPase membrane trafficking regulators Rab8a, Rab17 and Rab23 are known to be required for ciliogenesis, only Rab8 is reported to be present within the cilium [299]. Rab23 regulates Smo levels [582], while Rab8 localisation to the cilium requires CEP290 and PCM-1 [583] at the basal body. These interact with the BBSome (a regulator of Rab8 in ciliogenesis [333]) which also localises Rabin-8 to Rab11-positive vesicles in the centrosome [295]. These later promote membrane biogenesis, and axoneme extension, including the docking and fusion of vesicles at the base of the cilium [307]. Rab8A interacts with Cenexin/ODF2 of the basal body, indicating that the microtubule sub-structure of the basal body is vital for interactions of many downstream effectors.

Intra-flagellar component IFT22 is a RabL5-like protein regulating cellular pool size and number of IFT particles within the ciliary compartment in *Chlamydomonas reinhardtii* [359], indicating IFT components may also have ancillary active functions. The basal body appendages have been identified as sites where centriolin and cenexin regulate GTP-bound Rab11, its activator Evi5 and Exocyst component sec15, thereby influencing the localisation of the endosomal recycling compartment to the centrosome [584].

1.513 Rabs, Vesicular Processes and the Golgi

At present, the role of GTPases in chondrocyte function, signalling, differentiation and disease remains largely unknown [585, 586]. A number of Rab-GTPases share or have overlapping functions forming a complex network of regulatory pathways involving the cilium, cytoplasmic organelles and Golgi function within the cytosol [587]. Specific Rabs and their known interactions are summarised in Appendix II, while their involvement with organelles are tabulated in greater depth in Appendix V.

Secretion of materials derived from the endoplasmic reticulum is controlled by a set of Rab-GTPases. Reticulum to Golgi transport utilises Rab1 and Rab2 [588, 589]. Rab6 is involved in *trans*-Golgi and anterograde Golgi-ER microtubule transport [590], while Rab-Sec4p is active in the *trans*-Golgi derived vesicles (and is associated with the exocyst) [311]. Rab8 and Rab11 are involved in vesicular secretion, as well as ciliogenesis [591]. Rab6 is required to maintain cisternae number, and for trafficking of *trans*-Golgi 'coated protein' COPI-coated vesicles and Clathrin [592].

Rab1 is involved with endoplasmic reticulum exit sites while Rab2 is involved in pre-Golgi intermediates and Golgi to ER trafficking [581, 589]. Rab6 (liquid droplet formation) Rab18, and Rab24 [581, 593] function to expedite transport from the endoplasmic reticulum 'intermediate compartment' to the Golgi, which is known to utilise Rab6, Rab10, Rab22, Rab30, Rab33, and Rab40 to facilitate control of morphology and intra-Golgi trafficking [581] (Appendix II). Specific Rabs are also participate in compartments and periphery processes; Rab6, Rab24, Rab33 and Rab40 (*cis* edges [581]), Rab6, Rab33B (*medial*), Rab3D, Rab6, Rab8, Rab9, Rab14, Rab22, Rab31 (*trans*), Rab3D,

Rab11, Rab14, and Rab43 with the *trans*-Golgi-network (tabulated in Appendix II). Rabs and Golgins [594] coordinate the *trans*-Golgi network structure and interact with the cytoskeleton to create a functional Golgi [512].

Rab3, Rab8 and Rab11 [595] are involved with docking of secretory vesicles [596], while Rab18, Rab27 and Rab37 are concerned with secretory granules, although there appears to be some overlap in functionality [566]. Rab5A is occurs with coated pits (Rab5 controls endocytosis [597]), while Rab10, Rab18 and Rab35 play roles in the endosome, Rab4, Rab5C, Rab11, Rab15, Rab21 (Rab21 is involved in recycling integrin receptors [581]), Rab22 and Rab35 (early), Rab7, Rab9, Rab22, Rab24 and Rab25 (late) with Rab11, Rab15 and Rab35 in the recycling endosome (tabulated in Appendix II).

Rab-GTPases bridge membrane and cytoskeletal dynamics in both secretory and endocytotic pathways [598] as well as regulating the endoplasmic reticulum-Golgi intermediate compartment mobility through COPI coated pits, motor proteins and microtubules [599]. The role of small GTPase components and the Golgi has been recently reviewed by Baschieri et al., (2012) [539], pointing out spatial and temporal signalling controls the entry and egress of membrane bound components of the Golgi apparatus. Rabs are involved with organelle interactions in cellular processes, including the endosomal, lysosomal and phagocytic membrane processes tabulated in Appendices II and III.

Rab6 is critical to the function of the Golgi apparatus, where it not only interacts with numerous effectors for maintaining Golgi function and secretory processes, but also enables Golgi homeostasis, facilitation of vesicle transport, intra-Golgi cisternal fission, docking and tethering [527].

Golgins have several Rab binding partners within the Golgi and *trans*-Golgi network, where they are proposed to act as scaffolding molecules for regulating membrane recruitment and trafficking pathways by promoting cytoskeletal association with the Golgi membrane [512]. Golgins, predominant on the *cis* and *trans*-faces of the Golgi, are required for organising the network for secretion [600, 601].

1.514 Golgi Derived Transport: Targeting of Materials from the Golgi

The targeting of materials from the Golgi apparatus enables regulated secretion, exocytosis and transport to the endosomal and lysosomal systems. These depend on a host of regulatory processes from the *trans*-Golgi network [602]. Cross talk between GTPase family members for cargo selection and processing remains largely unknown; however, their intricate signalling, switching and cross-talk between components certainly influence a variety of cellular functions [536, 543 563, 603]. GTPases and their effectors are required for the ciliary targeting of Golgi derived vesicles for both ciliogenesis and normal ciliary function [563].

Protein trafficking from the Golgi to the primary cilium occurs through ‘ciliary localisation sequences’ utilising the terminal protein residue sequence V-x-P-x [325], commonly known as the ‘VxPx’ targeting motif [362]. These are recognised by ARF4 [563] in a transport ‘ciliogenesis

cascade' involving ARF4, Rab11 and effector FIP3 [563] involving components within the Golgi and *trans*-Golgi network. For example, in photoreceptor cells, Rab11 and effector FIP3 regulate the budding and sorting of vesicles in the *trans*-Golgi-network containing Rhodopsin [604] (Figure 1.21A). RP2 regulation of ARL3 is important for Golgi cohesion (loss of KIF3A, ARL3 or RP2 causes Golgi fragmentation) [605]. The retinitis pigmentosa protein RP2 may link centrosomal vesicle trafficking and the primary cilium, where it is found upon the periciliary ridge, and also co-localises with γ -tubulin and pericentrin [605]. Mutation of any ciliary protein may affect the targeting and action of other ciliary proteins, such as the retinitis pigmentosa GTPase regulator interacting protein 1 (RPGRIP1) 'interactome' complex, malfunction of which leads to specific retinal ciliopathies [606]. Understanding of the functional relationships of ciliary targeting and subsequent pathogenesis is not well established.

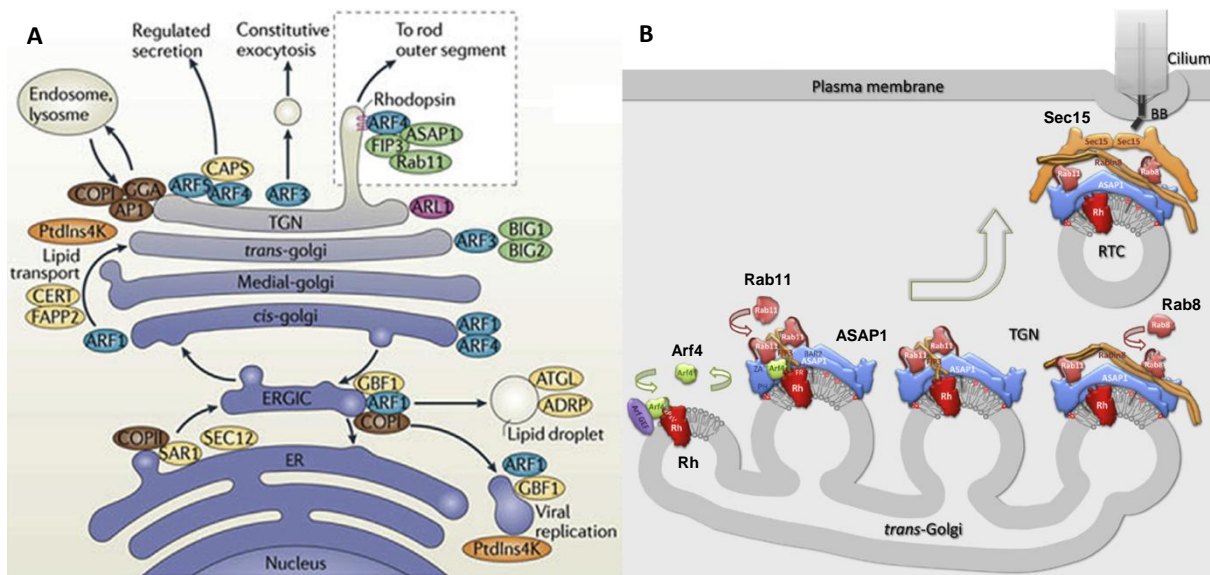


Figure 1.21: Regulated Golgi Transport and Signalling: [A] Materials are regulated in their passage from the endoplasmic reticulum to the intermediate compartment (ERGIC), before processing through the *cis*, *medial* and *trans* compartments, where the *trans*-Golgi network (TGN) directs them to specific locations via membrane complexes, targeting proteins and GTPases. Shown are the ARF-GTPase and its adaptor molecules, yet, the full mechanisms for Golgi regulatory control remain presently unknown. Reproduced with permission from Wang et al., (2013) [602]. GTPase 'Cross-Talk': [B] Cargo sorting and directed transport occurring from the *trans*-Golgi face requires the co-ordinated communication between effector molecules and the ARF and Rab-GTPases for the targeted delivery of the Rhodopsin (Rh) cargo to the primary cilium. Reproduced with permission from Deretic (2013) [563].

Ciliary components opsin, RP2, PC1 and PC2 also utilise the 'VxPx' localisation motif, and their trafficking utilises ARF4 [349, 350, 362, 563, 607-609], from the *trans*-Golgi ciliary trafficking (with the exception of PC2). PC2 however is sequestered directly to the cilium from the *cis*-Golgi side (GM130 co-localised), while PC2 not destined for the ciliary membrane passes directly through the Golgi [610]. PC1 ciliary directed trafficking is likely to be similar in both photoreceptors and renal epithelial cells, using a Golgi bound complex consisting of Rab6, Rab11 and ASAP1, while ARF4 and Rab8 are also utilised for ciliary trafficking [349].

IFT20 is functionally linked to the Golgi, where it is anchored by GMAP210 [259], and is known to localise with PC2, where it is necessary for ciliary assembly [332]. Rab3D reportedly

regulates a subset of the *trans*-Golgi-network [611], while Rab7 activates endosomal specific dynein motors through a Rab7-RILP-p150^{Glued}-ORP1L-spectrin complex [612]. ARF components are involved with the *trans*-Golgi, where ARF4, ARL3, ARL6, and ARL13B facilitate ciliary protein targeting [604] (Figure 1.21B).

1.515 Transport and the Golgi Apparatus

Golgi localisation requires the temporal and spatial coordination of the cytoskeleton, and a host of scaffold and adaptor protein interactions including GTPases and their effectors [563, 609]. Transport motors are vital for cellular processes, and loss of dynein or the microtubule cytoskeleton results in loss of Golgi function [519], since both dynein and kinesin are required for dispersion of the Golgi products. Rab6 acts as a recruiter for bicaudin-D, dynactin and dynein [525]. Dynactin can also bind microtubules to the COPII vesicle coat [520]. Bicaudal-D regulates aspects of COPI independent Golgi-to-ER traffic through recruitment of dynactin [525], where CDC42 may participate in dynein recruitment to COP1 vesicles [613]. Huntingtin plays a role in myosin and dynactin-dynein vesicle transport [614], as well as co-ordinating dynein mediated positioning of endosome and lysosomes [615]. Specific KIF-member motors facilitate interaction between cargo and a range of adapter proteins [270], are involved in divergent trafficking from the *trans*-Golgi [519] and probably share a level of redundancy and overlap in function [615].

1.60 Microtubule Roles During the Interphase

During interphase, microtubules mediate centrosome positioning, cell shape, organelle trafficking, planar cell polarity, endocytosis, secretion and extracellular matrix assembly [120, 616, 617] (Appendix V). Centrosomal derived microtubules appear to play a complex dynamic role, in which they are spatially and temporally regulated [618, 619] and simultaneously provide cytoskeletal resistance to compressive forces [142, 146, 152, 153].

Microtubules can be divided into distinct populations; those derived from the centrosome, those originating from the Golgi apparatus and free in the cytoplasm [518, 620, 621]. These are believed to have functionally different roles [622]. The centrosome provides a central focus for microtubules which form a transport conduit for vesicle transport between the endoplasmic reticulum and the Golgi, as well as other organelles. Appendix V gives Tables of kinesin and dynein motors, their effectors and roles in transport and regulation of the primary cilium, centrosome tensegrity and pericentrosomal vesicle recycling. Included are organelles of the endoplasmic reticulum, the Golgi, as well as the endosome, lysosome, melanosome, podosome, desmosome, nucleus and mitochondria. Transport motors are implicated in the regulation of cytosolic components, maintaining cytoskeletal shape, focal adhesions and matrix interactions. Re-arrangement of the cytoskeleton is required for the orderly movement of organelles, such as the Golgi complex [623] and nucleus [624]. Microtubule processes may interact with the cell membrane [625], nuclear membrane [624], endoplasmic

reticulum [626], mitochondria [627] and Golgi apparatus components and processes [622], although little is known about their regulation (Figure 1.22).

Microtubule dynamics and guidance [628] are controlled by protein regulators which include the promoter and stabiliser protein XMAP215 [629], the destabiliser XKCM1 and microtubule associated proteins EB1, APC, and CLIP170 [630, 631]. In *Drosophila*, kinesin-13 family members regulate microtubule dynamics and depolymerisation at the distal end [632]. Microtubule distal ends are involved in cytoskeletal support, and act as anchoring platforms through CLASPs allowing force transmission, a process where integrin receptors act as force couplers linking the extracellular matrix impinging upon the cell membrane to the cytoskeleton [633], and they also act as regulators of microtubule nucleation through MEK/ERK signalling [634]. Ran-GTP is known to coordinate regulation of microtubule nucleation [341, 634], since the attachment of microtubules to target binding sites may increase their stability. For a review of microtubule dynamics and their interaction partners in signalling see Tamura et al., (2012) [633]. Microtubule nucleation requires NEDD1 (GCP-WD) by way of involvement with γ -TuRC [533, 634], where it is believed discrete protein interaction networks within the centrosome govern interphase microtubules. This becomes evident upon transition to metaphase with the CDK1 kinase induced reorganisation, whose coordinated changes are not yet understood [631]. Organelle specific microtubule transport motors, their interactions and associated Rabs are tabulated within Appendix V.

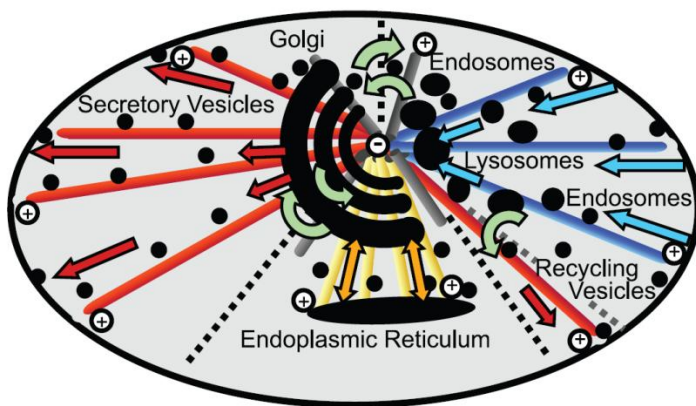


Figure 1.22 Microtubules and Vesicle Transport: Subsets of the centrosome microtubule network are believed to participate with transport processes and Golgi associated organelles. Microtubules are responsible for organelle homeostasis and function through bi-directional transport complexes allowing connectivity with the centrosome. Reproduced with permission from Klann et al., (2012) [635].

1.61 *The Cilium, Centrosome and the Golgi*

The intimate relationship between Golgi apparatus to the centrosome and the primary cilium during interphase is well documented [3, 26, 95-97]. For example, primary cilia and centrosome re-orientation are closely involved with the wound healing response [636, 637]. This involves cell migration, repositioning of the Golgi [638], the centrosome and nucleating microtubules [639]. During cell migration the primary cilium and centrosome are located close to the nucleus, with the Golgi apparatus aligned with the leading edge of the cell, in the direction of migration [518, 636] (Figure 1.23). This requires cytoskeletal re-organisation and polarisation of the Golgi that is initiated through CDC42 and the centrosome [529].

ARF1 and Rho protein CDC42 control dynein recruitment to the Golgi, and activating protein ARHGAP21 regulates ARF1 and CDC42 activity for microtubule and dynein dependent Golgi positioning [640]. For example, CDC42 activation is reported to control polarisation of the Golgi in migrating astrocytes [641].

Microtubule dynamics directing the bi-directional transport of vesicles and organelles remain poorly understood at present. Dynein, dynactin and kinesin family members are responsible for the polarised transport of various cargoes of materials and organelles within the cell, although the details of such processes remain elusive [145, 514], particularly their role in anchoring to and positioning the centrosome [121, 144].

Kinesin motors show preference for particular subsets of microtubules [642], although their selection, regulation, recycling and role in transport of organelles and polarisation of the cytoskeleton remains poorly understood. Microtubule disruption influences centrosome and Golgi localisation [643] as well as resulting in dispersal of the Golgi ribbon [644]. CAP350 centrosomal protein stabilises Golgi associated microtubules, and functions to maintain Golgi peri-centrosomal localisation [645], while CDC42 regulates microtubule Golgi positioning [640]. Klann et al., (2012) [635] has reviewed the modelling of vesicle transport processes and the cytoskeleton (see Figure 1.22).

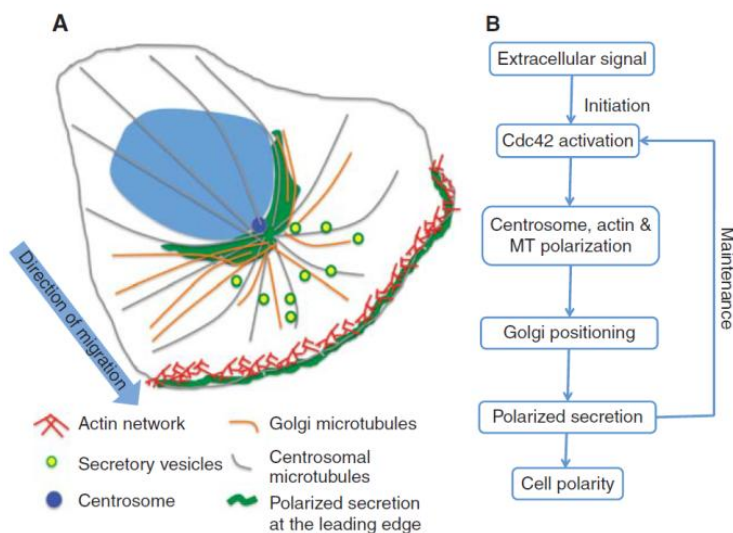


Figure 1.23 Polarisation of the Centrosome and Golgi in Cell Migration: **[A]** Migrating cells align the Golgi and centrosome with the cytoskeleton and leading edge aligned in the direction of migration. **[B]** Organisation of microtubule polarisation and secretion involves the centrosome and numerous pathways to achieve the required polarity. Reproduced and modified from Yadav et al., (2011) [518]. Different microtubule ends may be involved in planar cell polarity pathways and endocytosis. Within migrating cells, the Golgi and centrosome are constrained by the substrate [651].

Recent studies have shown that the Golgi apparatus also acts as a microtubule nucleating and organising centre [646,647], and that those microtubules are essential to the proper operation and behaviour of the Golgi [156, 622, 648]. Conversely, Golgi derived CLASP-dependent microtubules reciprocally influence Golgi polarisation and organisation [648]. Microtubule nucleation onto the *cis*-side of the Golgi requires proteins GM130 and AKAP450 [647], with *cis*-Golgi-network-associated-protein GMAP210 binding the (-) microtubule ends [649], while Golgi-derived CLASP-dependent microtubules control Golgi organisation and polarised trafficking [625, 648]. Components of microtubules and actin also regulate the *trans*-Golgi architecture: the *trans*-Golgi network

microtubules [512, 650] deliver vesicles containing precursor materials from the Golgi for directed secretion [636]. Many features of centrosome and Golgi positioning, regulation, secretory cargo transport, and exocytosis remain unclear.

1.62 Centrosome Positioning

Centrosome positioning requires a combination of pulling and pushing forces generated by microtubule motors applied to the cytoskeleton [144, 652]. Movement of the centrosome to adjust its position requires the timely balancing of forces generated upon the microtubule network by dynein and myosin [653, 654]. The close association of the centrosome with the nucleus is balanced by KIF9 and dynein [493, 653, 655, 656], where dynein is involved in rotation of the nucleus [504]. Kinesins KIFC3, KIF2A and KIF2C are thought to be involved in targeting CEP170 to the centrosome [479].

1.63 Intracellular Transport

Intracellular transport of organelles and materials uses specific proteins, GTPases, kinesin and dynein motors that are involved in the processes of transport, signalling and cytoskeletal rearrangement tabulated in Appendices II, III and V. The Golgi apparatus requires the bi-directional trafficking of materials derived from endoplasmic reticulum exit sites to the intermediate ER-Golgi compartments. This then requires orderly transport through the *cis*, *medial* and *trans*-compartments, to the *trans*-Golgi network, making the product available for either direct secretion, recycling or storage.

1.64 Transport of Vesicles

The steps of vesicle budding, tethering, transport and targeted delivery of vesicles require GTPases, with Rab proteins representing the most commonly known group. These also control transport motors allowing for the temporal and spatial controlled transport [502]. The transport of cytoplasmic vesicles, materials and organelles requires three classes of molecular transport motors; kinesins, dyneins and myosins [477, 657]. KIF3 members and dynein have vital roles in both ciliary and organelle transport, while dynein contributes to receptor transportation [503] (Appendices III and V).

1.65 Rabs and Microtubule Motors

Rab-GTPases have been identified as key regulators of microtubule transport of cargo and organelles [448] - however, their specific interactions remain poorly understood. Jordens et al., (2005) [502], reviewed Rab-GTPases and their interactions with protein motors. The early endosome utilises Rab4 (with transport motors KIF3B and dynein), and Rab5 (with KIF16B and dynein), while the Golgi exclusively uses Rab6 (p50, p150 and Rab6-kinesin). Rab7 is involved with the late endosome and lysosome with protein sorting [658], and in recruiting dynein/dynactin to the lysosome [502, 659]. Rab5 modulates endocytotic membrane docking and fusion, as well as microtubule interactions within

the microtubule network [660, 661] where the positioning and translocation of endosomal and lysosomal clusters depends upon microtubules [662]. Rab6-kinesin is involved with the Golgi and endosomal processing [502, 663], while Rab6A activates the idle dynein complex, dislocating LIS1 in the process [500]. In addition, Rab6 is involved with actin and microtubule motors in regulating trafficking from the endosomes (reviewed by Goud et al., (2012) [527]).

Rab6C (specific to *Hominidae*) is involved in a subset of tissues and has been identified in centrioles in the centrosome, where its depletion gives rise to tetraploid cells and over-expression in G1-phase arrest, indicating a significant role in centrosomal function [664]. Rab6 centrosome associated activating protein GAPCenA complexes with γ -tubulin, where it may regulate Golgi and microtubule dynamics [563]. Rab6 also reportedly functions as a modulator of the Golgi redistribution response to hypotonic stress [665], and as part of the secretory apparatus, linking endosomal function to secretion.

1.66 Myosin Motors and Rabs

Myosin motor protein structure and function has been reviewed by Sweeny et al., (2010) [666]. The myosin protein consists of a motor head, attached to a variable calmodulin tail that allows for specific interactions with cargo and demonstrates actin-dependent ATPase activity [502, 667, 668]. Myosin family members I, V, VI and VII are involved in transport, with myosin-V members regarded as the most prominent [502, 657]. Myosin-V member tails exhibit tissue specific splice variations [669] and contain three distinct Rab-binding domains, which are reported to interact with specific members [670]. Myosin-Va also interacts with a subset of the Rab-GTPases that are associated with the Golgi secretory and endocytic recycling systems. Rab10 and Rab11 play a role in membrane recruitment, while endocytic recycling and post-Golgi transport processes use Rab11 and Rab14 [668]. Rab-GTPases are also reported to be involved with subsets of myosin motors; the Golgi utilises Rab8 (with myosin-VI), the recycling compartment Rab11 (with myosin-Vb), while the melanosome uses Rab27 (with myosin-Va) and Rab27A (with myosin-VIIa) [502]. The transport of secretory vesicles from the *trans*-Golgi by Myosin-V also uses components of the Exocyst [671]. During interphase, myosin-V is reported to be localised to the pericentriolar matrix and centrioles through the myosin tail, enabling targeting of the centrosome [668]. The myosin regulatory chain reportedly phosphorylates Rho-kinase [672], with myosin activity being regulated by CP190 within the centrosome [673].

1.67 The Golgi Apparatus: Transport Motors

Kinesins, dyneins, the dynactin complex, myosin motors, Rabs and their effectors govern many aspects of vesicular transport and organelle movements. Distinct subsets of motors, Rabs and effectors are involved in Golgi apparatus positioning, and bi-directional transport from the endoplasmic reticulum compartments to the Golgi intermediate compartment for processing into the

apparatus. Further components are involved with discrete vesicle transport from the *trans*-Golgi to a network including the endosome, the lysosome, as well as the melanosome and podosome compartments.

The positioning of the Golgi apparatus involves complex motor coordination of myosins (II and VI) [502], kinesins (KIFC3) [674] and the dynein-dynactin complex. Dynein (which is recruited to the Golgi by Golgin160, mediated through ARF1 [675]) participates in the centrosomal localisation of the Golgi complex [676], with Kinesin-13 reported to be associated with the stacks of the Golgi [677]. The transport of materials synthesised in the endoplasmic reticulum to the Golgi requires the coordination of transport motors. Materials which bud from the endoplasmic reticulum require dynein/dynactin for transport, with kinesin-1 serving a role in reticulum elongation and positioning. Hiro et al., (2009) [270] extensively reviewed the kinesin superfamily and concluded that ER-to-Golgi transport requires cytoplasmic dynein and kinesins KIF3, KIF5 and KIF1C. Transport complexes KIF3 and KIF5 are believed to operate bi-directionally and synergistically between the endoplasmic reticulum and the Golgi [678, 679]. Endoplasmic reticulum to Golgi transport (COPII) is known to utilise KIF5B and dynein/dynactin, while Golgi-ER (COPI) involves KIF5B, Kinesin-2, KIF1C [598], with Bicaudal-D believed to regulate transport through recruiting the dynein-dynactin motor complex [525] (Appendix V).

Golgi vesicular processing utilises KIF5 and KIF20 (with Rab6 [468]) although the exact role of kinesins and dyneins with respect to Rabs is still elusive. Vesicles and their materials are recruited to the pre-Golgi intermediate compartment (endoplasmic-reticulum-Golgi complex ERGIC) via involvement of kinesin-2 members and the dynein heavy chain. Golgi derived materials for export to the cell membrane entering the *trans*-Golgi-network rely upon components of myosin, KIF1A, KIF1B, KIF5B, KIF5C, KIF13A, KIF17, KIFC3 and dynein-dynactin for their delivery (tabulated in Appendices III and V). Many vesicle transport-dependent processes utilise different subsets of motors and GTPases for the transport and positioning of materials to, and secretion from, the Golgi apparatus [598]. For example, the direct polarised apical transport of the neurotrophin receptor uses KIF1A, KIF1B β and KIF5B, for selected transport in MDCK cells [680]. Endosomal positioning uses KIF16B (which anchors the endosome [681]), while the secretory endosome entails KIF5B, KIF13A and Myosin-1b, and the recycling endosome involves KIF5B and dynein/dynactin [270, 598]. These many processes remain largely unexplored, but known components are selectively tabulated in Appendices III and V.

1.70 A Brief History of the Golgi Apparatus

Camillo Golgi first described the organelle that now bears his name in 1897 [682, 683], which he termed the ‘internal reticular apparatus’ and in 1909 [684] described structural changes of the apparatus in mucosal gastric cells related to the cell cycle [685]. It was not until electron microscopy studies that the Golgi became more structurally defined, from two dimensional images by Bahr et al., (1981) [686] and Olins et al. (1983) [687]. Many unknowns remain today regarding its function. Golgi occur in both plant and animal cells and are composed of a series of individual stacks (or dictyosomes) with singular membranes known as cisternae (singular cisterna) [141]. Usually from four to eight cisternae are present in any given stack, which is comprised of enclosed membranous discs that transport, modify and export cellular materials [141]. These are divided into a basic Golgi network comprising *cis*, *medial* and *trans* compartments, each containing enzymes that selectively modify the contents [688], depending on where they reside (Krieger et al. 2004) [689]. These compartments can vary in size and when adjoined appear as continuous ‘ribbons’, and undergo cell-cycle dependent changes [690]. During interphase, the Golgi stacks are observed arranged in an interconnected network in close proximity to the centrosome [691, 692].

The Golgi is involved in the orderly post-translational modification of endoplasmic-reticulum-derived proteins (and materials) through acylation, glycosylation [693], phosphorylation [694], sulphation [695] and proteolytic cleavage [141, 696, 697]. Golgi associated transport vesicles have been identified; COPI [698] and COPII [699] vesicles are involved with endoplasmic reticulum and Golgi transport, while clathrin coated vesicles are also associated with the Golgi and *trans*-Golgi network [700].

Processed materials are delivered to their final destinations through the *trans*-Golgi network, which is associated with the endosome, lysosome and storage granule systems [141, 701, 702]. The *early* and *late* endosome functions to sort and reprocess internalised materials [703, 704], before degradation in the lysosome [705] (Figure 1.24). Multi-vesicular bodies internalise ligands, receptors and nutrients through the endosomal system [705], with macropinosome and phagosome processes involved in aspects of materials processing [141, 706]. A number of diseases are associated with disruption or dys-regulation of Golgi processes from achondrogenesis to types of congenital muscular dystrophy [707].

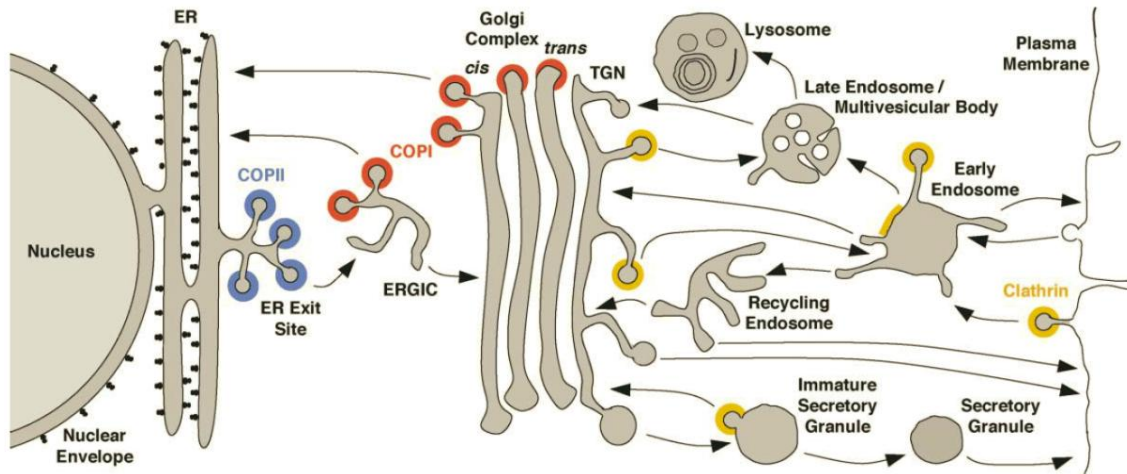


Figure 1.24 The Golgi Intracellular Transport Pathways: Details of the intracellular transport pathway for secretion. Materials derived from the endoplasmic reticulum (ER) pass to the Golgi intermediate compartment (ERGIC) [520] as vesicles decorated with ‘coat proteins’ (COP) [598] enabling directed transport (arrows). Adaptor proteins are colour coded as COPI (red), COPII (blue) and Clathrin (orange). Materials are transported through the *cis*, *medial* and *trans*-Golgi compartments, whence they are available, for direct secretion, the formation of secretory granules, or to components of the endosomal and lysosomal systems. Reproduced with permission from Bonifacino et al., (2004) [702].

1.71 Models of Transport Through The Golgi

Two intra-Golgi transport mechanisms have been proposed for the way in which endoplasmic reticulum derived vesicles are transported through the Golgi stacks for post-translational modification and processing [141, 700, 708]. Current evidence suggests this occurs via *both* mechanisms [709], with ample evidence supporting both models [700].

The Vesicular Transport Model is built around the concept of the Golgi as a distinct organelle divided into cisternal compartments in which smaller vesicles shuttle materials through the stack [708]. Vesicles budding from between the stacks are restricted in their movements due to fine filamentous proteins tethering the budded vesicles [141, 702].

The Cisternal Transport Model is based upon the premise that vesicles are continually transported to the *cis*-face where they coalesce and fuse to form cisternae along the pre *cis*-face. This model is supported by observations of pre-processed materials moving into the stacks from vesicles (ie collagen fibrils [692]), along with evidence of coat protein (COP) vesicles (Figure 1.24) [141, 710, 711].

Different appearances of the Golgi between species result from evolutionary divergence (extending to matrix proteins [712, 713]) so that a complete unified model of Golgi organelle function remains unclear [712, 714]. The architecture of the Golgi is also known to differ between cell types revealing that the Golgi is a dynamic specialised organelle with complex membranes, recycling and key signalling properties [715]. It has been suggested that the Golgi has evolved to become co-dependent with other cellular signalling and regulating processes [716-718].

In most cells, the Golgi apparatus fragments and dissolves upon the onset of mitosis (G2) (reviewed by Colanzi et al., (2003) [692]) [719], only to re-appear during telophase [720]. The re-appearance of the Golgi usually takes place during the onset of interphase, where its morphology and function are dependent on reassembly of the centrosomal network of microtubules [108]. Assembly of the Golgi is achieved by centrosome driven microtubule transport (or by self-organisation) where microtubules complement formation, with two populations being involved in its polarisation [156, 518].

1.72 The Golgi: Regulated Processing and Secretion

The basic model of vesicular transport through the cell begins with the synthesis of membrane bound materials transported from the endoplasmic reticulum to the Golgi intermediate compartment (ERGIC), which consists of vesicles and tubular structures coalescing with the *cis*-Golgi cisternae face, which is commonly highly fenestrated [520, 721]. Bi-directional Golgi transport is believed to be mediated by coated protein (COP) vesicles [722], where cisternae are thought to be in continuous turnover [723, 724]. COPI vesicles are involved in retrograde membrane trafficking from the *cis*-Golgi to the ER, while COPII vesicles are involved in anterograde trafficking from the ER to the Golgi. The progression of materials through the cisternae appears to be dependent upon the peripheral generation of COPI vesicles [702, 722, 725].

The *trans*-Golgi also interfaces with the endosomal and lysosomal systems through bi-directional transport [726] although the budding, tethering, cargo selection and fusion of vesicles is not well understood [702] (Figure 1.24). Retrograde and anterograde transport of materials between the *cis* and the *trans*-compartments, is probably facilitated by inter-connecting tubules and vesicles [716, 727]. Studies indicate compact cisternae are perforated, and interconnected by vesicular tubular linkage formations [728], which are observed to form between cisternae as a result of Golgi secretory trafficking [729]. Vesicle buds are evident upon the *medial* and the *trans*-compartments where enzymes are enriched within the perforated zone, but found to be depleted in COPI vesicles [728]. Materials are processed through the *medial*, and then *trans*-compartments before being delivered to its required destination (see Figs 1.21 A and 1.24).

The *trans*-Golgi network partakes in dynamic cargo-dependent packaging and sorting contents to their final destinations where the temporal morphology is dependent upon trafficking of materials [730]. One function of the Golgi is the sequential glycosylation of proteins and lipids of which there are at least 200 glyco-transferases [731] and several enzymes may occupy the same sub-compartment membrane [693]. These are recycled in the *trans* to *cis*-direction [732] in association with COPI vesicles [698], However recent studies have identified structural evidence that transport mechanisms throughout the Golgi are more complicated, with evidence for multiple transport mechanisms (Marsh et al. 2001) [715] including direct ER-*trans*-Golgi transport by-passing most of

the apparatus [724]. Curiously, some proteins bypass the Golgi altogether such as the cystic fibrosis trans-membrane conductance regulator (CFTR), CD45, FGF2, and Galectins 1 and 3 [733].

Microtubule disruption influences both centrosome and Golgi localisation, resulting in Golgi dispersal [643]. Golgi function and organisation is interdependent with other organelles on the actin and microtubule cytoskeleton [700], where the membrane shape is maintained through the roles of Grasp and Golgin proteins [734]. Golgi assembly is held together with oligomers of Grasp55/65, while glycosylation and sorting is also believed to be regulated by GRASP55/65 proteins [725, 735]. Clathrin proteins are involved in the endocytosis and internalisation of materials through the formation of 'coated pits' [141, 702], where their activity also enhances microtubule α -tubulin acetylation at pit sites [736]. Many aspects of the Golgi apparatus, its transport models and their networked structures are actively debated.

1.73 Planar Cell Polarity: The Centrosome and the Golgi

Planar cell polarity is required for development, cell migration, polarisation and symmetrical cell division where unique pathways regulate cytoskeletal rearrangement, polarisation and modification of cell behaviour [292, 462, 737-740]. Mutations in these pathways lead to a number of genetic abnormalities [289, 739, 652]. Extracellular Wnt ligands bind to Frizzled family membrane receptors [739], allowing transduction through the protein Dishevelled [741]. Canonical Wnt signalling involves gene regulation (β -catenin pathway) [742], while non-canonical (planar cell polarity) pathways control cytoskeletal members and are involved in a host of functional cellular, organ development and pathological processes [289, 292, 612, 739, 743-745].

Inversin is required for recruiting Dishevelled in response to activated Frizzled, acting as a switch between the planar cell polarity and β -catenin signalling pathways where it inhibits canonical Wnt signalling by degrading translocated Dishevelled [746, 747].

Wnt sensory protein Vangl2 localises to the cilium [744] and is responsible for ciliary tilting and positioning [748], but it also interacts with BBS8 [749] in determining left-right asymmetry in development. Wnt partner Chibby binds Cenexin at the distal end of the basal body, linking Wnt function to the basal body, where it plays a role in microtubule regulation [744] (Appendix I).

Planar cell polarity has a role in ciliogenesis [290]. The Dishevelled protein links basal body docking and orientation in ciliated epithelial cells [750]. Primary cilia are required for polarisation of sensory kinocilia [751], for which Frizzled and Van Gogh provide polarity information [751-753]. Downstream of Wnt signalling, DAAM1 is required for centrosome and Golgi re-orientation during cell migration [754]. Curiously, polarisation of the Golgi has been observed to be influenced by an external electric field [755], which in turn influences the cytoskeleton to align the cell in the direction of the field [756, 757].

The Rho family of GTPases [758] participate in reorganising the cytoskeleton and cell adhesion [543, 759]. CDC42 is involved in polarity and migration mediated by integrin activation

[760]. Dishevelled and Inturned mediate Rho-GTPase activity at the basal body [289], while Dishevelled is also associated with Clathrin for endocytosis [752]. CDC42 regulates pathways for controlling cytoskeletal structures [744] (Figure 1.23). Polarisation of the Golgi is also believed to be influenced by intracellular pathways involving the Ras/Raf/MEK/ERK and the PI3K/Akt/mTOR pathways, with MEK/ERK components required for two-dimensional orientation, while PI3K contributes to three-dimensional polarisation [761].

1.74 Planar Cell Polarity, Wnts and Cartilage

For a review of proteins within the canonical and non-canonical Wnt planar cell polarity signalling pathways and the cilium, see reviews by May-Simera et al., (2012) [744], Schlessinger et al. (2009) [756] and Church et al., (2002) [762]. In cartilage, Wnt is involved with planar cell polarity signalling for control of growth and chondrocyte column formation [763, 764] as well as induction of hypertrophy [765]. Non-canonical Frizzled signalling regulates the plane of cell division in chondrocytes [747], whereby daughter cells divide horizontally and then arrange into vertical columns. Wnt family members also have roles in cartilage function and chondrocyte differentiation [766]. Church et al., (2002) [762] reported Wnt expression to be developmentally important in cartilage; with Wnt-5b and Wnt-11 being expressed in pre-hypertrophic chondrocytes, Wnt-5a in the joints and perichondrium, with Wnt-4 blocking chondrogenesis. In contrast, Wnt-5a and Wnt-5b promote chondrogenesis, while Wnt-5b and Wnt-11 have Indian Hedgehog functionality. Wnt-5b also acts to inhibit chondrocyte hypertrophy and regulates mesenchymal cell aggregation and migration [767].

1.75 The Cilium to Golgi Continuum: Summary

Proper functioning of the Matrix-Cilium-Golgi Continuum in chondrocytes necessitates that the centrosome senses the extracellular environment, and regulates the necessary cellular processes required for the production, transport and post-translational modification and exocytosis of matrix materials. The concept of the centrosome as a highly organised cytoplasmic ‘central processing unit’ for controlling microtubule dynamics, sorting vesicles and organelles through coordinating the networks of motors and signalling effectors has not yet been fully developed. To this end, the roles of GTPases, kinesins, dyneins, and their known organelle interaction pathways have been tabulated within the Appendices. Central to this premise, is the primary cilium, which is a functional and structural microtubule based extension of the basal body, and the centrosome. It may express specific membrane bound receptors, and is involved in processing a variety of extracellular communication and sensing modalities in a variety of cell types, including connective tissues. The exact dynamics of the control mechanisms responsible for centrosomal control of the Golgi in synergy with the cytoplasm and respective organelles remain to be identified.

Section III – A Biomechanical Connective Tissue: Cartilage

1.80 Introduction: Biomechanical Function of Connective Tissues

Connective tissues comprise a broad range of tissue types, from tension transmitters like tendons, ligaments and skin, through to load bearers like cartilage and bone, including those interstitial, reticular, elastic and basement membrane networks which support specialised cells found in most organ systems. *All vertebrates share a common integrated connective tissue network which spans the molecular, cellular and whole organ levels.*

Connective tissues consist of two basic parts, a complex extracellular matrix (ECM) which forms the vast bulk of the tissue, and a smaller enclosed volume of cells, which are solely responsible for its formation, maintenance and repair. The extracellular matrix performs biomechanical and physicochemical functions that are appropriately sensed by the cells, which respond by producing the correct cocktail of extracellular matrix macromolecules necessary to maintain its structure and mechanical function. The composition of the extracellular matrix of tendon under tension is distinctly different to that of the matrix composition of cartilage under load, and the mechanisms mediating these mechano-biological interactions remain unclear. Previous studies suggest that the primary cilium could play a central role in this feedback loop, since it is located *in an intermediate position* between the extracellular matrix and the Golgi apparatus (responsible for *matrix secretion*), and is inferred to be capable of sensing mechanical signals, transducing information for transcription, and polarising the cellular secretory response [26, 97].

To date, knowledge of this relationship between the extracellular matrix, the primary cilium and the Golgi apparatus derives from conventional ultrastructural methods which provide a two dimensional perspective of the *structural* anatomical relationship between these strikingly different biological components. Few studies have attempted an ultrastructural serial reconstruction of a primary cilium, and none have attempted to include the three dimensional extracellular matrix which interacts with the ciliary membrane. To fully understand the dynamic relationship between connective tissue cells and their mechanically functional extracellular matrix, an essential preliminary is to define the three dimensional structural relationships which link the matrix macromolecules, the ciliary components and the organelles responsible for matrix secretion.

1.81 Overview: Connective Tissues

Connective tissues respond to mechanical loads, but how they do this depends upon the complex nature and unique constituent properties of collagens, proteoglycans and glycoproteins [141, 768-777]. These differ greatly in proportion between connective tissues, from the extreme toughness of bone and tendon to the softer basement membrane of epithelia, and they vary within the matrix environment, depending upon age and pathogenesis [775-779].

Matrix is composed of varying amounts of proteins and polysaccharides, which serve not only as a biomechanical scaffold, but also have a complex role as a biochemical microenvironment [141]. The composition and architecture of the extracellular matrix dictates cell behaviour, influencing cell proliferation, morphology, migration, development, function and survival [780, 781]. The unique properties of bone, the optical transparency of the cornea, the tensile strength of tendon, and load bearing properties of cartilage are all due to the different combinations of the same components comprising the extracellular matrix [782-784]. Changes to matrix composition result from a host of host of processes, ranging from developmental, homeostasis, aging and disease [784, 785]. In this study electron tomography was used to investigate cartilage as a compressive load bearing connective tissue, using avian sternal cartilage as a model.

1.82 A Compressive Tissue Matrix: Hyaline Cartilage

Hyaline (derived from the Greek word for glass) cartilage is one of the most common forms of cartilage, the others being the elastic and fibro- cartilages. It is a hypoxic, avascular, aneural, low friction load bearing tissue, which transmits and dissipates applied mechanical forces. Hyaline cartilage comprises the surfaces of articulated diarthrodial joints, elastic cartilage occurs in the nose, ears, the trachea and growth plates, while fibrocartilage makes up the intervertebral discs and the meniscus of the knee [141, 786].

Articular cartilage consists of four distinct morphological and biochemical zones which are bound between the synovial cavity and the subchondral bone: the superficial (tangential), the intermediate (transitional), the deep (radial) and the calcified zones [768] (see Figure 1.25). The superficial layer of articular cartilage makes up 1-5% of the cartilage volume, consisting of the lamina splendens [787], containing small flattened chondrocytes, with a low proteoglycan content, and incorporating a dense collagen fibre mesh which results in the characteristic hyaline translucency [768]. The intermediate layer comprises 40-45% of the matrix volume, and contains rounded encapsulated cells within a collagen matrix [768]. The deep layer makes up almost 45% of the total matrix volume and is characterised by increased proteoglycan content, presence of a radially orientated collagen network aligned perpendicular to the articular surface, and chondrocytes aligned into vertical columns in the direction of the load [768, 788, 789]. Each chondrocyte is suspended within a gelatinous pericellular matrix, which is encompassed by a capsule forming a chondron. Each chondron is surrounded by a local territorial matrix, while clusters of chondrons are separated by interterritorial matrices [788, 790] (see Figure 1.25). The calcified cartilage zone makes up approximately 10% of the matrix and is characterised by the presence of a 'tidemark', marking the transition from the middle layer to the calcified matrix zone [791]. This zone contains spherical encapsulated chondrocytes, calcium and radial collagen fibres, but is noticeably deficient in proteoglycans [768, 791].

Adult articular cartilage is distinguished by an extensive extracellular matrix which comprises in excess of 95% of the tissue volume, consisting primarily of collagen type II and sulphated proteoglycans [141, 768]. Cartilage water content contributes between 68% and 85% of the net wet weight of the tissue (remainder being 10-20% collagen and 5-10% proteoglycan) [792-794]. A mechanical balance against the hydration swelling pressure of proteoglycans is provided by the tensile resistance of the collagen fibres, which also allows the cartilage network to bear loads hydrodynamically [795]. An irregular interface between the calcified zone and the subchondral bone provides increased surface area for adhesion of the two matrices [768, 788].

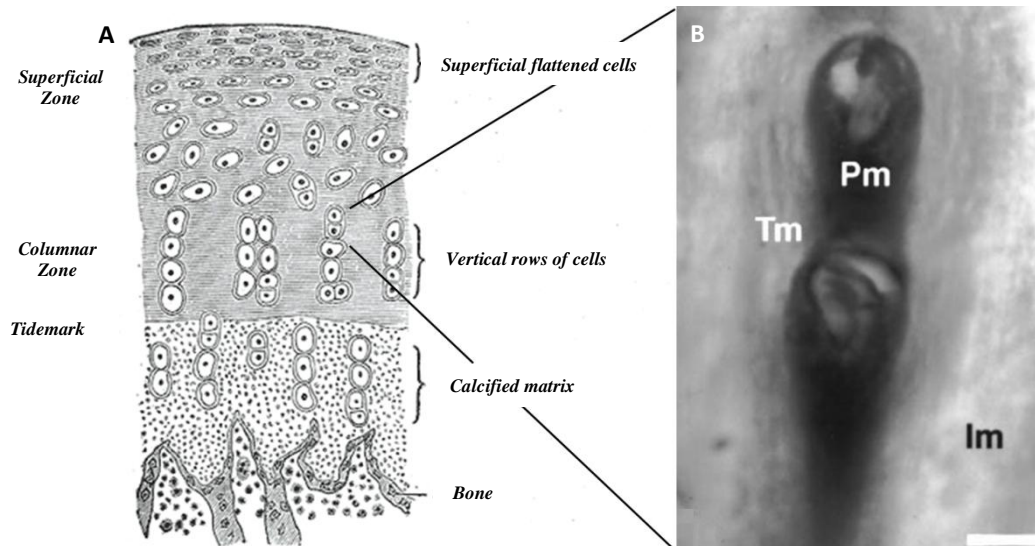


Figure 1.25 Hyaline Articular Cartilage: [A] Hyaline cartilage matrix morphology, showing the superficial zone (containing flattened cells), the deep columnar zone, the calcified zone (with tidemark) and the anchoring subchondral bone. Reproduced with from Gray's Anatomy. [B] Alignment of chondrocytes within the deep layer zone, detailing the pericellular matrix (**Pm**), the territorial matrix (**Tm**) and the interterritorial matrix (**Im**). Scale bar 10 μ m. Reproduced from Poole (1997) [789].

1.83 The Chondron

Benninghoff first described the chondron concept [796], which was later confirmed by Poole et al., (1987) [790], comprising a chondrocyte in hyaline cartilage surrounded by a zone of specialist matrix, the whole functioning as an essential structural component of mature cartilage. Here the chondron acts as a hydro-dynamically protective capsule surrounding the chondrocyte. The capsule consists mainly of tightly interwoven collagens of types II, VI, IX, XI [768, 797-800] and laminin [801]. The capsule is connected to the chondrocyte by type VI collagen while the pericellular glyocalyx contains aggrecan [802, 803], fibronectin [804], and laminin [801] as well as numerous minor components such as perlecan [805], biglycan, decorin [806], glypican, syndecan and link protein [807-809]. The capsule forms a boundary retaining the expansion of pericellular glyocalyx [800]. Chondron morphology varies between the superficial layer, the middle and deep layers, reflecting the local interterritorial matrix architecture, suggesting that zones experience different loads [789, 808, 809]. Fine channels of proteoglycan varying in diameter between 0.2 and 1.8 μ m extend

from the capsule into the adjacent territorial matrix, indicating intricate matrix specialisation around each chondron [768, 770, 771] (Figure 1.26).

It is widely accepted that chondrocytes actively modify their pericellular matrix in response to environmental influences [800, 809, 810]. In turn, the sequestered matrix affords protection to the chondrocyte from applied forces and associated osmotic challenges, limiting cell deformation under normal physiological conditions [771, 800, 811]. How a chondrocyte measures and responds to mechanical load has been proposed by Poole et al., (1985) [26] to involve the primary cilium as a 'cybernetic probe', where the cilium senses the extracellular environment, and enables the cell to respond to physiological signals and biomechanical forces, thereby producing a functional territorial and interterritorial matrix.

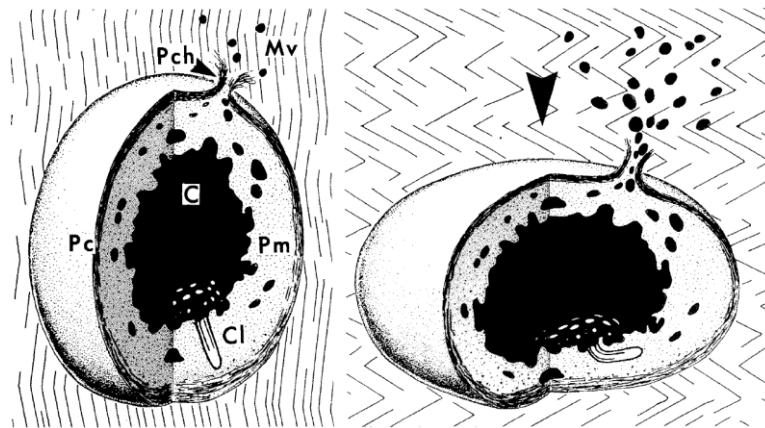


Figure 1.26: The Chondron: A conceptual diagram of the dynamic chondron microenvironment. The chondrocyte (C) and its primary cilium (Cl) is seen suspended within the pericellular matrix (Pm), encapsulated by the pericellular capsule (Pc), which has a pericellular channel (Pch) and matrix vesicles (Mv). Arrowhead indicates the direction of a matrix applied compressive force, which deforms the chondron, forcing mobile components out of the capsule into the surrounding territorial matrix. Note deflection of the primary cilium. Reproduced from Poole et al., (1988) [808].

1.84 Articular Cartilage Function

Cartilage functions as a viscoelastic matrix which provides a low friction surface allowing for movement, and also protects the underlying bone from mechanical impulses experienced from compressive shear, tensile forces and shock forces [456, 795, 814]. This is achieved through the high swelling tendency and low permeability of matrix proteoglycans, which are constrained by the collagen network [815]. The ability to deform is governed by the permeability of the hydrogel, which allows for the transmission and dissipation of load across the joint surface and the transmission of forces to the subchondral bone [788].

Compression of cartilage also results in shear stress, generating streaming potentials [817] by separating mobile cations (mainly Na^+ , Ca^{2+} and K^+) from the largely negatively fixed charge (SO_4^{2-}) of the matrix [818]. This results in a local osmolarity increase and decrease in pH [819]. The osmolarity of normal cartilage ranges between 350-450 milliOsm kg^{-1} , and with a pH between 6.6-6.9 (reviewed in Wilkins et al., (2000) [818]).

Under applied load, the deeper layers of the cartilage matrix deform, forcing water and low molecular weight solutes from around the proteoglycan components. Cessation of the applied force enables the displaced fluid to return to osmotic equilibrium [812]. The ability to successfully achieve this depends upon the unique interaction of the matrix components of collagen, proteoglycan and glycoproteins [769, 816, 820].

1.85 Cartilage Collagens

Collagen proteins represent the most abundant proteins in mammalian connective tissues [141, 769] and their fibres allow a plethora of connective tissues properties, spanning from the hard properties of bone to the flexibility of skin [821, 822]. Collagens belong to a ‘super-family’ of proteins whose genes are regulated to provide tissue specific expressions of fibrillar collagen, and comprise several subclasses [769]. Although the exact mechanism of genetic regulation of collagen composition remains unclear [823], a great deal is known about their chemical and physical properties [824-826]. For reviews of collagens, their synthesis and post-translational processing see Gelse et al., (2003) [827], Richard-Blum et al., (2011) [769] and Jalan et al., (2013) [825].

Mature cartilage principally consists of collagens of type II [828] (75% foetal, 90-95% adult [829]), together with and minor amounts of types III [830] (>10% adult) [829], VI [828, 829, 831, 832] (<1%) [829], IX [833, 834] (10% foetal, 1% adult [829, 835]), X [824] (hypertrophic cartilage only [828, 829]), XI (10% foetal, 3% adult) [829]. Lesser amounts of types XII, XIII (trans-membrane) and XIV [829] also contribute to the matrix.

Type II collagen is the most abundant collagen in cartilage and thus contributes most to the mechanical properties of the matrix [836]. Type II collagen fibres form around an inner core of type XI collagen, and sometimes occur externally decorated with type IX collagen, which auto-regulates type II fibre diameter [837], and is able to interact with the proteoglycan glycosaminoglycan (GAG) side chains [823, 838, 839]. Chondroitin and dermatan sulphate glycosaminoglycan side chains cross link to type II collagen, stabilising its structure [826]. Type III collagen associates with type II in the cartilage matrix [839], where it also binds von Willebrand factor [840].

Type VI collagen (1-3% [835]) mediates attachment of the chondrocyte to the pericellular matrix via integrin receptors, as well as hyaluronan [831, 841, 842], fibronectin [843], decorin [844], hyaluronan [842] and type II collagen [768, 838, 845]. Type VI is used as a marker to define the chondron microenvironment and identifies the chondron and bulk matrix [768, 799, 845].

Both type XI [846] and IX [847] interact and bind with glycosaminoglycan side chains. Type IX has a role in matrix stabilisation in association with fibronectin [848]. Type XI regulates collagen fibre and proteoglycan interactions making up 1-2% of the total collagen present in articular cartilage [849] where it is predominant in the chondron capsule and matrix [831]. Type X collagen is involved in the calcified cartilage zone [824].

1.86 Cartilage Glycosaminoglycans (GAGs)

The most significant glycosaminoglycans in hyaline cartilage are chondroitin sulphate (CS) [850], keratan sulphate (KS) [782, 851] and hyaluronic acid (HA) [852], all formed from unbranched long chain polysaccharides [770] (Figure 1.27). Chondroitin sulphate consists of repeating polymerised disaccharides composed of a hexose sugar, D-glucuronic acid and N-acetyl-D-galactosamine sulphation sites [850], while keratan sulphate consists of galactose and N-acetylglucosamine [782, 850]. Chondroitin and keratan sulphates are synthesised in the Golgi where they are covalently bound to a proteoglycan core protein and then sulphated prior to secretion. Post translational modification through the Golgi apparatus renders these as highly anionic polymers [853, 854] (see Figure 1.28). Hyaluronic acid is uniquely synthesised at the cell membrane, consisting of non-sulphated disaccharides of glucuronic acid and N-acetylglucosamine [772, 853, 855].

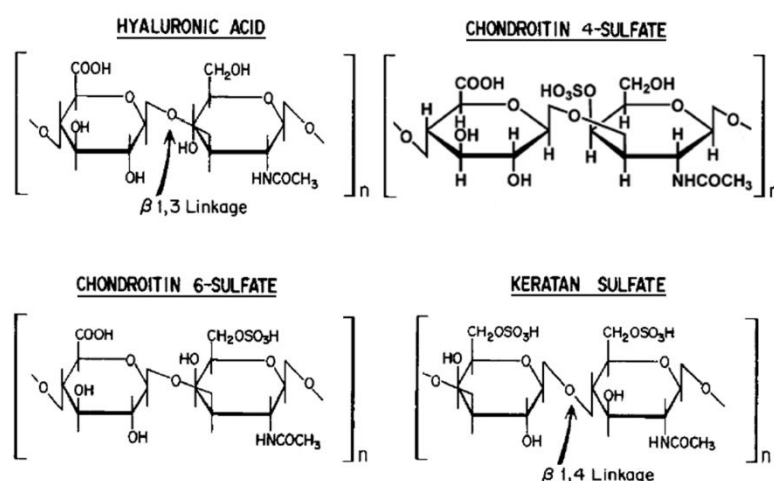


Figure 1.27 Disaccharide components of hyaluronic acid, chondroitin-4, -6, and keratan sulphates. Modified from Silbert et al., (1995) [772] and Oelker et al., (2008)[856].

1.87 Cartilage Proteoglycan Core Proteins and Glycoproteins

Proteoglycans are classified according to the leucine repeats present in their core proteins [787, 790] and exhibit a wide variety of molecular shapes and weights, resulting in their diverse structural and adhesive properties [773, 857-859]. The primary proteoglycan in cartilage, aggrecan consists of a protein core with highly charged modifiable glycosaminoglycan side-chains of chondroitin sulphate and keratan sulphate [802, 860] (Figs 1.27-1.29).

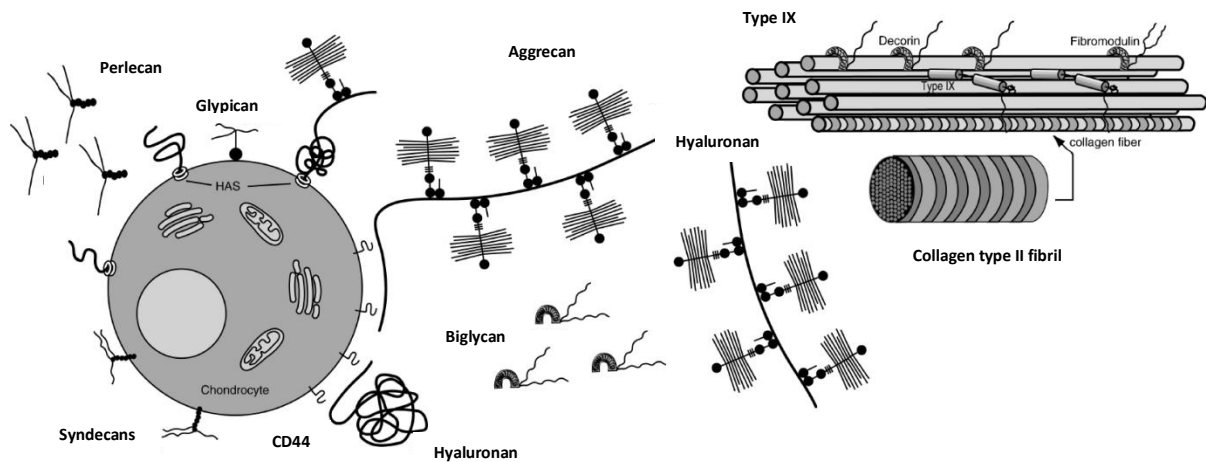


Figure 1.28 Cartilage Proteoglycans: Aggrecan represents the largest proteoglycan contributor in cartilage, binding to hyaluronan on the cell surface and within the matrix. Hyaluronan is produced at the cell membrane by hyaluronan synthase (HAS) where it acts as a binding site for aggrecan and can also interact with the CD44 receptor. Syndecans and glypican associate with the cell membrane, while fibromodulin, decorin, and type IX collagen interact with, and bind to collagen fibrils (of types II, IX and XI). Perlecan and biglycan are also present but their role is less well defined. Reproduced and modified with permission from Knudson et al., (2001) [862].

1.88 Aggrecan

Aggrecan is a high molecular weight protein which forms a multi-domain structure contributing 80-90% of the proteoglycan content of cartilage [835, 863, 864]. Alternative splicing sites add to aggrecan core protein variability [863]. Up to 150 chondroitin and keratan sulphate GAG chains can be attached [860, 865] to the protein core, each consisting of lengths up to 1000 disaccharide units [819]. Aggrecan assembles around a central fibre of hyaluronic acid, with up to 800 aggrecans [866] tethered via Link protein [867], contributing to the high GAG mass (87% CS, 6% KS and 7% protein [838]) [860] (Figure 1.29). The aggrecan domain possesses a hyaluronan binding site (the G1 domain interacts with hyaluronan acid and the Link protein [860, 865], see Figure 1.29). Once secreted by the Golgi, aggrecan undergoes post secretion maturation, altering its binding and physical properties. It can then diffuse from the chondron into the territorial matrix, where it may be subsequently modified [860, 868], reprocessed or lost through diffusion [860, 869, 870].

Proteoglycans are strongly hydrophilic, and their primary function in cartilage is thought to be to bind and retain water, providing the unique shock absorbing and lubricating properties of connective tissue. They are also vital for the formation, maintenance and functional support of chondrocytes within the pericellular microenvironment [835, 860]. Aggrecan is the predominant aggregating proteoglycan in cartilage, with minor amounts of versican, perlecan, aggrecan, syndecan, decorin, fibromodulin, biglycan and lumican. Cartilage glycoproteins include fibronectin, laminin, glypican, and tenascin [835, 861, 862, 838, 871, 872]. Cartilage contains only minor amounts of glycoproteins, where it is proposed that they function in matrix regulation [836, 872]. Proteoglycans decrease in size with age, and the glycosaminoglycan keratin sulphate content increases, while chondroitin sulphate respectively decreases [873, 874].

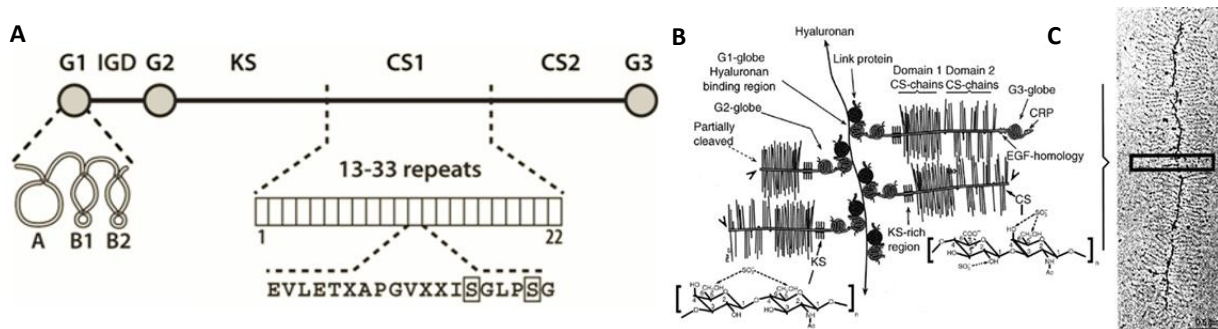


Figure 1.29 The Proteoglycan Aggrecan: [A] The aggrecan core protein consists of three globular domains (G1-G3), an interglobular domain (IGD), and spanning domains G1 and G2. Globular domain G1 may interact with link protein (A) or bind to hyaluronan (B1-B2), while the IGD region contains two main targets of cleavage enzymes. Beyond the G2 domain there are attachment sites for keratan sulphate (KS), chondroitin (CS1-2), while the G3 region contains an epidermal growth factor (EGF) like-domain, and a carbohydrate recognition domain [860]. Reproduced with permission from Roughley (2006) [875]. [B] Aggrecan core proteins (with their many variable glycosaminoglycan chains of chondroitin and keratan sulphate) are connected via Link protein to a central fibre of hyaluronan [860]. [C] An electron micrograph (scale bar 0.5 μm) detailing the aggregate structure of aggrecan. Modified from Lu et al., (2008) [456].

1.89 Synthesis of Extracellular Matrix: Proteoglycans, GAGs and Collagen

The Golgi apparatus acts as a shuttling centre in the secretory pathway, where proteins and lipids synthesised in the endoplasmic reticulum are sorted, post-translationally modified by families of specialist enzymes [141] and exported to their targeted destinations. Proteoglycan core proteins are sequentially assembled by specific transferases for the covalent addition of GAG components (reviewed in Prydz et al., (2000) [854]) and then undergo sulphation and increased charge density prior to export [141, 695, 772, 876-878]. Chondroitin sulphate attachment and synthesis upon proteoglycans occurs in the *medial* and *trans*-compartments [879] (see Figure 1.30) and involves at least 200 distinct glycotransferases and other enzymes [141, 693]. For a review of Golgi proteins involved in transport, signalling and tethering see Kümmel et al., (2011) [880], and on the sub-compartment organisation for N-glycan enzyme processes Schoberer et al., (2011) [881].

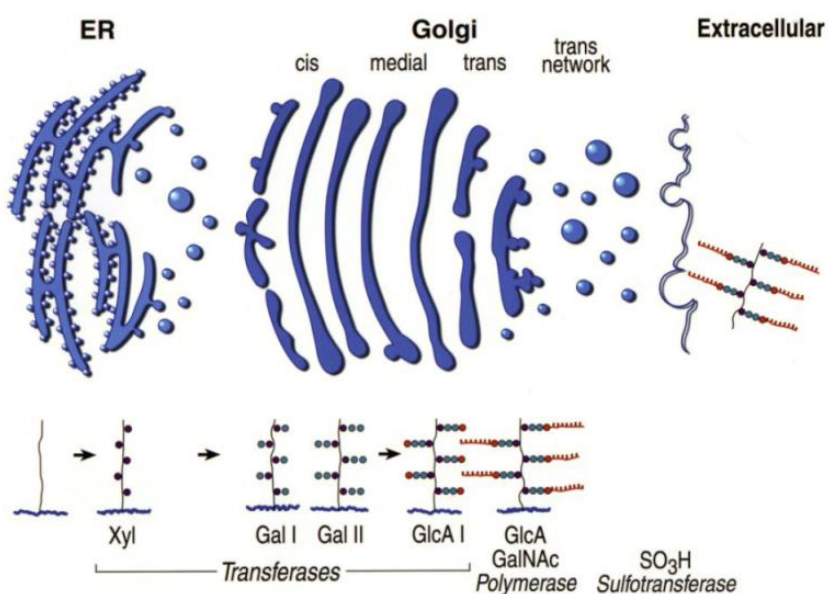


Figure 1.30 The Golgi Apparatus: The biosynthesis of GAGs that occurs in the Golgi apparatus allows for post-translational modification of endoplasmic reticulum (ER) derived matrix proteins through transferases, polymerases and finally sulphation, before packaging and exocytosis to the extracellular domain. Reproduced with permission from Silbert et al., (2002) [882]. Compartmentalisation of the Golgi into the *cis*, *medial* and *trans*-cisternal compartments allows for contained post-translational sequential enzymatic processes and sorting [141].

Collagen fibres consist of micro-fibrils composed of repeating specific amino acids of glycine, proline, hydroxyproline and arginine with a sequence pattern of Gly-Pro-X or Gly-X-Hyp (where X represents other amino acid residues). Peptide chains are synthesised upon the endoplasmic reticulum, where they undergo hydroxylation of lysine and proline amino acids, and glycosylation of specific hydroxylysine residues prior to formation of pro-collagens from pro- α chains (defined by three parallel left-handed helical coils) which are then transferred to the Golgi (see Figure 1.31) [141, 827]. The Golgi post-translationally modifies pro-collagens, arranging them into cylindrical membrane bound distensions, which are released from the *trans*-saccules to form secretory granules for export [141, 691]. Upon secretion into the extracellular microenvironment, pro-collagen is cleaved by peptidase to form tropocollagen, which self-assembles into collagen fibrils, these in turn aggregating to form larger collagen fibres [141, 883].

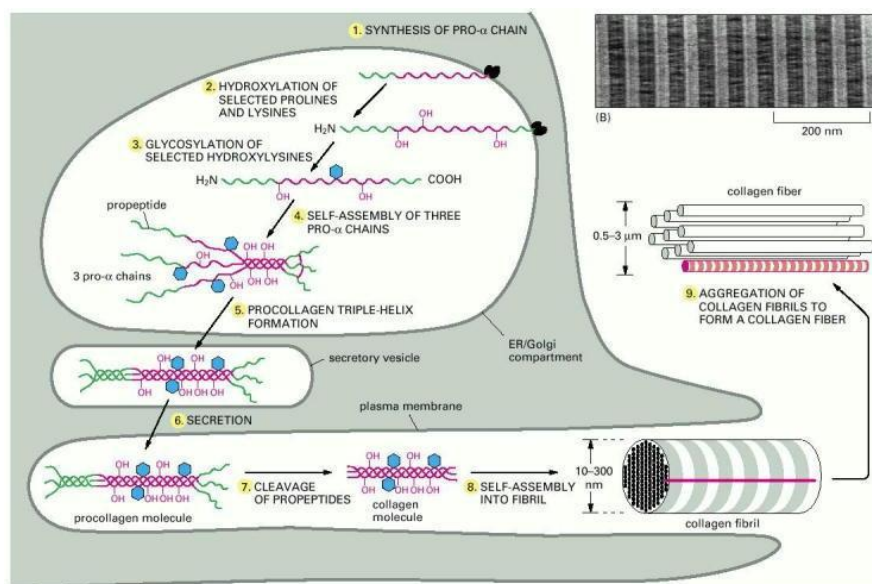


Figure 1.31 Synthesis and Formation of Collagen: (1) Synthesis of the pro- α chain in the endoplasmic reticulum (ER) results in its transport to the Golgi apparatus for the sequential hydroxylation (2) and glycosylation (3) for the formation of triple helix based pro-collagen (4, 5), which is then packaged for secretion (6), where upon peptide cleavage (7) it self-assembles into fibrils (8) which aggregate to form large collagen fibres (9). Reproduced with permission from Alberts et al., (1983) [141].

1.90 Binding the Matrix to the Cell Membrane

Cartilage is a tensegritous matrix that allows for the transmission of mechanical forces of applied load, to the cell and cytoskeleton, where the resultant stress is detected by matrix receptors [143, 153, 154, 457, 884, 886]. Each chondrocyte is enveloped in a specialised microenvironment of structured matrix macro-molecules which adhere to the cell membrane through families of specialist receptors [769, 862]. Some of these allow for the coupling of mechanical forces to the cell (Figure 1.32), while other receptor complexes are involved in the transduction of bio-chemical signals [153, 771, 886, 895].

Families of cell specific membrane receptors are responsible for the transduction of a wide spectrum of extracellular signals originating from the extracellular environment. These also have roles in adhesion to extracellular matrix for homeostasis and development [885-888]. They include

integrins [889], G-coupled proteins [353], CD44 [890], purinergic receptors [891], tyrosine and histidine kinases [348, 892], toll-like receptors [893], and intracellular receptors [894] that are closely associated with secondary messengers. Activators of cellular response pathways include such secondary messengers as cyclic adenosine monophosphate (cAMP) [445], Ca^{2+} [895] and the inositol triphosphate/diacylglycerol (IP3/DAG) pathway [782, 896], while extracellular signalling by receptor tyrosine kinases, integrins and ion channels results in activation of intracellular kinase/mitogen-activated protein kinase (ERK/MAPK) pathway [782, 897-900]. The chondrocyte cell membrane contains a rich ‘channel-ome’ of receptors and ion channels reviewed by Barrett-Jolley et al., (2010) [901].

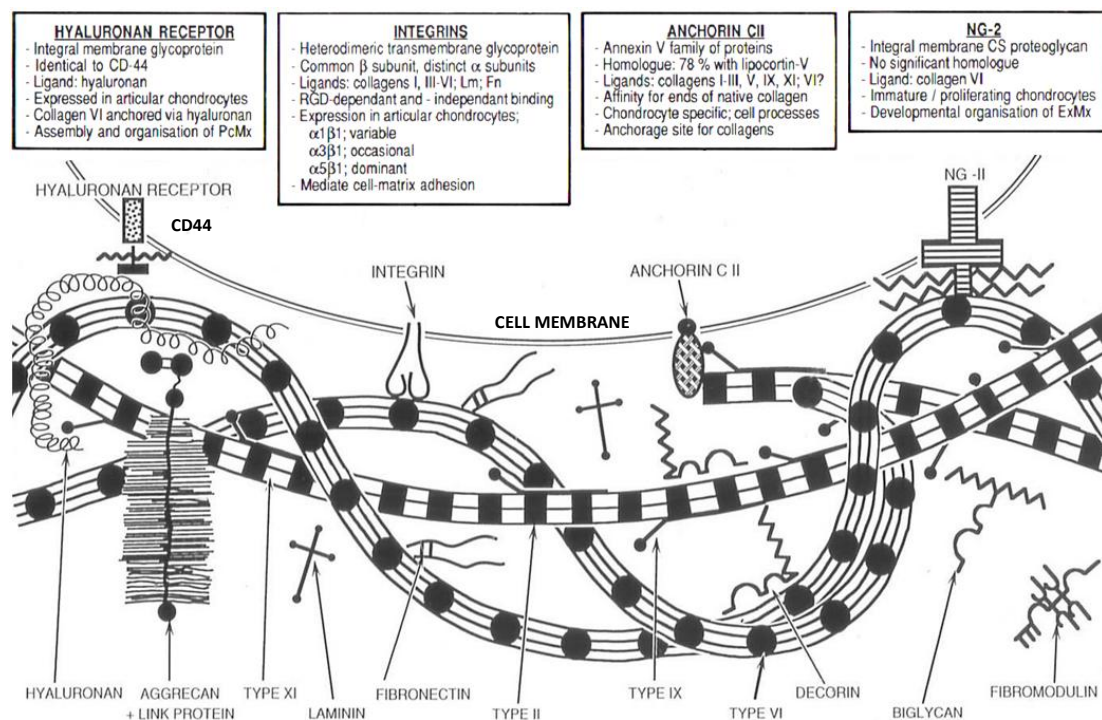


Figure 1.32 Chondrocyte Matrix Membrane Adhesion Receptors: Artistic visualisation of interactions between pericellular matrix components and the chondrocyte cell membranes. Matrix adhesion occurs through the hyaluronan receptor CD44, integrin, anchorin and NG-2. CD44 involves two chondroitin/heparin sulphate side chains which mediate hyaluronan binding of collagen type VI, which can in turn anchor collagens, proteoglycans and glycoproteins (see Figure 1.28). Integrins may bind directly to collagen type VI or through matrix molecules. Anchorin-CII binds collagen type II (which binds to type VI by its globular domain), while the NG2 receptor binds collagen type VI. Type XI collagen forms the core of type II collagen fibres, whose surface exhibits decorations of type IX collagen. Modified from Poole et al., (1992) [831].

1.91 Chondrocyte Matrix-Coupled Receptors

Integrin structure, interaction and activation has been reviewed by Campbell et al., (2011) [902]. Integrins interact with cartilage matrix proteins of collagens of types II, III, VI and XI, as well as fibronectin (which binds to $\alpha 5\beta 1$, $\alpha 1\beta 1$ and $\alpha v\beta 3$ [903, 904]) and laminin ($\alpha 3\beta 1$, $\alpha 6\beta 1$, $\alpha 7\beta 1$ and $\alpha 6\beta 1$ [905]), allowing for the physical coupling and the transmission of biomechanical impulses [769, 819, 904]. Type II collagen is known to bind to the cell via integrins $\alpha 2\beta 1$ [904] and $\alpha 10\beta 1$ [906], type III by $\alpha 1\beta 1$ and $\alpha 2\beta 1$ [906], type VI by $\alpha 1\beta 1$, $\alpha 10\beta 1$ [897] and $\alpha 3\beta 1$ [907] integrins. Type VI collagen also interacts with the neuron-glia-antigen-2 (NG2) proteoglycan receptor [907, 908], CD44

[909] and anchorin-CII (annexin-V via type II) [831]. NG2, $\alpha 3\beta 1$ integrin and Galectin-3 are reported to form a complex on the cell surface [910], with Galectin-3 reported to regulate $\alpha 2\beta 1$ -mediated adhesion to collagen IV [911]. Anchorin-CII also binds selectively to collagens types II and X [912]. CD44 interacts with collagen type VI (binding through hyaluronic acid) [831, 862] and it also binds aggrecan [862].

Versican is known to bind to hyaluronan and tenascin (which binds to decorin [913]), is involved with receptors CD44, $\beta 1$ -integrin and also contains an epidermal growth factor domain [914]. Syndecan binds to collagen type III, fibronectin and tenascin [807]. Decorin binds to type VI collagen [844], and is an antagonist of the epidermal growth factor receptor (EGFR) [915]. Biglycan interacts with type II collagen and BMP growth factors [916, 917], while glypican is involved with the Sonic Hedgehog (Shh) signalling pathway [416].

1.92 Cartilage Biomechanics: The Chondrocyte Microenvironment

Physiological compressive forces applied to cartilage are normally uni-directional, causing the normally spherical chondrons to deform laterally into oblate spheroid shapes. Proteoglycans are limited in their hydration to about 20% of their swelling potential by the collagen network. When load is applied, elastic deformation results in water loss from proteoglycans within the zone of deformation, which equilibrates when the change in osmotic pressure balances the applied load. Upon the cessation of load, this osmotic differential results in fluid restoration and recovery from the cartilage deformation [768]. Normal load bearing activities within cartilage may result in hydrostatic pressures ranging from 100-200 atmospheres (10-20 MPa) [810, 813] over millisecond time periods [819] during cartilage matrix deformation. Extreme sustained loads of between 15-20 MPa in bovine cartilage have been shown to disrupt collagen fibres and result in death of the enclosed chondrocytes [918]. However, apoptosis may be induced following pressures as low as 4.5 MPa [919], and collagen degradation may occur between 7-12 MPa [774, 919]. Degradation of matrix plays a key role in the progressive wearing of articular surfaces, resulting in the degenerative changes associated with osteoarthritis [365, 585, 774, 819, 919-920].

Chapter Two: Methods

2.0 *Overview*

The premise of electron microscopy is to adequately fix biological materials, to provide heavy metal contrast, process into resin, cure and section so as to examine thin slices of the preserved structure in vacuum with the use of transmitted electrons to generate images.

The ability to resolve structures is dependent upon the uptake of stain, and the resilience and preservation of delicate structures through a number of extreme chemical processes. As such, artefacts may be introduced at any stage of the process, raising the question as to how much of any structure retains its true form after processing, dehydration and embedding [921]. However, with careful attention to details and implementing appropriate strategies, one may expect to achieve a compromise, especially in cartilage. This has been achieved with the use of 'Ruthenium Red', which provides superior staining, and is also believed to reduce artefact formation through stabilisation of membrane structures.

2.10 *Introduction: Electron Tomography and Primary Cilia*

Electron Tomography (ET) is a technique for visualising cellular organelles and supra-molecular complexes at high resolution [922-928]. It entails the collection of a series of digital images at different known angular tilts ($\pm 70^\circ$) from a three dimensional specimen (200-450 nm thick) in a transmission electron microscope (TEM). Image projections are then processed to produce a tomogram which represents a three dimensional reconstruction of the object [929-933]. This method is analogous to modern medical tomography imaging technologies and is ideally suited for reproducing high resolution images otherwise unobtainable with conventional ultrathin TEM. In this study, a model connective tissue preparation was used to image chondrocyte primary cilia by ET, which generated tomograms with an average resolution of 1.2 nm (Figure 2.1).

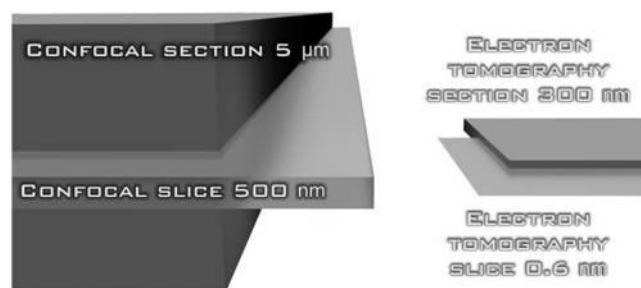


Figure 2.1 Imaging Resolution of Electron Tomography compared with Confocal Microscopy: Comparison of available 'slice' resolutions between light microscopy and electron tomography. Ultrathin (100 nm) and semithick (350 nm) sections are utilised for electron microscopy and tomography respectively. Reproduced and modified with permission from Dr Harland [934].

2.11 *Connective Tissue Models*

Chick embryo sternal cartilage and flexor tendon have previously served as connective tissue models to study primary cilia structure and function under both compressive and tensile loads [25,

26]. In this study it was found that tendon was extremely difficult to section reliably and cilia, when identified, were almost always acutely deflected and / or projecting out of the plane of section. Sternal cartilage was therefore chosen as the 'model connective tissue' with the chondrocyte as the model cell, both *in vivo* and *in vitro*.

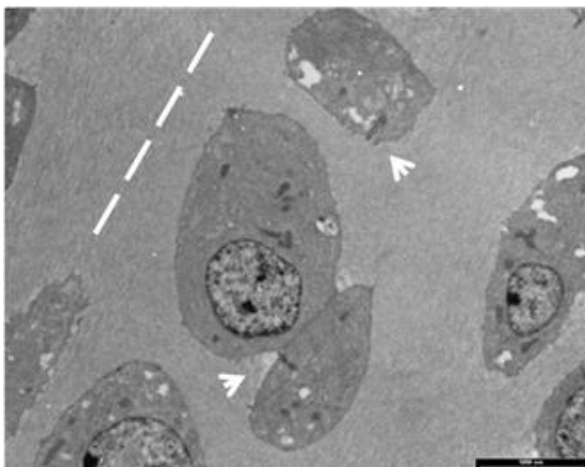
2.12 Embryonic Chick Sternal Cartilage: A Model Tissue

Embryonic sternal cartilage was chosen as a model tissue for a number of reasons. The three cartilage vanes of the chick embryo sterna were easy to dissect, prepare, fix and embed for electron microscopy. The presence of low cell numbers and a developing matrix allowed for smooth sectioning, providing excellent contrast and little obstruction for viewing between the extracellular matrix and the chondrocyte. Chondrocyte cilia appeared to be shorter and less deflected in their projections than those of other connective tissues, making chick embryonic sternal cartilage an ideal tissue model to investigate the relationship between the extracellular matrix, the primary cilium, cytoskeleton and the Golgi apparatus [97].

2.13 Chick Embryo Cartilage Fixation: *in vivo*

Chick embryo sternal cartilage was harvested after 15 days incubation at 39°C, and cut into 1 mm³ pieces for embedding (producing tri-lateral segments). They were fixed in 2.5% glutaraldehyde with 1600 ppm Ruthenium hexamine tri-chloride (RHT) for 16 hours at 37°C and post-fixed in 1% osmium tetroxide (OsO₄) with 1600 ppm RHT at 4 °C for 4 hours, followed by *en bloc* 4% uranyl acetate for 2 hours in 50% ethanol. RHT, commonly known as 'Ruthenium red', was used to complement the fixation of cartilage and to stabilise proteoglycan and glycoprotein in the extracellular matrix. Samples were stained with RHT, as previously described [26, 935-937], and semithick sections examined for staining quality (Figure 2.2).

Applications of cryogenic preservation techniques have demonstrated chondrocytes in their near 'native state' [938-943]. Hunziker et al., (1987) [939] indicated that this resulted in retention of extracellular matrix proteoglycans, although there was some migration of proteoglycan. Thus, the preservation and preparation of chondrocyte extracellular matrix for tomography through chemical or



cryogenic techniques represents a trade off in performance of available fixation strategies. With the need to find chondrocyte primary cilia by large scale serial sectioning, conventional resin processing was favoured over more complex and intricate cryogenic strategies.

Figure 2.2 Chick Embryo Cartilage: A semithick section of chick embryo sternal cartilage detailing the extracellular matrix, chondrocytes and their primary cilia. Axis of tissue indicated by dashed line, and the presence of primary cilia by arrowheads.

2.14 Chondrocyte Cell Culture: *in vitro*

Wild-type postnatal ovine chondrocytes were obtained from an ethically approved (AEC 88/07) cryogenic Bio-bank. Cells had been cryogenically preserved at a concentration of 1×10^6 cells/ml, with Advanced Dulbeccos' Modified Eagle Medium (aDMEM)/20% Foetal Calf Serum (FCS) (Invitrogen, New Zealand)/20% Di-Methyl-Sulphoxide (DMSO) for cryo-protection and stored in liquid nitrogen (-195°C) [941-943]. Reanimated cryotubes were thawed in a 37°C water-bath, wiped with ethanol, and washed in a 15 ml Fisher Falcon tube with aDMEM/Penicillin-Streptomycin-Glutamine (PSG). After centrifuging at 600g for 5 minutes, cells were resuspended in 100 μl of aDMEM and 2 μl extracted for cell counting and determination of cell viability using trypan blue exclusion. Primary cell lines were cultured in aDMEM with 1% PSG and 5% FCS. Cells were transferred to T75 flasks for culture (seeded with 200,000 viable cells) to expand cell numbers and plated upon 13 mm diameter ThermanoxTM or glass cover-slips (Thermo Scientific, USA), which were placed in 24 well plates and incubated at $37^\circ\text{C}/5\% \text{CO}_2$. Once at 80% confluence, they were 'serum starved' (aDMEM/PSG without FCS) for 3 days prior to fixation. This increases expression of primary cilia, which project down onto, and become aligned in parallel with, the substrate [31, 944] (Figure 2.3).



Figure 2.3 Cell Culture: Confluent serum starved chondrocytes prior to fixation, 40 \times magnification.

2.15 Fixation of Cultured Cells

Chondrocytes were grown upon Thermanox or glass cover-slips and subsequently processed through a variety of methods in line with several established protocols [26, 945-947]. A number of experimental variations were explored for their suitability for optimising the detection of primary cilia. After several trials the following protocol was adopted. Cells on cover-slips were fixed in 2% glutaraldehyde at 37°C , post-fixed in 1% OsO_4 with 1600 ppm RHT or 1% uranyl acetate *en bloc*, followed by dehydration through a progressive series of graded ethanol concentrations. After transfer to propylene oxide, samples were embedded in EMBED-812 resin and left to polymerise on a small resin chip at 60°C for 24 hours. Cover-slips were placed in specially designed Teflon holding canisters for processing. Thermanox was removed by heating on a hot plate or cooling in dry ice or

liquid nitrogen and then peeling it off. Glass cover-slips were removed by thermal shock, or by hydrofluoric acid, leaving the substrate side containing cells exposed at the resin surface for sectioning.

2.20 Fixation, Osmification, Ruthenium Red (RHT) and Artefacts

Fixation by glutaraldehyde primarily cross-links protein amino acids and deforms the α -helix structure, although it does cross-react to some degree with lipids, some carbohydrates and nucleic acids [948]. The large molecular size of glutaraldehyde results in a rate of penetration of less than 1 mm per hour into tissues [949]. Optimal fixation for tissues and cell cultures requires a constant temperature to avoid microtubule depolymerisation. OsO_4 is itself a microtubule destabilising agent and potent oxidiser [949-951]. It directly embeds into membranes due to reactions with phospholipids, preventing their coagulation during dehydration, and also serves as a heavy metal stain [950, 951]. It is believed that in fixed tissue, OsO_4 is initially covalently bound in both hexavalent and tetravalent states, but upon dehydration and embedding it forms a black dioxide of OsO_2 [952]. During dehydration, alcohol and propylene oxide further denature proteins and may cause further chemical modifications. Much attention has been paid to the roles of these solvents in creating secondary artefacts, in particular interactions with membranes, generating vesicle structures from free lipids [945]. Loqman et al., (2010) [946] demonstrated that adjusting fixative solutions to closely match the native extracellular osmotic pressure abolished a number of presumed artefacts and cell shrinkage arising from unmatched preparation. This osmotic protection extended to the use of RHT, which was shown to reduce artefacts, but samples still experienced some shrinkage effects. It is believed that RHT acts to stabilise cell membranes, reducing artefact formation, thus aiding in preserving structure during fixation.

2.21 Fixation with Ruthenium Complexes

Ruthenium hexa-amine-trichloride (RHT), or ammoniated Ruthenium oxy-chloride $[(\text{NH}_3)_5\text{Ru}-\text{O}-\text{Ru}(\text{NH}_3)_4-\text{O}-\text{Ru}(\text{NH}_3)_5]^{6+}$, commonly known as 'Ruthenium Red' (Mangin (1890) [947], prepared according to Fletcher et al., (1961) [953]), is a Platinum Group hexavalent inorganic dye (Figure 2.4). Originally used as an optical stain and cationic tracer, in combination with OsO_4 it has been extensively applied in electron microscopy. RHT has a relatively high molecular weight (858.5), a high charge density, and is opaque to electrons [935]. It exists in an ammoniated oxy-chloride complex of estimated volume of 0.762 nm^3 with an interpreted diameter of 1.13 nm [935, 954-956]. Theoretically, its small size allows for passing through some pores, but not coherent membranes, while its strong cationic charge lets it associate selectively with negatively charged structures and poly-anionic substances [957]. This is due to the close intercalation ability of RHT to electrostatically bind with interaction sites, where it may also facilitate catalytic electron transfer with substrate molecules.

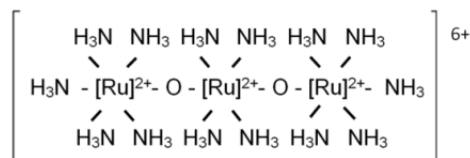


Figure 2.4 Ruthenium Hexa-amine-Trichloride: A proposed structure of the Ruthenium cation complex [958], $[(\text{NH}_3)_5\text{Ru}-\text{O}-\text{Ru}-(\text{NH}_3)_4-\text{O}-\text{Ru}(\text{NH}_3)_5]\text{Cl}_6$.

Ruthenium red has been used extensively as an electron-dense stain for muco-polysaccharides, glycoproteins and extracellular matrix components [935, 936, 954, 959-961]. Optimal results have been obtained by the inclusion of RHT with glutaraldehyde fixative, followed by a combination of RHT with OsO_4 prior to tissue osmication [935, 959-961]. RHT exists in equilibrium as a number of complex species (Ruthenium brown, red and violet cations), which also bind to anionic glycosaminoglycans and polysaccharide structures within tissues [935].

It is believed that ‘Ruthenium red’ is oxidised to ‘Ruthenium brown’ by OsO_4 , which is then available to oxidise polysaccharides (to which it is bound), reverting in the process back into ‘Ruthenium red’. This allows the process to be repeated at the reaction site, and also forms the insoluble electron opaque osmium dioxide (OsO_2) by-product. This mode of action allows for the deposition of multiple molecules of osmium oxide per saccharide interaction, but it only occurs in the presence of RHT [935, 936].

Many authors have reported variable results with RHT, which could reflect subtle variances in preparation techniques [936, 963]. Luft (1971) [936] indicated that the intracellular space was inaccessible to RHT penetration, although results could be indeterminate and controversial in this regard [960]. He also mentioned a number of exceptions, namely the nuclei of chondrocytes and oral epithelial cells, as well as mast cell granules, which have readily taken up the dye [936]. This effect appears to be due to the settling time of the RHT- OsO_4 mix prior to use, where it is believed OsO_4 generates Ruthenium coupled reactions resulting in enhanced cellular penetration. The effectiveness of the staining, as noted by Luft (1971) [936] and Hagiwara et al., (1992) [961], is of such density that further post-staining is unnecessary, as the effect is even optically visible in samples. In the present work, RHT together with OsO_4 , gave superior fine resolution imaging.

2.22 *Fixation of Extracellular Matrix Proteoglycans*

Glycosaminoglycans and muco-polyaccharide proteoglycans are not adequately fixed by treatments of glutaraldehyde or osmium tetroxide, resulting in loss of much of their respective vital structures during the process of dehydration and embedding. Hence, to accurately study extracellular matrices, one is faced with the problems of preventing not only artefact formation, but also fixing, retaining and staining members of extracellular matrix components. RHT is one of the most widely used dyes for localising proteoglycans [962], and, when used in combination with glutaraldehyde and OsO_4 , provides excellent stabilisation, staining and contrast of matrix components in cartilage [959,

961, 964-970]. This stabilising effect prevents degradation and loss of proteoglycans and carbohydrates during chemical fixation and processing, allowing preservation of their spatial structure for resin embedding. It is believed that chemically fixed ‘matrix granules’ (which are observed in the electron microscope) are precipitates of stained proteoglycans which have become condensed through the combined effects of the cationic dye and the dehydration process [966, 967]. Hunziker et al. (1981) [959] noted the presence of matrix granules after OsO₄/RHT treatment which produced repeatable superior results for preservation of cell membrane components and pericellular matrix proteoglycans. Other authors have noted improved ultra-structural cartilage fixation and prevention of proteoglycan loss during fixation using an RHT/OsO₄ combination [960, 966, 968-970]. Loqman et al., (2010) [946] and Swan et al., (1999) [971] have shown that careful attention to fixation strategies and osmolarity protection greatly reduced shrinkage issues and artefacts, resulting in improved overall preservation. Thus, although some matrix granule artefacts may result, RHT treatment preserves structures with which it interacts and represents the stain of choice for highlighting interactions between the matrix and cilia in chondrocytes [25, 26].

2.30 Serial Sectioning and Detection of Primary Cilia

Resin blocks were sectioned on a Reichert Ultra-Microtome E (Reichert, Austria) yielding a selection of candidate cilia which were completely contained within the semithick sections (350-550 nm) and therefore suitable for electron tomography. Sections were held together with improvised glue (formvar solution with dissolved Sellotape glue spray) before placement upon formvar-coated parallel slot copper electron microscope grids. Cell culture samples were cut into pieces to be mounted upon resin stubs for *en face* serial sectioning as above. Ultrathin sections were post-stained with 2 % uranyl acetate and 1 % lead citrate using the automated LKB 2168 Ultrastain grid stainer (LKB-Produkter AB, Bromma, Sweden, 1985).

Sternal chondrocytes were easier to serially section than tendon, and repeatedly produced excellent uniform ribbons (Figure 3.2A). During embedding sternal tissue sections were arranged in a known orientation with respect to the tri-lateral orientation of the cartilage, with blocks then being sectioned perpendicular to this. Mounting of serial ribbons onto parallel slot grids allowed for inspection in the direction of sectioning, for the identification of candidate cilia (Figure 3.2 A and B, arrows).

2.31 Semithick Sectioning of Sternal Cartilage

As a model connective tissue, sternal cartilage exhibits a low cell density ($2-5 \times 10^5$ cells/mm³ [28]), so that the probability of encountering a complete cilium within the plane of a semithick (350 nm) section is low. This is partially compensated for by chondrocytes usually having shorter cilia in comparison to other cell types [365, 972], thus increasing the odds of finding complete aligned cilia. The chance of obtaining a primary cilium fully aligned in the plane of an ultrathin (100 nm) section is

low [973], but increases proportionally with thickness. However, TEM imaging quality decreases with increasing specimen thickness, which is exaggerated at high tilt angles during tomography, influencing imaging data quality. Thus, the choice of section thickness represents a trade-off between cutting a section thick enough to contain a cilium, but thin enough to retain imaging quality, especially at high tilt angles [975]. In reality cilia are always to some degree bent in their projection within the matrix, complicating the search for candidate samples of aligned cilia suitable for tomography [25, 26, 100]. Since serial sectioning of chondrocyte connective tissue resulted in a low incidence of cilia in their longitudinal axis [973] due to their *pseudo random* projection within the matrix [31, 100, 973, 974], it became necessary to investigate cell culture techniques to increase the incidence of candidate cilia.

2.32 Tomography of Monolayer Cell Culture: Aligning Cilia With The Substrate

Analysis of primary cilia in cell culture has been aided by the observation that in many cells the cilia are aligned with the substrate [31, 63, 976] (Figure 2.5). It has been observed during cell culture that cell cycle arrest, through ‘serum starvation’ [986] increases the interphase expression of primary cilia [120, 977, 978, 985]. Albrecht-Buehler (1977) [979] examined large numbers of cells in culture and found that of their primary cilia, 73% ran parallel with the basement substrate whilst the other 27% were oriented apically upwards. Vorobjev et al., (1980) [980] examined 11 interphase cells, in which cilia were aligned not less than 75 degrees to the substrate ($P < 0.00125$), however this was not observed during G2-phase or mitosis [63].

An *in vitro* preparation represents a significant improvement in the incidence of usable cilia per section over *in situ* sectioning. The precise mechanisms by which chondrocytes cilia become aligned with the substrate presently remains unknown, however it is most likely due to a combination of a number of effects ranging from loss of micro-environment to culture media, and involving planar cell polarity and cytoskeletal rearrangement [981, 982]. Wheatley et al., (2000) [983] reported the presence of 5% bi-ciliated (and some multi-) ciliated centrosomes of cells in culture. It has been shown de-differentiation occurs during monolayer cell cultivation of chondrocytes [984], with Alieva et al., (2004) [985] indicating that unreliable data could result, as primary cilia *in vitro* may not be functioning correctly, since the cell is not in its native environment [986].

The application of cell culture allowed for the easy and accurate investigation of the proximal centriole with respect to the basal body, which was previously difficult to establish *in situ*. The correct polarisation of the orthogonal arrangement of the diplosomal centrioles has resulted in confusion within the literature, as many illustrations of them have been either vague or inaccurate [94].

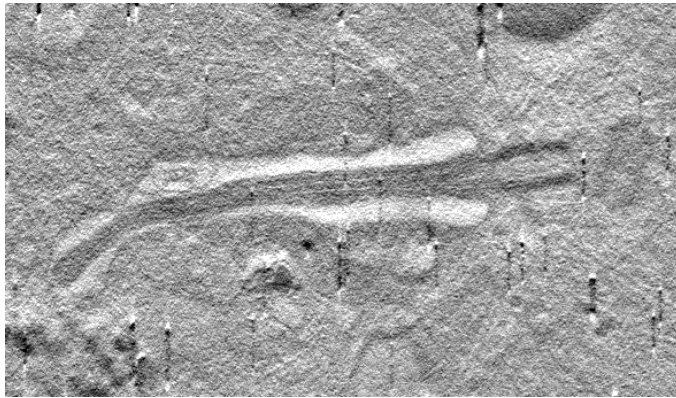


Figure 2.5 Tomography of a Primary Cilium Aligned with the Substrate: A tomogram optical section of an ovine chondrocyte in culture. The cilium is located beneath the cell, in a juxta-nuclear position, and is surrounded by a unique membrane encapsulate bound by the substrate. Centrosomal microtubules are aligned in a lateral radiating 'fan out' pattern, notably from the basal body, while the proximal centriole is seen tethered closely nearby.

2.40 *Investigative Electron Microscopy*

Investigative microscopy of semithick serial sections for candidate cilia was carried out using low voltage microscopy (100 kV on a Philips 410 with a LaB₆ filament) at low beam currents to prevent aging and damage to the resin. Detailed, image based maps of each electron microscope grid were constructed to aid in the re-identification of suitable cilia for electron tomography. These maps noted the position of cilia with respect to the cells in the section, and their relative positions on the grid. Captured images of primary cilia were measured using ImageJ [987].

2.41 *Fiducial Marker Application*

For accurate tomography reconstruction, electron-dense fiducial markers were added to the section for tracking purposes (Figure 2.6). Grids containing suitable candidate sections for tomography were labelled with 15 nm gold fiducial markers (British Bio-Cell, UK). Adequate application upon both sides of the electron microscope grid is required for use as electro-optical markers. Due to differences in material properties between the formvar and the resin of the section surfaces, gold fiducial applications require longer settling times upon formvar (by a factor of 30) in order to acquire suitable coverage densities for tomography.

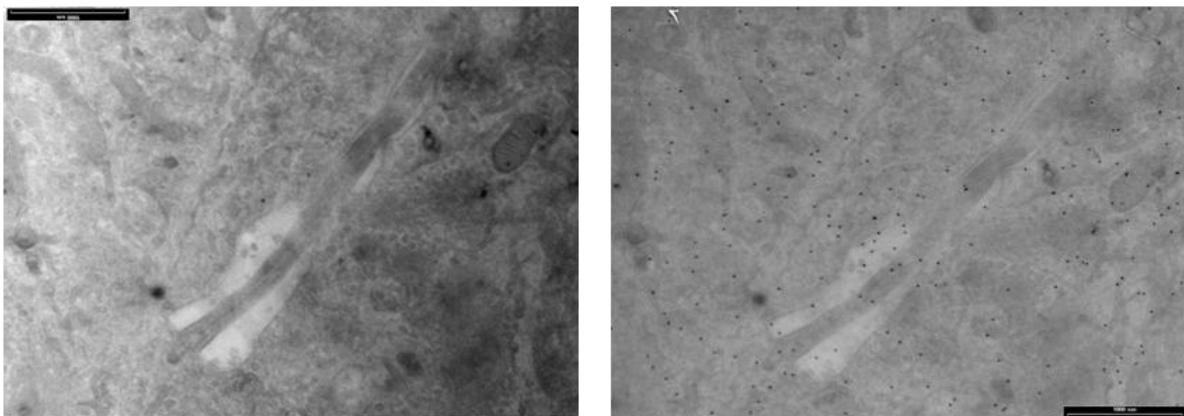


Figure 2.6 Fiducial Markers: Application of 15 nm gold markers upon a section containing a cultured chondrocyte primary cilium aligned in the direction of the substrate. Fiducial coverage aids in alignment and reconstruction of tilt series images. Scale bars 500 nm.

Fiducials were applied undiluted to the top (resin section) and bottom (formvar) sides of the electron microscope grid, for between 2-4 seconds, and 60 seconds respectively (rinsed off in distilled water) achieving a uniform distribution of 10-15 fiducials per square micron per side. Grids were inspected in a Philips 410 TEM to monitor application. Excess application of gold fiducials was found to make tomography impossible, as it ‘drowned out’ the signal to noise ratio of the images.

2.42 *Imaging Microscope*

Electron tomography was carried out at AgResearch Limited, Lincoln Research Centre, using a FEI Tecnai G² T30 300 kV transmission electron microscope (FEI Company, Oregon, USA) with a LaB₆ filament electron source. Single and dual axis tomography was undertaken at 300 kV, in a single axis tilted through $\pm 64.5^\circ$ at 1.5° increments. Images were collected with a Tietz camera (2048 by 2048 pixels, 12 bit). Not all specimens were suitable for dual axis tomography, as they were located in proximity to grid bars or close to the edge of sections Figure 3.2 (D- F). This sometimes resulted in occlusion of the image along one axis at higher tilt angles (Figure 3.2 E) or precluded imaging from contrast effects (Figure 3.2 F). During long data acquisition periods under the beam, electron heating aged the samples, leading to structural changes affecting the ability to reconstruct images into a tomogram.

2.43 *Remote Tomography*

Remote tomography was undertaken using the Kiwi Advanced Research Network (KAREN) between AgResearch Ltd in Lincoln and the Otago Centre for Electron Microscopy in Dunedin. This allowed the remote user to access the microscope via video-audio-link, to interact with technical personnel supporting the acquisition of the tomograms and to securely transfer images and data files offsite. This allowed for rapid feedback, as the user was able to quickly ascertain the quality of the data through remote viewing and reconstruction without being physically present at the AgResearch Lincoln Research Centre (Figure 2.7).

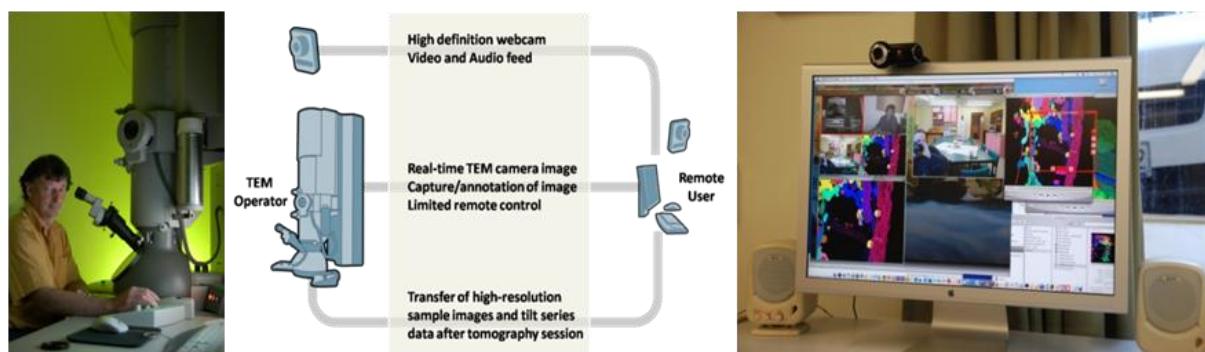


Figure 2.7 Remote Electron Tomography: Electron tomography undertaken over the KAREN network. Electron tomography data is acquired remotely, where monitoring of the process and tilt series data are transferred over the KAREN network for remote parties.

2.44 *Specimen Attrition*

Many otherwise excellent cilia were found to be unsuitable for tomography. For example, some were either too close to the grid bars, too close to the edge of the section or located at extremes towards the edges of the electron microscope grid which resulted in difficulty tracking during tilting or loss of imaging. Of those suitable cilia sampled at 300 kV, there was a high (50%) attrition rate during tomography, where sections physically failed under the microscope beam, or significant section aging resulted in failure to recombine the image alignments into a tomogram. Final inspection resulted in the discarding of many apparently suitable tomograms, as their quality proved inadequate for analysis. Handling and processing errors also destroyed specimens.

2.45 *Collection and Analysis*

Conventional electron microscopy provides projected spatial resolution in one dimension and is limited to ultrathin sections, while tomography provides a better spatial resolution. Single axis reconstructions result in missing geometric information known as the ‘missing wedge’ problem [988, 989] which is also present to a lesser extent in dual axis recombination [990-992] (Figure 2.8). Dual axis tomography provides improved resolution by the incorporation of two tomograms taken at orthogonal angles to each other and combining them into one, a more challenging task in terms of sample aging and distortion during acquisition.

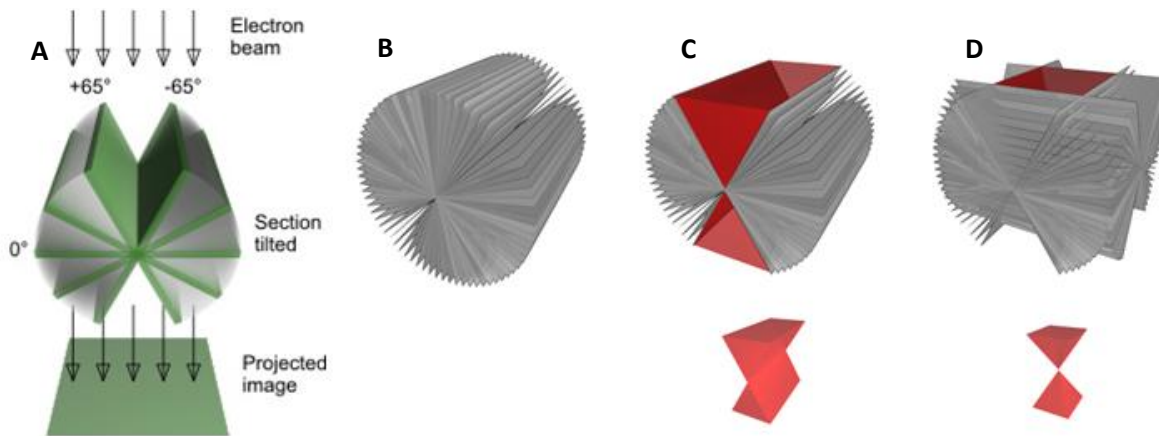


Figure 2.8 The ‘Missing Wedge’ Problem: A series of images of a sample section is gathered by the transmission of electrons onto a detector over a series of tilt angles ($\pm 65^\circ$) [A]. These are reconstructed so as to represent the volume imaged. However, it is not possible to tilt the specimen through all angles to reconstruct a full theoretical volume [B]. For a single axis acquisition, incomplete geometric information is represented as a ‘missing wedge’ (red) [C], which is reduced by incorporating dual axis images [D], taken at 90 degrees to each other. Reproduced and modified with permission from Dr Harland, AgResearch Ltd, Lincoln, personal correspondence.

Many parameters during tilt series image acquisition are under the control of the operator while others are automated processes within the microscope. Successful reconstruction of gathered data depends upon tracking each successive tilt series image with the aid of surface localised specialised markers on both sides of the section for determining the image axis and location through the full tilt range (Figure 2.9). Image series at known tilt angles are first processed, filtered, aligned and selected fiducial markers are then used to calculate an exact alignment solution to produce a

tomogram using digital software. The process of tilt series acquisitions are visualised as animations listed in Appendix VII, Section 7.1.

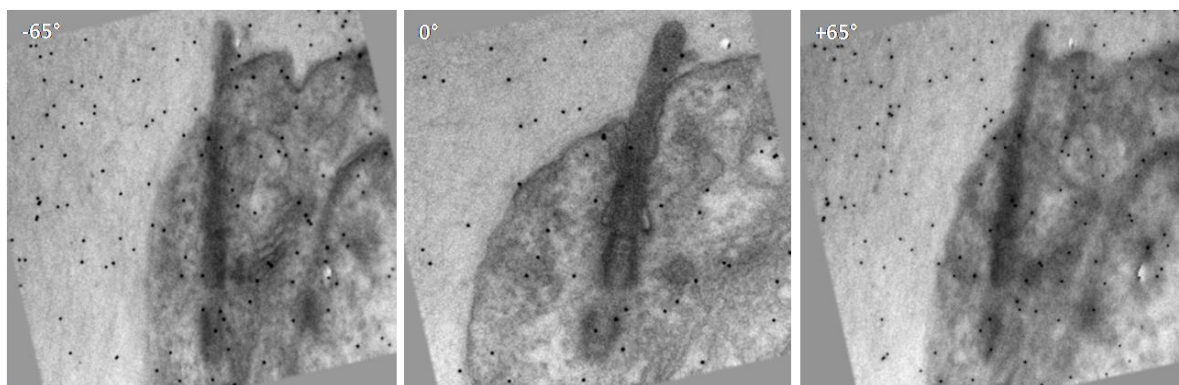


Figure 2.9 Data Acquisition: Tilt series images of a 300 nm semithick section containing a chick sternal chondrocyte primary cilium, taken in the Tecnai G² T30 electron microscope imaged at 300 kV. This tilt series is visualised as an animation <TiltSeries K10.avi>, listed in Appendix VII, Section 7.1.

Various software packages are available for aligning, tracking and reconstruction of a tomogram (such as IMOD [993], TomoJ [994, 995] and microscope specific packages) as well as for alignments without using fiducials [931]. IMOD, developed by Mastronarde and Gaudette and supported by the US National Centre for Research Resources [996], was chosen as a reconstruction and modelling package as it is recognised as the present standard freeware package. Tomograms are viewed as images conventionally in two dimensions as ‘optical slices’ (as seen in Figure 2.5) in the form of layered z-axis images. These differ from conventional ultrathin images in that their thickness is in the nanometer range (Figure 2.1). A series of optical slice images maintains structural information between consecutive images, allowing for precise determination of intricate features. Thus, ET provides detail of macromolecular assemblies such as membranes, microtubules, fibres and other complexes [924] at a resolution much greater than conventional TEM [932].

2.46 Data Processing

Data processing was carried out in the IMOD package (several upgrade versions) using an Intel® Core (TM2) Quad CPU Q8200 operating at 2.23 GHz with 4 GB of RAM. Single and dual axis tomograms were aligned and reconstructed using back projection and combined using IMOD [992]. Models were constructed using the ‘eTomo’ interface, allowing analysis and viewing of the biological volume in three dimensions [997].

2.47 Fiducial Tracking

To obtain the best tracking solutions, fiducials were chosen specifically for their ability to provide good contrast and visibility over the full range of imaging angles between consecutive frames, ensuring complete tracking solutions for all marker beads. This is necessary as many fiducials are not visible within the imaging field over all tilt angles, whilst others become occluded or obscured during tracking at higher tilt angles where the semithick section thickness increases, resulting in local

tracking errors (Figure 2.10). Fiducial tracking errors are visualised in series of animations listed in Appendix VII, Section 7.2, with animations of tomogram stacks in Section 7.3.

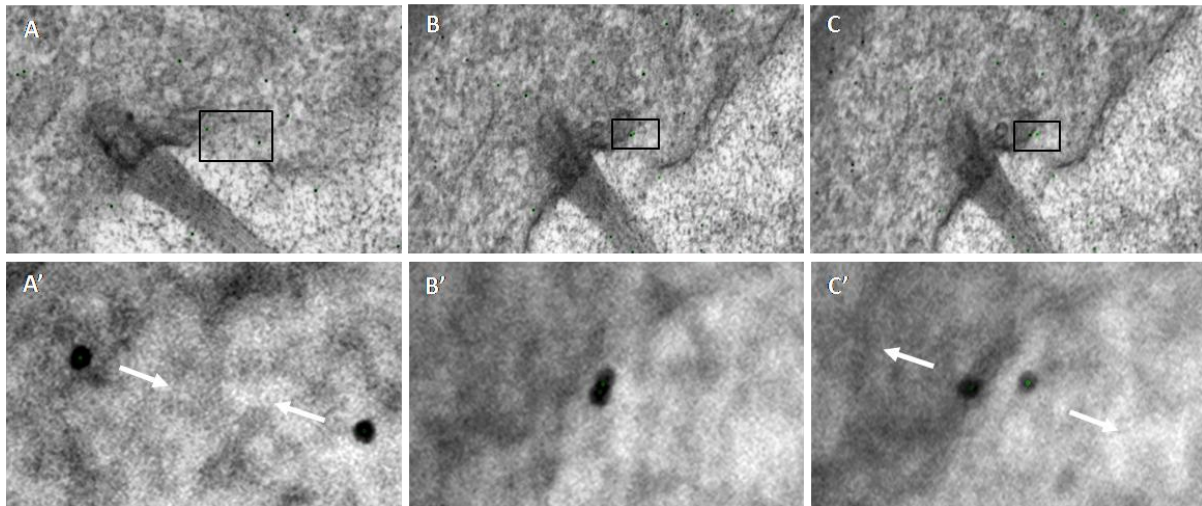


Figure 2.10 Fiducial Tracking in IMOD: [A-C] details tracking of gold markers across aligned tilt series prior to final tomogram formation. Enlarged views in [A', B' and C'] show the process of the induction of tracking errors (direction of motion, arrows) where fiducials come into occultation. Errors can also occur from background signal levels during tracking at higher tilt angles due to the increased effective imaging thickness. Animations are listed in Appendix VII, Section 7.2: <Fidtrackone.avi> and close up view in <Fidtracktwo.avi>.

2.50 Analysis and Modelling of the Tomogram

Visualisation of structures is achieved in IMOD (3DMod) through tracing components of interest, forming a three dimensional representation based on contour mapping and volume rendering. Vesicles were hand traced with drawing tools in the 'zap window' in the z-axis, with each new vesicle assigned a new unique model object number with selectable colour. Vesicle components of the Golgi apparatus were broken into their respective *cis*, *medial* and *trans* compartments, and were each grouped as distinct objects, while the nuclear and cell membranes and vesicles were each treated as individual objects. The ciliary pocket invagination was treated as a distinct structure, which also encompassed part of the ciliary membrane (due to the axis of the cilium within the section). The other half of the ciliary membrane was modelled as an extension of this structure, giving rise to the two element membrane model (Figure 2.11). The 'image slicer window' allows for visualisation of the tomogram ultrastructure in any plane, aiding the tracking and tracing of finer components, such as filaments and microtubules. Microtubule tracing within the axoneme and basal body was problematic due to the close spacing of microtubules and the twisting inward taper in their projections.

The 3DMod 'iso-surface' volume rendering function allowed complex electron-dense deposits and surfaces to be averaged and modelled as discrete volumes. Matrix granules, luminal deposits, microtubule deposits, y-shaped linkers, alar sheets and basal feet were modelled in this way.

Model construction was an intensive iterative process. Once structures had been meticulously traced, error checked and confirmed as accurate, they were saved as distinct objects. Model elements could be measured, spatial inter-relationships mapped and volumes ascertained. These processes are

time consuming, as manual tracing, control and input is required to generate model components and then display them. Automated image processing, data extraction and modelling for tomography is not yet possible. Animations of tomogram stacks are listed in Appendix VII, sections 1.3, while model constructions are listed in Section 7.5.

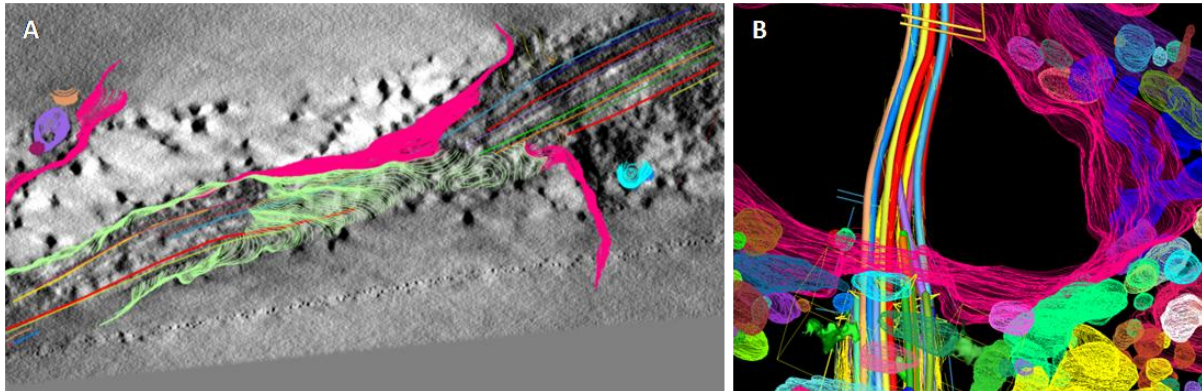


Figure 2.11 The Modelling Process: [A] Manual tracing of vesicles and microtubules produces a ‘raw’ layered view in 3DMod prior to meshing. Meticulous attention to detail ensured the accurate translation of information between successive optical slices of the tomogram for forming each object [B]. Details of the ciliary membrane surrounded by the extracellular matrix are seen in [A], with [B] detailing the ciliary pocket and cytosolic vesicles. Individual objects are assigned distinct distinguishing colours for clarity and identification. Animations of the coarse tracing process of model generation are listed within Appendix VII, Section 7.5.

2.51 *Model Display*

Objects were organized into groups defined by their ultra-structure. Tubes were used to form microtubules, intermediate filaments, actin and subdistal fibres, while vesicles and membranes were modelled as open or closed surfaces. Smaller electron dense deposits were displayed as solid volumetric renderings. Each object may be individually or selectively visualised by the user, with optional control over colour shading and transparency being possible. Object selection allows for individual or groups of objects to be examined, their spatial geometry and inter-relationships to be investigated. Screenshot capture sequences allowed for the generation of animations providing a three dimensional perspective.

2.6 *A Virtual Cilium: SolidWorks*

A classical reference image of an ultra-structural cross-section of a centriole from the frontispiece of Wheatley’s book *The Centriole: A Central Enigma of Cell Biology* [63] was imported into SolidWorks (Dassault Systèmes, SolidWorks Corp¹) for the purpose of forming an electronic template for the generation of a virtual cilium (Figure 2.12 A, B). Components could be extruded forming the triplets and inter-triplet linkages of a basal body (Figure 2.12 C and D) along with the axoneme sub-fibre doublets (Figure 2.12 E and F). The nine-fold (40°) symmetry of the model triplets should be noted, and also a slight distortion of the original image (which may be due to the technique used to generate the original image (Figure 2.10 A, B). Microtubule triplet and linkage lengths were

¹ <http://www.solidworks.com/>

extruded to match ultrastructural results (Figure 3.4), while doublet lengths were derived from the tomographic model data, providing an anatomical comparison in Figure 3.4 F.

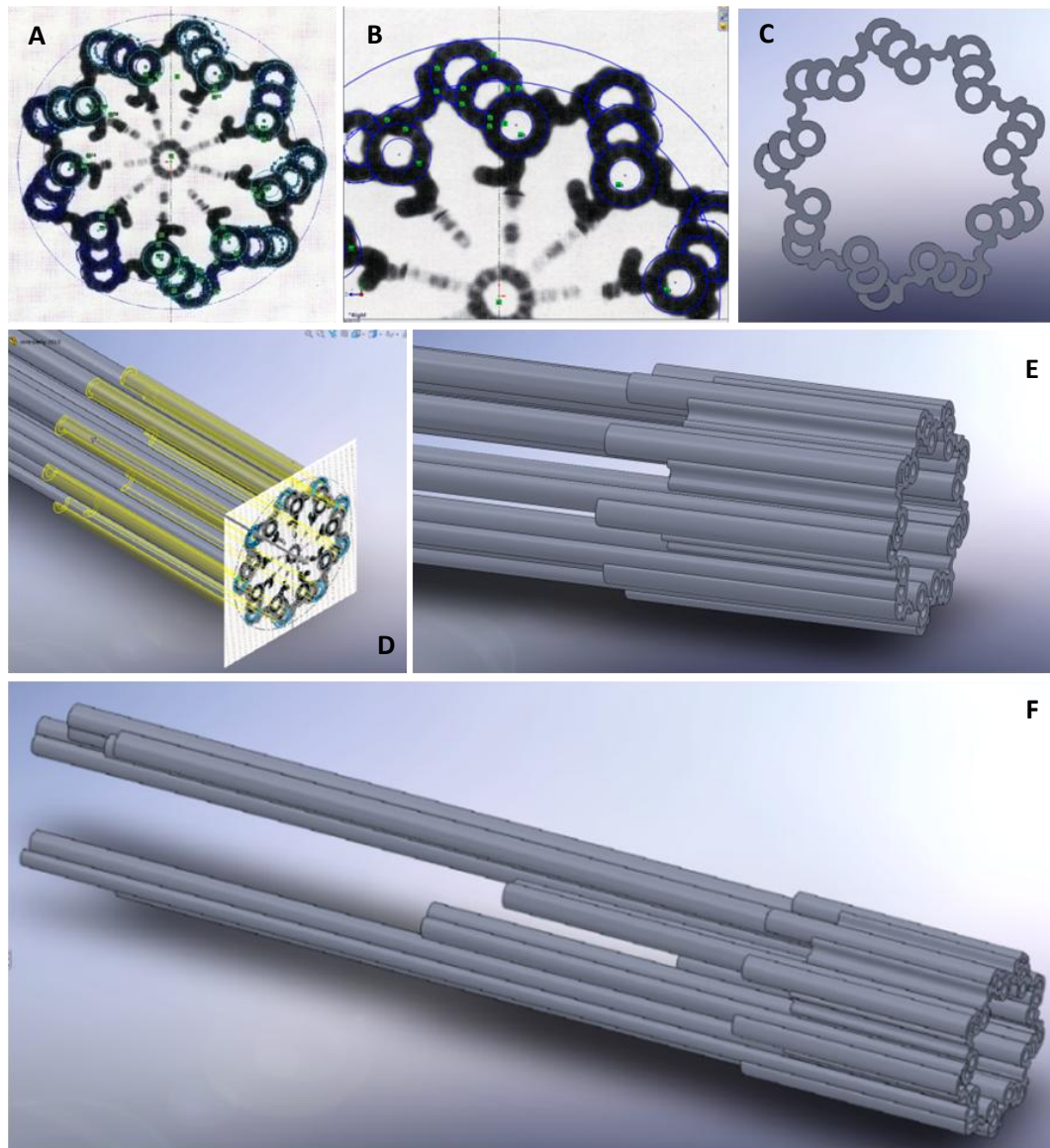


Figure 2.12 The Virtual Cilium: Extruded from a pictorial template into a structural likeness based upon tomographic data obtained from [A] and Figure 3.4. This model is visualised in animation <SolidWorksModel.avi> listed in Appendix VII, Section 7.7.

Chapter Three: Results

3.0 Introduction

All cells communicate with their extracellular microenvironment, yet up to the present the significant role of the primary cilium has been overlooked. Many researchers have studied primary cilia in the past, including using various biomechanically responsive connective tissues. In this work two connective tissue types have been investigated as a source of primary cilia: chick sternal cartilage and the flexor tendon of the chick *Gallus domesticus*. Flexor tendon was found to be too difficult to section reliably, hence sternal cartilage was utilised for tomographical investigation. Ovine chondrocyte cell culture served as a supplemental approach for investigating primary cilia.

3.1 Mechanical Connective Tissues: Tendon

Flexor tendon was sectioned longitudinally (with the grain of the collagen fibres) revealing highly aligned collagen bundles surrounded by tenocyte support cells (see Figure 3.1 A). Primary cilia were usually found to be deflected, and no cilia were found completely contained within a thick section. Some cilia were found seated within invaginations of the ciliary pocket, or protruding between bundles of collagen bundles. A high percentage of those observed were found to be highly deflected in their projection from the cell, so as to run parallel with the collagen fibres (Figure 3.1 B). This orientation made it virtually impossible to obtain a complete primary cilium within the plane of the section. A well-developed endoplasmic reticulum and sparse Golgi structures were observed within many cells. Transverse sectioning revealed tight bundles of highly polarised collagen bundles in the extracellular space, each consisting of hundreds of uniform arrays of collagen fibres, and with tenocyte cilia protruding between bundles (Figure 3.1 D-F).

3.2- 3.3 Mechanical Connective Tissues: Chondrocyte Cilia Morphology and Staining

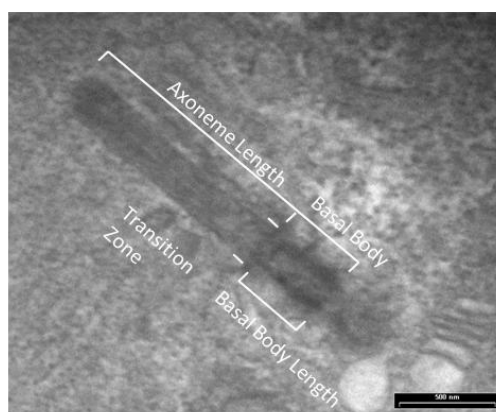
The choice of sternal cartilage was fortuitous, for investigation of chondrocyte primary cilia revealed they were generally undisturbed in their linear projections, increasing the odds of being completely contained within a semithick section (Figure 3.2). Two electron microscopy staining techniques were utilised for electron microscopy, conventional fixation with *en bloc* uranyl acetate, and 'Ruthenium Red', a platinum group transition metal utilised specifically for the fixation, retention and staining of extracellular proteoglycans and saccharides. Conventional electron microscopy staining revealed an interspersed network of collagens and some weakly stained structures, while the Ruthenium treated cartilage reveals not only this network, but the finer details of proteoglycans and matrix granules, which are not fixed or retained by conventional treatment techniques. Cilia were found in various projections, including being retracted (or invaginated) within the cell and being closely 'pocketed' by the membrane (see Figs 3.2 F, 3.3, and 3.5).

3.4 The Chondrocyte Primary Cilium: In vitro

The basal body form was similar to that described in other centriole studies [28, 29, 45, 998], as a longitudinal cylindrical barrel-shaped body comprised of nine semi-equidistant microtubule triplets, nominally 200 nm in diameter and inclined to the main ciliary axis with a left-hand ‘curl’ or twist in the positive microtubule direction. This allows for the determination of cilium microtubule direction in conventional ultra-thin sections, as viewed in the series from Figure 3.4 L-Q. The inner A and B-subfibres form the axoneme microtubule doublets, while the C-subfibre demarcates the basal body. Inter-triplet linkers are seen between the A and C-subfibres of adjoining triplets (Figure 3.4 L) as well as an inner A-subfibre ‘hook’ subtending into the lumen at the proximal end of the basal body (Figure 3.4 L and M) but do not appear to continue past the mid-body (Figure 3.4 N). The distal end the C-subfibre appears to become partially unattached from the B-subfibre (Figure 3.4 N) where the alar sheets appear to be extended from an amorphous ‘basement’ zone across the triplets, focused upon the B-subfibre. These sheets run to fine points of contact upon the axoneme membrane (Figure 3.4 N to O) anchoring the basal body to the cell membrane, and also demarcates the end of the C-subfibre and the start of the axoneme. Throughout this region the inclination of the microtubules transition in their pitch from the triplet structure of the basal body to axonemal configuration as seen in (Figure 3.4 P, Q). In this transition zone, y-shaped linkers were identified spanning between the doublets and the ciliary membrane, becoming infrequent further along the axoneme.

3.5 The Chondrocyte Primary Cilium: In Situ

The general morphology of all chondrocyte primary cilia examined conformed to work by earlier investigators [25-29] and where visible, the Golgi network was found to be located in proximity to the centrosome. The cilia themselves varied in their degree of projection and deflection into the matrix, with respect to the basal body (Figure 3.3), ranging from a full interactive extension, to a partially retracted invagination, and even to fully reclined extension (with less matrix present) against the cell membrane. Of hundreds of semithick serial ribbons inspected, 167 primary cilia were found to be completely contained within the plane of their section. Of these, 19 were prepared for electron tomography at 300 kV. Specimen attrition resulted in a total of 9 single axis and 5 dual axis tilt series of cilia being reconstructed, with only the most suitable (contained within section, location on grid, and with good contrast) chosen for modelling. Measurements were taken of the candidate cilia membrane length, axoneme, basal body length and width of transition zone, where it was possible to do so accurately (see Table 3.1). Ciliary membranes varied in length between 0.7-2.41 μm with an average length of 1.38 μm . Basal body lengths were found to average 0.365 μm , with the average transition zone width of 0.26 μm . Dual ciliary length measurements were taken due to discrepancies arising from the transition zone, in measuring between the cilium membrane and the full microtubule lengths of the cilium.



	μm	1σ	n
Axoneme Length	1.38	0.385	167
Axoneme & Basal Body	1.80	0.395	148
Basal Body Length	0.365	0.01	144
Width of Transition Zone	0.262	0.015	155

Table 3.1 Measurements of Chondrocyte Primary Cilia

3.6 Tomography of Native Sternal Chondrocytes

The majority of tomograms undertaken were not fully successful primarily due to the combined effects of aging upon the semithick section during tomography, such as failure of the section under beam, or alignments were rendered unsuitable for tomogram reconstruction. Others failed to deliver adequate contrast upon reconstruction, or occasionally were lost through attrition of the electron microscope grids or handling errors. Initially, the process of post-staining in some cases caused loss of stain on section, and precipitate fouling of the grids. This step was subsequently dropped, in favour of the use of *en bloc* staining alone, which proved more than sufficient with the RHT treatment. Fiducial application times were also reduced to minimise aqueous interactions and ‘wash out’ of stain. Once generated, tomograms provided high resolution optical slices of the imaged volume, however reconstruction results were found to vary somewhat, compared with conventionally stained samples (Figure 3.5). With enhanced staining from ‘Ruthenium Red’ treated samples (Figure 3.5 C’), the extracellular matrix was preserved revealing the abundant presence of matrix granules (Figure 3.5 C). The presence of collagen fibres was noted within the matrix, however these were largely obscured by granules within the Ruthenium treated samples (Figure 3.5 C, C’). The presence of luminal vesicles within the basal body of cilia was noted on numerous occasions and is in line with observations of previous researchers (see Section 1.11).

In this study a total of 9 single and dual axis tomograms of chondrocyte primary cilia were successfully reconstructed. A single axis tomogram ($\pm 65^\circ$ in 0.5° steps, 350 nm thick) was chosen to model as it showed excellent contrast of a near complete cilium located within an indentation in the cell membrane (see Figs 3.6 and 3.7). As an aid to understanding, a series of animations have been constructed and are included in Appendix VII.

3.7-3.9 A Single Axis Model

The model in this study was created based upon a single axis tomogram. Inspection revealed that not only was the cilium almost completely within the plane of the section, but suitable components, the extracellular matrix interacting with the cilium, along with other organelles; the Centrosome, Golgi Apparatus, Endoplasmic Reticulum and Nuclear Membrane were also within the tomogram (Figures 3.6, 3.7 and 3.8). The ultrastructural anatomy of the axoneme and basal body of the cilium is detailed in Figure 3.9. It was found however that a part of the distal tip of the cilium, along with a portion of the basal body and proximal centriole were missing, being out of the plane of section. During modelling, each structure within the tomogram was carefully considered, error checked and compared with ultrathin sections before being accepted as an element. The resulting model consists of roughly 2200 objects totalling 240 megabytes in size, taking 3000 hours to construct. The model is also in broad agreement with previous studies of primary ciliary ultrastructure [25-29], and chondrocyte ultrastructural observations (Figure 3.4).

3.10 Tomographical Modelling of the Extracellular Matrix and Matrix Granules

Cartilage connective tissue consists of chondrocytes surrounded by a pericellular capsule containing a complex mix of proteoglycans, collagens, osmolytes and signalling molecules. Specimens treated with RHT prior to and / or during osmication demonstrated greater contrast of proteoglycans compared to conventional treatment with *en bloc* uranyl-acetate alone, revealing fine structure content of the matrix granules and their fine inter-linkages (Figure 3.5 C'). Stained granules in the extracellular matrix were composed of condensed collections of interconnected minor aggregates, forming a complex three dimensional web of tensile proteoglycans which were modelled as 'condensates'. These are believed to be composed of Aggrecan and Link protein. Dual-axis tomography of these granules (Figure 3.10 D-G) revealed their fine structure and inter-connectivity but when seen in three dimensions they appear as 'coarse nuggety' structures (Figure 3.10 H-L). These were found to be usually distorted in the direction of their attached filaments. The proteoglycan matrix exists inside a 'vacuole like' indentation of the cell membrane located in the pericellular space. This surrounds the protruding cilium uniformly and is very similar in appearance to an enlarged ciliary pocket [325], however the matrix differs as it is less dense than the pericellular environment (Figs 3.6 and 3.7).

3.11 Matrix Ciliary Membrane Interactions

The ciliary membrane was found to be decorated on both sides with stained components which may represent receptors, trans-membrane proteins, channels and attachment complexes for unknown tethered structures (Figure 3.10). Extracellular matrix granules were found to be physically tethered via filaments to the membrane by unknown receptors along the full length of the axoneme, in some cases being the foci of localised distortions in the membrane created by matrix forces (Figs 3.11

and 3.12). Many densely stained structures were identified on both sides of the lipid membrane (Figure 3.11 F-M) which were associated with extracellular connecting filaments (Figure 3.11 G-J) and membrane-spanning particles (Figure 3.11 K-M).

3.12 Matrix to Ciliary Membrane to Microtubule Interactions

Matrix-membrane interaction sites were sometimes observed as local ‘dimples’ in the local membrane (Figs 3.11 and 3.12). These were connected via fine strands to matrix granules apparently under load from the external environment. These unknown receptor mediated ciliary membrane connections were matched nearby by complex protein linkages between the membrane and the microtubule doublets, and between individual doublets and (Figs 3.12 A, B and 3.15 A, C, arrow). Microtubules were also observed with microtubule-associated proteins, as well as accumulations of densely stained materials (Figure 3.12). Matrix forces upon the membrane are potentially able to be transmitted through these prominent linkers, allowing these forces to be transmitted to the microtubule doublets beneath. The membrane of the cilium was modelled in two parts, permitting a simple view of its internal structure. It was found to neatly cover its internal contents, while having a ripple texture, with a number of the distortions within the membrane being attributed to tensile matrix components (Figure 3.12 C and D).

3.13-3.15 The Axoneme Microtubules

The cilium axoneme was divided into three zones; The Distal, Middle and Transition Zones (Figure 3.13). The tomogram revealed the cilium’s unique three-dimensional microtubule nine-fold architecture, which is determined by the basal body (basal body triplet architecture is seen in Figure 3.20 G). The cilium is composed of a total of 27 unique subfibre assemblies of various lengths (from the basal body triplets), with the axoneme making up to 18 microtubule subfibre components (depending upon numbers projected). The microtubule doublets reduced in number along the axoneme (from 9 to 5), were twisted and inclined inward with a ‘left-handed inclination’ in their projection from the basal body triplets, resulting in the cilium tapering towards its distal end. The morphology of the axoneme appears deflected under the combined influence of external environmental loads of the local matrix (viewed longitudinally in Figure 3.13).

The localisation of macromolecular complexes identified within the axoneme are detailed in Figure 3.14. These were found concentrated upon specific microtubules within the ciliary lumen, located primarily in areas of the distal-to near mid-zone of the axoneme. While it is not possible to fully identify with any certainty the objects identified, it is possible to classify objects into broad categories. These were defined as membrane to microtubule linkers; microtubule to microtubule linkers, filaments and ‘rafts’ of periodic materials resembling intra-flagellar transport particles, tabulated with Figure 3.29.

Many smaller deposits upon the membrane and microtubules were also noted, however many were below the threshold chosen for modelling. Figure 3.15 details a number of objects and densely stained periodic microtubule associated structures interacting with the ciliary membrane (Figure 3.15 A, F) which are reminiscent of IFT-like transport materials. Membrane to microtubule linkages located near matrix induced ciliary distortions are seen decorated with unknown materials (Figure 3.15 E-F''), however these materials were curiously absent near the distortion in (Figure 3.15 E).

3.151 Localisation of Intra Ciliary Transport Materials

Figure 3.14 (A'-E') detail linear 'rafts' or trains of periodic electron-dense 'IFT-like materials' (marked by arrowheads and confined by bars '||'). These were located between (and sometimes inter-connecting) the microtubule doublets and the ciliary membrane (Figs 3.16 E and 3.17) and interspersed with connecting filaments (Figure 3.17 A, arrowhead). IFT 'rafts' or 'trains' were of variable length, the longest length of 400 nm, and with smaller 150, 80 and 30 nm collections. These were comprised of periodic groups of 20-45 nm elements, with shorter periodicities seen making up the longer rafts. These materials were primarily located upon microtubules 2, 3, 6, 7, and 8, with the highest concentrations observed upon 3, 6 and 8 (Figure 3.29, where microtubule triplets, doublets and their assorted components are listed). Triplet numbering convention followed from under the middle of a basal appendage, in a clockwise direction when viewed in the positive microtubule direction.

3.16 The Distal Axoneme

The structural tip of the cilium is unique as it is the termination zone of the microtubule doublets, the terminus for IFT-transit and an accumulation point for materials. An oblique part of the membrane of the tip was missing from the section (Figure 3.16), thus the model provided a 'cut-away view' of the distal tip of the axoneme revealing the termination zone of four microtubule doublets (the fifth falling just short, Figure 3.16 C and E). The distal ends of the microtubule doublets were associated with dense deposits coating the internal membrane of the cilium tip (Figure 3.16 A-A''). Electron dense materials and filamentous structures were identified between the ends of the doublets and the membrane (Figure 3.16 A and D). A perspective of the distal zone is seen in (Figure 3.16 E), which details the microtubule doublets emerging into the middle zone, associated with IFT-like 'rafts' of materials.

3.17 The Middle Axoneme

This zone is classically the long slender component of the cilium (Figure 3.3 A) which changes little in its uniformity over some distance. Bounding boxes detail linear zones of accumulations of materials decorating the microtubule doublets and the surrounding luminal space (Figure 3.17, A and B). The finer structure of 'raft-like' accumulations reveals semi-regular

periodicities which are interspersed in clusters along both the distal and middle axoneme microtubules. The termination zone of microtubule doublet one (Figure 3.17 A, arrow) is decorated with small structures at its end. Manipulation of the model allows perspective views of the axoneme that would be seen conventionally contained within an ultra-thin sections (Fig 3.17 C and D, viz, Fig 3.4 P and Q). The middle zone contains two microtubule doublets, both of which contain greater accumulations of dense particles than the others (doublets 3 and 6) (Figs 3.17 B (arrow), E (arrowhead) and 3.29).

3.18 The Transition Zone - One

The transition zone represents the first region where the cilium projects into the extracellular domain, and can be divided into two parts. In the first part the cell membrane joins the ciliary membrane at a tight right angle (or at a highly curved interface in the case of the ciliary pocket (Figure 3.5 B) where the basal body is attached to the transition membrane, demarcating the transition from the cytosolic to the ciliary domain. The second part is the tapering zone, where the microtubules reduce in number, and merge into the axoneme. Two small ciliary-membrane-associated vesicles were identified (35-40 nm in diameter) within the extra cellular matrix, closely associated with the membrane of the transition zone (Figure 3.18 A and B). Trans-membrane densities are associated with both vesicles. Notably absent was the zone of the 'ciliary necklace' [51] suggesting that the 'y-shaped linkers' were not present at the time of fixation, were not adequately resolved, or were destabilised by the Ruthenium Red treatment. Dense deposits were attached to microtubule doublets as well as fine filaments (Figure 3.18 C and D). The microtubules were also found to have their greatest inward inclination within the transition zone (Figure 3.18 E and F).

3.19 The Transition Zone - Two

The curvature of the transition from ciliary to periciliary membrane is illustrated in Figure 3.19 A, where cell and ciliary membranes merge at a right angle. Intense staining of the membrane is apparent, with heavy decorations and fine fibres present upon the inner surface (Figure 3.19 B and C). Fibres were found radiating from microtubule doublets and triplets to the ciliary and periciliary membrane surface along the length of the transition zone and adjoining basal body (Figure 3.19 B''). Other fibres made up a number of subdistal appendages (Figure 3.19 D, F and G), were connected to the basal body microtubule triplets and associated with dense deposits (Figure 3.19 F, centre, green). These dense deposits proved difficult to resolve adequately. The alar sheets occupy a zone spanning the microtubules near the terminating end of the C-subfibre and are each drawn to tethered apexes firmly held within the transition zone membrane (Figure 3.19 G, H and I). The fine granular structure of the alar sheets were also difficult to resolve.

3.20 The Basal Body Microtubule Triplets

The basal body contains a unique nine-fold symmetric 'barrel like' structure made up of the inclined vanes of microtubule triplet subfibres. The A and B-subfibres project longitudinally to form the axoneme, while the C-subfibre demarcates the centriole zone. Microtubules were aligned and traced within 3DMod carefully due to their respective close spatial proximities within the sections. Each subfibre was traced and modelled using intersecting tubes to best represent the circular tubulin components making up the microtubule. This proved difficult due to their inclination and slightly curved nature within the tomogram. This is apparent where perspective optical slices parallel the model (Figure 3.20, A-C, D and F). Of particular interest is the curvature in Figure 3.20 E, which is also seen in a 'cut-away' view in Figure 3.20 F. The basal body microtubule triplets were observed to be inclined with a left-handed polarisation and curve giving the basal body a 'barrel like structure' and 'vane' appearance, and were found to reduce in their inclination angle, as they tapered into the axoneme. As part of the basal body was missing, it has been reconstructed for viewing by projecting the nine-fold symmetry in Figure 3.20 G.

3.21-3.22 Internal Structures, Luminal Disc, Fibres and Vesicle

The basal body cavity contained numerous electron densities associated with lumen and microtubule faces (Figure 3.21). Numerous densely stained deposits of different size were found decorating the basal body triplets, including a larger opaque complex visible as a 'band' spanning inside the distal end of the basal body between microtubule triplets (only some deposits are shown for clarity of viewing, Figure 3.21 B, C and E). This was termed a 'luminal disc' like structure, and was associated with nearby fine fibres and macromolecular deposits attached to the microtubule triplet luminal faces. Not all the structures present were modelled within the proximal region of the basal body, as these proved to be too complex. Included with these structures, a luminal vesicle was identified and modelled (Figure 3.22). It was firmly attached to the microtubule face, and was found to be facing in the direction of the axoneme, appearing as if against a flow (Figure 3.22 E). This study identified three tomograms containing basal body luminal vesicles (see Figs 3.5 B and 3.22).

3.23-34 Basal Appendage One

Surrounding the basal body is the pericentriolar environment, which is made up of stained deposits of structures which include the alar sheets, subdistal appendages, and basal appendages (also known as basal feet). Two basal appendages were attached to the basal body. Each basal appendage consisted of three components; a basal anchoring complex attached to the basement microtubule triplets, an appendage arm and a docking head. The basal appendages extend centripetally not only to anchor and structurally support the microtubular network, but also to provide access to a zone away from the basal body. Examination of the ultrastructure of basal appendages revealed them to be intensely stained linear structures protruding at near right angles from the basal body (Figure 3.23 A-

H). Each appendage revealed over-staining of the docking complex and arm, but exposed an amorphous composition of the basement structures. This is seen in the model of Basal Appendage One (BA1, Figure 3.23 I-L) in its attachment to the centriole. The extending appendage arm and microtubule docking complex was modelled as a single component. The anchoring complex consisted of an amorphous support network comprised of three basement zones, each of which were inclined across their basal body triplets at inclination (Figure 3.24, C-F, arrows) to anchor the appendage. A low density zone was observed underneath the basal appendage, directly above the microtubule triplet upon which it was centred (also seen in Figure 3.25 F).

The basal appendage projects outside the pericentriolar environment to interact with the surrounding centrosome, where vesicles interact with the basal body and basal appendages through fine tethering linkages (Figure 3.25 A-D). The basal arm contains indentations (Figure 3.25 E) and fine protrusions extending along its length (Figure 3.25 F, H and I) until merging with the docking complexes upon its distal end. The docking complexes consist of two nodular projections, to which microtubules (Figure 3.25 G and G') and vesicles are tethered (Figure 3.25 B). Vesicles are associated with the basal appendage, the connecting microtubules, and also the pericentriolar basal body zone (Figure 3.25 D). Three microtubules are seen radiating from the docking complexes (two from one) in (Figure 3.25 F, H and G) and interacting with nearby centrosomal vesicles (Figure 3.25 H, J). The ultrastructural perspective in (Figure 3.25 G* and H) shows the vesicles modelled in (Figure 3.25 J*). Note the basal body longitudinal structure (Figure 3.25 J) detailing the basal appendage, the subdistal appendages, the alar sheets (attached to the transition zone membrane). Points of interest include the vesicles attached to basal appendage (Figure 3.25 C) and the basal body (Figure 3.25 D), as well as the inclination of the basal appendage which may be influenced by torque from the attached microtubules.

3.26-3.27 Basal Appendage Two (BA2)

Longitudinal optical sections of Basal Appendage Two (BA2) are seen in Figure 3.26 A-H. The docking complex and arm were modelled in the same way as basal appendage one and appear to have similar anatomical likenesses, possessing a similar cantilever projection (Figure 3.26 J and L). The basal appendage had an inclination which appears to also indicate a possible contribution of torsion from attached microtubules (Figure 3.27 A). The docking complex was found to have only two docking sites upon it (with no double nodular protrusions like BA1) tethering three and two microtubules respectively (Figure 3.27 A and B). The ultrastructure of two of these microtubules was examined around the docking complex (Figure 3.27 C-E). These were tethered to the docking head at their negative end, and extended positively outwards (Figure 3.27 E'). Densities are noted upon microtubule bases and docking heads (Figure 3.27 C', D and E') including linkages connecting the microtubule to nearby vesicles.

The basement anchoring complex substrate was modelled as numerous discrete components to investigate its finer amorphous form. Three attachment zones to the microtubule triplet substrates were identified, including a 'hollow' zone underneath the base arm above the central triplet it was attached to (Figs 3.27 A). Views detailed in Figure 3.26 I-L reveal a similar amorphous morphology to basal appendage one.

3.28 A Review of Basal Appendages One and Two

The basal appendage model perspectives are visualised in Figure 3.28 to compare their anatomical characteristics. Respective lateral views of basal appendages Figure 3.28 BA1 A-E and BA2 F-J detail the appendages docking head, arm and the basement complexes. Comparison of the basement anchoring sites reveals: 1) Low density areas located under the basal appendage, forming a longitudinal 'groove' (Figure 3.28 C and H). 2) Three distinct attachment areas or 'basement zones' corresponding to three separate microtubule triplet attachment regions (Figure 3.28 A and F). 3) The basement materials were highly amorphous in their nature, indicating a porous higher order structure (Figure 3.28 E and I). Rotational views of the appendage docking heads and arms (Figure 3.28 BA1 K-O and BA2 P-T) reveal subtle differences. The docking heads of BA1 are bifurcated (compared to the singular head on BA2) however their size and aspect ratios are similar, including the general architecture of the arms. The indentation on the arm of BA2 (Figure 3.28 R, arrow) should be noted. The presence of thorny projections from the lower arms (arrowheads) was also recorded (Figure 3.28 K, P, O and T).

In summary, both basal appendages share highly similar structural morphologies. Their basement anchoring complexes consist of finely porous materials, with supporting long tapering arms, whose head docking complexes consist of fine spiny protrusions, some of which anchor cytosolic microtubules and vesicles (Figure 3.25). Microtubules anchored to the basal appendage docking complexes are visualised as being decorated with numerous microtubule associates deposits, complexes and fine fibres linking to nearby vesicles which they carry (Figs 3.34 and 3.37). An area of exclusion is noted extending in a zone surrounding the perimeter of cytosolic microtubules, which are uncluttered except for the close proximity of vesicles and microtubule associated proteins (detailed in Figs 3.34, 3.36 and 3.37).

3.29 The Cilium, Basal Body Materials and Orientation

The positional relationship of the basal appendages (Basal Appendage One, Basal Appendage Two and their associated cytosolic microtubules) were investigated with respect to the microtubule triplet structure of the basal body (Figure 3.29 A, seen in the positive microtubule direction). Each appendage radially spanned across three microtubule triplets, and appeared to be symmetrically spaced around the basal body, so as to not overlap their basement complexes. This would imply a

number of rotational orders are possible, based upon the nine fold triplets, and the possibility of subtending at least three symmetric basal appendages.

The contents of the axoneme and basal body microtubules were interpreted using both the model and tomogram ultrastructure to establish the nature of their features, and their relative microtubule doublet association. Generalised categories were defined for luminal microtubule components: IFT-like materials (localised to membrane side outer, microtubule side inner), internal linkers (interconnecting microtubule doublets), membrane linkers (between the microtubules and the membrane), internal filaments (attached to microtubules projecting into the lumen (membrane side external, microtubule side internal), y-shaped linkers, alar sheets and the length of each microtubule doublet. The position of each basal appendage, the relative numbers and radial distribution of luminal materials upon the microtubules of the axoneme, including the basal body and transition zone vesicles, are visualised in Figure 3.29 B and tabulated in C. While these were collated from the model and tomogram, it is difficult to ascertain with absolute certainty their identity and functional significance.

Microtubule doublets that were derived from triplets associated with the basal appendages of the basal body were found to have the highest densities of materials associated with them. Doublets 2, 3, 6, 7, and 8, contained the most materials, while 4, 5, 9 and 1 contained lesser amounts. Extracellular matrix vesicles [999] were found to be associated with the ciliary membrane near microtubules 6 and 7 (Figure 3.18), while the basal body luminal vesicle was tethered to the inner surface of microtubule triplet 2. The position of extracellular matrix and luminal vesicles should be noted with respect to the basal appendages of the basal body (BA1 which covers triplets 6, 7 and 8 and BA2 9, 1 and 2), and the internal luminal disc (spanning 1 and 6). Numerous electron dense materials were also associated with the triplet faces.

3.30 The Proximal Centriole

The proximal centriole was modelled in the same way as the basal body. Although only half of the centriole was contained within the tomogram, it was possible to determine the polarisation and inclination of the microtubule triplets (Figure 3.30). The modelling revealed a nearly identical structure to the basal body. The microtubule triplets maintained their inclination along the proximal centriole but did not taper, as with the basal body. Also lacking were any external appendages or microtubule attachment sites. Similarly to the basal body, there was also a 'luminal disc' like structure located at the distal end of the proximal centriole (Figure 3.30 E and L). Electron-dense materials decorated the microtubule triplets, with larger complexes found present on the outside (Figure 3.30 C (G, model view), I and K). Structures linking microtubule triplets were also noted (Figure 3.30 F and G). Axial perspectives are seen in Figure 3.31 A-C and H showing the luminal disc and radial distribution of materials attached to and bridging the microtubule triplets. These pericentriolar

materials can be seen interacting within the nearby centrosome, and also the nearby nuclear membrane, in proximity to several nuclear pores (Figure 3.31 D-I).

3.31 Proximal Centriole Radial Components

The distributions of electron dense microtubule associated materials upon the proximal centriole are shown in Figure 3.31 A and B. These decorated the exterior microtubule surfaces, and included the presence of an oblique luminal disc like structure Figure 3.31 C. The centrosomal environment surrounding the proximal centriole contained numerous dense deposits (not all of which were modelled, Figure 3.31 D, E). The nuclear membrane was modelled to reveal nuclear pore complexes and found to be in close proximity to the centrosome (Figure 3.31 F). Linkages were identified connecting from the distal end of the centriole to the nearby nuclear membrane in proximity to several nuclear pore complexes shown in Figure 3.31 G-I (see Figs 3.33 E and 3.34 A). The nuclear pores were found to contain stained proteins, and their closeness to the centrosome, and the proximal centriole should be noted suggesting possible involvement with ciliary activity.

3.32 The Centrosome (1) Ultrastructure and Modelling

Selected serial optical slices of the centrosome overlaid with the model (Figure 3.32 A-H) revealed the position of the centrosome between the cell and nuclear membranes. At its core is the basal body, from which protrudes the primary cilium, and the sub-tending proximal centriole. Each is encompassed by its own pericentriolar environment, which in turn is surrounded by a complex zone of interacting vesicles. These were modelled individually to reveal a field of vesicles associated with the basal body, the basal appendages, their attached microtubules, and the cell and nuclear membrane (Figure 3.32 I-L). A notable gradient of vesicle sizes was noted with smaller vesicles generally being involved with the centrosome and its processes, and with vesicle size usually increasing further away from the centrosome. Vesicles were noted usually in clusters in proximity to cytosolic microtubules where they sometimes appeared to be distended as ellipsoids (Figure 3.32 K and L) with smaller vesicles usually found grouped as clusters (Figure 3.32 I and K).

3.33 The Centrosome (2) The Centrosomal Torus

During modelling a unique centrosomal vesicle was identified (Figure 3.33), which would not have been possible to discern adequately with conventional ultrastructural analysis. During tracing it revealed itself to be a circular 'tubular' or annular structure occupying an orbital equidistant 'toroid' volume in a zone midway between the basal body and the proximal centriole (Figs 3.32 A-K, blue outline and 3.33 A, B and G) . Although the structure continued out of section, it was called a torus. The 'Torus' was found to be tubular in structure, spanning a lateral zone of the centrosome with bud like protrusions located at one end, and a larger 'vesicle' at the other (Figure 3.33 G). The membrane protrusions were associated with a prominent field of interacting smaller vesicles, including a larger

vesicle which was attached by fine linkages to the torus membrane (Figure 3.33 C and D). This zone is prominent in its association with a larger field of pre-Golgi vesicles. Perspectives of the torus are seen (Figure 3.33 G-K) in relation to the basal body and proximal centrioles, where interactions with their pericentriolar environments are also seen ultrastructurally (Figure 3.33 E and box, F), with deposits being noted upon the membrane. These were not modelled as they were outside the scope of this study. However a microtubule nucleation site upon the torus membrane was identified (seen in Figure 3.33 E, I, J and K). The torus was also found to interact with a microtubule derived from basal appendage two (BA2) which spanned the centrosome to connect with arrays of pre-Golgi vesicles (Figure 3.33 A and K). The torus was found to contain the smallest amount of internal contrast of any vesicle within the tomogram (Figure 3.33 E and F).

3.34 The Centrosome (3) The Pericentriolar Environment

The pericentriolar environment consists of fine amorphous materials which decorate the surface of centrioles and interconnects them at their negative microtubule ends. This inter-connective region was found to be bound by the torus vesicle (Figure 3.34), with the centrioles radiating in a series of fine filaments linking these structures. A densely stained deposit was also found within this region (Figs 3.35 E and 3.35 E'), although this area was not investigated further. The pericentriolar zone was found to be the focus of short lengths of intermediate filaments focussed around the proximal centriole. Longer filaments were observed to radiate from this area, one to the pre-Golgi zone, another toward the cell membrane.

3.35 The Centrosome (4) Basal Body, Proximal Centriole within the MTOC

Selected detailed ultrastructural perspectives of centrosomal components interlaced with the wireframe of the model aid in revealing the confined nature of the centrosome, the basal body and proximal centriole and the relationship between the materials and vesicles surrounding them (Figure 3.35 A-E). The close proximity of the torus to the centrioles and nearby associated vesicles and microtubules should be noted. Electron dense materials upon the proximal end of the proximal centriole were modelled interacting with the torus and nearby vesicles (Figure 3.35 F). The basal appendages show distinct clusters of microtubule associated vesicles surrounding their docking heads, in close proximity to the basal body and transition zone membrane. Intermediate filaments (green) originated from a zone around the proximal centriole (Figure 3.35 F) (also identified in Figure 3.34 D and E). The composite model image of the centrosome (shown in Figure 3.35 F) is comparable to the optical slice of the tomogram stack visualised in Figure 3.8.

3.36-3.40 The Cytosolic Microtubules; Centrosome to Golgi Connectivity; The Cis-, Medial- and Trans-Golgi Compartments; Transport of Matrix from the Golgi

The majority of microtubules identified within the tomogram were physically associated within, and originating from, the centrosome and the basal appendages. Many of those that were traced originated out of the tomogram section, but were aligned to intersect with the centrosome, suggesting that they radiated from the greater pericentriolar zone surrounding it. Independent microtubules were found freely existing within the cytoplasm associated with local structures (or associated with the Golgi apparatus). Many of these were observed attached to vesicles or decorated with finer structures. A high degree of connectivity between microtubules and the Golgi apparatus was observed. A cluster of aligned microtubules was found to run parallel with the pre-Golgi *cis*-face (in the direction of the centrosome), and were involved with a large vesicle field (Figs 3.36 I-L and 3.37 B). Both basal appendages had microtubules interacting with the pre-Golgi and the *medial* cisternal stacks (Figure 3.37 B and D). An intermediate filament was also found running parallel to microtubules involved with the pre-Golgi vesicles (Figure 3.38 K). The Golgi itself was traced out, and modelling divided into *cis*-, *medial*- and *trans*-compartments. These were surrounded by an assortment of vesicles, which were in close proximity to the centrosome, and the cell membrane. The compartments consisted of a series of layers of perforated stacks, forming a highly aligned structure interspersed with smaller vesicles budding around their edges (Figure 3.38 A-J).

Unidentified materials were observed within some of the Golgi vesicles, and these were also accumulated in larger vesicles near the *trans*-face (Figure 3.39 A-B). These were surrounded by a transport process (Figure 3.39 C', E, F and F') involved with the cell membrane. Not far from these structures, the blunt tip of the primary cilium was found to be interacting with the cell membrane (Figure 3.40 A). Within this zone, numbers of clathrin-coated pits were identified in the process of undergoing receptor mediated endocytosis, with their contents being visible (Figure 3.40 B-D). These were modelled to reveal a series of active cell membrane processes in proximity to the Golgi and a number of tubular structures resembling endosomal transport conduits [1000] (Figure 3.40 A). A Caveoli like structure was identified in (Figure 3.40 E and E').

3.41-3.42 The Complete Model: The Matrix Cilium Golgi Continuum

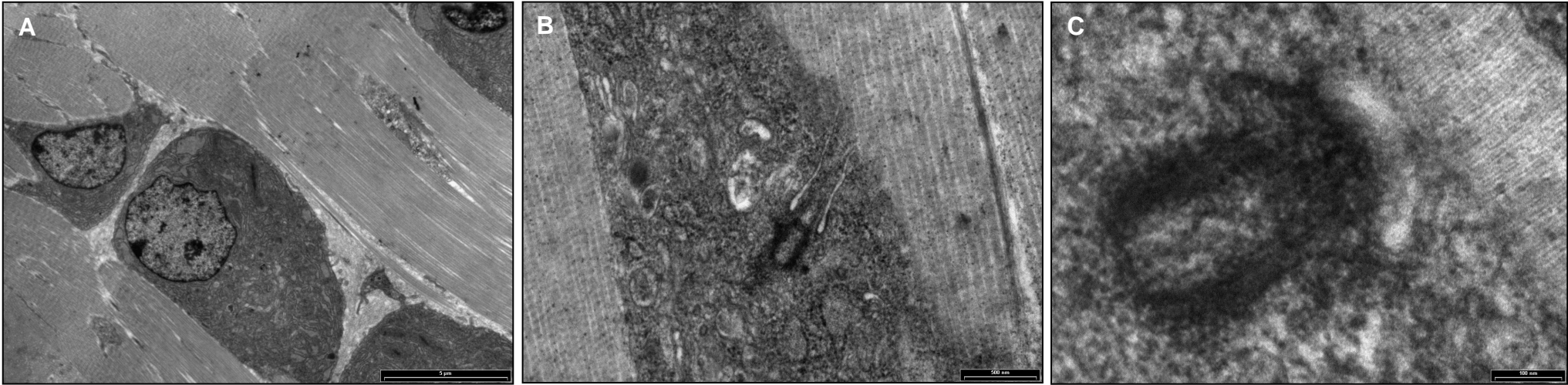
The full model of the chondrocyte primary cilium is illustrated in Figs 3.41-3.42. This details the extracellular matrix interacting with the primary cilium, the anatomy of the axoneme, the centrosome and the centrosomal connectivity to the Golgi apparatus. A tight physical continuum exists between the extracellular environment, the primary cilium, the centrosome and the Golgi apparatus, which makes possible the regulated processing and orderly exocytosis of the correct materials for maintaining a bio-mechanically functional extra-cellular environment.

3.43 The Continuum: The Cilium and Centrosome

The Cilium-Centrosome-Continuum is illustrated in Figure 3.43, which overviews the details of the ciliary axoneme, stemming from its distal tip to the adjoining centrosome. The unique microtubular architecture of the cilium is revealed, along with its internal cargoes and extra-cellular interaction with the matrix and a coated pit. The basal body is firmly tethered by basal appendage to radiating microtubules, and is also supported by the centrosome and proximal centriole. Some structures have been omitted for clarity. Detailed are the core microtubule based structures of the cilium, proximal centriole, and microtubule ‘interactome’ of the centrosome. This is the first three-dimensional reconstruction of a primary cilium at high resolution. It forms a template for the assignment of function to the described structures.

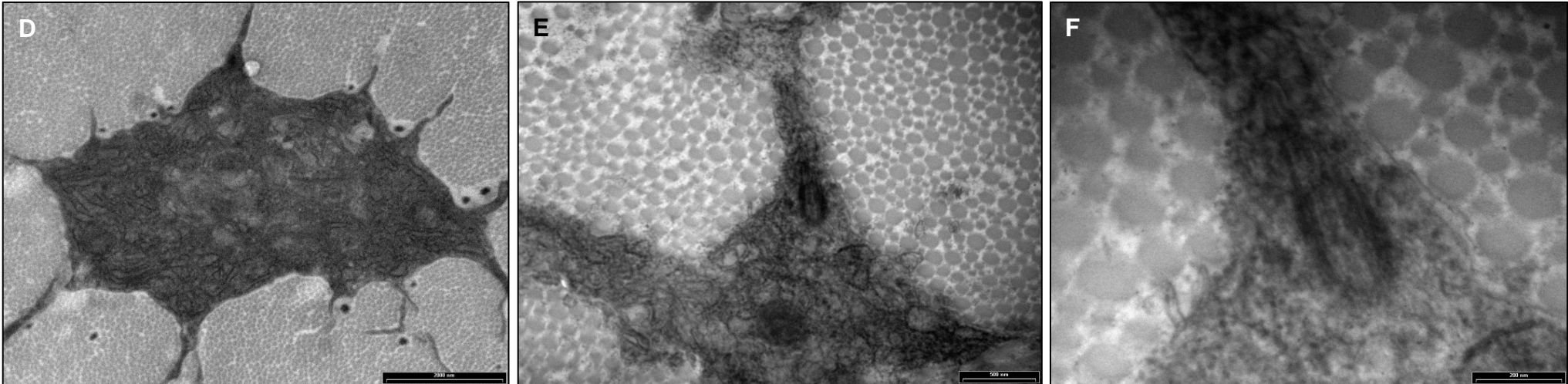
Figure 3.1 Connective Tissue Primary Cilia Sectioning of Tendon

Flexor Tendon Longitudinal Sectioning



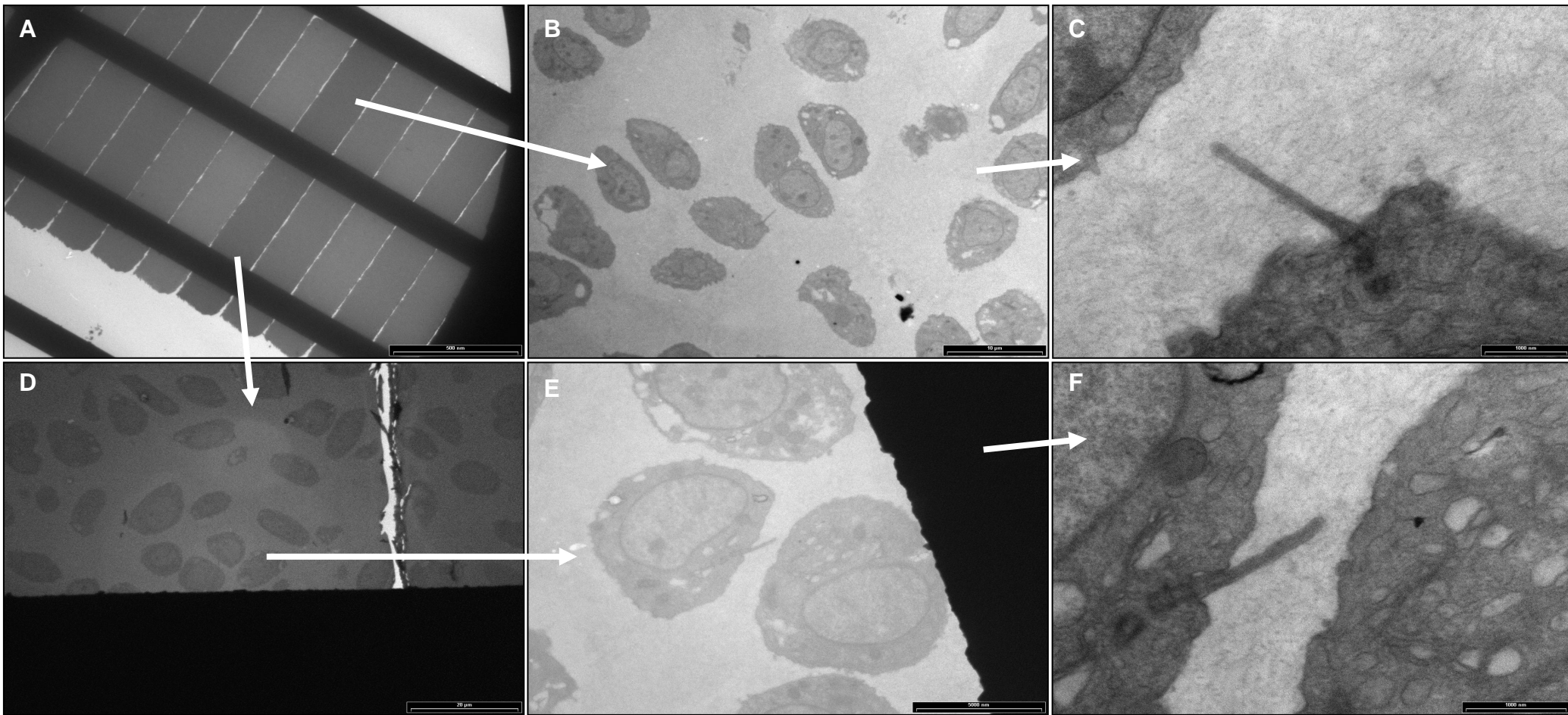
[A] Flexor tendon longitudinal sections, showing tenocytes amongst aligned collagen fibre bundles. Cilia were found to be highly deflected by the collagen fibres [B, C].

Flexor Tendon Transverse Sectioning



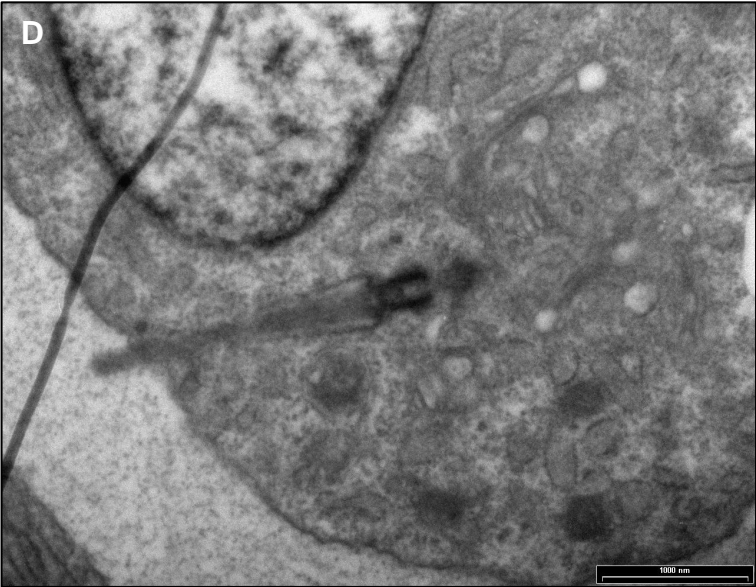
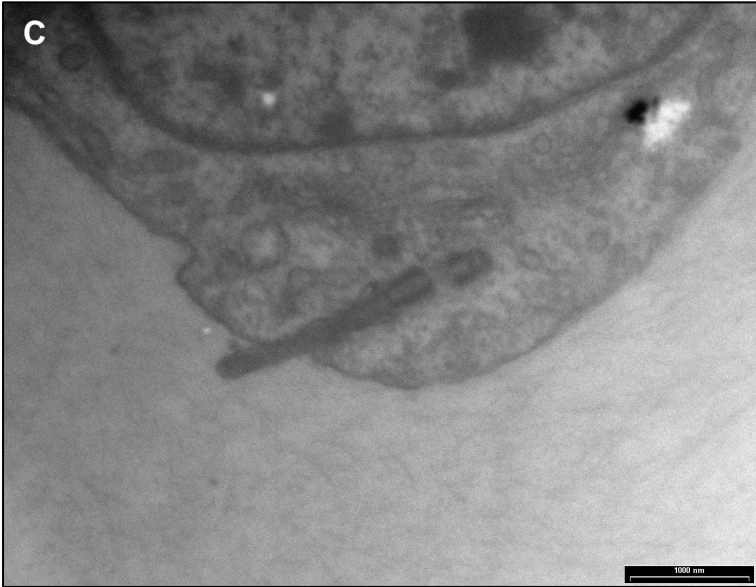
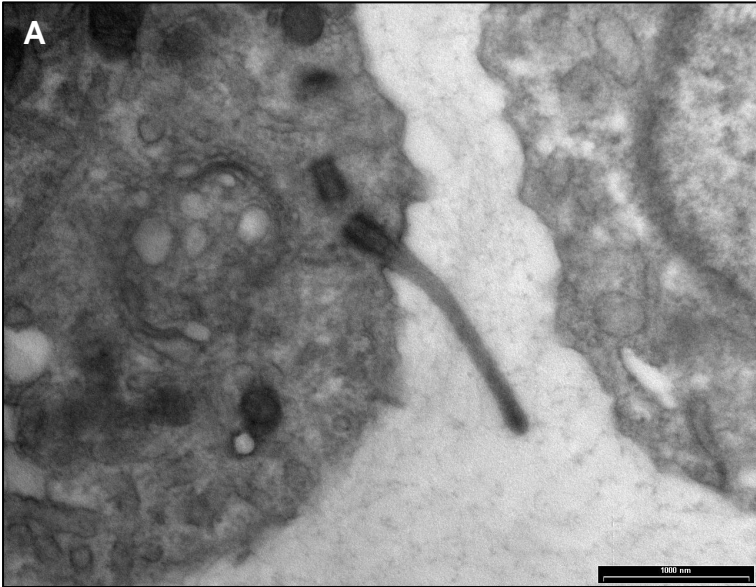
Cross section of a tenocyte surrounded by columnar collagen bundles [D], with cellular processes extending into gaps around the edges [E] along with a primary cilium [F].

Figure 3.2 Serial Sectioning of Chick Sternal Cartilage



Chick sternal cartilage semithick serial sections [A, D] containing primary cilia aligned within the section [B, C, E and F]. Scale bars [A] 500 μm , [B] 10 μm , [C], 1 μm , [D] 20 μm , [E] 5 μm and [F] 1 μm .

Figure 3.3 Projection Types of Chondrocyte Primary Cilia

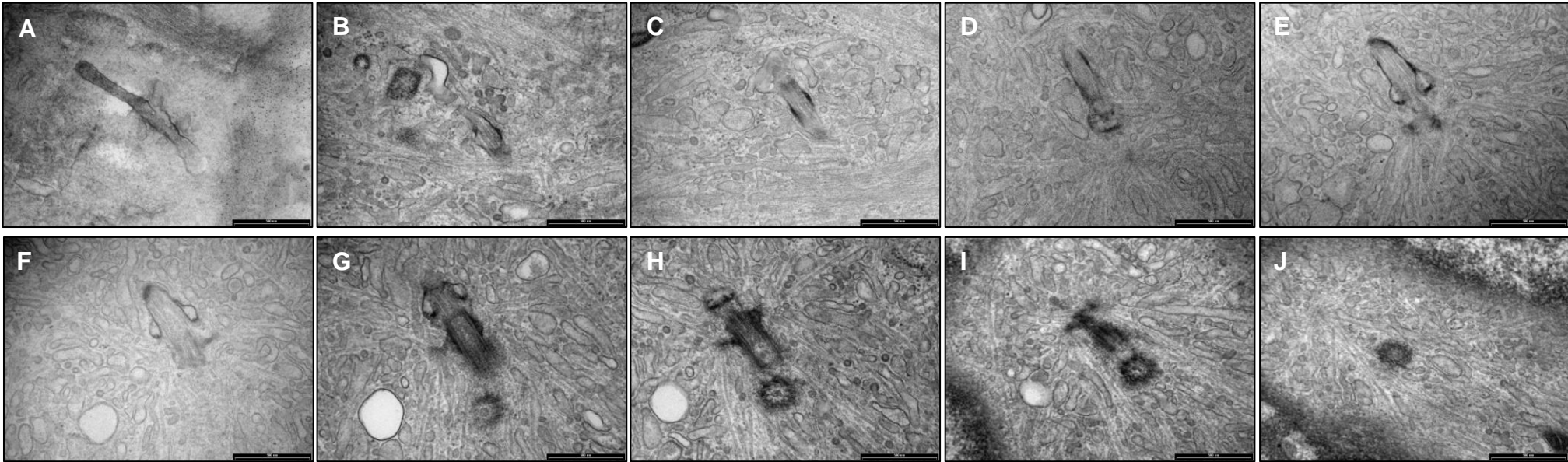


Conventional electron microscopy staining of sternal cartilage with OsO_4 and *en bloc* uranylacetate [A] in comparison to the Ruthenium Hexa-amine Trichloride (RHT) treatment [B], revealing an extensive matrix granule network, and stabilisation of the cell membrane seen in [B-D]. Cilia were found to displaying three classical projections; fully extended from the cell membrane [A], reclined against the membrane in a localised pocket [B], or partially or fully retracted into the cell [C and D].

Scale bars [A, C and D] 1 μm and [B] 0.5 μm

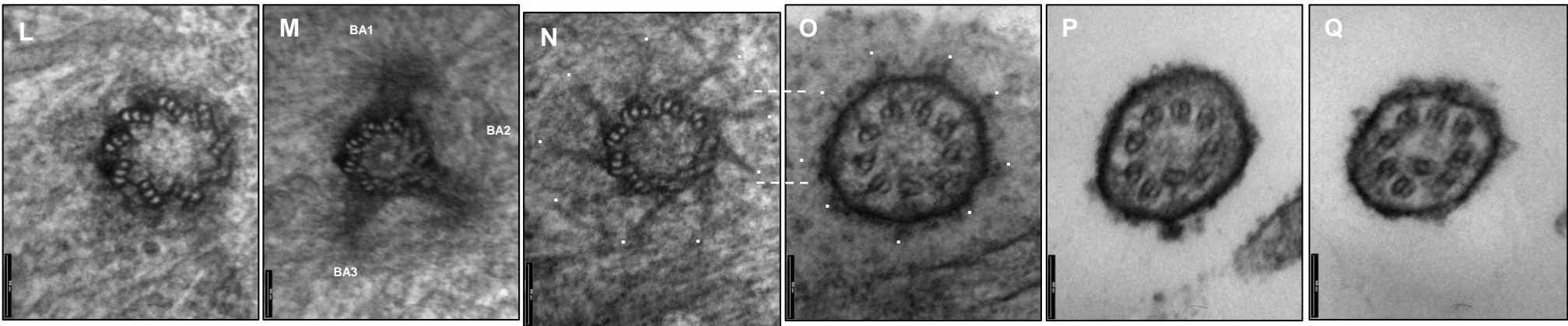
Figure 3.4 Cilium-Centrosome Serial Sectioning of Cultured Chondrocytes

Longitudinal Serial Sections



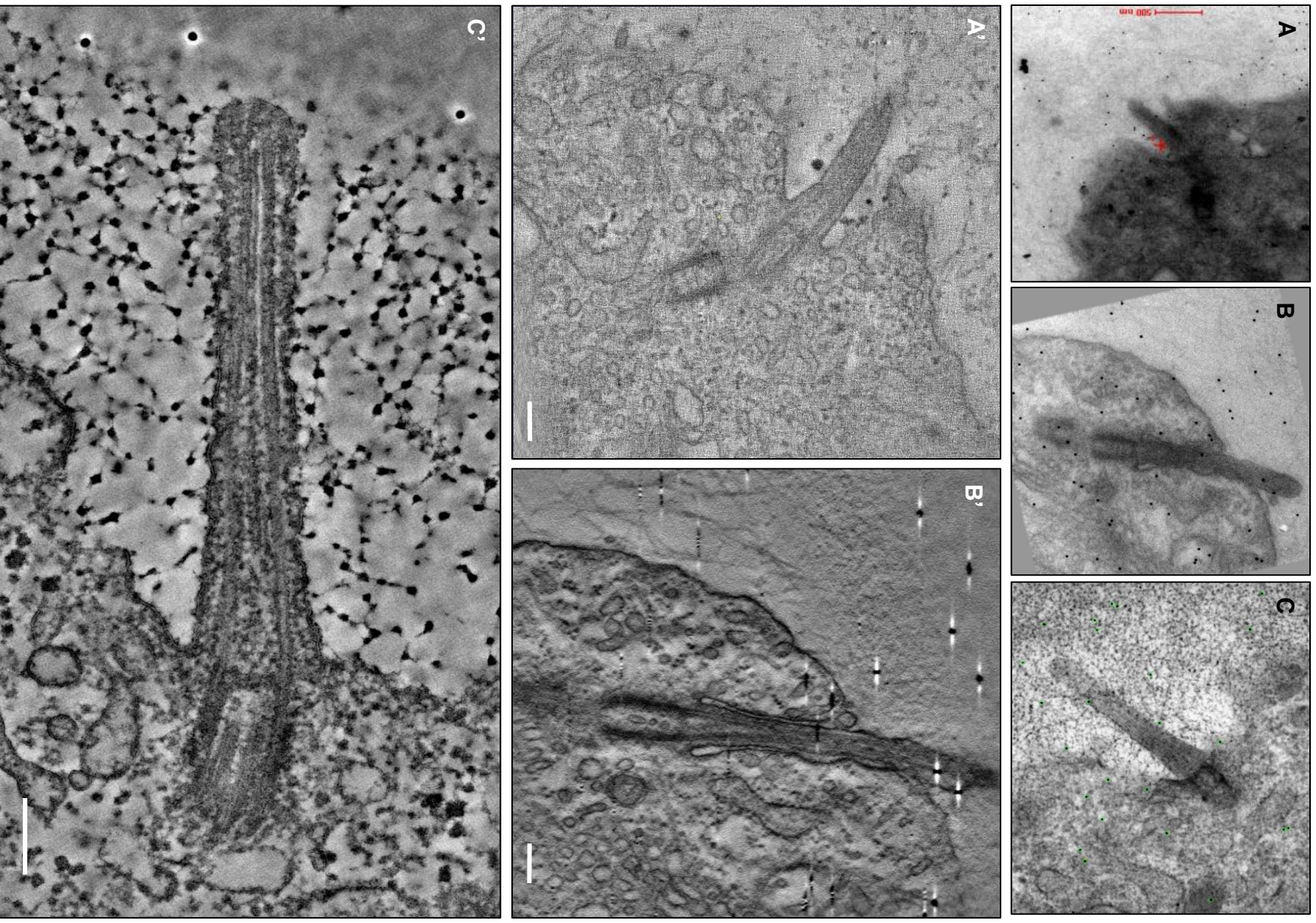
Longitudinal ultra-thin serial sections of cultured chondrocytes showing the cilium aligned in parallel with the substrate [A-J]. Note [A, D] shows the cilium extended, sheathed by the ciliary pocket and projected from the basal body, whose appendages [H] are attached to cytosolic microtubules. Closely subtending the basal body is the proximal centriole [G-J] making up the diplosome. Scale bar 0.5 μ m.

Transverse Serial Sections



Transverse serial ultra-thin sections of a basal body (in the + microtubule direction) [L-Q] showing the triplet subfibre structure [A] with attached basal feet (BA1-3) [B], the alar-sheet fibres [N] tethering individual subfibres to the transition zone membrane [O]. Note the presence of y-shaped linkers [O-Q] linking microtubule doublets to the axonemal membrane as they incline inwards in their projection. Scale bar 100 nm.

Figure 3.5 Selection of Tomograms and their Z-Axis Optical Sections



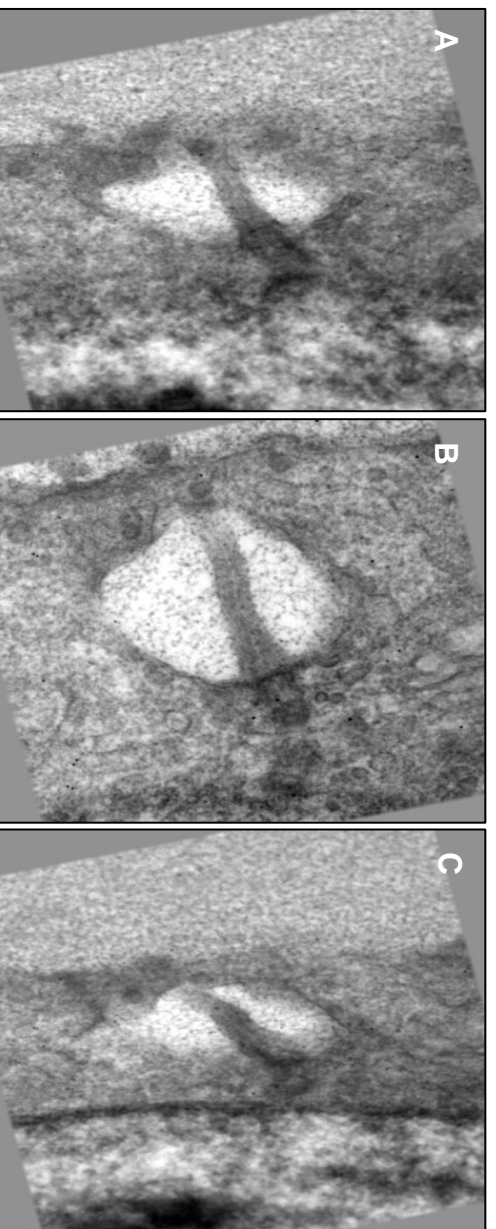
Select tomograms of chondrocyte cilia labelled with fiducial markers [A-C] and their corresponding optical slices [A',C']. Note poor contrast of single axis tomograms in [A'] in comparison to [B'] and dual axis reconstruction [C']. Note collagen fibres within the ECM [A', B'] and increased contrast and resolution from Ruthenium staining in [C'] showing connectivity between matrix granules and membranes. Also note three small luminal vesicles contained within the basal body of image [B']. Scale bars 200 nm.

Figure 3.6 A Semithick Section Containing a Primary Cilium



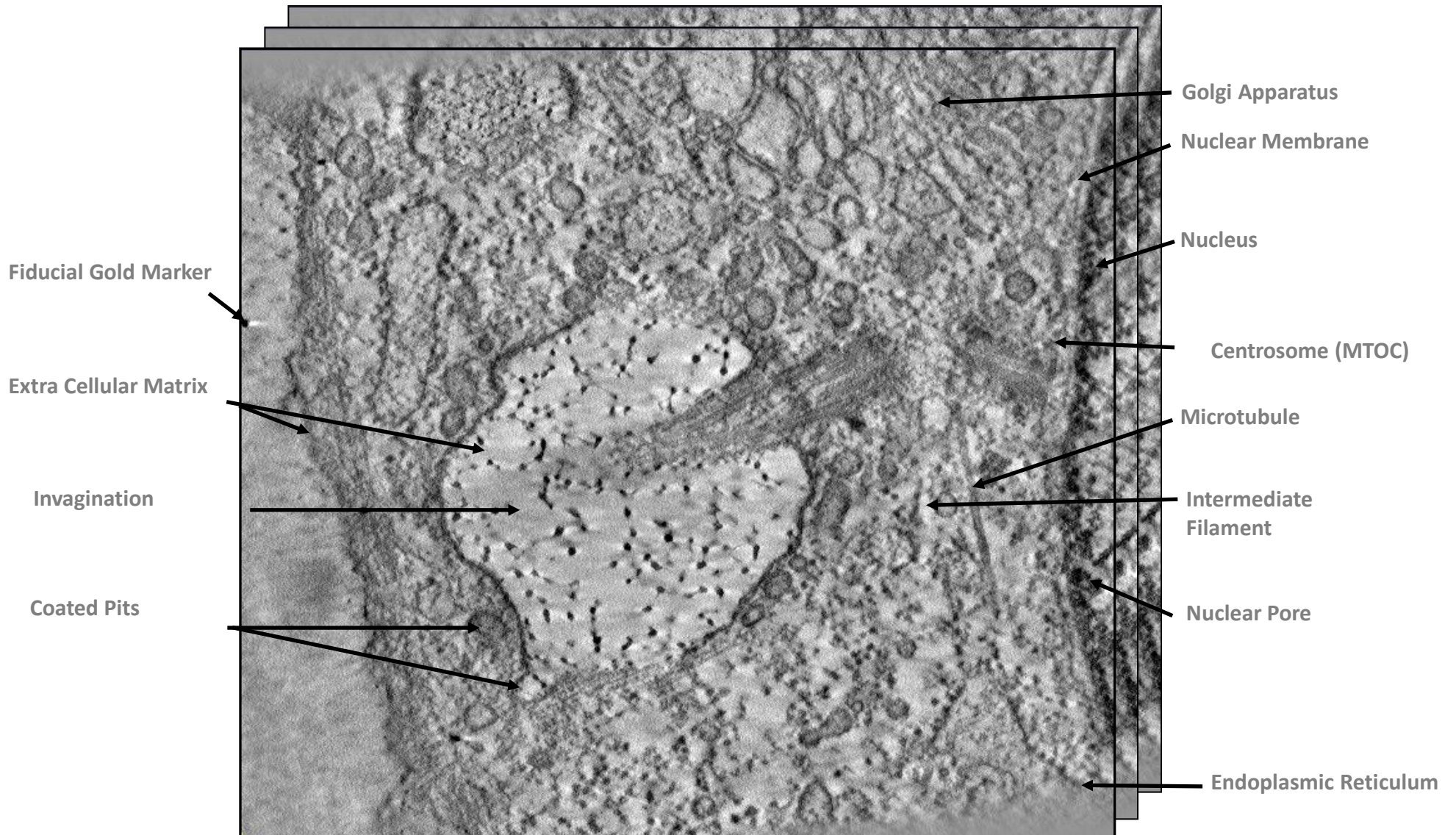
A 100 kV image of a 350 nm semithick section of a chick sternal chondrocyte fixed in Ruthenium Red/OsO₄ with *en bloc* uranyl acetate. The cilium is located within an invagination (similar to the ciliary pocket) in the cell membrane which contains a uniform but highly stained matrix comprised of matrix granules (in comparison to the pericellular matrix). Note the thicker section image characteristics (in comparison to ultra-thin sections) with less clarity due to heavy staining.

Figure 3.7 Alignment of Tomogram Dataset



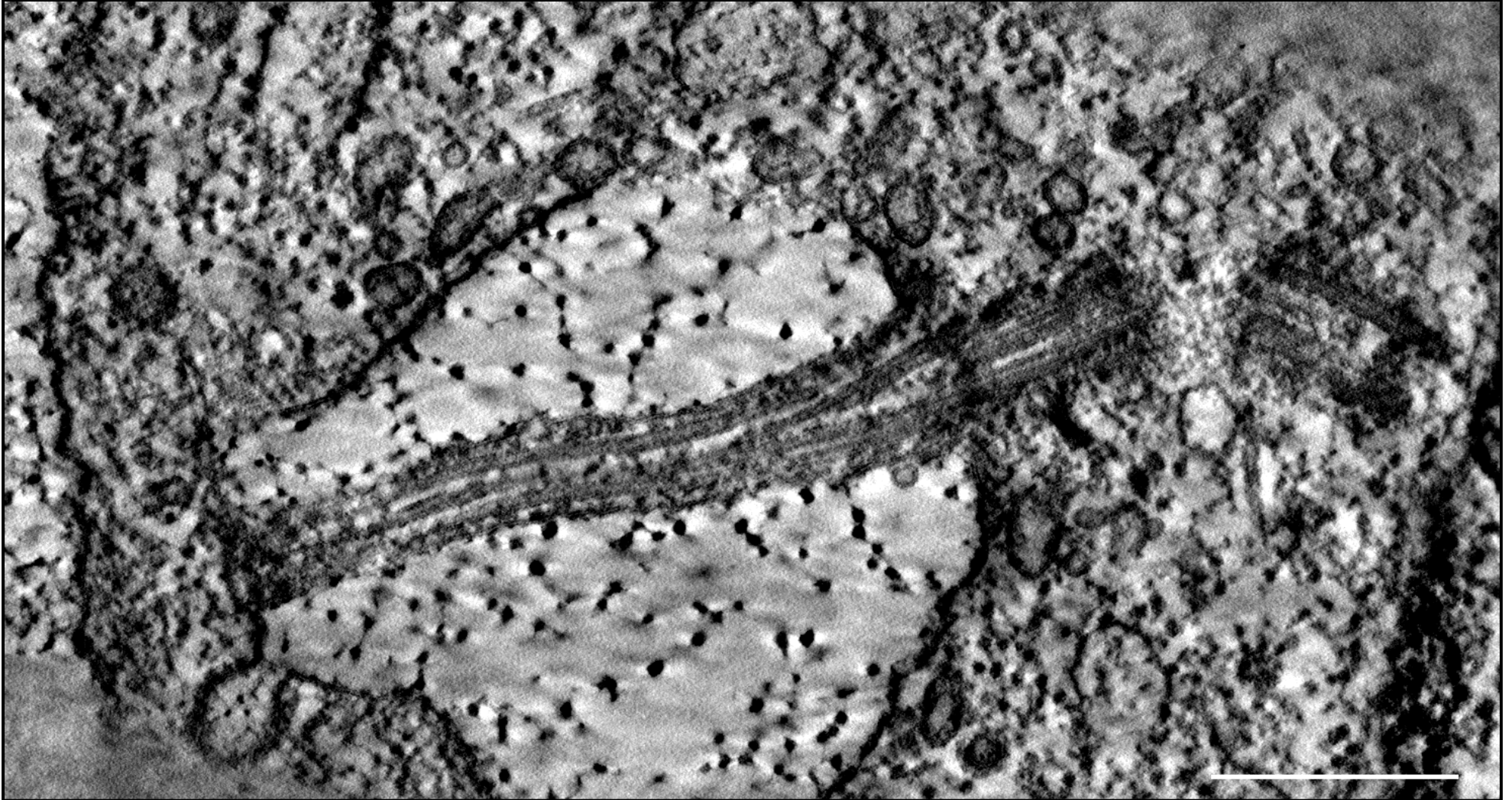
Aligned tilt series images of from full negative to full positive tilt [A-C]. An animation of this sample, <TiltSeriesB4-3.avi> is detailed in Appendix VII, Section 7.1

Figure 3.8 Tomogram Z-Axis Stack



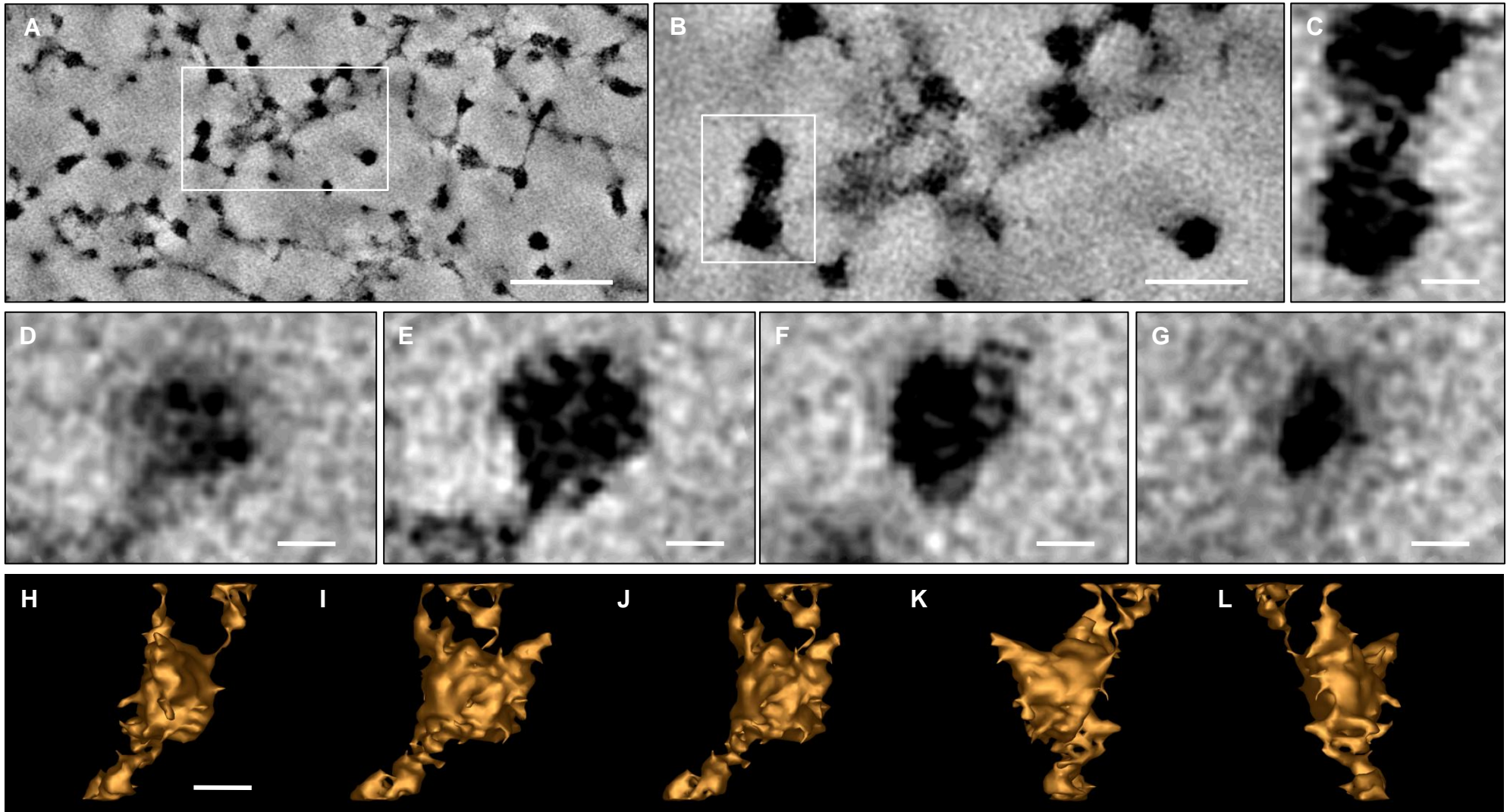
A series of optical sections showing features of the extra-cellular matrix, cilium and the Golgi apparatus as well as the nearby nuclear membrane. Visualisation of this stack is contained in movies <StackTomogramB4.avi, StackAxoneme.avi and StackCentrosomeB4.avi>, detailed in Appendix VII, Section 7.3.

Figure 3.9 An Optical Section of the Cilium Axoneme



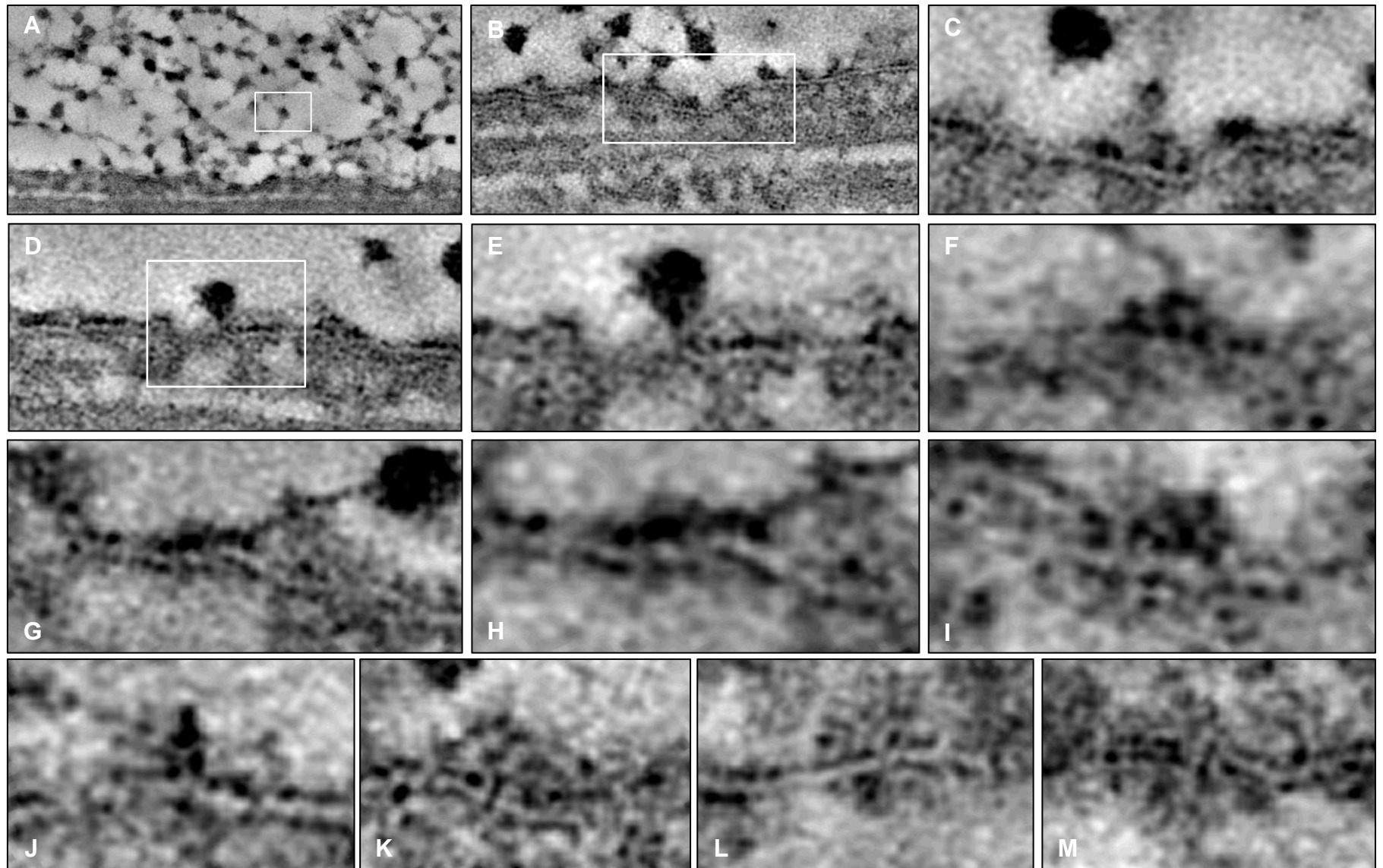
A slice through the tomogram aligned along the axis of the cilium showing the complete cilium and basal body, proximal centriole and detail of numerous processes. Scale bar 500 nm.

Figure 3.10 Tomographical Modelling of Extracellular Matrix and Matrix Granules



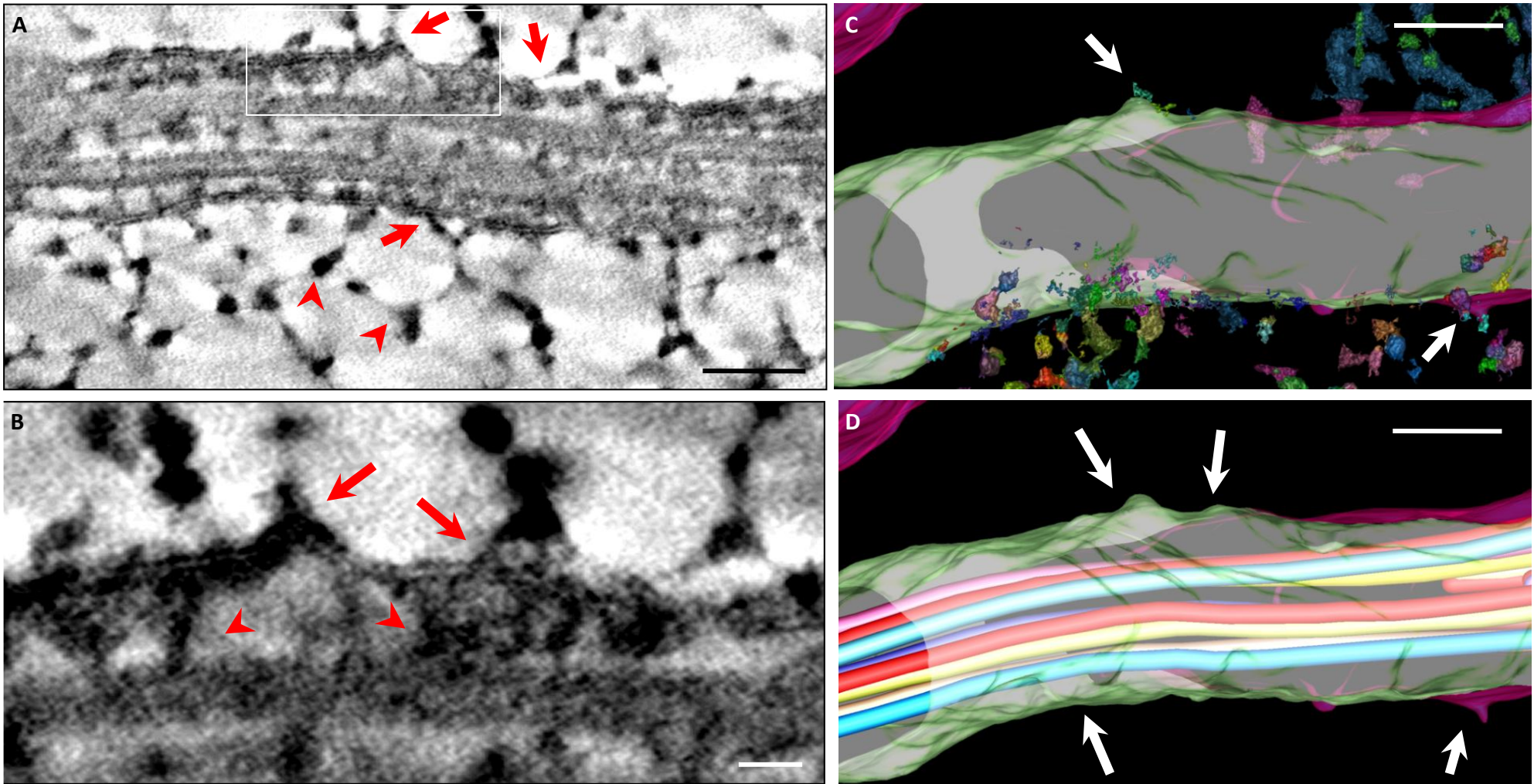
An optical section of extracellular ‘matrix granules’ [A], magnified in [B] and [C] (offset in z-axis). These are comprised of numerous tightly packed aggregates of smaller densely stained matrix components [C] which are inter-linked by fine filamentous fibres to at least 4 other granules within the matrix. [D-G] A series of slices of the matrix granule inset in Figure 3.11 [A] showing their fine structure and a series of rotations of the model based upon the granule [H-L]. Scale bars [A] 200 nm, [B] 50 nm and [C-L] 10 nm.

Figure 3.11 Matrix Ciliary Membrane Interactions



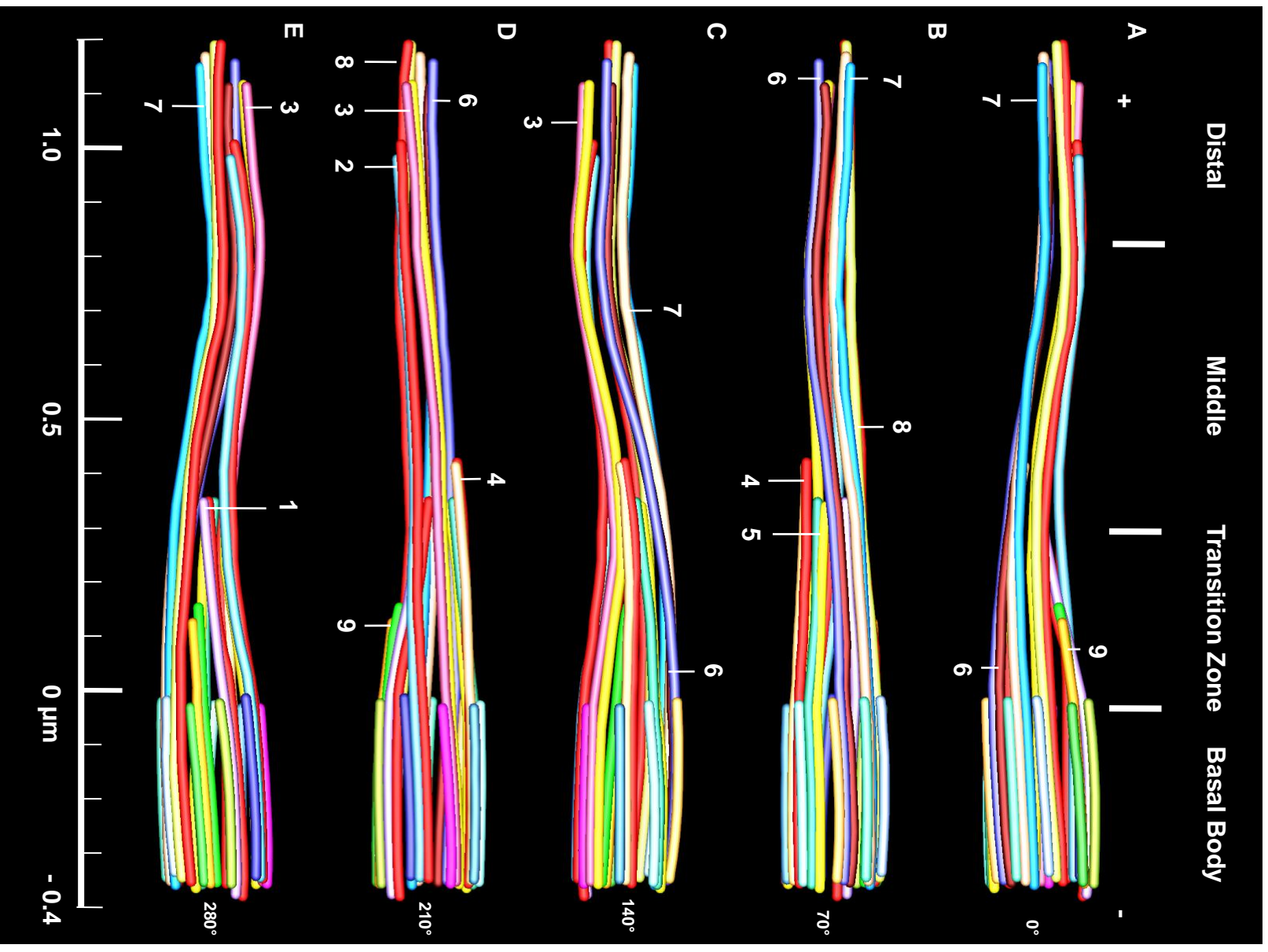
[A] An optical slice showing networks of highly filamentous interconnected matrix granules surrounding and linking to the ciliary axoneme (see Figure 3.14 [C']). A dimple in the membrane [B], which is seen enlarged and offset in the z-axis in [C] detailing attachment sites of unidentified extracellular components. [D, E] Detail of attachment of a matrix granule to the cilium membrane and [F-I] showing fibres to tethered to the lipid membrane [G], enlarged in [H]. [I, J] show the attachment of tethers with unknown membrane associated structures. Images [K-M] show numerous bound densities on both sides of the lipid membrane, some which span it. Scale: membrane thickness believed to be ~4.5 nm.

Figure 3.12 Matrix Ciliary Membrane Microtubule Interactions



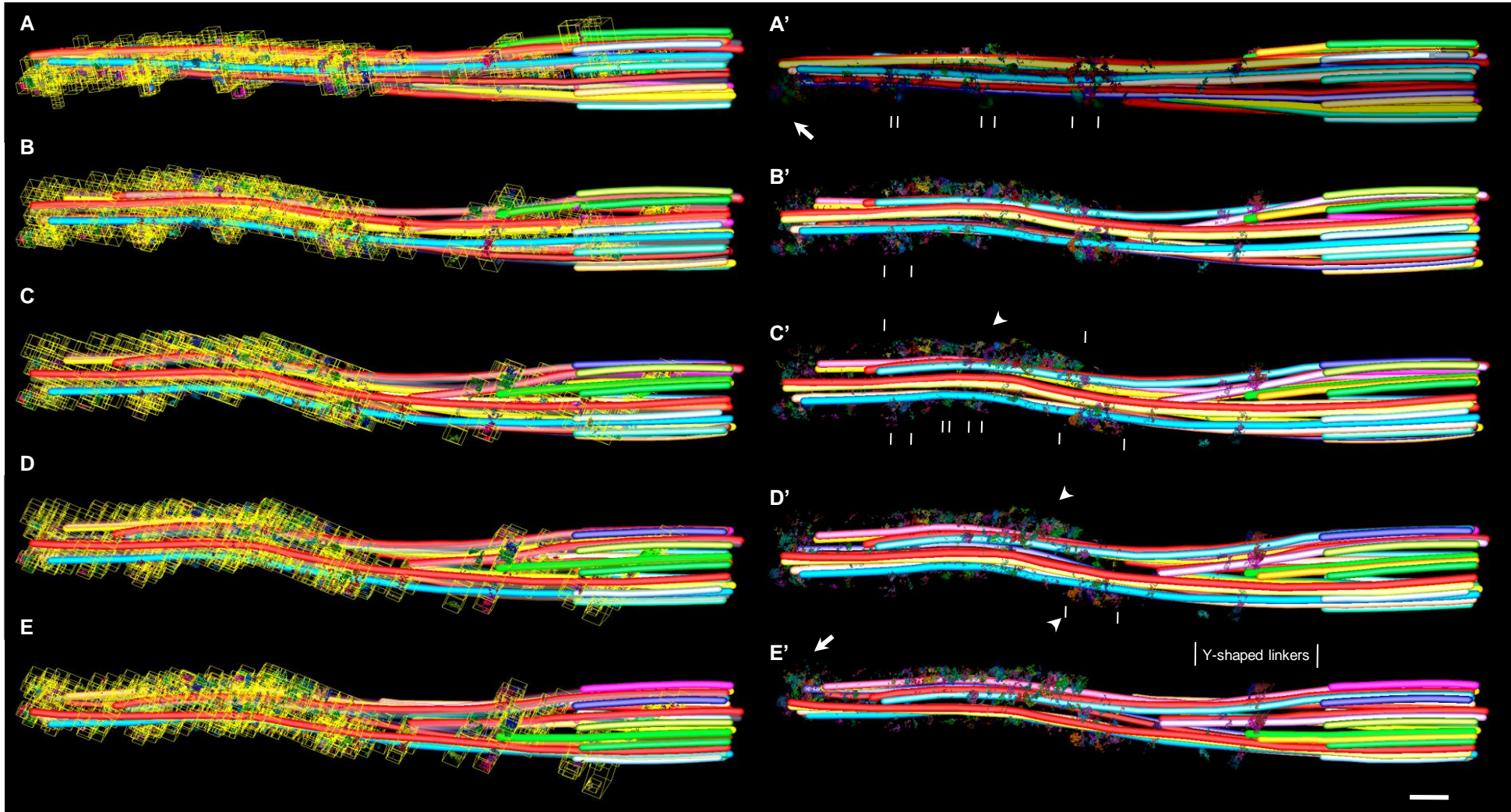
[A] An optical slice of the axoneme interacting with extracellular matrix granules (arrows) of aggrecan (arrowheads) which has been stained with Ruthenium Red. Each consists of multiple minor precipitates within each granule (see Figure 3.10). [B] Extracellular matrix granules interact with the ciliary membrane (arrows), and electron dense membrane associated proteins. Membrane to microtubule bridges connect the ciliary membrane to the microtubule doublets (arrowheads). [C] Components of the three dimensional aggrecan matrix were modelled interacting with the ciliary membrane (arrows). [D] The ciliary membrane is distorted from the combined forces of matrix connections (arrows) and bending of the microtubule core, causing dimpling and rippling of the membrane. Scale bar [A, C and D] 100 nm and [B] 25 nm.

Figure 3.13 Microtubule Doublet Nine-Fold Architecture



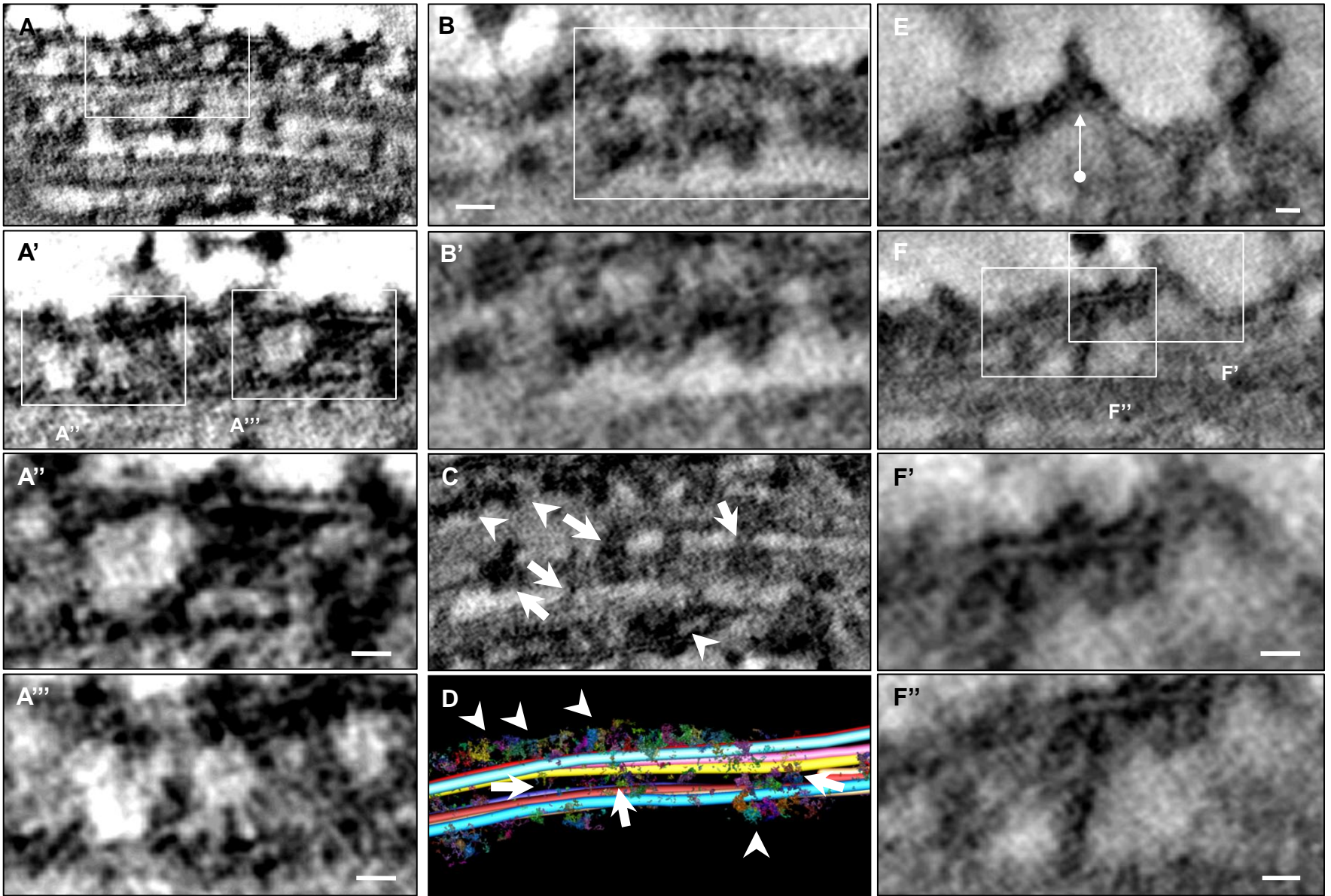
[A] The nine-fold microtubule architecture of the axoneme was traced out in 3DMod in the (-) to (+) microtubule subfibre direction. Each fibre is represented as a single object, individually coloured (for clarity) which are axially rotated in 70° increments [A-E]. Note the left handed inclination of the basal body which is translated in the projection of the microtubule doublets. Not all microtubule doublets reach to the end of the cilium, many are seen falling short (with an inward inclination) causing the tapered appearance of the axoneme. The following measurements were found: Maximum microtubule length of: 1.14-1.2 μm, Distal diameter: 0.12 μm, Medial diameter: (0.15 μm) and Transition Zone diameter: (0.18 μm). The Transition zone width (membrane to membrane) was found to be: (0.28-0.31 μm), while the Basal Body length was: (0.33-0.36 μm) and width found to be: (0.19-0.24 μm).

Figure 3.14 Localisation of Materials within the Axoneme



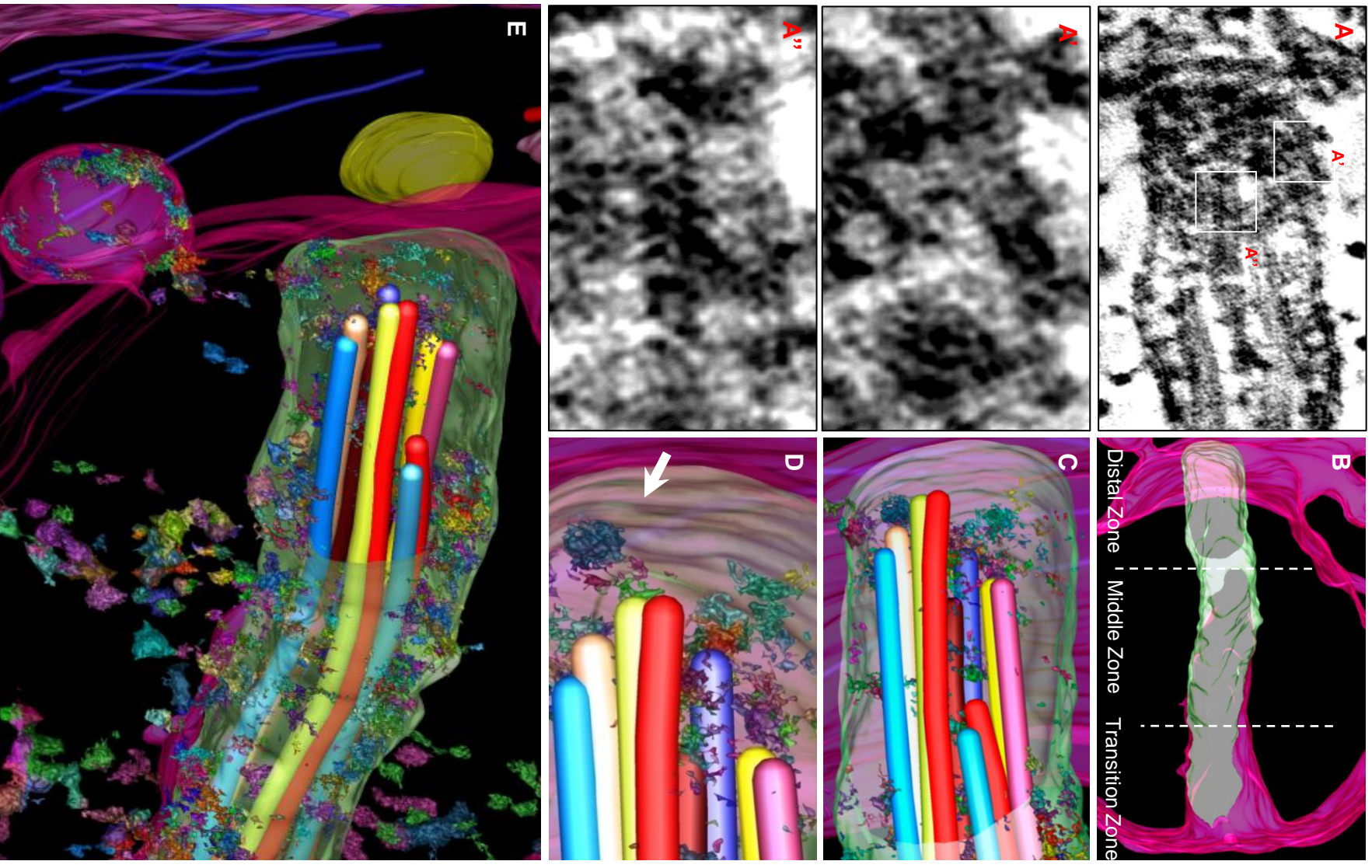
Localisation of yellow 3DMod iso-surface bounding boxes ([A-E]) of ciliary structures of interest which surround and attach to the microtubule doublets of the axoneme [A'-E']. Note some microtubules in series [A-E] are translucent to show details, whereas [A'-E'] are opaque. IFT trains and larger 'rafts' are indicated in [A'-E'] by '|' and arrowheads, with terminal tip associated deposits (arrows). Y-shaped linkers are seen surrounding the transition zone. Scale bar 100 nm.

Figure 3.15 The Luminal Axoneme: Intra-Ciliary ‘Rafts’ and Microtubule-Microtubule Interactions



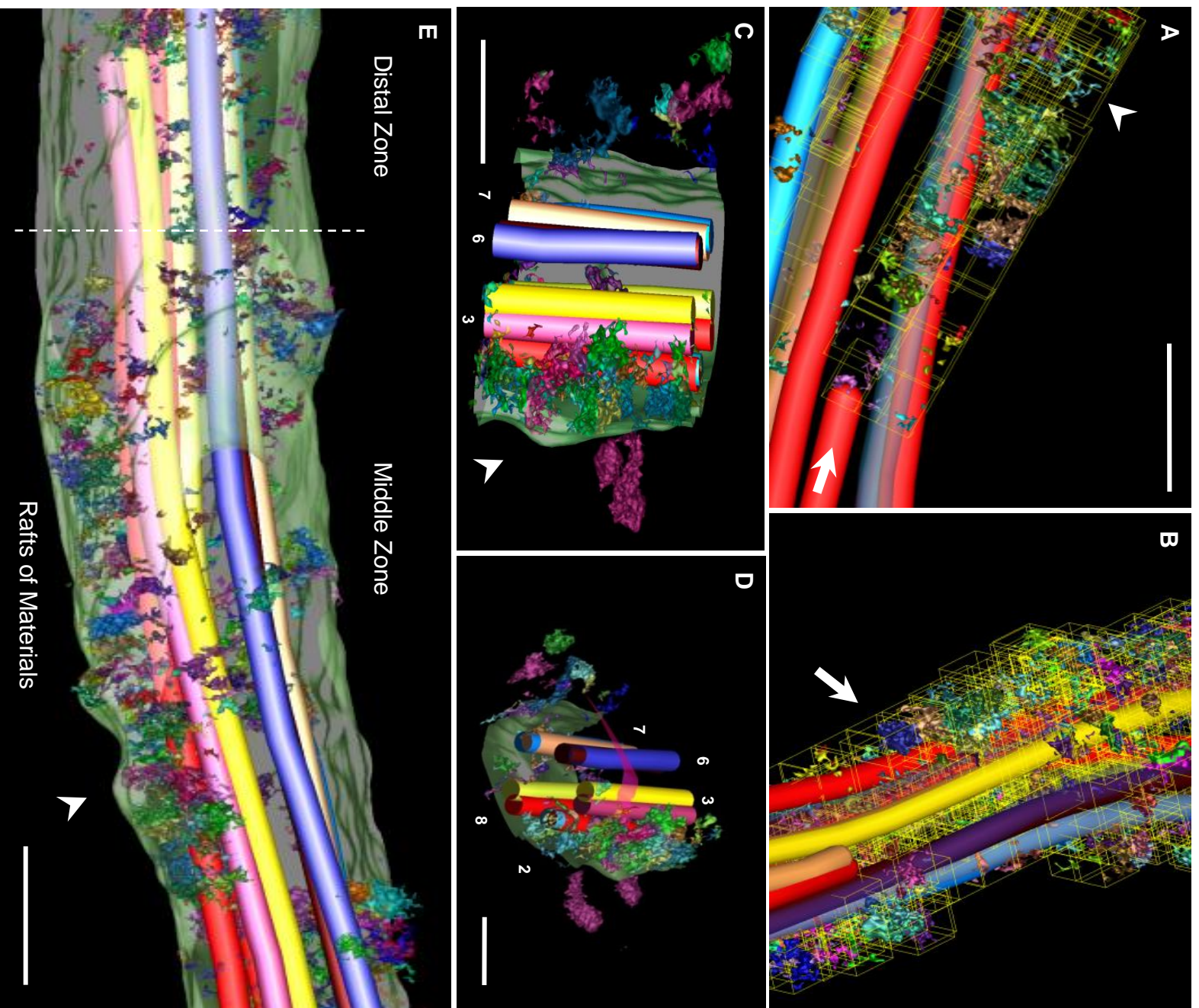
Ciliary luminal components [A] enlarged in [A' to A'''] showing densely stained unknown macromolecular complexes attached to the ciliary membrane and the nearby microtubule doublets. These were defined into two categories: 'linkers' which were seen connecting the ciliary membrane to the microtubules, and 'rafts' of densely stained materials which were grouped into the luminal space between membrane and some microtubule doublets. 'Rafts' of periodic electron dense deposits were found accumulated along some microtubules [B, B', C (arrowheads)] as seen in fully modelled in [D] (arrowheads). Microtubule to microtubule linkers are seen bridging doublets along the axoneme (arrowheads) in [C] and modelled in [D] (microtubules removed for clarity). Smaller unknown structures decorate ciliary lumen, microtubule faces and membrane surfaces [D]. A local matrix generated distortion in the ciliary membrane is seen (arrow), however with a noted lack of luminal components seen in nearby the vicinity [E]. A nearby linker [F] is seen connecting between the membrane and microtubule doublet, which is decorated along its length with finely stained components, while surrounding the both sides of the membrane attachment site dense complexes should be noted [F', F'']. Scale bars [A'', A''', B, E, F' and F''] 10 nm.

Figure 3.16 The Distal Axoneme (1)



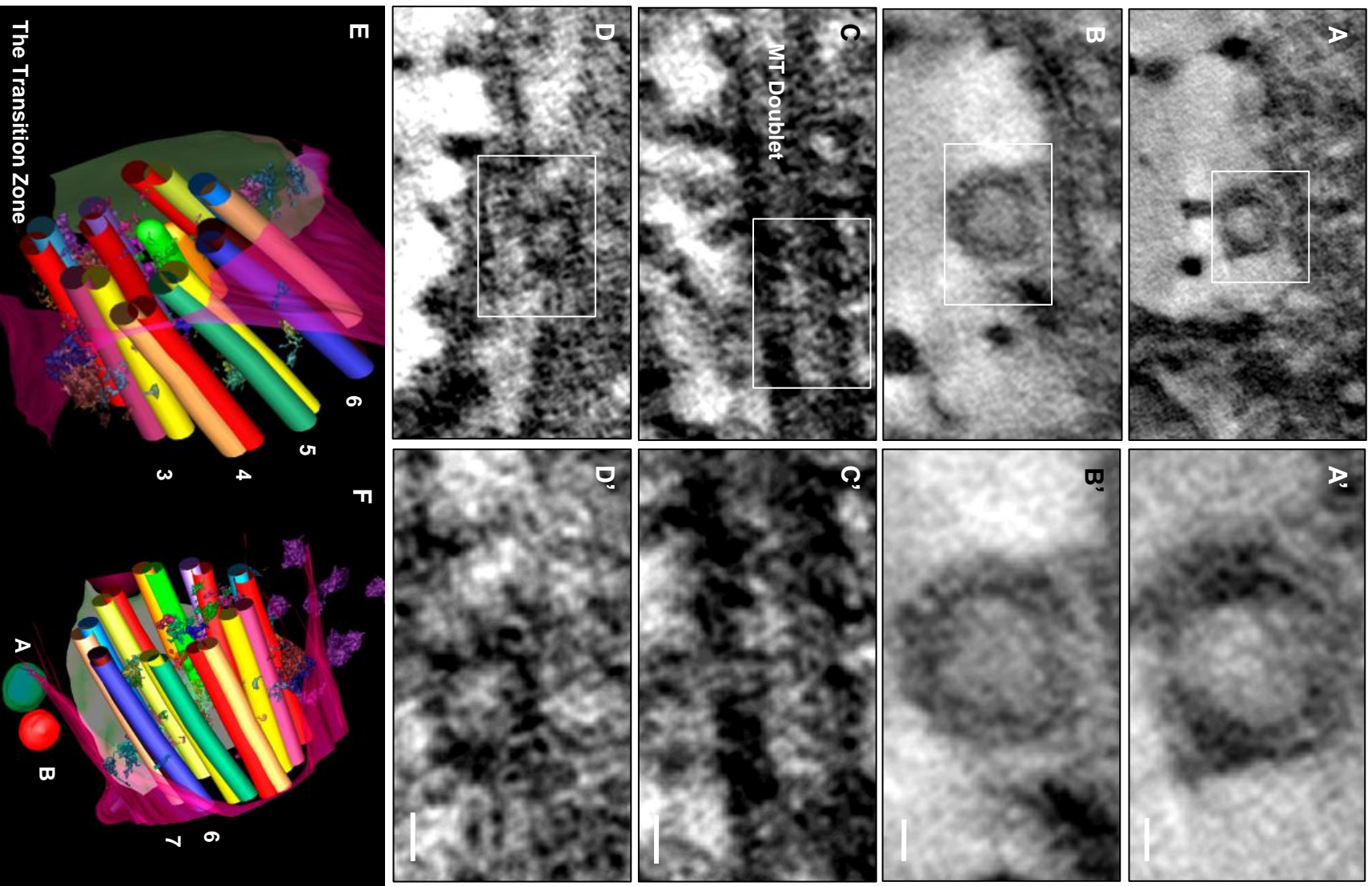
The cilium has been broken into three zones: The Distal zone, the Middle zone and the Transition zone [B]. The ciliary tip is located in close proximity to the cell membrane of the invagination (see Figure 3.9) [A]. Membrane associated densities were identified in [A'] in the terminal zone between the tips of the microtubule doublets [A'], which were found to contain materials at or near their terminal ends [A']. These were modelled in [C, D] (note overlap of structures may cause viewing confusion). Structures seen in [A''] corresponds to the dark blue microtubule in [D]. An oblique view of the model ciliary distal tip is seen in [E] detailing the terminal microtubule zone, the membrane tip and their associated densities. Interactions of the distal tip with the cell membrane, matrix and nearby coated pit should be noted.

Figure 3.17 The Middle Axoneme (2)



The middle axoneme consists of a longitudinal zone of longer gently tapering microtubules, seen with adjoining the distal tip in [E] minus the proximal membrane section (for clarity). Note the presence of periodic ‘rafts’ of densely stained materials (arrowhead) decorating the membrane and microtubules, microtubule to membrane / microtubule linkers and fine filaments. Yellow iso-surface bounding boxes designate individual model structures in [A, B (arrow)] which are enclosed by the ciliary membrane, including a membrane to microtubule linker (blue) seen in [A] (arrowhead). Cut away views of the axoneme are reminiscent of materials which would be contained within conventional 120 nm ultrathin serial sections (see Figure 3.4). Note intra-ciliary raft like deposits (arrowhead), numbered microtubules and nearby membrane associated extracellular matrix [C, D]. Scale bars [A, C, D and E] 100 nm.

Figure 3.18 The Transition Zone (1) – Tapered Zone



The transition zone represents the first domain where the cilium is projected from within the cell to interact with the extracellular environment. It is an area which the ciliary necklace has been noted [51] which consists of γ -shaped linkers connecting the microtubule doublets to the ciliary membrane (see Figure 3.4 N). Two small vesicles were found closely associated with the membrane whose diameters were normally comparable to some of the observed distances between matrix granules [A, B]. Microtubule doublets (MT Doublet) were found to be decorated with dense punctuations, with filamentous materials seen linking to the transition membrane [C and D]. Modelled in [E], and with opposed view [F] for vesicles A and B. Scale bars [A'-D'] 10 nm.

Figure 3.19 The Transition Zone (2) – Alar Sheets / Transition Fibres

Longitudinal views showing the cell to ciliary transition zone [A], with heavily stained membranes [B], y-shaped linkers [B'] and multiple fine linkages connecting membrane to the microtubules [B'' (arrow), C]. These are seen within the model interacting with the cell membrane and basal body triplets along with the sub-distal appendages [D]. The montage in [E (see A)] shows filaments originating around subfibres linking to the membrane. These are seen in close ups of the sub-distal zone as shown in [F and G] along with densities decorating the surfaces of the nearby basal body triplets. Alar sheets proved difficult to model [G] as they were stained diffusely, but can be seen attached to the transition membrane in [H, I]. Scale bars [B-C, E, H, and I] 20 nm.

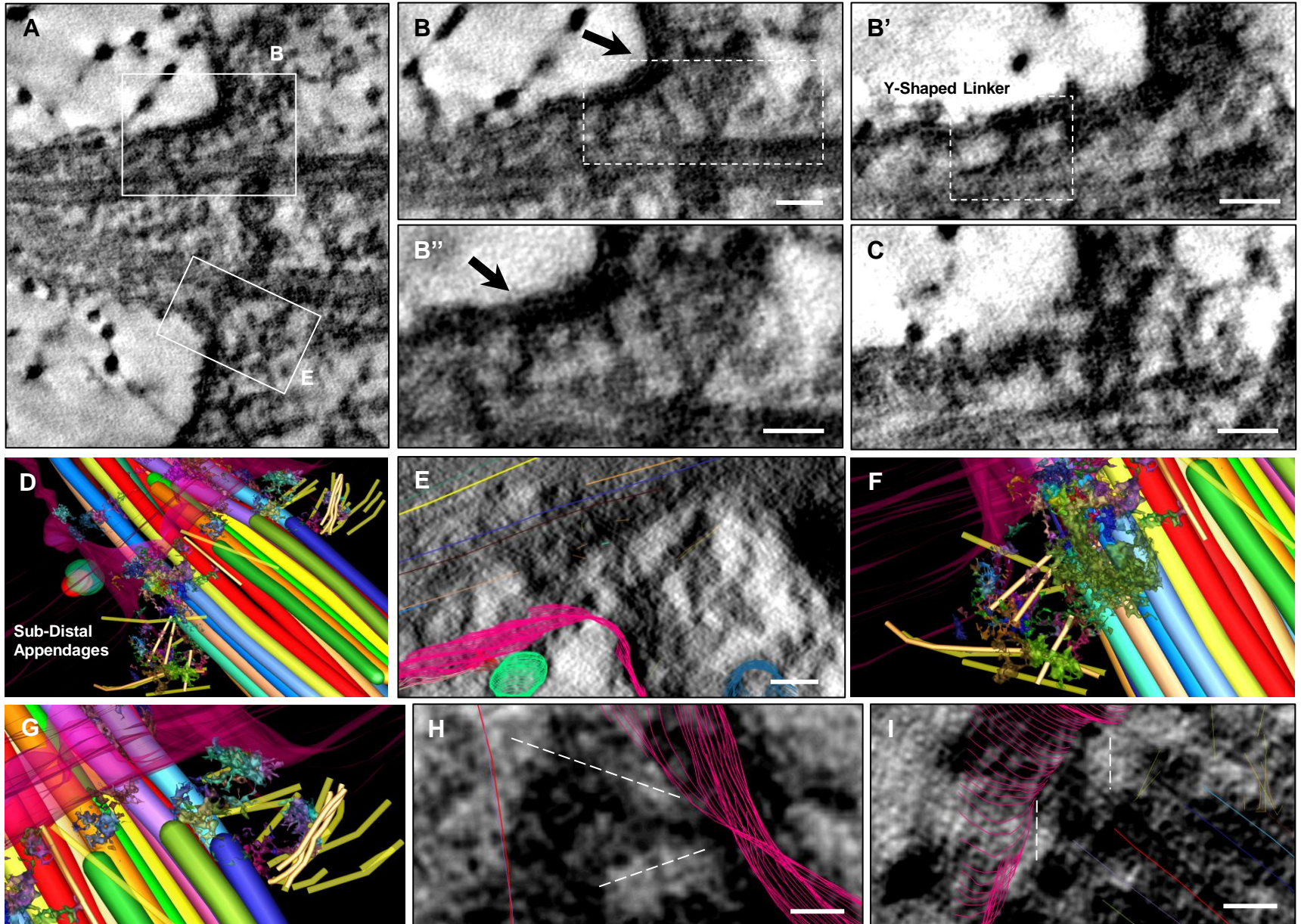
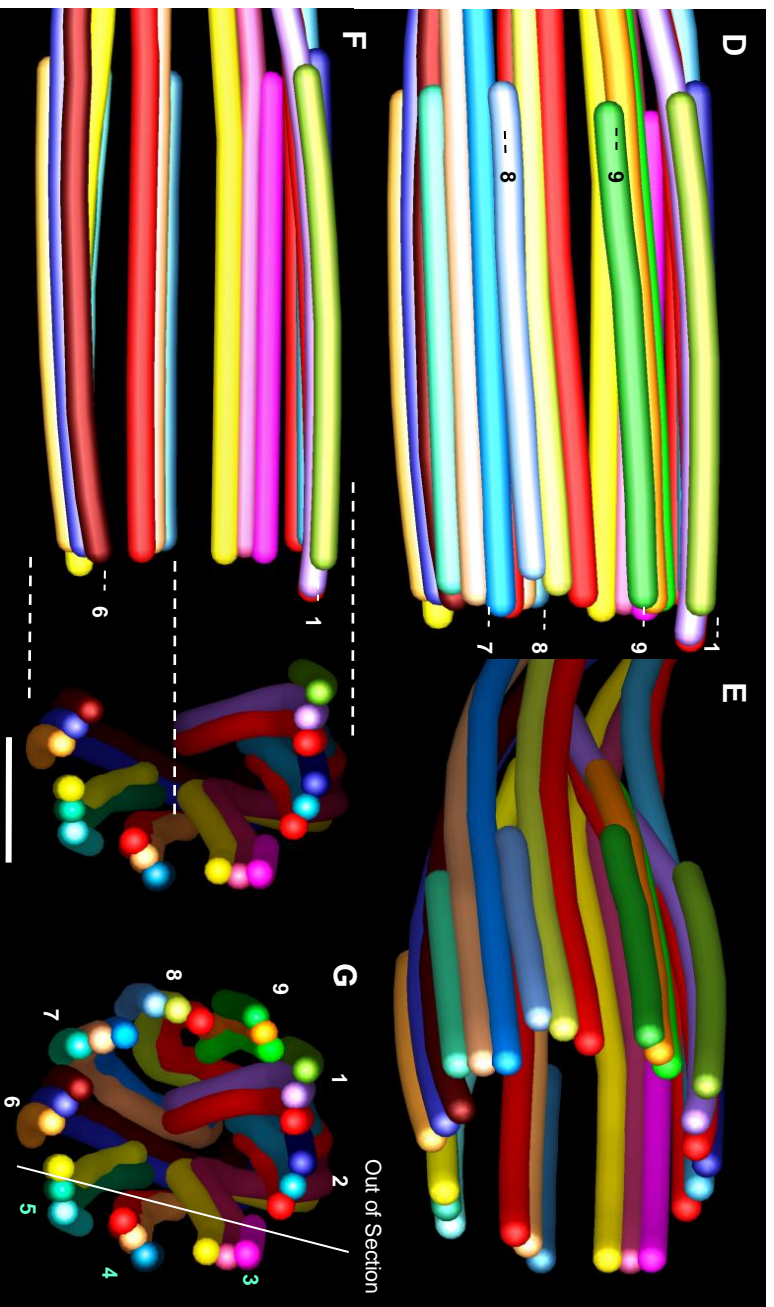
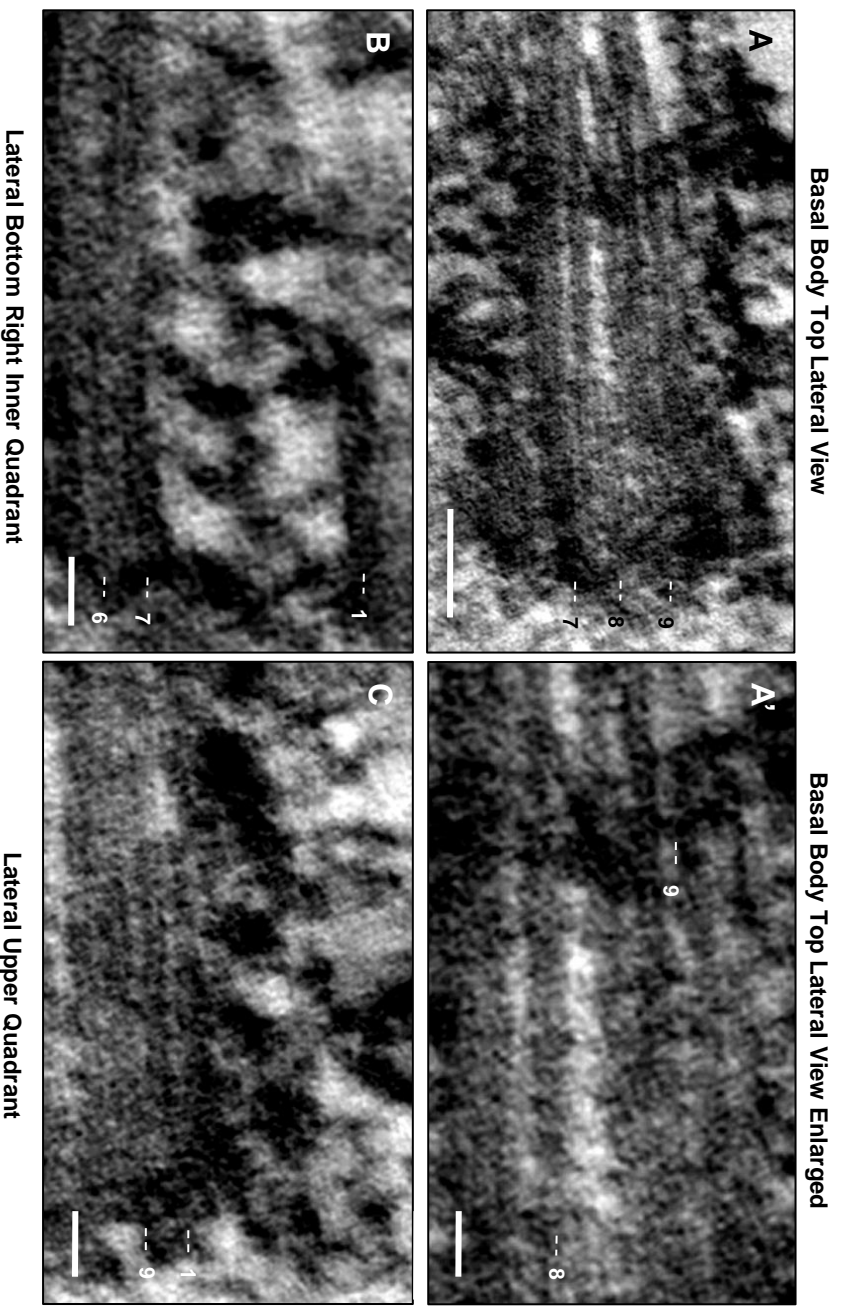
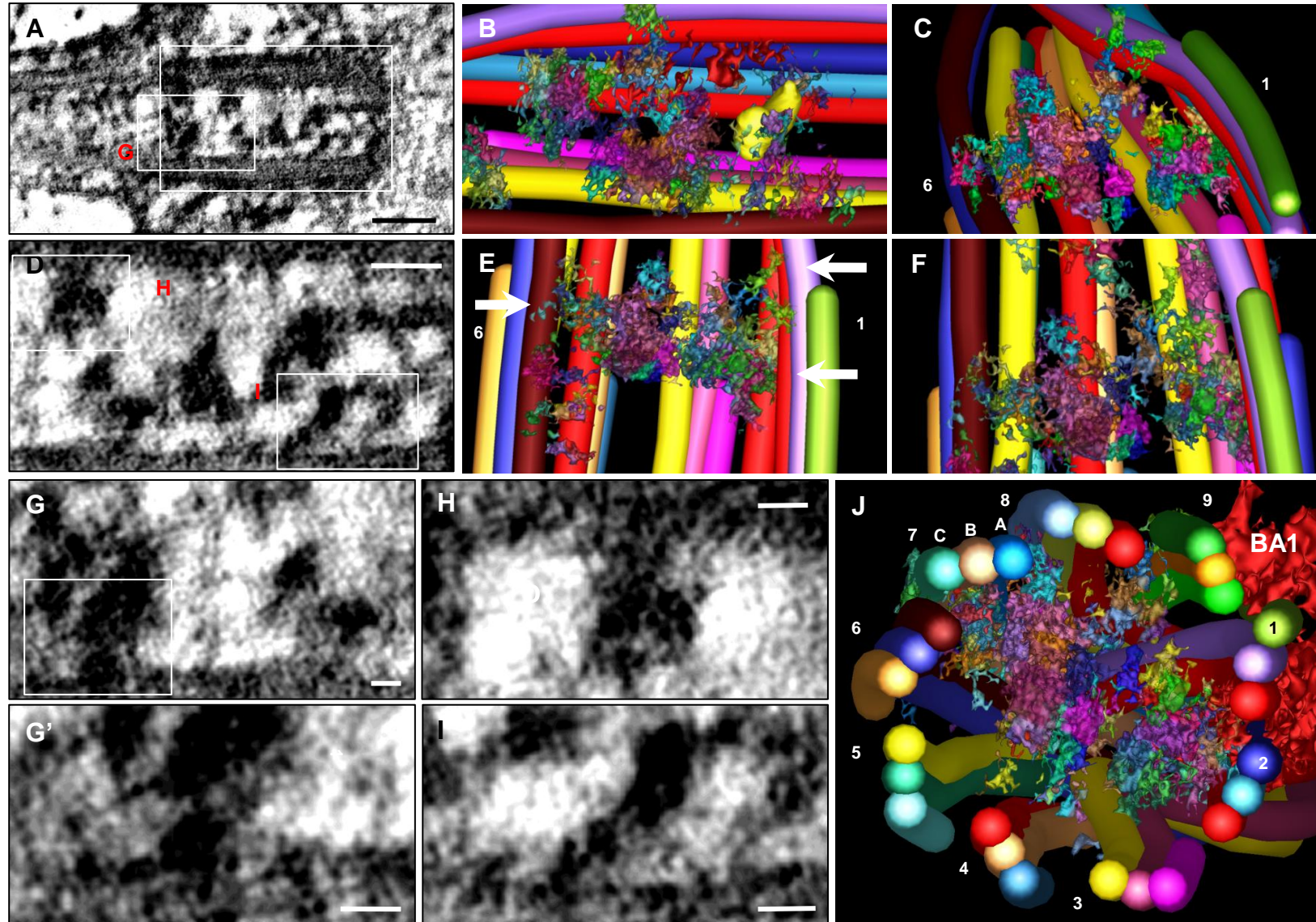


Figure 3.20 The Basal Body (1) Microtubule Triplets



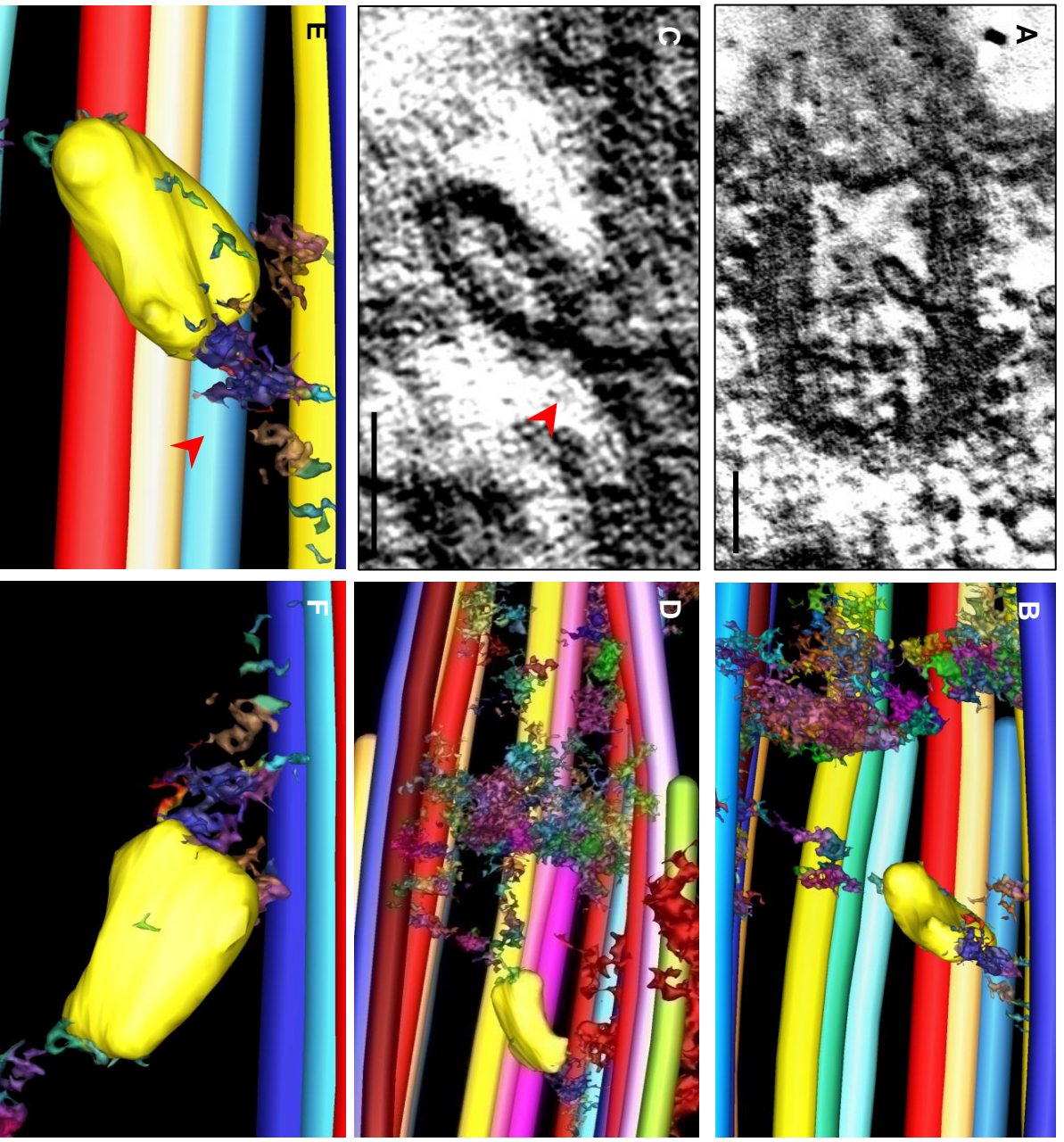
Selected aligned ultrastructural images of the microtubule subfibre triplets of the basal body. Their fine microtubule structure, close interconnectivity and separate inclinations are seen in [A, A'] making identification difficult. The curved nature of the triplets is seen in [B (7, 6)] while the closeness of triplet subfibre 'vanes' is seen in [C (1, 9)]. Note the unique barrel-shaped structure of the basal body [D] and its left-handed symmetry in projection of the microtubule triplets obliquely seen [E]. A cut away view [F] showing individual triplet's orientation highlights ultrastructural observations. Part of the basal body was found to be missing (out of plane of section [G]) and was reconstructed (partial triplets 3, 4 and 5) for completeness in the model owing to the basal body having a unique nine-fold symmetry. Scale bars [A, F] 100 nm, [A', B' and C'] 50 nm.

Figure 3.21 The Basal Body (2) Luminal Discs, Deposits and Fibers



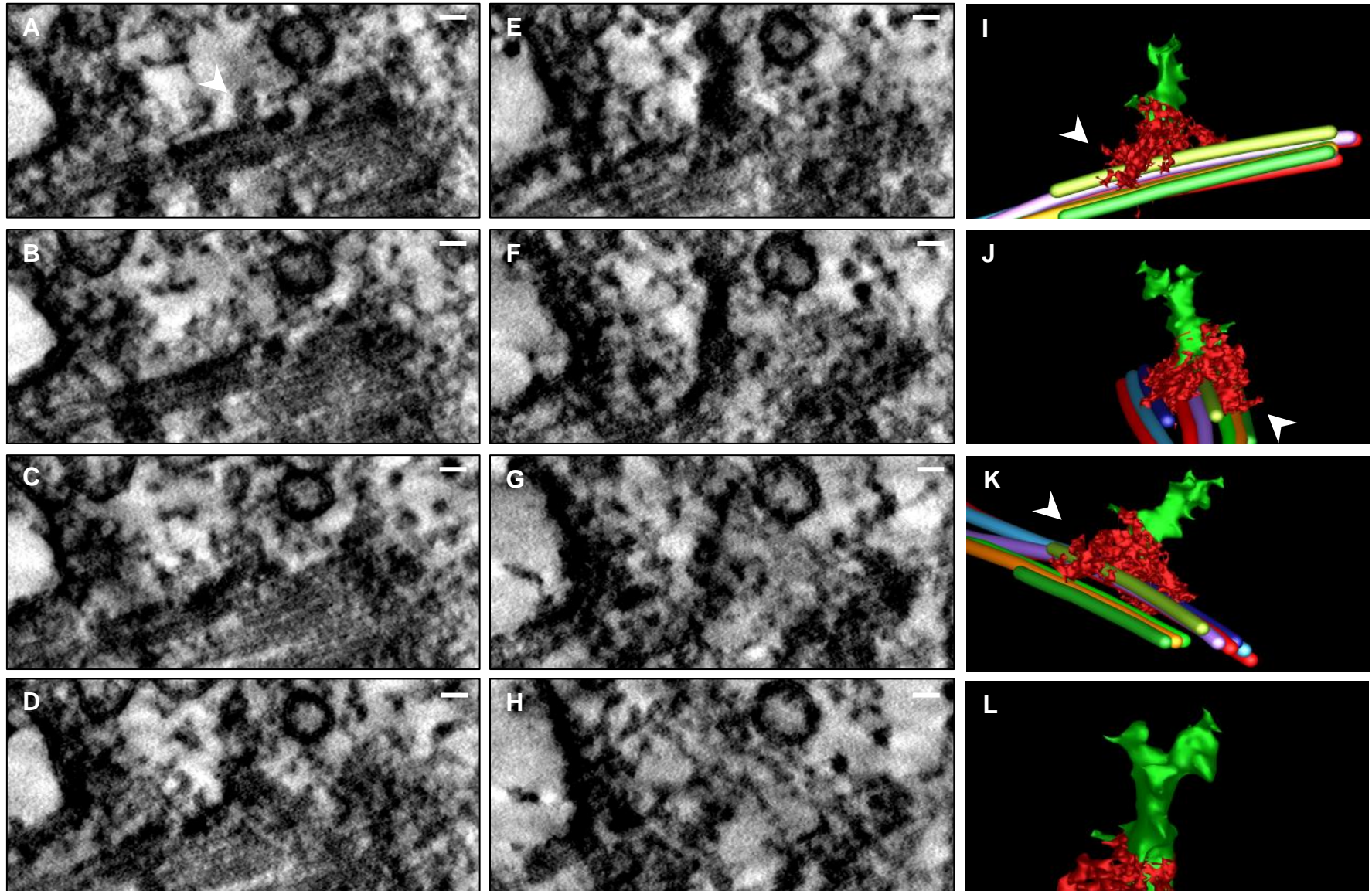
Intra-luminal deposits were found inside the basal body, decorating the microtubule triplet faces with some spanning between them [A, B, C]. Numerous densely stained accretions of macromolecular complexes were identified attached to the triplet faces [D, G, H], including fine filaments [D, G] and tethered structures [D, I] (which are seen modelled in [B, C]). A luminal disc-like structure was revealed [E (arrows), F] attached to the triplets by fine linkages whose attachment points encompass several triplet faces at the distal end of the basal body [F]. [J] An end on view of the basal body reveals the angular dispersal of many structures within the lumen and their relation to the triplet architecture. Materials are seen interconnecting between triplets (2, 3, 4 and 9) from the A-C subfibres. These are seen in proximity to Basal Appendage One (BA1). Scale bars [A] 100 nm, [D] 50 nm, [G, G', H and I] 20 nm.

Figure 3.22 Basal Body (3) Internal Structures and Vesicle



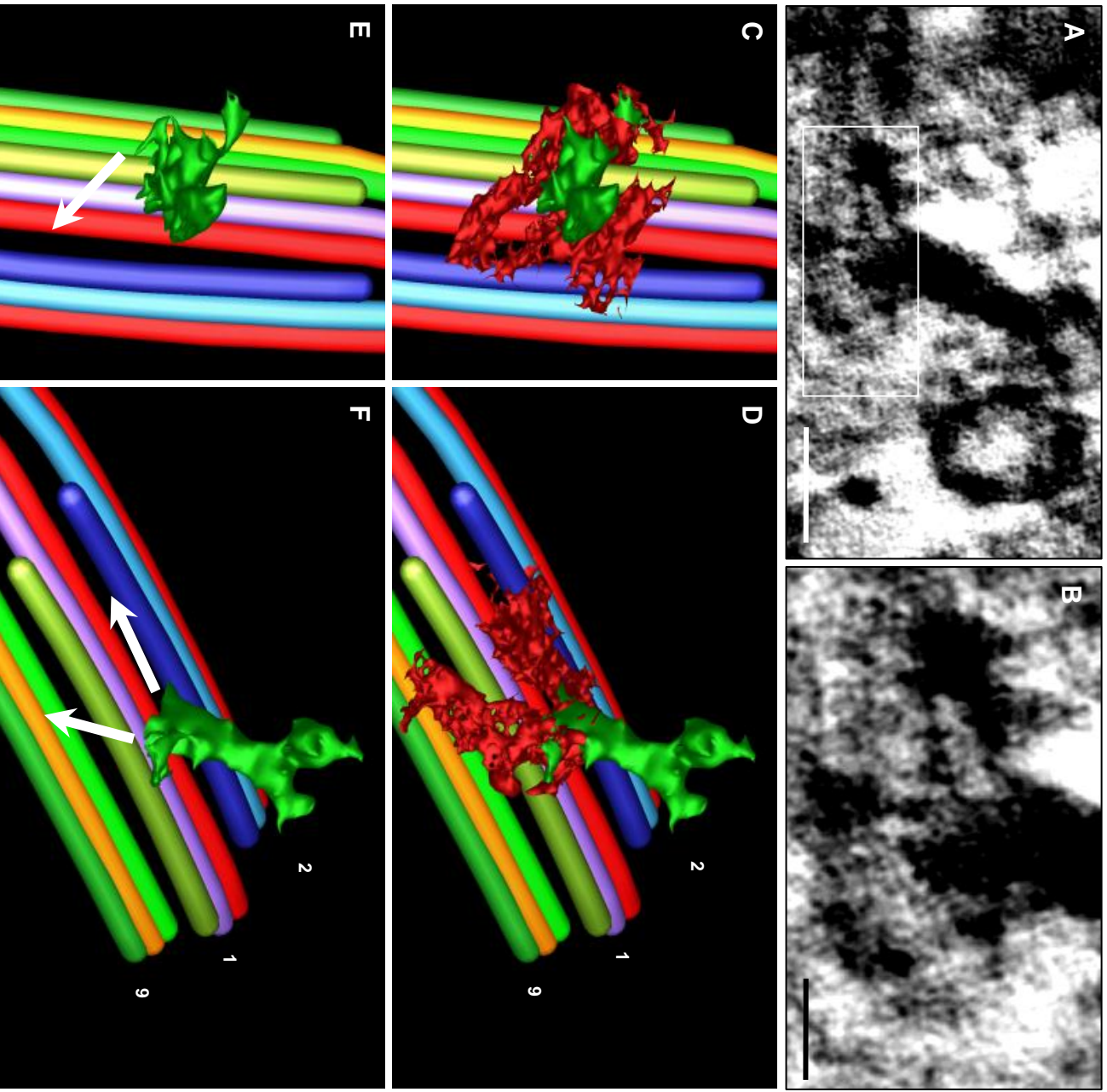
A vesicle was noted firmly attached to an inner microtubule triplet [A], enlarged in [C] (arrowhead). The model [B] shows a less cluttered view of the vesicle with respect to the basal body and the luminal disc. Filamentous linkages from the vesicle are seen interacting with the nearby luminal disc and microtubule triplet [D]. The surface of the vesicle contains densities upon its membrane and is firmly feathered to the microtubule doublet [E, F]. Scale bars [A] 100 nm and [C] 50 nm.

Figure 3.23 Basal Appendage One: Optical Sectioning and Reconstruction
Serial optical slices through Basal Appendage One (BA1)



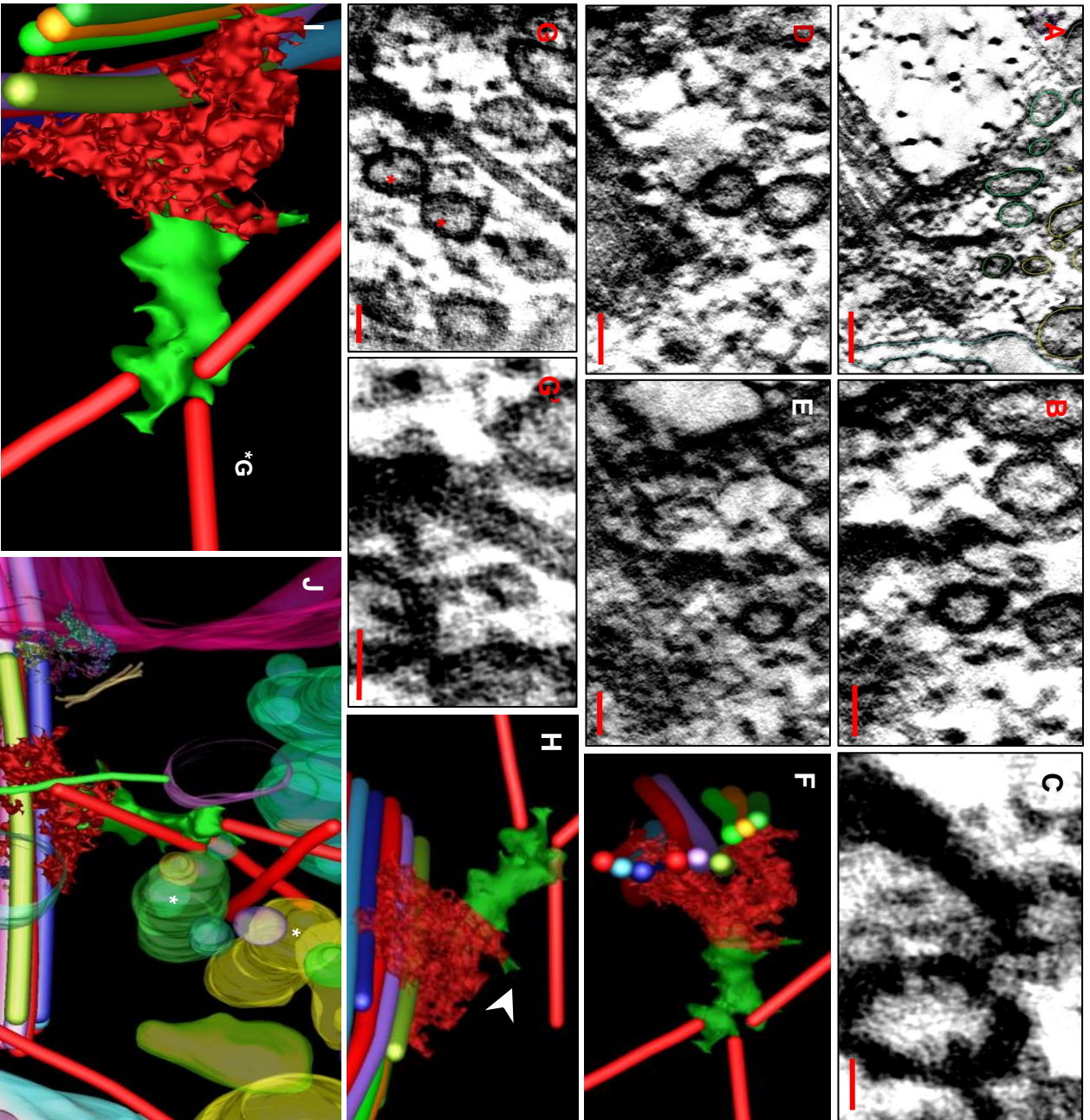
Selection of serial optical sections of the Basal Body Appendage (BA1) [A-H]. The basal appendage was reconstructed in two pieces, the docking complex and extending arm (green) and the basement complex (red). Note the localisation of a density in [A] which is seen on [I, J and K] (arrowheads). Details of the docking complex and basal arm are seen in [L]. Note electron dense materials surrounding the proximal end of the basal body microtubules. Scale bar 20 nm.

Figure 3.24 Basal Appendage One (1) Alignment of Basal Appendage Basement Structures



A longitudinal section of the basal appendage [A] showing cross sectional fine detail of the basement structure [B]. A plan [C] (and an oblique view [D]) of the basal appendage showing detail of the zones of attachment to the basement microtubule triplets. Three directional basement attachment sites were identified (arrows) [E, F]. Note the fine structure of the docking complex head showing fine thorny protrusions, the long docking arm and the perforated nature of the basement materials. Scale bars [A] 100 nm and [B] 50 nm.

Figure 3.25 Basal Appendage One (2) Ultrastructure of Arm, Docking Station and Substrate

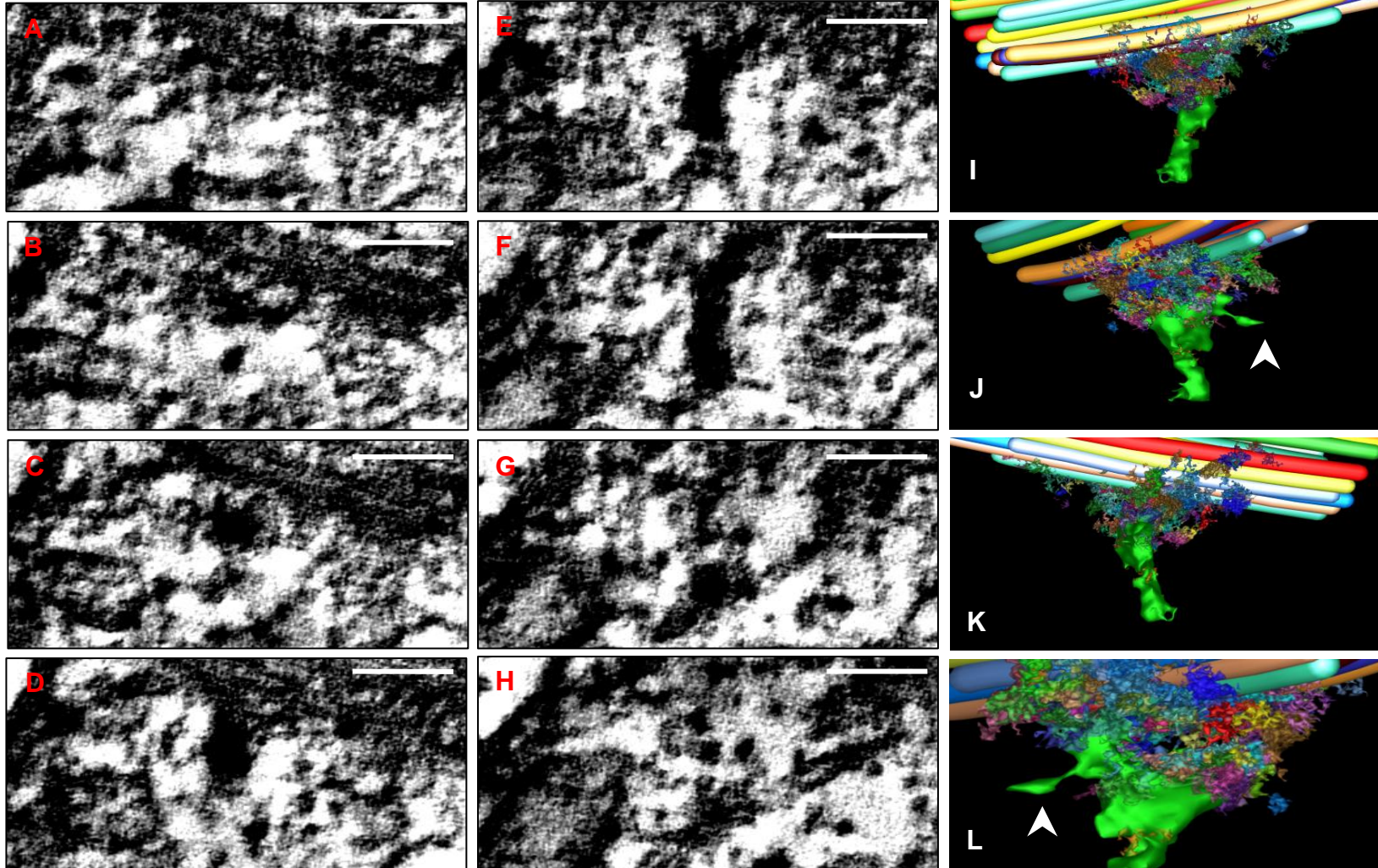


The basal appendage is seen projecting from the basal body (out of plane) where the docking head is able to interact with a local field of vesicles (within the centrosome) [A]. The docking head contains dense fine spiny protrusions [B] at one point tethering a vesicle [C] and nearby basal body associated densities [D]. Note indentations within the basal appendage arm [E]. Some docking head protrusions tether cytosolic microtubules (red) which act as conduits for vesicle transport [G, G*]. Note the presence of vesicle and microtubule associated materials noted in [J]. Microtubule orientation is seen in [F, H] giving the basal appendage a ‘swept back’ perspective at a slight angle [F, H] possibly from combined effects microtubule and ciliary loads. Note protrusion [H] (arrowhead). An extended view of the basal appendage detailing microtubule attachment sites, the head complex structure [I]. The full model with the basal appendage is seen in [J] interacting with a number of smaller vesicles associated with the docking complex and attached microtubules. Note the extra unattached microtubule interacting with nearby vesicles (ultra-structure of vesicles seen in [G] translate to those marked in [J]) and the area around basal body devoid of vesicles. Scale bars [A] 100 nm, [B, D, E, G, G*] 50 nm and [C] 25 nm.

Figure 3.26 Basal Appendage Two (1) Ultrastructure and Modelling

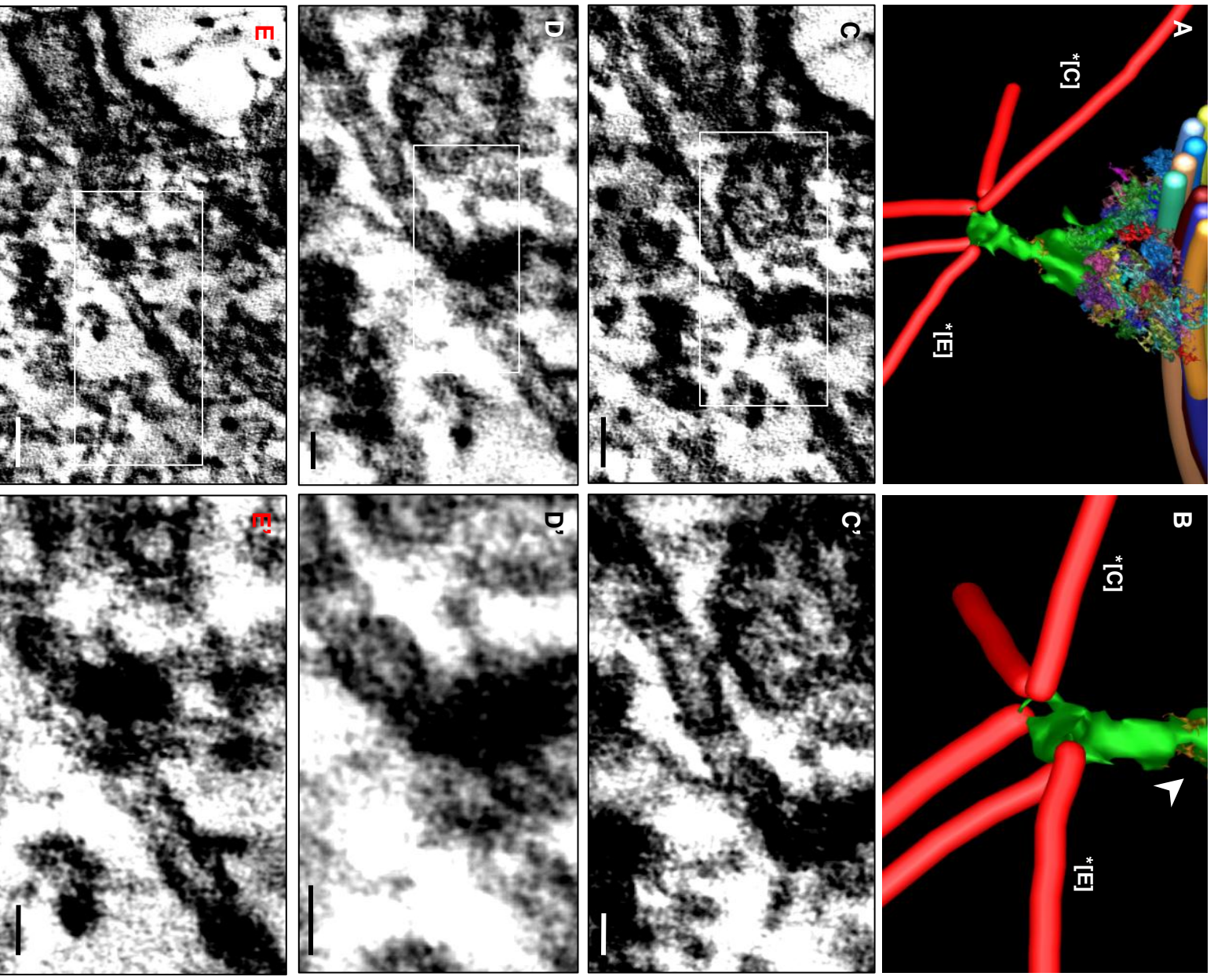
Serial optical slices through Basal Appendage Two (BA2)

Model Perspectives



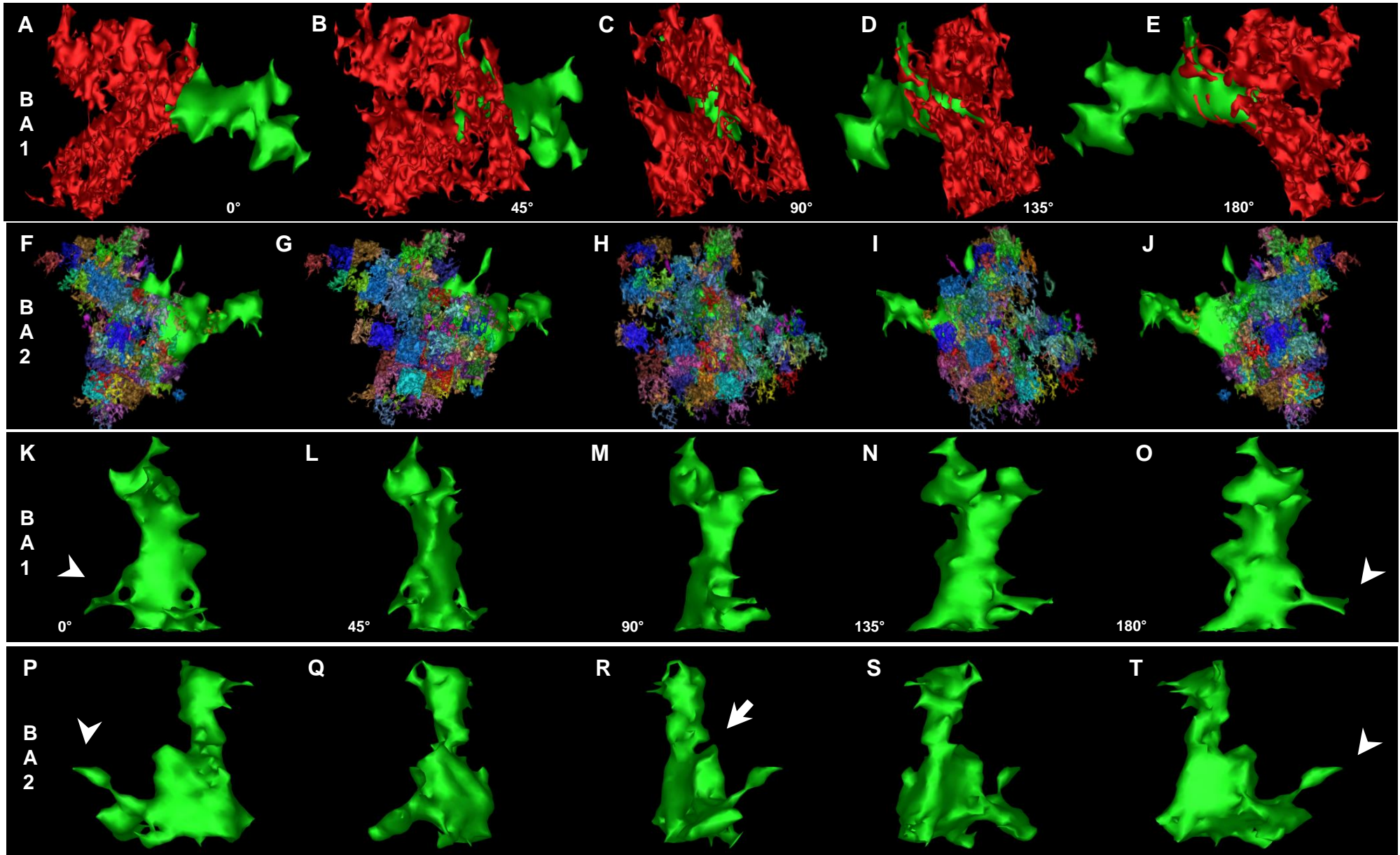
Serial optical sections of Basal Body Appendage Two (projecting downwards) [A-H]. The docking complex and arm were modelled the same way as for Basal Appendage One revealing similar anatomical features, however the basement structures were explored finer detail [I-L]. A similar basement profile was found, made up of three 'attachment zones' to the microtubule triplet substrates. Note fine linkages connecting the edge of the basement zone of the basal appendage to the outer surfaces of basal body microtubule triplets, and that the basal arm has a similar spiny protrusion as seen in Basal Appendage One (arrowheads) [J, L]. Scale bar 100 nm.

Figure 3.27 Basal Appendage Two (2) Docking Complexes



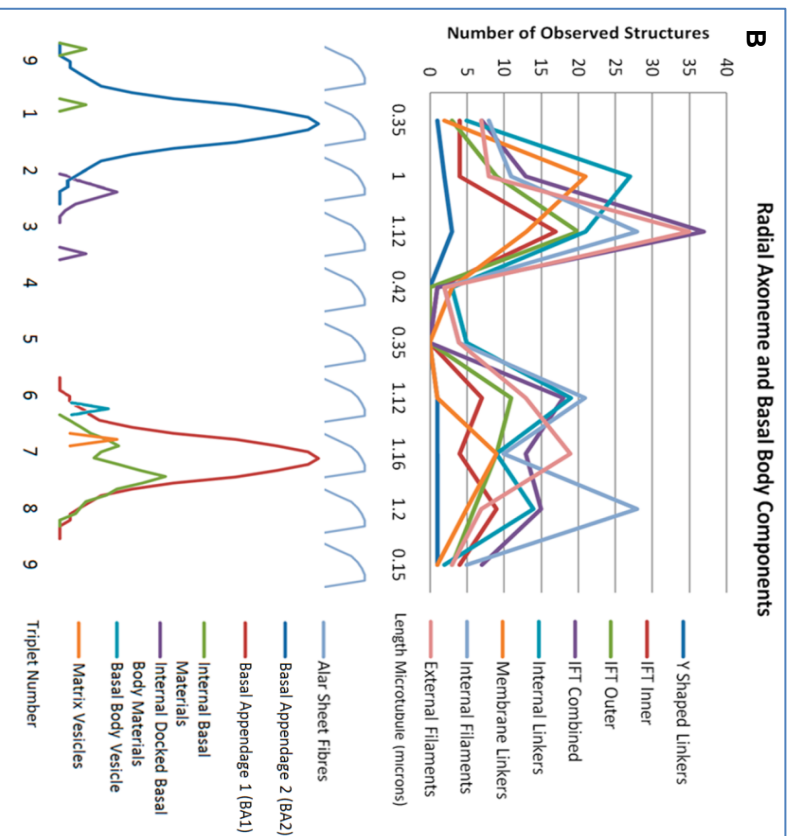
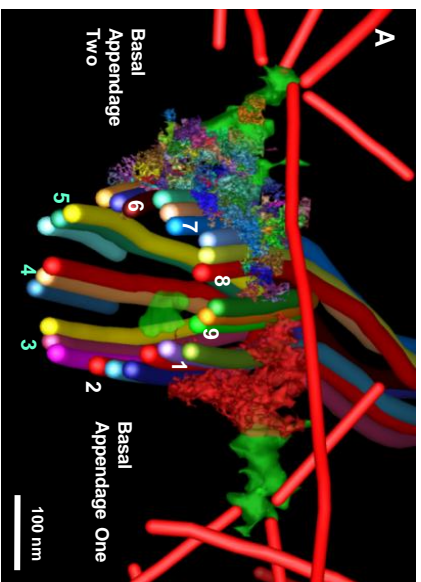
Examination of Basal Appendage Two reveals that it is slightly 'swept back' in its project [A] and has five cytosolic microtubules attached to its docking complex [B]. Ultrastructural details of the docking head attachment sites for two cytosolic microtubules (labelled in [A and B]) reveal a number of finer linkages radiating from along the microtubule to local vesicles [C, D]. Note the offset images [D, D'] are derived from [C] showing greater detail of the attached microtubules to the docking head. The second microtubule is seen aligned attached to the docking head complex [E]. Note staining densities upon microtubules and docking head [C', D' and E']. Note finer structures within the indentation in the basal arm [B] (arrowhead). Scale bar [C, E] 50 nm and [D, D', C' and E'] 25 nm.

Figure 3.28 Basal Body: Appendages Summary; Basement Structures, Basal Arm and Docking Complex



A review of Basal Body Appendages, One [A-E] and Two [F-J] detailing the finer perspectives and structures of their respective basement structures, basal arms and docking complexes. Rotational perspectives of the basal arms and docking complexes are detailed in [K-T].

Figure 3.29 Basal Body And Cilium Radial Components



C

Axoneme Sub-Fibre	Length (µm)	Yshaped Linkers	Basal Feet	Basal Body Densities	Triplet Sub-Fibre	IFT Internal & External	Membrane to MT Linkers	MT to MT Linkers	Filaments Internal & External	Comments	
1	2.1	1	BF1	*	1A	2	1	2	3	3	Turns inward sharply within the axoneme
			BF1		1B	2	2	2	3	3	
			BF1		1C				2	5	
2	1.0	2	BF1	*	2A	2	7	20	18	5	2
			BF1		2B	2	2	3	9	6	6
			BF1	*	2C				9	6	6
3	1.12	2	*	*	3A	9	2	25	10	10	20
			*	*	3B	8	18	17	11	18	15
			*	*	3C						
4	0.44	0	*	*	4A	1	0	5	1	1	1
			*	*	4B	0	0	4	2	1	1
			*	*	4C				2	1	1
5	0.35	0	*	*	5A	0	0	3	4	2	4
			*	*	5B	0	0	0	1	2	0
			*	*	5C						
6	1.12		BF2	*	6A	5	4	13	9	9	5
			BF2	*	6B	2	7	12	10	12	7
			BF2		6C						
7	1.16	1	BF2	*	7A	1	7	14	4	2	4
			BF2	*	7B	3	2	16	5	8	15
			BF2	*	7C				5	8	15
8	1.2	1	BF2	*	8A	4	4	4	9	8	2
			BF2	*	8B	5	2	6	5	20	5
			BF2		8C						
9	0.18	1	BF1	*	9A	4	3	0	1	2	2
			BF1		9B	0	0	2	1	3	1
			BF1		9C						

Close to Ciliary Matrix Vesicles

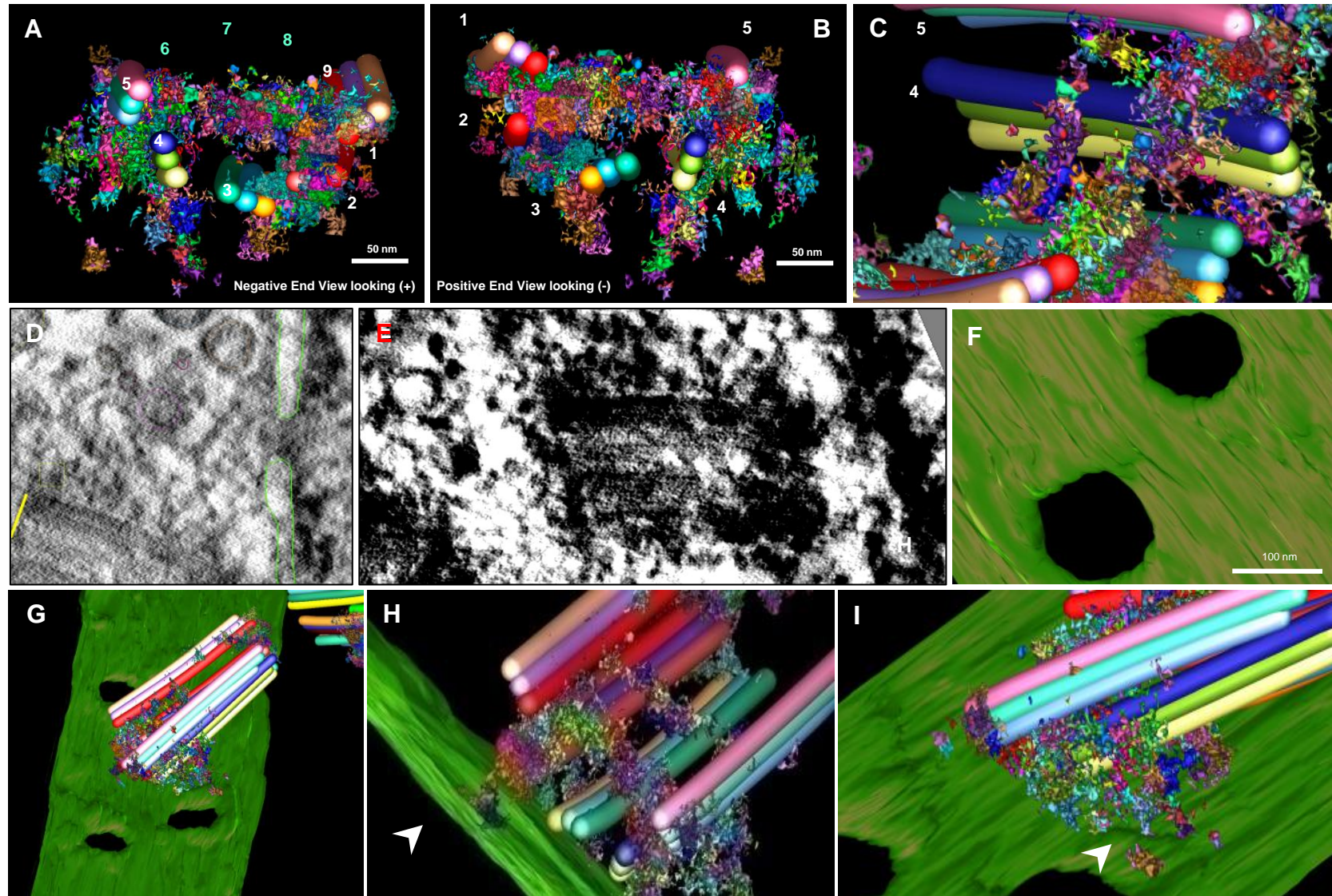
Longest doublet, significant ICT like materials

Fine filaments on BB

Longest observed microtubule doublet

Shortest MT

Figure 3.31 Proximal Centriole Radial Components and Proximity to Nuclear Pores



The distribution of materials associated with the proximal centriole are shown in [A, B], including a disc like structure spanning the distal end [C]. The centrosomal environment surrounding the proximal centriole contained numerous dense deposits (not all of them were modelled) [D, E]. The nuclear membrane was in close proximity to the centrosome and was modelled to reveal nuclear pore complexes [F]. Linkages were identified connecting from the distal end of the centriole to the nearby nuclear membrane in proximity to several nuclear pore complexes [G-I]. Scale bar 50 nm.

Figure 3.32 The Centrosome (1) Ultrastructure and Modelling

Selected ultrastructural serial slices (overlaid with model) of the centrosome detail the basal body, the proximal centriole, vesicles, microtubules, intermediate filaments and numerous electron dense structures which are bound between the cell and nuclear membranes [A-H]. By meticulously tracing objects through each optical slice it has been possible to ascertain the relationship between vesicles within the centrosome, which were observed interacting in zones associated with microtubules and the local cell membrane [I, L] as well as near the basal feet. Note nuclear pore proximity to centrosome [I and J]. Scale bars 100 nm.

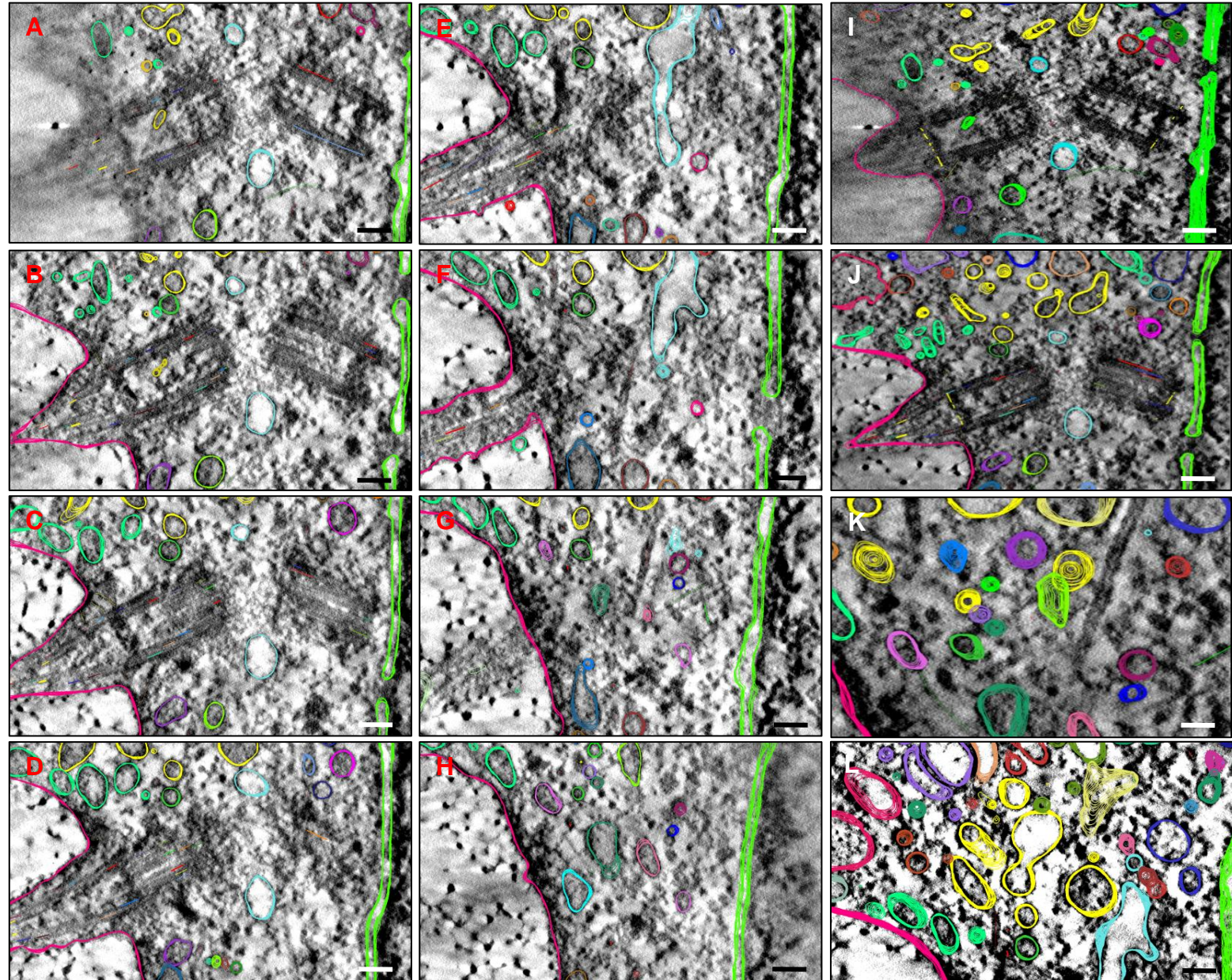
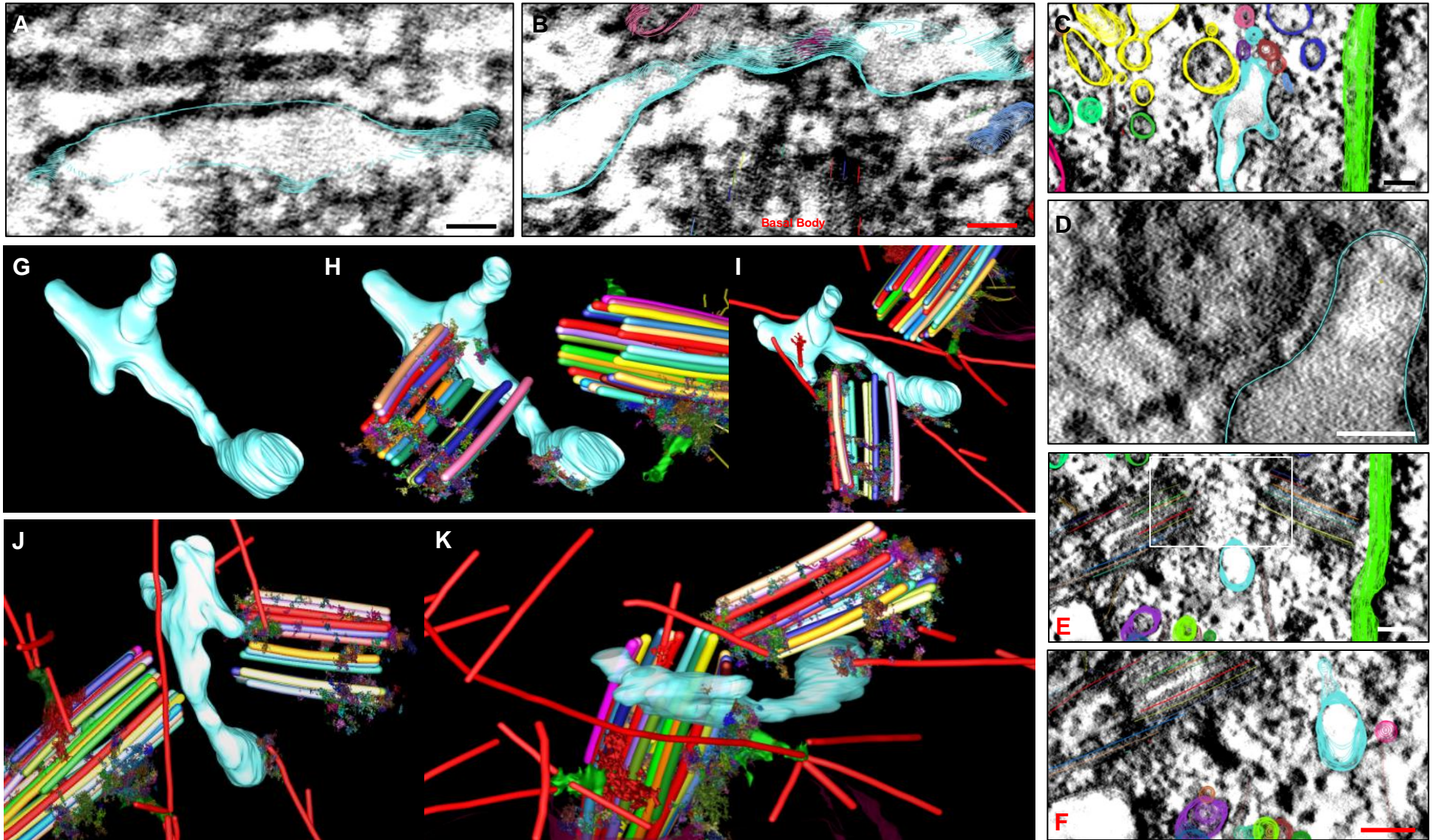
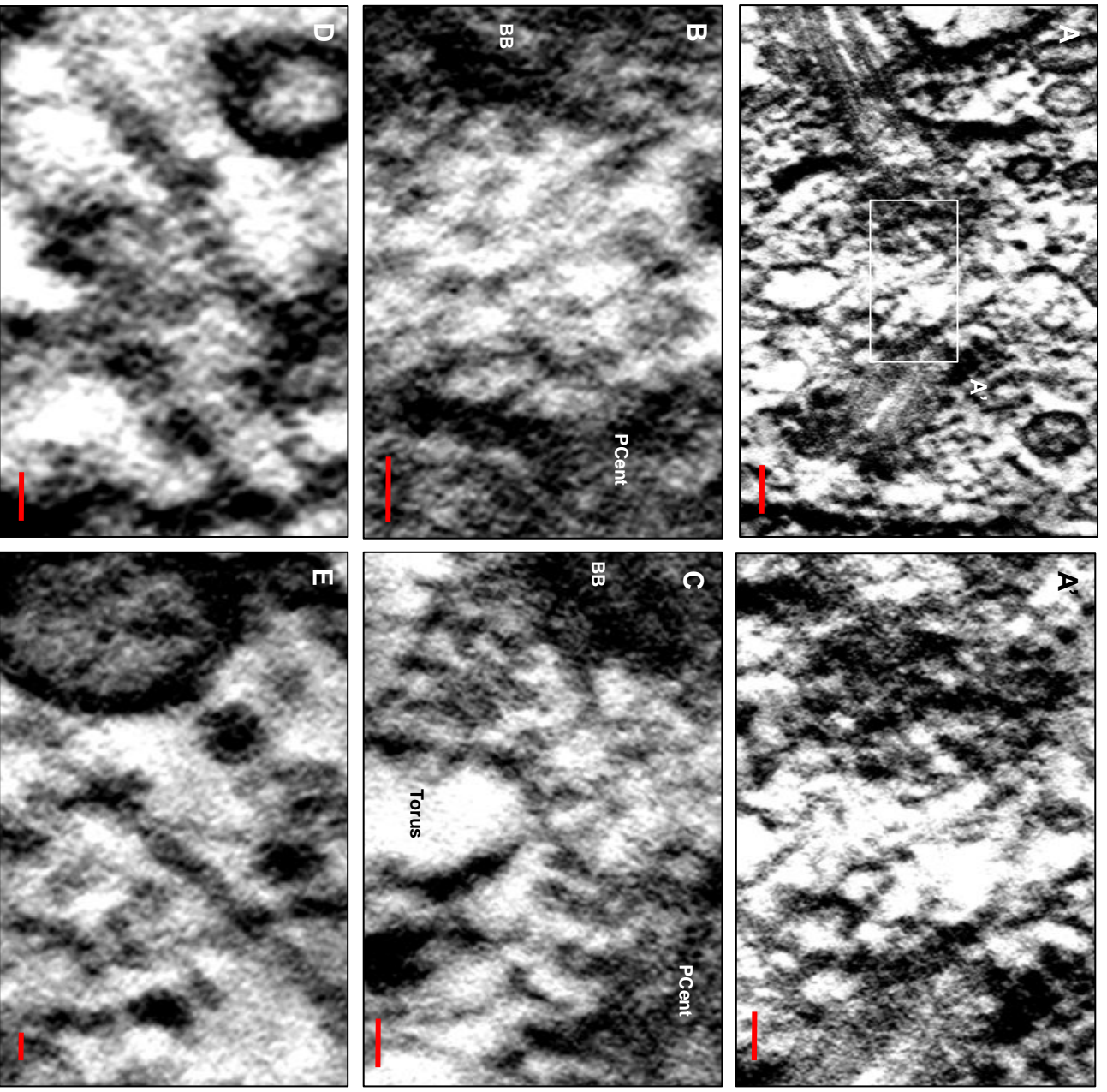


Figure 3.33 The Centrosome (2) The Centrosomal Torus



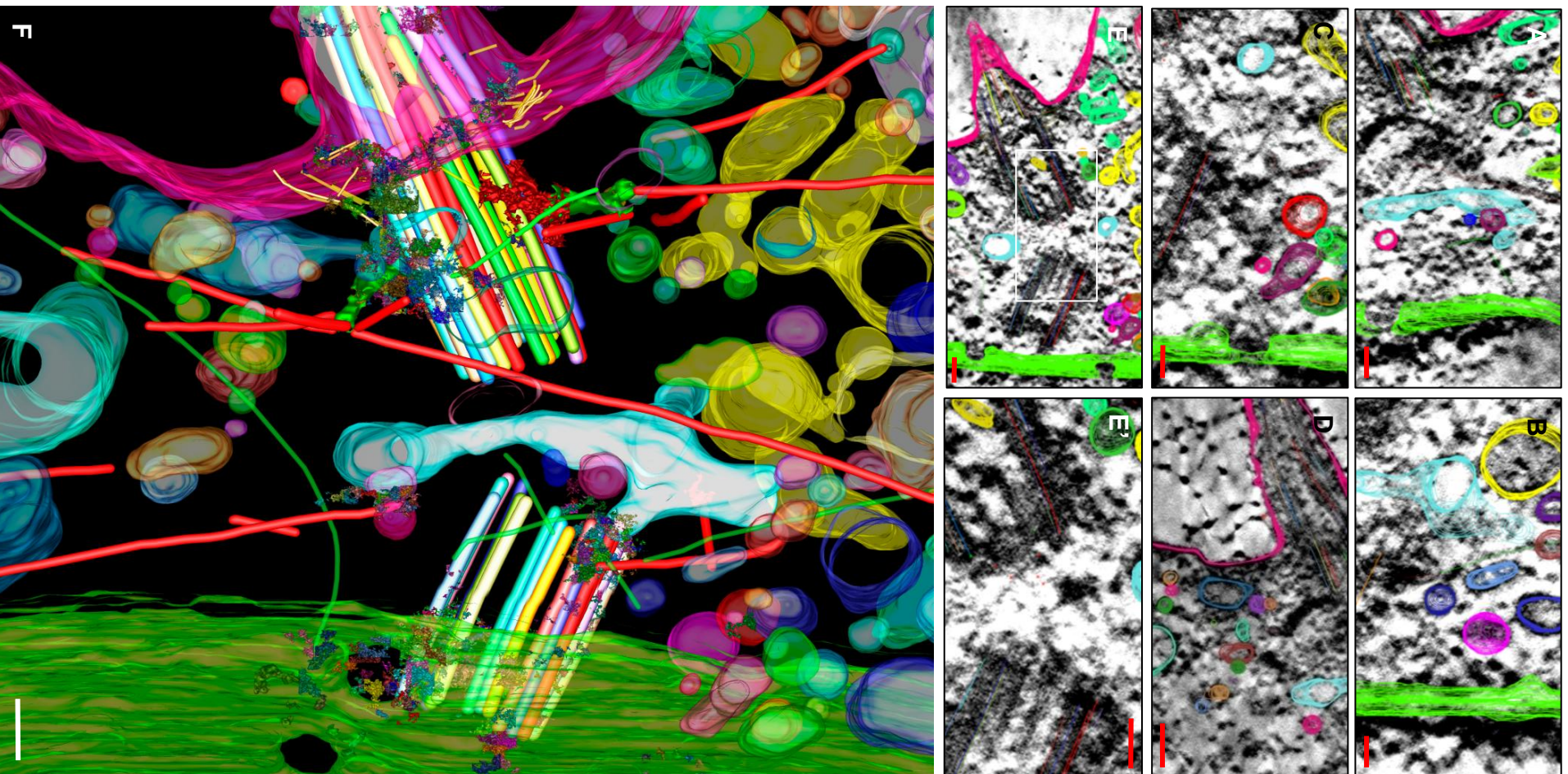
A circular ‘torus like’ structure (blue) was identified encompassing an orbital volume between the basal body and the proximal centriole (see Figure 3.32) and is shown obliquely in [A, B]. The centrosomal torus continued out of the plane of the tomogram and was found to consist of a near semi-circular volume with several process of ‘bud like’ projections [D, G]. It was found interacting with vesicles (associated with both ends) [C, D] and with microtubules [A, B]. Electron dense materials were noted upon the surface, interacting with the surrounding environment, and as a nucleation site for a microtubule [E, I, J, K]. Visual perspectives of the torus with respect to the basal body, proximal centriole and surround microtubules are seen [G-K]. It should be noted that the torus lumen, unlike other vesicles, contained very few electron dense materials. Scale bars [A] 50 nm and [B-F] 100 nm.

Figure 3.34 The Centrosome (3) The Pericentriolar Environment



The pericentriolar environment encompasses an area surrounding of the basal body (BB) and proximal centriole (PCent). It consists of an amorphous filamentous mass of fine materials linking the two centrioles at their (-) microtubule ends, and denser microtubule associated materials surrounding the centrioles themselves (see Figs 3.30, 3.32). The filamentous inter-centriolar zone is seen in [A, A'] and again in [B] where it is in proximity to, and seen interacting with, the centrosomal torus [C]. An area surrounding the proximal centriole was noted as a nucleation site for intermediate filaments [D, E]. Note intermediate fine structure. Scale bars [A] 100 nm, [A', B, C] 50 nm, and [D and E] 10 nm.

Figure 3.35 The Centrosome (4) Basal Body, Proximal Centriole within the MTOC



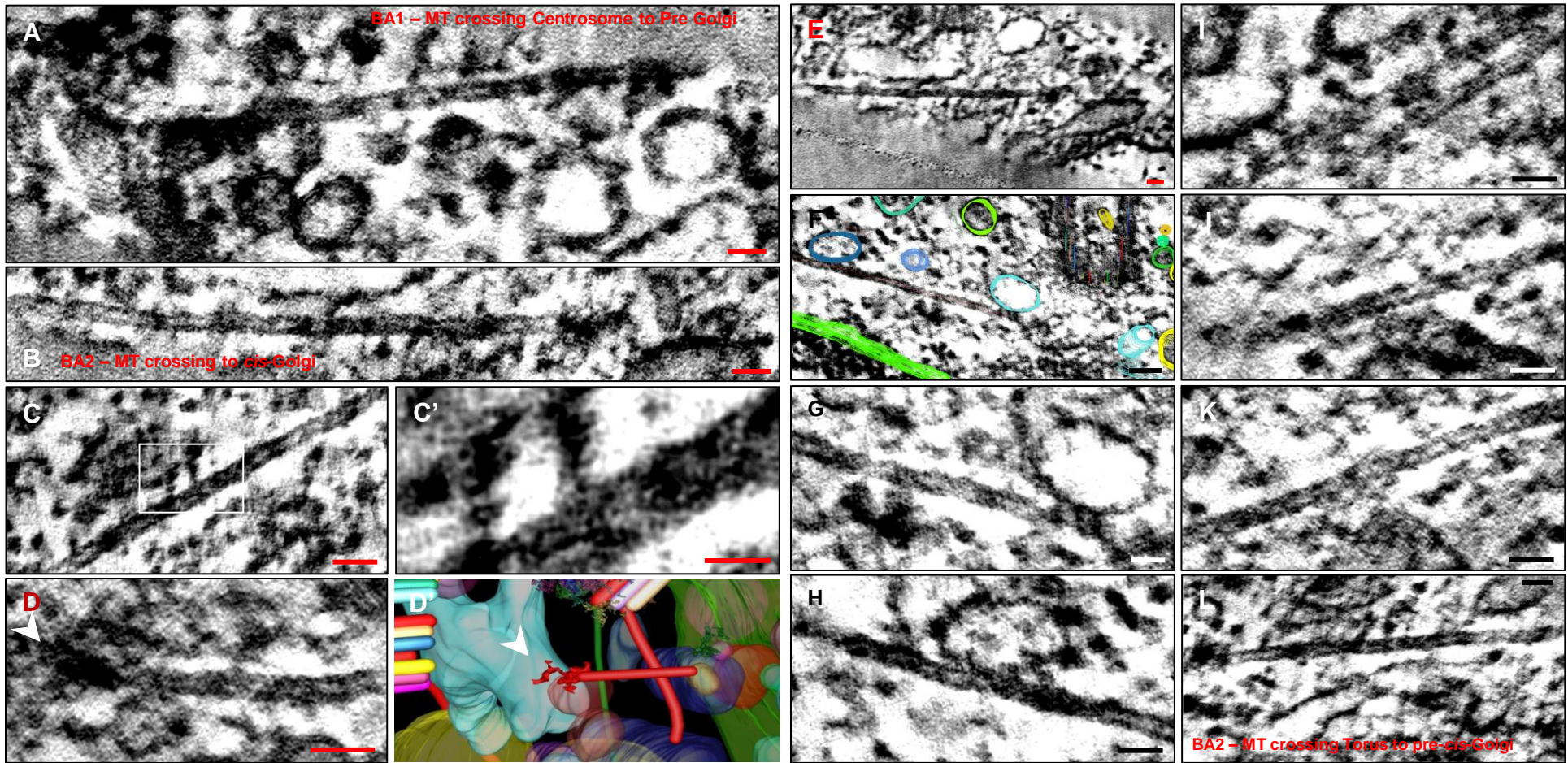
A selection of centrosomal images [A-E¹]. [A] The torus in proximity to a microtubule. [B, C] Vesicles interacting with electron dense materials of the pericentriolar environment (near the proximal centriole) and nearby a nuclear membrane pore. [D] Numbers of small vesicles collecting and budding around the microtubule network associated with Basal Appendage Two (BA2). [E, E¹] An enlargement of the pericentriolar zone detailing an electron dense structure located between the two centrioles. [F] A three dimensional model of the centrosome showing numbers of small vesicles around microtubule (red) trafficking zones. Note basal appendages, the centrosomal 'torus', intermediate filaments (green), the nearby nuclear membrane and nuclear pores. Scale bars 100 nm.

Figure 3.36 The Cytosolic Microtubules

Microtubules Originating from the Centrosome

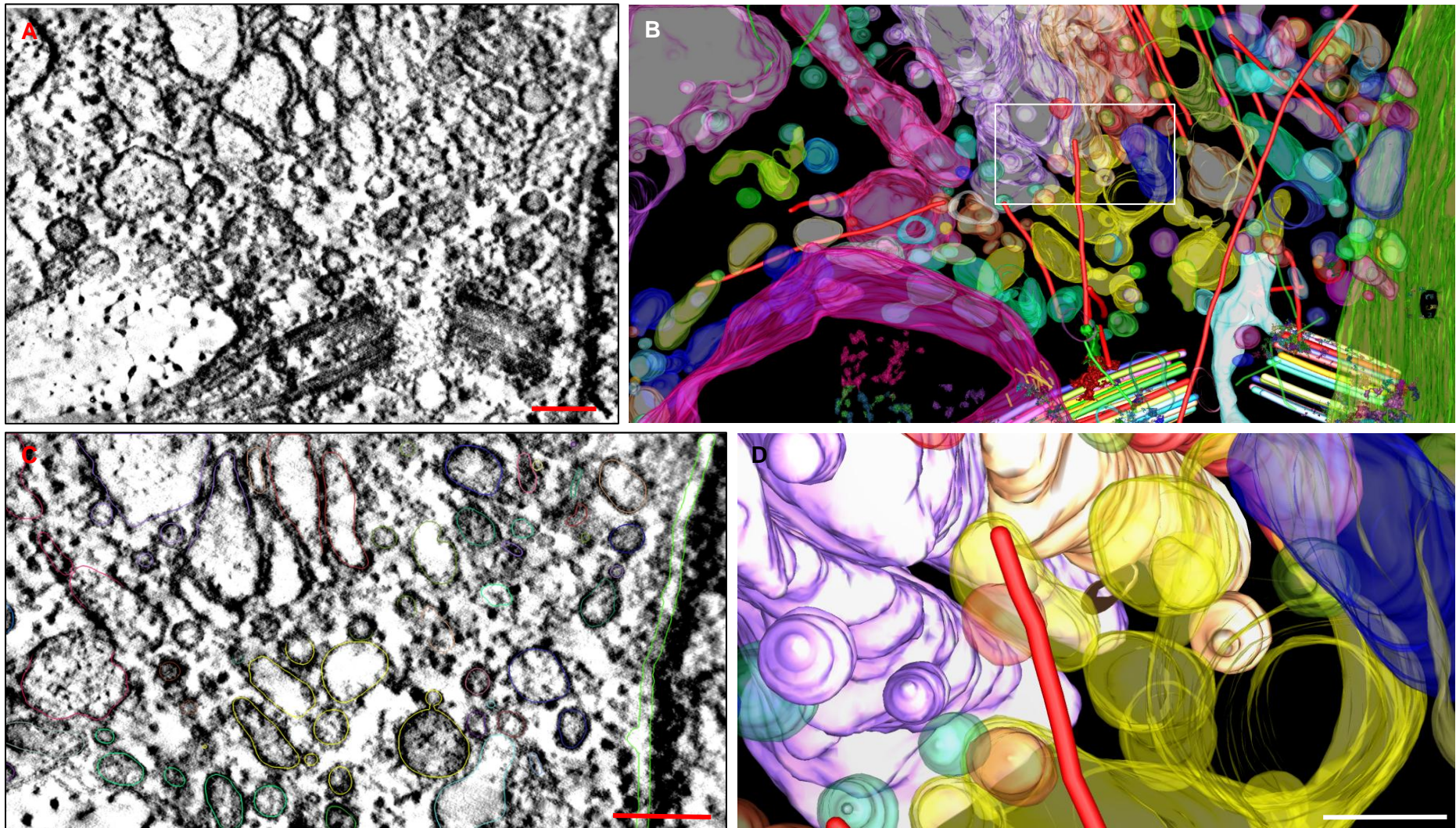
Centrosomal Torus Microtubule

Golgi Associated Microtubules



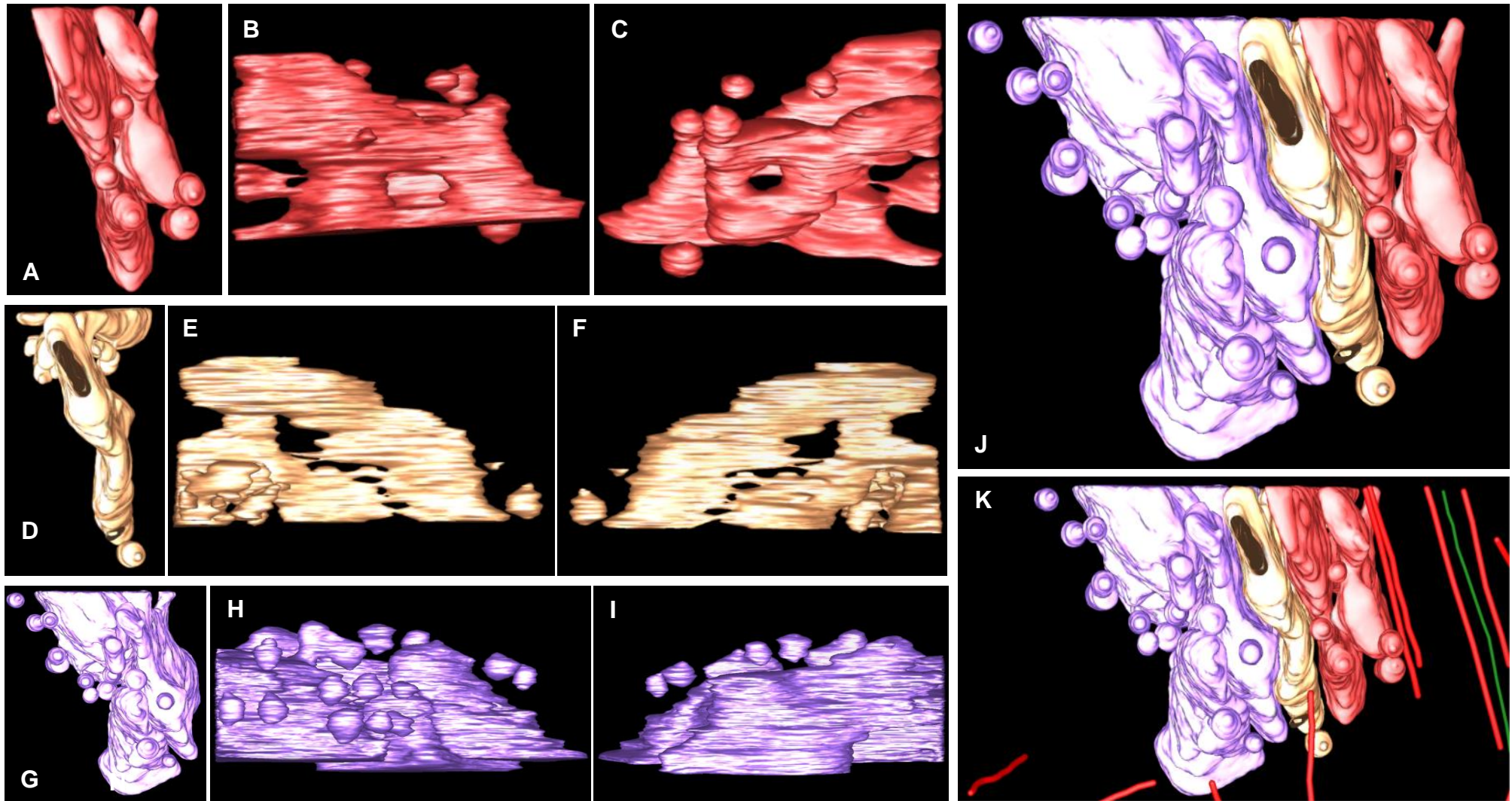
Microtubules were imaged and divided into three categories; those originating from 1) the basal body appendages 2) the centrosome, and 3) from the cytosol. [A] details a microtubule radiating from basal appendage one (BA1) which interacts at its distal end with the *cis*-Golgi apparatus. Note associated vesicles and areas of density along the microtubule. [B] A microtubule from basal appendage two (BA2) seen crossing the centrosome towards and terminating in an area of the pre-Golgi (see model in Figure 3.26 [F]). This microtubule is unique in that it passes near microtubules involved in the pre-*cis* face of the Golgi [M]. Vesicles were observed interacting with microtubules by what could be Dynein/Dynactin or Kinesin transport complexes [C, C']. A short microtubule was seen within the centrosome [D] and modelled [D']. Note electron dense materials at one end (arrowheads). Another microtubule observed radiating from the centrosome was identified firmly attached to the centrosomal torus [E, F, G] and also had vesicular activity associated with it [H]. Parallel sets of microtubules were noted being associated with the pre-*cis* face of the Golgi apparatus and were found to have numerous smaller vesicles associated with them [I, J and K] which were modelled in Figure 3.37 [B]. Scale bars [A, B, C, D and E-L] 50 nm and [C'] 25 nm.

Figure 3.37 Centrosome to Golgi Connectivity



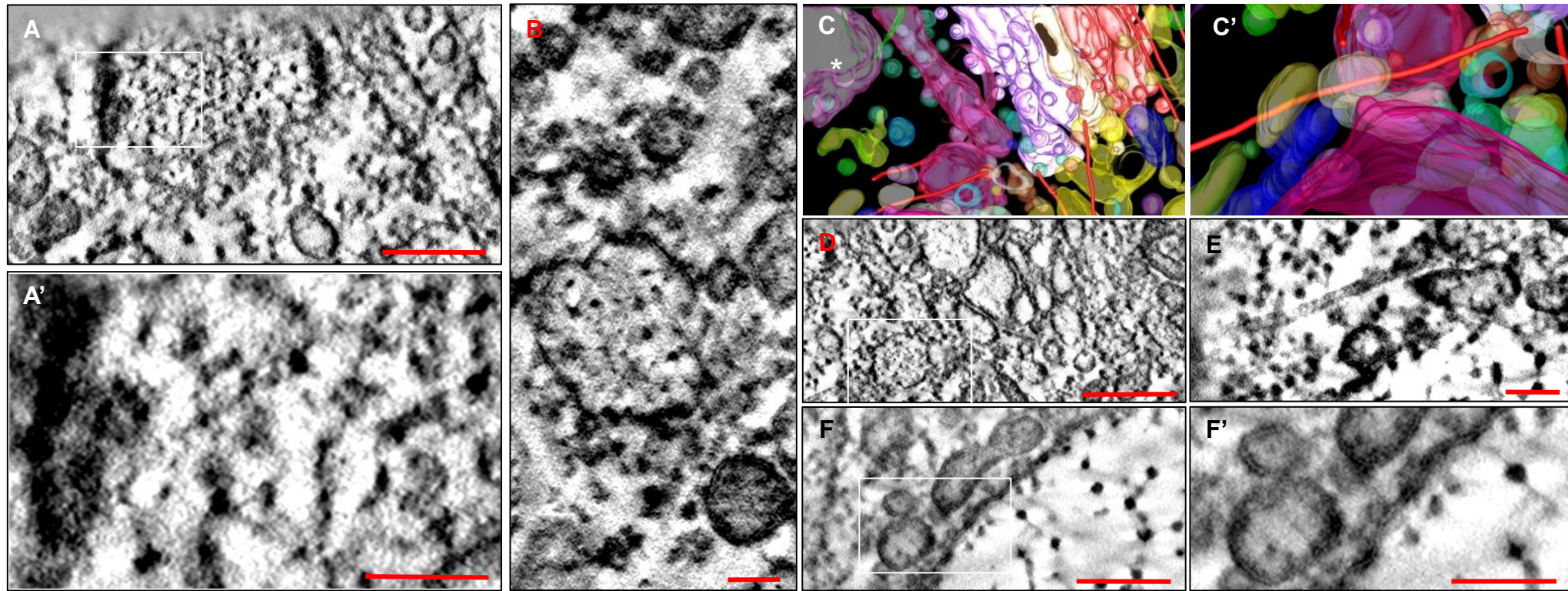
The periphery of the centrosome was found to be closely associated with the nearby Golgi apparatus, which is bound closely on both sides by the nuclear and cell membranes [A]. The pre-*cis*-Golgi face was found to be highly aligned with parallel microtubules (with a single intermediate filament (green)), mixed with clusters of numerous small vesicles [B]. The complexity of the interaction zone is detailed in [C], where a field of vesicles may be seen surrounding the Golgi have been traced. Although little detail is available within a single slice, combination of many slices reveals significant 3D information in a model. [D] An enlarged perspective of the translucent model in [B], however with the Golgi turned opaque to aid viewing. Note the microtubule (red) originating from the basal appendage (BA1) is seen interacting and terminating within a zone around the *medial* to *trans*-compartments. It was found to be specifically associated with a vesicle (red) amongst a field of ‘budding’ vesicles from the edges of the cisternae (see Figure 3.36 [A] for an ultrastructural view of the microtubule). Scale bar 200 nm.

Figure 3.38 The *Cis*, *Medial* and *Trans* Golgi Compartments



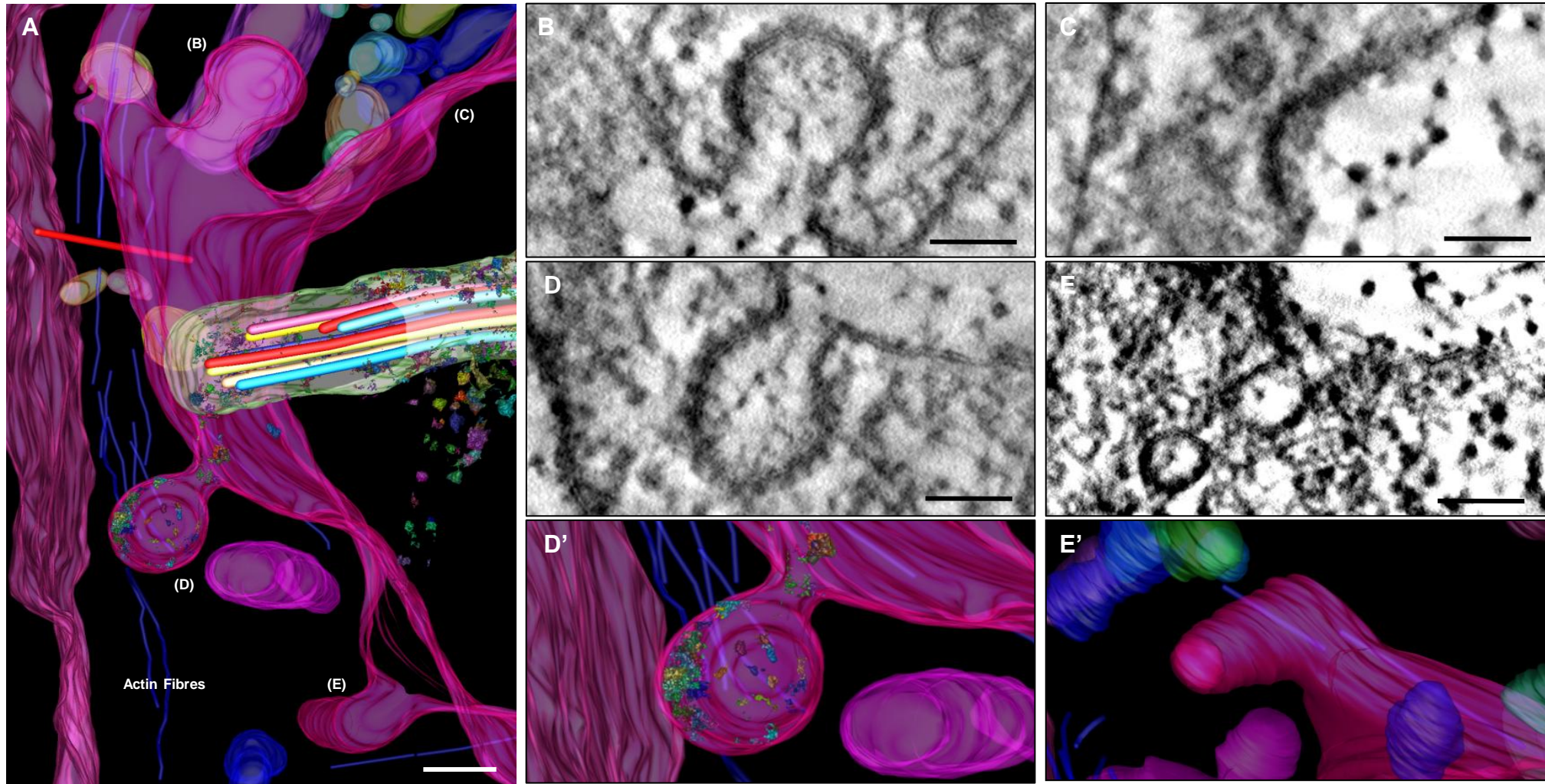
A series of vertical and lateral views of the Golgi *cis*, *medial* and *trans* compartments which were traced manually (as seen Figure 3.37 C). The *cis* compartments were found to have budding protrusions [B] and holes penetrating through the *cis* stacks [C]. The slender *medial* compartment was found to contain several fine holes forming a zone of perforation running diagonally within medial stack [E, F]. The *trans* compartment contained numerous vesicles budding from the *trans* face [G, H and J]. Combined stacks [J], are seen with respect to a microtubule array near the *cis* compartments [K]. Vesicles were found to normally be associated with the faces or peripheral edges of cisternae, while finer holes and fenestrations were observed in portions of the stack.

Figure 3.39 Transport of Matrix from the Golgi



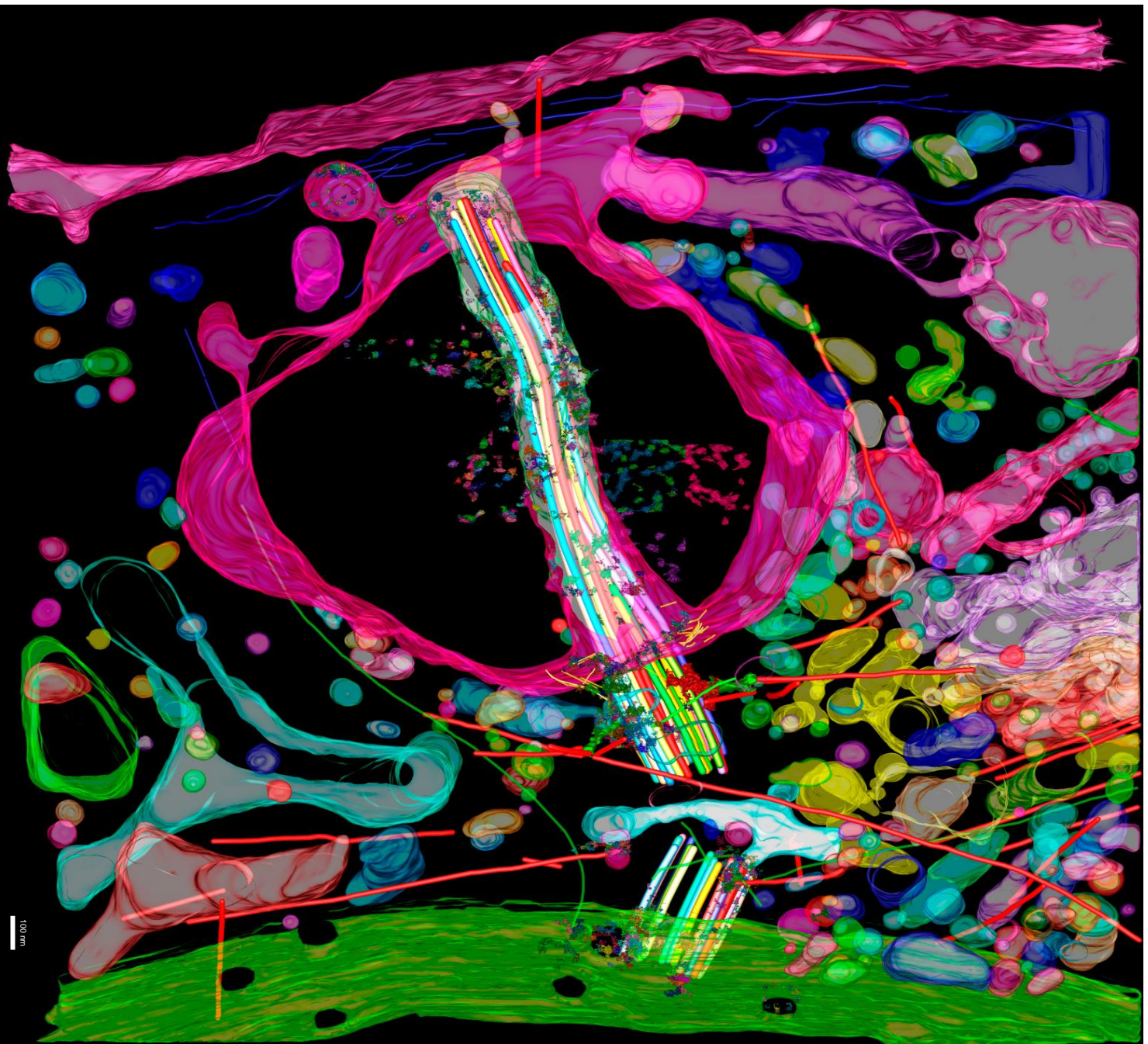
A large storage vesicle was identified containing tightly packed granular material (reminiscent of matrix granules) however at a higher density greater than the surround extracellular matrix [A, A' and C*]. An assortment of vesicles packed with similar granules were observed near the *trans* face of the Golgi [B, D], including a long tubular structure that could have 'shed' from the face (purple) [C]. Part of the *trans*-face was connected to the cell membrane via a microtubule [E] where a collection of vesicles were closely associated with the cell membrane [F, F'] (seen merging in [E]) and modelled in [C']. Scale bar [A, D, F] 200 nm and [A', B, E and F'] 100 nm.

Figure 3.40 The Cilium, Coated Pits and Caveolae



The distal tip of the cilium is seen interacting with the cell membrane [A] where a number of receptor-mediated endocytotic processes were identified and labelled in [A] as (B), (C) and (E). Coated pits labelled as (B, C, and D) are seen in their corresponding ultrastructural plates [B, C, D] with an enlarged view in [D']. Note the circular nature of coated pits, unknown structures decorating the membrane surfaces, and the extracellular contents of the pits, in the process of endocytosis (see Figure 3.43 for alternative field of [D']). A semi-circular 'pitted' membrane indentation, believed to be a coated pit in the process of formation, is seen in [C]. Structures revealing caveolae are identified in [E] and [F]. Scale bars 100 nm.

Figure 3.41 The Matrix Cilium Golgi Continuum



A combined overview of all features modelled from the tomogram (see Figure 3.8 for comparison) detailing matrix interactions with the cilium, its axonemal microtubule structure, the diplosomal centrosome, the radiating cytosolic microtubule network and the nearby Golgi apparatus. Cytosolic microtubules are shown in red, intermediate filaments in green, and actin fibres in blue.

Figure 3.42 Plan of Tomogram Features

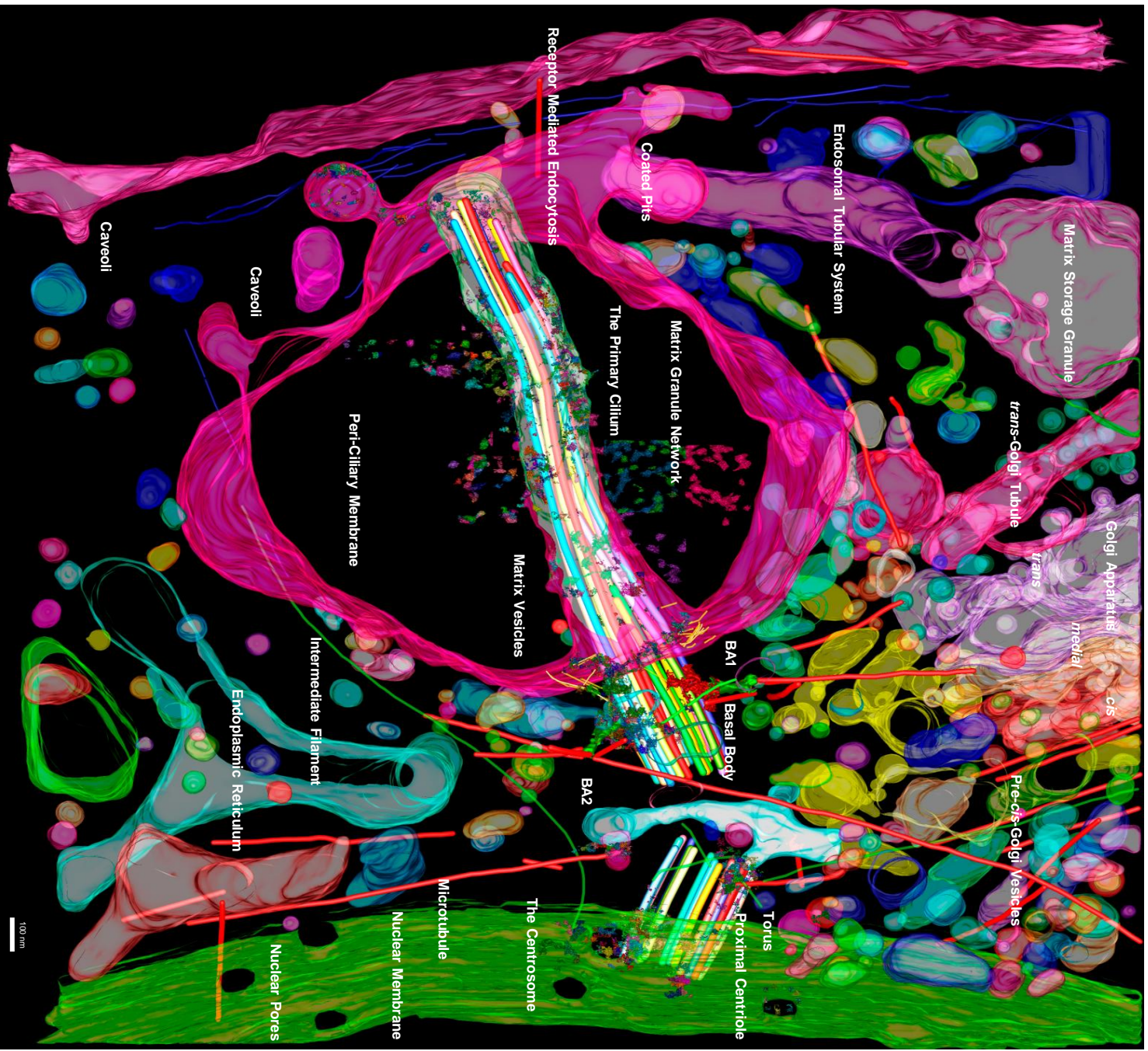
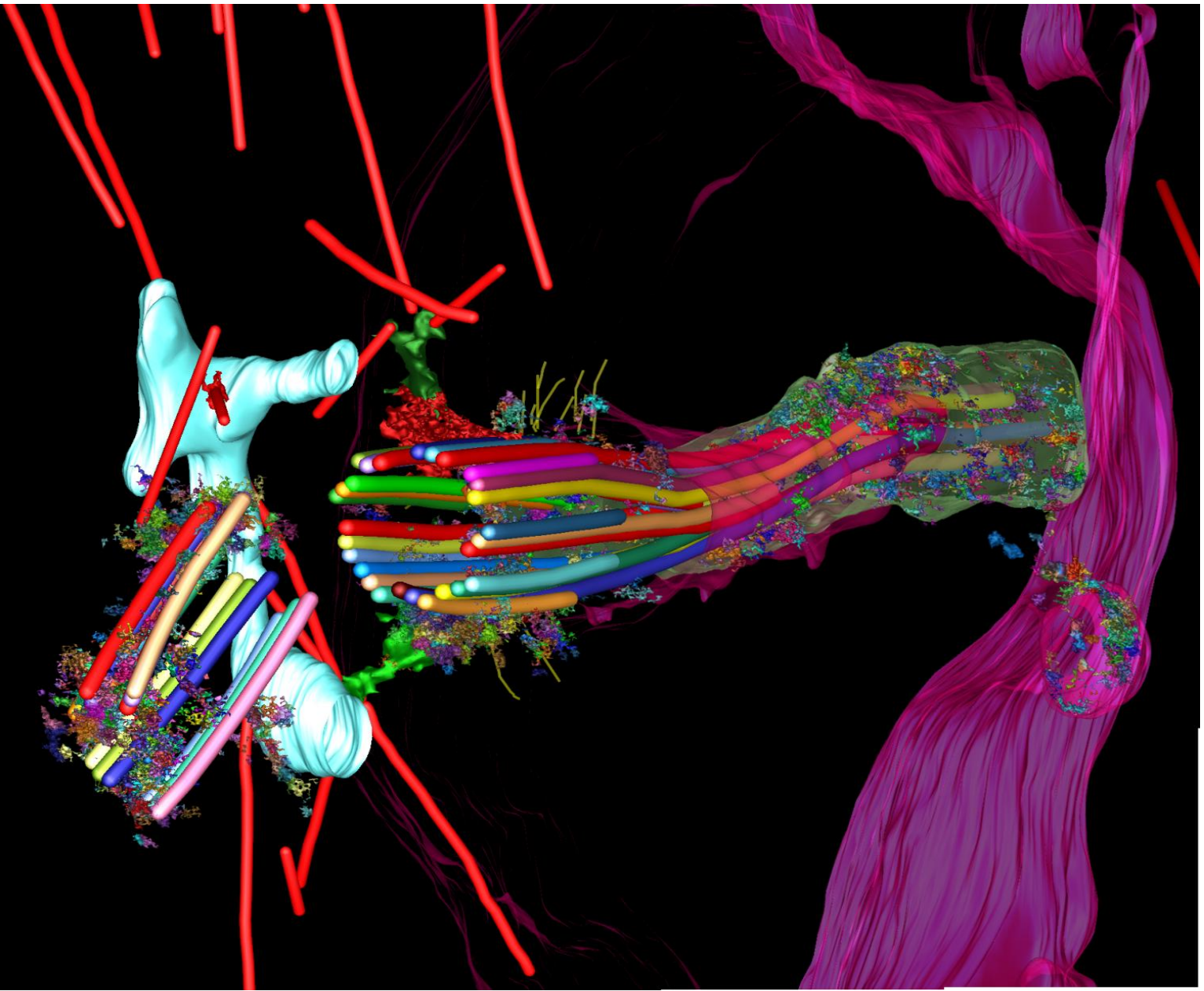


Figure 3.43 The Cilium-Centrosome Continuum



A perspective view along the axoneme, the basal body, the proximal centriole (with the centrosomal torus) and attached microtubules of the centrosome. Note the fine structures, inclination of the axoneme and a coated pit near the tip of the cilium. This details a physical continuum between the extracellular environment, and the centrosome, which is comprised of as yet many unknown proteins. Note the presence of microtubules which would intersect atop the basal body, where a third basal appendage would be, if continued out of section.

Chapter Four: Discussion

4.0 Introduction and Overview

Despite an ever growing body of knowledge of primary cilia as specialist sensors, many questions remain about their role as mechanical transducers and the means by which they influence cellular responses. The introductory chapters of this thesis have provided an overview of the previously known ultrastructure of primary cilia, a profile of their sensory capabilities, and their relationship within the extracellular matrix, cilium and the Golgi continuum. In summary, primary cilia occur nearly ubiquitously in eukaryotic cells and although known of for many years have recently been acknowledged as an organelle to epigenesis, physiological function, and several disease processes [1, 85, 229, 460, 1001]. Primary cilia express a unique (9+0) microtubule doublet symmetry nucleated from the maternal basal body, which is subtended by a proximal centriole, and the two together forming the diplosome of the centrosome. The centrosome is the microtubule organising centre of the cell, and is responsible for controlling many cellular functions [120]. During interphase it is located in a juxta-nuclear position, and is important for organisation of the Golgi apparatus [96, 97, 1002] and determining cell polarity [1003, 1004].

The hypothesis that the cilium acts as a ‘cybernetic probe’ in connective tissues [26] has since been supported by studies which show that primary cilia are unique sensory organelles within a variety of tissue types, capable of adaptation for sensing a host of mechanical, chemical, osmotic, photonic, polarity and other significant changes in the cellular microenvironment [33]. Norbert Wiener [99] coined the term ‘cybernetic’, derived from the Greek κυβερνητικός, literally the ‘steerer of a rowing boat’, which is appropriately describes the role of the primary cilium in detecting external signals, and directing an appropriate response.

Current concepts of ciliary structure are based upon data derived from conventional ultrathin electron microscope studies of cells and tissues containing predominantly motile cilia [45, 49, 51]. Fewer ultrastructural studies have been made of connective tissue primary cilia, as analysis is difficult due to the small size of the cilium relative to the volume of the cell, singular occurrence and unknown orientation within tissues [973, 1005-1006]. However, extensive ultrastructural analysis of chondrocyte primary cilia [26, 27, 96, 97] culminated in the first electron tomographical study by Jensen et al., (2004) [25], realising many accurate anatomical details.

Extracellular matrix of connective tissues plays a dynamic and integral role in cellular adhesion, signalling, proliferation, differentiation, apoptosis and mechanotransduction, through providing interactions with cell surface receptors such as integrins, which are physically or chemically coupled to the cytoskeleton [25, 1007-1009]. These tissue specific macromolecular architectures are influenced functionally by the application of biomechanical forces [1009]. The precise types of molecular connections and their relative abundance depend largely on the biomechanical function of the tissue and the required cellular response to biomechanical forces [1010]. Developmentally,

mechanical forces drive mesenchymal cells down a particular lineage [1011], while conversely cyclic hydrostatic pressure initiates chondrogenic differentiation and matrix secretion [1012].

In cartilage, chondrocytes are believed to sense their extracellular environment through their primary cilia, transducing this information to the centrosome, which responds appropriately by polarising the Golgi apparatus. This pathway involves a number of unique proteins and biochemical signalling cascades spanning from the cilium to the centrosome, allowing intracellular regulation and polarisation of the Golgi for the directed regulated secretion of appropriate extracellular matrix macromolecules for maintaining the extracellular microenvironment. Many of these known protein constituents and interactions are tabulated within the Appendices. The rapid increase in knowledge of these proteins and their dynamic association with the structure of primary cilia make this a truly unique study.

4.10 Limitations of Study

This study has primarily focussed upon tomography of *in situ* embryo sternal chondrocytes and has relied upon conventional chemical fixation and osmication, enhanced with RHT and *en bloc* uranyl-acetate stain. Inevitably, the presence of a certain degree of chemically induced artefact, shrinkage and distortion is expected, when compared to cryo-tomography techniques [938-943]. As such, RHT represents a trade off in fixation strategies, providing the ability to optimally stain, stabilise and retain extracellular matrix components that are not conventionally preserved. In addition, the enhanced resolution provided by RHT allowed resolution of fine structure never before seen. The time required to chemically fix, prepare and examine samples makes electron microscopy a highly involved process, however this is compensated for by the improved resolution which tomography can provide.

This study did not attempt to ascertain the preferential orientation of chondrocyte primary cilia within cartilage, which has been previously been investigated by Farnum et al, (2011) [973]. Measurement of cilia was carried out in ImageJ, however, there are limitations in measurement accuracy with semithick as compared to ultra-thin sections. As yet, *in situ* chondrocyte primary cilia have not undergone the same level of tomographical investigation as other cilia types (Appendix VI).

This is the first study to carry out both tomography and full modelling of a chondrocyte cilium, as well as incorporating the Golgi apparatus for visualisation of the ‘matrix-cilium-Golgi continuum’ as a functional entity. While only a single-axis tomogram was used to construct the model, it is believed to represent the anatomical and structural characteristics common to most chondrocyte primary cilia, agrees with, and improves on previous studies [27]. However, it should not serve as a sole reference interpret or represent all chondrocyte primary cilia. Further models would be a useful complement, however at present their construction is an intensive, though rewarding, undertaking.

4.11 Ruthenium Interactions with Cells and Membrane Bound Structures

The combined ability of RHT and its osmication products to interact with, stain and contrast membrane proteins and receptor channel complexes remains uncertain. Several authors have reported the penetration of RHT into living cells at fixation [960, 1013], including the biological effect of inhibiting T-cell activation [1014] RHT is reported to interact with a wide variety of membrane proteins and ion channels, many of which are reported upon cilia and flagella, however its ability to stain and contrast these structures remains unclear. Ruthenium Red also displays a high affinity for phospho-lipid membranes, specifically for *L-alpha-phosphatidyl serine*, where its action upon membranes has been modelled [1015, 1016].

Following RHT treatment, the ciliary membrane was observed to contain numerous heavy stained structures, as detailed in Figs 3.11 D-M, 3.12 and 3.15. These may represent numerous potential membrane bound components of matrix receptors, channels and their associated components upon the chondrocyte primary cilium. RHT has been used by Czukas et al., (2007) [1017], demonstrating an ability to resolve fine structures, when using it to identify fine linkages between stereo-cilia in alligator lizard auditory hair cells. In contrast, RHT in the present work led to such heavy staining of the periciliary membrane that it rendered some parts of those areas too opaque to adequately resolve any structure.

4.12 Occurrence and Morphology of Chondrocyte Primary Cilia

The incidence, length, morphology and orientation of primary cilia have been analysed in many connective tissue studies of fibroblasts [30, 95], tendon [26, 1018] and cartilage [26, 27]. It has been found that normally only one primary cilium is expressed per *in situ* interphase cell [30] as originally noted by Zimmerman [9]. This is believed to hold generally, however recent observations of primary cilia metaplasia on the apical surface of renal proximal tubules [1019] raises interesting perspectives as to the role of the primary cilium in these epithelial cells. Observations of cells containing bi-ciliated primary cilia have been made in many cell types, though the reasons for, and the dynamics of multi-ciliated centrosomes remain largely unknown [944, 978, 1020-1022]. Although their presence is reported associated with both cancerous and benign cells [248, 249, 1023, 1024].

Most chick sternal chondrocyte primary cilia were found to be surrounded by fields of matrix granules with only a sparse presence of collagen fibres near the cilium. The most significant discrepancy in measuring axoneme lengths may arise from the effect of sectioning, where the lengths of bent or longer cilia are not included, skewing the results slightly in favour of a shorter average length. Discrepancies in measuring basal body lengths may result from inclusion of incomplete or misaligned cilia in sampling (which is difficult to determine with semithick sections, especially in respect to the basal body) as well as errors from microscope settings, shrinkage and choice of measurement points. Basal body lengths were measured from the proximal base to the end of the C-

subfibre, near the alar sheet attachment site. This leaves the interpretation of the end-point of the basal body between the start of the transition zone and the ciliary membrane, subject to error.

Many authors have studied chondrocyte primary cilia in articular, growth plate, sternal and mandibular cartilage [26, 27, 42, 96, 1005, 1025-1026], with Rich et al., (2012) [365] having reviewed their incidences and lengths. Earlier studies of the presence, length and morphology of chondrocyte cilia revealed that ciliary length varies little between species [27, 28, 365, 973]. The measurements of chondrocyte primary cilia by Wilsman in 1978 [28] ($1.76 \mu\text{m}$, $\sigma 0.80$) closely match the results of this study ($1.80 \mu\text{m}$, $\sigma 0.36$) except for lengths of basal bodies ($0.5 \mu\text{m}$ $\sigma 0.03$ to this study $0.365 \mu\text{m}$, $\sigma 0.01$) and the range of axoneme lengths were similar (0.28 - 3.29 to this study 0.7 - 2.41) μm , respectively. On the other hand, primary ciliary length can vary greatly between cell types, from those expressing minimal extension of the axoneme (such as in the T-cell immunological synapse [1027]), to a length of $4.2 \pm 2.2 \mu\text{m}$ in the rat flexor tendon [1018], and to extremes of 20 - $30 \mu\text{m}$ (in Ovine Meckel-Grueber MKS3 fibroblasts [1028]). The depth of semithick sections prevented reliable measurement of basal body widths. However, transition membrane widths were measured ($0.262 \mu\text{m}$ $\sigma 0.015$, Section 3.5) in comparison to basal body width ($0.21 \mu\text{m}$, $\sigma 0.01$) as reported by Wilsman [28]. This indicates a 26 nm wide 'inlet zone' extending between the membrane and the microtubules of the transition zone. Anderson (1972) [45] reported a variable luminal diameter of the basal body (0.13 - $0.15 \mu\text{m}$), indicating the luminal end surface area is at least 1.25 times that of the transition zone.

4.13 Chick Sternal Cartilage Tomogram Selection

Of the many tomograms acquired, it was decided to model a single-axis dataset that contained a near complete ciliary axoneme, laying within an indentation resembling an enlarged 'ciliary pocket' [1029] (Figure 3.6). This section contained a near complete cilium and proximal centrioles of the microtubule organising centre and was positioned adjacent to the nucleus, in close proximity to the Golgi apparatus. The 'pocket' itself offers a striking comparison with an image published by Wheatley (Figure 6.1, pg 149 [3]) [1030] of a cilium extending into a large luminal vacuole with the centrosome positioned against the nuclear membrane. In the chondrocyte tomogram, the matrix surrounding the cilium within the indentation is of a lower staining density than that of the extracellular matrix, and is uniquely devoid of collagen fibres.

4.14 Defining the Cilium and its Relation to the Golgi

Numerous detailed tomographical studies have focussed upon the finer molecular aspects of the microtubule-based architecture of the motile axoneme, with none attempting to explore either its complete structure, or the relationship of the cilium within the centrosome and its relationship to other organelles. The modelling of a continuum between the matrix, the primary cilium, the centrosome and the Golgi within one tomogram, as achieved in the present study, uniquely indicates the presence of a

highly ordered microtubule-based structural continuum mechanically linking the cilium with the Golgi apparatus. The interrogative and inclusive model enables a three dimensional understanding of the architecture of the primary cilium not available from conventional ultra-thin studies.

4.20 Interpretation of the Model Structure

In an effort to understand the structural components of the model, and their functional significance, it is necessary to compare features already described in the literature on cilia, the cytoskeleton and cellular organelles, including the Golgi apparatus. Appendix VI contains a selected review of tomographic and modelling studies of components of the extracellular matrix, of cilia, flagella, the cytoskeleton and the organelles of various species. While many studies have focussed exclusively upon motile cilia, only Jensen et al., (2004) [25] has utilised tomography to study chondrocyte primary cilia, investigating linkages between the ciliary membrane and with the extracellular matrix.

While the microtubule architecture of centrioles, basal bodies and axonemes have been extensively reviewed, only recently have they been the focus of higher resolution studies [1031, 1032]. While it is not possible to know with any certainty, which proteins make up the structures detailed within the model, it is possible to deduce what these may be, with some degree of certainty. Studies based upon lower resolution immunofluorescence and electron microscopical localisation of known proteins can serve as a bridge for interpretation. Selections of known structural and signalling proteins specific to primary cilia are included in Appendices, and form an essential basis for translating ultrastructural based information into putative function. While electron tomography studies have greatly aided the analysis of cellular organelles, the construction of large-scale models from datasets remains a laborious process, and is not usually undertaken.

4.21 The Matrix of the Ciliary Pocket

Areas of lower density matrix were frequently observed in a zone surrounding chondrocyte cilia, which also express various degrees of deflection and invagination of their projection with the cell membrane. The molecular structure and functionality of this ‘ciliary matrix zone’ remains to be determined. The matrix granule density within the ciliary pocket is less than the external pericellular matrix environment (Figs 3.5 C and 3.7). This may indicate an area of special matrix properties, or that freshly secreted matrix materials are less inter-connected. Knudson (1993) [861] showed that pericellular matrix assembly occurs in a zone near the cell membrane directed by hyaluronan in an ‘aggrecan rich chondrocyte pericellular matrix’ (sic) anchored by interaction between hyaluronan and its receptors [1033, 1034]. All tomograms revealed the pericellular matrix usually consisted of a complex mix of collagen and proteoglycans (Figure 3.5, A’, B’), and a number of cilia were characterised by a distinct absence of collagen fibres in their vicinity. The periciliary matrix of the model presented consisted solely of regular arrays of matrix granules (Figs 3.5 and 3.6) 30-45 nm in

diameter, each connected to at least 4 others via fine filaments (thought to be hyaluronic acid or Link protein). It is believed that the basic inter-connectivity and structure of the granule network was preserved by RHT treatment, rather than being a post-fixational artefact. Tomography revealed the individual granules to consist of aggregates of multiple minor precipitates of stained proteoglycan components that may have coalesced due to dehydration during processing (Figure 3.10) [967, 1034].

Thyberg et al., (1973) [1034] analysed epiphyseal cartilage matrix granules, reporting them to be polygonal in shape, ranging in size between 100-500 Å (10-50 nm), while Phillips et al., (1989) [967] noted connectivity of up to 7 filaments per granule. Matrix granule substructure consists of densely stained aggregates, reported by Matukas et al., (1968) [1035] to vary from 15 to 40 Å (1.5 to 4 nm) which closely matches observations from tomogram ultrastructure in this present study of matrix granules (Figs 3.10 and 3.11), where similar sized punctate deposits were also identified on fibres linking the matrix granules.

In adult cartilage, matrix granules have been found to have a greater concentration in the pericellular capsule than in either the pericellular or territorial matrices [788] (Figure 1.25). Slightly greater numbers of granules of larger diameter are reported within the proliferative compared with the hypertrophic zone (viz 27 to 24 nm) [1034]. The functional importance of the distribution, inter-connectivity and size of these granules within cartilage remains to be determined.

Modelling of the matrix granule network within the pocket surrounding the cilium indicates that both the granules, and their network, contain a regular higher ordered structure (Figs 3.5 C', 3.12 and 3.41). Such a uniform inter-connective 'mesh-work', represents a unique architecture likely to enable the transmission of mechanical forces to the cell and ciliary membranes [1036]. Zhu et al., (1996) [1037] established that proteoglycans, *in vitro*, form tensile networks which exhibit complex proteoglycan to proteoglycan shear moduli (where Link proteins determine their viscoelastic properties) and their stabilisation increases the average strength of the reaction sites in the network [1038-1041]. How these interact with and transmit forces from their bulk matrix via linkages to the ciliary and cell membrane offers interesting opportunities for further study.

Of particular interest are the properties of the granule network 'packing density', and its mechanical role in influencing ciliary movement, as well as allowing the diffusion of solutes and ligands. Matrix components such as proteoglycan residues form integral parts of a number of cellular pathways associated with receptors known to primary cilia [1042-1044], which also influence Wnt proteins [419].

4.22 The Periciliary Membrane and the Ciliary Pocket

The periciliary membrane and the ciliary pocket encompass an area spanning from the transition zone, extending into the cell membrane around the cilium and centrosome. In many cases this is contained within the ciliary pocket, due to the mechanisms of ciliogenesis [295, 1045], or potentially as the result of movement of the basal body internally within the cell. The ciliary pocket has been previously described [978] as a tightly enclosed active endocytotic zone [420] surrounding the base of the cilium. It may express degrees of invagination, and is normally observed sheathing the primary cilium (Figs 3.3, 3.4 and 3.5).

Examination of numerous candidate cilia shows that the degree of invagination of the cilium within the ciliary pocket of the chondrocytes varies substantially. This may allow controlled reduction of the gain of extracellular signals, where the cilium acts as an adaptive antenna. This may also function to protect the cilium from the external environment while positioning the cell, or repositioning of the centrosome for other functions. How this process occurs, and how ciliary receptors and signal transduction function during invagination, is unknown.

Numerous vesicles are closely opposed to the periciliary membrane surrounding the cilium, that may be inferred to have been derived from the Golgi apparatus (Figure 3.42). The periciliary membrane was observed to be devoid of actin filaments. Actin clearance is required for centrosome and basal body docking in the ‘immunological synapse’ in T cells [1027, 1046], which thus becomes a focus for the endo- and exocytosis of materials [1027, 1047, 1048]. Depletion of actin severing components is reported to inhibit ciliogenesis [255, 297]. The membrane of the pocket is known to be involved in ciliary protein sorting and entry [326, 1027], while TGF- β signalling is associated with endocytosis in the pocket, and also at the interaction sites of the distal tip of the cilium [420]. The model illustrates the periciliary membrane of the chondrocyte in close proximity with the distal tip of the cilium, which is associated with an active zone of clathrin-coated pits, presumably undergoing receptor-mediated endocytosis [26, 978] (Figs 3.8, 3.9, and 3.40-3.43).

4.23 The Ciliary Membrane

The ciliary membrane provides a huge surface area to volume ratio ($\sim 4 \times 10^7 \text{ m}^{-1}$), potentially acting as a high sensitivity sensor for detecting and amplifying external stimuli. Due to its small size, a complete analysis probably lies within the realms of quantum physics for interpretation of nanoscale interactions of its protein-based components [376, 1049-1051].

Analysis of chondrocyte ciliary membranes revealed that intra-membranous matrix granules were inter-connected via fine linkages, forming a complex web of tensile proteoglycans, which generated localised distortions or ‘dimples’ in the membrane, similar to observations by Jensen et al., (2004) [25]. These matrix connections were matched by protein complexes decorating both sides of the ciliary membrane. These are most likely trans-membrane proteins or complexes closely associated with extracellular linkages (Figure 3.11 E-J). Some unknown structures not associated with linkages

were also identified (Figure 3.11 J-L). Internal luminal linkers were found to be physically connecting the ciliary membrane to microtubule doublets (Figure 3.12). These connections together serve to physically connect the extracellular matrix to the membrane, the membrane to the axoneme microtubules, and they also link the microtubules to each other.

Freeze fracture of motile ciliary membranes revealed arrays of intra-membranous materials consisting of longitudinal rows, rosettes, plaques, and necklaces with attachment sites associated with the microtubule doublets beneath [51, 52, 345]. Differences in ciliary patterns reportedly exist between cell types, with higher densities of materials in sensory cilia [52], however the details of the identity and targeting of membrane proteins has remained largely unknown until recently [345, 376]. This present study has revealed the presence of numerous punctate electron dense materials of unknown function associated with, and spanning the ciliary membrane (Figs 3.11 and 3.15).

While it is tempting to speculate about the localisation of membrane receptors, it could be inferred that any potential specific distributions of these may be closely related to the presence of microtubule IFT-like materials (Figure 3.14). How membrane receptors are organised in relation to membrane-microtubule linkages is not yet established. The inability at the present time to identify these proteins within the membrane could to some degree be resolved in future with specialist immuno-histochemical investigation [385], in combination with higher resolution tomography and immuno-gold labelling.

4.231 Linking Matrix to the Ciliary Membrane and Transduction

Literature on chondrocyte ciliary receptors is relatively unknown; however, they probably utilise sensors receptive to tonicity and physical forces appropriate to maintaining cartilage tissue function. Activation of chondrocyte membrane receptors may occur directly by membrane tension from physical force impulse transduction, pressure induced deformation resulting from compression, electrical differences from streaming potentials [817, 1008], and from receptor-ligand signalling [422].

The reported presence of integrin receptors upon chondrocyte primary cilia provides a putative physical link to the tethering extracellular matrix components. Furthermore, integrin receptors are known to exhibit cross-talk with other components, such as growth factor receptors [1052]. β 1-integrins in primary cilia of MDCK cells are reported to potentiate fibronectin-induced Ca^{2+} signalling [458] and have been found to associate with PC2 [406], where ciliary bending has been shown to increase intracellular calcium levels [34]. Although their role in chondrocyte cilia remains to be determined, the study of receptors provides a putative framework for focussing upon the role of potential receptors, their transport, inclusion and functional role within the cilium.

Resident ciliary membrane receptors and their associated peptides may vary in their temporal expression, providing an adaptive ability to detect a range of signals, ligands and matrix effects, which may potentially influence function appropriate to their role. Well-known mechanotransductive

proteins of ciliary membranes already discussed include the sodium channel, ENac, the universal polycystin protein complex of PC1 and PC2, and the TRPV4-cation channel (Figs 1.16-1.18).

Receptors such as insulin growth factor IGF-1R also possess an extracellular ligand-binding domain, and a luminal region with enzyme linked components [1055]. Curiously, IGF-1R regulates G β signalling, which is reported to aid in G1-S phase progression by inducing ciliary resorption, linking ciliary signalling functionality to the cell cycle [1054].

In fibroblasts, platelet derived growth factor tyrosine kinase receptor signalling is regulated through primary cilia, and utilises the MEK1/2-ERK1/2 pathways [344, 1055]. In addition, vascular endothelial growth factor (VEGF) receptor complexes have been visualised through electron microscopy [1056], in which direct contacts are required with matrix for their activation and signalling [1057]. The epidermal growth factor (EGF) receptor contains both extracellular and luminal components [1058] and may have a sensory function with TRP family member PKD2 on the cilium [1059]. Other signalling receptors, such as Smoothed, whose sequence is similar to Frizzled, have recently been modelled [1060], while the structures of TRPV1 [1061] and TRPV4 [1062] have also been investigated. Receptors within chondrocyte cilia are likely specific to their sensory functions, for example Interleukin-1 β is reported to sequester hypoxia inducible factor-2 α (HIF2 α) to the cilium in chondrocytes [1063], vital for anabolic sensation for the phenotype.

While many proteins are known to be localised to the cilium, it is not possible in this study to identify unequivocally any within the ultrastructure of the chondrocyte or the model. The linking of membrane receptors to ciliary sensory function, and their signalling pathways represents a new endeavour of visualisation encompassing the specialist aspects of the mechanisms of transduction, which lie outside of the scope of this present study, but present fruitful opportunity for future work, building on the model presented here.

4.232 Cilia, ENac and Mechanotransduction

The sodium channel ENac participates in a diverse range of functions, from maintaining intracellular sodium levels, to registration of nociception and mechanotransduction [1064-1066], and has been found localised upon cilia [1066]. The ENac channel also shares compositional similarity with the P2X receptor family members implicated in ciliary mechanotransduction [422]. Evidence suggests they respond to flow [1067] as a sensitive membrane shear sensor, activated from membrane tension, or in combination with impulses from nearby matrix connections [1068, 1069]. Speculatively, they operate by altering permeability to sodium, thus inducing transient depolarisation, and are influenced by their order and lipid interactions within the membrane [1070, 1071], where their signalling and regulation utilises catalytic kinases and their messengers [1072, 1073]. While they have not yet been reported to be present upon chondrocyte primary cilia, evidence that these structures transduce mechanical stimuli suggests they will be found there.

4.233 The Axoneme Membrane

The translucent three-dimensional model view of the ciliary mid-section (Figs 2.11 A and 3.12) illustrates the cilium laying in matrix within a membrane pocket and shows the tapering of the proximal transition zone towards the distal end (right to left) of the axoneme. Only selected matrix zones were modeled here (depicted in Figs 3.12, 3.16 E and 3.41). These impinge upon the membrane along its length, and where connected by filaments they form localised ‘dimples’, suggesting the membrane is under tension locally, so that changes in applied force could alter this tension. The net combination of these forces within the matrix is translated to produce the bending and torsional moments upon the cilium (Figs 3.12 and 3.13).

The membrane displays a remarkable ‘rippled’ texture, which neatly and uniformly covers the axonemal contents. Curiously, only small numbers of y-shaped linkers were observed attached to the membrane in the transition zone. Their low presence could result from functional reasons or from RHT treatment at the time of fixation. Two small vesicles were found located close to the membrane of the transition zone (Figure 3.18), closely associated with the membrane, which nearby tapers into the pericellular membrane at a sharp right angle (Figure 3.35). It remains unclear whether they represent artefacts of fixation, however exosome-like vesicles containing PC1, PC2 and Fibrocystin have been discovered associated with the ciliary membrane, indicating that cilia are also possibly receivers of packages of more complex information [1074]. Thus, the presence of vesicles apparently emerging from the cilium may represent a normal mode of temporal receptor control and clearance.

4.234 Ciliary Membrane Forces

Forces upon the cilium are visible as localised distortions in the membrane, but also in the twisting and deflection of the axoneme transferred from the surrounding periciliary matrix. The radii of the ciliary membrane were found to be generally more consistently uniform between the middle and distal segments, where the microtubule doublet numbers were reduced to 5, and many IFT-like materials were located. Osmotic or mechanical loads result in membrane changes that are constrained by both the matrix and ciliary microtubule structure. Particle attachment to membranes is responsible for membrane deformation, and results in changes to the elastic energy of the membrane [1075].

The generation of curvature in membranes is intrinsic for both ciliary activity and protein function [1075-1079]. A number of proteins are involved in influencing the development of membrane curvature [1075], sorting of lipid components [1080], controlling rigidity [1081], membrane deformation [1082- 1084] and gradient formation [1085], where it is probable specialist curvatures of the ciliary membrane influence and have a role in aiding receptor and GTPase function [1083, 1084, 1086].

4.24 The 9+0 Microtubule Axoneme

The microtubule doublets were found to taper luminally inwards in their projection along the length of the axoneme, reducing in number distally (from 9 to 5, detailed in Figs 3.4 (O-Q) and 3.13), and were also deflected and twisted from the net effects of applied extracellular load. A strong morphological similarity is seen in comparison with the artistic representation by Wilsman (1978) [27] of the chondrocyte cilium (Figure 1.2).

4.241 The Flexural Rigidity of Primary Cilia

Models of axoneme bending behaviour exist for both primary and motile cilia [1087, 1088]. Schwartz et al., (1997) [1089] calculated the flexural rigidity of the primary cilium in the rat nephron in response to fluid shear of $3.1 \pm 0.8 \times 10^{-23} \text{ Nm}^2$, which fitted the ‘heavy elastica’ model (1) in predicting the bending behaviour. The cilium was assumed to be a cylindrical cantilever beam subject to fluid drag, where $\psi (s)$ is the slope angle at point s along the beam, and k is dependent upon the applied load and the material properties of the beam (valid for $\psi < 15^\circ$).

$$\frac{d^2\psi}{ds^2} + k^2 \cos\psi = 0 \quad (1)$$

For fluid drag experienced upon the cilium, modelled as a ‘cylinder’ for laminar flow condition per unit length (ω), Re is the Reynolds number, ρ the density (kg/m^3), v the velocity (m/s) and d the diameter (m) of the axoneme is given by Schwartz et al., (1997) [1089] (2).

$$\omega = \frac{4\pi\rho v^2 d}{Re[2.002 - \ln Re]} \quad (2)$$

Downs et al., (2012) [1087] carried out an experimental analysis of cilium deflection from fluid flow and found the flexural rigidity *in vitro* to be near $2 \times 10^{-22} \text{ Nm}^2$ (larger than previously reported by Schwartz et al. (1997) [1089], viz $3.1 \pm 0.8 \times 10^{-23} \text{ Nm}^2$) and also provided analysis of rotational bending and non-linear effects. In comparison, motile cilia express rigidities an order of magnitude greater. Fluid drag forces upon renal primary epithelial cilia from 2 Hz orbital shaking are estimated to be $5.2 \times 10^{-15} \text{ N}$ [1090].

Computational modelling of fluid dynamics of both active rotating and passive cilia in the mammalian embryo node revealed maximal shear stress and pressure upon cilia occurs at their tip [1189]. Finite element fluid flow modelling by Rydholm et al., (2010) [1092] identified the ciliary transition zone membrane and microtubules around the base of the cilium as experiencing the greatest stress in response to flow. The dynamics of ciliary bending in flow are reviewed by Young et al., (2012) [1093] where 80 cilia from the inner medullary collecting duct were found to have an average length $3.9 \mu\text{m}$ with a bending rigidity spanning between $1\text{-}5 \times 10^{-23} \text{ Nm}^2$. It was found longer cilia experience greater drag forces, and thus bend more easily [1089].

Within the cilium model described here, five microtubule doublets run almost the full length of the axoneme (Figure 3.14), which using Downs et al., 2012 [1087] figure for primary cilia flexural rigidity ($2 \times 10^{-22} \text{ Nm}^2$) would give rise to a doublet rigidity of around $4 \times 10^{-23} \text{ Nm}^2$, assuming similar

that the cilium architecture. This is in line with flexural rigidity observations for motile cilia doublets by Gittes et al., (1993) [1094] of $5 \times 10^{-23} \text{ Nm}^2$, and with Aoyama et al., (2005) [1095], estimate of the sperm axoneme microtubule doublet rigidity being around $6.0 \times 10^{-23} \text{ Nm}^2$. The value of such comparisons between motile and non-motile cilia remains unclear. In comparison, the steady state deformation and mechanical properties of cytosolic microtubules have been studied extensively [1193], although measurements of microtubule flexural rigidity by various authors has given rise to a range of conflicting results ($0.27\text{-}3.0 \times 10^{-23} \text{ Nm}^2$) [1094, 1097-1100].

Observations in this study of independent microtubule doublet lengths within the cilium may explain variances of flow induced non-linear ciliary bending and reports of the presence of 'kinked' axonemes [1087]. Such variances in observations of rigidity and nonlinear effects are to be expected between cell types if cilia can dynamically vary their lengths and microtubule numbers. Measurements of ciliary rigidity to date have taken place within a less viscous medium of aqueous saline, however rigidities for chondrocyte cilia are constrained by their embedding within a gel-like extracellular matrix, and remain unreported. This places chondrocyte primary cilia in a unique category amongst ciliated cells.

4.242 Distribution of Materials upon the Axoneme Doublets

Materials associated with each microtubule doublet were interpreted and classified according to their shape and possible function. These are tabulated within Figure 3.29, with respect to which microtubule doublet, its length, and position relative to the basal appendages, while their linear distributions are visualised in Figure 3.14.

The distal tip of the cilium may be viewed as a 'turn-around' terminus zone for the transport of materials to the end of the microtubule doublets and has received little ultrastructural investigation. The membrane luminal surface was coated with a number of structures associated with the microtubule terminations, some of which were connected by fine linkages and dense deposits (Figure 3.16). Along the axoneme fibre 'linkers' connecting microtubule doublets to the membrane, and shorter non-connecting filaments were identified, decorating both the membrane and luminal sides of the microtubules (Figure 3.15). These were similar to fine 10 nm long fibres that have been reported associated with cytoplasmic microtubules [166], and it is likely similar proteins may also act as scaffolds upon the basal body. Between microtubules of the axoneme, the fine filaments and inter-connecting linkages were primarily associated with the A-subfibre, for microtubule to membrane linkers (A:B 86:62), while inter-microtubule linkers being found to be more evenly associated with the B-subfibre (A:B 46:59). Filaments which decorated the membrane and luminal faces of the microtubule surfaces, but did not connect to membranes or other components were of higher incidence upon the B-subfibre (internal A:B 42:75) and external filaments (A:B 43:54) respectively (tabulated in Figure 3.29 B and C). At present, the nature of these structures remains obscure.

4.243 Distribution of IFT-like Particles

This is the first study to take a detailed look at IFT particles within the chondrocyte primary cilium. A significant limitation of electron microscopy is the difficulty of matching known or anticipated functions, determined by techniques of molecular biology, to the micro-morphology exposed by staining with heavy metals. It is however possible to speculate on that relationship, since recent proteomic analysis of cilia and primary cilia in particular has revealed many of their structural, transport and signalling protein components [41, 132, 270, 468, 1101-1104]. Maintenance of ciliary function requires continual turnover of material within the cilium, which only be achieved by transport from the cell into the ciliary lumen.

Identification of IFT-like particles as macromolecular protein complexes located between the microtubule doublets and the ciliary membrane resulted from comparison with previous ultrastructural findings of Rosenbaum et al., (2002) [1105]. Figure 3.29 tabulates the relative doublet position, their lengths, accumulations of materials, including 'rafts' of IFT-like particles, with reference to the positions of the basal appendages. Distributions of IFT-like 'rafts' of materials were identified predominantly upon longer microtubule doublets, and were clustered towards the distal end of the axoneme (Figure 3.14).

The choice of microtubule triplet numbering on the chondrocyte cilium was in reference to the presence of Basal Appendage One (BA1), and incremented in convention with motile cilia. IFT-like accumulations were predominantly concentrated upon microtubule doublets 2, 3, 6, 7 and 8 with 1, 4, 5 and 9 being less populated or free, while basal appendages spanned microtubule triplets 1, 9 and 2 and 6, 7 and 8 (Figure 3.29). In comparison, Buisson et al., (2013) [261] noted IFT in the flagellum *Trypanosoma brucei* was restricted to microtubule doublets 3, 4, 7 and 8, with 1, 2 and 9 being available for transport, while Absalon et al., (2008) [284] noted IFT restriction predominantly to doublets 3, 4, 7 and 8.

Curiously, Basal Appendage Two (BA2) contained the greatest number of anchored cytosolic microtubules involved in active transport processes (visualised in Figure 3.27), and it is closely associated with microtubule doublet 3, which carries the greatest number of IFT-like materials. This might indicate that within the chondrocyte cilium, transport may be preferential upon distinct radial populations of microtubule doublets, and the distribution of basal appendages may influence their loading. This discrete transport relationship and assignment of cargoes upon specific microtubule doublets is likely to be structurally defined, and may depend on the relative proximity of the triplet to the basal appendage basement structure, for access of vesicles and fine materials from docked microtubules (detailed in Figs 3.24, 3.25 and 3.27).

This relationship may be further developed through the observed variances in microtubule length, which requires IFT for their polymerisation and stabilisation [320]. Curiously, Gluenz et al., (2010) [1006] established that certain microtubule doublets may undergo preferential collapse, and

furthermore, that the pro-centriole is commonly tethered to a preferred microtubule triplet, indicating discrete polarisation of basal body processes.

While it is not possible to identify proteins within the tomogram with any certainty, the chondrocyte model indicated the presence of IFT-like structures accumulating within two laterally opposed zones (Figure 3.14 arrows). Structures were noted upon both the A and B-subfibres, (with a slightly higher association with the B-subfibre), including on the internal lumen side, while shorter microtubules of the axoneme were generally bereft of IFT-like particles. In motile cilia, the A-subfibre contains motile dynein machinery, while IFT-trains are observed to be tightly contained between the B-subfibre and the membrane [269, 322]. In comparison with primary cilia, the A-subfibre is free, and thus could be used for discrete transport (detailed in Figs 1.9, 3.12, 3.15, and 3.17). IFT-complex particles must first be transported to the basal body microtubule substrate, where they become selected and activated to transport their cargoes to their respective destinations, before being recycled [261-264]. IFT-complexes and transport motors have been reported to be concentrated around the transition zone and basal body, where their interaction dynamics are discussed by Pedersen et al., (2008) [103].

Chondrocyte IFT collections were found to have 20-45 nm periodicities, with the longest 'raft' measuring 400 nm, with 150, 80 and 30 nm lengths also being observed, distributed with the highest concentrations observed upon microtubule doublets 3, 6 and 8 (Figure 3.29). Tomography by Pigino et al., (2009) [269] identified, in *Chlamydomonas reinhardtii*, IFT 'trains' consisting of both 'short and long' trains containing 12-27 particles per train, with mean lengths of 250 and 700 nm with a periodicity of 16 nm for the short, and 50 nm for the long train, respectively. Engle et al., (2009) [264] indicated transport particle size was inversely related to flagellar length. Recently, Buisson et al., (2013) [261] reported anterograde transport trains of 393 ± 51 nm, with retrograde trains 250 ± 51 nm in *Trypanosoma brucei* [261], with dual anterograde populations exhibiting velocities of 2.22 and 3.12 $\mu\text{m/s}$ (a small population exhibiting low velocities of 0.5 $\mu\text{m/s}$) and retrograde speeds of up to 7.42 $\mu\text{m/s}$. Such variable velocities may indicate a more complex microtubule-motor-IFT cargo relationship, which is yet to be addressed. Anterograde transport frequencies of around 1 Hz were observed for anterograde trains, whilst retrograde frequencies are three times higher [261]. It has been proposed that different anterograde velocities result from the actions of different motors [1106].

Given the number of transport motors that have been identified associated with the cilium, there remains the likelihood of finding further ciliary motor interactions. These may possibly include KIF12 and KIF13A [103], as well as a greater role of KIF7 and KIF17 motors in the distal region [47, 270]. Furthermore, Ou et al., (2007) [285] indicated that IFT-components and transport may be influenced by cell phenotype. This may indicate that chondrocytes display unique structural and ciliary functionality, as evidenced by close anatomical similarities between the model and the architecture described originally by Wilsman [27].

In conclusion, ciliary morphology affords a strong inference that IFT-trains travel upon restricted sets of microtubule doublets, individually controlled by discrete mechanisms from the basal body, akin to a train marshalling yard. This would explain variances in doublet length and cargo size.

4.25 The Transition Zone

The transition zone consists of linking structures of three distinct types: y-shaped linkers, alar sheets, and interspersed fine filamentous fibres. The term ‘distal’ or ‘transitional fibres’ has also been used in the literature to describe ‘alar sheets’. Alar sheets function to attach the basal body to the periciliary membrane, while y-shaped linkers connect the microtubule doublets to the ciliary membrane. Both are considered to act as both a physical barrier and a regulatory zone. The transition zone is formed from two distinct compartments: the alar sheet zone from the axoneme juncture to the basal body and the y-shaped linker zone (Figs 3.18 and 3.19). However, descriptions of these structures vary between cilia types and between cell types [48, 49, 1107]. Horst et al., (1987) [1108] identified the presence of cell surface glyco-conjugates linking the microtubule doublets to the ciliary surface glycocalyx, in rat photoreceptors, indicating the possibility of extracellular interactions in these cells.

In the present work, tomography revealed densely stained accretions decorating both the microtubule doublets, and the membrane within this zone, interpreted as indicating the presence of proteinaceous complexes. Two small membrane associated vesicles were located nearby closely associated with the ciliary membrane (Figure 3.18). Their small diameter would allow them to migrate through the ciliary matrix granule zone, but they could also represent used or superfluous ciliary receptors shed from the membrane.

This zone contains many protein structures whose identities and functions remain obscure (Figs 3.18 and 3.19). The distribution of ciliary proteins within the transition zone compartment has been reviewed by Szymanska et al., (2012) [65], Czarnecki et al., (2012) [55] and Garcia-Gonzalo et al., (2011) [70]. Ciliary transition zone components have recently been likened to a nuclear pore complex [68], where it is proposed to function both as a regulatory zone and a diffusion barrier [1109] for the orderly processing and exclusion of materials [66, 297, 1109]. Whether this zone is permeable to vesicle transport remains to be seen.

4.251 Y-shaped Linker Structure

The presence of few identifiable y-shaped linkers within the ciliary transition zone in the tomogram was a surprise in view of previous studies [49, 51] and given their very visible presence in the *in vitro* work (Figure 3.4). This may reflect the effects of RHT and fixative influencing their preservation, or temporal variation within the cilium at the time of fixation. Y-shaped linkers were hard to discern and translate to the model adequately in the tomogram due to poor contrast. Curiously,

no y-shaped linkers were identified upon two of the shorter microtubule doublets 4 and 5 (Figure 3.29 C), indicating a possible absence of these structures upon dynamic microtubules.

4.252 Sub-Distal Fibres: Filamentous Structures

A number of fine filaments were observed within both the transition zone and basal body, linking the microtubules to the membrane. These were investigated and modelled (Figure 3.19) revealing them to be concentrated in a sub-distal zone upon the basal body, in proximity to the alar sheets and associated with denser depositions along the microtubule surface (Figure 3.19 D-G). The composition and function of these fibres remains unknown, as such structures have not been commonly reported in the literature [49].

4.253 The Alar-Sheets Structure

The alar sheets are believed to function as a regulatory entry barrier for active transport into the cilium [297, 308], from where the doublet subfibres of the triplets transition to form microtubule conduits on which transport complexes transfer structural, signalling and receptor proteins to their required locations, and are recycled back to the centrosome.

Within the tomogram the alar sheets, like the y-shaped linkers, were difficult to discern, unlike the earlier *in vitro* ultrastructural investigations (see Figure 3.4 N and O). Each consisted of lightly stained fine amorphous granules that tether the basal body to points within the periciliary membrane. Originating from an attachment zone near the distal end of the C-subfibre, the alar sheets evenly span across each doublet face, focussed upon the B-subfibre base (50 nm wide and 90-100 nm in length), tapering outwards at right angles from the surface of the triplets, to focus upon anchoring points within the ciliary membrane (see Figs 3.4 and 3.19). The transition zone membrane width was found to average 262 nm in diameter (Section 3.5), with the entire alar sheet and basal body docking system measuring an estimated 500 nm in diameter, in line with observations by Sillibourne et al., (2011) [1110].

The tomogram provides perspectives of the alar sheets, which were modelled selectively due to their lower density structure, consisting of fine inter-dispersed granules (Figure 3.19 H). There was little evidence to support the alar sheet structure as consisting of ‘wings’, that is frequently reported in the literature [25, 45, 297]. The model shows the presence of vesicles in proximity to the alar sheets, however these occur in close association with basal appendage microtubule transport processes. The full role, structure and function of the alar sheet complexes remains unknown, although they are known to be composed of the proteins ODF1, ODF2, CEP164 and CCDC123/CEP123 (Appendix D). CEP123 associated with CEP164 [1110], which in turn associates with CEP170 [293] and HYL1 [70].

Materials entering the cilium must pass the alar sheets, by active or passive transport mechanisms into the axoneme. A ‘ciliary gate’ gap of 60 nm is reported [65] around the transition

zone, which allows for active transport into, and out of the cilium, regulated from the basal body (Figure 3.29). It is not clear if this precludes vesicle transport. Lin et al., (2013) [327] established that the interior of the cilium was accessible to proteins as large as 7.9 nm, through the base of the cilium, while low molecular weight dextrans (<40 kDa) have been shown to be able to enter the cilium [68], although information about the shape of these molecules was not reported.

A number of proteins have been located within the transition zone [55, 70, 302, 1111] where they are believed to contribute to ciliary gating, ciliogenesis [65] as well as membrane composition [70]. Specific details of their structure and roles have only recently been established [62, 65, 70, 1112, 1113]. Mutations to any of these key proteins within the zone give rise to pathologies ranging from lethal embryonic conditions to impaired ciliary function (Figure 4.1) resulting in a spectrum of ciliopathies [1, 55, 1114, 1115]. Some of the common ciliopathies have been assigned to a structural site of action within the transition zone, illustrated in Figure 4.3.

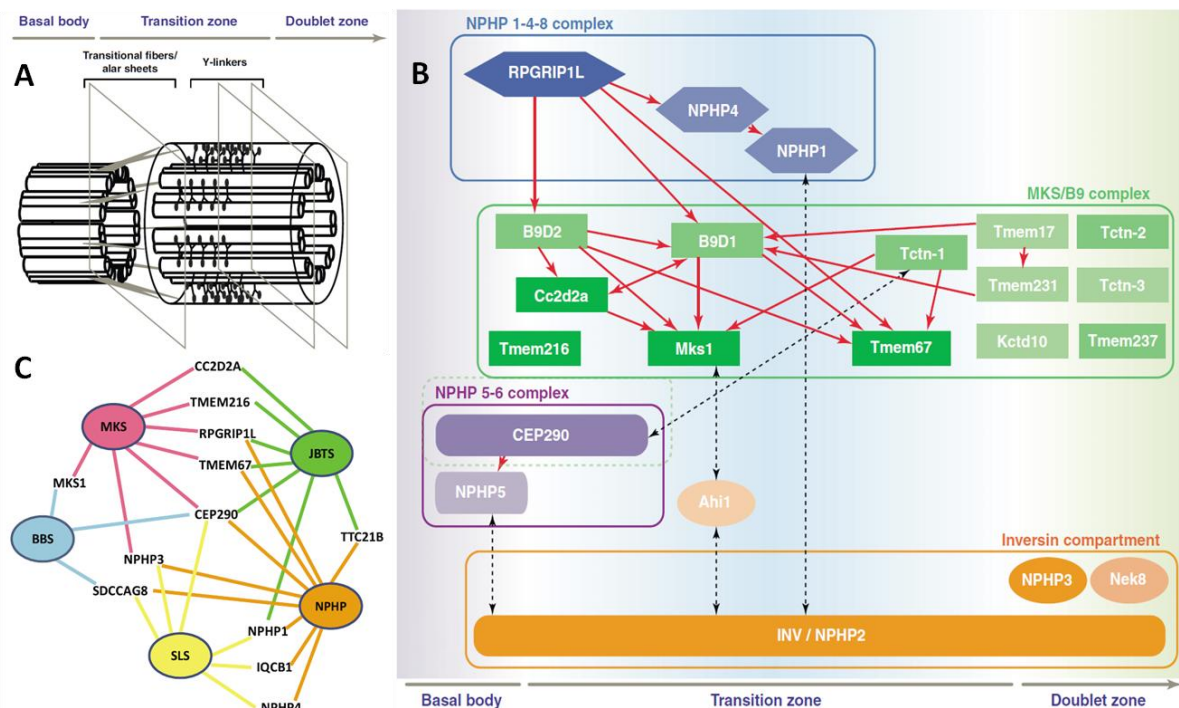


Figure 4.1 The Transition Zone ‘Compartment’: **[A]** A model of the transition zone located between the basal body and the axoneme, where alar sheets tether the basal body to the periciliary membrane, and y-shaped linkers connect the axoneme microtubules to the ciliary membrane. The zone is divided into modules which contain distinct components. Reproduced and edited from Czarnecki et al., (2012) [55]. **[B]** Organisation of the Transition Zone Modules are based around protein complexes; **The NPHP1-4-8 Complex**: NPHP1,4 and 8, the **MKS/B9 Complex**: (B9D1, B9D2, CC2D2A, MKS1, KCTD10, TCTN 1, 2 and 3, including trans membrane proteins TMEM17, TMEM67 TMEM216, TMEM231 [1116], TMEM67, TMEM237), and the **NPHP5-6 Complex**: (CEP290 and NPHP5) and the **Inversin compartment** (NPHP2, 3, NEK8, and INV). The vertical height associates complexity of component interactions, while the colour intensity indicates pathology complexity, while arrows shows associations between molecules. The horizontal axis indicates dispersal of respective complexes from the basal body along the axoneme. Reproduced with permission from Czarnecki et al., (2012) [55], who noted the shared elements of the transition compartment in ciliogenesis and disease[70, 1111]. **[C]** Reviews of five ciliopathy proteins: MKS (Meckel-Grueber), JBT5 (Joubert syndrome), NPHP (Nephronophthisis), BBS (Bardet-Biedl Syndrome) and SLS (Senior-Loken Syndrome). Interactive protein partners included CC2D2A, TMEM216, RPGRIP1L, TMEM67, CEP290, NPHP3, SDCCAG8, NPHP1, IQCB1 and NPHP4. Mutation of any of these proteins may generate particular aspects of these ciliopathies, which are joined by common lines. Reproduced with permission from Szymanska et al., (2012) [65]. The exact functional roles of many of these proteins remains unknown (see Appendix I).

4.30 The Centrosome

The centrosome has been simply but accurately described as a ‘polyfunctional multi-protein cell complex’ by Alieva et al., (2008) [120], a structural processing unit for the regulated control of cytosolic materials, organelles and cell cycle. During interphase, it acts a cytoskeletal microtubule nucleating and organising centre, where the primary cilium functions as a physical extension of the basal body, with the proximal centriole subtending it. Components may be broken into three groups: *structural*, either involved in the microtubule structure, or localised with it, *centrosomal proteins* associated with the centrosome and cell cycle, or *functional proteins* such as transport motors and regulatory complexes [120].

Analysis of the centrosome in Figure 3.32 A-H demonstrates a series of slices detailing the microtubule architecture, the pericentriolar matrix, the basal appendages, and the nearby nuclear membrane. Surrounding the centrosome are fields of vesicles shown in Figure 3.32 I-L. These are interspersed with microtubules, indicating the centrosome as a central organiser of vesicular based processes. Modelling of the microtubule based architecture of the basal body, proximal centriole and cytosol surrounding them is illustrated in perspective views in Figure 3.33, uniquely including the presence of the nucleating microtubule upon the vesicular ‘torus’.

Figs 3.34 and 3.35 detail further ultrastructural and model views of the relationship of centrosomal components. These images contain large amounts of information covering spatial components of the centrosome, the tubulin based basal body and the proximal centriole, microtubule nucleation and attachment points of the basal appendages and pericentriolar matrix, intermediate filaments and fields of vesicles in the process of directed transport, docking and sorting of materials.

Limitations to interpretation of ultrastructure stem inevitably from the use of a single axis tomogram containing a complete cilium for model generation. It is possible to expand into great detail on many of the proteins and molecular pathways associated with aspects of the model components of the primary cilium, and also the centrosome. These protein components are too numerous to mention in this discussion, but some of these are tabulated within the Appendices aiding in linking the structural components that have been visualised, with function. Many of these represent *speculative* findings in the literature, and need to be interpreted carefully. However, the focus of this discussion must be limited, brief and upon technical aspects resolved in the model, to which *function* could be attributed. The few previously undertaken tomography based modelling studies of centrosomes, have focussed upon aspects of centriole structure, pro-centriole formation, microtubule networks and nucleation or mitotic processes (see Appendix VI).

4.31 The Basal Body

The microtubule based architecture of the maternal basal body and its subtending proximal centriole form the core of the centrosome. These were carefully traced within the tomogram to ensure the accuracy of each element. Individual triplet subfibres were depicted as simple intersecting tubes, each extruded to represent the microtubule doublets of the axoneme (Figure 3.20). This provided a simple basis for modelling all microtubule based components, however it unfortunately constrained the presentation of the basal body fine structure.

The structure of the microtubule triplet unit and its position within the basal body is similar to previous basal body studies (Appendix VI). Anderson (1972) [45] and Wilsman et al, (1978) [27] produced artistic representations of the basal body triplet architecture. These are visualised in the model, with each microtubule triplets 'left-handed' polarisation and decreasing angle observed in their distal projection along the basal body, detailed in Figs 3.20 and 3.21 J. The microtubule triplet angle decreases uniformly along the basal body, where each triplet merges into the doublet of the axoneme, retaining a slight left-handed rotation or 'curl'. The basal body is observed to be slightly wider at its centre, giving the appearance of having a 'barrel' shaped structure (Figure 3.20), as described by previous authors [27, 45] (Appendix VI).

4.32 The Microtubule Triplet Structure

The model presented in this study did not fully investigate the basal body triplet fine structure. This requires higher resolution visualisation, to establish finer details of the whole centriole, its longitudinal structure, triplet architecture, and the inter-triplet relationship with their associated proteins. Simple investigative microscopy of primary cilia utilising cell culture was used to define the basal body subfibres, their inter-linkages and 'hooks' (Figure 3.4), but only at a relatively low resolution.

The A-subfibre feet appear to be functional remnants of centriole assembly, which exist only within the proximal zone. The A-C-subfibre linkages tether the respective proximal ends of the triplets, providing mechanical inter-triplet support to the basal body (Figs 1.8 and 3.4) and disappear towards the distal end of the basal body near the termination of the C-subfibres. It is a matter for further investigation whether each of the A and A-C subfibre structures are of continuous form like the A-B-subfibres, or are represented as individual periodic linkages, as observed within the triplet structure by Li et al., (2011) [89]. These connections occur within the luminal environment of the cilium, and may function as attachment and regulatory sites upon the inner surface. The longitudinal fine unfolding protofilament structure of the C-subfibre has received little attention since being described by Wilsman et al., (1983) [88], as its fine 'hook' structure gradually disappears distally along the cilium.

4.33 Luminal Vesicles

Numerous observations have been made of cilia and basal bodies containing vesicles, ranging in diameter from 25 to 150 nm, however they have customarily been regarded as artefacts of fixation [95, 1117-1120]. Luminal vesicles observed within the primary cilia of chondrocytes have received less attention, despite previous mention in ultrastructural and tomographic investigations [25, 26]. In this study, no vesicles were observed within the axoneme of primary cilia. However, the basal bodies of three cilia contained vesicles (Figs 3.5 A, B and 3.22), with one distinctly containing three small vesicles (Figure 3.5 B).

Vesicle size ranged from 35 to 50 nm, curiously similar size distributions to the ciliary membrane vesicles observed within the matrix (Figure 3.18 for comparison). The single oval shaped vesicle contained within the model appeared to be firmly attached to the luminal face of a triplet of the basal body, suggesting internal transport may be possible within the lumen (Figure 3.22). The vesicle was found to interact with proteinaceous materials contained within the lumen.

Presumably cilia undergo chemical fixation rapidly, so the probability of observing vesicles using ciliary transport should be low, due to their relatively short axonemal transit periods. However, frequent observations exist of vesicles throughout the cilium, including from within the transition zone [25, 26]. The presence of a base plate and central microtubule doublet in motile cilia may hinder luminal vesicular transport, although vesicles have been noted in the motile cilia of patients with bronchiectasis [1121].

In primary cilia, a large intra-luminal zone does not preclude potential vesicular accumulation or transport. If these vesicles represent the true structure, and are not artefacts, then it may be concluded that they are in fact part of the normal transport processes of moving membrane bound materials to and from the cilium. Thus, the lumen of the primary cilium basal body may represent a novel conduit between the cilium and the centrosome.

4.34 Basal Luminal Discs and Internal Structures

Various electron dense structures have been commonly occur within the lumen of centrioles of many species. Formations such as the pro-centriole replication 'cartwheel' complex [237] disappear within the mature centriole [1122, 1123], while other indeterminate structures are frequently noted within the lumen [1124], including those termed luminal discs [124, 237, 253, 597, 1125]. The tomogram has revealed a presence of granular structures spanning the distal ends of both the basal body (Figure 3.21) and the proximal centriole (Figs 3.30-3.32). The basal body lumen also contains numerous deposits and filaments of unknown electron dense materials, many of which are often attached to the triplet faces.

It is probable that the lumen of the basal body functions as a tightly regulated 'hangar and conduit' for the storage, modification and signalling of key ciliary and centrosomal components, which are protected from the active cytosolic environment by the microtubule triplets. Key proteins

involved during pro-centriole biogenesis [237] include the lumenally located components of CP110, Centrin, CPAP and CEP135, while Centrobin [1126], CEP110, 120, 135 and 192 are known to have microtubule associations [120, 122, 237]. The presence of centrosomal RNAs (cnRNA) have been reported, however their exact roles and localisation with respect to the basal body are still to be determined [1127, 1128]. It is likely that many proteins share both temporal and spatial locations around and within the basal body during normal cilium operation and the cell cycle.

4.35 The Basal Appendages

Within the tomogram, basal appendages appear as extremely heavily stained electron dense structures that leave little contrast to their fine structure (spanning Figs 3.23-3.27). Each consists of three parts, the *basement complex*, the *appendage arm*, and a distal *docking complex*, with attached cytosolic microtubules. The three 'basement zones' were found to obliquely span at least three microtubule triplets, each consisting of fine porous materials forming a perforated structure. These were investigated through volume rendering approaches (Basal Appendage One, Figs 3.23 and 3.24) and (Basal Appendage Two, Figure 3.26). Each is attached obliquely to three microtubule triplets, comprising of a collection of fine amorphous materials, detailed in Figs 3.24, 3.25 and compared in Figure 3.28, sharing a strong similarity in their shape, structure and disposition.

A 'hollow' low density zone is located in the middle of the basement zones, located under the appendage arm, which extends perpendicularly outwards, resembling findings by Kunimoto et al., (2012) [74]. The arm itself is uniformly extremely electron dense, containing pockets and thorny protrusions. The docking complex heads appear as finer spiny complexes, some of which are bifurcated (Figure 3.27), and also act as mechanical attachment points for microtubules. Vesicles were noted in close proximity to both microtubules and the basal appendage, with one of these being physically linked via fine fibres to the anchoring complex, and the nearby basal body (Figs 3.23-3.25).

The basal appendages may experience loads resulting from the interplay of combined forces upon the cilium, and those applied by their anchored cytosolic microtubules. These radiate outward from the docking complexes and appear to interact with a number of vesicles and organelles (Figs 3.25, 3.27 and 3.35). Other microtubules were observed radiating from the centrosome and these may function together with intermediate filaments to act as part of a cytoplasmic tensegity network required to maintain cellular shape. The possible presence of another basal appendage was identified outside the plane of section of the tomogram, indicated by the occurrence of intersecting trajectories of cytosolic microtubules within the section (Figure 3.43). If present, this extra appendage could easily span triplets 3 to 5 (Figure 3.29), and would provide the cilium with a third additional anchoring point.

Basal appendages are a marker of the formation of the mature basal body, where they act as a tethering apparatus for the attachment of cytosolic microtubules (Figs 1.9-1.11), and are ubiquitously associated with both motile and primary cilia. Descriptions in the literature of basal appendage

structure and relationship to the basal body are multifarious and imaginative. This present study finds little evidence to support these, although there exists abundant opportunity for further study.

The protein components constituting the basal appendages, and which are involved with the mechanisms of microtubule nucleation and anchoring within the centrosome are not yet fully understood [120]. Some discrete protein members have been identified and their roles are listed in Appendix I. Basal appendages are known to contain the proteins Cenexin [1129], Ninein [160], CEP170 [1130], CEP110 and ϵ -tubulin [1131], although there are undoubtedly many more awaiting discovery. The basal appendage anchoring head complexes are believed to be comprised of Cenexin, Centriolin, CEP170 and ϵ -tubulin [120], where Ninein may also act as a molecular link for anchoring of γ -TuRC complexes in the centrosome [160, 198]. It is believed CEP192 may act as a scaffold for γ -TuRC microtubule nucleation, while NEDD-1 (GCP-WD) is required for γ -TuRC complex centrosomal localisation and binding [1132]. CG-NAP and Pericentrin are believed to play roles in anchoring nucleation sites within the centrosome. Centrosomin is known to interact with γ -tubulin [1133], while Pericentrin provides a physical scaffold that interacts with GCP2 and the γ -tubulin nucleating component [1134, 1135]. BBS4 functions as a critical adaptor link between PCM-1 and p150^{Glued}, and also influences microtubule attachment [120]. IFT-complex motor KIF3A recruits Dynactin (p150^{Glued}) to organise the appendages, where depletion of p150^{Glued} results in loss of KIF3A and Ninein giving rise to ciliary dysfunction [523]. Striated parallel bandings are sometimes reported decorating basal appendage arms [1120], however their composition remains unknown.

4.36 *The Proximal Centriole*

Naming conventions for the proximal centriole as a ‘daughter’ centriole (with respect to the ‘mother’ basal body) have resulted in much confusion, with centriole replication pro-centrioles being referred to as ‘daughter centrioles’. The centrioles of the diplosome exhibit dynamic spatial and separation inter-relationships throughout the cell cycle [236]. The proximal centriole was only partially contained within the tomography section, resulting in an open ‘cusp’ like appearance in model projections (Figs 3.30-3.32) revealing the triplet architecture is similar to the basal body in structure, handedness and polarisation [64, 94]. However, a notable exception is the absence of the gentle distal straightening of the triplet angle during their projection, as in the basal body. It is oriented in the positive microtubule direction away from the axis of the basal body at 135°. Importantly, it is devoid of any alar-sheets, subdistal fibres or basal appendages, and lacks microtubules attached to or nucleating from its surface.

Dense areas of heavy stain decorate materials upon both the external and luminal surfaces of the proximal centriole, indicating a substantial collection of proteins. A series of dense luminal disc-like accumulations was identified spanning the near distal end of the proximal centriole (Figs 3.30-3.32) in striking similarity to structures contained within the basal body.

The proximal centriole closely subtends the basal body within the centrosome, connected to it by fine linkages of pericentriolar material connecting their respective proximal ends (detailed in Figure 3.34 A and B). The proximal end is in close proximity to a vesicular bud projecting from the centrosomal annulus (Figure 3.33). The distal end of the proximal centriole contains proteinaceous tendrils linking to the nuclear membrane and to a nearby nuclear pore, one of three in close proximity (Figure 3.31). Within the literature, centrioles have been commonly reported associated with the nuclear membrane [1002, 1154]. Proteins Ninein, NEK2 and δ -tubulin are known to be localised to the proximal ends of the basal body and proximal centriole, while Centrin localises to their respective distal ends [120]. The function of the proximal centriole remains elusive, however is a vital component of centrosomal dynamics, where its structure appears every bit as intricate as that of the basal body.

4.40 Microtubule Populations

Three distinct cytosolic microtubule populations were observed; those derived from the basal body appendages, those from within the centrosome pericentriolar matrix, and those originating from within the cytoplasm. The pericentriolar matrix acts as a ‘scaffolding lattice’ for many proteins, as well as acting as a nucleating site for microtubule ‘minus’ ends (Figs 1.11, 1.12, 3.35 and 3.36). These are spatially distributed within the matrix surrounding the centrosome, where it has been suggested that a limited number of nucleation sites exist [124, 135].

Visualisation of microtubule surfaces in their long axis revealed decorations of fine speckled deposits, denser globular structures, and fine tethers linking to vesicles (Figure 3.36). These were intimately clustered on microtubules surrounding the basal appendage anchoring heads and the centrosome (Figs 3.25 and 3.27). These microtubule-associated materials of unknown function may represent directed motor dependent transport processes of the basal body, the centrosome and the Golgi apparatus. This raises further questions about the role of the appendage derived microtubules within the centrosome, their interactions with organelles, and the regulation of transport motors responsible for their many transport and signaling mechanisms.

Basal Appendage One-derived microtubules were identified extending to the Golgi apparatus, associated with vesicle fields of the pre-*cis* compartment area, and both the *cis*- and *medial*-compartment edges (Figs 3.35, 3.37 and 3.41). It is likely that the terminal ends of the microtubules also interact with the Golgi membrane and resident proteins [53]. For example, Hoff et al., (2011) [610] has shown that proteins destined for the cilium, such as PC2, may emerge exclusively from the *cis*-Golgi. Microtubule transport of such ciliary derived PC2 can be readily envisaged from the components detailed in Figure 3.37 B and D.

Basal Appendage Two-derived microtubules appear to have a selection of assorted protein structures and vesicles associated with them, some in close association with the nearby periciliary

membrane. These microtubules display surface variances in staining, and exhibit a number of putative motor-associated tethers attached to them, with some linked to nearby vesicles (Figure 3.27).

A long microtubule originating from Basal Appendage Two transects the centrosome to span a field of assorted vesicles (including the torus) bound by the nuclear membrane and the *cis*-Golgi face (Figure 3.41). These areas appear to direct trafficking of vesicles into the Golgi cisternae, from components of the ERGIC. As Golgi cisternae are also highly dynamic, it is likely that many microtubule processes are also involved in interfacing the Golgi with the centrosome in this region.

A subset of non-basal appendage, centrosome-derived microtubule fields are observed running closely parallel to the pre-*cis*-Golgi face, which appears to be actively involved with a high-density field of pre-*cis* face vesicles (Figure 3.37, 3.38 K). Such arrays could easily transit materials along the 'building face' of the Golgi, and also be involved in the spatial organisation and signalling to the apparatus. It is tempting to speculate basal body derived microtubules may exclusively source materials from the Golgi as part of their normal centrosome function.

Microtubules from the basal appendages are intimately associated with Golgi cisternae and the *pre*-Golgi vesicle fields. Centrosome derived microtubules are associated closely together with the *cis*-face, indicating that they are involved with specific aspects of the Golgi. Transport upon these may be both spatially refined and restricted, while other centrosome microtubules appear to facilitate the bulk transfer of materials from the endoplasmic reticulum to the Golgi.

4.41 The Intermediate Filament Organisation Centre (IFOC)

Intermediate filaments have been shown to originate within the centrosome from an organisation centre within the pericentriolar matrix, surrounding the proximal centriole (observed structurally in Figure 3.34 D and E and modelled in Figs 3.35 F, 3.37 B and 3.41), where intermediate filaments have long been associated with the centrosome [115, 120, 236]. Examination of the model reveals that the intermediate filament network originates in a condensed zone within the centrosome surrounding the proximal centriole. This model concurs with observations of Alieva et al., (1992) [115], who reported intermediate filaments originating in a zone, with no single focus, contained within 0.3 μm of the proximal centriole. Filaments were observed attached by fine linkages to materials within the pericentriolar matrix (Figure 3.34 D, E). Some filaments ran in parallel with the microtubule network, with one filament originating from near the proximal centriole, radiating into the pre-*cis*-Golgi area (Figure 3.35, 3.37 and 3.41), perhaps indicating a functional relationship.

As a component of the cellular tensegrity network, intermediate filaments can be deformed under strain, and are involved in the dynamic regulation and maintenance of cytoskeletal architecture [1136-1139]. Their keratin and vimentin members are known to be associated with the centrosome [1136, 1140, 1141], influencing its stability [1142], with vimentin being reported to be necessary for the maintenance of the chondrocyte phenotype [139]. De-tyrosinated microtubules reportedly interact with vimentin intermediate filaments [1143], while the cytoskeletal protein Plectin mediates their

interaction [1144]. The centrosome shares both the microtubule and intermediate filament organising centres, each sharing a zone surrounding the basal body and the proximal centriole, where they each play an intrinsic regulatory and nano-mechanical role in bearing compressive forces upon the cell.

4.42 Order in the Pericentriolar Matrix

In the electron microscope, the pericentriolar matrix appears as a zone of finely stained filamentous material that surrounds the diplosome, inter-connecting the distal ends of the centrioles (Figs 3.32, 3.33 and 3.34). The use of RHT gave an enhancement of contrast deficient in earlier studies. The matrix is now revealed to be an intricate lattice, made up of many fine interlinked components, dispersed with small electron dense granules. These linkages inter-connect the basal body and the proximal centriole, where they also decorate and coat the microtubule triplets. The luminal contents of the proximal ends of the basal body and the proximal centriole also merge into this matrix, which permeates around the diplosome. The lattice extends outwards to interact with a variety of nearby objects, including microtubules, intermediate filaments and vesicles. It is constrained by the presence of the vesicular centrosomal torus, to which it also binds (Figure 3.34 C). No striated rootlets or inter-centriolar linkers were observed within the tomogram. The known protein components of the centriole anchoring complexes are tabulated in Appendix I (see Centriole Anchoring Complexes).

Two distinct PCM domains appear to exist surrounding the diplosome: a near zone that is reported to be based upon pericentrin-like-protein fibrils aligned with the centriole wall, and a larger extended zone linking to the larger pericentriolar-centrosomal matrix [122]. Materials accumulated upon the microtubule triplets have been proposed to have both higher order structures and functions [464]. The PCM contains PCM-1, which interacts with a wide range of proteins as well as with the γ -TuRC nucleation complex [128, 138, 459]. The PCM acts as nucleation site for microtubules, and tethers centrioles [126], as well as containing key proteins involved in the cell cycle [134], cell regulation, ciliary formation and regulation [62]. The role of the PCM in supporting interphase function is less well known [128, 466, 1126] where it varies during the cell cycle [112, 128].

Recent visualisation of numerous key centrosomal proteins during interphase by high resolution three dimensional microscopy has revealed the detailed organisation of many of these proteins within a highly organised 'PCM tube' and lattice, which are confined in spatial layers surrounding the basal body [104, 122, 464]. The relationship of this centrosomal matrix to the vesicular torus described in this study remains unknown.

4.43 The Centrosomal 'Torus'

This study has identified a unique vesicular annular structure surrounding the centrosome that has not been previously described. It occupies an orbital volume (torus) between the proximal and distal centrioles, spanning an intermediate position in association with vesicle fields of the pre *cis*-

Golgi to the endoplasmic reticulum. Smaller vesicles are involved with the end zones surrounding the annulus, and with the nearby microtubule transport conduits around the basal appendages (Figure 3.33, 3.35 and 3.41). The Golgi associated end of the annulus was found to have small budding membrane protrusions associated with a vesicle fields and a nearby larger vesicle that is tethered to the surface by a series of fine connections (Figure 3.33 D). Centrally, the membrane is near to a microtubule derived from basal appendage two (Figure 3.33 A), which also interacts with the distant Golgi vesicle field Figure (3.35 F). The pericentriolar matrix of the basal body interacts closely with the membrane surface (Figs 3.33, 3.34 B and C), while nearby on the lateral side a membrane protrusion is juxtaposed to a number of electron-dense accumulations on the end of the proximal centriole, in association with two small vesicles. Opposed at 180°, the annulus was found to contain a microtubule-nucleating site that is closely associated with smaller vesicles and electron dense materials (Figure 3.35 F). The presence of smaller vesicles in close proximity to both centrioles is novel, and offers a possible source for explaining translocation to the basal body.

The close proximity of such a large vesicle engaged closely with the centrosome and centrioles raises questions as to its function, however the transport of larger vesicles by the microtubule network is common [1145]. It may function in part as a novel pericentriolar matrix protein trafficking network of the centrosome. Curiously, Wang et al., (2009) [1116] noted a novel pericentriolar compartment enriched with ceramide that was located at the base of the primary cilium, whose transport was associated with the *cis*-Golgi. Equally, it may be an extension of the 'ER to Golgi intermediate compartment' (ERGIC), whose defined role between the endoplasmic reticulum and Golgi has so far remained elusive [520, 1147, 1148]. Uniquely, it shares a physical location, shape and most likely interacts with the 'PCM tube', which is an ordered tubular pericentriolar matrix accumulation of specific materials and protein species required for centrosomal function [122, 129]. Thus, the torus represents a unique, but likely temporary structure, which serves to function as an interface with the pericentriolar matrix of the centrosome and the Golgi.

4.44 Nuclear Pores

Nuclear pores act as conduits for the transfer of RNA, and also for signalling proteins shuttling between the nucleus, the cytoplasm and the centrosome [141, 1149, 1150], which are known to be involved in the regulation of gene expression [1149, 1152]. Within the model, the centrosome, and in particular the proximal centriole, are positioned in close proximity to several nuclear pores, and protein based tendrils are observed to connect the distal end of the proximal centriole to the nuclear membrane, and nearby nuclear pores (Figure 3.31 and 3.32). The association of centrioles with the nuclear membrane has been previously reported [1001, 1150, 1503], where Bolhy et al., (2011) [1154] described the attachment of the centrosome to the nuclear membrane via Nup133-dependent anchoring. A vesicle cluster is located in the model near a nuclear pore, upon the periphery of pericentriolar matrix and proximal centriole (Figure 3.35 C and F). The significance of such

relationships remains unknown. Burakov et al., (2013) [1150] reviewed centrosome positioning and mechanisms of attachment to the nucleus, mediated by SUN-1 and ZYG-12 [1155]. The close presence of the centrosome to the nucleus with respect to signalling, transcription and cellular regulation are intriguing and suggestive.

4.50 The Golgi Apparatus

Current concepts of Golgi structure and organisation have been derived from conventional electron microscopy studies [724], with images similar in appearance to optical sections visualised in Figure 3.37. The Golgi apparatus is the central organelle of the secretory pathway, which receives its materials from the endoplasmic reticulum. It contains the classical description of flattened cisternae, of *cis*, *medial* and *trans*-compartments [691] (Figure 3.38). The *cis*-cisternae contain large fenestrations, some significant branching and a small number of COP-like vesicles around the periphery (Figure 3.37). The *medial*-compartment is tightly layered, containing finer fenestrations, a marked discontinuity running across the compartment and fewer peripheral COP-like vesicles. Fine tubules, 30-40 nm in diameter, were noted connecting cisternae, which are reportedly triggered by secretory traffic [729, 1156]. The *trans*-cisternae are composed of larger compartments, with a number of 'exit faces', with defined fields of COP-like vesicles appearing to bud and emanating from the faces. Occasionally, fine electron dense material was noted within compartments of the Golgi cisternae, however no collagen-like precursors were observed within the Golgi network. The *trans*-Golgi face was observed to be adjacent to larger vesicular granules and tubular structures, where it is presumed that cargoes were being sorted for their respective destinations and secretion (Figure 3.41).

Utilisation of tomography has resolved many of the aspects of fine form and understanding of the Golgi between species (Appendix VI). Recent electron tomography studies examining the three-dimensional architecture using dual-axis tomography (Ladinsky et al., (1994) [1157], Marsh et al., (2001, 2005) [1158, 714]) revealed detail of highly complex, yet conserved structures. These and others revealed the close relationship between the cytoskeleton and the Golgi apparatus, and also raised questions about the exact nature of how the Golgi processes materials.

4.51 The trans-Golgi Network

The *trans*-Golgi network is an inter-connected arrangement of vesicles and membrane compartments associated with the *trans*-face of the Golgi, and is an area where vesicles containing proteins are sorted and then shipped to their intended destinations [691, 1159-1161]. It was originally defined as a 'specialised organelle' on the *trans*-side of the Golgi stack that is responsible for the routing of proteins to lysosomes, secretory vesicles, from the Golgi to the plasma membrane [1162]. Novikoff (1964) [1163] described the 'Golgi-Endoplasmic Reticulum-Lysosome' (GERL) hypothesis, which he used to describe structures related to the Golgi *sacculae*, which is part of the endoplasmic reticulum and *trans*-Golgi, and which form lysosomes.

Post-translationally modified materials are transported into the *trans*-Golgi, and then organised for their respective directed secretion [1159]. A large cylindrical tubular process was located in parallel with the face of the *trans*-Golgi, being surrounded by a cluster of COP-like vesicles (Figure 3.39 C). It is not known if this represents a migrating *trans*-Golgi fragment, or a ‘*trans*-Golgi tubule’ (Figure 3.42), or if it is part of the *trans*-tubular network, described by Clermont et al., (1995) [1161]. It most likely represents a process of the *trans*-Golgi network tubule in the process of being shed [1159].

Microtubules were modelled associated with presumed active transport to the plasma and periciliary membrane from locations close to the *trans*-Golgi face (Figure 3.37), demonstrating a role for the Golgi as a MTOC [646]. These were observed apparently undergoing active transport, with some vesicles in close contact and others merging with the plasma membrane, indicative of secretory processes being undertaken (Figure 3.39 E). Examination of individual vesicle membranes revealed the presence of electron dense coatings (Figure 3.39 F) indicative of membrane mediated processes. The occurrence of vesicles packed with densely stained ‘matrix granule-like precursor materials’ were identified predominantly associated with the *trans*-Golgi network. These were similar in nature to the extracellular granules, but were contained within their compartments at a higher packing density than the extracellular matrix granule network (Figure 3.39 A, A’, B and D).

The matrix-granule-containing vesicles were easily recognised by their contents, with the largest storage granule being of appreciable diameter (600 nm), comparable with the nearby Golgi stack (Figure 3.42). This vesicle is closely surrounded by a number of *trans*-Golgi derived vesicles, and was observed apparently undergoing active transfer processes in close proximity to a long tubular structure, assumed to be part of the endosomal system. The distal end of the tube was closely associated with active receptor mediated coated pit processes.

Novikoff (1976) [1164] described the biochemical and cytochemical processes of the endoplasmic reticulum for the formation of melanosomes and lysosomes, for the metabolism and secretion of materials for various systems and association with the *trans*-Golgi. Marsh (2005) [714] described these processes as being analogous to a ‘distillation tower’, in which cisternae of the *trans*-Golgi are sorted with their ‘refined fractions’ for further distribution. In the model, the *trans*-faces appear to be residual fragments of the *trans*-Golgi stack (Figs 3.37 and 3.41). Clermont et al. (1995) [1161] discussed differences in *trans*-Golgi network structures, which were found to vary extensively in size and shape between species. Furthermore, Ladinsky et al., (1999) [727] reported an association of the endoplasmic reticulum with the *trans*-face, suggesting that localised post-processing was also occurring. A full picture of the Golgi apparatus is certain to be complicated, as it has been found that Golgi and *trans*-Golgi components are not permanent structures, but dynamically changeable, and continuously undergoing breakdown and renewal [721].

4.52 Coated Pits and Caveoli

A number of coated pits were observed to occur clustered within a zone of the plasma membrane, in close proximity to the ciliary tip (Figure 3.40). Such relationships have previously been reported [26], however this is the first functional tomography model of receptor-mediated coated pits to clearly show the mediated endocytosis of matrix material in proximity of the cilium. Included is a nearby membrane process in the early stages of initiating pit formation. Endocytosed ‘coated pit’ materials accumulate within endosomes, *en route* to the Golgi [1165], where they engage with processes of the *trans*-Golgi, and its associated network [1166]. Sorting occurs within the early and late endosomal systems that display a tubular morphology and close *trans*-Golgi network association [1167] (Figure 3.42).

The mechanisms of clathrin coating, vesicle budding and fusion have been described [702, 1168], while the processes of endosomal sorting and retrograde transport to the *trans*-Golgi have been reviewed by Bonifacino et al., (2006) [1000].

Caveolae were identified in the model in proximity to the field of coated pits, consisting of fine finger like indentation into the cell membrane (Figure 3.40 E). Wolfgang et al., (1999) [1169] identified numerous caveoli-like invaginations along the plasmalemmal membrane of chondrocytes [1170], where they have been described functionally as *trans*-endothelial channels [1171], however their functional importance remains to be determined.

4.53 Are Primary Cilia Both Displacement Detectors and Pressure Sensors?

Recent research has clearly identified the role of primary cilia as receptors for a raft of specialised modalities, transducing external stimuli, into internal information, and enabling an appropriate response. The primary cilium of the chondrocyte is embedded distally in the surrounding matrix, and thus almost certainly distorts under applied force to that matrix. The level of distortion required to trigger transduction remains uncertain.

Attachment of the matrix to the ciliary membrane may physically trigger membrane receptors, raising the issue of the threshold of displacement required for transduction (Figure 3.43). The three-dimensional nanoscopic nature of this matrix may possess a novel property of being a negative Poisson material, offering interesting material and mechanical properties [1172, 1173]. This arises due to the semi-crystalline properties of a regular three-dimensional ‘mesh-like’ material, which may possibly be similar to the matrix structures making up the zone of the ‘ciliary pit’.

Bell [1174] raised the interesting example of ciliated cochlea hair cells detecting sound pressure and displacement, but it remains subject to further investigation to see if the difference in properties between the fluid of the pit and the surrounding medium enables efficient pressure detection. This may partially help resolve the concept of the cilium as being both a deflection and pressure sensor within the matrix [1175]. It also allows the cilium flexibility of movement and permits chemotactic signalling by enabling the migration of solutes and ligands [455].

4.54 Matrix-Cilium-Golgi Continuum in Chondrocytes

Cilia function as highly specialised sensors, where the targeting, functionality of specific receptors upon the cilium and their pathways are usually specific to cell type, and sensory requirements [352, 1176, 1177]. For example, chondrocyte primary cilia are specialised for the detection of applied force. Ciliary membrane integrin-matrix receptors allow the physical coupling of external matrix forces to the ciliary membrane, which contains receptors that allow for signal transduction. The application of larger forces induces extreme deflection of the membrane and axonemal microtubules, which translates through the basal body to the cytoskeletal network, which dissipates the load via complex cytoskeletal tensegrity interactions. The cilium acts as a specialist conduit where intra-ciliary transport maintains and adaptively services physiochemical-signalling components. It is possible signalling pathways within the cilium possibly function similar to a 'phase-locked-loop' for the adaptive amplification of both discrete and continuous signals, tailoring the physical properties and sensory detection capacity of the cilium to discriminate and adaptively respond effectively to weak environmental signals. The results in an appropriate response such as directed growth through matrix secretion and deposition. The refined perspective available with tomography and advanced image reconstruction software reveals a structural relationship between the mechanically functional extracellular matrix, the primary cilium, the centrosome, and the Golgi apparatus. This unique relationship is proposed to be responsible for maintenance of cartilage matrix integrity, which occurs independently of the physiological activity of the rest of the body.

4.60 Modelling the Primary Cilium

This thesis aimed to investigate the structural continuum between the extracellular matrix and the primary cilium using electron tomography. The ability of hyaline cartilage connective tissue to absorb, re-distribute and transmit compressive and shear forces to the subchondral bone renders it an ideal functional tissue in which to investigate the mechanical relationship between the matrix, the primary cilium, and the Golgi apparatus. This study is the first to generate and characterise an anatomically accurate three dimensional ultrastructural tomographic model of an *in situ* interphase chondrocyte primary cilium in relation to the extracellular matrix, the centrosome, and the Golgi apparatus. The ability to interrogate an anatomically accurate model allows investigation of the architecture of the primary cilium and its relationship with other cellular organelles in a detail that has not been previously available through conventional studies.

The cilium architecture shows remarkable consistency with previous ultrastructural investigations of chondrocyte primary cilia [27]. Many aspects of the centrosome, microtubule networks, and the Golgi conform to findings of previous investigators tomographical findings (Appendix VI). While single axis reconstruction resolution was limited, the contrast and staining from Ruthenium Red treatment allowed identification of much finer structural features and their physical relationship than had previously been obtained.

This model clearly demonstrates the existence of a structural continuum between the primary cilium and the centrosome, allowing for the detection, conduction and translation of biomechanical signals. The Golgi apparatus lies in close proximity to the centrosome, which intimately interacts with its microtubules, their cargoes, and vesicle fields. Central to the premise of a functional continuum is the cilium's role in detecting and transducing extracellular information to the centrosome, which then regulates not only the cytoskeleton, but is also believed to be responsible for polarising the Golgi for the regulated, directed secretion of matrix materials to maintain the local microenvironment.

In the process of curiosity led investigation and modelling of the cilium, a great number of new questions arise about the many processes, which govern its nano-biomechanical function, its sensory role within the cell and its highly conserved evolutionary history. While it is difficult to conclusively infer function from structure alone, a mounting body of literature has been reviewed to complement the interpretation offered in this thesis. These publications are selectively tabulated within the Appendices, and provide a basis for the interpretation of many of the biochemical networks responsible for regulating the cilium, the centrosome, and the intracellular response pathways for directed organelle regulation and vesicle transport. The model structure thus provides a scaffold on which function may be superimposed.

In consequence, the primary cilium is becoming the focus of interest in understanding of a wide spectrum of developmental maladies and common inherited genetic diseases. These may include milder pathologies ranging from satiety, obesity, and depression, to age related changes in connective tissues such as cartilage, necessitating joint replacement [1, 920, 1177, 1178].

4.7 Future Work

Further electron microscopy based investigation relies upon the ability to find candidate cilia, as the detection rate for *in situ* sectioning remains low. It has been demonstrated that *in vitro* techniques viably increase cilia numbers, at the expense of loss of their native environment. Further investigation requires more advanced electron microscopy techniques for improved imaging resolution. These may be further complemented with discrete studies focussed upon anatomical areas of interest that would provide higher levels of molecular detail. As microscopy imaging resolving power increases, individual molecules will become visible, however full understanding of the molecular properties of these ciliary constituents will only be elicited through understanding the quantum mechanical interactions of the many protein based components that govern their function.

The role of quantum physics in biology is necessary for an understanding the function and structure of many molecular machines, ranging from receptors to transport motors [757, 1179-1181]. The study of nanoscale biological materials, their interactions, and structures under 200 nm in size are governed by the influences of quantum mechanical effects. These affect a host of small-scale interactions from molecules, influencing many processes through evolution [757, 1179]. Many

structures and microtubule motors discussed within this study are nanoscale machines, where understanding of their structure will elicit insights into their functional properties.

Further insights into understanding of the three dimensional 'centrosomal processing unit' of the cell, its proteins and control hierarchy may have a myriad of applications. Marriage of biochemistry with ultrastructure can lead to new understandings of the aetiology of diseases and the opportunity to develop novel mechanisms of treatment.

References

- [1] Badano JL, Mitsuma N, Beales PL, Katsanis N. (2006) The ciliopathies: an emerging class of human genetic disorders. *Annual Review of Genomics and Human Genetics*, **7**, 125-148.
- [2] Bloodgood RA. (2009) From Central to Rudimentary to Primary: The History of an Underappreciated Organelle Whose Time Has Come - The Primary Cilium. *Methods in Cell Biology*, **94**, Elsevier, Amsterdam, New York.
- [3] Wheatley DN. (1982) *The Centriole: a Central Enigma of Cell Biology*. Elsevier Biomedical Press, Amsterdam, New York.
- [4] Leeuwenhoek A. (1677) Concerning little animals observed in rain-, well-, sea- and snow-water; as also in water wherein pepper had lain infused. *Philosophical Transactions of the Royal Society of London*, **12**, 821-831.
- [5] Clifford D. (1932) *Antony van Leeuwenhoek and his "Little Animals"*. John Bale, Sons and Danielsson, London. Reprinted by Dover, New York, 1958.
- [6] Muller OF. (1786) Animalcula infusoria; fluvia tilia et marina, que detexit, systematice descripsit et ad vivum delineari curavit. Hauniae, Typis N, Molleri.
- [7] Langerhans P. (1876) Zur Anatomie des *Amphioxus*. *Archiv für Mikroskopische Anatomie*, **12**, 290-348.
- [8] Zimmerman KW. (1894) Demonstration: Plastische reconstruction des hirnrohres; Schnittserie, Kaninch-enembryo; Photogramm; Präparate von Uterus, Nebenhoden, Darm, Ureter, Niere, Thranendruse. Verhandlungen der Anatomischen Gesellschaft auf der achten Versammlung zu Strassburg, **13-16**, 244-245.
- [9] Zimmerman KW. (1898) Beiträge zur Kenntniss einiger Drüsen und Epithelien. *Archiv für Mikroskopische Anatomie*, **52**, 552-706.
- [10] Bloodgood RA. (2012) The future of ciliary and flagellar membrane research. *Molecular Biology of the Cell*, **23**, 2407-2411.
- [11] Flemming W. (1875) Studien über die Entwicklungsgeschichte der Najaden. *Sitzungsbeber Akad Wissensch Wien*, **71**, 81-147.
- [12] Schatten H. (2008) The mammalian centrosome and its functional significance. *Histochemistry and Cell Biology*, **129**, 667-686.
- [13] Boveri T. (1888) Zellenstudien II. Die Befruchtung und Teilung des Eies von *Ascaris megalcephala*. *Jena Zeitschrift für Naturwissenschaft*, **22**, 685-882.
- [14] Chapman MJ. (1998) One hundred years of centrioles: the Henneguy-Lenhossek theory. *International Microbiology*, **1**, 233-236.
- [15] Jennings HS. (1899) Studies on reactions to stimuli in unicellular organisms. II. The mechanism of the motor reactions of *Paramecium*. *American Journal of Physiology*, **2**, 311-341.
- [16] Jennings HS. (1906) *Behavior of the Lower Organisms*. Columbia University Press, New York.
- [17] Bloodgood RA. (2010) Sensory reception is an attribute of both primary cilia and motile cilia. *Journal of Cell Science*, **123**, 505-509.

- [18] Cowhig J. (1974) *The World Under the Microscope*. Bounty Books, New York.
- [19] Abbe E. (1873) Beitrage zur theorie des mikroskops und der mikroskopischen wahrnehmung. *Archiv für Mikroskopische Anatomie*, **9**, 413-420.
- [20] Ruska E. (1986) *Ernst Ruska Autobiography*. Nobel Foundation.
- [21] Palade GE. (1952) A study of fixation for electron microscopy. *Journal of Experimental Medicine*, **95**, 285-298.
- [22] Luft JH, (1961) Improvements in epoxy resin embedding methods, *Journal of Biophysical and Biochemical Cytology*, **9**, 409-414.
- [23] Silverman MA, Leroux MR. (2009) Intraflagellar transport and the generation of dynamic, structurally and functionally diverse cilia. *Trends in Cell Biology*, **19**, 306-316.
- [24] Wheatley DN. (2005) Landmarks in the first hundred years of primary (9+0) cilium research. *Cell Biology International*, **29**, 333-339.
- [25] Jensen CG, Poole CA, McGlashan SR, Marko M, Issa ZI, Vujcich KV, Bowser SS. (2004) Ultrastructural, tomographic and confocal imaging of the chondrocyte primary cilium *in situ*. *Cell Biology International*, **28**, 101-110.
- [26] Poole C A, Flint MH, Beaumont BW. (1985) Analysis of the morphology and function of primary cilia in connective tissues: a cellular cybernetic probe? *Cell Motility*, **5**, 175-193.
- [27] Wilsman NJ. (1978) Cilia of adult canine articular chondrocytes. *Journal of Ultrastructural Research*, **64**, 270-281.
- [28] Wislman NJ, Fletcher TF. (1978) Cilia of neonatal articular chondrocytes: incidence and morphology. *Anatomical Record*, **190**, 871-889.
- [29] Wilsman NJ, Farnum CE, Reed-Aksamit DK. (1980) Incidence and morphology of equine and murine chondrocytic cilia. *Anatomical Record*, **197**, 355-366.
- [30] Archer FL, Wheatley N. (1971) Cilia in cell-cultured fibroblasts. 11. Incidence in mitotic and post mitotic BHK 21/C13 fibroblasts. *Journal of Anatomy*, **109**, 277-292.
- [31] Albrecht-Buehle, G, Bushnell A. (1979) The orientation of centrioles in migrating 3T3 cells. *Experimental Cell Research*, **120**, 111-118.
- [32] Jensen CG, Jensen LC, Rieder CL. (1979) The occurrence and structure of primary cilia in a subline of *Potorous tridactylus*. *Experimental Cell Research*, **123**, 444-449.
- [33] Anderson CT, Stearns T. (2007) The primary cilium: what once did nothing, now does everything. *Journal of Musculoskeletal and Neuronal Interactions*, **7**, 299.
- [34] Praetorius HA, Spring KR. (2001) Bending the MDCK cell primary cilium increases intracellular calcium. *Journal of Membrane Biology*, **184**, 71-79.
- [35] Praetorius HA, Spring KR. (2003) The renal cell primary cilium functions as a flow sensor. *Current Opinion in Nephrology and Hypertension*, **12**, 517-520.

- [36] De Robertis E. (1960) Some observations on the ultrastructure and morphogenesis of photoreceptors. *Journal of General Physiology*, **43**, 1-13.
- [37] Inglis PN, Borojevich KA, Leroux MR. (2006) Piecing together a ciliome. *Trends in Genetics*, **22**, 491-500.
- [38] Ishikawa H, Thompson J, Yates JR, Marshall WF. (2012) Proteomic analysis of mammalian primary cilia. *Current Biology*, **22**, 414-419.
- [39] Thomas J, Morle L, Soulavie F, Laurencon A, Sagnol S, Durand B. (2010) Transcriptional control of genes involved in ciliogenesis: a first step in making cilia. *Biology of the Cell*, **102**, 499-513.
- [40] Gherman A, Davis EE, Katsanis N. (2006) The ciliary proteome database: an integrated community resource for the genetic and functional dissection of cilia. *Nature Genetics*, **38**, 961-962.
- [41] Pazour G J, Agrin N, Leszyk J, Witman G B. (2005) Proteomic analysis of a eukaryotic cilium. *Journal of Cell Biology*, **170**, 103-113.
- [42] Scherft JP, Daems WT. (1967) Single cilia in chondrocytes. *Journal of Ultrastructural Research*, **19**, 546-555.
- [43] Hart JAL. (1968) Cilia in articular cartilage. *Journal of Anatomy*, **103**, 222.
- [44] Federman M, Nichols G. (1974) Bone cell cilia: vestigial or functional organelles. *Calcified Tissue Research*, **17**, 81-85.
- [45] Anderson RG. (1972) The three-dimensional structure of the basal body from the rhesus monkey oviduct. *Journal of Cell Biology*, **54**, 246-265.
- [46] Wei Q, Zhang Y, Li Y, Zhang Q, Ling K, Hu J. (2012) The BBSome controls IFT assembly and turnaround in cilia. *Nature Cell Biology*, **14**, 950-957.
- [47] Bader JR, Kusik BW, Besharse JC. (2012) Analysis of KIF17 distal tip trafficking in zebrafish cone photoreceptors. *Vision Research*, **75**, 37-43.
- [48] Berbari NF, O'Connor AK, Haycraft CJ, Yoder BK. (2009) The primary cilium as a complex signaling center. *Current Biology*, **19**, R526-R535.
- [49] Fisch C, Dupuis-Williams P. (2011) Ultrastructure of cilia and flagella - back to the future! *Biology of the Cell*, **103**, 249-270.
- [50] Portman RW, LeCluyse EL, Dentler WL. (1987) Development of microtubule capping structures in ciliated epithelial cells. *Journal of Cell Science*, **87**, 85-94
- [51] Gilula NB, Satir P. (1972) The ciliary necklace. A ciliary membrane specialization. *Journal of Cell Biology*, **53**, 494-509.
- [52] Bardele CF. (1981) Functional and phylogenetic aspects of the ciliary membrane: a comparative freeze-fracture study. *Biosystems*, **14**, 403-421.
- [53] Stephens DJ. (2012) Functional coupling of microtubules to membranes - implications for membrane structure and dynamics. *Journal of Cell Science*, **125**, 2795-2804.

- [54] Gibbons IR. (1961) The relationship between the fine structure and direction of beat in gill cilia of a lamellibranch mollusc. *Journal of Biophysical and Biochemical Cytology*, **11**, 179-205.
- [55] Czarnecki PG, Shah JV. (2012) The ciliary transition zone: from morphology and molecules to medicine. *Trends in Cell Biology*, **22**, 201-210.
- [56] Lin J, Heuser T, Song K, Fu X, Nicastro D. (2012) One of the nine doublet microtubules of eukaryotic flagella exhibits unique and partially conserved structures. *PLoS One*, **7**(10):e46494.
- [57] Kitagawa D, Vakonakis I, Olieric N, Hilbert M, Keller D, Olieric V, Bortfeld M, Erat MC, Flückiger I, Gönczy P, Steinmetz MO. (2011) Structural basis of the 9-fold symmetry of centrioles. *Cell*, **144**, 364-375.
- [58] Sotelo JR, Trujillo-Cenoz O. (1958) Electron microscope study on the development of ciliary components of the neural epithelium of the chick embryo. *Zeitschrift für Zellforschung und mikroskopische Anatomie*, **49**, 1-12.
- [59] Carvalho-Santos Z, Azimzadeh J, Pereira-Leal JB, Bettencourt-Dias M. (2011) Evolution: Tracing the origins of centrioles, cilia, and flagella. *Journal of Cell Biology*, **194**, 165-175.
- [60] Manton I, Clarke B. (1952) An electron microscope study of the spermatozoid of *Sphagnum*. *Journal of Experimental Botany*, **3**, 265-275.
- [61] Afzelius BA, Dallai R, Lanzavecchia S, Bellon PL. (1995) Flagellar structure in normal human spermatozoa and in spermatozoa that lack dynein arms. *Tissue and Cell*, **27**, 241-247.
- [62] Ishikawa H, Marshall W F. (2011) Ciliogenesis: building the cell's antenna. *Nature Reviews, Molecular and Cell Biology*, **12**, 222-234.
- [63] Vorobjev I A, Chentsov S. (1982) Centrioles in the cell cycle. I. Epithelial cells. *Journal of Cell Biology*, **93**, 938-949.
- [64] Uzbekov RE, Maurel DB, Aveline PC, Pallu S, Benhamou CL, Rochefort GY. (2012) Centrosome fine ultrastructure of the osteocyte mechanosensitive primary cilium. *Microscopy and Microanalysis*, **18**, 1430-1441.
- [65] Szymanska K, Johnson CA. (2012) The transition zone: an essential functional compartment of cilia. *Cilia*, **1**, 10.
- [66] Reiter JF, Blacque OE, Leroux MR. (2012) The base of the cilium: roles for transition fibres and the transition zone in ciliary formation, maintenance and compartmentalization. *EMBO Report*, **13**, 608-618.
- [67] Kee HL, Verhey KJ. (2013) Molecular connections between nuclear and ciliary import processes. *Cilia*, **2**, 11.
- [68] Kee HL, Dishinger JF, Blasius TL, Liu CJ, Margolis B, Verhey KJ. (2012) A size-exclusion permeability barrier and nucleoporins characterize a ciliary pore complex that regulates transport into cilia. *Nature Cell Biology*, **14**, 431-437.
- [69] Zhang D, Aravind L. (2012) Novel transglutaminase-like peptidase and C2 domains elucidate the structure, biogenesis and evolution of the ciliary compartment. *Cell Cycle*, **11**, 3861-3875.
- [70] Garcia-Gonzalo FR, Corbit KC, Sirerol-Piquer MS, Ramaswami G, Otto EA, Noriega TR, Seol AD, Robinson JF, Bennett CL, Josifova DJ, García-Verdugo JM, Katsanis N, Hildebrandt F, Reiter

- JF. (2011) A transition zone complex regulates mammalian ciliogenesis and ciliary membrane composition. *Nature Genetics*, **43**, 776-784.
- [71] Andersen R A, Barr DJS, Lynn DH, Melkonian M, Moestrup Ø, Sleight MA. (1991). Terminology and nomenclature of the cytoskeletal elements associated with the flagellar/ciliary apparatus in protists. *Protoplasma*, **164**, 1-8.
- [72] Alieva I B, Vorobjev A. (1994) Centrosome behavior under the action of a mitochondrial uncoupler and the effect of disruption of cytoskeleton elements on the uncoupler-induced alterations. *Journal of Structural Biology*, **113**, 217-224.
- [73] Hoyer-Fender S. (2010) Centriole maturation and transformation to basal body. *Seminars in Cellular and Developmental Biology*, **21**, 142-147.
- [74] Kunimoto K, Yamazaki Y, Nishida T, Shinohara K, Ishikawa H, Hasegawa T, Okanoué T, Hamada H, Noda T, Tamura A, Tsukita S, Tsukita S. (2012) Coordinated ciliary beating requires Odf2-mediated polarization of basal bodies via basal feet. *Cell*, **148**, 189-200.
- [75] Guirao B, Meunier A, Mortaud S, Aguilar A, Corsi JM, Strehl L, Hirota Y, Desoeuvre A, Boutin C, Han YG, Mirzadeh Z, Cremer H, Montcouquiol M, Sawamoto K, Spassky N. (2010) Coupling between hydrodynamic forces and planar cell polarity orients mammalian motile cilia. *Nature Cell Biology*, **12**, 341-350.
- [76] Wallingford JB. (2010) Planar cell polarity signalling, cilia and polarized ciliary beating. *Current Opinion in Cell Biology*, **22**, 597-604.
- [77] Wittmann T, Waterman-Storer CM. (2001) Cell motility: can Rho GTPases and microtubules point the way? *Journal of Cell Science*, **114**, 3795-3803.
- [78] Hagiwara H, Aoki T, Ohwada N, Fujimoto T. (1997) Development of striated rootlets during ciliogenesis in the human oviduct epithelium. *Cell and Tissue Research*, **290**, 39-42.
- [79] Yang J, Gao J, Adamian M, Wen XH, Pawlyk B, Zhang L, Sanderson MJ, Zuo J, Makino CL, Li T. (2005) The ciliary rootlet maintains long-term stability of sensory cilia. *Molecular and Cellular Biology*, **25**, 4129-4137.
- [80] Gonobobleva E, Maldonado M. (2009) Choanocyte ultrastructure in *Halisarca dujardini* (Demospongiae, Halisarcida). *Journal of Morphology*, **270**, 615-627.
- [81] Kano A, Hagiwara H, Takata K, Mogi K. (2001) Immunolocalization of centriole-associated striated rootlets in human submandibular gland cells with and without solitary cilia. *Histochemical Journal*, **33**, 613-620.
- [82] Hagiwara H, Takata K. (2002) Depolymerization of microtubules by colcemid induces the formation of elongated and centriole-nonassociated striated rootlets in PtK(2) cells. *Cell and Tissue Research*, **309**, 287-292.
- [83] Hagiwara H, Harada S, Maeda S, Aoki T, Ohwada N, Takata K. (2002) Ultrastructural and immunohistochemical study of the basal apparatus of solitary cilia in the human oviduct epithelium. *Journal of Anatomy*, **200**, 89-96.
- [84] Delattre P, Gonczy J. (2004) The arithmetic of centrosome biogenesis. *Cell Science*, **117**, 1619-1630.

- [85] Palermo G, Colombero LT, Rosenwaks Z. (1997) The human sperm centrosome is responsible for normal syngamy and early embryonic development. *Journals of Reproduction and Fertility*, **2**, 19-27.
- [86] Carvalho-Santos Z, Machado P, Branco P, Tavares-Cadete F, Rodrigues-Martins A, Pereira-Leal JB, Bettencourt-Dias M. (2010) Stepwise evolution of the centriole-assembly pathway. *Journal of Cell Science*, **123**, 1414-1426.
- [87] Marshall W F. (2009) Centriole evolution. *Current Opinion in Cell Biology*, **21**, 14-19.
- [88] Wilsman NJ, Farnum CE. (1983) Arrangement of C-tubule protofilaments in mammalian basal bodies. *Journal of Ultrastructural Research*, **84**, 205-212.
- [89] Li S, Fernandez JJ, Marshall WF, Agard DA. (2011) Three-dimensional structure of basal body triplet revealed by electron cryo-tomography. *EMBO Journal*, **31**, 552-562.
- [90] Gönczy P. (2012) Towards a molecular architecture of centriole assembly. *Nature Reviews, Molecular and Cellular Biology*, **13**, 425-436.
- [91] McNitt R. (1974) Centriole ultrastructure and its possible role in microtubule formation in an aquatic fungus. *Protoplasma*, **80**, 91-108.
- [92] Nogales E, Wolf SG, Downing KH. (1998) Structure of the alpha beta tubulin dimer by electron crystallography. *Nature*, **391**, 199-203.
- [93] Linck RW, Stephens RE. (2007) Functional protofilament numbering of ciliary, flagellar, and centriolar microtubules. *Cell Motility and Cytoskeleton*, **64**, 489-495.
- [94] Uzbekov R, Prigent C. (2007) Clockwise or anticlockwise? Turning the centriole triplets in the right direction! *FEBS Letters*, **581**, 1251-1254.
- [95] Sorokin S. (1962) Centrioles and the formation of rudimentary cilia by fibroblasts and smooth muscle cells. *Journal of Cell Biology*, **15**, 363-377.
- [96] Poole CA, Jensen CG, Snyder JA, Gray CG, Hermanutz VL, Wheatley DN. (1997) Confocal analysis of primary cilia structure and colocalization with the Golgi apparatus in chondrocytes and aortic smooth muscle cells. *Cell Biology International*, **21**, 483-494.
- [97] Poole CA, Zhang ZJ, Ross JM. (2001) The differential distribution of acetylated and deetyrosinated alpha-tubulin in the microtubular cytoskeleton and primary cilia of hyaline cartilage chondrocytes. *Journal of Anatomy*, **199**, 393-405.
- [98] Tenkova T, Chaldakov GN. (1988) Golgi-cilium complex in rabbit ciliary process cells. *Cell Structure and Function*, **13**, 455-458.
- [99] Wiener N. (1948) *Cybernetics: Or Control and Communication in the Animal and the Machine*. MIT Press, 2nd revised ed. 1961, Paris, (Hermann & Cie) & Cambridge, Massachusetts.
- [100] McGlashan SR, Jensen CG, Poole CA. (2006) Localization of extracellular matrix receptors on the chondrocyte primary cilium. *Journal of Histochemistry and Cytochemistry*, **54**, 1005-1014.
- [101] Qin H, Diener DR, Geimer S, Cole DG, Rosenbaum JL. (2004) Intraflagellar transport (IFT) cargo: IFT transports flagellar precursors to the tip and turnover products to the cell body *Journal of Cell Biology*, **164**, 255-266.

- [102] Hou Y, Pazour GJ, Witman GB. (2004) A dynein light intermediate chain, D1bLIC, is required for retrograde intraflagellar transport. *Molecular Biology of the Cell*, **15**, 4382-4394.
- [103] Lotte B, Pedersen JL, Rosenbaum JL. (2008) Intraflagellar transport (IFT) role in ciliary assembly, resorption and signalling. *Current Topics in Developmental Biology*, **85**, 23-61.
- [104] Lawo S, Hasegan M, Gupta GD, Pelletier L. (2012) Subdiffraction imaging of centrosomes reveals higher-order organizational features of pericentriolar material. *Nature Cell Biology*, **11**, 1148-1158.
- [105] Bornens M. (2012) The centrosome in cells and organisms. *Science*, **335**, 422-426.
- [106] Bartolini F, Gundersen GG (2006) Generation of noncentrosomal microtubule arrays. *Journal of Cell Science*, **119**, 4155-4163.
- [107] Kulic IM, Brown AE, Kim H, Kural C, Blehm B, Selvin PR, Nelson PC, Gelfand VI. (2008) The role of microtubule movement in bidirectional organelle transport. *Proceedings of the National Academy of Sciences, USA*, **105**, 10011-10016.
- [108] Thyberg J, Moskalewski S. (1999) Role of microtubules in the organization of the Golgi complex. *Experimental Cell Research*, **246**, 263-279.
- [109] Bettencourt-Dias M, Glover DM. (2007) Centrosome biogenesis and function: centrosomics brings new understanding. *Nature Reviews of Molecular Cell Biology*, **8**, 451-463.
- [110] Hinchcliffe EH, Miller FJ, Cham M, Khodjakov A, Sluder G. (2001) Requirement of a centrosomal activity for cell cycle progression through G(1) into S phase. *Science*, **291**, 1547-1550.
- [111] Kochanski RS, Borisy GG. (1990) Mode of centriole duplication and distribution. *Journal of Cell Biology*, **110**, 1599-1605.
- [112] Conduit PT, Brunk K, Dobbelaere J, Dix CI, Lucas EP, Raff JW. (2010) Centrioles regulate centrosome size by controlling the rate of Cnn incorporation into the PCM. *Current Biology*, **20**, 2178-2186.
- [113] Barenz F, Mayilo D, Gruss OJ. (2011) Centriolar satellites: Busy orbits around the centrosome. *European Journal of Cell Biology*, **90**, 983-989.
- [114] Kubo AH, Sasaki, H, Yuba-Kubo A, Tsukita S, Shiina N. (1999) Centriolar satellites: molecular characterization, ATP-dependent movement toward centrioles and possible involvement in ciliogenesis. *Journal of Cell Biology*, **147**, 969-980.
- [115] Alieva IB, Nadezhdina ES, Vaisberg EA, Vorobjev A. (1992) Microtubule and Intermediate Filament Patterns around the Centrosome in Interphase Cells. *The Centrosome*, **15**, 103-129.
- [116] Dammermann A, Desai A, Oegema K. (2003) The minus end in sight. *Current Biology*, **13**, R614-R624.
- [117] Desai A, Mitchison TJ. (1997) Microtubule polymerization dynamics. *Annual Reviews of Cell and Developmental Biology*, **13**, 83-117.
- [118] Bornens M. (2002) Centrosome composition and microtubule anchoring mechanisms. *Current Opinions in Cell Biology*, **14**, 25-34.

- [119] Wadsworth P, McGrail M. (1990) Interphase microtubule dynamics are cell type-specific. *Journal of Cell Science*, **95**, 23-32.
- [120] Alieva IB, Uzbekov RE. (2008) The centrosome is a polyfunctional multiprotein cell complex. *Biochemistry (Moscow)* **73**, 626-643.
- [121] Kollman JM, Merdes A, Mourey L, Agard DA. (2011) Microtubule nucleation by γ -tubulin complexes. *Nature Reviews of Molecular and Cell Biology*, **12**, 709-721.
- [122] Mennella V, Keszthelyi B, McDonald KL, Chhun B, Kan F, Rogers GC, Huang B, Agard DA. (2012) Subdiffraction resolution fluorescence microscopy reveals a domain of the centrosome critical for pericentriolar material organization. *Nature Cell Biology*, **14**, 1159-1168.
- [123] Sonnen KF, Schermelie L, Leonhardt H, Nigg EA. (2012) 3D-structured illumination microscopy provides novel insight into architecture of human centrosome. *Biology Open*, **1**, 965-976.
- [124] Azimzadeh J, Bornens M. (2007) Structure and duplication of the centrosome. *Journal of Cell Science*, **120**, 2139-2142.
- [125] Ou Y, Zhang M, Rattner JB. (2004) The centrosome: The centriole-PCM coalition. *Cell Motility and the Cytoskeleton*, **57**, 1-7.
- [126] Graser S, Stierhof YD, Nigg EA. (2007) Cep68 and Cep215 (Cdk5rap2) are required for centrosome cohesion. *Journal of Cell Science*, **120**, 4321-4331.
- [127] Kashina AS, Semenova IV, Ivanov PA, Potekhina ES, Zaliapin I, Rodionov VI. (2004). Protein kinase A, which regulates intracellular transport, forms complexes with molecular motors on organelles. *Current Biology*, **14**, 1877-1881.
- [128] Moser JJ, Fritzler MJ, Ou Y, Rattner JB. (2010) The PCM-basal body/primary cilium coalition. *Seminars in Cellular and Developmental Biology*, **21**, 148-155.
- [129] Fu J, Glover DM. (2012) Structured illumination of the interface between centriole and pericentriolar material. *Open Biology* **2**, 120104.
- [130] Jakobsen L, Vanselow K, Skogs M, Toyoda Y, Lundberg E, Poser I, Falkenby LG, Bennetzen M, Westendorf J, Nigg EA, Uhlen M, Hyman AA, Andersen JJ. (2011). Novel asymmetrically localizing components of human centrosomes identified by complementary proteomics methods. *EMBO Journal*, **30**, 1520-1535.
- [131] Nogales-Cadenas R, Abascal F, Díez-Pérez J, Carazo JM, Pascual-Montano A. (2009) CentrosomeDB: a human centrosomal proteins database. *Nucleic Acids Research*, **37**, D175-D180.
- [132] Liu Q, Tan G, Levenkova N, Li T, Pugh EN Jr, Rux JJ, Speicher DW, Pierce EA. (2007) The proteome of the mouse photoreceptor sensory cilium complex. *Molecular Cell Proteomics*, **6**, 1299-1317.
- [133] Sakakibara A1, Sato T, Ando R, Noguchi N, Masaoka M, Miyata T. (2014) Dynamics of centrosome translocation and microtubule organization in neocortical neurons during distinct modes of polarization. *Cerebral Cortex*, **24**, 1301-10
- [134] Baumann K. (2012) Cell cycle: Order in the pericentriolar material. *Nature Reviews of Molecular and Cellular Biology*, **13**, 749.

- [135] Moritz M, Braunfeld MB, Fung JC, Sedat JW, Alberts BM, Agard DA. (1995) Three-dimensional structural characterization of centrosomes from early *Drosophila* embryos. *Journal of Cell Biology*, **130**, 1149-1159.
- [136] Pelletier L1, O'Toole E, Schwager A, Hyman AA, Müller-Reichert T. (2006) Centriole assembly in *Caenorhabditis elegans*. *Nature*, **444**, 619-623.
- [137] Megraw TL, Kilaru S, Turner FR, Kaufman TC. (2002) The centrosome is a dynamic structure that ejects PCM flares. *Journal of Cell Science*, **115**, 4707-4718.
- [138] O'Toole E, Greenan G, Lange KI, Srayko M, Muller-Reichert T. (2012) The role of γ -tubulin in centrosomal microtubule organization. *PLoS One*, **7**(1):e29795.
- [139] Blain EJ. (2009) Involvement of the cytoskeletal elements in articular cartilage homeostasis and pathology. *International Journal of Experimental Pathology*, **90**, 1-15.
- [140] Langelier E, Suetterlin R, Hoemann CD, Aebi U, Buschmann MD. (2000) The chondrocyte cytoskeleton in mature articular cartilage: structure and distribution of actin, tubulin, and vimentin filaments. *Journal of Histochemistry and Cytochemistry*, **48**, 1307-1320.
- [141] Alberts B, Johnson A, Lewis J, Raff M, Roberts K, Walter P. (2002) *Molecular Biology of the Cell*. 4th edn. Garland Science, New York.
- [142] Brangwynne CP1, MacKintosh FC, Kumar S, Geisse NA, Talbot J, Mahadevan L, Parker KK, Ingber DE, Weitz DA. (2006) Microtubules can bear enhanced compressive loads in living cells because of lateral reinforcement. *Journal of Cell Biology*, **173**, 733-741.
- [143] Ingber DE. (1997) Tensegrity: the architectural basis of cellular mechanotransduction. *Annual Reviews of Physiology*, **59**, 575-599.
- [144] Burakov A, Nadezhdina E, Slepchenko B, Rodionov V. (2003) Centrosome positioning in interphase cells. *Journal of Cell Biology*, **162**, 963-969.
- [145] Lüders J, Stearns T. (2007) Microtubule-organizing centres: a re-evaluation. *Nature Reviews of Molecular and Cell Biology*, **8**, 161-167.
- [146] Brangwynne CP, MacKintosh FC, Weitz DA. (2007) Force fluctuations and polymerization dynamics of intracellular microtubules. *Proceedings of the National Academy of Sciences, USA*, **104**, 16128-16133.
- [147] Stehbens S, Wittmann T. (2012) Targeting and transport: how microtubules control focal adhesion dynamics. *Journal of Cell Biology*, **198**, 481-489.
- [148] Schopferer M, Bär H, Hochstein B, Sharma S, Mücke N, Herrmann H, Willenbacher N. (2009) Desmin and vimentin intermediate filament networks: their viscoelastic properties investigated by mechanical rheometry. *Journal of Molecular Biology*, **388**, 133-143.
- [149] Herrmann H, Aebi U. (2004) Intermediate filaments: molecular structure, assembly mechanism, and integration into functionally distinct intracellular Scaffolds. *Annual Reviews of Biochemistry*, **73**, 749-89.
- [150] Herrmann H, Strelkov SV, Burkhard P, Aebi U. (2009) Intermediate filaments: primary determinants of cell architecture and plasticity. *Journal of Clinical Investigations*, **119**, 1772-1783.

- [151] Bursa J, Lebis R, Holata J. (2012) Tensegrity finite element models of mechanical tests of individual cells. *Technology of Health Care*, **20**, 135-150.
- [152] Ingber DE. (2003) Tensegrity I. Cell structure and hierarchical systems biology. *Journal of Cell Science*, **116**, 1157-1173.
- [153] Ingber DE. (2003) Tensegrity II. How structural networks influence cellular information-processing networks. *Journal of Cell Science*, **116**, 1397-1408.
- [154] Ingber DE. (2006) Cellular mechanotransduction: putting all the pieces together again. *FASEB Journal*, **20**, 811-827.
- [155] Chen TJ, Wu CC, Tang MJ, Huang JS, Su FC. (2010) Complexity of the tensegrity structure for dynamic energy and force distribution of cytoskeleton during cell spreading. *PLoS One*, **5**(12):e14392.
- [156] Vinogradova T, Paul R, Grimaldi AD, Loncarek J, Miller PM, Yampolsky D, Magidson V, Khodjakov A, Mogilner A, Kaverina I. (2012) Concerted effort of centrosomal and Golgi-derived microtubules is required for proper Golgi complex assembly but not for maintenance. *Molecular Biology of the Cell*, **23**, 820-833.
- [157] Hughes JR, Meireles AM, Fisher KH, Garcia A, Antrobus PR, Wainman A, Zitzmann N, Deane C, Ohkura H, Wakefield JG. (2008) A microtubule interactome: complexes with roles in cell cycle and mitosis. *PLoS Biology*, **6**(4):e98.
- [158] Syred HM, Welburn J, Rappsilber J, Ohkura H. (2013) Cell cycle regulation of microtubule interactomes: multi-layered regulation is critical for the interphase/mitosis transition. *Molecular and Cell Proteomics*, **12**, 3135-3147.
- [159] Moritz M, Braunfeld MB, Sedat JW, Alberts B, Agard DA. (1995) Microtubule nucleation by γ -tubulin-containing rings in the centrosome. *Nature*, **378**, 638-640.
- [160] Mogensen MM, Malik A, Piel M, Bouckson-Castaing V, Bornens M. (2000) Microtubule minus-end anchorage at centrosomal and non-centrosomal sites: the role of ninein. *Journal of Cell Science*, **113**, 3013-3023.
- [161] Guilak F, Tedrow J, Burgkart, R. (2000) Viscoelastic properties of the cell nucleus. *Biochemical and Biophysical Research Communications*, **269**, 781-786.
- [162] Ofek G, Natoli RM, Athanasiou KA. (2009) *In situ* mechanical properties of the chondrocyte cytoplasm and nucleus. *Journal of Biomechanics*, **42**, 873-877.
- [163] Guilak F. (1995) Compression-induced changes in the shape and volume of the chondrocyte nucleus. *Journal of Biomechanics*, **28**, 1529-1541.
- [164] Buschmann MD, Hunziker EB, Kim YJ, Grodzinsky AJ. (1996) Altered aggrecan synthesis correlates with cell and nucleus structure in statically compressed cartilage. *Journal of Cell Science*, **109**, 499-508.
- [165] Löwe J, Li H, Downing KH, Nogales E. (2001) Refined structure of alpha beta-tubulin at 3.5 Å resolution. *Journal of Molecular Biology*, **313**, 1045-1057.
- [166] Unger E, Böhm KJ, Vater W (1990) Structural diversity and dynamics of microtubules and polymorphic tubulin assemblies. *Electron Microscopy Reviews*, **3**, 355-395.

- [167] Wu Z, Wang HW, Mu W, Ouyang Z, Nogales E, Xing J. (2009) Simulations of tubulin sheet polymers as possible structural intermediates in microtubule assembly. *PLoS One*, **4**(10):e7291.
- [168] Tilney LG, Bryan J, Bush DJ, Fujiwara K, Mooseker MS, Murphy DB, Snyder DH. (1973) Microtubules: evidence for 13 protofilaments. *Journal of Cell Biology*, **59**, 267-275.
- [169] Karsenti E, Nédélec F, Surrey T. (2006) Modelling microtubule patterns. *Nature Cell Biology*, **8**, 1204-1211.
- [170] Dutcher, SK. (2001) The tubulin fraternity: alpha to eta. *Current Opinion in Cell Biology*, **13**, 49-54.
- [171] Downing K, Nogales E. (1998) Tubulin and microtubule structure. *Current Opinion in Structural Biology*, **8**, 785-791.
- [172] Saillour Y1, Broix L, Bruel-Jungerman E, Lebrun N, Muraca G, Rucci J, Poirier K, Belvindrah R, Francis F, Chelly J. (2014) Beta tubulin isoforms are not interchangeable for rescuing impaired radial migration due to Tubb3 knockdown. *Human Molecular Genetics*, **23**, 1516-1526.
- [173] Denoulet P, Filliatreau G, de Nechaud B, Gross F, di Giamferardino L. (1989) Differential axonal transport of isotubulins in the motor axons of the rat sciatic nerve. *Journal of Cell Biology*, **108**, 965-971.
- [174] Ludwig SR, Oppenheimer DG, Silflow CD, Snustad DP. (1987) Characterization of the alpha-tubulin gene family of *Arabidopsis thaliana*. *Proceedings of the National Academy of Sciences, USA*, **84**, 5833-5837.
- [175] Hurd DD, Miller RM, Núñez L, Portman DS. (2010) Specific alpha- and beta-tubulin isotypes optimize the functions of sensory cilia in *Caenorhabditis elegans*. *Genetics*, **185**, 883-896.
- [176] Million K, Larcher J, Laoukili J, Bourguignon D, Marano F, Tournier F. (1999) Polyglutamylation and polyglycylation of alpha- and beta-tubulins during in vitro ciliated cell differentiation of human respiratory epithelial cells. *Journal Cell Science*, **112**, 4357-4366
- [177] Westermann S, Weber K. (2003) Post-translational modifications regulate microtubule function. *Nature Reviews Molecular and Cell Biology*, **4**, 938-947.
- [178] Janke C, Rogowski R, van Dijk J. (2008) Polyglutamylation: a fine-regulator of protein function? 'Protein Modifications: Beyond the Usual Suspects'. *EMBO Reports*, **9**, 636-641.
- [179] Janke C, Rogowski K, Wloga D, Regnard C, Kajava A, Strub J, Temurak N, Van Dijk J, Boucher D, Van Dorsselaer A, Survavanshi S, Gaertia J, Edde B. (2005) Tubulin polyglutamylase enzymes are members of the TTL domain protein family. *Science*, **308**, 1758-1762.
- [180] Wiese C, Zheng Y (2006) Microtubule nucleation: gamma-tubulin and beyond. *Journal of Cell Science*, **119**, 4143-4153.
- [181] Teixidó-Travesa N, Roig J, Lüders J. (2012) The where, when and how of microtubule nucleation - one ring to rule them all. *Journal of Cell Science*, **125**, 4445-4456.
- [182] Prokop A. (2013) The intricate relationship between microtubules and their associated motor proteins during axon growth and maintenance. *Neural Development*, **8**, 17.
- [183] Mishra RK, Chakraborty P, Arnaoutov A, Fontoura BM, Dasso M. (2010) The Nup107-160 complex and gamma-TuRC regulate microtubule polymerization at kinetochores. *Nature Cell Biology*, **12**, 164-169.

- [184] Guillet V, Knibiehler M, Gregory-Pauron L, Remy MH, Chemin C, Raynaud-Messina B, Bon C, Kollman JM, Agard DA, Merdes A, Mourey L. (2011) Crystal structure of γ -tubulin complex protein GCP4 provides insight into microtubule nucleation. *Nature Structural Molecular Biology*, **18**, 915-919.
- [185] vanBuren V, Cassimeris L, Odde DJ. (2005) Mechanochemical model of microtubule structure and self-assembly kinetics. *Biophysical Journal*, **89**, 2911-2926.
- [186] Conde C, Cáceres A. (2009) Microtubule assembly, organization and dynamics in axons and dendrites. *Nature Reviews Neuroscience*, **10**, 319-332.
- [187] Sandblad L, Busch KE, Tittmann P, Gross H, Damian Brunner D, Hoenger A. (2006) The *Schizosaccharomyces pombe* EB1 homolog Mal3p binds and stabilizes the microtubule lattice seam. *Cell*, **127**, 1415-1424.
- [188] Kikkawa M, Ishikawa T, Nakata T, Wakabayashi T, Hirokawa N. (1994) Direct Visualization of Microtubule Lattice Seam Both in vitro and in vivo. *Journal of Cell Biology*, **127**, 1965-1971.
- [189] Moritz M, Braunfeld MB, Guenebaut V, Heuser J, Agard DA. (2000) Structure of the γ -tubulin ring complex: a template for microtubule nucleation. *Nature Cell Biology*, **2**, 365-370.
- [190] Katsuki M1, Drummond DR, Cross RA. (2014) Ectopic A-lattice seams destabilize microtubules. *Nature Communications*, **5**, 3094.
- [191] Stephens RE. (2000) Preferential incorporation of tubulin into the junctional region of ciliary outer doublet microtubules: a model for treadmilling by lattice dislocation. *Cell Motility and the Cytoskeleton*, **47**, 130-140.
- [192] Song YH, Mandelkow E. (1993) Recombinant kinesin motor domain binds to β -tubulin and decorates microtubules with a B surface lattice. *Proceedings of the National Academy of Sciences, USA*, **90**, 1671-1675.
- [193] Satir P. (1968) Studies on cilia. 3. Further studies on the cilium tip and a "sliding filament" model of ciliary motility. *Journal of Cell Biology*, **39**, 77-94.
- [194] Kamimura S, Mandelkow E. (1992) Tubulin protofilaments and kinesin-dependent motility. *Journal of Cell Biology*, **118**, 865-875.
- [195] Nicastro D, Fu X, Heuser T, Tso A, Porter ME, Linck RW. (2011) Cryo-electron tomography reveals conserved features of doublet microtubules in flagella. *Proceedings of the National Academy of Sciences, USA*, **108**, E845-E853.
- [196] Linck RW, Norrander JM. (2003) Protofilament ribbon compartments of ciliary and flagellar microtubules. *Protist*, **154**, 299-311.
- [197] Vaughan S, Shaw M, Gull K. (2006) A post-assembly structural modification to the lumen of flagellar microtubule doublets. *Current Biology*, **16**, R449-R450.
- [198] Delgehyr N, Sillibourne J, Bornens M. (2005) Microtubule nucleation and anchoring at the centrosome are independent processes linked by ninein function. *Journal Cell Science*, **118**, 1565-75.
- [199] Janke C, Bulinski JC. (2011) Post-translational regulation of the microtubule cytoskeleton: mechanisms and functions. *Nature Reviews Molecular Cell Biology*, **12**, 773-786.

- [200] Wloga D, Gaertig J. (2010) Post-translational modifications of microtubules. *Journal of Cell Science*, **123**, 3447-3455.
- [201] Cambray-Deakin M, Burgoyne RD. (1987) Acetylated and detyrosinated alpha-tubulins are co-localized in stable microtubules in rat meningeal fibroblasts. *Cell Motility and the Cytoskeleton*, **8**, 284-291.
- [202] Sadoul K, Boyault C, Pabion M, Khochbin S. (2008) Regulation of protein turnover by acetyltransferases and deacetylases. *Biochimie*, **90**, 306-312.
- [203] Zambito AM, Wolff J. (1997) Palmitoylation of tubulin. *Biochemical and Biophysical Research Communications*, **239**, 650-654.
- [204] Luduena RF, Zimmermann HP, Little M. (1988) Identification of the phosphorylated beta-tubulin isotype in differentiated neuroblastoma cells. *FEBS Letters*, **230**, 142-146.
- [205] van Dijk J, Miro J, Strub JM, Lacroix B, Van Dorselaer A, Edde' B, Janke C. (2008) Polyglutamylation is a post-translational modification with a broad range of substrates. *Journal of Biological Chemistry*, **283**, 3915-3922.
- [206] Iftode F, Clerot JC, Levilliers N, Bré MH. (2000) Tubulin polyglycylation: a morphogenetic marker in ciliates. *Biology of the Cell*, **92**, 615-628.
- [207] Quinones GB, Danowski BA, Devaraj A, Singh V, Ligon LA. (2011) The posttranslational modification of tubulin undergoes a switch from detyrosination to acetylation as epithelial cells become polarized. *Molecular Biology of the Cell*, **22**, 1045-1057.
- [208] Peris L, Thery M, Fauré J, Saoudi Y, Lafanechère L, Chilton JK, Gordon-Weeks P, Galjart N, Bornens M, Wordeman L, Wehland J, Andrieux A, Job D. (2006) Tubulin tyrosination is a major factor affecting the recruitment of CAP-Gly proteins at microtubule plus ends. *Journal of Cell Biology*, **174**, 839-849.
- [209] Nakamura S, Takino H, Kojima MK. (1987) Effect of lithium on flagellar length in *Chlamydomonas reinhardtii*. *Cell Structure and Function*, **12**, 369-374.
- [210] Barra HS, Arce C, Argaraña CE. (1988) Posttranslational tyrosination/detyrosination of tubulin. *Molecular Neurobiology*, **2**, 133-153.
- [211] Hammond JC, Cai D, Verhey KJ. (2008) Tubulin modifications and their cellular functions. *Current Opinion in Cell Biology*, **20**, 71-76.
- [212] Sirajuddin M, Rice LM, Vale RD. (2014) Regulation of microtubule motors by tubulin isotypes and post-translational modifications. *Nature Cell Biology*, **16**, 335-344.
- [213] Lehtreck KF, Geimer S. (2000) Distribution of polyglutamylated tubulin in the flagellar apparatus of green flagellates. *Cell Motility and the Cytoskeleton*, **47**, 219-235.
- [214] Plessmann U, Weber K. (1997) Mammalian sperm tubulin: an exceptionally large number of variants based on several posttranslational modifications. *Journal of Protein Chemistry*, **16**, 385-390.
- [215] Dossou SJ, Bré MH, Hallworth R. (2007) Mammalian cilia function is independent of the polymeric state of tubulin glycylation. *Cell Motility and the Cytoskeleton*, **64**, 847-855.

- [216] Bosch Grau M, Gonzalez Curto G, Rocha C, Magiera MM, Marques Sousa P, Giordano T, Spassky N, Janke C. (2013) Tubulin glycyllases and glutamylases have distinct functions in stabilization and motility of ependymal cilia. *Journal of Cell Biology*, **202**, 441-451.
- [217] Regnard C, Desbruyeres E, Denoulet P, Eddé B. (1999) Tubulin polyglutamylase: isozymic variants and regulation during the cell cycle in HeLa cells. *Journal of Cell Science*, **112**, 4281-4289.
- [218] Utreras E, Jiménez-Mateos EM, Contreras-Vallejos E, Tortosa E, Pérez M, Rojas S, Saragoni L, Maccioni RB, Avila J, González-Billault C. (2008) Microtubule-associated protein 1B interaction with tubulin tyrosine ligase contributes to the control of microtubule tyrosination. *Developmental Neuroscience*, **30**, 200-210.
- [219] Takemura R, Okabe S, Umeyama T, Kanai Y, Cowan NJ, Hirokawa N. (1992) Increased microtubule stability and alpha tubulin acetylation in cells transfected with microtubule associated proteins. *Journal of Cell Science*, **103**, 953-964.
- [220] Reed NA, Cai D, Blasius TL, Jih GT, Meyhofer E, Gaertig J, Verhey KJ. (2006) Microtubule acetylation promotes kinesin-1 binding and transport. *Current Biology*, **16**, 2166-2172.
- [221] Johnson KA. (1998) The axonemal microtubules of the *Chlamydomonas* flagellum differ in tubulin isoform content. *Journal of Cell Science*, **111**, 313-320.
- [222] Jensen CG, Davison EA, Bowser SS, Rieder CL. (1987) Primary cilia cycle in PtK1 cells: Effects of colcemid and taxol on cilia formation and resorption. *Cell Motility and the Cytoskeleton*, **7**, 187-197.
- [223] Santos N, Reiter JF. (2008) Building it up and taking it down: the regulation of vertebrate ciliogenesis. *Developmental Dynamics*, **237**, 1972-1981.
- [224] Gerdes JM, Davis EE, Katsanis N. (2009) The vertebrate primary cilium in development, homeostasis, and disease. *Cell*, **137**, 32-45.
- [225] Gerdes JM, Liu Y, Zaghoul NAS, Leitch CC, Lawson SS, Kato M, Beachy PA, Beales PL, De Martinoi GN, Fisher S, Badano JL, Katsanis N. (2007) Disruption of the basal body compromises proteasomal function and perturbs intracellular Wnt response. *Nature Genetics*, **39**, 1350-1360.
- [226] Hodges ME, Wickstead B, Gull K, Langdale JA. (2011) Conservation of ciliary proteins in plants with no cilia. *BMC Plant Biology*, **11**, 185.
- [227] Yamashita YM (2009) The centrosome and asymmetric cell division. *Prion*, **3**, 84-88.
- [228] Christensen ST1, Pedersen SF, Satir P, Veland IR, Schneider L. (2008) The primary cilium coordinates signaling pathways in cell cycle control and migration during development and tissue repair. *Current Topics in Developmental Biology*, **85**, 261-301.
- [229] Sun QY, Schatten H. (2007) Centrosome Inheritance after Fertilization and Nuclear Transfer in Mammals. *Advances in Experimental Biology and Medicine*, **591**, 58-71.
- [230] Rodrigues-Martins A, Riparbelli M, Callaini G, Glover DM, Bettencourt-Dias M. (2007) Revisiting the role of the mother centriole in centriole biogenesis. *Science*, **316**, 1046-1050.
- [231] Rodrigues-Martins A, Riparbelli M, Callaini G, Glover DM, Bettencourt-Dias M. (2008) From centriole biogenesis to cellular function: centrioles are essential for cell division at critical developmental stages. *Cell Cycle*, **7**, 11-16.

- [232] Cavalier-Smith, T. (2009) Predation and eukaryote cell origins: A coevolutionary perspective. *International Journal of Biochemistry and Cell Biology*, **41**, 307-322.
- [233] Koonin EV. (2010) The origin and early evolution of eukaryotes in the light of phylogenomics. *Genome Biology*, **5**, 209.
- [234] Bornens M, Azimzadeh J. (2007) Origin and evolution of the centrosome. *Advances in Experimental Biology and Medicine*, **607**, 119-129.
- [235] Pan J, Snell W. (2007) The primary cilium: keeper of the key to cell division. *Cell*, **129**, 1255-1257.
- [236] Piel M, Meyer P, Khodjakov A, Rieder CL, Bornens M. (2000) The respective contributions of the mother and daughter centrioles to centrosome activity and behavior in vertebrate cells. *Journal of Cell Biology*, **149**, 317-330.
- [237] Strnad P, Gönczy P. (2008) Mechanisms of procentriole formation. *Trends in Cell Biology*, **18**, 389-396.
- [238] Guichard P, Chretien D, Marco S, Tassin, AM. (2010) Procentriole assembly revealed by cryo-electron tomography. *EMBO Journal*, **29**, 1565-1572.
- [239] Salisbury JL. (2007) A mechanistic view on the evolutionary origin for centrin-based control of centriole duplication. *Journal of Cell Physiology*, **213**, 420-428.
- [240] Plotnikova OV, Pugacheva OV, Golemis EA. (2009) Primary cilia and the cell cycle. *Methods in Cell Biology*, **94**, 137-160.
- [241] Parker JD, Hilton LK, Diener DR, Rasi MQ, Mahjoub MR, Rosenbaum JL, Quarmby LM. (2010) Centrioles are freed from cilia by severing prior to mitosis. *Cytoskeleton*, **67**, 425-430.
- [242] Rieder CL, Jensen CG, Jensen LC. (1979) The resorption of primary cilia during mitosis in a vertebrate (PtK1) cell line. *Journal of Ultrastructure Research*, **68**, 173-185.
- [243] Sung CH, Li A. (2011) Ciliary resorption modulates G1 length and cell cycle progression. *Cell Cycle*, **10**, 2825-2826.
- [244] Kobayashi T, Dynlacht BD. (2011) Regulating the transition from centriole to basal body. *Journal of Cell Biology*, **193**, 435-444.
- [245] Paridaen JT1, Wilsch-Bräuninger M, Huttner WB. (2013) Asymmetric inheritance of centrosome-associated primary cilium membrane directs ciliogenesis after cell division. *Cell*, **155**, 333-344.
- [246] Li A, Blow JJ. (2001) The origin of CDK regulation. *Nature Cell Biology*, **3**, E182-E184.
- [247] Nishitani H, Lygerou Z. (2002) Control of DNA replication licensing in a cell cycle. *Genes to Cells*, **7**, 523-534.
- [248] Nigg EA. (2002) Centrosome aberrations: cause or consequence of cancer progression? *Nature Reviews Cancer*, **2**, 815-825.
- [249] Nigg EA. (2007) Centrosome duplication: of rules and licenses. *Trends in Cell Biology*, **17**, 344-354.

- [250] Hinchcliffe EH, Sluder G. (2001) Centrosome duplication: Three kinases come up a winner! *Current Biology*, **11**, R698-R701.
- [251] Goto H, Inoko A, Inagaki M. (2013) Cell cycle progression by the repression of primary cilia formation in proliferating cells. *Cellular and Molecular Life Sciences*, **70**, 3893-3905.
- [252] Schibler L, Gibbs L, Benoist-Lassel C, Decraene C, Martinovic J, Loget P, Delezoide AL, Gonzales M, Munnich A, Jais JP, Legeai-Mallet L. (2009) New insight on FGFR3-related chondrodysplasias molecular physiopathology revealed by human chondrocyte gene expression profiling. *PLoS One*, **4**(10):e7633.
- [253] Azimzadeh J, Marshall WF. (2010) Building the Centriole. *Current Biology*, **20**, R816-R825.
- [254] Hinchcliffe EH, Sluder G. (2001) "It takes two to tango": understanding how centrosome duplication is regulated throughout the cell cycle. *Genes and Development*, **15**, 1167-1181.
- [255] Kim J, Lee JE, Heynen-Genel S, Suyama E, Ono K, Lee K, Ideker T, Aza-Blanc P, Gleeson JG. (2010) Functional genomic screen for modulators of ciliogenesis and cilium length. *Nature*, **464**, 1048-1051.
- [256] Avasthi P, Marshall WF. (2012) Stages of ciliogenesis and regulation of ciliary length. *Differentiation*, **83**, S30-S42.
- [257] Hao L, Scholey J M. (2009) Intraflagellar transport at a glance. *Journal of Cell Science*, **122**, 889-892.
- [258] Baldari CT, Rosenbaum J. (2009) Intraflagellar transport: it's not just for cilia anymore. *Current Opinion Cell Biology*, **2022**, 75-80.
- [259] Follit JA, San Agustin JT, Xu F, Jonassen JA, Samtani R, Lo CW, Pazour GJ. (2008) The Golgin GMAP210/TRIP11 anchors IFT20 to the Golgi complex. *PLoS Genetics*, **4**(12):e1000315
- [260] Richey EA, Qin H. (2012) Dissecting the sequential assembly and localization of intraflagellar transport particle complex B in *Chlamydomonas*. *PLoS One*, **27**(8):e43118.
- [261] Buisson J, Chenouard N, Lagache T, Blisnick T, Olivo-Marin JC, Bastin P. (2013) Intraflagellar transport proteins cycle between the flagellum and its base. *Journal of Cell Science*, **126**, 327-338.
- [262] Ou G, Blacque O E, Snow JJ, Leroux M R, Scholey JM. (2005) Functional coordination of intraflagellar transport motors. *Nature*, **436**, 583-587.
- [263] Zhao C, Malicki J. (2011) Nephrocystins and MKS proteins interact with IFT particle and facilitate transport of selected ciliary cargos. *EMBO Journal*, **30**, 2532-2544.
- [264] Engel BD, Ludington WB, Marshall WF. (2009) Intra-agellar transport particle size scales inversely with flagellar length: revisiting the balance-point length control model. *Journal of Cell Biology*, **187**, 81-89.
- [265] Short B. (2009) BBS proteins run an export business. *Journal of Cell Biology*, **187**, 936.
- [266] Signor D, Wedaman KP, Orozco JT, Dwyer ND, Bargmann CI, Rose LS, Scholey JM. (1999) Role of a class DHC1b dynein in retrograde transport of IFT motors and IFT raft particles along cilia, but not dendrites, in chemosensory neurons of living *Caenorhabditis elegans*. *Journal of Cell Biology*, **147**, 519-530.

- [267] Tsao C, Gorovsky M A. (2008) Different effects of *Tetrahymena* IFT172 domains on anterograde and retrograde intraflagellar transport. *Molecular Biology of the Cell*, **19**, 1450-1461.
- [268] Pedersen L B, Miller MS, Geimer S, Leitch JM, Rosenbaum JL, Cole DG. (2005) *Chlamydomonas* IFT172 is encoded by FLA11, interacts with CrEB1, and regulates IFT at the flagellar tip. *Current Biology*, **15**, 262-266.
- [269] Pigino G, Geimer S, Lanzavecchia S, Paccagnini E, Cantele F, Diener DR, Rosenbaum JL, Lupetti P. (2009) Electron-tomographic analysis of intraflagellar transport particle trains in situ. *Journal of Cell Biology*, **187**, 135-148.
- [270] Hirokawa N, Noda Y, Tanaka Y, Niwa S. (2009) Kinesin superfamily motor proteins and intracellular transport. *Nature Reviews Molecular and Cellular Biology*, **10**, 682-696.
- [271] Insinna C, Pathak N, Perkins B, Drummond I, Besharse JC. (2008) The homodimeric kinesin, Kif17, is essential for vertebrate photoreceptor sensory outer segment development. *Developmental Biology*, **316**, 160-170.
- [272] Cheung HO, Zhang X, Ribeiro A, Mo R, Makino S, Puviindran V, Law KK, Briscoe J, Hui CC. (2009) The kinesin protein Kif7 is a critical regulator of Gli transcription factors in mammalian hedgehog signaling. *Science Signalling*, **2**, ra29.
- [273] Nozawa YI, Lin C, Chuang PT. (2013) Hedgehog signalling from the primary cilium to the nucleus: an emerging picture of ciliary localization, trafficking and transduction. *Current Opinion in Genetics and Development*, **23**, 429-437.
- [274] Endoh-Yamagami S, Evangelista M, Wilson D, Wen X, Theunissen JW, Phamluong K, Davis M, Scales SJ, Solloway MJ, de Sauvage FJ, Peterson AS. (2009) The mammalian Cos2 homolog Kif7 plays an essential role in modulating Hh signal transduction during development. *Current Biology*, **19**, 1320-1326.
- [275] Goetz SC, Anderson KV. (2010) The primary cilium: a signalling centre during vertebrate development. *Nature Reviews Genetics*, **11**, 331-344.
- [276] Maurya AK, Ben J, Zhao Z, Lee RT, Niah W, Ng AS, Iyu A, Yu W, Elworthy S, van Eeden FJ, Ingham PW. (2013) Positive and negative regulation of Gli activity by Kif7 in the zebrafish embryo. *PLoS Genet*, **9**, e1003955.
- [277] Hsu SH, Zhang X, Yu C, Li ZJ, Wunder JS, Hui CC, Alman BA. (2011) Kif7 promotes hedgehog signaling in growth plate chondrocytes by restricting the inhibitory function of Sufu. *Development*, **138**, 3791-3801.
- [278] Mukhopadhyay S, Wen X, Chih B, Nelson CD, Lane WS, Scales SJ, Jackson PK. (2010) TULP3 bridges the IFT-A complex and membrane phosphoinositides to promote trafficking of G protein-coupled receptors into primary cilia. *Genes and Development*, **24**, 2180-2193.
- [279] Mukhopadhyay S, Wen X, Chih B, Nelson CD, Lane WS, Scales SJ, Jackson PK. (2010) TULP3 bridges the IFT-A complex and membrane phosphoinositides to promote trafficking of G protein-coupled receptors into primary cilia. *Genes and Development*, **24**, 2180-2193.
- [280] Berbari N F, J. S. Lewis JS, Bishop GA, Askwith CC, Mykytyn K. (2008) Bardet-Biedl syndrome proteins are required for the localization of G protein-coupled receptors to primary cilia. *Proceedings of the National Academy of Sciences, USA*, **105**, 4242-4246.

- [281] Liem KF Jr, Ashe A, He M, Satir P, Moran J, Beier D, Wicking C, Anderson KV. (2012) The IFT-A complex regulates Shh signaling through cilia structure and membrane protein trafficking. *Journal of Cell Biology*, **197**, 789-800.
- [282] Seo S, Zhang Q, Bugge K, Breslow DK, Searby CC, Nachury MV, Sheffield VC. (2011) A novel protein LZTFL1 regulates ciliary trafficking of the BBSome and Smoothed. *PLoS Genetics*, **7**(11):e1002358.
- [283] Jin H, White SR, Shida T, Schulz S, Aguiar M, Gygi SP, Bazan JF, Nachury MV. (2010) The conserved Bardet-Biedl syndrome proteins assemble a coat that traffics membrane proteins to cilia. *Cell*, **141**, 1208-1219.
- [284] Absalon S, Blisnick T, Kohl L, Toutirais G, Dore' G, Julkowska D, Tavenet A, Bastin P. (2008). Intraflagellar transport and functional analysis of genes required for flagellum formation in trypanosomes. *Molecular Biology of the Cell*, **19**, 929-944.
- [285] Ou G, Koga M, Blacque OE, Murayama T, Ohshima Y, Schafer JC, Li C, Yoder BK, Leroux MR, Scholey JM. (2007) Sensory ciliogenesis in *Caenorhabditis elegans*: assignment of IFT components into distinct modules based on transport and phenotypic profiles. *Molecular Biology of the Cell*, **18**, 1554-1569.
- [286] Gorivodsky M, Mukhopadhyay M, Wilsch-Braeuninger M, Phillips M, Teufel A, Kim C, Malik N, Huttner W, Westphal H. (2009) Intraflagellar transport protein 172 is essential for primary cilia formation and plays a vital role in patterning the mammalian brain. *Developmental Biology*, **325**, 24-32.
- [287] Caspary T, Larkins CE, Anderson KV. (2007) The graded response to Sonic Hedgehog depends on cilia architecture. *Development of the Cell*, **12**, 767-778.
- [288] Incardona, JP, Gruenberg J, Roelink H. (2002) Sonic hedgehog induces the segregation of patched and smoothed in endosomes. *Current Biology*, **12**, 983-995.
- [289] Oishi I, Kawakami Y, Raya A, Callol-Massot C, Izpisua Belmonte JC. (2006) Regulation of primary cilia formation and left-right patterning in zebrafish by a noncanonical Wnt signaling mediator, *duboraya*. *Nature Genetics*, **38**, 1316-1322.
- [290] Park TJ, Mitchell BJ, Abitua PB, Kintner C, Wallingford JB. (2008) Dishevelled controls apical docking and planar polarization of basal bodies in ciliated epithelial cells. *Nature Genetics*, **40**, 871-879.
- [291] Fan S, Hurd TW, Liu CJ, Straight SW, Weimbs T, Hurd EA, Domino SE, Margolis B. (2004) Polarity proteins control ciliogenesis via kinesin motor interactions. *Current Biology*, **14**, 1451-1461.
- [292] Wallingford JB, Mitchell B. (2011) Strange as it may seem: the many links between Wnt signaling, planar cell polarity, and cilia. *Genes and Development*, **25**, 201-213.
- [293] Graser S, Stierhof YD, Lavoie SB, Gassner OS, Lamla S, Le Clech M, Nigg EA. (2007) Cep164, a novel centriole appendage protein required for primary cilium formation. *Journal of Cell Biology*, **179**, 321-330.
- [294] Schmidt KN, Kuhns S, Neuner A, Hub B, Zentgraf H, Pereira G. (2012) Cep164 mediates vesicular docking to the mother centriole during early steps of ciliogenesis. *Journal of Cell Biology*, **199**, 1083-1101.

- [295] Westlake CJ, Baye LM, Nachury MV, Wright KJ, Ervin KE, Phu L, Chalouni C, Beck JS, Kirkpatrick DS, Slusarski DC, Sheffield VC, Scheller RH, Jackson PK. (2011) Primary cilia membrane assembly is initiated by Rab11 and transport protein particle II (TRAPP2) complex-dependent trafficking of Rabin8 to the centrosome. *Proceedings of the National Academy of Sciences, USA*, **108**, 2759-2764.
- [296] Kaplan OI, Molla-Herman A, Cevik S, Ghossoub R, Kida K, Kimura Y, Jenkins P, Martens JR, Setou M, Benmerah A, Blacque OE. (2010) The AP-1 clathrin adaptor facilitates cilium formation and functions with RAB-8 in *C. elegans* ciliary membrane transport. *Journal of Cell Science*, **123**, 3966-3977.
- [297] Nachury MV, Seeley ES, Jin H. (2010) Trafficking to the ciliary membrane: how to get across the periciliary diffusion barrier? *Annual Review of Cell and Developmental Biology*, **26**, 59-87.
- [298] Nachury MV, Loktev AV, Zhang Q, Westlake CJ, Peranen J, Merdes A, Slusarski DC, Scheller RH, Bazan JF, Sheffield VC, Jackson PK. (2007). A core complex of BBS proteins cooperates with the GTPase Rab8 to promote ciliary membrane biogenesis. *Cell*, **129**, 1201-1213.
- [299] Yoshimura S, Egerer J, Fuchs E, Haas AK, Barr FA. (2007) Functional dissection of Rab GTPases involved in primary cilium formation. *Journal of Cell Biology*, **178**, 363-369.
- [300] Hsiao Y, Tuz K, Ferland RJ. (2012) Trafficking in and to the primary cilium. *Cilia*, **1**, 4.
- [301] Zuo X, Guo W, Lipschutz JH. 2009. The exocyst protein Sec10 is necessary for primary ciliogenesis and cystogenesis *in vitro*. *Molecular Biology of the Cell*, **20**, 2522-2529.
- [302] Garcia-Gonzalez FR, Reiter JF. (2012) Scoring a backstage pass: mechanisms of ciliogenesis and ciliary access. *Journal of Cell Biology*, **197**, 697-709.
- [303] Spektor A, Tsang WY, Khoo D, Dynlacht BD. (2007) Cep97 and CP110 suppress a cilia assembly program. *Cell*, **130**, 678-690.
- [304] Tsang WY, Bossard C, Khanna H, Peränen J, Swaroop A, Malhotra V, Dynlacht BD. (2008) CP110 suppresses primary cilia formation through its interaction with CEP290, a protein deficient in human ciliary disease. *Developmental Cell*, **15**, 187-197.
- [305] Kobayashi T, Tsang WY, Li J, Lane W, Dynlacht BD. (2011) Centriolar kinesin Kif24 interacts with CP110 to remodel microtubules and regulate ciliogenesis. *Cell*, **145**, 914-925.
- [306] Tsang WY, Dynlacht BD. (2013) CP110 and its network of partners coordinately regulate cilia assembly. *Cilia*, **2**, 9.
- [307] Leroux MR. (2007) Taking vesicular transport to the cilium. *Cell*, **129**, 1041-1043.
- [308] Deane JA, Cole DG, Seeley ES, Diener DR, Rosenbaum JL. (2001) Localization of intraflagellar transport protein IFT52 identifies basal body transitional fibers as the docking site for IFT particles. *Current Biology*, **11**, 1586-1590.
- [309] Wiens CJ, Tong Y, Esmail MA, Oh E, Gerdes JM, Wang J, Tempel W, Rattner JB, Katsanis N, Park HW, Leroux MR. (2010) Bardet-Biedl syndrome-associated small GTPase ARL6 (BBS3) functions at or near the ciliary gate and modulates Wnt signaling. *Journal of Biological Chemistry*, **285**, 16218-16230.

- [310] Rogers KK, Wilson PD, Snyder RW, Zhang X, Guo W, Burrow, CR, Lipschutz JH, (2004) The exocyst localizes to the primary cilium in MDCK cells. *Biochemical and Biophysical Research Communications*, **319**, 138-143.
- [311] Das A, Guo W. (2011) Rabs and the exocyst in ciliogenesis, tubulogenesis and beyond. *Trends in Cell Biology*, **21**, 383-386.
- [312] Kuhns S, Schmidt KN, Reymann J, Gilbert DF, Neuner A, Hub B, Carvalho R, Wiedemann P, Zentgraf H, Erfle H, Klingmüller U, Boutros M, Pereira G. (2013) The microtubule affinity regulating kinase MARK4 promotes axoneme extension during early ciliogenesis. *Journal of Cell Biology*, **200**, 505-522.
- [313] Schroder JM, Schneider L, Christensen ST, Pedersen LB. (2007) EB1 is required for primary cilia assembly in fibroblasts. *Current Biology*, **17**, 1134-1139.
- [314] Tsang WY, Dynlacht BD. (2013) CP110 and its network of partners coordinately regulate cilia assembly. *Cilia*, **2**, 9.
- [315] Haycraft CJ, Schafer JC, Zhang Q, Taulman PD, Yoder BK. Identification of CHE-13, a novel intraflagellar transport protein required for cilia formation. *Experimental Cell Research*, **284**, 251-263.
- [316] Wloga D, Webster DM, Rogowski K, Bré MH, Levilliers N, Jerka-Dziadosz M, Janke C, Dougan ST, Gaertig J. (2009) TTLL3 is a tubulin glycine ligase that regulates the assembly of cilia. *Developmental Cell*, **16**, 867-876.
- [317] Pathak N, Austin CA, Drummond IA. (2011) Tubulin tyrosine ligase-like genes *tll3* and *tll6* maintain zebrafish cilia structure and motility. *Journal of Biological Chemistry*, **286**, 11685-11695.
- [318] Sharma N, Bryant J, Wloga D, Donaldson R, Davis RC, Jerka-Dziadosz M, Gaertig J. (2007). Katanin regulates dynamics of microtubules and biogenesis of motile cilia. *Journal of Cell Biology*, **178**, 1065-1079.
- [319] Blaineau C, Tessier M, Dubessay P, Tasse L, Crobu L, Pagès M, Bastien P. (2007) A novel microtubule-depolymerizing kinesin involved in length control of a eukaryotic flagellum. *Current Biology*, **217**, 778-782.
- [320] Walter WJ, Koonce MP, Brenner B, Steffen W. (2012) Two independent switches regulate cytoplasmic dynein's processivity and directionality. *Proceedings of the National Academy of Sciences, USA*, **109**, 5289-5293.
- [321] Bhogaraju S, Cajanek L, Fort C, Blisnick T, Weber K, Taschner M, Mizuno N, Lamla S, Bastin P, Nigg EA, Lorentzen E. (2013) Molecular basis of tubulin transport within the cilium by IFT74 and IFT81. *Science*, **341**(6149),1009-1012.
- [322] Hao L, Thein M, Brust-Mascher I, Civelekoglu-Scholey G, Lu Y, Acar S, Prevo B, Shaham S, Scholey JM. (2011) Intraflagellar transport delivers tubulin isotypes to sensory cilium middle and distal segments. *Nature Cell Biology*, **13**, 790-798.
- [323] Marshall WF, and Rosenbaum JL. (2001) Intraflagellar transport balances continuous turnover of outer double microtubules: Implications for flagellar length control. *Journal of Cell Biology*, **155**, 405-414.
- [324] Milenkovic L, Scott MP, Rohatgi R. (2009) Lateral transport of Smoothed from the plasma membrane to the membrane of the cilium. *Journal of Cell Biology*, **187**, 365-374.

- [325] Pazour GJ, Bloodgood RA. (2008) Targeting proteins to the ciliary membrane. *Current Topics in Developmental Biology*, **85**, 115-149.
- [326] Francis SS, Sfakianos J, Lo B, Mellman I. (2011) A hierarchy of signals regulates entry of membrane proteins into the ciliary membrane domain in epithelial cells. *Journal of Cell Biology*, **193**, 219-233.
- [327] Lin YC, Niewiadowski P, Lin B, Nakamura H, Phua SC, Jiao J, Levchenko A, Inoue T, Rohatgi R, Inoue T. (2013) Chemically inducible diffusion trap at cilia reveals molecular sieve-like barrier. *Nature Chemical Biology*, **9**, 437-443.
- [328] Omori Y, Zhao C, Saras A, Mukhopadhyay S, Kim W, Furukawa T, Sengupta P, Veraksa A, Malicki J. (2008) Elipsa is an early determinant of ciliogenesis that links the IFT particle to membrane associated small GTPase Rab8. *Nature Cell Biology*, **10**, 437-444.
- [329] Silva DA, Huang X, Behal RH, Cole DG, Qin H. (2012) The RABL5 homolog IFT22 regulates the cellular pool size and the amount of IFT particles partitioned to the flagellar compartment in *Chlamydomonas reinhardtii*. *Cytoskeleton*, **69**, 33-48.
- [330] Qin H, Wang Z, Diener D, Rosenbaum J. (2007) Intraflagellar transport protein 27 is a small G protein involved in cell-cycle control. *Current Biology*, **17**, 193-202.
- [331] Wood CR, Wang Z, Diener D, Zones JM, Rosenbaum J, Umen JG. (2012) IFT proteins accumulate during cell division and localize to the cleavage furrow in *Chlamydomonas*. *PLoS One*, **7**(2):e30729.
- [332] Follit JA, Tuft RA, Fogarty KE, Pazour GJ. (2006) The intraflagellar transport protein IFT20 is associated with the Golgi complex and is required for cilia assembly. *Molecular Biology of the Cell*, **17**, 3781-3792.
- [333] Nachury MV. (2008) Tandem affinity purification of the BBSome, a critical regulator of Rab8 in ciliogenesis. *Methods in Enzymology*, **439**, 501-513.
- [334] Mokrzan EM, Lewis JS, Mykityn K. (2007) Differences in Renal Tubule Primary Cilia Length in a Mouse Model of Bardet-Biedl Syndrome. *Nephron Experimental Nephrology*, **106**, e88-e96.
- [335] Kim JC, Badano JL, Sibold S, Esmail M, Hill J, Hoskins B, Leitch CC, Venner K, Ansley SJ, Ross AJ, Leroux MR, Katsanis N, Beales PL. (2004) The Bardet-Biedl protein BBS4 targets cargo to the pericentriolar region and is required for microtubule anchoring and cell cycle progression. *Nature Genetics*, **36**, 462-470.
- [336] Forsythe E, Beales PL. (2013) Bardet-Biedl syndrome. *European Journal of Human Genetics*, **21**, 8-13.
- [337] Corbit KC, Shyer AE, Dowdle WE, Gaulden J, Singla V, Chen MH, Chuang PT, Reiter JF. (2008) Kif3a constrains beta-catenin-dependent Wnt signalling through dual ciliary and non-ciliary mechanisms. *Nature Cell Biology*, **10**, 70-76.
- [338] Ross AJ, May-Simera H, Eichers ER, Kai M, Hill J, Jagger DJ, Leitch CC, Chapple JP, Munro PM, Fisher S, Tan PL, Phillips HM, Leroux MR, Henderson DJ, Murdoch JN, Copp AJ, Eliot MM, Lupski JR, Kemp DT, Dollfus H, Tada M, Katsanis N, Forge A, Beales PL. (2005) Disruption of Bardet-Biedl syndrome ciliary proteins perturbs planar cell polarity in vertebrates. *Nature Genetics*, **37**, 1135-1140.

- [339] Dishinger JF, Kee H, Jenkins PM, Fan S, Hurd TW, Hammond JW, Truong YN, Margolis B, Martens JR, Verhey KJ. (2010) Ciliary entry of the kinesin-2 motor KIF17 is regulated by importin-beta2 and RanGTP. *Nature Cell Biology*, **12**, 703-710.
- [340] Verhey KJ, Dishinger J, Kee HL. (2011) Kinesin motors and primary cilia. *Biochemical Society Transactions*, **39**, 1120-1125.
- [341] Fan S, Whiteman EL, Hurd TW, McIntyre JC, Dishinger JF, Liu CJ, Martens JR, Verhey KJ, Sajjan U, Margolis B. (2011) Induction of Ran GTP drives ciliogenesis. *Molecular Biology of the Cell*, **22**, 4539-4548.
- [342] Cai Y, Singh BB, Aslanukov A, Zhao H, Ferreira PA. (2001) The docking of kinesins, KIF5B and KIF5C, to Ran-binding protein 2 (RanBP2) is mediated via a novel RanBP2 domain. *Journal of Biological Chemistry*, **276**, 41594-41602.
- [343] Molla-Herman A, Boularan C, Ghossoub R, Scott MG, Burtey A, Zarka M, Saunier S, Concordet JP, Marullo S, Benmerah A. (2008) Targeting of beta-arrestin2 to the centrosome and primary cilium: role in cell proliferation control. *PLoS One*, **3**(11):e3728.
- [344] Schneider L, Clement CA, Teilmann SC, Pazour GJ, Hoffmann EK, Satir P, Christensen ST. (2005) PDGFRalpha signaling is regulated through the primary cilium in fibroblasts. *Current Biology*, **15**, 1861-1866.
- [345] Rohatgi R, Snell WJ. (2010) The ciliary membrane. *Current Opinions in Cell Biology*, **22**, 541-546.
- [346] Berbari NF, Johnson AD, Lewis JS, Askwith CC, Mykytyn K (2008) Identification of ciliary localization sequences within the third intracellular loop of G protein-coupled receptors. *Molecular Biology of the Cell*, **19**, 1540-1547.
- [347] Humbert MC, Weihbrecht K, Searby CC, Li Y, Pope RM, Sheffield VC, Seo S. (2012) ARL13B, PDE6D, and CEP164 form a functional network for INPP5E ciliary targeting. *Proceedings of the National Academy of Sciences*, **109**, 19691-19696.
- [348] Christensen ST, Clement CA, Satir P, Pedersen LB. (2012) Primary cilia and coordination of receptor tyrosine kinase (RTK) signalling. *Journal of Pathology*, **226**, 172-184.
- [349] Ward HH, Brown-Glaberman U, Wang J, Morita Y, Alper SL, Bedrick EJ, Gattone VH 2nd, Deretic D, Wandinger-Ness A. (2011) A conserved signal and GTPase complex are required for the ciliary transport of polycystin-1. *Cell*, **22**, 3289-3305.
- [350] Geng L, Okuhara D, Yu Z, Tian X, Cai Y, Shibazak, S, Somlo S. (2006). Polycystin-2 traffics to cilia independently of polycystin-1 by using an N-terminal RVxP motif. *Journal of Cell Science*, **119**, 1383-1395.
- [351] Wolfrum U, Schmitt A. (2000) Rhodopsin transport in the membrane of the connecting cilium of mammalian photoreceptor cells. *Cell Motility and the Cytoskeleton*, **46**, 95-107.
- [352] Follit JA, Li L, Vucica Y, Pazour GJ. (2010) The cytoplasmic tail of fibrocystin contains a ciliary targeting sequence. *Journal of Cell Biology*, **188**, 21-28.
- [353] Lin H, Sassano MF, Roth BL, Shoichet BK. (2013) A pharmacological organization of G protein-coupled receptors. *Nature Methods*, **10**, 140-146.

- [354] Nagata A, Hamamoto A, Horikawa M, Yoshimura K, Takeda S, Saito Y. (2013) Characterization of ciliary targeting sequence of rat melanin-concentrating hormone receptor 1. *General and Comparative Endocrinology*, **188**, 159-165.
- [355] Ezak MJ, Ferkey DM. (2011) A functional nuclear localization sequence in the *C. elegans* TRPV channel OCR-2. *PLoS One*, **6**(9):e25047.
- [356] Chapin HC, Rajendran V, Capasso A, Caplan MJ. (2009) Detecting the surface localization and cytoplasmic cleavage of membrane-bound proteins. *Methods in Cell Biology*, **94**, 223-239.
- [357] Hatayama M1, Aruga J. (2012) Gli protein nuclear localization signal. *Vitamins and Hormones*, **88**, 73-89.
- [358] Johnson LR, Robinson JD, Lester KN, Pitcher JA. (2013) Distinct structural features of G protein-coupled receptor kinase 5 (GRK5) regulate its nuclear localization and DNA-binding ability. *PLoS One*, **8**(5):e62508.
- [359] Jeffries, S, Capobianco AJ. (2000) Neoplastic transformation by Notch requires nuclear localization. *Molecular and Cellular Biology*, **20**, 3928-3941.
- [360] Itoh K, Brott BK, Bae GU, Ratcliffe MJ, Sokol SY. (2005) Nuclear localization is required for Dishevelled function in Wnt/beta-catenin signaling. *Journal of Biology*, **4**, 3.
- [361] Sheng T, Chi S, Zhang X, Xie J. (2006) Regulation of Gli1 localization by the cAMP/protein kinase A signaling axis through a site near the nuclear localization signal. *Journal of Biological Chemistry*, **281**, 9-12.
- [362] Mazelova J, Astuto-Gribble L, Inoue H, Tam BM, Schonteich E, Prekeris R, Moritz OL, Randazzo PA, Deretic D. (2009) Ciliary targeting motif VxPx directs assembly of a trafficking module through Arf4. *EMBO Journal*, **28**, 183-192.
- [363] Miyoshi K, Kasahara K, Miyazaki I, Asanuma M. (2011) Factors that influence primary cilium length. *Acta Medica Okayama*, **65**(5), 279-285.
- [364] Prodromou NV, Thompson CL, Osborn DP, Cogger KF, Ashworth R, Knight MM, Beales PL, Chapple JP. (2012) Heat shock induces rapid resorption of primary cilia. *Journal of Cell Science*, **125**, 4297-4305.
- [365] Rich DR, Clark AL. (2012) Chondrocyte primary cilia shorten in response to osmotic challenge and are sites for endocytosis. *Osteoarthritis and Cartilage*, **20**, 923-930.
- [366] Wann AK, Knight MM. (2012) Primary cilia elongation in response to interleukin-1 mediates the inflammatory response. *Cellular and Molecular Life Sciences*, **69**, 2967-2977.
- [367] Broekhuis JR, Leong WY, Jansen G. (2013) Regulation of cilium length and intraflagellar transport. *International Review of Cellular and Molecular Biology*, **303**, 101-138.
- [368] Hilton LK, Gunawardane K, Kim JW, Schwarz MC, Quarmby LM. (2013) The Kinases LF4 and CNK2 Control Ciliary Length by Feedback Regulation of Assembly and Disassembly Rates. *Current Biology*, **23**, 2208-2214.
- [369] Pan J, Snell WJ. (2005) *Chlamydomonas* shortens its flagella by activating axonemal disassembly, stimulating IFT particle trafficking, and blocking anterograde cargo loading. *Developmental Cell*, **9**, 431-438.

- [370] Ghossoub R, Hu Q, Failler M, Rouyez MC, Spitzbarth B, Mostowy S, Wolfrum U, Saunier S, Cossart P, Nelson WJ, Benmerah A. (2013) Septins 2, 7, and 9 and MAP4 co-localize along the axoneme in the primary cilium and control ciliary length. *Journal of Cell Science*, **126**, 2583-2594.
- [371] Rondanino C, Poland PA, Kinlough CL, Li H, Rbaibi Y, Myerburg MM, Al-Bataineh MM, Kashlan OB, Pastor-Soler NM, Hallows KR, Weisz OA, Apodaca G, Hughey RP. (2011) Galectin-7 modulates the length of the primary cilia and wound repair in polarised kidney epithelial cells. *American Journal of Physiology*, **301**, F622-F633.
- [372] Niwa S, Nakajima K, Miki H, Minato Y, Wang D, Hirokawa N. (2012) KIF19A is a microtubule-depolymerizing kinesin for ciliary length control. *Developmental Cell*, **23**, 1167-1175.
- [373] Jurisch-Yaksi N, Rose AJ, Lu H, Raemaekers T, Munck S, Baatsen P, Baert V, Vermeire W, Scales SJ, Verleyen D, Vandepoel R, Tylzanowski P, Yaksi E, de Ravel T, Yost HJ, Froyen G, Arrington CB, Annaert W. (2013) Rer1p maintains ciliary length and signaling by regulating γ -secretase activity and Foxj1a levels. *Journal of Cell Biology*, **200**, 709-720.
- [374] Sato K, Sato M, Nakano A. (2001) Rer1p, a retrieval receptor for endoplasmic reticulum membrane proteins, is dynamically localized to the Golgi apparatus by coatmer. *Journal of Cell Biology*, **152**, 935-944.
- [375] Wojtyniak M, Brear AG, O'Halloran DM, Sengupta P. (2013) Cell- and subunit-specific mechanisms of CNG channel ciliary trafficking and localization in *C. elegans*. *Journal of Cell Science*, **126**, 4381-4395.
- [376] Emmer BT, Maric D, Engman DM. (2010) Molecular mechanisms of protein and lipid targeting to ciliary membranes. *Journal of Cell Science*, **123**, 529-536.
- [377] Tyler K M, Fridberg A, Toriello K M, Olson C L, Cieslak JA, Hazlett T L, Engman D M. (2009) Flagellar membrane localization via association with lipid rafts. *Journal of Cell Science*, **122**, 859-866.
- [378] Ott C, Elia N, Jeong SY, Insinna C, Sengupta P, Lippincott-Schwartz J. (2012) Primary cilia utilize glycoprotein-dependent adhesion mechanisms to stabilize long-lasting cilia-cilia contacts. *Cilia*, **1**, 3.
- [379] Kooijman R, de Wildt P, Beumer S, van der Vliet G, Homan W, Kalshoven H, Musgrave A, van den Ende H. (1989) Wheat germ agglutinin induces mating reactions in *Chlamydomonas* eugametes by cross-linking agglutinin-associated glycoproteins in the flagellar membrane. *Journal of Cell Biology*, **109**, 1677-1687.
- [380] Schmidt-Rohlfing B, Schneider U, Goost H, Silny J. (2002) Mechanically induced electrical potentials of articular cartilage. *Journal of Biomechanics*, **35**, 475-482.
- [381] Moller PC, Chang JP, Partridge LR. (1981) The distribution of cationized ferritin receptors on ciliated epithelial cells of rat trachea. *Tissue and Cell*, **13**, 731-737.
- [382] Anderson RG, Hein CE. (1977) Distribution of anionic sites on the oviduct ciliary membrane. *Journal of Cell Biology*, **72**, 482-492.
- [383] Ye F, Breslow DK, Koslover EF, Spakowitz AJ, Nelson WJ, Nachury MV. (2013) Single molecule imaging reveals a major role for diffusion in the exploration of ciliary space by signaling receptors. *Elife*, **2**, e00654.

- [384] Green JA, Gu C, Mykytyn K (2012) Heteromerization of Ciliary G Protein-Coupled Receptors in the Mouse Brain. *PLoS ONE*, **7**(9):e46304
- [385] Follit JA, Pazour GJ. (2013) Analysis of ciliary membrane protein dynamics using SNAP technology. *Methods in Enzymology*, **524**,195-204.
- [386] Schaub JR, Stearns T. (2013) The Rilp-like proteins Rilpl1 and Rilpl2 regulate ciliary membrane content. *Molecular Biology of the Cell*, **26**, 453-464.
- [387] Abulrob A, Lu Z, Baumann E, Vobornik D, Taylor R, Stanimirovic D, Johnston LJ. (2010) Nanoscale imaging of epidermal growth factor receptor clustering: effects of inhibitors. *Journal of Biological Chemistry*, **285**, 3145-3156.
- [388] Li Q, Montalbetti N, Wu Y, Ramos A, Raychowdhury MK, Chen XZ, Cantiello HF. (2006) Polycystin-2 cation channel function is under the control of microtubular structures in primary cilia of renal epithelial cells. *Journal of Biological Chemistry*, **281**, 37566-37575.
- [389] Phan MN, Leddy HA, Votta BJ, Kumar S, Levy DS, Lipshutz DB, Lee SH, Liedtke W, Guilak F. (2009) Functional characterization of TRPV4 as an osmotically sensitive ion channel in porcine articular chondrocytes. *Arthritis and Rheumatology*, **60**, 3028-3037.
- [390] Goswami C, Kuhn J, Heptall PA, Hucho T. (2010) Importance of non-selective cation channel TRPV4 interaction with cytoskeleton and their reciprocal regulations in cultured cells. *PLoS One*, **5**(7):e11654.
- [391] Bloodgood RA. (1984) Preferential turnover of membrane proteins in the intact *Chlamydomonas* flagellum. *Experimental Cell Research*, **150**, 488-493.
- [392] Besharse JC, Hollyfield JG, Rayborn ME. (1977) Turnover of rod photoreceptor outer segments. II. Membrane addition and loss in relationship to light. *Journal of Cell Biology*, **75**, 507-527.
- [393] Besharse JC, Horst CJ. (1990) The photoreceptor connecting cilium: a model for the transition zone. In: Bloodgood, RA. (ed). *Ciliary and flagellar membranes*. Plenum Press, New York, pp. 409-431.
- [394] Trivedi D, Colin E, Louie CM, Williams DS. (2012) Live-cell imaging evidence for the ciliary transport of rod photoreceptor opsin by heterotrimeric kinesin-2. *Journal of Neuroscience*, **32**, 10587-10593.
- [395] Ezratty EJ, Stokes N, Chai S, Shah AS, Williams SE, Fuchs E. (2011) A role for the primary cilium in Notch signaling and epidermal differentiation during skin development. *Cell*, **145**, 1129-1141.
- [396] Lancaster MA, Schroth J, Gleeson JG. (2011) Subcellular spatial regulation of canonical Wnt signalling at the primary cilium. *Nature Cell Biology*, **13**, 700-707.
- [397] Haycraft CJ, Banizs B, Aydin-Son Y, Zhang Q, Michaud EJ, Yoder BK. (2005) Gli2 and gli3 localize to cilia and require the intraflagellar transport protein polaris for processing and function. *PLoS Genetics*, **1**, e53.
- [398] Varjosalo M, Taipale J. (2008) Hedgehog: functions and mechanisms. *Genes and Development*, **22**, 2454-2472.

- [399] Wen X, Lai CK, Evangelista M, Hongo JA, de Sauvage FJ, Scales SJ. (2010) Kinetics of hedgehog-dependent full-length gli3 accumulation in primary cilia and subsequent degradation. *Molecular and Cellular Biology*, **30**, 1910-1922.
- [400] Zhang Q, Seo S, Bugge K, Stone EM, Sheffield VC. (2012) BBS proteins interact genetically with the IFT pathway to influence SHH-related phenotypes. *Human Molecular Genetics*, **21**, 1945-1953.
- [401] Rohatgi R, Milenkovic L, Scott MP. (2007) Patched1 regulates hedgehog signaling at the primary cilium. *Science*, **317**, 372-373.
- [402] Seeger-Nukpezah T, Golemis EA. (2012) The extracellular matrix and ciliary signaling. *Current Opinion in Cell Biology*, **24**, 652-661.
- [403] Wu LN, Genge BR, Lloyd GC, Wuthier RE. (1991) Collagen-binding proteins in collagenase-released matrix vesicles from cartilage. Interaction between matrix vesicle proteins and different types of collagen. *Journal of Biological Chemistry*, **266**, 1195-1203.
- [404] Brochhausen C, Zehbe R, Watzer B, Halstenberg S, Schubert H, Kirkpatrick CJ. (2010) Growth Factors and Signalling Molecules for Cartilage Tissue Engineering - from Embryology to Innovative Release Strategies for Guided Tissue Engineering, In: *Tissue Engineering*, Daniel Eberli (Ed.).
- [405] Adams SL, Cohen AJ, Lassová L. (2007) Integration of signaling pathways regulating chondrocyte differentiation during endochondral bone formation. *Journal of Cell Physiology*, **213**, 635-641.
- [406] Wang S, Zhang J, Nauli SM, Li X, Starremans PG, Luo Y, Roberts KA, Zhou J. (2007) Fibrocystin/polyductin, found in the same protein complex with polycystin-2, regulates calcium responses in kidney epithelia. *Molecular and Cell. Biology*, **27**, 3241-3252.
- [407] Anyatonwu GI, Ehrlich BE. (2004) Calcium signaling and polycystin-2. *Biochemical and Biophysical Research Communications*, **322**, 1364-1373.
- [408] Minina E, Kreschel C, Naski MC, Ornitz DM, Vortkamp A. (2002) Interaction of FGF, Ihh/Pthlh, and BMP signaling integrates chondrocyte proliferation and hypertrophic differentiation. *Journal of Cellular Biochemistry*, **114**, 735-742.
- [409] Viviano BL, Paine-Saunders S, Gasiunas N, Gallagher J, Saunders S (2004) Domain-specific modification of heparan sulfate by Qsulf1 modulates the binding of the bone morphogenetic protein antagonist Noggin. *Journal of Biological Chemistry*, **279**, 5604-5611.
- [410] Kirn-Safran CB, Gomes RR, Brown AJ, Carson DD. (2004) Heparan sulfate proteoglycans: coordinators of multiple signaling pathways during chondrogenesis. *Birth Defects Research, C Embryo Today*, **72**, 69-88.
- [411] French MM, Gomes RR Jr, Timpl R, Höök M, Czymmek K, Farach-Carson MC, Carson DD. (2002) Chondrogenic activity of the heparan sulfate proteoglycan perlecan maps to the N-terminal domain I. *Journal of Bone Mineral Research*, **17**, 48-55.
- [412] Hecht JT, Hayes E, Haynes R, Cole WG, Long RJ, Farach-Carson MC, Carson DD. (2005) Differentiation-induced loss of heparan sulfate in human exostosis derived chondrocytes. *Differentiation*, **73**, 212-221.
- [413] Wells S, Ayer A. (2006) Heparan sulfate proteoglycan expression in differentiating chondrocyte cultures. *FASEB Journal*, **20**, LB57.

- [414] Witt RM, Hecht ML, Pazyra-Murphy MF, Cohen SM, Noti C, van Kuppevelt TH, Fuller M, Chan JA, Hopwood JJ, Seeberger PH, Segal RA. (2013) Heparan sulfate proteoglycans containing a glypican 5 core and 2-O-sulfo-iduronic acid function as sonic hedgehog co-receptors to promote proliferation. *Journal of Biological Chemistry*, **288**, 26275-26288.
- [415] Li F, Shi W, Capurro M, Filmus J. (2011) Glypican-5 stimulates rhabdomyosarcoma cell proliferation by activating Hedgehog signaling. *Journal of Cell Biology*, **192**, 691-704.
- [416] Capurro MI, Xu P, Shi W, Li F, Jia A, Filmus J. (2008) Glypican-3 inhibits Hedgehog signaling during development by competing with patched for Hedgehog binding. *Developmental Cell*, **14**, 700-711.
- [417] Ohlig S, Pickhinke U, Sirko S, Bandari S, Hoffmann D, Dreier R, Farshi P, Götz M, Grobe K. (2012) An emerging role of Sonic hedgehog shedding as a modulator of heparan sulfate interactions. *Journal of Biological Chemistry*, **287**, 43708-43719.
- [418] Callejo A, Torroja C, Quijada L, Guerrero I. (2006) Hedgehog lipid modifications are required for Hedgehog stabilization in the extracellular matrix. *Development*, **133**, 471-783.
- [419] Fuerer C, Habib SJ, Nusse R. (2010) A study on the interactions between heparan sulfate proteoglycans and Wnt proteins. *Developmental Dynamics*, **239**, 184-190.
- [420] Clement CA, Ajbro KD, Koefoed K, Vestergaard ML, Veland IR, Henriques de Jesus MP, Pedersen LB, Benmerah A, Andersen CY, Larsen LA, Christensen ST. (2013) TGF- β signaling is associated with endocytosis at the pocket region of the primary cilium. *Cell Reports*, **3**, 1806-1814.
- [421] Kleene NK, Kleene SJ. (2012) A method for measuring electrical signals in a primary cilium. *Cilia*, **1**, 17.
- [422] Wann AK, Zuo N, Haycraft CJ, Jensen CG, Poole CA, McGlashan SR, Knight MM. (2012) Primary cilia mediate mechanotransduction through control of ATP-induced Ca²⁺ signaling in compressed chondrocytes. *FASEB Journal*, **26**, 1663-1671.
- [423] Mobasher A, Barrett-Jolley B. (2011) Transient receptor potential channels: emerging roles in health and disease. *The Veterinary Journal*, **187**, 145-146.
- [424] Clapham DE. (2003) TRP channels as cellular sensors. *Nature*, **426**, 517-524.
- [425] Nauli SM, Alenghat FJ, Luo Y, et al. (2003) Polycystins 1 and 2 mediate mechanosensation in the primary cilium of kidney cells. *Nature Genetics*, **33**, 129-137.
- [426] Gradilone SA, Masyuk AI, Splinter PL, Banales J, Huang BQ, Tiet, PS, Masyuk TV, LaRusso NF. (2007) Cholangiocyte cilia express TRPV4 and detect changes in luminal tonicity inducing bicarbonate secretion. *Proceedings of the National Academy of Sciences, USA*, **104**, 19138-19143.
- [427] Bargmann CI. Chemosensation in *C. elegans*. *WormBook*, **2006**, 1-29.
- [428] Kottgen M, Buchholz B, Garcia-Gonzalez MA, Kotsis F, Fu X, Doerken M, Boehlke C, Steffl D, Tauber R, Wegierski T, Nitschke R, Suzuki M, Kramer-Zucker A, Germino GG, Watnick T, Prenen J, Nilius B, Kuehn EW, Walz G. (2008) TRPP2 and TRPV4 form a polymodal sensory channel complex. *Journal of Cell Biology*, **182**, 437-447.
- [429] Zhou J. (2009) Polycystins and primary cilia: primers for cell cycle progression. *Annual Reviews of Physiology*, **71**, 83-113.

- [430] Qian F, (2013) Handbook of Proteolytic Enzymes (Third Edition) *ELSEVIER*, 3728-3736. ISBN: 9780123822192
- [431] Forman JR, Qamar S, Paci E, Sandford RN, Clarke J. (2005) The remarkable mechanical strength of polycystin-1 supports a direct role in mechanotransduction. *Journal of Molecular Biology*, **349**, 861-871.
- [432] Osborn DPS, Boucher C, Wilson P, Gattone V, Beales PL, Drummond I, Sandford R. (2012) A novel 9 kDa phosphoprotein is a component of the primary cilium and interacts with polycystin-1. *Cilia*, **1**, P74.
- [433] Foy RL, Chitalia VC, Panchenko MV, Zeng L, Lopez D, Lee JW, Rana SV, Boletta A, Qian F, Tsiokas L, Piontek KB, Germino GG, Zhou MI, Cohen HT. (2012) Polycystin-1 regulates the stability and ubiquitination of transcription factor Jade-1. *Human Molecular Genetics*, **21**, 5456-5471.
- [434] Du J, Ding M, Sours-Brothers S, Graham S, Ma R. (2008) Mediation of angiotensin II-induced Ca²⁺ signaling by polycystin 2 in glomerular mesangial cells. *American Journal of Physiology*, **294**, 909-918.
- [435] Zhang ZR, Chu WF, Song B, Goo M, Zhang JN. (2013) TRPP2 and TRPV4 Form an EGF-Activated Calcium Permeable Channel at the Apical Membrane of Renal Collecting Duct Cells. *PLoS One*, **8**(8), e73424.
- [436] Clark AL, Votta BJ, Kumar S, Liedtke W, Guilak F. (2010) Chondroprotective role of the osmotically sensitive ion channel transient receptor potential vanilloid 4: age- and sex-dependent progression of osteoarthritis in Trpv4-deficient mice. *Arthritis and Rheumatology*, **62**, 2973-2983.
- [437] Muramatsu S, Wakabayashi M, Ohno T, Amano K, Ooishi R, Sugahara T, Shiojiri S, Tashiro K, Suzuki Y, Nishimura R, Kuhara S, Sugano S, Yoneda T, Matsuda A. (2007) Functional gene screening system identified TRPV4 as a regulator of chondrogenic differentiation. *Journal of Biological Chemistry*, **282**, 32158-32167.
- [438] Knight MM, McGlashan SR, Garcia M, Jensen CG, Poole CA. (2009) Articular chondrocytes express connexin 43 hemichannels and P2 receptors - a putative mechanoreceptor complex involving the primary cilium? *Journal of Anatomy*, **214**, 275-283.
- [439] Chowdhury TT, Knight MM. (2006) Purinergic pathway suppresses the release of NO and stimulates proteoglycan synthesis in chondrocyte/agarose constructs to dynamic compression. *Journal of Cell Physiology*, **290**, 845-853.
- [440] Masyuk AI, Gradilone SA, Banales JM, Huang BQ, Masyuk TV, Lee SO, Splinter PL, Stroope AJ, Larusso NF. (2008) Cholangiocyte primary cilia are chemosensory organelles that detect biliary nucleotides via P2Y12 purinergic receptors. *American Journal of Physiology*, **295**, G725-G734.
- [441] Pinguan-Murphy B, El-Azzeh M, Bader DL, Knight MM. (2006) Cyclic compression of chondrocytes modulates a purinergic calcium signalling pathway in a strain rate- and frequency-dependent manner. *Journal of Cell Physiology*, **209**, 389-397.
- [442] Low SH, Vasanth S, Larson CH, Mukherjee S, Sharma N, Kinter MT, Kane ME, Obara T, Weimbs T. (2006) Polycystin-1, STAT6, and P100 function in a pathway that transduces ciliary mechanosensation and is activated in polycystic kidney disease. *Developmental Cell*, **10**, 57-69.
- [443] Philipp M, Caron MG. (2009) Hedgehog signaling: is Smo a G protein-coupled receptor? *Current Biology*, **19**, R125-R127.

- [444] McMahon AP, Ingham PW, Tabin CJ. (2003) Developmental roles and clinical significance of hedgehog signaling. *Current Topics in Developmental Biology*, **53**, 1-114.
- [445] Mukhopadhyay S, Wen X, Ratti N, Loktev A, Rangell L, Scales SJ, Jackson PK. (2013) The ciliary G-protein-coupled receptor Gpr161 negatively regulates the Sonic hedgehog pathway via cAMP signaling. *Cell*, **152**, 210-222.
- [446] Farnum CE, Wilsman NJ. (2011) Axonemal positioning and orientation in three-dimensional space for primary cilia: what is known, what is assumed, and what needs clarification. *Developmental Dynamics*, **240**, 2405-2431.
- [447] Kwon RY, Hoey DA, Jacobs CR. (2011) Mechanobiology of primary cilia. *Cellular and Biomolecular Mechanics and Mechanobiology*, Vol 4. Gefen, A. (ed) SpringerLink, Heidelberg: pp 99-124.
- [448] Hoey DA, Chen JC, Jacobs CR. (2012) The primary cilium as a novel extracellular sensor in bone. *Frontiers in Endocrinology (Lausanne)*, **3**, 75.
- [449] Kwon RY, Temiyasathit S, Tummala P, Quah CC, Jacobs CR. (2010) Primary cilium-dependent mechanosensing is mediated by adenylyl cyclase 6 and cyclic AMP in bone cells. *FASEB Journal*, **24**, 2859-2868.
- [450] Malone AMD, Anderson CT, Tummala P, Kwon RY, Johnston TR, Stearns T, Jacobs CR. (2007) Primary cilia mediate mechanosensing in bone cells by a calcium independent mechanism. *Proceedings of the National Academy of Sciences, USA*, **104**, 13325-13330.
- [451] Puri S, Magenheimer BS, Maser RL, Ryan EM, Zien CA, Walker DD, Wallace DP, Hempson SJ, Calvet JP. (2004) Polycystin-1 activates the calcineurin/NFAT (nuclear factor of activated T-cells) signaling pathway. *Journal of Biological Chemistry*, **279**, 55455-55464.
- [452] Yoder BK, Hou X, Guay-Woodford LM. (2002) The polycystic kidney disease proteins, polycystin-1, polycystin-2, polaris, and cystin, are co-localized in renal cilia. *Journal of the American Society of Nephrology*, **13**, 2508-2516.
- [453] Ma M, Tian X, Igarashi P, Pazour GJ, Somlo S. (2013) Loss of cilia suppresses cyst growth in genetic models of autosomal dominant polycystic kidney disease. *Nature Genetics*, **45**, 1004-1012.
- [454] Alenghat FJ, Nauli SM, Kolb R, Zhou J, Ingber DE. (2004) Global cytoskeletal control of mechanotransduction in kidney epithelial cells. *Experimental Cell Research*, **301**, 23-30.
- [455] Kaimori JY, Nagasawa Y, Menezes LF, Garcia-Gonzalez MA, Deng J, Imai E, Onuchic LF, Guay-Woodford LM, Germino GG. (2007) Polyductin undergoes notch-like processing and regulated release from primary cilia. *Human Molecular Genetics*, **16**, 942-956.
- [456] Lu XL, Mow VC. (2008) Biomechanics of articular cartilage and determination of material properties. *Medicine and Science in Sports and Exercise*, **40**, 193-199.
- [457] Chen CS, Ingber DE. (1999) Tensegrity and mechanoregulation: from skeleton to cytoskeleton. *Osteoarthritis and Cartilage*, **7**, 81-94.
- [458] Praetorius HA, Praetorius J, Nielsen S, Frokiaer J, Spring KR. (2004) Beta1-integrins in the primary cilium of MDCK cells potentiate fibronectin-induced Ca²⁺ signaling. *American Journal of Physiology*, **287**, F969-F978.

- [459] Wilson PG. (2008) Centriole inheritance. *Prion*, **2**, 9-16.
- [460] Sathananthan AH, Ratnam SS, Ng SC, Tarin JJ, Gianaroli L, Trounson A. (1996) The sperm centriole: its inheritance, replication and perpetuation in early human embryos. *Human Reproduction*, **11**, 345-356.
- [461] Doxsey S, Zimmerman W, Mikule K. (2005) Centrosome control of the cell cycle. *Trends in Cell Biology*, **15**, 303-311.
- [462] Tang N, Marshall WF. (2012) Centrosome positioning in vertebrate development. *Journal of Cell Science*, **125**, 4951-4961.
- [463] Mitchison T, Kirschner M. (1984) Dynamic instability of microtubule growth. *Nature*, **312**, 237-242.
- [464] Ou YY, Zhang M, Chi S, Matyas JR, Rattner JB. (2003) Higher Order Structure of the PCM Adjacent to the Centriole. *Cell Motility and the Cytoskeleton*, **55**, 125-133.
- [465] Conduit PT, Feng Z, Richens JH, Baumbach J, Wainman A, Bakshi SD, Dobbelaere J, Johnson S, Lea SM, Raff JW. (2014) The centrosome-specific phosphorylation of Cnn by Polo/Plk1 drives Cnn scaffold assembly and centrosome maturation. *Developmental Cell*, **28**, 659-669.
- [466] Ou Y, Rattner JB. (2004) The centrosome in higher organisms: structure, composition, and duplication. *International Reviews of Cytology*, **238**, 119-182.
- [467] Vallee RB, Williams JC, Varma D, Barnhart LE. (2004) Dynein: an ancient motor protein involved in multiple modes of transport. *Journal of Neurobiology*, **58**, 189-200.
- [468] Hirokawa N, Noda Y. (2008) Intracellular transport and kinesin superfamily proteins, KIFs: structure, function, and dynamics. *Physiological Reviews*, **88**, 1089-1118.
- [469] Kapitein LC, van Bergeijk P, Lipka J, Keijzer N, Wulf PS, Katrukha EA, Akhmanova A, Hoogenraad CC. (2013) Myosin-V opposes microtubule-based cargo transport and drives directional motility on cortical actin. *Current Biology*, **23**, 828-834.
- [470] Welte MA. (2004) Bidirectional transport along microtubules. *Current Biology*, **14**, R525-R537.
- [471] Vale RD. (2003) The molecular motor toolbox for intracellular transport. *Cell*, **112**, 467-480.
- [472] Vale RD, Milligan RA. (2000) The way things move: looking under the hood of molecular motor proteins. *Science*, **288**, 88-95.
- [473] Kardon JR, Vale RD. (2009) Regulators of the cytoplasmic dynein motor. *Nature Reviews Molecular Cellular Biology*, **10**, 854-865.
- [474] Marx A, Hoenger A, Mandelkow E. (2009) Structures of kinesin motor proteins. *Cell Motility and the Cytoskeleton*, **66**, 958-966.
- [475] Yun M, Bronner CE, Park C, Cha S, Park H, Endow SA (2003) Rotation of the stalk/neck and one head in a new crystal structure of the kinesin motor protein, ncd. *EMBO Journal*, **22**, 1.
- [476] Kon T, Oyama T, Shimo-Kon R, Imamula K, Shima T, Sutoh K, Kurisu G. (2012) The 2.8Å crystal structure of the dynein motor domain. *Nature*, **484**, 345-350.

- [477] Karcher RL, Deacon SW, Gelfand VI. (2002) Motor-cargo interactions: the key to transport specificity. *Trends in Cell Biology*, **12**, 21-27.
- [478] Caviston JP, Holzbaaur EL. (2006) Microtubule motors at the intersection of trafficking and transport. *Trends in Cell Biology*, **16**, 530-537.
- [479] Maliga Z, Junqueira M, Toyoda Y, Ettinger A, Mora-Bermúdez F, Klemm RW, Vasilij A, Guhr E, Ibarlucea-Benitez I, Poser I, Bonifacio E, Huttner WB, Shevchenko A, Hyman AA. (2013) A genomic toolkit to investigate kinesin and myosin motor function in cells. *Nature Cell Biology*, **15**, 325-334.
- [480] Tikhonenko I, Nag DK, Robinson DN, Koonce MP. (2009) Microtubule-nucleus interactions in *Dictyostelium discoideum* mediated by central motor kinesins. *Eukaryotic Cell*, **8**, 723-731.
- [481] Kull FJ, Sablin EP, Lau R, Fletterick RJ, Vale RD. (1996) Crystal structure of the kinesin motor domain reveals a structural similarity to myosin. *Nature*, **380**, 550-550.
- [482] Sack S, Müller J, Marx A, Thormählen M, Mandelkow EM, Brady ST, Mandelkow E. (1997) X-ray structure of motor and neck somains of rat brain kinesin. *Biochemistry*, **36**, 16155-16165.
- [483] Marx A. Müller J, Mandelkow EM, Hoenger A, Mandelkow E. (2006) Interaction of kinesin motors, microtubules, and MAPs. *Journal of Muscle Research and Cell Motility*, **27**, 125-137.
- [484] Holzwarth G, Bonin K, Hill DB. (2002) Forces required of kinesin during processive transport through cytoplasm. *Biophysical Journal*, **82**, 1784-1790.
- [485] Böhm KJ, Stracke R, Unger E. (2000). Speeding up kinesin-driven microtubule gliding in vitro by variation of cofactor composition and physicochemical parameters. *Cell Biology International*, **24**, 335-341.
- [486] Berman HM, Henrick K, Nakamura H. (2003) Announcing the worldwide Protein Data Bank. *Nature Structural Biology*, **10**, 98.
- [487] Guex N, Peitsch MC. (1997) SWISS-MODEL and the Swiss-PdbViewer: An environment for comparative protein modeling. *Electrophoresis*, **18**, 2714-2723.
- [488] Kikkawa M. (2013) Big steps toward understanding dynein. *Journal of Cell Biology*, **202**, 15-23.
- [489] Sakakibara H, Oiwa K. (2011) Molecular organization and force-generating mechanism of dynein. *FEBS Journal*, **278**, 2964-2979.
- [490] King SM. (2010) Axonemal dyneins winch the cilium. *Nature Structural and Molecular Biology*, **17**, 673-674.
- [491] Pfister KK, Fisher EM, Gibbons IR, Hays TS, Holzbaaur EL, McIntosh JR, Porter ME, Schroer TA, Vaughan KT, Witman GB, King SM, Vallee RB. (2005) Cytoplasmic Dynein nomenclature. *Journal of Cell Biology*, **17**, 411-413.
- [492] Palmer KJ, Hughes H, Stephens DJ. (2009) Specificity of cytoplasmic dynein subunits in discrete membrane-trafficking steps. *Molecular Biology of the Cell*, **20**, 2885-2899.
- [493] Mallik R, Carter BC, Lex SA, King SJ, Gross SP. (2004) Cytoplasmic dynein functions as a gear in response to load. *Nature*, **427**, 649-652.

- [494] Schmidt H, Gleave ES, Carter AP. (2012) Insights into dynein motor domain function from a 3.3-Å crystal structure. *Nature Structural and Molecular Biology*, **19**, 492-497.
- [495] Reck-Peterson SL, Yildiz A, Carter AP, Gennerich A, Zhang N, Vale RD. (2006) Single molecule analysis of dynein processivity and stepping behavior. *Cell*, **126**, 335-348.
- [496] Roberts AJ, Kon T, Knight PJ, Sutoh K, Burgess SA. (2013) Functions and mechanics of dynein motor proteins. *Nature Reviews Molecular Cell Biology*, **14**, 713-726.
- [497] Vallee RB, McKenney RJ, Ori-McKenney KM. (2012) Multiple modes of cytoplasmic dynein regulation. *Nature Cell Biology*, **14**, 224-230.
- [498] Gagnon JA, Kreiling JA, Powrie EA, Wood TR, Mowry KL. (2013) Directional transport is mediated by a Dynein-dependent step in an RNA localization pathway. *PLoS Biology*, **11**, e1001551.
- [499] Tsai JW, Bremner KH, Vallee RB. (2007) Dual subcellular roles for LIS1 and dynein in radial neuronal migration in live brain tissue. *Nature Neuroscience*, **10**, 970-979.
- [500] Yamada M, Kumamoto K, Mikuni S, Arai Y, Kinjo M, Nagai T, Tsukasaki Y, Watanabe TM, Fukui M, Jin M, Toba S, Hirotsune S. (2013) Rab6a releases LIS1 from a dynein idling complex and activates dynein for retrograde movement. *Nature Communications*, **4**, 2033.
- [501] McKenney RJ, Vershinin M, Kunwar A, Vallee RB, Gross SP. (2010) LIS1 and NudE induce a persistent dynein force-producing state. *Cell*, **141**, 304-314.
- [502] Jordens I, Marsman M, Kuijl C, Neefjes J. (2005) Rab proteins, connecting transport and vesicle fusion. *Traffic*, **6**, 1070-1077.
- [503] Harrell JM, Murphy PJ, Morishima Y, Chen H, Mansfield JF, Galigniana MD, Pratt WB. (2004) Evidence for glucocorticoid receptor transport on microtubules by dynein. *Journal of Biological Chemistry*, **279**, 54647-54654.
- [504] Wu J, Lee KC, Dickinson RB, Lele TP. (2011) How dynein and microtubules rotate the nucleus. *Journal of Cell Physiology*, **226**, 2666-2674.
- [505] Harada A, Takei Y, Kanai Y, Tanaka Y, Nonaka S, Hirokawa N. (1998) Golgi vesiculation and lysosome dispersion in cells lacking cytoplasmic dynein. *Journal of Cell Biology*, **141**, 51-59.
- [506] Kimura N, Okabayashi S, Ono F. (2012) Dynein dysfunction disrupts intracellular vesicle trafficking bidirectionally and perturbs synaptic vesicle docking via endocytic disturbances a potential mechanism underlying age-dependent impairment of cognitive function. *American Journal of Pathology*, **180**, 550-561.
- [507] Hammesfahr B, Kollmar M. (2012) Evolution of the eukaryotic dynactin complex, the activator of cytoplasmic dynein. *BMC Evolutionary Biology*, **12**, 95.
- [508] Schafer DA, Gill SR, Cooper JA, Heuser JE, Schroer TA. (1994) Ultrastructural analysis of the dynactin complex: an actin-related protein is a component of a filament that resembles F-actin. *Journal of Cell Biology*, **126**, 403-412.
- [509] Deacon SW, Serpinskaya AS, Vaughan PS, Fanarraga ML, Vernos I, Vaughan KT, Gelfand VI. (2003) Dynactin is required for bidirectional organelle transport. *Journal of Cell Biology*, **160**, 297-301.

- [510] Holleran EA, Ligon LA, Tokito M, Stankewich MC, Morrow JS, Holzbaur ELF. (2001). β III Spectrin Binds to the Arp1 Subunit of Dynactin. *Journal of Biological Chemistry*, **276**, 36598-36605.
- [511] Zhapparova ON, Burakov AV, Nadezhdina S. (2007) The centrosome keeps nucleating microtubules but loses the ability to anchor them after the inhibition of dynein-dynactin complex. *Biochemistry (Moscow)*, **72**, 1233-1240.
- [512] Cobbold C, Coventry J, Ponnambalam S, Monaco AP. (2004) Actin and microtubule regulation of trans-Golgi network architecture, and copper-dependent protein transport to the cell surface. *Molecular Membrane Biology* **21**, 59-66.
- [513] Muresan V, Stankewich MC, Steffen W, Morrow JS, Holzbaur EL, Schnapp BJ. (2001) Dynactin-dependent, dynein-driven vesicle transport in the absence of membrane proteins. *Molecular Cell*, **7**, 173-183.
- [514] Quintyne NJ, Schroer TA. (2002) Distinct cell cycle-dependent roles for dynactin and dynein at centrosomes. *Journal of Cell Biology*, **159**, 245-254.
- [515] Ozaki Y, Matsui H, Nagamachi A, Asou H, Aki D, Inaba T. (2011) The dynactin complex maintains the integrity of metaphasic centrosomes to ensure transition to anaphase. *Journal of Biological Chemistry*, **286**, 5589-5598.
- [516] Karki S, Holzbaur ELF. (1999) Cytoplasmic dynein and dynactin in cell division and intracellular transport. *Current Opinion in Cell Biology*, **11**, 45-53.
- [517] Vaughan KT, Vallee RB. (1995) Cytoplasmic dynein binds dynactin through a direct interaction between the intermediate chains and p150^{Glued}. *Journal of Cell Biology*, **131**, 1507-1516.
- [518] Yadav S, Linstedt AD. (2011) Golgi positioning. *Cold Spring Harbour Perspectives in Biology*, **1**, 3 a005322.
- [519] Allan VJ, Thompson HM, McNiven MA. (2002) Motoring around the Golgi. *Nature Cell Biology*, **4**, E236-E242.
- [520] Appenzeller-Herzog C, Hauri HP. (2006) The ER-Golgi intermediate compartment (ERGIC): in search of its identity and function. *Journal of Cell Science*, **119**, 2173-2183.
- [521] Salcedo-Sicilia L, Granell S, Jovic M, Sicart A, Mato E, Johannes L, Balla T, Egea G. (2013) β III spectrin regulates the structural integrity and the secretory protein transport of the Golgi complex. *Journal of Biological Chemistry*, **288**, 2157-2166.
- [522] Habermann A, Schroer TA, Griffiths G, Burkhardt JK. (2001) Immunolocalization of cytoplasmic dynein and dynactin subunits in cultured macrophages: enrichment on early endocytic organelles. *Journal of Cell Science*, **114**, 229-240.
- [523] Kodani A, Salomé Sirerol-Piquer M, Seol A, Garcia-Verdugo JM, Reiter JF. (2013) Kif3a interacts with Dynactin subunit p150^{Glued} to organize centriole subdistal appendages. *EMBO Journal*, **32**, 597-607.
- [524] Uetake Y, Terada Y, Matuliene J, Kuriyama R. (2004) Interaction of Cep135 with a p50 dynactin subunit in mammalian centrosomes. *Cell Motility and the Cytoskeleton*, **58**, 53-66.
- [525] Matanis T, Akhmanova A, Wulf P, Del Nery E, Weide T, Stepanova T, Galjart N, Grosveld F, Goud B, De Zeeuw CI, Barnekow A, Hoogenraad CC. (2002) Bicaudal-D regulates COPI-

independent Golgi-ER transport by recruiting the dynein-dynactin motor complex. *Nature Cell Biology*, **4**, 986-992.

[526] Short B, Preisinger C, Schaletzky J, Kopajtich R, Barr FA. (2002) The Rab6 GTPase regulates recruitment of the dynactin complex to Golgi membranes. *Current Biology*, **12**, 1792-1795.

[527] Goud B, Askhanova A. (2012) Rab GTPase. In: *Rab GTPases and Membrane Trafficking*. Eds: Li G, Segev N. Bentham Science Publishing, USA. pp. 34-46.

[528] Quintyne NJ, Gill SR, Eckley DM, Crego CL, Compton DA, Schroer TA. (1999) Dynactin is required for microtubule anchoring at fibroblast centrosomes. *Journal of Cell Biology*, **147**, 321-334.

[529] Palazzo AF, Joseph HL, Chen YJ, Dujardin DL, Alberts AS, Pfister KK, Vallee RB, Gundersen GG. (2001) Cdc42, dynein, and dynactin regulate MTOC reorientation independent of Rho-regulated microtubule stabilization. *Current Biology*, **11**, 1536-1541.

[530] Deneka M, Neeft M, van der Sluijs P. (2003) Regulation of membrane transport by rab GTPases. *Critical Reviews in Biochemistry and Molecular Biology*, **38**, 121-114.

[531] Etienne-Manneville S, Hall A. (2002) Rho GTPases in cell biology. *Nature*, **420**, 629-635.

[532] Rojas AM, Fuentes G, Rausell A, Valencia A. (2012) The Ras protein superfamily: evolutionary tree and role of conserved amino acids. *Journal of Cell Biology*, **196**, 189-201.

[533] Carazo-Salas RE, Gruss OJ, Mattaj IW, Karsenti E. (2001) Ran-GTP coordinates regulation of microtubule nucleation and dynamics during mitotic-spindle assembly. *Nature Cell Biology*, **3**, 228-234.

[534] Bourne HR, Sanders DA, McCormick F. (1991) The GTPase superfamily: conserved structure and molecular mechanism. *Nature*, **349**, 117-127.

[535] Brighouse A, Dacks JB, Field MC. (2010) Rab protein evolution and the history of the eukaryotic endomembrane system. *Cellular and Molecular Life Sciences*, **67**, 3449-3465.

[536] Grosshans B, Ortiz D, Novick P. (2006) Rabs and their effectors: achieving specificity in membrane traffic. *Proceedings of the National Academy of Sciences, USA*, **103**, 11821-11827.

[537] Iden S, Collard JG. (2008) Crosstalk between small GTPases and polarity proteins in cell polarization. *Nature Reviews Molecular and Cellular Biology*, **9**, 846-859.

[538] Schwartz SL, Cao C, Pylypenko O, Rak A, Wandinger-Ness A. (2007) Rab GTPases at a glance. *Journal of Cell Science*, **120**, 3905-3910.

[539] Baschieri F, Farhan H. (2012) Crosstalk of small GTPases at the Golgi apparatus. *Small GTPases*, **3**, 80-90.

[540] Feig LA. (2003) Ral-GTPases: approaching their 15 minutes of fame. *Trends in Cell Biology*, **13**, 419-425.

[541] Heo WD, Meyer T. (2003) Switch-of-function mutants based on morphology classification of Ras superfamily small GTPases. *Cell*, **113**, 315-328.

[542] Goud B, Gleeson PA. (2010) TGN golgins, Rabs and cytoskeleton: regulating the Golgi trafficking highways. *Trends in Cell Biology*, **20**, 329-336.

- [542] Kaibuchi K1, Kuroda S, Amano M. (1999) Regulation of the cytoskeleton and cell adhesion by the Rho family GTPases in mammalian cells. *Annual Reviews in Biochemistry*, **68**, 459-486.
- [543] Kang J, Pervaiz S. (2013) Crosstalk between Bcl-2 family and Ras family small GTPases: potential cell fate regulation? *Frontiers in Oncology*, **2**, 206.
- [544] Bustelo XR, Sauzeau V, Berenjeno IM. (2007) GTP-binding proteins of the Rho/Rac family: regulation, effectors and functions *in vivo*. *BioEssays*, **29**, 356-370.
- [545] Pan J, You Y, Huang T, Brody SL. (2007) RhoA-mediated apical actin enrichment is required for ciliogenesis and promoted by Foxj1. *Journal of Cell Science*, **120**, 1868-1876.
- [546] Dawe H R, Smith U M, Cullinane A R, Gerrelli D, Cox P, Badano J L, Blair-Reid S, Sriram N, Katsanis N, Attie-Bitach T, Afford SC, Copp AJ, Kelly DA, Gull K, Johnson, CA. (2007). The Meckel-Gruber Syndrome proteins MKS1 and meckelin interact and are required for primary cilium formation. *Human and Molecular Genetics*, **16**, 173-186.
- [547] Dawe H, Adams M, Whewey G, Szymanska K, Logan CV, Noegel AA, Gull K, Johnson CA. (2009) Nesprin-2 interacts with meckelin and mediates ciliogenesis via remodelling of the actin cytoskeleton. *Journal of Cell Science*, **122**, 2716-2726.
- [548] Nayak RC, Chang KH, Vaitinadin NS, Cancelas JA. (2013) Rho GTPases control specific cytoskeleton-dependent functions of hematopoietic stem cells. *Immunological Reviews*, **256**, 255-268.
- [549] Chevrier V, Piel M, Collomb N, Saoudi Y, Frank R, Paintrand M, Narumiya S, Bornens M, Job D. (2002) The Rho-associated protein kinase p160ROCK is required for centrosome positioning. *Journal of Cell Biology*, **157**, 807-817.
- [550] Huvneers S, Danen EH. (2009) Adhesion signaling - crosstalk between integrins, Src and Rho. *Journal of Cell Science*, **122**, 1059-1069.
- [551] Maeda M, Hasegawa H, Hyodo T, Ito S, Asano E, Yuang H, Funasaka K, Shimokata K, Hasegawa Y, Hamaguchi M, Senga T. (2011) ARHGAP18, a GTPase-activating protein for RhoA, controls cell shape, spreading, and motility. *Molecular Biology of the Cell*, **22**, 3840-3852.
- [552] Ridley AJ, Schwartz MA, Burridge K, Firtel RA, Ginsberg MH, Borisy G, Parsons JT, Horwitz AR. (2003) Cell migration: integrating signals from front to back. *Science*, **302**, 1704-1709.
- [553] Nobes CD, Hall A. (1999) Rho GTPases control polarity, protrusion, and adhesion during cell movement. *Journal of Cell Biology*, **144**, 1235-1244.
- [554] Tapon N, Hall A. (1997) Rho, Rac and Cdc42 GTPases regulate the organization of the actin cytoskeleton. *Current Opinion in Cell Biology*, **9**, 86-92.
- [555] Fan S, Margolis B. (2011) The Ran importin system in cilia trafficking. *Organogenesis*, **7**, 147-153.
- [556] Di Fiore B, Ciciarello M, Mangiacasale R, Palena A, Tassin AM, Cundari E, Lavia P. (2003) Mammalian RanBP1 regulates centrosome cohesion during mitosis. *Journal of Cell Science*, **116**, 3399-3411.
- [557] Quimby BB, Lamitina T, L'Hernault SW, Corbett AH. (2000) The mechanism of ran import into the nucleus by nuclear transport factor 2. *Journal of Biological Chemistry*, **275**, 28575-28582.

- [558] Keryer G, Di Fiore B, Celati C, Lechtreck KF, Mogensen M, Delouvee A, Lavia P, Bornens M, Tassin AM. (2003) Part of Ran is associated with AKAP450 at the centrosome: involvement in microtubule-organizing activity. *Molecular Biology of the Cell*, **14**, 4260-4271.
- [559] Kahn RA1, Volpicelli-Daley L, Bowzard B, Shrivastava-Ranjan P, Li Y, Zhou C, Cunningham L. (2005) Arf family GTPases: roles in membrane traffic and microtubule dynamics. *Biochemical Society Transactions*, **33**, 1269-1272.
- [560] Zhou C, Cunningham L, Marcus AI, Li Y, Kahn RA. (2006) Arl2 and Arl3 regulate different microtubule-dependent processes. *Molecular Biology of the Cell*, **17**, 2476-2487.
- [561] Zhang Q, Hu J, Ling K. (2013) Molecular views of Arf-like small GTPases in cilia and ciliopathies. *Experimental Cell Research*, **319**, 2316-2322.
- [562] Li Y, Zhang Q, Wei Q, Zhang Y, Ling K, Hu J. (2012) SUMOylation of the small GTPase ARL-13 promotes ciliary targeting of sensory receptors. *Journal of Cell Biology*, **199**, 589-598.
- [563] Deretic D. (2013) Crosstalk of Arf and Rab GTPases en route to cilia. *Small GTPases*. **4**, 70-77.
- [564] Cuif MH, Possmayer F, Zander H, Bordes N, Jollivet F, Couedel-Courteille A, Janoueix-Lerosey I, Langsley G, Bornens M, Goud B. (1999) Characterization of GAPCenA, a GTPase activating protein for Rab6, part of which associates with the centrosome. *EMBO Journal*, **18**, 1772-1782.
- [565] Horgan CP, McCaffrey MW. (2011) Rab GTPases and microtubule motors. *Biochemical Society Transactions*, **39**, 1202-1206.
- [566] Stenmark H. (2009) Rab GTPases as coordinators of vesicle traffic. *Nature Reviews Molecular and Cellular Biology*, **10**, 513-525.
- [567] Hutagalung AH, Novick PJ. (2011) Role of Rab GTPases in membrane traffic and cell physiology. *Physiological Reviews*, **91**, 119-149.
- [568] Lim YS, Chua CE, Tang BL. (2011) Rabs and other small GTPases in ciliary transport. *Biology of the Cell*, **103**, 209-221.
- [569] Wanschers B, Van de Vorstenbosch R, Wijers M, Wieringa B, King SM, Fransen J. (2008) Rab6 family proteins interact with the dynein light chain protein DYNLRB1. *Cell Motility and Cytoskeleton*, **65**, 183-196.
- [570] Jahn R, Scheller RH. (2006) SNAREs--engines for membrane fusion. *Nature Reviews Molecular and Cellular Biology*, **7**, 631-643.
- [571] Hammer JA 3rd, Wu XS. (2002) Rabs grab motors: defining the connections between Rab GTPases and motor proteins. *Current Opinion in Cell Biology*, **14**, 69-75.
- [572] Goldenberg NM, Grinstein S, Silverman M. (2007) Golgi-bound Rab34 Is a Novel Member of the Secretory Pathway *Molecular Biology of the Cell*, **18**, 4762-4771.
- [573] Cai H, Reinisch K, Ferro-Novick S. (2007) Coats, tethers, Rabs, and SNAREs work together to mediate the intracellular destination of a transport vesicle. *Developmental Cell*, **12**, 671-682.
- [574] Rodman JS, Wandinger-Ness A. (2000) Rab GTPases coordinate endocytosis. *Journal of Cell Science*, **113**, 183-192.

- [575] Tolmachova T, Anders R, Stinchcombe J, Bossi G, Griffiths GM, Huxley C, Seabra MC. (2004) A general role for Rab27a in secretory cells. *Molecular Biology of the Cell*, **15**, 332-344.
- [576] Berg-Larsen A, Landsverk OJ, Progida C, Gregers TF, Bakke O. (2013) Differential regulation of Rab GTPase expression in monocyte-derived dendritic cells upon lipopolysaccharide activation: a correlation to maturation-dependent functional properties. *PLoS One*, **8**(9):e73538.
- [577] Kelly EE, Horgan CP, Goud B, McCaffrey MW. (2012) The Rab family of proteins: 25 years on. *Biochemical Society Transactions*, **40**, 1337-1347.
- [578] Sklan EH, Serrano L, Einav S, Pfeffer SR, Lambright DG, Glenn JS. (2007) TBC1D20 is a Rab1 GTPase-activating protein that mediates hepatitis C virus replication. *Journal of Biological Chemistry*, **282**, 36354-36361.
- [579] Corbeel L, Freson K. (2008) Rab proteins and Rab-associated proteins: major actors in the mechanism of protein-trafficking disorders. *European Journal of Pediatrics*, **167**, 723-729.
- [580] Hou Q, Wu YH, Grabsch H, Zhu Y, Leong SH, Ganesa, K, Cross D, Tan LK, Tao J, Gopalakrishnan V, Tang L, Ko, OL, Tan P. (2008) Integrative genomics identifies RAB23 as an invasion mediator gene in diffuse-type gastric cancer. *Cancer Research*, **68**, 4623-4630.
- [581] Stenmark H, Olkkonen VM. (2001) The Rab GTPase family. *Genome Biology*, **2**, REVIEWS3007.
- [582] Boehlke C, Bashkurov M, Buescher A, Krick T, John AK, Nitschke R, Walz G, Kuehn EW. (2010) Differential role of Rab proteins in ciliary trafficking: Rab23 regulates smoothed levels. *Journal of Cell Science*, **123**, 1460-1467.
- [583] Kim J, Krishnaswami SR, Gleeson JG. (2008) CEP290 interacts with the centriolar satellite component PCM-1 and is required for Rab8 localization to the primary cilium. *Human Molecular Genetics*, **17**, 3796-3805.
- [584] Hehnlly H, Chen CT, Powers CM, Liu HL, Doxsey S. (2012) The centrosome regulates the Rab11- dependent recycling endosome pathway at appendages of the mother centriole. *Current Biology*, **22**, 1944-1950.
- [585] Zhu S, Liu H, Wu Y, Heng BC, Chen P, Liu H, Ouyang HW. (2013) Wnt and Rho GTPase signaling in osteoarthritis development and intervention: implications for diagnosis and therapy. *Arthritis Research and Therapy*, **15**, 217.
- [586] Wang G, Beier F. (2005) Rac1/Cdc42 and RhoA GTPases antagonistically regulate chondrocyte proliferation, hypertrophy, and apoptosis. *Journal of Bone and Mineral Research*, **20**, 1022-1031.
- [587] Barr FA, Egerer J. (2005) Golgi positioning: are we looking at the right MAP? *Journal of Cell Biology*, **168**, 993-998.
- [588] Watson P, Forster R, Palmer KJ, Pepperkok R, Stephens DJ. (2004) Coupling of ER exit to microtubules through direct interaction of COPII with dynactin. *Nature Cell Biology*, **7**, 48-55.
- [589] Tisdale EJ, Balch WE. (1996) Rab2 is essential for the maturation of pre-Golgi intermediates. *Journal of Biological Chemistry*, **271**, 29372-29379.
- [590] Young JI, Stauber T, del Nery E, Vernos I, Pepperkok R, Nilsson T. (2005) Regulation of microtubule-dependent recycling at the trans-Golgi network by Rab6A and Rab6A'. *Molecular Biology of the Cell*, **16**, 162-177.

- [591] Knödler A1, Feng S, Zhang J, Zhang X, Das A, Peränen J, Guo W. (2010) Coordination of Rab8 and Rab11 in primary ciliogenesis. *Proceedings of the National Academy of Sciences, USA*, **107**, 6346-6351.
- [592] Storrie B, Micaroni M, Morgan GP, Jones N, Kamykowski JA, Wilkins N, Pan TH, Marsh BJ. (2012) Electron tomography reveals Rab6 is essential to the trafficking of trans-Golgi clathrin and COPI-coated vesicles and the maintenance of Golgi cisternal number. *Traffic*, **13**, 727-744.
- [593] Martinez O, Goud B. (1998) Rab proteins. *Biochimica Biophysica Acta*, **1404**, 101-112.
- [594] Barr FA, Short B. (2003) Golgins in the structure and dynamics of the Golgi apparatus. *Current Opinion in Cell Biology*, **15**, 405-413.
- [595] Khandelwal P, Prakasam HS, Clayton DR, Ruiz WG, Gallo LI, van Roekel D, Lukianov S, Peränen J, Goldenring JR, Apodaca G. (2013) A Rab11a-Rab8a-Myo5B network promotes stretch-regulated exocytosis in bladder umbrella cells. *Molecular Biology of the Cell*, **24**, 1007-1019.
- [596] Grigoriev I, Yu KL, Martinez-Sanchez E, Serra-Marques A, Smal I, Meijering E, Demmers J, Peränen J, Pasterkamp RJ, van der Sluijs, P, Hoogenraad CC, Akhmanova A. (2011) Rab6, Rab8, and MICAL3 cooperate in controlling docking and fusion of exocytotic carriers. *Current Biology*, **21**, 967-974.
- [597] Ibrahim R, Messaoudi C, Chichon FJ, Celati C, Marco S. (2009) Electron tomography study of isolated human centrioles. *Microscopic Research Techniques*, **72**, 42-48.
- [598] Anitei M, Hoflack B. (2011) Bridging membrane and cytoskeleton dynamics in the secretory and endocytic pathways. *Nature Cell Biology*, **14**, 11-19.
- [599] Tomás M, Martínez-Alonso E, Ballesta J, Martínez-Menárguez JA. (2010) Regulation of ER-Golgi intermediate compartment tubulation and mobility by COPI coats, motor proteins and microtubules. *Traffic*, **11**, 616-625.
- [600] Bard F, Malhotra V. (2006) The formation of TGN-to-plasma-membrane transport carriers. *Annual Review of Cellular and Developmental Biology*, **22**, 439-455.
- [601] Lieu ZZ, Lock JG, Hammond LA, La Gruta NL, Stow JL, Gleeson PA. (2008) A trans-Golgi network golgin is required for the regulated secretion of TNF in activated macrophages *in vivo*. *Proceedings of the National Academy of Sciences, USA*, **105**, 3351-3356.
- [602] Wang J, Deretic D. (2013) Molecular complexes that direct rhodopsin transport to primary cilia. *Progress in Retinitis Eye Research*, **14**, S1350-S9462.
- [603] Kang BH, Nielsen E, Preuss ML, Mastronarde D, Staehelin LA. (2011) Electron tomography of RabA4b- and PI-4K β 1-labeled trans Golgi network compartments in *Arabidopsis*. *Traffic*, **12**, 313-329.
- [604] Li Y, Ling K, Hu J. (2012) The emerging role of Arf/Arl small GTPases in cilia and ciliopathies. *Journal of Cellular Biochemistry*, **113**, 2201-2207.
- [605] Evans RJ, Schwarz N, Nagel-Wolfrum K, Wolfrum U, Hardcastle AJ, Cheetham ME. (2010) The retinitis pigmentosa protein RP2 links pericentriolar vesicle transport between the Golgi and the primary cilium. *Human and Molecular Genetics*, **19**, 1358-1367.

- [606] Patil H, Tserentsoodol N, Saha A, Hao Y, Webb M, Ferreira PA. (2012) Selective loss of RPGRIP1-dependent ciliary targeting of NPHP4, RPGR and SDCCAG8 underlies the degeneration of photoreceptor neurons. *Cell Death and Disease*, **3**, e355.
- [607] Mazelova J, Ransom N, Astuto-Gribble L, Wilson MC, Deretic D. (2009) Syntaxin 3 and SNAP-25 pairing, regulated by omega-3 docosahexaenoic acid, controls the delivery of rhodopsin for the biogenesis of cilia-derived sensory organelles, the rod outer segments. *Journal of Cell Science*, **122**, 2003-2013.
- [608] Deretic D, Williams AH, Ransom N, Morel V, Hargrave PA, Arendt A. (2005) Rhodopsin C terminus, the site of mutations causing retinal disease, regulates trafficking by binding to ADP-ribosylation factor 4 (ARF4). *Proceedings of the National Academy of Sciences, USA*, **102**, 3301-3306.
- [609] Ward HH, Peterson B, Romero E, Deretic D, Wandinger-Ness A. (2008) Polycystin-1 trafficking from Golgi to cilia. *The FASEB Journal*, **22**, 464.3.
- [610] Hoffmeister H, Babinger K, Gürster S, Cedzich A, Meese C, Schadendorf K, Osten L, de Vries U, Rasche A, Witzgall R. (2011) Polycystin-2 takes different routes to the somatic and ciliary plasma membrane. *Journal of Cell Biology*, **192**, 631-645.
- [611] Pavlos NJ, Xu J, Riedel D, Yeoh JS, Teitelbaum S, Papadimitriou JM, Jahn R, Ross P, Zhen, MH. (2005) Rab3D regulates a novel vesicular trafficking pathway that is required for osteoclastic bone resorption. *Molecular and Cellular Biology*, **25**, 5253-5269.
- [612] Johansson M, Rocha N, Zwart W, Jordens I, Janssen L, Kuijl C, Olkkonen VM, Neefjes J. (2007) Activation of endosomal dynein motors by stepwise assembly of Rab7-RILP-p150Glued, ORP1L, and the receptor betalll spectrin. *Journal of Cell Biology*, **176**, 459-471.
- [613] Chen JL, Fucini RV, Lacomis L, Erdjument-Bromage H, Tempst P, Stamnes M. (2005) Coatamer-bound Cdc42 regulates dynein recruitment to COPI vesicles. *Journal of Cell Biology*, **169**, 383-389.
- [614] Caviston JP, Holzbaur EL. (2009) Huntingtin as an essential integrator of intracellular vesicular trafficking. *Trends in Cell Biology*, **19**, 147-155.
- [615] Caviston JP, Zajac AL, Tokito M, Holzbaur EL. (2011) Huntingtin coordinates the dynein-mediated dynamic positioning of endosomes and lysosomes. *Molecular Biology of the Cell*, **22**, 478-492.
- [616] Kimura A, Onami S. (2010) Modeling microtubule-mediated forces and centrosome positioning in *Caenorhabditis elegans* embryos. *Methods in Cell Biology*, **97**, 437-453.
- [617] Kimura K, Kimura A. (2011) Intracellular organelles mediate cytoplasmic pulling force for centrosome centration in the *Caenorhabditis elegans* early embryo. *Proceedings of the National Academy of Sciences, USA*, **108**, 137-142.
- [618] Shiina N, Tsukita S. (1999) Regulation of microtubule organization during interphase and M phase. *Cell Structure and Function*, **24**, 385-391.
- [619] Sellin ME, Holmfeldt P, Stenmark S, Gullberg M. (2008) Global regulation of the interphase microtubule system by abundantly expressed Op18/stathmin. *Molecular Biology of the Cell*, **19**, 2897-2906.

- [620] Sumigray KD, Foote HP, Lechler T. (2012) Noncentrosomal microtubules and type II myosins potentiate epidermal cell adhesion and barrier formation. *Journal of Cell Biology*, **199**, 513-525.
- [621] Keating TJ, Borisy GG. (1999) Centrosomal and non-centrosomal microtubules. *Biology of the Cell*, **91**, 321-329.
- [622] Nagae S, Meng W, Takeichi M. (2013) Non-centrosomal microtubules regulate F-actin organization through the suppression of GEF-H1 activity. *Genes and Cells*, **18**, 387-396
- [623] Rivero S, Cardenas J, Bornens M, Rios RM. (2009) Microtubule nucleation at the cis-side of the Golgi apparatus requires AKAP450 and GM130. *The EMBO Journal*, **28**, 1016-1028.
- [624] King MC, Drivas TG, Blobel G. (2008) A network of nuclear envelope membrane proteins linking centromeres to microtubules. *Cell*, **134**, 427-438.
- [625] Efimov A, Kharitonov A, Efimova N, Loncarek J, Miller PM, Andreyeva N, Gleeson P, Galjart N, Maia AR, McLeod IX, Yates JR 3rd, Maiato H, Khodjakov A, Akhmanova A, Kaverina I. (2007) Asymmetric CLASP-dependent nucleation of noncentrosomal microtubules at the trans-Golgi network. *Developmental Cell*, **12**, 917-930.
- [626] Terasaki M, Chen LB, Fujiwara K. (1986) Microtubules and the endoplasmic reticulum are highly interdependent structures. *Journal of Cell Biology*, **103**, 1557-1568.
- [627] Misawa T, Takahama M, Kozaki T, Lee H, Zou J, Saitoh T, Akira S. (2013) Microtubule-driven spatial arrangement of mitochondria promotes activation of the NLRP3 inflammasome. *Nature Immunology*, **14**, 454-460.
- [628] Huda S, Soh S, Pilans D, Byrska-Bishop M, Kim J, Wilk G, Borisy GG, Kandere-Grzybowska K, Grzybowski BA. (2012) Microtubule guidance tested through controlled cell geometry. *Journal of Cell Science*, **125**, 5790-5799.
- [629] Brouhard GJ, Stear JH, Noetzel TL, Al-Bassam J, Kinoshita K, Harrison SC, Howard J, Hyman AA. (2008) XMAP215 is a processive microtubule polymerase. *Cell*, **132**, 79-88.
- [630] Fukata M, Watanabe T, Noritake J, Nakagawa M, Yamaga M, Kuroda S, Matsuura Y, Iwamatsu A, Perez F, Kaibuchi K. (2002) Rac1 and Cdc42 capture microtubules through IQGAP1 and CLIP-170. *Cell*, **109**, 873-885.
- [631] Niethammer P, Kronja I, Kandels-Lewis S, Rybina S, Bastiaens P, Karsenti E. (2007) Discrete states of a protein interaction network govern interphase and mitotic microtubule dynamics. *PLoS Biology*, **5**(2):e29.
- [632] Mennella V, Rogers GC, Rogers SL, Buster DW, Vale RD, Sharp DJ. (2005) Functionally distinct kinesin-13 family members cooperate to regulate microtubule dynamics during interphase. *Nature Cell Biology*, **7**, 235-245.
- [633] Tamura N, Draviam VM. (2012) Microtubule plus-ends within a mitotic cell are 'moving platforms' with anchoring, signalling and force-coupling roles. *Open Biology*, **2**, 120132.
- [634] Colello D, Mathew S, Ward R, Pumiglia K, LaFlamme SE. (2012) Integrins regulate microtubule nucleating activity of centrosome through mitogen-activated protein kinase/extracellular signal-regulated kinase/extracellular signal-regulated kinase (MEK/ERK) signaling. *Journal of Biological Chemistry*, **287**, 2520-2530.

- [635] Klann M, Koepl H, Reuss M. (2012) Spatial modeling of vesicle transport and the cytoskeleton: the challenge of hitting the right road. *PLoS One*, **7** (1):e29645.
- [636] Sütterlin C, Colanzi A. (2010) The Golgi and the centrosome: building a functional partnership. *Journal Cell Biology*, **18**, 621-628.
- [637] Schneider L, Cammer M, Lehman J, Nielsen SK, Guerra CF, Veland IR, Stock C, Hoffmann EK, Yoder BK, Schwab A, Satir P, Christensen ST. (2010) Directional cell migration and chemotaxis in wound healing response to PDGF-AA are coordinated by the primary cilium in fibroblasts. *Cell Physiol Biochem*. **25**, 279-292.
- [638] Yadav, S. et al. (2009) A primary role for Golgi positioning in directed secretion, cell polarity, and wound healing. *Molecular Biology of the Cell*, **20**, 1728-173.
- [639] Salaycik KJ, Fagerstrom CJ, Murthy K, Tulu US, Wadsworth P. (2005). Quantification of microtubule nucleation, growth and dynamics in wound-edge cells. *Journal of Cell Science*, **118**, 4113-4122
- [640] Hehny H, Xu W, Chen JL, Stamnes M. (2010) Cdc42 regulates microtubule-dependent Golgi positioning. *Traffic*, **11**, 1067-1078.
- [641] Etienne-Manneville S, Hall A. (2001) Integrin-mediated activation of Cdc42 controls cell polarity in migrating astrocytes through PKCzeta. *Cell*, **106**, 489-498.
- [642] Cai D, McEwen DP, Martens JR, Meyhofer E, Verhey KJ (2009) Single molecule imaging reveals differences in microtubule track selection between kinesin motors. *PLoS Biology*, **7**(10):e1000216.
- [643] Cole NB, Sciaky N, Marotta A, Song J, Lippincott-Schwartz J. (1996) Golgi dispersal during microtubule disruption: regeneration of Golgi stacks at peripheral endoplasmic reticulum exit sites. *Molecular Biology of the Cell*, **7**, 631-650.
- [644] Storrie B, White J, Röttger S, Stelzer EHK, Saganuma T, Nilsson T. (1998) Recycling of Golgi-resident glycosyltransferases through the ER reveals a novel pathway and provides an explanation for nocodazole-induced Golgi scattering. *Journal of Cell Biology*, **143**, 1505-1521.
- [645] Hoppeler-Lebel A, Celati C, Bellett G, Mogensen MM, Klein-Hitpass L, Bornens M, Tassin AM. (2007) Centrosomal CAP350 protein stabilises microtubules associated with the Golgi complex. *Journal of Cell Science*, **120**, 3299-32308.
- [646] Chabin-Brion K, Marceiller J, Perez F, Settegrana C, Drechou A, Durand G, Pous C. (2001) The Golgi complex is a microtubule-organizing organelle. *Molecular Biology of the Cell*, **12**, 2047-2060.
- [647] Rivero S, Cardenas J, Bornens M, Rios RM. (2009) Microtubule nucleation at the cis-side of the Golgi apparatus requires AKAP450 and GM130. *EMBO Journal*, **28**, 1016-1028.
- [648] Miller PM, Folkmann AW, Maia AR, Efimova N, Efimov A, Kaverina I. (2009) Golgi-derived CLASP dependent microtubules control Golgi organization and polarized trafficking in motile cells. *Nature Cell Biology*, **11**, 1069-1080.
- [649] Infante C, Ramos-Morales F, Fedriani C, Bornens M, Rios RM. (1999) GMAP-210, A cis-Golgi network associated protein, is a minus end microtubule-binding protein. *Journal of Cell Biology*, **145**, 83-98.

- [650] Liu Z, Vong QP, Zheng Y. (2007) CLASPIing microtubules at the trans-Golgi network. *Developmental Cell*, **12**, 839-40.
- [651] Pouthas F, Girard P, Lecaudey V, Ly TB, Gilmour D, Boulin C, Pepperkok R, Reynaud EG. (2008) In migrating cells, the Golgi complex and the position of the centrosome depend on geometrical constraints of the substratum. *Journal of Cell Science*, **121**, 2406-2414.
- [652] Happé H, de Heer E, Peters DJ. (2012) Morphometric analysis of centrosome position in tissues. *Methods in Molecular Biology*, **839**, 249-255.
- [653] Shekhar N, Wu J, Dickinson RB, Lele TP. (2013) Cytoplasmic dynein: tension generation on microtubules and the nucleus. *Cellular and Molecular Bioengineering*, **6**, 74-81.
- [654] Zhu J, Burakov A, Rodionov V, Mogilner A. (2010) Finding the cell center by a balance of dynein and myosin pulling and microtubule pushing: a computational study. *Molecular Biology of the Cell*, **21**, 4418-4427.
- [655] Tikhonenko I, Magidson V, Gräf R, Khodjakov A, Koonce MP. (2013) A kinesin-mediated mechanism that couples centrosomes to nuclei. *Cellular and Molecular Life Sciences*, **70**, 1285-1296.
- [656] Tanenbaum ME, Akhmanova A, Medema RH. (2011) Bi-directional transport of the nucleus by dynein and kinesin-1. *Communicative and Integrative Biology*, **4**, 21-25.
- [657] Hirokawa N. (1998) Kinesin and dynein superfamily proteins and the mechanism of organelle transport. *Science*, **279**, 519-526.
- [658] Deinhardt K, Salinas S, Verastegui C, Watson R, Worth D, Hanrahan S, Bucci C, Schiavo G. (2006) Rab5 and Rab7 control endocytic sorting along the axonal retrograde transport pathway. *Neuron*, **52**, 293-305.
- [659] Jordens I, Fernandez-Borja M, Marsman M, Dusseljee S, Janssen L, Calafat J, Janssen H, Wubbolts R, Neefjes J. (2001) The Rab7 effector protein RILP controls lysosomal transport by inducing the recruitment of dynein-dynactin motors. *Current Biology*, **11**, 1680-1685.
- [660] Nielsen E, Severin F, Backer JM, Hyman AA, Zerial M. (1999) Rab5 regulates motility of early endosomes on microtubules. *Nature Cell Biology*, **1**, 376-382.
- [661] Ding Q, Wang Z, Chen Y. (2009) Endocytosis of adiponectin receptor 1 through a clathrin- and Rab5-dependent pathway. *Cell Research*, **19**, 317-327.
- [662] Matteoni, Kreis TE. (1987) Translocation and clustering of endosomes and lysosomes depends on microtubules. *Journal of Cell Biology*, **105**, 1253-1265.
- [663] Echard A, Jollivet F, Martinez O, Lacapere JJ, Rousselet A, Janoueix-Lerosey I, Goud B. (1998) Interaction of a Golgi-associated kinesin-like protein with Rab6. *Science*, **279**, 580-585.
- [664] Young J, Ménétrey J, Goud B. (2010) RAB6C is a retrogene that encodes a centrosomal protein involved in cell cycle progression. *Journal of Molecular Biology*, **397**, 69-88.
- [665] Jiang S, Storrie B. (2005) Cisternal rab proteins regulate Golgi apparatus redistribution in response to hypotonic stress. *Molecular Biology of the Cell*, **16**, 2586-2596.
- [666] Sweeney HL, Houdusse A. (2010) Structural and functional insights into the Myosin motor mechanism. *Annual Review of Biophysics*, **39**, 539-557.

- [667] Berg JS, Powell BC, Cheney RE. (2001) A millennial myosin census. *Molecular Biology of the Cell*, **12**, 780-794.
- [668] Espreafico EM, Coling DE, Tsakraklides V, Krogh K, Wolenski JS, Kalinec G, Kachar B. (1998) Localization of myosin-V in the centrosome. *Proceedings of the National Academy of Sciences, USA*, **95**, 8636-8641.
- [669] Roland JT, Lapierre LA, Goldenring JR. (2009) Alternative splicing in class V myosins determines association with Rab10. *Journal of Biological Chemistry*, **284**, 1213-1223.
- [670] Lindsay AJ, Jollivet F, Horgan CP, Khan AR, Raposo G, McCaffrey MW, Goud B. (2013) Identification and characterisation of multiple novel Rab-myosin Va interactions. *Molecular Biology of the Cell*, **24**, 3420-3434.
- [671] Jin Y, Sultana A, Gandhi P, Franklin E, Hamamoto S, Khan AR, Munson M, Schekman R, Weisman LS. (2011) Myosin V transports secretory vesicles via a Rab GTPase cascade and interaction with the exocyst complex. *Development and Cell*, **21**, 1156-1170.
- [672] Liu X, Kapoor TM, Chen JK, Huse M. (2013) Diacylglycerol promotes centrosome polarization in T cells via reciprocal localization of dynein and myosin II. *Proceedings of the National Academy of Sciences, USA*, **110**, 11976-11981.
- [673] Chodagam S, Royou A, Whitfield W, Karess R, Raff JW. (2005) The centrosomal protein CP190 regulates myosin function during early *Drosophila* development. *Current Biology*, **15**, 1308-1313.
- [674] Xu Y, Takeda S, Nakata T, Noda Y, Tanaka Y, Hirokawa N. (2002) Role of KIFC3 motor protein in Golgi positioning and integration. *Journal of Cell Biology*, **158**, 293-303.
- [675] Yadav S, Puthenveedu MA, Linstedt AD. (2012) Golgin160 recruits the dynein motor to position the Golgi apparatus. *Development and Cell*, **23**, 153-165.
- [676] Corthésy-Theulaz I, Pauloin A, Pfeffer SR. (1992) Cytoplasmic dynein participates in the centrosomal localization of the Golgi complex. *Journal of Cell Biology*, **118**, 1333-1345.
- [677] Lu L, Lee YR, Pan R, Maloof JN, Liu B. (2005) An internal motor kinesin is associated with the Golgi apparatus and plays a role in trichome morphogenesis in *Arabidopsis*. *Molecular Biology of the Cell*, **16**, 811-823.
- [678] Hirota Y, Meunier A, Huang S, Shimozawa T, Yamada O, Kida YS, Inoue M, Ito T, Kato H, Sakaguchi M, Sunabori T, Nakaya MA, Nonaka S, Ogura T, Higuchi H, Okano H, Spassky N, Sawamoto K. (2010) Planar polarity of multiciliated ependymal cells involves the anterior migration of basal bodies regulated by non-muscle myosin II. *Development*, **137**, 3037-3046.
- [679] Wozniak, M. J. Allan, V. J. (2006) Cargo selection by specific kinesin light chain 1 isoforms. *EMBO Journal*, **25**, 5457-5468.
- [680] Xue X, Jaulin F, Espenel C, Kreitzer G. (2010) PH-domain-dependent selective transport of p75 by kinesin-3 family motors in non-polarized MDCK cells. *Journal of Cell Science*, **123**, 1732-1741.
- [681] Blatner NR1, Wilson MI, Lei C, Hong W, Murray D, Williams RL, Cho W. (2007) The structural basis of novel endosome anchoring activity of KIF16B kinesin. *EMBO Journal*, **26**, 3709-3719.

- [682] Golgi, C. (1898) Sur la structure des cellules nerveuses des ganglions spinaux. *Archives Italiennes de Biologie*, **30**, 278-286.
- [683] Golgi, C. (1898) Intorno alla struttura delle cellule nervose, *Bollettino della Società Medico-Chirurgica di Pavia*, **13**, 3-16.
- [684] Golgi, C. (1909) Sur une fine particularité de structure de l'épithélium de la muqueuse gastrique et intestinale de quelques vertèbres. *Archives Italiennes de Biologie*, **51**, 213-245.
- [685] Pavelk M, Mironov AA. (2008) *The Golgi Apparatus: State of the art 110 years after Camillo Golgi's discovery*. Springer, Berlin.
- [686] Bahr GF, Schell, BE, Engler WF. (1981) Instrumentation for the three dimensional reconstruction of cellular organelles by electron microscopy, *Ultramicroscopy*, **6**, 251-258.
- [687] Olins DE, Olins AL, Levy HA, Durfee RC, Margle SM, Tinnel EP, Dover SD. (1983) Electron microscope tomography: transcription in three dimensions, *Science*, **220**, 498- 500.
- [688] Glick BS, Malhotra V. (1998) The curious status of the Golgi apparatus. *Cell*, **95**, 883-889.
- [689] Krieger M, Scott MP, Matsudaira PT, Lodish HF, Darnell JE. Lawrence Z, Kaiser C, Arnold B. (2004). *Molecular Cell Biology* (5th edn) W.H. Freeman and Co, New York.
- [690] Seguí-Simarro JM, Staehelin LA. (2006) Cell cycle-dependent changes in Golgi stacks, vacuoles, clathrin-coated vesicles and multivesicular bodies in meristematic cells of *Arabidopsis thaliana*: a quantitative and spatial analysis. *Planta* **223**, 223-236.
- [691] Leblond CP. (1989) Synthesis and secretion of collagen by cells of connective tissue, bone, and dentin. *Anatomical Record*, **224**, 123-138.
- [692] Colanzi A, Suetterlin C, Malhotra V. (2003) Cell-cycle-specific Golgi fragmentation: how and why? *Current Opinion in Cell Biology*, **15**, 462-467.
- [693] Nilsson T, Au CE, Bergeron JJ. (2009) Sorting out glycosylation enzymes in the Golgi apparatus. *FEBS Letters*, **583**, 3764-3769.
- [694] Capasso JM, Keenan TW, Abeijon C, Hirschberg CB. (1989) Mechanism of phosphorylation in the lumen of the Golgi apparatus. Translocation of adenosine 5'-triphosphate into Golgi vesicles from rat liver and mammary gland. *Journal of Biological Chemistry*, **264**, 5233-5240.
- [695] Capasso JM, Hirschberg CB. (1984) Mechanisms of glycosylation and sulfation in the Golgi apparatus: evidence for nucleotide sugar/nucleoside monophosphate and nucleotide sulfate/nucleoside monophosphate antiports in the Golgi apparatus membrane. *Proceedings of the National Academy of Sciences, USA*, **81**, 7051-7055.
- [696] Lodish H, Berk A, Zipursky SL, Zipursky L, Matsudaira P, Baltimore D, Darnell J. (2000) *Molecular Cell Biology*. 4th edn W. H. Freeman, New York, Section 17.8, Golgi and Post-Golgi Protein Sorting and Proteolytic Processing. Available from: <http://www.ncbi.nlm.nih.gov/books/NBK21487/>
- [697] Tartakoff A M. (1983) The confined function model of the Golgi complex: centre for ordered processing of biosynthetic products of the rough endoplasmic reticulum. *International Review of Cytology*, **85**, 221-252.

- [698] Serafini T, Orci L, Amherdt M, Brunner M, Kahn RA, Rothman JE (1991) ADP-ribosylation factor is a subunit of the coat of Golgi-derived COP-coated vesicles: a novel role for a GTP-binding protein. *Cell*, **67**, 239-253.
- [699] Hughes H, Stephens DJ. (2007) Assembly, organization, and function of the COPII coat. *Histochemistry and Cell Biology*, **129**, 129-151.
- [700] Martínez-Menárguez JA. (2013) Intra-Golgi transport: roles for vesicles, tubules, and cisternae. *ISRN Cell Biology*, **2013**, Article ID 126731.
- [701] Griffliths G, Pfeiffer S, Simons K, Marlin K. (1985) Exit of newly synthesized membrane proteins from the trans-cisternae of the Golgi complex to the plasma membrane. *Journal of Cell Biology*, **101**, 949-964.
- [702] Bonifacino JS, Glick BS. (2004) The mechanisms of vesicle budding and fusion. *Cell*, **116**, 153-166.
- [703] Xu H, Shields D. (1993) Prohormone processing in the trans-Golgi network: endoproteolytic cleavage of prosomatostatin and formation of nascent secretory vesicles in permeabilized cells. *Journal of Cell Biology*, **122**, 1169-1184.
- [704] Snider MD, Rogers C. (1985) Intracellular movement of cell surface receptors after endocytosis: resialylation of asyalo-transferrin receptor in human erythroleukemia cells. *Journal of Cell Biology*, **100**, 826-834.
- [705] Saftig P, Klumperman J. (2009) Lysosome biogenesis and lysosomal membrane proteins: trafficking meets function. *Nature Reviews, Molecular and Cellular Biology*, **10**, 623-635.
- [706] Fader CM, Colombo MI. (2009) Autophagy and multivesicular bodies: two closely related partners. *Cell Death and Differentiation*, **16**, 70-78.
- [707] Freeze HH, Ng BG. (2011) Golgi glycosylation and human inherited diseases. *Cold Spring Harbour Perspectives in Biology*, **3**(9):a005371.
- [708] Palade G. (1975) Intracellular aspects of the process of protein synthesis. *Science*, **189**, 347-358.
- [709] Pelham RB, Rothman, JE. (2000) The debate about transport in the golgi—two sides of the same coin? *Cell*, **102**, 713-719.
- [710] Pfeffer SR. (2001) Constructing a Golgi complex. *Journal of Cell Biology*, **155**, 873-875.
- [711] Rizzo R, Parashuraman S, Mirabelli P, Puri C, Lucocq J, Luini A. (2013). The dynamics of engineered resident proteins in the mammalian Golgi complex relies on cisternal maturation. *Journal of Cell Biology*, **201**, 1027-1036.
- [712] Klute MJ, Melançon P, Dacks JB. (2011) Evolution and diversity of the Golgi. *Cold Spring Harbour Perspectives in Biology*, **3**(8):a007849.
- [713] Varki A. (2011) Evolutionary forces shaping the Golgi glycosylation machinery: why cell surface glycans are universal to living cells. *Cold Spring Harbour Perspectives in Biology*, **3**(6). pii: a005462.
- [714] Marsh B J. (2005) Lessons from tomographic studies of the mammalian Golgi. *Biochimica et Biophysica Acta*, **1744**, 273-292.

- [715] Marsh BJ, Howell KE. (2002) The mammalian Golgi-complex debates. *Nature Reviews, Molecular and Cellular Biology*, **3**, 789-795.
- [716] Mironov AA, Banin VV, Sesorova IS, Dolgikh VV, Luini A, Beznoussenko GV. (2007) Evolution of the endoplasmic reticulum and the Golgi complex. *Advances in Experimental Medicine and Biology*, **607**, 61-72.
- [717] Jékely G. (2007) Origin of eukaryotic endomembranes: a critical evaluation of different model scenarios. *Advances in Experimental Medicine and Biology*, **607**, 38-51.
- [718] Makarova KS, Wolf YI, Mekhedov SL, Mirkin BG, Koonin EV. (2005) Ancestral paralogs and pseudoparalogs and their role in the emergence of the eukaryotic cell. *Nucleic Acids Research*, **33**, 4626-4638.
- [719] Lucocq JM, Pryde JG, Berger EG, Warren G (1987) A mitotic form of the Golgi apparatus in HeLa cells. *Journal of Cell Biology*, **104**, 865-874.
- [720] Souter E, Pypaert M, Warren G. (1993) The Golgi stack reassembles during telophase before arrival of proteins transported from the endoplasmic reticulum. *Journal of Cell Biology*, **122**, 533-540.
- [721] Klumperman J. (2011) Architecture of the mammalian Golgi. *Cold Spring Harbour Perspectives in Biology*, **3**(7) pii: a005181.
- [722] Orci L, Ravazzola M, Volchuk A, Engel T, Gmachl M, Amherdt M, Perrelet A, Sollner TH, Rothman JE. (2000) Anterograde flow of cargo across the golgi stack potentially mediated via bidirectional "percolating" COPI vesicles. *Proceedings of the National Academy of Sciences, USA*. **97**, 10400-10405.
- [723] Adolf F, Herrmann A, Hellwig A, Beck R, Brügger B, Wieland FT. (2013) Scission of COPI and COPII vesicles is independent of GTP hydrolysis. *Traffic*, **8**, 922-932.
- [724] Mogelsvang S, Marsh B, Ladinsky MS, Howell KE. (2004). Predicting function from structure: 3D structure studies of the mammalian Golgi complex. *Traffic*, **5**, 338-345.
- [725] Wang Y, Seemann J. (2011) Golgi biogenesis. *Cold Spring Harbour Perspectives in Biology*, **3**(10):a005330.
- [726] Rohn WM, Rouillé Y, Waguri S, Hoflack B. (2000) Bi-directional trafficking between the trans-Golgi network and the endosomal/lysosomal system. *Journal of Cell Science*, **113**, 2093-2101.
- [727] Ladinsky MS, Mastronarde DN, McIntosh JR, Howell KE, Staehelin LA. (1999) Golgi structure in three dimensions: functional insights from the normal rat kidney cell. *Journal of Cell Biology*, **144**, 1135-1149.
- [728] Kweon HS, Beznoussenko GV, Micaroni M, Polishchuk RS, Trucco A, Martella O, Di Giandomenico D, Marra P, Fusella A, Di Pentima A, Berger EG, Geerts WJ, Koster AJ, Burger KN, Luini A, Mironov AA. (2004) Golgi enzymes are enriched in perforated zones of golgi cisternae but are depleted in COPI vesicles. *Molecular Biology of the Cell*, **15**, 4710-4724.
- [729] Trucco A, Polishchuk RS, Martella O, Di Pentima A, Fusella A, Di Giandomenico D, San Pietro E, Beznoussenko GV, Polishchuk EV, Baldassarre M, Buccione R, Geerts WJ, Koster AJ, Burger KN, Mironov AA, Luini, A. (2004) Secretory traffic triggers the formation of tubular continuities across Golgi sub-compartments. *Nature Cell Biology*, **6**, 1071-1081.

- [730] Griffiths G, Fuller SD, Back R, Hollinshead M, Pfeiffer S, Simons K. (1989) The dynamic nature of the Golgi complex. *Journal of Cell Biology*, **108**, 277-297.
- [731] Opat AS, Van Vliet C, Gleeson PA. (2001) Trafficking and localisation of resident Golgi glycosylation enzymes, *Biochimie*, **83**, 763-773.
- [732] Glick BS, Elston T, Oster G. (1997) A cisternal maturation mechanism can explain the asymmetry of the Golgi stack. *FEBS Letters*, **414**, 177-181.
- [733] Nickel W, Rabouille C. (2009) Mechanisms of regulated unconventional protein secretion. *Nature Reviews Molecular and Cellular Biology*, **10**, 148-155.
- [734] Tang D, Wang Y. (2013) Cell cycle regulation of Golgi membrane dynamics. *Trends in Cell Biology*, **23**, 296-304.
- [735] Xiang Y, Zhang X, Nix DB, Katoh T, Aoki K, Tiemeyer M, Wang Y. (2013) Regulation of protein glycosylation and sorting by the Golgi matrix proteins GRASP55/65. *Nature Communications*, **4**, 1659.
- [736] Montagnac G, Meas-Yedid V, Irondelle M, Castro-Castro A, Franco M, Shida T, Nachury MV, Benmerah A, Olivo-Marin JC, Chavrier P. (2013) aTAT1 catalyses microtubule acetylation at clathrin-coated pits. *Nature*, **502**, 567-570.
- [737] Babayeva S, Zilber Y, Torban E. (2011) Planar cell polarity pathway regulates actin rearrangement, cell shape, motility and nephrin distribution in podocytes. *American Journal of Physiology*, **300**, F549-F560.
- [738] Werner ME, Hwang P, Huisman F, Taborek P, Yu CC, Mitchell BJ. (2011) Actin and microtubules drive differential aspects of planar cell polarity in multiciliated cells. *Journal of Cell Biology*, **195**, 19-26.
- [739] Jenny A, Reynolds-Kenneally J, Das G, Burnett M, Mlodzik M. (2005) Diego and Prickle regulate Frizzled planar cell polarity signalling by competing for Dishevelled binding. *Nature Cell Biology*, **7**, 691-697.
- [740] Sugiyama Y, Lovicu FJ, McAvoy JW. (2011) Planar cell polarity in the mammalian eye lens. *Organogenesis*. **3**, 191-201.
- [741] Gao C, Chen YG. (2010) Dishevelled: The hub of Wnt signaling. *Cell Signalling*, **22**, 717-727.
- [742] He X. (2008) Cilia put a brake on Wnt signalling. *Nature Cell Biology*, **10**, 11-13.
- [743] Komiya Y, Habas R. (2008) Wnt signal transduction pathways. *Organogenesis*, **4**, 68-75.
- [744] May-Simera HL, Kelley MW. (2012) Cilia, Wnt signaling, and the cytoskeleton. *Cilia*, **1**, 7.
- [745] Kaldis P, Pagano M. (2009) Wnt Signaling in mitosis. *Developmental Cell*, **17**, 749-750.
- [746] Lienkamp S, Ganner A, Walz G. (2012) Inversin, Wnt signaling and primary cilia. *Differentiation*, **83**, S49-S55.
- [747] Li Y, Dudley AT. (2009) Noncanonical frizzled signaling regulates cell polarity of growth plate chondrocytes. *Development*, **136**, 1083-1092.

- [748] Borovina A, Superina S, Voskas D, Ciruna B. (2010) Vangl2 directs the posterior tilting and asymmetric localization of motile primary cilia. *Nature Cell Biology*, **12**, 407-412.
- [749] May-Simera HL, Kai M, Hernandez V, Osborn DP, Tada M, Beales PL. (2010) Bbs8, together with the planar cell polarity protein Vangl2, is required to establish left-right asymmetry in zebrafish. *Developmental Biology*, **345**, 215-225.
- [750] Vladar EK, Axelrod JD. (2008) Dishevelled links basal body docking and orientation in ciliated epithelial cells. *Trends in Cell Biology*, **18**, 517-520.
- [751] Axelrod JD. (2008) Basal bodies, kinocilia and planar cell polarity. *Nature Genetics*, **40**, 10-11.
- [752] Yu A, Rual JF, Tamai K, Harada Y, Vidal M, He X, Kirchhausen T. (2007) Association of Dishevelled with the clathrin AP-2 adaptor is required for Frizzled endocytosis and planar cell polarity signaling. *Developmental Cell*, **12**, 129-141.
- [753] Warrington SJ1, Strutt H, Strutt D. (2013) The Frizzled-dependent planar polarity pathway locally promotes E-cadherin turnover via recruitment of RhoGEF2. *Development*, **140**, 1045-1054.
- [754] Ang SF, Zhao ZS, Lim L, Manser E. (2010) DAAM1 is a formin required for centrosome re-orientation during cell migration. *PLoS One*, **5**(9):e13064.
- [755] Pu J, Zhao M. (2005) Golgi polarization in a strong electric field. *Journal of Cell Science*, **118**, 1117-1128.
- [756] Onuma EK, Hui SW. (1988) Electric field-directed cell shape changes, displacement, and cytoskeletal reorganization are calcium dependent. *Journal of Cell Biology*, **106**, 2067-2075.
- [757] Havelka D, Cifra M, Kucera O, Pokorný J, Vrba J. (2011) High-frequency electric field and radiation characteristics of cellular microtubule network. *Journal of Theoretical Biology*, **286**, 31-40.
- [758] Schlessinger K, Hall A, Tolwinski N. (2009) Wnt signaling pathways meet Rho GTPases. *Genes and Development*, **23**, 265-277.
- [759] Hall A. (1998) Rho GTPases and the actin cytoskeleton. *Science*, **279**, 509-514.
- [760] Etienne-Manneville S. (2004) Cdc42-the centre of polarity. *Journal of Cell Science*, **117**, 1291-1300.
- [761] Bisel B, Calamai M, Vanzi F, Pavone FS (2013) Decoupling Polarization of the Golgi Apparatus and GM1 in the Plasma Membrane. *PLoS One*, **8**(12):e80446.
- [762] Church V, Nohno T, Linker C, Marcelle C, Francis-West P. (2002) Wnt regulation of chondrocyte differentiation. *Journal of Cell Science*, **115**, 4809-4818.
- [763] Randall RM, Shao YY, Wang L, Ballock RT. (2012) Activation of Wnt Planar Cell Polarity (PCP) signaling promotes growth plate column formation *in vitro*. *Journal of Orthopaedic Research*, **30**, 1906-1914.
- [764] Ma B, Landman EB, Miclea RL, Wit JM, Robanus-Maandag EC, Post JN, Karperien M. (2013) WNT signaling and cartilage: of mice and men. *Calcified Tissue International*, **92**, 399-411.
- [765] Dong YF, Soung Y, Schwarz, EM, O'Keefe RJ, Drissi H. (2006) Wnt induction of chondrocyte hypertrophy through the Runx2 transcription factor. *Journal of Cell Physiology*, **208**, 77-86.

- [766] Yates KE, Shortkroff S, Reish RG. (2005) Wnt influence on chondrocyte differentiation and cartilage function. *DNA and Cell Biology*, **24**, 446-457.
- [767] Bradley EW, Drissi MH. (2011) Wnt5b regulates mesenchymal cell aggregation and chondrocyte differentiation through the planar cell polarity pathway. *Journal of Cell Physiology*, **226**, 1683-1693.
- [768] Poole CA. (1993) The structure and Function of Articular cartilage Matrices. In: *Joint Cartilage degradation: Basic and Clinical Aspects*. Eds: Woessner JF, Howell DS. Marcel Dekker, Inc, New York, NY.
- [769] Ricard-Blum S. (2011) The collagen family. *Cold Spring Harbour Perspectives in Biology*, **23**, a004978.
- [770] Esko JD, Kimata K, Lindahl U. (2009) Proteoglycans and Sulfated Glycosaminoglycans. Ch.16 In: *Essentials of Glycobiology. 2nd edition*. Ed: Varka A. Cold Spring Harbor Laboratory Press, Cold Spring Harbor (NY).
- [771] Guilak F, Alexopoulos LG, Upton ML, Youn I, Choi JB, Cao L, Setton LA, Haider MA. (2006) The pericellular matrix as a transducer of biomechanical and biochemical signals in articular cartilage. *Annals of the New York Academy of Sciences*, **1068**, 498-512.
- [772] Silbert JE, Sugumaran G. (1995) Intracellular membranes in the synthesis, transport, and metabolism of proteoglycans. *Biochimica Biophysica Acta*, **1241**, 371-384.
- [773] Schaefer L, Schaefer RM. (2010) Proteoglycans: from structural compounds to signaling molecules. *Cell and Tissue Research*, **339**, 237-246.
- [774] Bader DL, Salter DM, Chowdhury TT. (2011) Biomechanical influence of cartilage homeostasis in health and disease. *Arthritis*, 2011:979-1032.
- [775] Maldonado M, Nam J. (2013) The role of changes in extracellular matrix of cartilage in the presence of inflammation on the pathology of osteoarthritis. *Biomedical Research International*, **2013**, 284873.
- [776] Cavalcante FS, Ito S, Brewer K, Sakai H, Alencar AM, Almeida MP, Andrade JS Jr, Majumdar A, Ingenito EP, Suki B. (2005) Mechanical interactions between collagen and proteoglycans: implications for the stability of lung tissue. *Journal of Applied Physiology*, **98**, 672-679.
- [777] Lee PH, Trowbridge JM, Taylor KR, Morhenn VB, Gallo RL. (2004) Dermatan sulfate proteoglycan and glycosaminoglycan synthesis is induced in fibroblasts by transfer to a three-dimensional extracellular environment. *Journal of Biological Chemistry*, **279**, 48640-48646.
- [778] Hari G, Garg PJ, Roughley R, Hales CA. (2005) *Proteoglycans in Lung Disease*. Marcel Dekker, New York.
- [779] Wells RG. (2008) The role of matrix stiffness in regulating cell behavior. *Hepatology*, **47**, 1394-4000.
- [780] Li S, Guan JL, Chien S. (2005) Biochemistry and biomechanics of cell motility. *Annual Reviews of Biomedical Engineering*, **7**, 105-150.
- [781] Schrader J, Gordon-Walker TT, Aucott RL, van Deemter M, Quaas A, Walsh S, Benten D, Forbes SJ, Wells RG, Iredale JP. (2011) Matrix stiffness modulates proliferation, chemotherapeutic response, and dormancy in hepatocellular carcinoma cells. *Hepatology*, **53**, 1192-205.

- [782] Funderburgh JL. (2000) Keratan sulfate: structure, biosynthesis, and function. Mini Review. *Glycobiology*, **10**, 951-958.
- [783] Funderburgh JL, Mann MM, Funderburgh ML. (2003). Keratocyte phenotype mediates proteoglycan structure: a role for fibroblasts in corneal fibrosis. *Journal of Biological Chemistry*, **278**, 45629-45637.
- [784] Martin JA, Buckwalter JA. (2002) Aging, articular cartilage chondrocyte senescence and osteoarthritis. *Biogerontology*, **3**, 257-264.
- [785] Basu R, Kassiri Z. (2013) Extracellular Matrix Remodelling and Abdominal Aortic Aneurysm. *Journal of Clinical and Experimental Cardiology*, **4**, 259.
- [786] Hunziker EB, Schenk RK, Cruz-Orive LM. (1987) Quantitation of chondrocyte performance in growth-plate cartilage during longitudinal bone growth. *Journal of Bone and Joint Surgery*, **69**, 162-173.
- [787] Aspden RM, Hukins DW. (1979) The lamina splendens of articular cartilage is an artefact of phase contrast microscopy. *Proceedings of the Royal Society of London, B, Biological Sciences*, **206**, 109-113.
- [788] Poole CA, Flint MH, Beaumont BW. (1984) Morphological and functional interrelationships of articular cartilage matrices. *Journal of Anatomy*, **138**, 113-138.
- [789] Poole CA. (1997) Articular cartilage chondrons: form, function and failure. *Journal of Anatomy*, **191**, 1-13.
- [790] Poole CA, Flint MH, Beaumont BW. (1987) Chondrons in cartilage: ultrastructural analysis of the pericellular microenvironment in adult human articular cartilages. *Journal of Orthopaedic Research*, **5**, 509-522.
- [791] Dmitrovsky E, Lane LB, Bullough PG. (1978) The characterisation of the tidemark in human articular cartilage. *Metabolic Bone Disease and Related Research*, **1**, 115-118.
- [792] Maroudas A, Bullough P. (1968) Permeability of articular cartilage. *Nature*, **219**, 1260-1261.
- [793] Ateshian GA, Costa KD, Hung CT. (2007) A theoretical analysis of water transport through chondrocytes. *Biomechanics and Modelling in Mechanobiology*, **6**, 91-101.
- [794] Mow VC, Gu WY, Chen FH. (2005) Structure and function of articular cartilage and meniscus. In: MowVC, Huiskes R. (Eds.), *Basic Orthopaedic Biomechanics and Mechano-biology*. Lippincott Williams and Wilkins, Philadelphia, pp.181-258.
- [795] Kovach IS. (1995) The importance of polysaccharide configurational entropy in determining the osmotic swelling pressure of concentrated proteoglycan solution and the bulk compressive modulus of articular cartilage. *Biophysical Chemistry*, **53**, 181-187.
- [796] Benninghoff, A. (1925) Form und Bau der Gelenkknorpel in ihren Beziehungen zur Funktion. *Zeitschrift für Anatomie und Entwicklungsgeschichte*, **75**, 783-862.
- [797] Sherwin AF, Carter DH, Poole CA, Hoyland JA, Ayad S. (1999) The distribution of type VI collagen in the developing tissues of the bovine femoral head. *Histochemical Journal*, **31**, 623-632.

- [798] Poole CA, Ayad S, Schofield, JR. (1988) Chondrons from articular cartilage: I. Immunolocalization of type VI collagen in the pericellular capsule of isolated canine tibial chondrons. *Journal of Cell Science*, **90**, 635-643.
- [799] Poole CA, Gilbert RT, Herbage D, Hartmann DJ. (1997). Immunolocalization of type IX collagen in normal and spontaneously osteoarthritic canine tibial cartilage and isolated chondrons. *Osteoarthritis and Cartilage*, **5**, 191-204.
- [800] Hing WA, Sherwin AF, Poole CA. (2002) The influence of the pericellular microenvironment on the chondrocyte response to osmotic challenge. *Osteoarthritis and Cartilage*, **10**, 297-307.
- [801] Durr J, Lammi P, Goodman SL, Aigner T, von der Mark K. (1996) Identification and immunolocalization of laminin in cartilage. *Experimental Cell Research*, **222**, 225-233.
- [802] Luo W, Guo C, Zheng J, Chen TL, Wang PY, Vertel BM, Tanzer ML. (2000) Aggrecan from start to finish. *Journal of Bone and Mineral Metabolism*, **18**, 51-56.
- [803] Ng L, Hung HH, Sprunt A, Chubinskaya S, Ortiz C, Grodzinsky A. (2007) Nanomechanical properties of individual chondrocytes and their developing growth factor-stimulated pericellular matrix. *Journal of Biomechanics*, **240**, 1011-1023.
- [804] Glant TT, Hadhazy CS, Mikecz K, Sipos A (1985) Appearance and persistence of fibronectin in cartilage. Specific interaction of fibronectin with collagen type II. *Histochemistry*, **82**, 149-158.
- [805] Wilusz RE, Defrate LE, Guilak F. (2012) A biomechanical role for perlecan in the pericellular matrix of articular cartilage. *Matrix Biology*, **31**, 320-327.
- [806] Miosge N, Flachsbarth K, Goetz W, Schultz W, Kresse H, Herken R. (1994) Light and electron microscopical immunohistochemical localization of the small proteoglycan core proteins decorin and biglycan in human knee joint cartilage. *Histochemical Journal*, **26**, 939-945.
- [807] Pap T, Bertrand J. (2013) Syndecans in cartilage breakdown and synovial inflammation. *Nature Reviews Rheumatology*, **9**, 43-55.
- [808] Poole CA, Flint MH, Beaumont BW. (1988a) Chondrons extracted from canine tibial cartilage: Preliminary report on their isolation and structure. *Journal of Orthopaedic Research*, **6**, 408-419.
- [809] Lotz MK, Otsuki S, Grogan SP, Sah R, Terkeltaub RD, Lima D. (2010) Cartilage cell clusters. *Arthritis and Rheumatology*, **62**, 2206-2218.
- [810] Bachrach NM, Mow VC, Guilak F. (1998) Incompressibility of the solid matrix of articular cartilage under high hydrostatic pressures. *Journal of Biomechanics*, **31**, 445-451.
- [811] Guilak F, Erickson GR, Ting-Beall HP. (2002) The effects of osmotic stress on the viscoelastic and physical properties of articular chondrocytes. *Biophysica Journal*. **2**, 720-727.
- [812] Poole CA. (1992) The Chondrocyte and its pericellular Microenvironment. *Articular Cartilage and Osteoarthritis*. Ed, Kuettner KE, Raven Press, New York. pp.221-240.
- [813] Hall AC, Horwitz ER, Wilkins RJ. (1996) The cellular physiology of articular cartilage. *Experimental Physiology*, **81**, 535-545.
- [814] Morris NP, Keene DR, Horton WA. (2002) Morphology of connective tissue: cartilage, In: *Connective Tissue and Its Heritable Disorders* Eds. Royce PM. and Steinmann B. Wiley-Liss Inc, New York. pp.41-66.

- [815] Maroudas A. (1979) Physiochemical properties of articular cartilage. *Adult Articular Cartilage*. Ed. Freeman MAR. Pitman Medical, London.
- [816] Roughley PJ, Lee ER. (1994) Cartilage proteoglycans: structure and potential functions. *Microscopy Research and Techniques*, **28**, 385-397.
- [817] Chen AC, Nguyen TT, Sah RL. (1997) Streaming potentials during the confined compression creep test of normal and proteoglycan-depleted cartilage. *Annals of Biomedical Engineering*, **25**, 269-277.
- [818] Wilkins RJ, Browning JA, Urban JP. (2000) Chondrocyte regulation by mechanical load. *Biorheology*, **37**, 67-74.
- [819] Milner PI, Wilkins RJ, Gibson JS. (2012) Cellular Physiology of Articular Cartilage in Health and Disease. In: *Principles of Osteoarthritis - Its Definition, Character, Derivation and Modality-Related Recognition*. Ed, Rothschild BM, Intech, Croatia.
- [820] Fassbender HG. (1987) Role of chondrocytes in the development of osteoarthritis. *American Journal of Medicine*, **83**, 17-24.
- [821] Viguet-Carrin S, Garnero P, Delmas PD. (2006) The role of collagen in bone strength. *Osteoporosis International*, **17**, 319-336.
- [822] Keene DR, McDonald K. (1993) The ultrastructure of the connective tissue matrix of skin and cartilage after high-pressure freezing and freeze-substitution. *Journal of Histochemistry and Cytochemistry*, **41**, 1141-1153.
- [823] Olsen B, Reino O. (1995) New insights into the function of collagens from genetic analysis. *Current Opinion in Cell Biology*, **7**, 720-727.
- [824] Iyama KI, Ninomiya Y, Olsen BR, Linsenmayer TF, Trelstad RL, Hayashi M. (1991) Spatio-temporal pattern of type X collagen gene expression and collagen deposition in embryonic chick vertebrae undergoing endochondral ossification. *Anatomical Record*, **229**, 462-472.
- [825] Jalan AA, Demeler B, Hartgerink JD. (2013) Hydroxyproline-free single composition ABC collagen heterotrimer. *Journal of the American Chemical Society*, **135**, 6014-6017.
- [826] Olsen B R. (1992) *Molecular Biology of Cartilage Collagens, Articular Cartilage and Osteoarthritis*. Raven Press, New York.
- [827] Gelse K, Pöschl E, Aigner T. (2003) Collagens structure, function, and biosynthesis. *Advances in Drug Delivery Reviews*, **55**, 1531-1546.
- [828] Eyre, D. (2002) Collagen of articular cartilage. *Arthritis Research*, **4**, 30-35.
- [829] Eyre DR, Weis MA, Wu JJ. (2006) Articular cartilage collagen: an irreplaceable framework? *European Cells and Materials*, **12**, 57-63.
- [830] Wu JJ, Weis MA, Kim LS, Eyre DR. (2010) Type III collagen, a fibril network modifier in articular cartilage. *Journal of Biological Chemistry*, **285**, 18537-18544.
- [831] Poole CA, Ayad S, Gilbert RT. (1992) Chondrons from articular cartilage. V. Immunohistochemical evaluation of type VI collagen organisation in isolated chondrons by light, confocal and electron microscopy. *Journal of Cell Science*, **103**, 1101-1110.

- [832] Chang J, Nakajima H, Poole CA. (1997) Structural colocalisation of type VI collagen and fibronectin in agarose cultured chondrocytes and isolated chondrons extracted from adult canine tibial cartilage. *Journal of Anatomy*, **190**, 523-532.
- [833] Poole CA, Wotton SF, Duance VC. (1988) Localization of type IX collagen in chondrons isolated from porcine articular cartilage and rat chondrosarcoma. *Histochemical Journal*, **20**, 567-574.
- [834] Blumbach K, Bastiaansen-Jenniskens YM, DeGroot J, Paulsson M, van Osch GJ, Zaucke F. (2009) Combined role of type IX collagen and cartilage oligomeric matrix protein in cartilage matrix assembly: cartilage oligomeric matrix protein counteracts type IX collagen-induced limitation of cartilage collagen fibril growth in mouse chondrocyte cultures. *Arthritis and Rheumatology*, **60**, 3676-3685.
- [835] Gahunia HK, Pritzker KP. (2012) Effect of exercise on articular cartilage. *Orthopedic Clinics of North America*, **43**, 187-199.
- [836] Hagg R, Bruckner P, Hedbom E. (1998) Cartilage fibrils of mammals are biochemically heterogeneous: differential distribution of decorin and collagen IX. *Journal of Cell Biology*, **142**, 285-294.
- [837] Eikenberry EF, Mendler M, Bürgin KH, Winterhalter P, Bruckner P. (1992) *Fibrillar organization in cartilage. In Articular Cartilage and Osteoarthritis*. Eds. Kuettner KE, Schleyerbach R, Peyron JG, Hascall VC. Raven Press, Ltd, New York. pp.133-149.
- [838] Ayad S, Boot-Handford R, Humphries MJ, Kadler KE, Shuttleworth A. (Eds) (1998) *The Extracellular Matrix Facts Book* (Second Edition) Elsevier Inc.
- [839] Wu MH, Urban JP, Cui F, Cui Z, Xu X. (2007) Effect of extracellular pH on matrix synthesis by chondrocytes in 3D agarose gel. *Biotechnology Progress*, **23**, 430-434.
- [840] van der Plas RM, Gomes L, Marquart JA, Vink T, Meijers JC, de Groot PG, Sixma JJ, Huizinga EG. (2000) Binding of von Willebrand factor to collagen type III: role of specific amino acids in the collagen binding domain of vWF and effects of neighboring domains. *Journal of Thrombosis and Haemostasis*, **84**, 1005-1011.
- [841] Kielty CM, Whittaker SP, Grant ME, Shuttleworth CA. (1992) Type VI collagen microfibrils: evidence for a structural association with hyaluronan. *Journal of Cell Biology*, **118**, 979-990.
- [842] McDevitt CA, Marcelino J, Tucker L. (1991) Interaction of intact type VI collagen with hyaluronan. *FEBS Letters*, **294**, 167-170.
- [843] Burton-Wurster N, Lust G, Macleod JN (1997) Cartilage fibronectin isoforms: in search of functions for a special population of matrix glycoproteins. *Matrix Biology*, **15**, 441-454.
- [844] Bidanset DJ, Guidry C, Rosenberg LC, Choi HU, Timpl R, Hook M. (1992) Binding of the proteoglycan decorin to collagen type VI. *Journal of Biological Chemistry*, **267**, 5250-5256.
- [845] Söder S, Hambach L, Lissner R, Kirchner T, Aigner T. (2002) Ultrastructural localization of type VI collagen in normal adult and osteoarthritic human articular cartilage. *Osteoarthritis and Cartilage*, **10**, 464-470.
- [846] Vaughan-Thomas A, Young RD, Phillips AC, Duance VC. (2001) Characterization of type XI collagen-glycosaminoglycan interactions. *Journal of Biological Chemistry*, **276**, 5303-5309.

- [847] Bruckner P, Vaughan L, Winterhalter KH. (1985) Type IX collagen from sternal cartilage of chicken embryo contains covalently bound glycosaminoglycans. *Proceedings of the National Academy of Sciences*, **182**, 2608-2612.
- [848] Parsons P, Gilbert SJ, Vaughan-Thomas A, Sorrell DA, Notman R, Bishop M, Hayes AJ, Mason DJ, Duance VC. (2011) Type IX collagen interacts with fibronectin providing an important molecular bridge in articular cartilage. *Journal of Biological Chemistry*, **286**, 34986-34997.
- [849] Mendler M, Eich-Bender SG, Vaughan L, Winterhalter KH, Bruckner P. (1989) Cartilage contains mixed fibrils of collagen types II, IX, and XI. *Journal of Cell Biology*, **108**, 191-197.
- [850] Silbert JE, Freilich S. (1980) Biosynthesis of chondroitin sulphate by a Golgi-apparatus-enriched preparation from cultures of mouse mastocytoma cells. *Biochemical Journal*, **190**, 307-313.
- [851] Quantock AJ, Young RD, Akama TO. (2010) Structural and biochemical aspects of keratan sulphate in the cornea. *Cell and Molecular Life Sciences*. **67**, 891-906.
- [852] Carole E, Schanté GZ, Herlin C, Vandamme TF. (2011) Chemical modifications of hyaluronic acid for the synthesis of derivatives for a broad range of biomedical applications. *Carbohydrate Polymers*, **85**, 469-489.
- [853] Otsuki S, Hanson SR, Miyaki S, Grogan SP, Kinoshita M, Asahara H, Wong CH, Lotz MK. (2010) Extracellular sulfatases support cartilage homeostasis by regulating BMP and FGF signaling pathways. *Proceedings of the National Academy of Sciences, USA*, **107**, 10202-10207.
- [854] Prydz K, Dalen KT. (2000) Synthesis and sorting of proteoglycans. *Journal of Cell Science*, **113**, 193-205.
- [855] Weigel PH, DeAngelis PL. (2007) Hyaluronan synthases: a decade-plus of novel glycosyltransferases. *Journal of Biological Chemistry*, **282**, 36777-36781.
- [856] Oelker AM, Grinstaff MW. (2008) Ophthalmic adhesives: a materials chemistry perspective. *Journal of Materials Chemistry*, **18**, 2521-2536.
- [857] Lohmander S. (1988) Proteoglycans of joint cartilage. Structure, function, turnover and role as markers of joint disease. *Baillieres Clinical Rheumatology*, **2**, 37-62.
- [858] Etzler ME. (2009) *Essentials of Glycobiology*. 2nd edition. Eds. Varki A, Cummings RD, Esko JD, Freeze HH, Stanley P, Bertozzi CR, Cold Spring Harbor Laboratory Press, Cold Spring Harbor (NY).
- [859] Couchman JR, Pataki CA. (2012) An introduction to proteoglycans and their localization. *Journal of Histochemistry and Cytochemistry*, **60**, 885-897.
- [860] Kiani C, Chen L, Wu YJ, Yee AJ, Yang BB. (2002) Structure and function of aggrecan. *Cell Research*, **12**, 19-32.
- [861] Knudson CB. (1993) Hyaluronan receptor-directed assembly of chondrocyte pericellular matrix. *Journal of Cell Biology*, **120**, 825-834.
- [862] Knudson CB, Knudson W. (2001) Cartilage proteoglycans. *Seminars on Cell and Developmental Biology*, **12**, 69-78.

- [863] Doege KJ, Sasaki M, Kimura T, Yamada Y. (1991) Complete coding sequence and deduced primary structure of the human cartilage large aggregating proteoglycan, aggrecan. Human-specific repeats, and additional alternatively spliced forms. *Journal of Biological Chemistry*, **266**, 894-902.
- [864] Zhu W, Iatridis JC, Hlibczuk V, Ratcliffe A, Mow VC. (1996) Determination of collagen-proteoglycan interactions *in vitro*. *Journal of Biomechanics*, **29**, 773-783.
- [865] Hardingham TE. (1979) The role of link-protein in the structure of cartilage proteoglycan aggregates. *Biochemical Journal*, **177**, 237-247.
- [866] Lee GM, Johnstone B, Jacobson K, Caterson B. (1993) The dynamic structure of the pericellular matrix on living cells. *Journal of Cell Biology*, **123**, 1899-1907.
- [867] Shi S, Grothe S, Zhang Y, O'Connor-McCourt MD, Poole AR, Roughley PJ, Mort JS. (2004) Link protein has greater affinity for versican than aggrecan. *Journal of Biological Chemistry*, **279**, 12060-12066.
- [868] Hauser NM, Paulsson M, Heinegard R, Morgelin M. (1995) Crosslinking of cartilage matrix protein to aggrecan increases with maturation. *Acta Orthopaedica Scandinavica*, (Suppl. 266) **66**, 71-79.
- [869] Sandy JD. (1992) *Extracellular Metabolism of Aggrecan. Articular Cartilage and Osteoarthritis*. Raven Press, New York.
- [870] Winter G M, Poole CA, Ilic MZ, Ross JM, Robinson HC, Handley CJ. (1998) Identification of distinct metabolic pools of aggrecan and their relationship to type VI collagen in the chondrons of mature bovine articular cartilage explants. *Connective Tissue Research*. **37**, 277-293.
- [871] Roughley PJ, White RJ, Cs-Szabó G, Mort JS. (1996) Changes with age in the structure of fibromodulin in human articular cartilage. *Osteoarthritis and Cartilage*, **4**, 153-161.
- [872] Rhee DK, Marcelino J, Baker M, Gong Y, Smits P, Lefebvre V, Jay GD, Stewart M, Wang H, Warman ML, Carpten JD. (2005) The secreted glycoprotein lubricin protects cartilage surfaces and inhibits synovial cell overgrowth. *Journal of Clinical Investigation*, **115**, 622-631.
- [873] Li Y, Wei X, Zhou J, Wei L. (2013) The age-related changes in cartilage and osteoarthritis. *Biomedical Research International*, **2013**, 916530.
- [874] Inerot S, Heinegard D, Audell L, Olsson SE. (1978) Articular-cartilage proteoglycans in aging and osteoarthritis. *Biochemical Journal*, **169**, 143-156.
- [875] Roughley PJ. (2006) The structure and function of cartilage proteoglycans. *European Cells and Materials*, **12**, 92-101.
- [876] Dick G, Akslen-Hoel LK, Grøndahl F, Kjos I, Prydz K. (2012) Proteoglycan synthesis and Golgi organization in polarized epithelial cells. *Journal of Histochemistry and Cytochemistry* **60**, 926-935.
- [877] Anower-E-Khuda MF, Habuchi H, Nagai N, Habuchi O, Yokochi T, Kimata K. (2013) Heparan sulfate 6-O-sulfotransferase isoform-dependent regulatory effects of heparin on the activities of various proteases in mast cells and the biosynthesis of 6-O-sulfated heparin. *Journal of Biological Chemistry*, **288**, 3705-3717.
- [878] Mulhaupt HA, Couchman JR. (2012) Heparan sulfate biosynthesis: methods for investigation of the heparanosome. *Journal of Histochemistry and Cytochemistry*, **60**, 908-915.

- [879] Ratcliffe A, Fryer PR, Hardingham TE. (1985) Proteoglycan biosynthesis in chondrocytes: protein A-gold localization of proteoglycan protein core and chondroitin sulfate within Golgi subcompartments. *Journal of Cell Biology*, **101**, 2355-2365.
- [880] Kümmel D, Reinisch KM. (2011) Structure of Golgi transport proteins. *Cold Spring Harbour Perspectives in Biology*, **3**(12). pii: a007609.
- [881] Schoberer J, Strasser R. (2011) Sub-compartmental organization of Golgi-resident N-glycan processing enzymes in plants. *Molecular Plant*, **4**, 220-228.
- [882] Silbert JE, Sugumaran G. (2002) Biosynthesis of chondroitin/dermatan sulfate. *IUBMB Life*, **54**, 177-186.
- [883] Shoulders MD, Raines RT. (2009) Collagen structure and stability. *Annual Review of Biochemistry*, **78**, 929-958.
- [884] Mow VC, Ratcliffe A, Poole R. (1992) Cartilage and diarthrodial joints as paradigms for hierarchical materials and structures. *Biomaterials*, **13**, 67-97.
- [885] Rivelino D, Zamir E, Balaban NQ, Schwarz US, Ishizaki T, Narumiya S, Kam Z, Geiger B, Bershadsky AD. (2001) Focal contacts as mechanosensors: externally applied local mechanical force induces growth of focal contacts by an mDial-dependent and ROCK-independent mechanism. *Journal of Cell Biology*, **153**, 1175-1186.
- [886] Wolfenson H, Bershadsky A, Henis YI, Geiger B. (2011) Actomyosin-generated tension controls the molecular kinetics of focal adhesions. *Journal of Cell Science*, **124**, 1425-1432.
- [887] Heino J, Käpylä J. (2009) Cellular receptors of extracellular matrix molecules. *Current Pharmaceutical Design*. **15**, 1309-1317.
- [888] Hynes RO. (2002) Integrins: bidirectional, allosteric signaling machines. *Cell*, **110**, 673-687.
- [889] Hehlhans S, Haase M, Cordes N. (2007) Signaling via integrins: Implications for cell survival and anticancer strategies. *Biochimica Biophysica Acta*, **1775**, 163-180.
- [890] Ishida O, Tanaka Y, Morimoto I, Takigawa M, Eto S. (1997) Chondrocytes are regulated by cellular adhesion through CD44 and hyaluronic acid pathway. *Journal of Bone and Mineral Research*, **12**, 1657-1663.
- [891] Varani K, De Mattei M, Vincenzi F, Tosi A, Gessi S, Merighi S, Pellati A, Masieri F, Ongaro A, Borea PA. (2008) Pharmacological characterization of P2X1 and P2X3 purinergic receptors in bovine chondrocytes. *Osteoarthritis and Cartilage*, **16**, 1421-1429.
- [892] Maslennikov I, Klammt C, Hwang E, Kefala G, Okamura M, Esquivies L, Mörs K, Glaubitz C, Kwiatkowski W, Jeon YH, Choe S. (2010) Membrane domain structures of three classes of histidine kinase receptors by cell-free expression and rapid NMR analysis. *Proceedings of the National Academy of Sciences, USA*, **107**, 10902-10907.
- [893] Barton GM, Kagan JC (2009) A cell biological view of Toll-like receptor function: regulation through compartmentalization. *Nature Reviews Immunology*, **9**, 535-542.
- [894] Bosanac I, Alattia JR, Mal TK, Chan J, Talarico S, Tong FK, Tong KI, Yoshikawa F, Furuichi T, Iwai M, Michikawa T, Mikoshiba K, Ikura M. (2002) Structure of the inositol 1,4,5-trisphosphate receptor binding core in complex with its ligand. *Nature*, **420**, 696-700.

- [895] Berridge MJ, Bootman MD, Roderick HL. (2003) Calcium signalling: dynamics, homeostasis and remodelling. *Nature Reviews Molecular and Cellular Biology*, **4**, 517-529.
- [896] Bosanac I, Michikawa T, Mikoshiba K, Ikura M, (2004) Structural insights into the regulatory mechanism of IP3 receptor. *Biochimica Biophysica Acta - Molecular Cell Research*, **1742**, 89-102.
- [897] Díaz J, Martínez-Mekler G. (2005) Interaction of the IP3-Ca²⁺ and MAPK signaling systems in the *Xenopus* blastomere: a possible frequency encoding mechanism for the control of the Xbra gene expression. *Bulletin of Mathematical Biology*, **67**, 433-465.
- [898] Kim K, Choi EJ (2010) Pathological roles of MAPK signaling pathways in human diseases. *Biochimica Biophysica Acta*, **1802**, 396-405.
- [899] Mendoza MC, Er EE, Blenis J. (2011) The Ras-ERK and PI3K-mTOR pathways: cross-talk and compensation. *Trends in Biochemical Sciences*, **36**, 320-328.
- [900] Corrigan RM, Gründling A. (2013) Cyclic di-AMP: another second messenger enters the fray. *Nature Reviews Microbiology*, **11**, 513-524.
- [901] Barrett-Jolley R, Lewis R, Fallman R, Mobasher A. (2010) The emerging chondrocyte channelome. *Frontiers in Physiology*, **1**, 135.
- [902] Campbell ID, Humphries MJ. (2011) Integrin structure, activation, and interactions. *Cold Spring Harbour Perspectives in Biology*, **3**(3). pii: a004994.
- [903] Danen EH, Sonneveld P, Brakebusch C, Fassler R, Sonnenberg A. (2002) The fibronectin-binding integrins alpha5beta1 and alphabeta3 differentially modulate RhoA-GTP loading, organization of cell matrix adhesions, and fibronectin fibrillogenesis. *Journal of Cell Biology*, **159**, 1071-1086.
- [904] Tuckwell DS, Ayad S, Grant ME, Takigawa M, Humphries MJ. (1994) Conformation dependence of integrin-type II collagen binding. Inability of collagen peptides to support alpha 2 beta 1 binding, and mediation of adhesion to denatured collagen by a novel alpha 5 beta 1-fibronectin bridge. *Journal of Cell Science*, **107**, 993-1005.
- [905] Nishiuchi R, Takagi J, Hayashi M, Ido H, Yagi Y, Sanzen N, Tsuji T, Yamada M, Sekiguchi K. (2006) Ligand-binding specificities of laminin-binding integrins: a comprehensive survey of laminin-integrin interactions using recombinant alpha3beta1, alpha6beta1, alpha7beta1 and alpha6beta4 integrins. *Matrix Biology*, **25**, 189-197.
- [906] Leitinger B, Hohenester E. (2007) Mammalian collagen receptors. *Matrix Biology*, **26**, 146-155.
- [907] Doane KJ, Howell SJ, Birk DE. (1998) Identification and functional characterization of two type VI collagen receptors, alpha 3 beta 1 integrin and NG2, during avian corneal stromal development. *Investigative Ophthalmology and Vision Science*, **39**, 263-275.
- [908] Fukushi J, Makagiansar IT, Stallcup WB. (2004) NG2 proteoglycan promotes endothelial cell motility and angiogenesis via engagement of galectin-3 and alpha3beta1 integrin. *Molecular Biology of the Cell*, **15**, 3580-3590.
- [909] Knudson W, Loeser F. (2002) CD44 and integrin matrix receptors participate in cartilage homeostasis. *Cellular and Molecular Life Sciences*, **59**, 36-44.

- [910] Tillet E, Gential B, Garrone R, Stallcup WB. (2002) NG2 proteoglycan mediates beta1 integrin-independent cell adhesion and spreading on collagen VI. *Journal of Cell Biochemistry*, **86**, 726-736.
- [911] Friedrichs JI, Manninen A, Muller DJ, Helenius J. (2008) Galectin-3 regulates integrin alpha2beta1-mediated adhesion to collagen-I and -IV. *Journal of Biological Chemistry*, **283**, 32264-32272.
- [912] Kirsch T, Pfäffle M. (1992) Selective binding of anchorin CII (annexin V) to type II and X collagen and to chondrocalcin (C-propeptide of type II collagen). Implications for anchoring function between matrix vesicles and matrix proteins. *FEBS Letters*, **310**, 143-147.
- [913] Elefteriou F, Exposito JY, Garrone R, Lethias C. (2001) Binding of tenascin-X to decorin. *FEBS Letters*, **495**, 44-47.
- [914] Matsumoto K, SMasafumi S, Mitiko G, Katsuji S, Tamayuki S, Koji K, Hideto W. (2003) Distinct interaction of versican/PG-M with hyaluronan and link protein. *Journal of Biological Chemistry*, **278**, 41205-41212.
- [915] Santra M, Reed CC, Iozzo RV. (2002) Decorin binds to a narrow region of the epidermal growth factor (EGF) receptor, partially overlapping but distinct from the EGF-binding epitope. *Journal of Biological Chemistry*, **277**, 35671-35681.
- [916] Moreno M, Muñoz R, Aroca F, Labarca M, Brandan E, Larraín J. (2005) Biglycan is a new extracellular component of the Chordin-BMP4 signaling pathway. *EMBO Journal*, **24**, 1397-1405.
- [917] Vynios DH, Papageorgakopoulou N, Sazakli H, Tsiganos CP. (2001) The interactions of cartilage proteoglycans with collagens are determined by their structures. *Biochimie*, **83**, 899-906.
- [918] Torzilli PA, Grigiene R, Borrelli J Jr, Helfet DL. (1999) Effect of impact load on articular cartilage: cell metabolism and viability, and matrix water content. *Journal of Biomechanical Engineering*, **121**, 433-441.
- [919] Loening AM, James IE, Levenston ME, Badger AM, Frank EH, Kurz B, Nuttall ME, Hung HH, Blake SM, Grodzinsky AJ, Lark MW. (2000) Injurious mechanical compression of bovine articular cartilage induces chondrocyte apoptosis. *Archives of Biochemistry and Biophysics*, **381**, 205-212.
- [920] Poole AR. (1986) Changes in the collagen and proteoglycan of articular cartilage in arthritis. *Rheumatology* **10**, 316-371.
- [921] Crang FE, Klomparens L. (1988) *Artifacts in Biological Electron Microscopy*. Plenum Press, New York.
- [922] Baumeister W, Grimm R, Walz J. (1999) Electron tomography of molecules and cells, *Trends in Cell Biology*, **9**, 81-85.
- [923] McEwen BF, Marko M. (2001) The emergence of electron tomography as an important tool for investigating cellular ultrastructure, *Journal of Histochemistry and Cytochemistry*, **49**, 553-563.
- [924] McIntosh R, Nicastro D, Mastronarde, D. (2005) New views of cells in 3D: an introduction to electron tomography. *Trends in Cell Biology* **15**, 43-51.
- [925] Medalia O, Weber I, Frangakis AS, Nicastro D, Gerisch G, Baumeister W. (2002) Macromolecular architecture in eukaryotic cells visualized by cryoelectron tomography. *Science*, **298**, 1209-1213.

- [926] Frank J. (1992) Introduction: principles of electron tomography. In *Electron Tomography: Three Dimensional Imaging with the Transmission Electron Microscope*. J. Frank, ed. Plenum Press, New York.
- [927] Koster AJ, Grimm R, Typke D, Hegerl R, Stoschek A, Walz, J, Baumeister W. (1997) Perspectives of molecular and cellular electron tomography. *Journal of Structural Biology*, **120**, 276-308.
- [928] Baumeister W. (2002) Electron tomography: towards visualizing the molecular organization of the cytoplasm. *Current Opinion in Structural Biology*, **12**, 679-684.
- [929] Radon J. (1917) U`ber die Bestimmung von Funktionendurch ihre Integralwertel`angsgewisser Mannigfaltigkeiten Ber. Verh. Sachsische Akademie der Wissenschaften zu Leipzig - Math. Natur. Kl, **69**, 262-277.
- [930] Crowther R, DeRosier D, Klug A. (1970) The reconstruction of a three-dimensional structure from projections and its application to electron microscopy. *Proceedings of the Royal Society of London, Series. A*, **317**, 319-340.
- [931] Castaño-Díez D, Al-Amoudi A, Glynn AM, Seybert A, Frangakis AS. (2007) Fiducial-less alignment of cryo-sections. *Journal of Structural Biology*, **159**, 413-423.
- [932] Lucic V, Förster, Baumeister W. (2005) Structural studies by electron tomography: from cells to molecules. *Annual Review of Biochemistry*, **74**, 833-865.
- [933] Yang C, Zhang HB, Li JJ, Takaoka, A. (2005) The top-bottom effect of a tilted thick specimen and its influence on electron tomography. *Journal of Electron Microscopy*, **54**, 367-371.
- [934] Dr Duane Harland, Lincoln Research Centre, AgResearch Lincoln, New Zealand.
- [935] Luft JH. (1971) Ruthenium red and violet. I. Chemistry, purification, methods of use for electron microscopy and mechanism of action. *Anatomical Record*, **171**, 347-368.
- [936] Luft JH. (1971) Ruthenium red and violet. II. Fine structural localization in animal tissues. *Anatomical Record*, **171**, 369-415.
- [937] Poole CA, Reilly HC, Flint MH. (1982) The adverse effects of HEPES, TES, and BES zwitterion buffers on the ultrastructure of cultured chick embryo epiphyseal chondrocytes. *In Vitro*, **18**, 755-765.
- [938] Hunziker EB. (1993). Application of cryotechniques in cartilage tissue preservation and immunoelectron microscopy: potentials and problems. *Microscopic Research Techniques*, **24**, 457-464.
- [939] Hunziker EB, Herrmann W. (1987). In situ localization of cartilage extracellular matrix components by immunoelectron microscopy after cryotechnical tissue processing. *Journal of Histochemistry and Cytochemistry*, **35**, 647-655.
- [940] Akisaka T, Subita G P, Kawaguchi H, Shigenaga Y. (1987) Improved ultrastructural preservation of epiphyseal chondrocytes by the freeze-substitution method. *Journal of Anatomy*, **219**, 347-355.
- [941] Kielberg V. (1995) Cryopreservation of mammalian cells. *Nunc Technical Note*, **2**, 14.

- [942] Oegema TR, Deloria LB, Fedewa MM, Bischof JC, Lewis JL. (2000) A simple cryopreservation method for the maintenance of cell viability and mechanical integrity of a cultured cartilage analog. *Cryobiology*, **40**, 370-375.
- [943] Rendal-Vázquez ME, Maneiro-Pampín E, Rodríguez-Cabarcos M, Fernández-Mallo O, López de Ullibarri I, Andión-Núñez C, Blanco FJ. (2001) Effect of cryopreservation on human articular chondrocyte viability, proliferation, and collagen expression. *Cryobiology*, **42**, 2-10.
- [944] Albrecht-Buehler G, Bushnell A. (1980) The ultrastructure of primary cilia in quiescent 3T3 cells. *Experimental Cell Research*, **126**, 427-437.
- [945] Mollenhauer HH. (1993) Artifacts caused by dehydration and epoxy embedding in transmission electron microscopy. *Microscopic Research Techniques*, **26**, 496-512.
- [946] Loqman MY, Bush G, Farquharson C, Hall AC. (2010) A cell shrinkage artefact in growth plate chondrocytes with common fixative solutions: importance of fixative osmolarity for maintaining morphology. *European Cells and Materials*, **19**, 214-227.
- [947] Mangin L. (1890) Sur les reactifs colorants des substances fondamentales de la membrane. *Comptes Rendus de l'Académie des Sciences*, **111**, 120-123.
- [948] Bozzola JJ, Russell D. (1999) *Specimen Preparation for Transmission Electron Microscopy. Electron microscopy: Principles and Techniques for Biologists*. Jones and Bartlett, Sudbury, Massachusetts.
- [949] Hayat MA. (1981) *Fixation for Electron Microscopy*, Academic Press, New York.
- [950] Hayat MA. (1986) Glutaraldehyde: Role in electron microscopy *Micron and Microscopica Acta*, **17**, 115-135.
- [951] Hayat MA. (2000) *Principles and Techniques of Electron Microscopy: Biological Applications*. Cambridge University Press, 45-62.
- [952] Glauert AM, Lewis PR. (1998) *Biological Specimen Preparation for Transmission Electron Microscopy*. Princeton University Press, USA.
- [953] Fletcher JM, Greenfield BF, Hardy CJ, Scargill D, Woodhead JL. (1961) Ruthenium Red. *Journal of Chemical Society*, 2000-2006.
- [954] Luft JH. (1964) Electron microscopy of cell extraneous coats as revealed by ruthenium red staining. *Journal of Cell Biology*, **23**, 54A-55A.
- [955] Luft J H. (1965) The fine structure of hyaline cartilage matrix following ruthenium red fixation and staining. *Journal of Cell Biology*, **27**, 37-51.
- [956] Tani E, Ametani T. (1970) Substructure of microtubules in brain nerve cells as revealed by ruthenium red. *Journal of Cell Biology*, **46**, 159-165.
- [957] Monis B, Rovasio RA, Valentich MA. (1975) Ultrastructural characterization by ruthenium red of the surface of the fat globule membrane of human and rat milk with data on carbohydrates of fractions of rat milk. *Cell and Tissue Research*, **157**, 17-24.
- [958] Carrondo MA, Griffith WP, Hall JP, Skapski AC. (1980) X-ray structure of $[\text{Ru}_3 \text{O}_2 (\text{NH}_3)_{14}]^{6+}$, cation of the cytological reagent Ruthenium Red. *Biochimica Biophysica Acta*, **627**, 332-334.

- [959] Hunziker EB, Herrmann W, Schenk RK. (1981) Improved cartilage fixation by ruthenium hexamminetrichloride (RR). A prerequisite for morphometry in growth cartilage. *Journal of Ultrastructural Research*, **81**, 1-12.
- [960] Handley DA, Chien S. (1981) Oxidation of ruthenium red for use as an intercellular tracer. *Histochemistry*, **71**, 249-258.
- [961] Hagiwara H. (1992) Immunoelectron microscopic study of proteoglycans in rat epiphyseal growth plate cartilage after fixation with ruthenium hexamine trichloride (RR). *Histochemistry*, **98**, 305-309.
- [962] Colombo PM, Rascio N. (1977) Ruthenium red staining for electron microscopy of plant material. *Journal of Ultrastructural Research*, **60**, 135-139.
- [963] Gebbers JO, Otto HF. (1974) Electron microscope studies on the intestine using ruthenium red. *Zeitschrift für Zellforschung und mikroskopische Anatomie*, **147**, 271-283.
- [964] Ruggeri A, Dell'orbo C, Quacci D. (1977) Electron microscopic visualisation of proteoglycans with Ruthenium Red. *Histochemical Journal*, **9**, 249-252. Letter to Editor.
- [965] Hunziker EB, Ludi A, Hermann W. (1992) Preservation of cartilage matrix proteoglycans using cationic dyes chemically related to ruthenium hexaamminetrichloride. *Journal of Histochemistry and Cytochemistry*, **40**, 909-917.
- [966] Matukas VJ, Panner BJ, Orbison JL. (1967) Studies on ultrastructural identification and distribution of protein-polysaccharide in cartilage matrix. *Journal of Cell Biology*, **32**, 365-377.
- [967] Phillips FM, Pottenger LA. (1989) *In vitro* reconstruction of a cartilage matrix granule network. *Anatomical Record*, **225**, 26-34.
- [968] Hunziker EB, Herrmann W, Schenk RK. (1983) Ruthenium hexamminetrichloride (RR)-mediated interaction between plasmalemmal components and pericellular matrix proteoglycans is responsible for the preservation of chondrocytic plasma membranes in situ during cartilage fixation. *Journal of Histochemistry and Cytochemistry*, **31**, 717-727.
- [969] Nuehring LP, Steffens WL, Rowland GN. (1991) Comparison of the Ruthenium hexamminetrichloride method to other methods of chemical fixation for preservation of avian physeal cartilage. *Histochemical Journal*, **23**, 201-214.
- [970] Buschmann MD, Maurer A, Berger E, Perumbuli P, Hunziker EB. (2000) Ruthenium hexaammine trichloride chemography for aggrecan mapping in cartilage is a sensitive indicator of matrix degradation. *Journal of Histochemistry and Cytochemistry*, **48**, 81-88.
- [971] Swan MA. (1999) Improved ultrastructural preservation: a role for osmoprotection during cellular fixation. *Microscopy and Analysis, Asia/Pacific*, **72**, 21-24 ISSN: 0958-1952.
- [972] Jennings M, Parker K, Eccles M, Poole CA, McGlashan SR, Jensen CG. (2008) Fibroblast primary cilia in a sheep model of ARPKD. *Queenstown Molecular Biology Meeting: Molecular mechanisms of kidney disease*, Queenstown.
- [973] Farnum CE, Wilsman NJ. (2011) Orientation of primary cilia of articular chondrocytes in three-dimensional space. *Anatomical Record*, **294**, 533-549.

- [974] Ascenzi MG, Blanco C, Drayer I, Kim H, Wilson R, Retting KN, Lyons KM, Mohler G. (2011) Effect of localization, length and orientation of chondrocytic primary cilium on murine growth plate organization. *Journal of Theoretical Biology*, **285**, 147-155.
- [975] Ziese U1, Geerts WJ, Van Der Krift TP, Verkleij AJ, Koster AJ. (2003) Correction of autofocusing errors due to specimen tilt for automated electron tomography. *Journal of Microscopy*, **211**, 179-185.
- [976] Wheatley DN, Feilen E, Yin Z, Wheatley SP. (1994) Primary cilia in cultured mammalian cells: detection with an antibody against deetyrosinated α -tubulin (ID5) and by electron microscopy. *Journal of Submicroscopic Cytology and Pathology*, **126**, 91-102.
- [977] Egeberg DL1, Lethan M, Manguso R, Schneider L, Awan A, Jørgensen TS, Byskov AG, Pedersen LB, Christensen ST. (2012) Primary cilia and aberrant cell signalling in epithelial ovarian cancer. *Cilia*, **1**, 1-15.
- [978] Molla-Herman A, Ghossoub R, Blisnick T, Meunier A, Serres C, Silbermann F, Emmerson C, Romeo K, Bourdoncle P, Schmitt A, Saunier S, Spassky N, Bastin P, Benmerah A. (2010) The ciliary pocket: an endocytic membrane domain at the base of primary and motile cilia. *Journal of Cell Science*, **123**, 1785-1795.
- [979] Albrecht-Buehler G. (1977) Phagokinetic tracks of 3T3 cells: Parallels between the orientation of track segments and of cellular structures which contain actin or tubulin. *Cell*, **12**, 333-339.
- [980] Vorobjev IA, Chentsov YS. (1980) The ultrastructure of centriole in mammalian tissue culture cells. *Cell Biological International Report*, **14**, 1037-1044.
- [981] Dawe H R, H. Farr H, Gull K. (2007) Centriole/basal body morphogenesis and migration during ciliogenesis in animal cells. *Journal of Cell Science*, **120**, 7-15.
- [982] McMurray RJ, Wann AK1, Thompson CL, Connelly JT, Knight MM. (2013) Surface topography regulates wnt signaling through control of primary cilia structure in mesenchymal stem cells. *Science Report*, **3**, 3545.
- [983] Wheatley DN, Bowser SS. (2000) Length control of primary cilia: analysis of monociliate and multiciliate PtK1 cells. *Biology of the Cell*, **92**, 573-582.
- [984] Lin Z, Fitzgerald JB, Xu J, Willers C, Wood D, Grodzinsky AJ, Zheng MH. (2008) Gene expression profiles of human chondrocytes during passaged monolayer cultivation. *Journal of Orthopaedic Research*, **26**, 1230-1237.
- [985] Alieva IB, Vorobjev IA. (2004) Vertebrate primary cilia: a sensory part of centrosomal complex in tissue cells, but a "sleeping beauty" in cultured cells? *Cell Biology International*, **28**, 139-150.
- [986] Pirkmajer S, Chibalin AV. (2011) Serum starvation: caveat emptor. *American Journal Cell Physiology*, **301**, C272-9.
- [987] Rasband WS. (1997-2012) ImageJ, U. S. National Institutes of Health, Bethesda, Maryland, USA, <http://imagej.nih.gov/ij/>
- [988] Bartesaghi A, Sprechmann P, Liu J, Randall G, Sapiro G, Subramaniam S. (2008) Classification and 3D averaging with missing wedge correction in biological electron tomography. *Journal of Structural Biology*, **162**, 436-450.

- [989] Frank J. (2006) *Electron Tomography: Methods for Three-Dimensional Visualization of Structures in the Cell*, 2nd edn, Springer, New York.
- [990] Kobayashi A, Fujigaya T, Itoh M, Taguchi T, Takano H. (2009) Technical note: a tool for determining rotational tilt axis with or without fiducial markers. *Ultramicroscopy*, **110**, 1-6.
- [991] Arslan I, Tong JR, Midgley, PA. (2006) Reducing the missing wedge: High-resolution dual axis tomography of inorganic materials. *Ultramicroscopy*, **106**, 994-1000.
- [992] Mastrorade DN. 1997. Dual-axis tomography: An approach with alignment methods that preserve resolution. *Journal of Structural Biology*, **120**, 343-352.
- [993] <http://bio3d.colorado.edu/imod>
- [994] <http://rsb.info.nih.gov/ij/index.html>
- [995] <http://u759.curie.fr/fr/telechargements/softwares/tomoj/tomoj-00733>
- [996] <http://bio3d.colorado.edu/imod> and personal correspondence.
- [997] Kremer J, Mastrorade DN, McIntosh JR. (1996) Computer visualisation of three-dimensional image data using IMOD. *Journal of Structural Biology*, **116**, 71-76.
- [998] Farnum CE, Wilsman NJ. (1986) Three dimensional orientation of chondrocytic cilia in adult articular cartilage. In: Proceedings of the 32nd *Orthopaedic Research Society*, New Orleans, 486.
- [999] Wuthier RE, Chin JE, Hale JE, Register TC, Hale LV, Ishikawa Y. (1985). Isolation and characterization of calcium-accumulating matrix vesicles from chondrocytes of chicken epiphyseal growth plate cartilage in primary culture. *Journal Biological Chemistry*, **260**, 15972-15979.
- [1000] Bonifacino JS, Rojas R. (2006) Retrograde transport from endosomes to the trans-Golgi network. *Nature Reviews Molecular Cell Biology*, **7**, 568-579.
- [1001] Riparbelli MG, Callaini G, Megraw TL. (2012) Assembly and persistence of primary cilia in dividing *Drosophila* spermatocytes. *Developmental Cell*, **23**, 425-432.
- [1002] Nadezhdina ES, Fais D, Chentsov YS. (1979) On the association of centrioles with the interphase nucleus. *European Journal of Cell Biology*, **19**, 109-115.
- [1003] Jones C, Chen P. (2008) Primary cilia in planar cell polarity regulation of the inner ear. *Current Topics in Developmental Biology*, **85**, 197-224.
- [1004] Bisgrove BW, Yost HJ. (2006) The roles of cilia in developmental disorders and disease. *Development*, **133**, 4131-4143.
- [1005] Ascenzi MG, Lenox M, Farnum C. (2007) Analysis of the orientation of primary cilia in growth plate cartilage: a mathematical method based on multiphoton microscopical images. *Journal of Structural Biology*, **158**, 293-306.
- [1006] Gluenz E, Höög JL, Smith AE, Dawe HR, Shaw MK, Gull K. (2010) Beyond 9+0: noncanonical axoneme structures characterize sensory cilia from protists to humans. *FASEB Journal*, **24**, 3117-3121.

- [1007] Kim, Y-J, Bonassar, LJ, Grodzinsky AJ. (1995) The role of cartilage streaming potential, fluid flow and pressure in the stimulation of chondrocyte biosynthesis during dynamic compression. *Journal of Biomechanics*, **28**, 1055-1066.
- [1008] Kim SH, Turnbull J, Guimond S. (2011) Extracellular matrix and cell signalling: the dynamic cooperation of integrin, proteoglycan and growth factor receptor. *Journal of Endocrinology*, **209**, 139-151.
- [1009] Muiznieks LD, Keeley FW. (2013) Molecular assembly and mechanical properties of the extracellular matrix: A fibrous protein perspective. *Biochimica Biophysica Acta*, **1832**, 866-875.
- [1010] Culav EM, Clark CH, Merrilees MJ. (1999) Connective tissues: matrix composition and its relevance to physical therapy. *Physical Therapy*, **79**, 308-319.
- [1011] Delaine-Smith RM, Reilly GC. (2012) Mesenchymal stem cell responses to mechanical stimuli. *Muscles, Ligaments and Tendons Journal*, **2**, 169-180.
- [1012] Puetzer J, Williams J, Gillies A, Bernacki S, Lobo EG. (2013) The effects of cyclic hydrostatic pressure on chondrogenesis and viability of human adipose- and bone marrow-derived mesenchymal stem cells in three-dimensional agarose constructs. *Tissue Engineering A*, **19**, 299-306.
- [1013] Gupta MP, Dixon IM, Zhao D, Dhalla NS. (1989) Influence of ruthenium red on rat heart subcellular calcium transport. *Canadian Journal of Cardiology*, **5**, 55-63.
- [1014] Dwyer DS, Gordon K, Jones B. (1995) Ruthenium Red potently inhibits immune responses both *in vitro* and *in vivo*. *International Journal of Immunopharmacology*, **17**, 931-940.
- [1015] Voelker D, Smejtek P. (1996) Adsorption of ruthenium red to phospholipid membranes. *Biophysical Journal*, **70**, 818-830.
- [1016] Szubinska B, Luft JH. (1971). Ruthenium red and violet. 3. Fine structure of the plasma membrane and extraneous coats in amoebae (*A. proteus* and *Chaos chaos*). *Anatomical Record*, **171**, 417-441.
- [1017] Czukas SR, Rosenquist TH, Mulroy MJ. (1987) Connections between stereocilia in auditory hair cells of the alligator lizard. *Hearing Research*, **30**, 147-155.
- [1018] Donnelly E, Ascenzi MG, Farnum C. (2010) Primary cilia are highly oriented with respect to collagen direction and long axis of extensor tendon *Journal of Orthopaedic Research*, **28**, 77-82.
- [1019] Hayek S, Parasuraman R, Desai HS, Samarapungavan D, Li W, Wolforth SC, Reddy GH, Cohn SR, Rocher LL, Dumler F, Rooney MT, Zhang PL. (2013) Primary Cilia Metaplasia in Renal Transplant Biopsies with Acute Tubular Injury. *Ultrastructural Pathology*, **37**, 159-163.
- [1020] Bird SD, Legge M, Walker RJ. (2004) Cultured peritoneal mesothelial cells exhibit apical primary cilia. *Cell Biology International*, **28**, 79-92.
- [1021] Wheatley D N. (1969) Cilia in cell-cultured fibroblasts. I. On their occurrence and relative frequencies in primary cultures and established cell lines. *Journal of Anatomy*, **105**, 351-362.
- [1022] Wheatley D N. (1967) Cells with two cilia in the rat adenohypophysis. *Journal of Anatomy*, **101**, 479-485.
- [1023] Wong C, Stearns T. (2005) Mammalian cells lack checkpoints for tetraploidy, aberrant centrosome number, and cytokinesis failure. *BMC Cell Biology*, **6**, 6.

- [1024] Wong C, Stearns T. (2003) Centrosome number is controlled by a centrosome-intrinsic block to reduplication. *Nature Cell Biology*, **5**, 539-544.
- [1025] Cox RW, Peacock MA. (1977) The fine structure of developing elastic cartilage. *Journal of Anatomy*, **123**, 283-296.
- [1026] McGlashan SR, Cluett EC, Jensen CG, Poole CA. (2008) Primary cilia in osteoarthritic chondrocytes: from chondrons to clusters. *Developmental Dynamics*, **237**, 2013e20.
- [1027] Griffiths GM, Tsun A, Stinchcombe JC. (2010) The immunological synapse: a focal point for endocytosis and exocytosis. *Journal of Cell Biology*, **189**, 399-406.
- [1028] Poole CA, Stayner C, McGlashan SR, Parker K, Wiles A, Jennings M, Jensen CG, Johnstone AC, Walker RJ, Eccles MR. (2012) Primary cilia defects in the polycystic kidneys from an ovine model of Meckel Gruber syndrome. *Cilia*, **1**, 97.
- [1029] Ghossoub R, Molla-Herman A, Bastin P, Benmerah A. (2011) The ciliary pocket: a once-forgotten membrane domain at the base of cilia. *Biology of the Cell*, **103**, 131-144.
- [1030] Wheatley DN. (1967) Cilia and centrioles of the rat adrenal cortex. *Journal of Anatomy*, **101**, 223-237.
- [1031] Nicastro D, Schwartz C, Pierson J, Gaudette R, Porter ME, McIntosh JR (2006) The molecular architecture of axonemes revealed by cryoelectron tomography. *Science*, **313**, 944-948.
- [1032] Bui, KH, Sakakibara H, Movassagh T, Oiwa, K, Ishikawa T. (2008) Molecular architecture of inner dynein arms in situ in *Chlamydomonas reinhardtii* flagella. *Journal of Cell Biology*, **183**, 923-932.
- [1033] Rilla K, Siiskonen H, Spicer AP, Hyttinen JM, Tammi MI, Tammi RH. (2005) Plasma membrane residence of hyaluronan synthase is coupled to its enzymatic activity. *Journal of Biological Chemistry*, **280**, 31890-31897.
- [1034] Thyberg J, Lohmander S, Friberg U. (1973) Electron microscopic demonstration of proteoglycans in guinea pig epiphyseal cartilage. *Journal of Ultrastructural Research*, **45**, 407-427.
- [1035] Matukas VJ, Panner BJ, Orbison JL. (1967) Studies on ultrastructural identification and distribution of protein-polysaccharide in cartilage matrix. *Journal of Cell Biology*, **32**, 365-377.
- [1036] Stamenovic D, Wang N, Ingber DE. (2006) Cellular Tensegrity Models and Cell-Substrate Interactions. *Principles of Cellular Engineering*, Ed King MR, Academic Press, New York.
- [1037] Zhu W, Lai WM, Mow VC. (1991) The density and strength of proteoglycan-proteoglycan interaction sites in concentrated solutions. *Journal of Biomechanics*, **24**, 1007-1018.
- [1038] Mow VC, Holmes MH, Lai WM. (1984) Fluid transport and mechanical properties of articular cartilage. *Journal Biomechanics*, **17**, 377-394.
- [1039] Mow VC, Mak, AF, Lai, WM, Rosenberg, LC, Tang, L. H. (1984) Viscoelastic properties of proteoglycan subunits and aggregates in varying solution concentrations. *Journal Biomechanics*, **17**, 325-338.

- [1040] Mow V C, Zhu W B, Lai W M, Hardingham T E, Hughes C, Muir H. (1989) The influence of link protein stabilisation on the viscometric properties of proteoglycan aggregate solutions. *Biochimica Biophysica Acta*, **992**, 201-208.
- [1041] Zhu WB, Lai WM, Mow VC, Tang LH, Roam LC, Hughes C, Hardingham TE, Muir, H. (1988) Influence of composition, size and structure of cartilage proteoglycan on the strength of molecular network formed in solution. *Zlvsurs. ortirop. Res. Sot.* **13**, 67.
- [1042] Carrasco H1, Olivares GH, Faunes F, Oliva C, Larraín J. (2005) Heparan sulfate proteoglycans exert positive and negative effects in Shh activity. *Journal of Cellular Biochemistry*, **96**, 831-838.
- [1043] Mitsi M, Hong Z, Costello CE, Nugent MA (2006) Heparin-mediated conformational changes in fibronectin expose vascular endothelial growth factor binding sites. *Biochemistry*, **45**, 10319-10328.
- [1044] Wang S, Ai X, Freeman SD, Pownall ME, Lu Q, Kessler DS, Emerson CP. (2004) QSulf1, a heparan sulfate 6-O-endosulfatase, inhibits fibroblast growth factor signalling in mesoderm induction and angiogenesis. *Proceedings of the National Academy of Sciences, USA*, **101**, 4833-4838.
- [1045] Westlake CJ, Rahajeng J, Lu Q, Scheller RH, Caplan S, Jackson PK. (2012) Building the primary cilium membrane. *Cilia*, **1**, O15.
- [1046] Tsun A, Qureshi I, Stinchcombe JC, Jenkins MR, de la Roche M, Kleczkowska J, Zamoyska R, Griffiths GM. (2011) Centrosome docking at the immunological synapse is controlled by Lck signaling. *Journal of Cell Biology*, **192**, 663-674.
- [1047] Kukulski W, Schorb M, Kaksonen M, Briggs JA. (2012) Plasma membrane reshaping during endocytosis is revealed by time-resolved electron tomography. *Cell*, **150**, 508-520.
- [1048] Kaplan OI, Doroquez DB, Cevik S, Bowie RV, Clarke L, Sanders AA, Kida K, Rappoport JZ, Sengupta P, Blacque OE. (2012) Endocytosis genes facilitate protein and membrane transport in *C. elegans* sensory cilia. *Current Biology*, **22**, 451-460.
- [1049] Cherfils J, Zeghouf M. (2011) Chronicles of the GTPase switch. *Nature Chemical Biology*, **7**, 493-495.
- [1050] Zhu F, Tajkhorshid E, Schulten K. (2004) Theory and simulation of water permeation in aquaporin-1. *Biophysical Journal*, **86**, 50-57.
- [1051] Singer SJ, Nicolson GL (1972) The fluid mosaic model of the structure of cell membranes. *Science*, **175** (4023), 720-731.
- [1052] Eliceiri BP. (2001) Integrin and growth factor receptor crosstalk. *Circulation Research*, **89**, 1104-1110.
- [1053] De Meyts P, Wallach B, Christoffersen CT, Ursø B, Grønskov K, Latus LJ, Yakushiji F, Ilondo MM, Shymko RM. (1994) The insulin-like growth factor-I receptor. Structure, ligand-binding mechanism and signal transduction. *Hormonal Research*, **42**, 152-169.
- [1054] Yeh C, Li A, Jen-Zen Chuang J, Saito M, Ca´ceres A, Sung C. (2013) IGF-1 activates a cilium-localized noncanonical Gbg signalling pathway that regulates cell-cycle progression. *Developmental Cell*, **26**, 358-368.

- [1055] Shim AH, Liu H, Focia PJ, Chen X, Lin PC, He X. (2010) Structures of a platelet-derived growth factor/propeptide complex and a platelet-derived growth factor/receptor complex. *Proceedings of the National Academy of Sciences, USA*, **107**, 11307-11312.
- [1056] Ruch C, Skiniotis G, Steinmetz MO, Walz T, Ballmer-Hofer K (2007) Structure of a VEGF-VEGF receptor complex determined by electron microscopy. *Nature Structural and Molecular Biology*, **14**, 249-250.
- [1057] Yang Y, Xie P, Opatowsky Y, Schlessinger J. (2010) Direct contacts between extracellular membrane-proximal domains are required for VEGF receptor activation and cell signaling. *Proceedings of the National Academy of Sciences, USA*, **107**, 1906-1911.
- [1058] Bessman NJ, Lemmon MA. (2012) Finding the missing links in EGFR. *Nature Structural and Molecular Biology*, **19**, 1-3.
- [1059] Ma R, Li WP, Rundle D, Kong J, Akbarali HI, Tsiokas L. (2005) PKD2 functions as an epidermal growth factor-activated plasma membrane channel. *Molecular and Cellular Biology*, **25**, 8285-8298.
- [1060] Wang C, Wu H, Katritch V, Han GW, Huang XP, Liu W, Siu FY, Roth BL, Cherezov V, Stevens RC. (2013) Structure of the human smoothed receptor bound to an antitumour agent. *Nature*, **497**, 338-343.
- [1061] Liao M, Cao E, Julius D, Cheng Y. (2013) Structure of the TRPV1 ion channel determined by electron cryo-microscopy. *Nature*, **504**, 107-112.
- [1062] Shigematsu H, Sokabe T, Danev R, Tominaga M, Nagayama K. (2010) A 3.5-nm structure of rat TRPV4 cation channel revealed by Zernike phase-contrast cryoelectron microscopy. *Journal of Biological Chemistry*, **285**, 11210-11218.
- [1063] Wann AK, Thompson CL, Chapple JP, Knight MM. (2012) Interleukin-1 β sequesters hypoxia inducible factor 2 α to the primary cilium. *Cilia*, **2**, 17.
- [1064] Mobasheri A, Martin-Vasallo P. (1999) Epithelial sodium channels in skeletal cells: a role in mechanotransduction? *Cell Biology International*, **23**, 237-240.
- [1065] Kashlan OB, Kleyman TR. (2011) ENaC structure and function in the wake of a resolved structure of a family member. *American Journal of Physiology*, **301**, F684-F696.
- [1066] Enuka Y, Hanukoglu I, Edelheit O, Vaknine H, Hanukoglu A. (2012) Epithelial sodium channels (ENaC) are uniformly distributed on motile cilia in the oviduct and the respiratory airways. *Histochemistry and Cell Biology*, **2137**, 339-353.
- [1067] Lisa M. Satlin LM, Sheng S, Woda CB, Kleyman TR. (2001) Epithelial Na⁺ channels are regulated by flow. *American Journal of Physiology*, **280**, F1010-F1018.
- [1068] Benos DJ. (2004) Sensing tension: recognizing ENaC as a stretch sensor. *Hypertension*, **44**, 616-617.
- [1069] Hamill OP, Martinac B. (2001) Molecular basis of mechanotransduction in living cells. *Physiological Reviews*, **81**, 685-740.
- [1070] Awayda MS1, Shao W, Guo F, Zeidel M, Hill WG. (2004) ENaC-membrane interactions: regulation of channel activity by membrane order. *Journal of general Physiology*, **123**, 709-727.

- [1071] Yoshimura K, Sokabe M. (2010) Mechanosensitivity of ion channels based on protein-lipid interactions. *Journal of the Royal Society Interface*. **7**, Suppl 3, S307-S320.
- [1072] Xu BE, Stippec S, Chu PY, Lazrak A, Li XJ, Lee BH, English JM, Ortega B, Huang CL, Cobb MH. (2005) WNK1 activates SGK1 to regulate the epithelial sodium channel. *Proceedings of the National Academy of Sciences, USA*, **102**, 10315-10320.
- [1073] Taruno A, Niisato N, Marunaka Y. (2008) Intracellular calcium plays a role as the second messenger of hypotonic stress in gene regulation of SGK1 and ENaC in renal epithelial A6 cells. *American Journal of Physiology*, **294**, F177-F186.
- [1074] Hogan MC, Manganelli L, Woollard JR, Masyuk AI, Masyuk TV, Tammachote R, Huang BQ, Leontovich AA, Beito TG, Madden BJ, Charlesworth MC, Torres VE, LaRusso NF, Harris PC, Ward CJ. (2009) Characterization of PKD protein-positive exosome-like vesicles. *Journal of the American Society of Nephrology*, **20**, 278-288.
- [1075] Bahrami AH, Lipowsky R, Weikl TR. (2012) Tubulation and aggregation of spherical nanoparticles adsorbed on vesicles. *Physical Review Letters*, **109**, 188102.
- [1076] Baumgart T1, Capraro BR, Zhu C, Das SL. (2011) Thermodynamics and mechanics of membrane curvature generation and sensing by proteins and lipids. *Annual Review of Physics and Chemistry*, **62**, 483-506.
- [1077] Shnyrova AV, Frolov VA, Zimmerberg J. (2009) Domain-driven morphogenesis of cellular membranes. *Current Biology*, **19**, R772-R780.
- [1078] Krauss M, Jia JY, Roux A, Beck R, Wieland FT, De Camilli P, Haucke V. (2008) Arf1-GTP-induced tubule formation suggests a function of Arf family proteins in curvature acquisition at sites of vesicle budding. *Journal of Biological Chemistry*, **283**, 27717-27723.
- [1079] Zimmerberg J1, Kozlov MM. (2006) How proteins produce cellular membrane curvature. *Nature Reviews Molecular and Cellular Biology*, **7**, 9-19.
- [1080] Tian A, Baumgart T. (2009) Sorting of lipids and proteins in membrane curvature gradients. *Biophysical Journal*, **96**, 2676-2688.
- [1081] Settles EI, Loftus AF, McKeown AN, Parthasarathy R. (2010) The vesicle trafficking protein Sar1 lowers lipid membrane rigidity. *Biophysical Journal*, **99**, 1539-1545.
- [1082] Farsad K, De Camilli P. (2003) Mechanisms of membrane deformation. *Current Opinion in Cell Biology*, **15**, 372-381.
- [1083] McMahon HT, Gallop JL. (2005) Membrane curvature and mechanisms of dynamic cell membrane remodelling. *Nature*, **438**, 590-596.
- [1084] Tian AW, Capraro BR, Esposito C, Baumgart T. 2009. Bending stiffness depends on curvature of ternary lipid mixture tubular membranes. *Biophysical Journal*, **97**, 1636-1646.
- [1085] Ambroggio E, Sorre B, Bassereau P, Goud B, Manneville JB, Antonny B. 2010. ArfGAP1 generates an Arf1 gradient on continuous lipid membranes displaying flat and curved regions. *EMBO Journal*, **29**, 292-303.
- [1086] Beck R, Sun Z, Adolf F, Rutz C, Bassler J, et al. 2008. Membrane curvature induced by Arf1-GTP is essential for vesicle formation. *Proceedings of the National Academy of Sciences, USA*, **105**, 11731-11736.

- [1087] Downs ME, Nguyen AM, Herzog FA, Hoey DA, Jacobs CR. (2012) An experimental and computational analysis of primary cilia deflection under fluid flow. *Computer Methods in Biomechanical and Biomedical Engineering*, **17**, 2-10.
- [1088] Hilfinger A, Chattopadhyay AK, Jülicher F. (2009) Nonlinear dynamics of cilia and flagella. *Physical Review. E, Statistical, Nonlinear, and Soft Matter Physics*, **79**, 051918.
- [1089] Schwartz EA, Leonard ML, Bizios R, Bowser SS. (1997) Analysis and modeling of the primary cilium bending response to fluid shear. *American Journal of Physiology*, **272**, F132-F138.
- [1090] Resnick A, Hopfer U. (2007) Force-response considerations in ciliary mechanosensation. *Biophysical Journal*, **93**, 1380-1390.
- [1091] Chen D, Norris D, Ventikos Y. (2009) The active and passive ciliary motion in the embryo node: a computational fluid dynamics model. *Journal of Biomechanics*, **242**, 210-216.
- [1092] Rydholm S, Zwartz G, Kowalewski JM, Kamali-Zare P, Frisk T, Brismar H. (2010) Mechanical properties of primary cilia regulate the response to fluid flow. *American Journal of Physiology*, **298**, F1096-F1102.
- [1093] Young YN, Downs M, Jacobs CR. (2012) Dynamics of the primary cilium in shear flow. *Biophysical Journal*, **103**, 629-639.
- [1094] Gittes F, Mickey B, Nettleton J, Howard J. (1993) Flexural rigidity of microtubules and actin filaments measured from thermal fluctuations in shape. *Journal of Cell Biology*, **120**, 923-934.
- [1095] Aoyama S, Kamiya R. (2005) Cyclical interactions between two outer doublet microtubules in split flagellar axonemes. *Biophysical Journal*, **89**, 3261-3268.
- [1096] Schaap IA, Carrasco C, de Pablo PJ, MacKintosh FC, Schmidt CF. (2006) Elastic response, buckling, and instability of microtubules under radial indentation. *Biophysical Journal*, **91**, 1521-1531.
- [1097] Felgner H, Frank R, Schliwa M. (1996) Flexural rigidity of microtubules measured with the use of optical tweezers. *Journal of Cell Science*, **109**, 509-516.
- [1098] Kikumoto M, Kurachi M, Tosa V, Tashiro H. (2006) Flexural rigidity of individual microtubules measured by a buckling force with optical traps. *Biophysical Journal*, **90**, 1687-1696.
- [1099] Ghavanloo E, Daneshmand F, Amabili M. (2010) Prediction of bending stiffness and deformed shape of non-axially compressed microtubule by a semi-analytical approach. *Journal of Biological Physics*, **36**, 427-435.
- [1100] Kurachi M, Hoshi M, Tashiro H. (1995) Buckling of a single microtubule by optical trapping forces: direct measurement of microtubule rigidity. *Cell Motility and Cytoskeleton*, **30**, 221-228.
- [1101] Andersen JS, Wilkinson CJ, Mayor T, Mortensen P, Nigg EA, Mann M. (2003) Proteomic characterization of the human centrosome by protein correlation profiling. *Nature*, **426**, 570-574.
- [1102] Keller LC, Romijn EP, Zamora I, Yates JR 3rd, Marshall WF. (2005) Proteomic analysis of isolated *Chlamydomonas* centrioles reveals orthologs of ciliary-disease genes. *Current Biology*, **15**, 1090-1098.

- [1103] Muller H, Schmidt D, Steinbrink S, Mirgorodskaya E, Lehmann V, Habermann K, Dreher F, Gustavsson N, Kessler T, Lehrach H, Herwig R, Gobom J, Ploubidou A, Boutros M, Lange BM. (2010) Proteomic and functional analysis of the mitotic *Drosophila* centrosome. *EMBO Journal*, **29**, 3344-3357.
- [1104] Li, J. B. Gerdes JM, Haycraft CJ, Fan Y, Teslovich TM, May-Simera H, Li H, Blacque OE, Li L, Leitch CC, Lewis RA, Green JS, Parfrey PS, Leroux MR, Davidson WS, Beales PL, Guay-Woodford LM, Yoder BK, Stormo GD, Katsanis N, Dutcher SK. (2004) Comparative genomics identifies a flagellar and basal body proteome that includes the BBS5 human disease gene. *Cell*, **117**, 541-552.
- [1105] Rosenbaum JL, Witman GB. (2002) Intraflagellar transport. *Nature Reviews Molecular and Cellular Biology*, **3**, 813-825.
- [1106] Snow JJ, Ou G, Gunnarson AL, Walker MR, Zhou HM, Brust-Mascher I, Scholey JM. (2004) Two anterograde intraflagellar transport motors cooperate to build sensory cilia on *C. elegans* neurons. *Nature Cell Biology*, **6**, 1109-1113.
- [1107] Besschetnova TY, Kolpakova-Hart E, Guan Y, Zhou J, Olsen BR, Shah JV. (2010) Identification of signaling pathways regulating primary cilium length and flow-mediated adaptation. *Current Biology*, **20**, 182-187.
- [1108] Horst CJ, Forestner DM, Besharse JC. (1987) Cytoskeletal-membrane interactions: a stable interaction between cell surface glycoconjugates and doublet microtubules of the photoreceptor connecting cilium. *Journal of Cell Biology*, **105**, 2973-2987.
- [1109] Hu Q, Nelson WJ (2011) Ciliary diffusion barrier: the gatekeeper for the primary cilium compartment. *Cytoskeleton*, **68**, 313-324.
- [1110] Sillibourne JE, Specht CG, Izeddin I, Hurbain I, Tran P, Triller A, Darzacq X, Dahan M, Bornens M. (2011) Assessing the localization of centrosomal proteins by PALM/STORM nanoscopy. *Cytoskeleton*, **68**, 619-627.
- [1111] Sang L, Miller JJ, Corbit KC, Giles RH, Brauer MJ, Otto EA, Baye LM, Wen X, Scales SJ, Kwong M, Huntzicker EG, Sfakianos MK, Sandoval W, Bazan JF, Kulkarni P, Garcia-Gonzalo FR, Seol AD, O'Toole JF, Held S, Reutter HM, Lane WS, Rafiq MA, Noor A, Ansar M, Devi AR, Sheffield VC, Slusarski DC, Vincent JB, Doherty DA, Hildebrandt F, Reiter JF, Jackson PK. (2011) Mapping the NPHP-JBTS-MKS protein network reveals ciliopathy disease genes and pathways. *Cell*, **145**, 513-528.
- [1112] Craige B, Tsao CC, Diener DR, Hou Y, Lechtreck KF, Rosenbaum JL, Witman GB. (2010) CEP290 tethers flagellar transition zone microtubules to the membrane and regulates flagellar protein content. *Journal of Cell Biology*, **190**, 927-940.
- [1113] Shiba D, Manning DK, Koga H, Beier DR, Yokoyama T. (2010) Inv acts as a molecular anchor for Nphp3 and Nek8 in the proximal segment of primary cilia. *Cytoskeleton*, **67**, 112-119.
- [1114] Williams CL, Masyukova SV, Yoder BK. (2010) Normal ciliogenesis requires synergy between the cystic kidney disease genes MKS-3 and NPHP-4. *Journal of the American Society of Nephrology*, **21**, 782-793.
- [1115] Fliegauf M, Benzing T, Omran H. (2007) When cilia go bad: cilia defects and ciliopathies. *Nature Reviews Molecular and Cellular Biology*, **8**, 880-893.

- [1116] Chih B, Liu P, Chinn Y, Chalouni C, Komuves LG, Hass PE, Sandoval W, Peterson AS. (2011) A ciliopathy complex at the transition zone protects the cilia as a privileged membrane domain. *Nature Cell Biology*, **14**, 61-72.
- [1117] Brooker BE, Goodwin LG, Guy MW. (1971) Ciliated fibroblasts in rabbit ear chambers. *Journal of Anatomy*, **110**, 363-365.
- [1118] Geerts WJ, Vocking K, Schoonen N, Haarbosch L, van Donselaar EG, Regan-Klapisz E, Post JA. (2011) Cobblestone HUVECs: a human model system for studying primary ciliogenesis. *Journal of Structural Biology*, **176**, 350-359.
- [1119] Reese TS (1965) Olfactory cilia in the frog. *Journal of Cell Biology*, **25**, 209-230.
- [1120] Doolin PF, Birge WJ. (1966) Ultrastructural organization of cilia and basal bodies of the epithelium of the choroid plexus in the chick embryo. *Journal of Cell Biology*, **29**, 333-345.
- [1121] Pifferi M, Cangiotti AM, Caramella D, Pietrobelli A, Ragazzo V, De Marco E, Macchia P, Cinti S, Boner AL. (2004) "Cyst-like" structures within the ciliary shafts in children with bronchiectasis. *European Respiratory Journal*, **23**, 857-860.
- [1122] Jerka-Dziadosz M1, Gogendeau D, Klotz C, Cohen J, Beisson J, Koll F. (2010) Basal body duplication in *Paramecium*: the key role of Bld10 in assembly and stability of the cartwheel. *Cytoskeleton*, **67**, 161-171.
- [1123] Alvey PL. (1986) Do adult centrioles contain cartwheels and lie at right angles to each other? *Cell Biology International Reports*, **10**, 589-589.
- [1124] Paintrand M, Moudjou M, Delacroix H, Bornens M. (1992) Centrosome organization and centriole architecture: their sensitivity to divalent cations. *Journal of Structural Biology*, **108**, 107-128.
- [1125] Ibrahim R, Messaoudi C, Chichon FJ, Celati C, Marco S. (2009) Electron tomography study of isolated human centrioles. *Microscopic Research Techniques*, **72**, 42-48.
- [1126] Jeffery JM, Grigoriev I, Poser I, van der Horst A, Hamilton N, Waterhouse N, Bleier J, Subramaniam VN, Maly IV, Akhmanova A, Khanna KK. (2013) Centrobin regulates centrosome function in interphase cells by limiting pericentriolar matrix recruitment. *Cell Cycle*, **12**, 899-906.
- [1127] Pederson T. (2006) The centrosome: built on an mRNA? *Nature Cell Biology*, **8**, 652-654.
- [1128] Tkemaladze JV, Chichinadze KN. (2005) Centriolar mechanisms of differentiation and replicative aging of higher animal cells. *Biochemistry*, **70**, 1288-1303.
- [1129] Tateishi K, Yamazaki Y, Nishida T, Watanabe S, Kunitomo K, Ishikawa H, Tsukita S. (2013) Two appendages homologous between basal bodies and centrioles are formed using distinct Odf2 domains. *Journal of Cell Biology*, **203**, 417-425.
- [1130] Guarguaglini G, Duncan PI, Stierhof YD, Holmström T, Duensing S, Nigg EA (2005) The forkhead-associated domain protein Cep170 interacts with Polo-like kinase 1 and serves as a marker for mature centrioles. *Molecular Biology of the Cell*, **16**, 1095-1107.
- [1131] Chang P, Giddings TM, Winey M, Stearns T. (2003) ϵ -Tubulin is required for centriole duplication and microtubule organization. *Nature Cell Biology*, **5**, 71-76.

- [1132] Gomez-Ferreria MA, Bashkurov M, Helbig AO, Larsen B, Pawson T, Gingras AC, Pelletier L. (2012) Novel NEDD1 phosphorylation sites regulate γ -tubulin binding and mitotic spindle assembly. *Journal of Cell Science*, **125**, 3745-3751.
- [1133] Terada Y, Uetake, Y, Kuriyama R. (2003) Interaction of Aurora-A and centrosomin at the microtubule-nucleating site in *Drosophila* and mammalian cells. *Journal of Cell Biology*, **162**, 757-763.
- [1134] Dichtenberg JB, Zimmerman W, Sparks CA, Young A, Vidar C, Zheng Y, Carrington W, Fay FS, Doxsey SJ (1998) Pericentrin and gamma-tubulin form a protein complex and are organized into a novel lattice at the centrosome. *Journal of Cell Biology*, **141**, 163-174.
- [1135] Takahashi M, Yamagiwa A, Nishimura T, Mukai H, Ono Y. (2002) Centrosomal proteins CG-NAP and kendrin provide microtubule nucleation sites by anchoring gamma-tubulin ring complex. *Molecular Biology of the Cell*, **13**, 3235-3245.
- [1136] Kreplak L, Buehler M J, Schnur JM. (2009) Structure Controls Nanomechanical Properties of Vimentin Intermediate Filaments Schnur, *PLoS One*, **4**(10):e7294.
- [1137] Lemullois M, Gounon P, Sandoz D. (1987) Relationships between cytokeratin filaments and centriolar derivatives during ciliogenesis in the quail oviduct. *Biology of the Cell*, **61**, 39-49.
- [1138] Trevor KT, McGuire JG, Leonova EV. (1995) Association of vimentin intermediate filaments with the centrosome. *Journal of Cell Science*, **108**, 343-356.
- [1139] Herrmann HH, Kreplak L, Strelkov SV, Aebi U. (2007) Intermediate filaments: from cell architecture to nanomechanics. *Nature Reviews Molecular Cell Biology*, **8**, 562-573.
- [1140] Eckert BS, Caputi SE, Brinkley BR. (1984) Localization of the centriole and keratin intermediate filaments in PtK1 cells by double immunofluorescence. *Cell Motility*, **4**, 241-247.
- [1141] Helfand BT, Chang L, Goldman RD. (2004) Intermediate filaments are dynamic and motile elements of cellular architecture. *Journal of Cell Science*, **117**, 133-141.
- [1142] Scliwa M, Höner B. (1993) Microtubules, centrosomes and intermediate filaments in directed cell movement. *Trends in Cell Biology*, **3**, 377-380.
- [1143] Kreitzer G, Liao G, Gundersen GG. (1999) Detyrosination of tubulin regulates the interaction of intermediate filaments with microtubules in vivo via a kinesin-dependent mechanism. *Molecular Biology of the Cell*, **10**, 1105-1118.
- [1144] Svitkina TM, Verkhovskiy AB, Borisy GG (1996) Plectin sidearms mediate interaction of intermediate filaments with microtubules and other components of the cytoskeleton. *Journal of Cell Biology*, **135**, 991-1007.
- [1145] Herold C, Leduc C, Stock R, Diez S, Schwille P. (2012) Long-range transport of giant vesicles along microtubule networks. *ChemPhysChem*, **13**, 1001-1006.
- [1146] Wang G, Krishnamurthy K, Bieberich E. (2009) Regulation of primary cilia formation by ceramide. *Journal of Lipid Research*, **50**, 2103-2110.
- [1147] Bannai H, Inoue T, Nakayama T, Hattori M, Mikoshiba K. (2004) Kinesin dependent, rapid, bi-directional transport of ER sub-compartment in dendrites of hippocampal neurons. *Journal of Cell Science*, **117**, 163-175.

- [1148] Simpson JC, Nilsson T, Pepperkok R. (2006) Biogenesis of tubular ER-to-Golgi transport intermediates. *Molecular Biology of the Cell*, **17**, 723-737.
- [1149] Resendes KK, Rasala BA, Forbes DJ. (2008) Centrin 2 localizes to the vertebrate nuclear pore and plays a role in mRNA and protein export. *Molecular Biology of the Cell*, **28**, 1755-1769.
- [1150] Burakov AV, Nadezhdina ES. (2013) Association of nucleus and centrosome: magnet or velcro? *Cell Biology International*, **37**, 95-104.
- [1151] Köhler A, Hurt E. (2010) Gene regulation by nucleoporins and links to cancer. *Molecular Cell*, **38**, 6-15.
- [1152] Capelson M, Liang Y, Schulte R, Mair W, Wagner U, Hetzer MW. (2010) Chromatin-bound nuclear pore components regulate gene expression in higher eukaryotes. *Cell*, **140**, 372-383.
- [1153] Kallenbach RJ, Mazia D. (1982) Origin and maturation of centrioles in association with the nuclear envelope in hypertonic-stressed sea urchin eggs. *European Journal of Cell Biology*, **28**, 68-76.
- [1154] Bolhy S, Bouhrel I, Dultz E, Nayak T, Zuccolo M, Gatti X, Vallee R, Ellenberg J, Doye V. (2011) A Nup133-dependent NPC-anchored network tethers centrosomes to the nuclear envelope in prophase. *Journal of Cell Biology*, **192**, 855-871.
- [1155] Minn IL, Rolls MM, Hanna-Rose W, Malone CJ. (2009) SUN-1 and ZYG-12, mediators of centrosome-nucleus attachment, are a functional SUN/KASH pair in *Caenorhabditis elegans*. *Molecular Biology of the Cell*, **20**, 4586-4595.
- [1156] Marsh BJ, Volkmann NV, McIntosh JR, Howell KE. (2004) Direct continuities between cisternae at different levels of the Golgi complex in glucose-stimulated mouse islet beta cells. *Proceedings of the National Academy of Sciences, USA*, **101**, 5565-5570.
- [1157] Ladinsky MS, Kremer JR, Furcinitti PS, McIntosh JR, Howell KE. (1994) HVEM tomography of the trans-Golgi network: structural insights and identification of a lace-like vesicle coat. *Journal of Cell Biology*, **127**, 29-38.
- [1158] Marsh BJ, Mastrorarde DN, Buttle KF, Howell KE, McIntosh JR. (2001). Organellar relationships in the Golgi region of pancreatic beta cell line, HIT-T15, visualized by high resolution electron tomography. *Proceedings of the National Academy of Sciences, USA*, **98**, 2399-2406.
- [1159] Ramirez IB, Lowe M. (2009) Golgins and GRASPs: holding the Golgi together. *Seminars in Cellular and Developmental Biology*, **20**, 770-779.
- [1160] Gu F, Crump CM, Thomas G. (2001) Trans-Golgi network sorting. *Cellular and Molecular Life Sciences*, **58**, 1067-1084.
- [1161] Clermont Y, Rambourg A, Hermo L. (1995) Trans-Golgi network (TGN) of different cell types: three-dimensional structural characteristics and variability. *Anatomical Record*, **242**, 289-301.
- [1162] Griffiths G, Simons K. (1986) The trans Golgi network: sorting at the exit site of the Golgi complex. *Science*, **234**, 438-443.
- [1163] Novikoff AB. (1964) GERL, its form and function in neurons of rat spinal ganglia, *Biological Bulletin*, **127**, 358.
- [1164] Novikoff AB. (1976) The endoplasmic reticulum: a cytochemist's view. *Proceedings of the National Academy of Sciences, USA*, **73**, 2781-2787.

- [1165] Nichols BJ. (2002) A distinct class of endosome mediates clathrin-independent endocytosis to the Golgi complex. *Nature Cell Biology*, **4**, 374-378.
- [1166] Pavelka M, Ellinger A, Debbage P, Loewe C, Vetterlein M, Roth J. (1998) Endocytic routes to the Golgi apparatus. *Histochemistry and Cellular Biology*, **109**, 555-570.
- [1167] Russell MR, Nickerson DP, Odorizzi G. (2006) Molecular mechanisms of late endosome morphology, identity and sorting. *Current Opinion in Cell Biology*, **18**, 422-428.
- [1168] Kirchhausen T. (2009) Imaging endocytic clathrin structures in living cells. *Trends in Cell Biology*, **19**, 596-605.
- [1169] Schwab W, Hempel U, Funk RH, Kasper M. (1999) Ultrastructural identification of caveolae and immunocytochemical as well as biochemical detection of caveolin in chondrocytes. *Histochemical Journal*, **31**, 315-320.
- [1170] Wilsman NJ, Farnum CE, Reed-Aksamit DK. (1981) Caveolar system of the articular chondrocyte. *Journal of Ultrastructural Research*, **74**, 1-10.
- [1171] Le PU, Nabi IR. (2003) Distinct caveolae-mediated endocytic pathways target the Golgi apparatus and the endoplasmic reticulum. *Journal of Cell Science*, **116**, 1059-1071.
- [1172] Lake RS. (1987) Negative Poisson's ratio materials, *Science*, **238**, 551.
- [1173] Lakes RS. (1987) Foam structures with a negative Poisson's ratio, *Science*, **235**, 1038-1040.
- [1174] Bell A. (2007) Detection without deflection? A hypothesis for direct sensing of sound pressure by hair cells. *Journal of Bioscience*, **32**, 385-404.
- [1175] Bell A. (2008) The pipe and the pinwheel: is pressure an effective stimulus for the 9+0 primary cilium? *Cell Biology International*, **32**, 462-468.
- [1176] Deretic D. (2010) Post-Golgi Trafficking and Ciliary Targetting of Rhodopsin. In *Encyclopedia of the Eye*, Ed Darlene AD, 480-487, Academic Press, Oxford.
- [1177] Mukhopadhyay S, Jackson PK. (2013) Cilia, tubby mice, and obesity. *Cilia*, **2**, 1.
- [1178] Ko HW. (2012) The primary cilium as a multiple cellular signalling scaffold in development and disease. *BMB Report*, **45**, 427-432.
- [1179] Martin-Delgado MA. (2012) On quantum effects in a theory of biological evolution. *Science Report*, **2**, 302.
- [1180] Gauger EM, Rieper E, Morton JLL, Benjamin SC, Vedral V. (2011) Sustained quantum coherence and entanglement in the avian compass, *Physical Review Letters*, **106**, 4, 040503.
- [1181] Vattay G, Kauffman S, Niiranen S. (2014) Quantum biology on the edge of quantum chaos. *PLoS One*, **9**(3):e89017.

Appendices

Supplemental Information to Thesis

These attached sections contain information collated during the thesis and is only a guide to supplement the reader with some of the many known receptors, their pathways and associated components within the cilium and the centrosome. References appropriate to each Appendix are listed in numerical order and at the end of each section.

Appendix I: Receptors and Signalling in the Cilium and Centrosome

Appendix II: The RabGTPases - Ciliary and Golgi Function

Appendix III: Kinesin and Dynein Microtubule Motors

Appendix IV: Intra-Flagellar Transport Complexes

Appendix V: Kinesin and Dynein Motors Responsible for Organelle Processes and Transport

Appendix VI: Select Review of Tomography and Modelling

Appendix VII: Animation List

Appendix VIII: Poster Presentations

Appendix I: Receptors and Signalling in the Cilium and Centrosome

1.1 Membrane Receptors, Luminal Components and Signalling Pathways

Membrane Associated Protein/Matrix Receptor	Interaction, Localisation and Signalling Cascade	Disease Implication / Ancillary Information
Integrins α2-integrin[1] α3-integrin[1, 2] α5-integrin[1, 2] β1-integrin[1, 2, 3]	Receptors which mediate attachment between the extracellular matrix and the cell membrane. Integrins bind ECM components of Collagen, Fibronectin, Laminin and Vitronectin [4] as part of the mechanosensory transduction process. β1-integrin potentiates Fibronectin-induced Ca²⁺ signalling through the primary cilium[3], while McGlashan et al., (2006)[200] observed the presence of α2, α3, β1-integrins and NG2 (but not CD44 and Annexin V) on chondrocyte primary cilia[1]. β1-integrins are involved in inter-connecting stereocilia[2]. It has been proposed by Praetorius et al., (2004)[3] that in MDCK cells β1-integrin is involved in ciliary mechanotransduction through fibronectin and was found localised to primary cilia in collecting ducts and proximal tubules and ascending limbs. β1, α3 and possibly α5-integrins were found localised to MDCK primary cilia[3].	Loss of α8-β1 integrin results in hearing loss in murines[1]. β1-integrins potentiate fluid flow sensing in endothelial cell primary cilia[3]. α3, α5, and β1-integrins are found upon primary cilia in Madin-Darby Canine Kidney cells[3]. α1, α5β1, and αvβ5 integrins mediate chondrocyte adhesion to cartilage[5].
NG2/CSP4 Neuron-Glial Antigen-2 (NG2) chondroitin sulphate proteoglycan-4	Interacts with Galectin-3 , and α3β1 integrin (forming a membrane complex)[6] in which the PDZ binding terminus motif binds to the seventh PDZ domain of GRIP1 in progenitor cells[7], and mediates activity of β1-integrins [8].	Involved in cell matrix interactions in tumour metastasis [9]
Tubby/TUB-1	TUB-1 is involved in ciliary transport[10,11].	Associated with obesity, life span and fat storage[10, 11].
TULP(Tulp1–Tulp4) Tubby-Like Proteins	TULP1 and TULP2 are expressed in the retina[12, 13], TULP3 bridges between the IFT complex and membrane. IFT-A directs TULP3 entry into the cilium with TULP3 promoting the transport of G-proteins (GPCRs), but not Smø [14]. Also involved in the negative regulation of Shh and in neural tube defects [14]. TULP1 interacts with F-Actin in photoreceptors, on the inner segments, on the connecting cilium and the outer membrane[15].	Involved in tissue development and patterning.
Sec6(EXCO3)/Sec8(EXCO4)	SEC6/SEC8 complex localises to the primary cilium[16], where SEC6 inhibits ciliary shedding and blocks down regulation of Claudin-2 and GP135/CNTN1 . Needed for de-ciliation [17].	See the Exocyst and Septins.
SEC10(EXO5) SEC15(EXO6)	The small GTPase CDC42 interacts with Sec10 [18]; is required for primary ciliogenesis and cystogenesis[18, 19]. Localises on the primary cilium[18]. Sec15 is a Rab11 effector which interacts with Rab8 and Rabin8 [20-22].	See the Exocyst. SEC10 is involved in ciliogenesis [23]. Interacts with PC2 where knock down causes PKD phenotypes [24].
Cystin	Membrane associated protein which localises to the cilium via micro-domains[25, 26].	Involved with Polycystic Kidney Disease [26].
Napa	N-ethylmaleimide-sensitive factor attachment protein. Interacts with SNARE protein SNAP23 (vesicle fusion)[27]. Involved with vesicle docking and adhesion[28].	
Tie-1/Tie-2	Expressed upon primary cilium[29]. Usually expressed as a cell surface marker, where TIE1 up-regulates E-Selectin, ICAM-1 and VCAM-1 through a p38 mediated process[30]. Involved in atherosclerosis in response to atherogenic shear-stress [31].	Associated with angiogenic factors. Tie-2 is the Angiopoietin receptor[32].
Somatostatin Receptors	G-coupling receptors[33]. SSTR3 is coupled into	The roles of Receptors 1-5 are not

(SSTR1/SSTR2/SSTR3)	regulation of hippocampal type 3 adenylyl-cyclase (AC3) in the cilium[34-37]; required for a number of neurological processes[38, 39]. SSTR1 and SSTR2 localise to retina in rats[40]. SSTR3 contains ciliary localisation sequences and is found in the primary cilium[36]. Somatostatin receptors in neuronal cilia are critical for object recognition learning[38] and in pancreatic islets for insulin and GH release through SSTRS1 and SSTRS5 [35]. Ciliary targeting of somatostatin receptor is mediated by the BBSome [41].	fully known.
5-Ht ₆ (Serotonin) Receptor	A G-protein–coupled receptor (GPCR), the Serotonin neurotransmitter receptor. Involved in ciliary driven motion through acetylcholine release [42]. Contains a ciliary localisation sequence[36]. Found localised to the membrane of neuronal cilia[32, 43].	Involved in a large number of biological processes and pathways.
EGFR Epidermal Growth Factor Receptor (EGFR)	Involved with PKD2 and localises to the cilium[44, 45]. EGFR is involved in a large number of interactions and signalling cascades.	
IGFR	Activated noncanonical Gβγ pathway regulating G1-S-phase cell cycle progression[46].	
PDGFR Platelet Derived Growth Factor (PDGFR)- α	Activates AKT and MEK1/2-ERK1/2 pathways. Mek1/2 is phosphorylated in the primary cilium and basal body[47]. Localises to the primary cilium[47]. NHE1 Na⁺/H⁺ ion exchanger is required for directional cell migration through PDGFR-α in the primary cilium [48].	PDGF/VEGF -signalling transduction pathways localise to the primary cilium[49].
PDGFA/PDGFB/PDGFC (Ligands)	PDGF/VEGF family growth factors. PDGFA and PDGFC may function as a ligands for PDGFR-α [50] PDGF-C interacts with PDGFR-α [51]. Associated with receptors found upon the ciliary membrane (see above).	PDGFC only recently identified with PDGFA and PDGFB . Maybe a pathway in Palatogenesis [50].
MEK1/2	MEK1/2 is phosphorylated in the cilium at the basal body[47].	Involved in cancers[52].
Signal Transduction		
CAMLG (Calcium signal-modulating cyclophilin ligand)	Interacts with fibrocystin and involved in calcium signalling. Interacts with fibrocystin and localizes to the primary cilium[53].	
STAT6 Signal Transducer and Activator of Transcription-6.	Involved in transcription control and in ciliary mechanosensing with Polycystin-1 , and P100 [54, 55]. Interacts with the transcription activator, the CREB-binding protein [56].	Interaction partners include many downstream proteins and pathways.
LKB1 (Serine-Threonine Kinase)	Localised to the cilium. Involved in activating the MTORC1 pathway and in cell size regulation [57].	Tumour-suppressor protein.
Purinergic P2 Receptors (P2)	ATP Activated Purinergic ATP Receptors (P2) are divided into two Families; P2X(1-7) which gate cations and P2Y(1-4,5, 11-14) which are G-coupled protein nucleotide receptors (GPCRs) for signal transduction[58, 59]. P2X receptors are heterodimeric ligand-gated channels which bind extracellular ATP and contain extracellular and membrane spanning domains within their structures[60-63]. P2Y receptors are involved in downstream signalling cascades[64]. P2 channels are involved in flow sensing in renal cilia [64]. The primary cilium appears to be necessary for flow-mediated release of ATP [65]. Cholangiocyte primary cilia detect biliary nuclides via the P2Y12 purinergic receptor[66].	There is cross talk between P1 and P2 receptor complexes[67]. There is some evidence for P family receptor complexes may be on the cilium[68]. P2X channels are susceptible to influence from cations[59] and can exhibit cross talk with other receptor types[58].
Connexin-43 Mechanosensitive ATP-release channel	Engages with lipid-raft membrane domains, known to interact with Caveolin-1 and -2 [69], found in gap junctions[70, 71]. Tight junction protein ZO-1 is associated with Connexin-43 and also localises with α	Involved with atherosclerotic plaques[73]. Articular chondrocyte cilia express Connexin 43 hemichannels and P2

	and β-tubulin [72]. Connexin-43 forms hemi-channels expressed in the primary cilium[68] where mechanical forces trigger ATP release . Expressed in the upper 200 microns of articular cartilage by connective tissue primary cilia[68].	receptors[68]. Changes in pressure on astrocytes vary the expression and phosphorylation of Connexin-43[74].
Rhodopsin (GPCR)	Fusion of Rhodopsin transport carriers to retinal photoreceptors is achieved via Ezrin and Rac2 phosphoinositides [75]. Syntaxin and SNAP-25 are involved with Rhodopsin transport carriers [76] derived from the trans-Golgi-Network , and are vectored by a ciliary-targeting complex , regulated by ARF4 and RAB11 [75, 77].	Syntaxin-3 and SNAP-25 are regulated by omega-3 docosahexaenoic acid, deliver rhodopsin for the ciliary biogenesis of rod outer segments[76].
FA2P	NIMA-related kinase . Localises to the proximal ends of the centrioles[78]. Role in axoneme deflagellation and in cell cycle [79].	
β -Arrestins (GPCR) (β -arr1 & β -arr2)	Versatile adapter proteins which bind GPCR proteins[80], where they act as scaffolds and recruiters for signaling AP2 and Clathrin . It has been proposed that β-arrestin-SRC complexes control GPCR mediated endocytosis, via ERK1/2 , JNK3 and MAP kinases [80]. β-arr2 localises to the primary cilium in quiescent cells and the centrosome in cycling cells[81]. Arrestin-β2 was found to co-localise to, and interact with 14-3-3 proteins, KIF3A [81] and also mediate the localisation of Smo [82]. Smo localisation in neuronal precursors has linked Sonic Hedgehog signalling to the cell cycle [81, 83].	Observed upon proximal ends of centrioles , associated with microtubules [81] and involved in signal transduction[84]. β -arrestins are responsible for regulating membrane bound receptors (including the majority of GPCRs) and some in the cilium, as well as for endocytosis [76, 81].
Collectrin/TMEM7 (Trans-membrane glycoprotein[186])	Localises to the cilium and basal body/pericentriolar region where it is involved in transport of vesicles. Interacts with and binds γ-actin-myosin-IIA , SNAREs , and polycystin-2-polaris complexes [85]. HNF-1β -targetted collectrin is involved in cell polarity and the maintenance of primary cilia in the renal collecting ducts, where the silencing of collectrin can result in loss of ciliary PKD2 [85, 86].	Angiotensin converting enzyme homologue (ACE-2)[85].
Septins (2, 7, 9) Filamentous guanine tri-phosphatases (GTPases)	Septins usually act as a diffusion barrier at the base of the cilium[87] where SEPT2 forms part of a diffusion barrier at the base of the ciliary membrane and is required for appropriate signalling[88] as well as control of planar cell polarity [89]. Septins 2, 7, 9 and microtubule associated protein MAP4 control ciliary length [90].	Interacts with the Exocyst components Sec6/Sec8 [91] which are required for ciliogenesis[91].
AVPR2 (Vasopressin) Arginine Vasopressin Receptor 2 (G-protein receptor)	Ciliary localisation with adenylyl cyclase (AC) type V/VI[92]. The cilium is required for vasopressin mediated transport of Aquaporin-2 (AQP2) in the renal collecting duct[93]. AVPR2 interacts with Calmodulin (for mediated Ca^{2+} mobilisation[94, 95]. Located in the primary cilium[96, 97].	Vasopressin Receptor 1A is referred as the ' Altruistic gene '[98, 99]. Role in osmo-regulation, insulin release memory and social behavior[100].
AQP2(Aquaporin2)	Localised along the ciliary shaft[93].	
AP1 (Adaptin)	Clathrin adaptor protein. Facilitates cilium formation and interacts with RAB8 for membrane transport in <i>C. elegans</i> [101].	
Bromi Broad Minded Protein	Involved in ciliary membrane assembly. Structurally links the axoneme to the membrane, interacts with IFT and is involved in the cell cycle. Influences Hedgehog signalling and membrane localisation of Gli2 [102].	
Fibrocystin (PKHD1)	The fibrocystin tail contains a ciliary targeting motif [1103] where it is found concentrated on the ciliary membrane and in the basal body area [104-106]. Undergoes Notch-like signalling (proteolytic cleavage of the extracellular domain) and regulated	Polycystin-2 and PKHD1 (fibrocystin/polyductin) are found localised together on the plasma membrane and primary cilium membrane in renal epithelia[107].

	release from the cilium[106] by ADAM (metallo-proteinase disintegrins) which cleaves the extracellular domain. Interacts with Ca²⁺ signalling protein CAML [53].	
Meckelin Type	Meckel and Nephrocystin proteins are involved within the transition zone[108].	
MKS1	A regulator of ciliary function[109], where it localises to the basal body/transition zone [110] where depletion or disruption of MKS1 and MKS3 result in ciliary and centrosomal defects[111]. MKS1 and Nesprin-2 mediate ciliogenesis via remodeling the actin cytoskeleton [112]. Murine models show MKS1 is required for Sonic-Hedgehog and ciliogenesis [113].	MKS1 mutations are associated with Meckel syndrome [114] or Bardet-Biedel syndrome [115]. Wnt signalling is influenced by MKS1 [116].
MKS2/JBTS6/C2CD3 (TMEM216)	Essential regulator of Sonic Hedgehog (Shh) and proteolytic processing of GLI3 . Localises to the basal body and ciliary membrane for intracellular transduction of the Hedgehog signals [117, 118]. Loss of TMEM216 function in mutants causes defective ciliogenesis , centrosomal docking and hyper-activation of RhoA and Disheveled [117]. Localises to the base of the cilium[117].	Mutations cause disruption of ciliogenesis[118]. Association with Meckel and Joubert Syndromes [119].
MKS3/TMEM67/JBTS6/ (Meckelin)	Putatively localises to ciliary membrane[108, 110, 112]; involved in centriole migration to the apical membrane, and with cilium formation. Requires interaction with NPHP-4 for normal ciliogenesis, chemo-taxis and ciliary length control, where it localises to the axonemal α-tubulin and to the membrane[120]. Required for ER protein-C degradation (tetraspan protein)[121]. Interacts with nesprin for ciliogenesis via remodeling actin [112].	Mutations cause loss of centriole cohesion and disruption of axonemal length regulation. Interacts with HDAC6 with a possible role in ciliary stability[122].
MKS4/JBTS5/NPHP6 (CEP290)	Involved in the formation of microtubule-to-membrane linkers in the transition zone where it may be involved in ciliary transport[123]. Localises to the cilium and centrosome[124] in a cell-cycle dependent manner [126]. Interacts with centriolar satellite protein PCM1 [127], which is required for RAB8 localisation as PCM-1 has a vital role in the microtubule organisation network. Loss of CEP290 causes loss of the MTOC network and results in defects of ciliary biogenesis and protein composition of photoreceptors [123-125]. Interacts with RPGR [124] and is expressed in all cilia[128, 129].	Transition zone membrane to microtubule linker[123]. See Rachel et al., (2012)[124]. Loss of CEP290 function leads to anosmia caused by the selective loss of G-proteins in sensory cilia and olfactory neurons[130].
MKS5/JBTS7/NPHP8	Interacts with NPHP4 and NPHP6 [131]; localises to basal bodies and the axoneme[132].	RPGRIP1L gene is mutated in Joubert Syndrome Type-B [132].
MKS6 /JST9 (CC2D2A)	Contains calcium binding domains ; localises to the transition zone ; has involvement in Opsin vesicle transport to the outer segments of photoreceptor rods and cones. Suggested that it facilitates protein transport through the role of RAB8 [133].	
MKS7	See NPHP3.	
TRPP-Family	Transient Receptor Potential Channels	
TRPP1 (PKD1) Polycystin-1	GPCR-activated channel . Polycystin-1 contains large extracellular glycoprotein binding domains in the ciliary membrane[134-136]. Interacts with Polycystin-2 (TRPP2) [136] where variations in the amounts of Polycystin-1 and 2 regulate pressure sensing [137] and is found co-localised on renal cilia[135, 138]. Involved in skeleto-genesis through stimulating RUNX2-II [139].	PKD1 and PKD2 are ciliary mechanosensors . Activated by shear stress and flow and involved in renal cystic disease[135, 137, 138, 140].
TRPP2 (PKD2) Polycystin-2	Localises to the primary cilium[141, 142]. Interacts with channel TRPC1 [143] and PKD1 [136]. TRPP2 and	PKD1 and PKD2 function as ciliary mechanosensors (shear stress,

	TRPC1 assemble to form a GPCR channel involving TRPP2 in mechano-sensation and cilium-based Ca²⁺ signalling [144]. Polycystin-2 interacts with filamin-A [150] and is also involved in pressure sensing[137, 145]. Polycystin-2 and TRPV4 form modal sensory channel[146]. Functions together with mucolipins TRPML [147].	flow and pressure activated[137]). Mutations are associated with retinal and renal defects[138, 142, 147, 149]. Probable mechano-transductive extracellular matrix-cell membrane receptor [150].
TRPP3/4/5	TRPP3/PKD2L2 may be expressed on kinocilia (with the role of 4 and 5 being poorly understood)[148]. TRPP3 / PKD2L1 functions as a sour taste receptor [151, 152].	Inhibited by amiloride [152].
TRPC Family (Transient Receptor Cation Channels)	Family members interact forming channels. TRPC2 associates with no known family members; however TRPC1 forms channels with TRPC4 and TRPC5 , while others form homo- or hetero-dimers TRPC4/5 and TRPC3/6/7 [153].	
TRPC1	GPCR-activated channel localised to the ciliary membrane in renal epithelial cells[149]. Interacts with PKD2 [154, 155], TRPC3 [156] and TRPC5 [156]. TRPP2 and TRPC1 form a heterotetramer complex [144]. Interacts with RhoA [157] TRPP1 , IP3 , Caveolin-1 , and PMCA [158, 159].	Ion channel activated by Ca²⁺ [159]. Characterised upon the primary cilium[134].
TRPC2	Interacts with TRPC6 (for erythropoietin control of Ca²⁺ flux)[160], with Calmodulin , IP3 and Enkurin [161, 162].	
TRPC3 (Possibly on cilia)	Erythropoietin regulated calcium channel[164, 165]. Interacts with TRPC1 and TRPC6 [153, 166]. Erythropoietin controls TRPC3 activation with IP3 and PLCγ [165], whilst protein kinase-C can inhibit TRPC3 channels[166, 167].	Pore forming signalling molecule involved in vaso-regulation [166]. TRPC3 and TRPC6 form mechano-transductive channels[168].
TRPC6 (Possibly on cilia)	Suspected upon cilia[160], but not proven.	
TRPM-Family	Transient Receptor Potential Mucopolypins	
TRPM1/MCHR1 (Melanin concentrating hormone receptor MCHR1)	Involved in the regulation of feeding and energy balance[169, 170]. Required for the depolarised light response of retinal cells [171, 172]. Localises to cilia and possibly regulates feeding behaviour and body-weight[169].	Possibly involved in satiety , obesity [169, 170] and melanoma progression[159].
TRPM2 (suspected on primary cilia)	Involved in insulin secretion[173] through cyclic ADP-ribose; Interacts with calmodulin and cADP-ribose hydrolase [159]. TRPM2 and TRPC5 detect oxidative stress inducing gene expression[176].	TRP Cation channel, function enhanced by hypo-osmolarity [159]. Involved in bipolar disorder [174].
TRPM3 (suspected on primary cilia)	Activated by the steroid pregnenolone sulphate and Ca²⁺ resulting in insulin release from β-islet cells [177, 178]. Hypotonic pressure sensor cation channel which results in cytoskeletal re-organisation[179]. Potential channel for renal Ca²⁺ absorption[159].	Volume regulated cation channel[179]. Potential renal role for Ca²⁺ absorption [159].
TRPM4 (suspected on primary cilia)	Melastatin-4 is a Ca²⁺ -activated non-selective cation channel[179-181]. Interacts with calmodulin , SUR1 [159]. Involved in dendritic cell migration[182].	Loss involved in increased anaphylactic responses[181].
TRPM5	Involved in taste sensation and insulin release [183, 184]. Regulated by PIP2 [185]. Expressed on olfactory cilia [186]. Regulates mucin secretion in goblet cells[187].	Impermeable to Ca²⁺ -/- murines cannot detect sweat , bitter or umami flavours [159].
TRPM6 (suspected on primary cilia)	Expressed on olfactory cilia[186]. Involved in Mg²⁺ transport[188] and is sensitive to acid pH [159, 189]. Interacts with TRPM7 [159, 190], and PIP2 [190]. Inhibited by Ruthenium Red [159].	Defects involved with hypomagnesia[188].
TRPM7 (suspected on P primary cilia)	Both an ion channel and a kinase (dependent upon intracellular ATP) capable of phosphorylating itself and translation factors eEF2 via eEF2-k [191]. Interacts with PLCβ1/2/3 , PLC-γ , TRMP6 [159] and is sensitive to	Involved in vascular hypertension[192].

	acid pH [159, 189].	
TRPM8 (suspected on primary cilia)	Involved in pain response. TRPM8 couples with TRPV1 and TRPA1 to inhibit their mechano-sensory and chemosensory functions[193]. Expressed on olfactory cilia[186].	
TRPML3	Similar intracellular localisation to TRPA1 ; mutations result in hearing loss in stereo-cilia[194]. Suspected role in cilia 'membrane to membrane' inter-connecting fibres[195]. Interacts with TRPML1 and TRPML2 [159].	pH sensitive channel[186].
TRPV-Family (Vanilloid)	Transient Receptor Potential Cation Channel	
TRPV1 (suspected on primary cilia)	Thermo-sensitive ion channel . Interactions with Calmodulin [196, 197] and tubulin, where TRPV1 C-terminal preferably binds with β-tubulin and less strongly with α-tubulin [198]. Antagonists involved in neuropathic pain, and the channel is involved in body temperature maintenance[196, 199]. Also involved in infra-red detection[200].	Non selective cation channel in nociceptive neurons of PNS and CNS . Hypotonicity and stretch activated[196]. Implicated in renal hypertension[138].
TRPV2 (suspected on primary cilia)	Thermo-sensitive ion channel involved in intracellular Ca^{2+} regulation[201]; regulated by insulin in pancreatic β -cells[202]. Blocked by Ruthenium Red and Lanthanum [159, 202] but activated by probenecid and cannabidiol [203].	Activated at temperatures $T > 53^{\circ}C$, hypotonicity, and possibly stretch[159].
TRPV3 (suspected on primary cilia)	Thermo-sensitive ion channel . Interacts with TRPV1 , expressed in skin, keratocytes and brain[148, 204]. Inhibited by Ruthenium Red [159].	Activated by $T > 30^{\circ}C$, vanilla and camphor type compounds[159].
TRPV4	Tyrosine protein ligase Lyn [205] provide a link between TRPV4 and the microtubular cytoskeleton in mechano-sensation [206]. Binds calmodulin [207]. TRPV4 is involved in osmolarity sensing[159]. Cholangiocyte primary cilia express TRPV4 and can detect changes in tonicity [208]. Interacts with TRPP2 (PC2) [209], MAP7 [210], aquaporin-5 [211], Calmodulin , and Pacsin3 (inhibits endocytosis)[212]	Hypotonicity and stretch activated, inhibited by Ruthenium Red [159, 208, 213]. TRPV4 is an osmo-sensitive channel in porcine chondrocytes[214].
TRPV5 (suspected on primary cilia)	Calcium selective channel, interacts with the Annexin-2-complex (p11)[215]. Involved in renal calcium re-absorption[216]. Interacts with TRPV6 and RAB11A [159]. Inhibited by Ruthenium Red , Mg²⁺ and Pb²⁺ [159].	Defects cause idiopathic hypercalciuria [138, 217]. Constitutively active[159].
TRPV6 (suspected on primary cilia)	Expression vitamin-D dependent (increased presence resulted in increased expression[218, 219]). Interacts with TRPV5 , Annexin II , and RAB11A (inhibited by Ruthenium Red)[159].	Role in cancer[219].
Other Channels/Receptors		
TRPA1 (suspected on primary cilia) (Transient receptor potential ankyrin-1[428])	Stress receptor ion channel[220], sensitive to range of chemical stimuli[221, 222], involved in pain response and hearing[223], blocked by gadolinium , amiloride , gentamicin , and Ruthenium Red [159, 223]. Involved in infra-red detection [224], mechanical and cold sensation [225].	Mechano-stress receptor/ Ca^{2+} channel in stereocilia[223, 226]. Conflicting mechanosensitive evidence[183].
Taurine Transporter (SLC6A6)	Na^{+} -dependent taurine transporter is localized to the primary cilium. Regulates cell volume , oxidative stress and Ca^{2+} levels[227].	
Note	For review of thermo-TRP ion channels see Wu et al., (2010)[377]. TRPV1 , TRPV2 , TRPV3 , TRPV4 , TRPM2 , TRPM4 , TRPM5 , TRPM8 , and TRPA1 are thermo sensitive TRP channels[228].	
Opsin	Membrane-bound G-protein receptors [229] which are transported via a connecting cilium to the ciliary photoreceptor stack [230].	Evolutionary functions in the brain[231].

ENac (Epithelial Sodium Channel)	Located on some ciliary membranes, permeable to Na⁺ ions[232]. Characterised upon primary cilia[233].	
ATP-2 (ATP synthase)	β -subunit of the ATP synthase interacts with LOV-1 and is involved in Polycystin-1 (PKD-1) signalling in <i>C. elegans</i> [234]. ATP indirectly activates the cilia conductance[235].	Part of a complex ATP synthesis and export system. Extracellular ATP drives a number of cilia related processes[236].
AC3(Adenylate Cyclase-3)	Expressed in the primary cilium in hippocampal neurons of the central nervous system . Somatostatin Receptor-3 SSTR3 is coupled into regulation of AC3 . Implicated in impaired learning, contextual conditioning and memory [39]. Li⁺ increases cilium length three fold by inhibiting AC3 [237].	Implicated in a host of neurological conditions. Suggests AC3 is involved in regulating primary cilia length [237].
AC4 (Adenylyl Cyclase-4)	Identified on the cilium[66].	
AC6 (Adenylyl Cyclase-6)	Involved in mechano-sensing in bone cells. Signal is transduced through Adenylate Cyclase-6 and cAMP . AC6 localises to the primary cilium, where activation from deflection by flow decreases cAMP and upregulates COX expression[238].	
AC8 (Adenylyl Cyclase-8)	Identified in the cilium[66].	
Galectins	Contain carbohydrate recognising domains specific for binding β-galactosides [239, 240]. Gal-3 localises exclusively to the primary cilium/centrosome and modulates cyst growth [240-242], Gal-7 localises to the cilium and modulates renal ciliary length and wound repair [243], Gal8 reportedly binds to integrins inhibiting cell adhesion and inducing apoptosis[244], however is unknown at present in the cilium.	Mediates the recognition of N-acetyl-galactosamine-containing glycoproteins . Mutation of NEK8 over-expresses Gal-1, sorcin and vimentin and urinary proteins in JCK murine renal cysts [240].
ARL13B (ADP-ribosylation factor-like protein-2-like 1)/JBTS8	ARF-Family GTPase ARL13B [245]. Required for ciliogenesis and sonic Hedgehog signalling . Interacts with membranes and IFT machinery involved in ciliary formation and maintenance[245, 246]. Found localised at the proximal end of the cilium associated with membranes through palmitoylation modification regulating trans-membrane proteins localisation and anterograde IFT stability [245]. In mutated forms (Jouberts), PKD2 is elevated, destabilising anterograde IFT [243].	Defects in ARL13B result in aberrant Shh signalling from BMPs and result in neural tube defects[247].
INPP5E/JBTS1 phosphatidylinositol-4,5-bisphosphate 5-phosphatase	Peripheral membrane protein which localises to the primary cilium and is involved in its formation[248-250]. ARL13B, PDE6D , and CEP164 form a network for INPP5E ciliary targeting[251].	Mutations in INPP5E cause primary cilium signalling defects causing ciliary instability and disease[453].
TMEM216/JBTS2	Trans-membrane protein localised to the base of the primary where it is proposed to be possibly with RhoA and Dishevelled signalling[117].	Mutations result in defective ciliogenesis[117].
AHI1/JBTS3	Interacts with nephrocytin-1 , expressed in cell-cell junctions, centrosomes, basal bodies and on primary cilia[252]. Colocalises with aquaporin-2 .	Associated with Schizophrenia [253] and Joubert Syndrome [254].
CRMP-2	Localises to the axoneme and basal body in fibroblasts. It is also involved with axon formation, neurite outgrowth and elongation in neuronal cells[255].	Involved with GSK-3β .
Par3 / Par6 / aPKC polarity cassette	The Crumbs -associated Par3/Par6/aPKC polarity cassette localises to cilia and regulates ciliogenesis[256].	
CRB3 (Crumbs)	Localises to cilia of renal epithelia[257]. Crumbs3 binds importin-β2 regulating ciliogenesis and cell division[257].	
Exocyst (EXCO1-8)	A multi-subunit rod-like complex involved in docking of post Golgi transport vesicles , membrane remodelling, cytoskeletal activation and desmosome	Components formerly known as Sec3 (EXCO1), Sec5 (EXCO2), Sec6 (EXCO3), Sec8 (EXCO4),

	assembly[258]. Localises to the primary cilium [16]. RAB10 interacts with the primary cilium and Exocyst[259] components; Sec15 (as an effector of Rab11 GTPase [22]), Sec10 (which is vital for ciliogenesis[19]) and Sec8 (is involved in binding to lipid rafts and vesicles [260]). Sec5 is involved in vesicle transport and in tethering vesicles to membranes [261, 262]. Sec10 interacts with PC2 [24].	Sec10 (EXCO5), Sec15 (EXCO6), Exo70 (EXCO7) and Exo84 (EXCO8). The RalB/Sec5 effector complex directly recruits and activates IkappaB-kinase family member TBK1 (innate immunity and cancer)[262]. See Septins .
Sonic Hedgehog Signalling	The Hedgehog Signalling family comprises three members: Indian , Sonic and Desert . Shh are morphogens responsible for signalling and patterning development[263-265]. Dysregulation of Hh signalling is involved in a broad range of conditions and disease[113, 266]. Interference of Sonic Hedgehog (specifically GLI signalling[267]) causes inhibition of cancer cell proliferation and tumour formation[267, 268]. Interacts with IFT122 [269] and inhibits p16 [270].	Implicated in synovial chondromatosis [271]. The Shh pathway is a target for clinical treatment of various diseases[272].
Smo (Smoothened)	Essential G-protein-receptor involved with Sonic Hedgehog pathway [273, 272] located in the primary cilium[275-277]. The Smo tail is involved with cAMP dependent kinases , and is extensively phosphorylated [277]. Involved in vesicle transport [278] Loss of retrograde IFT disrupts localisation of Smo preventing activator and repressor of Gli function [279]. Patched acts indirectly to regulate Smo function[280], in which Patch (Ptc) and Smoothened are transduction components of the Hedgehog receptor complex[281], suggesting Patched binds Hh without assistance from Smo , favouring Hh/PTCH1 binding inducing conformation release of Smo [281]. Smo is the teratogenic target of cyclopamine [276, 282].	
SuFu (Suppressor of Fused)	Smo activates Gli which is inhibited by dual binding mechanisms (SuFu)[283]. Hh stimulation releases SuFu in the cilium, since Hh dissociates the SuFu-Gli complex allowing Gli to target the nucleus [284, 285]. Protein-Kinase A (PKA) inhibits Shh signalling[284]. Interacts with Gli1 [285], Gli3 [286] and mediates the Gli3/SuFu/GSK3-β complex [286].	SuFu forms Gli-SuFu complexes within the cilium. Hh causes dissociation of permitting Gli to activate nuclear transcription pathways[284].
Patched/PTCH1	PTCH1 suppresses Hh signalling pathway by preventing trafficking of Smo into the cilium. On binding of the Hh ligand to PTCH1 , Smo relocates to the cilium[276] where it is responsible for activating the Hh pathway[287]. Smoothened and Patched are found in lipid raft domains. Patched interacts with Caveolin , but Smoothened does not[288]. Localises to cilia inhibiting Smo accumulation[289].	The sterol-sensing domain of Patched may be involved in vesicular trafficking in Smoothened regulation [278].
Gli1	Gli is a Hedgehog Signalling pathway effector [290, 291]. Involved in regulating transcription, cell fate determination and extra cellular sensing . Interacts with SuFu [285, 292, 293] and Shh activation of Gli1 is controlled by Gli3 [291]. KIF7 is a regulator of Gli transcription factors[294, 295].	Associated with cancers[296] and synovial chondromatosis [297].
Gli2 (α, β, γ and δ)	Transcriptional mediators of Shh signalling . GLI2 activates cytoplasmic PTCH1 [298, 299]. GLI2 is able to promote G1-S-phase progression[299], however it requires IFT component Polaris to function[298]. There are implications for Gli2 in cancer[300, 301]. Involved in neuronal patterning[302]. Localises to the primary cilium tip [298] being controlled by Broad Minded kinase BROMO [102]. Gli2 transcription factor binds and inhibits the p16 promoter[302].	Involved with polydactyly [303]. Gli1 and Gli2 are part of a positive-feedback mechanism in Basal Cell Carcinoma [304].

Gli3	Transcription repressor, full-length Gli3 localises at the tip of the cilium [305] and required for IFT Polaris to function[298]. Gli3 is an activator for Gli1 [291, 306], and interacts with SuFu in Hedgehog Signalling[307].	Pallister-Hall Syndrome [308].
Wnt Signalling	Wnt signalling factors are involved in cell-proliferation and differentiation. Wnt proteins interact with multiple receptors and pathways including the canonical Wnt/β-catenin pathway of transcription co-activator β -catenin. The non-canonical Wnt /planar cell polarity (PCP) pathway is involved with development[309-311].	
Frizzled Family(FZD1-10)	G-protein receptor family, trans-membrane domain proteins which act as receptors for Wnt signalling[230, 312]. Transmembrane receptors of FZD1-10 , LRP5 , LRP6 and ROR2 transduce WNT signals through endocytosis involving Caveolin or Clathrin [313, 314]. Wnt signals are involved in regulation of planar cell polarity , cell adhesion , and motility . CD44 and vimentin gene components of the non-Canonical WNT cascade [313]. These are part of, and interact with, Notch , FGF , BMP and Hedgehog signalling cascades [313, 314]. Frizzled activates cytoplasmic Disheveled [315].	Frizzled Family Members are expressed differentially in tissues and are being explored as platforms for tissue engineering [313].
Disheveled (Dvl)	Regulates canonical and non-canonical Wnt-β-catenin and planar cell polarity pathways; involved with basal body polarization and apical docking[316, 317] Dvl and Inturned mediate activity of Rho-GTPase upon basal bodies directing docking to the apical membrane. Docking also involves membrane bound vesicles and the vesicle trafficking protein Sec8 [318]. Interacts with Frizzled [315, 316].	Required for ciliogenesis
Chibby	Wnt/β-Catenin Pathway antagonist Chibby binds Conexin at the distal end of the basal body and functions in primary cilium formation [319]. Required for ciliogenesis and centriole formation in <i>Drosophila</i> but not WNT signalling[320].	
INV	Acts as a molecular anchor for NPHP3 and NEK8 in the proximal segment of the cilium[321].	
Notch Signalling		
Notch	Notch receptors and processing enzymes are co-localised with cilia[238]. Notch1 and 2 modify endochondral ossification in chondrocytes[323] as well as chondrogenic differentiation[324]. Notch signalling regulates imposition of left-right-asymmetry through ciliary length control[325], and suppresses nuclear factor NFat in T-cells and Nfatc in chondrocytes[326].	Involved in osteoarthritis [322].

[1] Littlewood Evans A, Müller U. (2000) Stereocilia defects in the sensory hair cells of the inner ear in mice deficient in integrin $\alpha 8 \beta 1$. *Nature Genetics*, **24**, 424-428.

[2] McGlashan SR, Jensen CG, Poole CA. (2006) Localisation of extracellular matrix receptors on the chondrocyte primary cilium. *Journal of Histochemistry and Cytochemistry*, **54**, 1005-1014.

[3] Praetorius HA, Praetorius J, Nielsen S, Frokiaer J, Spring KR. (2004) $\beta 1$ -integrins in the primary cilium of MDCK cells potentiate fibronectin-induced Ca^{2+} signalling. *American Journal of Physiology*, **287**, F969-F978.

[4] Brauchi S, Orio P, Latorre R. (2004) Clues to understanding cold sensation: Thermodynamics and electrophysiological analysis of the cold receptor TRPM8. *Proceedings of the National Academy of Sciences, USA*, **101**, 15494-15499.

- [5] Kurtis MS, Schmidt TA, Bugbee WD, Loeser RF, Sah RL. (2003) Integrin-mediated adhesion of human articular chondrocytes to cartilage. *Arthritis and Rheumatology*, **48**, 110-118.
- [6] Fukushi J, Makagiansar IT, Stallcup WB (2004) NG2 proteoglycan promotes endothelial cell motility and angiogenesis via engagement of galectin-3 and alpha3beta1 integrin. *Molecular Biology of the Cell*, **15**, 3580-3590.
- [7] Stegmüller J, Werner H, Nave KA, Trotter J (2003) The proteoglycan NG2 is complexed with alpha-amino-3-hydroxy-5-methyl-4-isoxazolepropionic acid (AMPA) receptors by the PDZ glutamate receptor interaction protein (GRIP) in glial progenitor cells. Implications for glial-neuronal signalling. *Journal of Biological Chemistry*, **278**, 3590-3598.
- [8] Stallcup WB, Huang FJ. (2008) A role for the NG2 proteoglycan in glioma progression. *Cell Adhesion and Migration*, **2**, 192-201.
- [9] Burg MA, Pasqualini R, Arap W, Ruoslahti E, Stallcup WB. (1999) NG2 proteoglycan-binding peptides target tumour neovasculature. *Cancer Research*, **59**, 2869-2874.
- [10] Mak HY, Nelson LS, Basson M, Johnson CD, Ruvkun G. (2006) Polygenic control of *Caenorhabditis elegans* fat storage. *Nature Genetics*, **38**, 363-368.
- [11] Mukhopadhyay A, Deplancke B, Walhout AJ, Tissenbaum HA. (2005) *C. elegans* tubby regulates life span and fat storage by two independent mechanisms. *Cell Metabolism*, **2**, 35-42.
- [12] North MA, Naggert JK, Yan Y, Noben-Trauth K, Nishina PM. (1997) Molecular characterization of TUB, TULP1, and TULP2, members of the novel tubby gene family and their possible relation to ocular diseases. *Proceedings of the National Academy of Sciences, USA*, **94**, 3128-3133.
- [13] Hagstrom SA, Adamian M, Scimeca M, Pawlyk BS, Yue G, Li T. (2001) A role for the Tubby-like protein 1 in rhodopsin transport. *Investigative Ophthalmology and Visual Science*, **42**, 1955-1962.
- [14] Mukhopadhyay S, Wen X, Chih B, Nelson CD, Lane WS, Scales SJ, Jackson PK. (2010) TULP3 bridges the IFT-A complex and membrane phosphoinositides to promote trafficking of G protein-coupled receptors into primary cilia. *Genes and Development*, **24**, 2180-2193.
- [15] Xi Q, Pauer GJ, Marmorstein AD, Crabb JW, Hagstrom SA. (2005) Tubby-like protein 1 (TULP1) interacts with F-actin in photoreceptor cells. *Investigative Ophthalmology and Visual Science*, **46**, 4754-4761.
- [16] Rogers KK, Wilson PD, Snyder RW, Zhang X, Guo W, Burrow CR, Lipschutz JH. (2004) The exocyst localises to the primary cilium in MDCK cells. *Biochemical and Biophysical Research Communications*, **319**, 138-143.
- [17] Overgaard CE, Sanzone KM, Spiczka KS, Sheff DR, Sandra A, Yeaman C. (2009) Deciliation is associated with dramatic remodeling of epithelial cell junctions and surface domains. *Molecular Biology of the Cell*, **20**, 102-113.
- [18] Zuo X, Fogelgren B, Lipschutz JH. (2011) The small GTPase Cdc42 is necessary for primary ciliogenesis in renal tubular epithelial cells. *Journal of Biological Chemistry*, **286**, 22469-22477.
- [19] Zuo X, Guo W, Lipschutz JH. (2009) The exocyst protein Sec10 is necessary for primary ciliogenesis and cystogenesis *in vitro*. *Molecular Biology of the Cell*, **20**, 2522-2529.

- [20] Westlake CJ, Baye LM, Nachury MV, Wright KJ, Ervin KE, Phu L, Chalouni C, Beck JS, Kirkpatrick DS, Slusarski DC, Sheffield VC, Scheller RH, Jackson PK. (2011) Primary cilia membrane assembly is initiated by Rab11 and transport protein particle II (TRAPP2) complex-dependent trafficking of Rabin8 to the centrosome. *Proceedings of the National Academy of Sciences, USA*, **108**, 2759-2764.
- [21] Knödler A, Feng S, Zhang J, Zhang X, Das A, Peränen J, Guo W. (2010) Coordination of Rab8 and Rab11 in primary ciliogenesis. *Proceedings of the National Academy of Sciences, USA*, **107**, 6346-6351.
- [22] Zhang XM, Ellis S, Sriratana A, Mitchell CA, Rowe T. (2004) Sec15 is an effector for the Rab11 GTPase in mammalian cells. *Journal of Biological Chemistry*, **279**, 43027-43034.
- [23] Choi SY, Chacon-Heszele MF, Huang L, McKenna S, Wilson FP, Zuo X, Lipschutz JH. (2013) Cdc42 deficiency causes ciliary abnormalities and cystic kidneys. *Journal of the American Society of Nephrology*, **24**, 1435-1450.
- [24] Fogelgren B, Lin SY, Zuo X, Jaffe KM, Park KM, Reichert RJ, Bell PD, Burdine RD, Lipschutz JH. (2010) The exocyst protein Sec10 interacts with polycystin-2 and knockdown causes PKD-phenotypes. *PLoS Genetics*, **7**(4):e1001361.
- [25] Tao B, Bu S, Yang Z, Siroky B, Kappes JC, Kispert A, Guay-Woodford LM. (2009) Cystin localises to primary cilia via membrane microdomains and a targeting motif. *Journal of the American Society of Nephrology*, **20**, 2570-2580.
- [26] Wu M, Yang C, Tao B, Bu S, Guay-Woodford LM. (2013) The ciliary protein Cystin forms a regulatory complex with Necdin to modulate Myc expression. *PLoS One*, **8**(12):e83062.
- [27] Chae TH, Kim S, Marz KE, Hanson PI, Walsh CA. (2004) The *hyh* mutation uncovers roles for alpha Snap in apical protein localisation and control of neural cell fate. *Nature Genetics*, **36**, 264-270.
- [28] McMahon HT, Missler M, Li C, Südhof TC. (1995) Complexins: cytosolic proteins that regulate SNAP receptor function. *Cell*, **83**, 111-119.
- [29] Teilmann SC, Christensen ST. (2005) Localization of the angiotensin receptors Tie-1 and Tie-2 on the primary cilia in the female reproductive organs. *Cell Biology International*, **29**, 340-346.
- [30] Chan B, Yuan HT, Ananth Karumanchi S, Sukhatme VP. (2008) Receptor tyrosine kinase Tie-1 over expression in endothelial cells upregulates adhesion molecules. *Biochemical and Biophysical Research Communications*, **371**, 475-479.
- [31] Woo KV, Qu X, Babaev VR, Linton MF, Guzman RJ, Fazio S, Baldwin HS. (2011) Tie1 attenuation reduces murine atherosclerosis in a dose-dependent and shear stress-specific manner. *Journal of Clinical Investigation*, **121**, 1624-1635.
- [32] Staton CA, Valluru M, Hoh L, Reed MW, Brown NJ. (2010) Angiotensin-1, angiotensin-2 and Tie-2 receptor expression in human dermal wound repair and scarring. *British Journal of Dermatology*, **163**, 920-927.
- [33] Fasciani A, Quilici P, Biscaldi E, Flamini M, Fioravanti A, Orlandi P, Oliviero J, Repetti F, Bandelloni R, Danesi R, Simoncini T, Bocci G (2010) Overexpression and functional relevance of somatostatin receptor-1, -2, and -5 in endometrium and endometriotic lesions. *Journal of Clinical Endocrinology and Metabolism*, **95**, 5315-5319.

- [34] Lai CK, Gupta N, Wen X, Rangell L, Chih B, Peterson AS, Bazan JF, Li L, Scales SJ. (2011) Functional characterization of putative cilia genes by high-content analysis. *Molecular Biology of the Cell*, **22**, 1104-1119.
- [35] Iwanaga T, Takashi Miki T, Takahashi-Iwanaga H. (2011) Restricted expression of somatostatin receptor 3 to primary cilia in the pancreatic islets and adenohypophysis of mice. *Biomedical Research*, **32**, 73-81.
- [36] Berbari NF, Johnson AD, Lewis JS, Askwith CC, Mykytyn K. (2008) Identification of ciliary localisation sequences within the third intracellular loop of G protein-coupled receptors. *Molecular Biology of the Cell*, **19**, 1540-1547.
- [37] Yoon SH, Ryu JY, Lee Y, Lee ZH, Kim HH. (2011) Adenylate cyclase and calmodulin-dependent kinase have opposite effects on osteoclastogenesis by regulating the PKA-NFATc1 pathway. *Journal of Bone and Mineral Research*, **26**, 1217-1229.
- [38] Einstein EB, Patterson CA, Hon BJ, Regan KA, Reddi J, Melnikoff DE, Mateer MJ, Schulz S, Johnson BN, Tallent MK. (2010) Somatostatin signalling in neuronal cilia is critical for object recognition memory. *Journal of Neuroscience*, **30**, 4306-4314.
- [39] Wang Z, Phan T, Storm DR. (2011) The type 3 Adenylyl Cyclase is required for novel object learning and extinction of contextual memory: role of cAMP signalling in primary cilia. *Journal of Neuroscience*, **31**, 5557-5561.
- [40] Helboe L, Møller M. (1999) Immunohistochemical localisation of somatostatin receptor subtypes sst1 and sst2 in the rat retina. *Investigative Ophthalmology and Vision Science*, **40**, 2376-2382.
- [41] Jin H, White SR, Shida T, Schulz S, Aguiar M, Gygi SP, Bazan JF, Nachury MV. (2010) The conserved Bardet-Biedl syndrome proteins assemble a coat that traffics membrane proteins to cilia. *Cell*, **141**, 1208-1219.
- [42] König P, Krain B, Krasteva G, Kummer W. (2009) Serotonin increases cilia-driven motion via an acetylcholine-independent pathway in the mouse trachea. *PLoS One*, **4**(3):e4938.
- [43] Brailov I, Bancila M, Brisorgueil MJ, Miquel MC, Harmon M, Verge D. (2000) Localisation of 5-HT(6) receptors at the plasma membrane of neuronal cilia in the rat brain. *Brain Research*, **872**, 271-275.
- [44] Wu J, Du H, Wang X, Mei C, Sieck GC, Qian Q. (2009) Characterization of primary cilia in human airway smooth muscle cells. *Chest*, **136**, 561-570.
- [45] Ma R, Li WP, Rundle D, Kong J, Akbarali HI, Tsiokas L. (2005) PKD2 functions as an epidermal growth factor-activated plasma membrane channel. *Molecular and Cellular Biology*, **25**, 8285-8298.
- [46] Yeh C, Li A, Jen-Zen Chuang J, Saito M, Caceres A, Sung C. (2013) IGF-1 activates a cilium-localized noncanonical Gbg signaling pathway that regulates cell-cycle progression. *Developmental Cell*, **26**, 358-368.
- [47] Schneider L, Clement CA, Teilmann SC, Pazour GJ, Hoffmann EK, Satir P, Christensen ST. (2005) PDGFRalpha signalling is regulated through the primary cilium in fibroblasts. *Current Biology*, **15**, 1861-1866.

- [48] Schneider L, Stock C, Dieterich P, Jensen BH, Pedersen B, Satir P, Schwab A, Christensen ST, Pedersen SF. (2009) The Na⁺/H⁺ exchanger NHE1 is required for directional migration stimulated via PDGFR- α in the primary cilium. *Journal of Cell Biology Home Archive*, **185**, 163-176.
- [49] Michaud EJ, Yoder BK. (2006) The primary cilium in cell signalling and cancer. *Cancer Research*, **66**, 6463-6467.
- [50] Choi SJ, Marazita ML, Hart PS, Sulima PP, Field LL, McHenry TG, Govil M, Cooper ME, Letra A, Menezes R, Narayanan S, Mansilla MA, Granjeiro JM, Vieira AR, Lidral AC, Murray JC, Hart TC. (2009) The PDGF-C regulatory region SNP rs28999109 decreases promoter transcriptional activity and is associated with CL/P. *European Journal of Human Genetics*, **17**, 774-784.
- [51] Gilbertson DG, Duff ME, West JW, Kelly JD, Sheppard PO, Hofstrand PD, Gao Z, Shoemaker K, Bukowski TR, Moore M, Feldhaus AL, Humes JM, Palmer TE, Hart CE. (2001) Platelet-derived growth factor C (PDGF-C), a novel growth factor that binds to PDGF α and β receptor. *Journal of Biological Chemistry*, **276**, 27406-27414.
- [52] Frémin C, Meloche S. (2010) From basic research to clinical development of MEK1/2 inhibitors for cancer therapy. *Journal of Hematological Oncology*, **3**, 8.
- [53] Nagano J, Kitamura K, Hujer KM, Ward CJ, Bram RJ, Hopfer U, Tomita K, Huang C, Miller RT. (2005) Fibrocystin interacts with CAML, a protein involved in Ca²⁺ signaling. *Biochemical and Biophysical Research Communications*, **338**, 880-889.
- [54] Low SH, Vasanth S, Larson CH, Mukherjee S, Sharma N, Kinter MT, Kane ME, Obara T, Weimbs T. (2006) Polycystin-1, STAT6, and P100 function in a pathway that transduces ciliary mechanosensation and is activated in polycystic kidney disease. *Developmental Cell*, **10**, 57-69.
- [55] Paukku K, Yang J, Silvennoinen O. (2003) Tudor and nuclease-like domains containing protein p100 function as coactivators for signal transducer and activator of transcription 5. *Molecular Endocrinology*, **17**, 1805-1814.
- [56] Välineva T, Yang J, Palovuori R, Silvennoinen O. (2005) The transcriptional co-activator protein p100 recruits histone acetyltransferase activity to STAT6 and mediates interaction between the CREB-binding protein and STAT6. *Journal of Biological Chemistry*, **280**, 14989-14996.
- [57] Boehlke C, Kotsis F, Patel V, Braeg S, Voelker H, Bredt S, Beyer T, Janusch H, Hamann C, Gödel M, Müller K, Herbst M, Hornung M, Doerken M, Köttgen M, Nitschke R, Igarashi P, Walz G, Kuehn EW. (2010) Primary cilia regulate mTORC1 activity and cell size through Lkb1. *Nature Cell Biology*, **12**, 1115-1122.
- [58] Abbracchio MP, Burnstock G, Boeynaems JM, Barnard EA, Boyer JL, Kennedy C, Knight GE, Fumagalli M, Gachet C, Jacobson KA, Weisman GA. (2006) International Union of Pharmacology LVIII: update on the P2Y G protein-coupled nucleotide receptors: from molecular mechanisms and pathophysiology to therapy. *Pharmacology Reviews*, **58**, 281-341.
- [59] Gever JR, Cockayne DA, Dillon MP, Burnstock G, Ford AP. (2006) Pharmacology of P2X channels. *European Journal of Physiology*, **452**, 513-537.
- [60] North RA. (2002) Molecular physiology of P2X receptors. *Physiology Reviews*, **82**, 1013-1067.
- [61] Egan TM, Samways DS, Li Z. (2006) Biophysics of P2X receptors. *European Journal of Physiology*, **452**, 501-512.

- [62] Roberts JA, Vial C, Digby HR, Agboh KC, Wen H, Atterbury-Thomas A, Evans RJ. (2006) Molecular properties of P2X receptors. *European Journal of Physiology*, **452**, 486-500.
- [63] Nicke A, Baumert HG, Rettinger J, Eichele A, Lambrecht G, Mutschler E, Schmalzing G. (1998) P2X1 and P2X3 receptors form stable trimers: a novel structural motif of ligand-gated ion channels. *EMBO Journal*, **17**, 3016-3028.
- [64] Praetorius HA, Leipziger J. (2009) Released nucleotides amplify the cilium-dependent, flow-induced $[Ca^{2+}]$ response in MDCK cells. *Acta Physiologica*, **197**, 241-251.
- [65] Leipziger J. (2011) Luminal nucleotides are tonic inhibitors of renal tubular transport. *Current Opinion in Nephrology and Hypertension*, **20**, 518-522.
- [66] Masyuk AI, Gradilone SA, Banales JM, Huang BQ, Masyuk TV, Lee SO, Splinter PL, Stroope AJ, Larusso NF. (2008) Cholangiocyte primary cilia are chemosensory organelles that detect biliary nucleotides via P2Y12 purinergic receptors. *American Journal of Physiology*, **295**, G725-G734.
- [67] Morales B, Barrera N, Uribe P, Mora C, Villalón M. (2000) Functional cross talk after activation of P2 and P1 receptors in oviductal ciliated cells. *American Journal of Physiology*, **279**, C658-C669.
- [68] Knight MM, McGlashan SR, Garcia M, Jensen CG, Poole CA. (2009) Articular chondrocytes express connexin 43 hemichannels and P2 receptors - a putative mechanoreceptor complex involving the primary cilium? *Journal of Anatomy*, **214**, 275-283.
- [69] Langlois S, Cowan KN, Shao Q, Cowan BJ, Laird DW. (2008) Caveolin-1 and -2 interact with connexin43 and regulate gap junctional intercellular communication in keratinocytes. *Molecular Biology of the Cell*, **19**, 912-928.
- [70] Cooper CD, Lampe PD. (2002) Casein kinase 1 regulates connexin-43 gap junction assembly. *Journal of Biological Chemistry*, **277**, 44962-44968.
- [71] Rhett JM, Jourdan J, Gourdie RG. (2011) Connexin 43 connexon to gap junction transition is regulated by zonula occludens-1. *Molecular Biology of the Cell*, **22**, 1516-1528.
- [72] Giepmans BN, Verlaan I, Moolenaar WH. (2001) Connexin-43 interactions with ZO-1 and alpha- and beta-tubulin. *Cell Communication and Adhesion*, **8**, 219-223.
- [73] Kwak BR, Veillard N, Pelli G, Mulhaupt F, James RW, Chanson M, Mach F. (2003) Reduced connexin43 expression inhibits atherosclerotic lesion formation in low-density lipoprotein receptor-deficient mice. *Circulation*, **107**, 1033-1039.
- [74] Malone P, Miao H, Parker A, Juarez S, Hernandez MR. (2007) Pressure induces loss of gap junction communication and redistribution of connexin 43 in astrocytes. *Glia*, **55**, 1085-1098
- [75] Deretic D, Traverso V, Parkins N, Jackson F, Rodriguez de Turco EB, Ransom N. (2004) Phosphoinositides, ezrin/moesin, and rac1 regulate fusion of rhodopsin transport carriers in retinal photoreceptors. *Molecular Biology of the Cell*, **15**, 359-370.
- [76] Mazelova J, Ransom N, Astuto-Gribble L, Wilson MC, Deretic D. (2009) Syntaxin 3 and SNAP-25 pairing, regulated by omega-3 docosahexaenoic acid, controls the delivery of rhodopsin for the biogenesis of cilia-derived sensory organelles, the rod outer segments. *Journal of Cell Science*, **122**, 2003-2013.
- [77] Wang J, Deretic D. (2013) Molecular complexes that direct rhodopsin transport to primary cilia. *Progress in Retinal and Eye Research*, pii: S1350-9462(13)00060-8.

- [78] Mahjoub MR, Qasim Rasi M, Quarmby LM. (2004) A NIMA-related kinase, Fa2p, localises to a novel site in the proximal cilia of Chlamydomonas and mouse kidney cells. *Molecular Biology of the Cell*, **15**, 5172-5186.
- [79] Quarmby LM, Parker JD. (2005) Cilia and the cell cycle? *Journal of Cell Biology*, **6**, 707-710.
- [80] Luttrell LM, Lefkowitz RJ. (2002) The role of beta-arrestins in the termination and transduction of G-protein-coupled receptor signals. *Journal of Cell Science*, **115**, 455-465.
- [81] Molla-Herman A, Boularan C, Ghossoub R, Scott MG, Burtey A, Zarka M, Saunier S, Concordet JP, Marullo S, Benmerah A. (2008) Targeting of beta-arrestin2 to the centrosome and primary cilium: role in cell proliferation control. *PLoS One*, **3**(11):e3728.
- [82] Kovacs JJ, Whalen EJ, Liu R, Xiao K, Kim J, Chen M, Wang J, Chen W, Lefkowitz RJ. (2008) Beta-arrestin-mediated localisation of smoothened to the primary cilium. *Science*, **320**(5884), 1777-1781.
- [83] Parathath SR, Mainwaring LA, Fernandez-L A, Guldal CG, Nahlé Z, Kenney AM. (2010) β -Arrestin-1 links mitogenic sonic Hedgehog signalling to the cell cycle exit machinery in neural precursors. *Cell Cycle*, **9**, 4013-4024.
- [84] Lefkowitz RJ, Shenoy SK (2005) Transduction of receptor signals by beta-arrestins. *Science*, **308** (5721), 512-517.
- [85] Zhang Y, Wada J, Yasuhara A, Iseda I, Eguchi J, Fukui K, Yang Q, Yamagata K, Hiesberger T, Igarashi P, Zhang H, Wang H, Akagi S, Kanwar YS, Makino H. (2007) The role for HNF-1beta-targeted collectrin in maintenance of primary cilia and cell polarity in collecting duct cells. *PLoS One*, **2**(5):e414.
- [86] Zhang, H, Wada, J, Hida, K, Tsuchiyama, Y, Hiragushi, K, Shikata, K, Wang, H, Lin, S, Kanwar, Y.S, Makino, H. (2001) Collectrin, a collecting duct-specific transmembrane glycoprotein, is a novel homolog of ACE2 and is developmentally regulated in embryonic kidneys. *Journal of Biological Chemistry*, **276**, 17132-17139.
- [87] Hu Q, Nelson WJ. (2011) Ciliary diffusion barrier: the gatekeeper for the primary cilium compartment. *Cytoskeleton*, **68**, 313-324.
- [88] Hu Q, Milenkovic L, Jin H, Scott MP, Nachury MV, Spiliotis ET, Nelson WJ. (2010) A septin diffusion barrier at the base of the primary cilium maintains ciliary membrane protein distribution. *Science*, **329**, 436-439.
- [89] Kim SK, Shindo A, Park TJ, Oh EC, Ghosh S, Gray RS, Lewis RA, Johnson CA, Attie-Bittach T, Katsanis N, Wallingford JB. (2010) Planar cell polarity acts through septins to control collective cell movement and ciliogenesis. *Science*, **329**(5997), 1337-1340.
- [90] Ghossoub R, Hu Q, Failler M, Rouyez MC, Spitzbarth B, Mostowy S, Wolfrum U, Saunier S, Cossart P, Nelson WJ, Benmerah A. (2013) Septins 2, 7, and 9 and MAP4 co-localize along the axoneme in the primary cilium and control ciliary length. *Journal of Cell Science*, **126**, 2583-2594.
- [91] Hsu SC, Hazuka CD, Roth R, Foletti DL, Heuser J, Scheller RH. (1998) Subunit composition, protein interactions, and structures of the mammalian brain sec6/8 complex and septin filaments. *Neuron*, **20**, 1111-1122.

- [92] Raychowdhury MK, Ramos AJ, Zhang P, McLaughlin M, Dai XQ, Chen XZ, Montalbetti N, Del Rocío Cantero M, Ausiello DA, Cantiello HF. (2009) Vasopressin receptor-mediated functional signaling pathway in primary cilia of renal epithelial cells. *American Journal of Physiology*, **296**, F87-F97.
- [93] Saigusa T, Bell PD, Kolb RJ. (2010) Primary cilium is required for vasopressin mediated aquaporin-2 trafficking. *FASEB Journal*, **24**, 1024.23.
- [94] Marion V, Schlicht D, Mockel A, Caillard S, Imhoff O, Stoetzel C, van Dijk P, Brandt C, Moulin B, Dollfus H. (2011) Bardet-Biedl syndrome highlights the major role of the primary cilium in efficient water reabsorption. *Kidney International*, **79**, 1013-1025.
- [95] Nickols HH, Shah VN, Chazin WJ, Limbird LE. (2004) Calmodulin interacts with the V2 vasopressin receptor: elimination of binding to the C terminus also eliminates arginine vasopressin-stimulated elevation of intracellular calcium. *Journal of Biological Chemistry*, **279**, 46969-46980.
- [96] Innamorati G, Whang MI, Molteni R, Le Gouill C, Birnbaumer M. (2002) GIP, a G-protein-coupled receptor interacting protein. *Regulatory Peptides*, **109**, 173-179.
- [97] Raychowdhury MK, Ramos AJ, Zhang P, McLaughlin M, Dai XQ, Chen XZ, Montalbetti N, Del Rocío Cantero M, Ausiello DA, Cantiello HF. (2009) Vasopressin receptor-mediated functional signalling pathway in primary cilia of renal epithelial cells. *American Journal of Physiology*, **296**, F87-F97.
- [98] Knafo A, Israel S, Darvasi A, Bachner-Melman R, Uzefovsky F, Cohen L, Feldman E, Lerer E, Laiba E, Raz Y, Nemanov L, Gritsenko I, Dina C, Agam G, Dean B, Bornstein G, Ebstein RP. (2008) Individual differences in allocation of funds in the dictator game associated with length of the arginine vasopressin 1a receptor RS3 promoter region and correlation between RS3 length and hippocampal mRNA. *Genes, Brain and Behavior*, **7**, 266-275.
- [99] Knafo A, Israel S, Darvasi A, Bachner-Melman R, Uzefovsky F, Cohen L, Feldman E, Lerer E, Laiba E, Raz Y, Nemanov L, Gritsenko I, Dina C, Agam G, Dean B, Bornstein G, Ebstein RP. (2008) Individual differences in allocation of funds in the dictator game associated with length of the arginine vasopressin 1a receptor RS3 promoter region and correlation between RS3 length and hippocampal mRNA. *Genes, Brain and Behavior*, **7**, 266-275.
- [100] Vincent JL, Su F. (2008) Physiology and pathophysiology of the vasopressinergic system. *Best Practice and Research Clinical Anaesthesiology*, **22**, 243-252.
- [101] Kaplan OI, Molla-Herman A, Cevik S, Ghossoub R, Kida K, Kimura Y, Jenkins P, Martens JR, Setou M, Benmerah A, Blacque OE. (2010) The AP-1 clathrin adaptor facilitates cilium formation and functions with RAB-8 in *C. elegans* ciliary membrane transport. *Journal of Cell Science*, **123**, 3966-3977.
- [102] Ko HW, Norman RX, Tran J, Fuller KP, Fukuda M, Eggenschwiler JT. (2010) Broad-minded links cell cycle-related kinase to cilia assembly and Hedgehog signal transduction. *Developmental Cell*, **18**, 237-247.
- [103] Follit JA, Li L, Vucica Y, Pazour GJ. (2010) The cytoplasmic tail of fibrocystin contains a ciliary targeting sequence. *Journal of Cell Biology*, **188**, 21-28.
- [104] Wang S, Luo Y, Wilson PD, Witman GB, Zhou J. (2004) The autosomal recessive polycystic kidney disease protein is localized to primary cilia, with concentration in the basal body area. *Journal of the American Society of Nephrology*, **15**, 592-602.

- [105] Zhang M, Mai W, Li C, Cho S, Hao C, Moeckel G, Zhao R, Kim I, Wang J, Xiong H, Wang H, Sato Y, Wu Y, Nakanuma Y, Lilova M, Pei Y, Harris R, Li S, Coffey R, Sun L, Wu D, Chen X, Breyer M, Zhao Z, McKanna J, Wu G. (2004) PKHD1 protein encoded by the gene for autosomal recessive polycystic kidney disease associates with basal bodies and primary cilia in renal epithelial cells. *Proceedings of the National Academy of Sciences, USA*, **101**, 2311-2316.
- [106] Kaimori JY, Nagasawa Y, Menezes LF, Garcia-Gonzalez MA, Deng J, Imai, E, Onuchic LF, Guay-Woodford, LM, Germino GG. (2007) Polyductin undergoes notch-like processing and regulated release from primary cilia. *Human Molecular Genetics*, **16**, 942-956.
- [107] Wang S, Zhang J, Nauli SM, Li X, Starremans PG, Luo Y, Roberts KA, Zhou J. (2007) Fibrocystin/polyductin, found in the same protein complex with polycystin-2, regulates calcium responses in kidney epithelia. *Molecular Cell Biology*, **27**, 3241-3252.
- [108] Williams CL, Li C, Kida K, Inglis PN, Mohan S, Semenec L, Bialas NJ, Stupay RM, Chen N, Blacque OE, Yoder BK, Leroux MR. (2011) MKS and NPHP modules cooperate to establish basal body/transition zone membrane associations and ciliary gate function during ciliogenesis. *Journal of Cell Biology*, **192**, 1023-1041.
- [109] Leightner AC, Hommerding CJ, Peng Y, Salisbury JL, Gainullin VG, Czarnecki PG, Sussman CR, Harris PC. (2013) The Meckel syndrome protein meckelin (TMEM67) is a key regulator of cilia function but is not required for tissue planar polarity. *Human Molecular Genetics*, **22**, 2024-2040.
- [110] Dawe HR, Smith UM, Cullinane AR, Gerrelli D, Cox P, Badano JL, Blair-Reid S, Sriram N, Katsanis N, Attie-Bitach T, Afford SC, Copp AJ, Kelly DA, Gull K, Johnson CA. (2006) The Meckel-Gruber Syndrome proteins MKS1 and meckelin interact and are required for primary cilium formation. *Human Molecular Genetics*, **16**, 173-186.
- [111] Tammachote R, Hommerding CJ, Sindere RM, Miller CA, Czarnecki PG, Leightner AC, Salisbury JL, Ward CJ, Torres VE, Gattone VH, Harris PC. (2009) Ciliary and centrosomal defects associated with mutation and depletion of the Meckel syndrome genes MKS1 and MKS3. *Human Molecular Genetics*, **18**, 3311-3323.
- [112] Dawe HR, Adams M, Wheway G, Szymanska K, Logan CV, Noegel AA, Gull K, Johnson CA. (2009) Nesprin-2 interacts with meckelin and mediates ciliogenesis via remodelling of the actin cytoskeleton. *Journal of Cell Science*, **122**, 2716-2726
- [113] Weatherbee SD, Niswander LA, Anderson KV (2009) A mouse model for Meckel syndrome reveals Mks1 is required for ciliogenesis and Hedgehog signalling. *Human Molecular Genetics*, **18**, 4565-4575.
- [114] Kyttala M, Tallila J, Salonen R, Kopra O, Kohlschmidt N, Paavola-Sakki P, Peltonen L, Kestila M. (2006) MKS1, encoding a component of the flagellar apparatus basal body proteome, is mutated in Meckel syndrome. *Nature Genetics*, **38**, 155-157.
- [115] Leitch CC, Zaghoul NA, Davis EE, Stoetzel C, Diaz-Font A, Rix S, Alfadhel M, Al-Fadhel M, Lewis RA, Eyaid W, Banin E, Dollfus H, Beales PL, Badano JL, Katsanis N. (2008) Hypomorphic mutations in syndromic encephalocele genes are associated with Bardet-Biedl syndrome. *Nature Genetics*, **40**, 443-438.
- [116] Wheway G, Abdelhamed Z, Natarajan S, Toomes C, Inglehearn C, Johnson CA. (2013) Aberrant Wnt signalling and cellular over-proliferation in a novel mouse model of Meckel-Gruber syndrome. *Developmental Biology*, **377**, 55-66.

- [117] Valente EM, Logan CV, Mougou-Zerelli S, Lee JH, Silhavy JL, Brancati F, Iannicelli M, Travaglini L, Romani S, Illi B, Adams M, Szymanska K, Mazzotta A, Lee JE, Tolentino JC, Swistun D, Salpietro CD, Fede C, Gabriel S, Russ C, Cibulskis K, Sougnez C, Hildebrandt F, Otto EA, Held S, Diplas BH, Davis EE, Mikula M, Strom CM, Ben-Zeev B, Lev D, Sagie TL, Michelson M, Yaron Y, Krause A, Boltshauser E, Elkhartoufi N, Roume J, Shalev S, Munnich A, Saunier S, Inglehearn C, Saad A, Alkindy A, Thomas S, Vekemans M, Dallapiccola B, Katsanis N, Johnson CA, Attié-Bitach T, Gleeson JG. (2010) Mutations in TMEM216 perturb ciliogenesis and cause Joubert, Meckel and related syndromes. *Nature Genetics*, **42**, 619-625.
- [118] Hoover AN, Wynkoop A, Zeng H, Jia J, Niswander LA, Liu A. (2008) C2cd3 is required for cilia formation and Hedgehog signalling in mouse. *Development*, **135**, 4049-4058.
- [119] Wang A. (2010) TMEM216 joins its ciliary cousins in ciliopathies. *Clinical Genetics*, **79**, 45-47.
- [120] Williams CL, Masyukova SV, Yoder BK. (2010) Normal ciliogenesis requires synergy between the cystic kidney disease genes MKS-3 and NPHP-4. *Journal of the American Society of Nephrology*, **21**, 782-793.
- [121] Wang M, Bridges JP, Na CL, Xu Y, Weaver TE. (2009) Meckel-Gruber syndrome protein MKS3 is required for endoplasmic reticulum-associated degradation of surfactant protein C. *Journal of Biological Chemistry*, **284**, 33377-33383.
- [122] De Mori R, Illi B, Romani S, Valente S, Johnson CA, Mai A, Valente EM. (2012) The ciliary protein Meckelin/TMEM67 interacts with HDAC6: possible implications for primary cilia stability. *Cilia*, **1**, 20.
- [123] Craige B, Tsao CC, Diener DR, Hou Y, Lechtreck KF, Rosenbaum JL, Witman GB. (2010) CEP290 tethers flagellar transition zone microtubules to the membrane and regulates flagellar protein content. *Journal of Cell Biology*, **190**, 927-940.
- [124] Rachel RA, Li T, Swaroop A. (2012) Photoreceptor sensory cilia and ciliopathies: focus on CEP290, RPGR and their interacting proteins. *Cilia*, **1**, 22.
- [125] Chang B, Khanna H, Hawes N, Jimeno D, He S, Lillo C, Parapuram SK, Cheng H, Scott A, Hurd RE, Sayer JA, Otto EA, Attanasio M, O'Toole JF, Jin G, Shou C, Hildebrandt F, Williams DS, Heckenlively JR, Swaroop A. (2006) In-frame deletion in a novel centrosomal/ciliary protein CEP290/NPHP6 perturbs its interaction with RPGR and results in early-onset retinal degeneration in the rd16 mouse. *Human Molecular Genetics*, **15**, 1847-1857.
- [126] Sayer JA, Otto EA, O'Toole JF, Nurnberg G, Kennedy MA, Becker C, Hennies HC, Helou J, Attanasio M, Fausett BV, Utsch B, Khanna H, Liu Y, Drummond I, Kawakami I, Kusakabe T, Tsuda M, Ma L, Lee H, Larson RG, Allen SJ, Wilkinson CJ, Nigg EA, Shou C, Lillo C, Williams DS, Hoppe B, Kemper MJ, Neuhaus T, Parisi MA, Glass IA, Petry M, Kispert A, Gloy J, Ganner A, Walz G, Zhu X, Goldman D, Nurnberg P, Swaroop A, Leroux MR, Hildebrandt F. (2006) The centrosomal protein nephrocystin-6 is mutated in Joubert syndrome and activates transcription factor ATF4. *Nature Genetics*, **38**, 674-681.
- [127] Kim J, Krishnaswami SR, Gleeson JG. (2008) CEP290 interacts with the centriolar satellite component PCM-1 and is required for Rab8 localisation to the primary cilium. *Human Molecular Genetics*, **17**, 3796-3805.
- [128] Schäfer T, Pütz M, Lienkamp S, Ganner A, Bergbreiter A, Ramachandran H, Gieloff V, Gerner M, Mattonet C, Czarnecki PG, Sayer JA, Otto EA, Hildebrandt F, Kramer-Zucker A, Walz G. (2008) Genetic and physical interaction between the NPHP5 and NPHP6 gene products. *Human Molecular Genetics*, **17**, 3655-3662.

- [129] Cideciyan AV, Rachel RA, Aleman TS, Swider M, Schwartz SB, Sumaroka A, Roman AJ, Stone EM, Jacobson SG, Swaroop A. (2011) Cone photoreceptors are the main targets for gene therapy of NPHP5 (IQCB1) or NPHP6 (CEP290) blindness: generation of an all-cone Nphp6 hypomorph mouse that mimics the human retinal ciliopathy. *Human Molecular Genetics*, **20**, 1411-1423.
- [130] McEwen DP, Koenekoop RK, Khanna H, Jenkins PM, Lopez I, Swaroop A, Martens JR. (2007) Hypomorphic CEP290/NPHP6 mutations result in anosmia caused by the selective loss of G proteins in cilia of olfactory sensory neurons. *Proceedings of the National Academy of Sciences, USA*, **104**, 15917-15922.
- [131] Delous M, Baala L, Salomon R, Laclef C, Vierkotten J, Tory K, Golzio C, Lacoste T, Besse L, Ozilou C, Moutkine I, Hellman NE, Anselme I, Silbermann F, Vesque C, Gerhardt C, Rattenberry E, Wolf MT, Gubler MC, Martinovic J, Encha-Razavi F, Boddart N, Gonzales M, Macher MA, Nivet H, Champion G, Berthélemy JP, Niaudet P, McDonald F, Hildebrandt F, Johnson CA, Vekemans M, Antignac C, Rüther U, Schneider-Maunoury S, Attié-Bitach T, Saunier S. (2007) The ciliary gene RPGRIPL1 is mutated in cerebello-oculo-renal syndrome (Joubert syndrome type B) and Meckel syndrome. *Nature Genetics*, **39**, 875-881.
- [132] Arts HH, Doherty D, van Beersum SE, Parisi MA, Letteboer SJ, Gorden NT, Peters TA, Märker T, Voeselek K, Kartono A, Ozyurek H, Farin FM, Kroes HY, Wolfrum U, Brunner HG, Cremers FP, Glass IA, Knoers NV, Roepman R. (2007) Mutations in the gene encoding the basal body protein RPKRIPL1, a nephrocystin-4 interactor, cause Joubert syndrome. *Nature Genetics*, **39**, 882-888.
- [133] Bachmann-Gagescu R, Phelps IG, Stearns G, Link BA, Brockerhoff SE, Moens CB, Doherty D. (2011) The ciliopathy gene cc2d2a controls zebrafish photoreceptor outer segment development through a role in Rab8-dependent vesicle trafficking. *Human Molecular Genetics*, **20**, 4041-4055.
- [134] Raychowdhury MK, McLaughlin M, Ramos AJ, Montalbetti N, Bouley R, Ausiello DA, Cantiello HF. (2005) Characterization of single channel currents from primary cilia of renal epithelial cells. *Journal of Biological Chemistry*, **280**, 34718-34722.
- [135] Yoder BK, Hou X, Guay-Woodford LM. (2002) The polycystic kidney disease proteins, polycystin-1, polycystin-2, polaris, and cystin, are colocalized in renal cilia. *Journal of the American Society of Nephrology*, **13**, 2508-2516.
- [136] Zhou J. (2009) Polycystins and primary cilia: primers for cell cycle progression. *Annual Reviews of Physiology*, **71**, 83-113.
- [137] Sharif-Naeini R, Folgering JH, Bichet D, Duprat F, Lauritzen I, Arhatte M, Jodar M, Dedman A, Chatelain FC, Schulte U, Retailleau K, Loufrani L, Patel A, Sachs F, Delmas P, Peters DJ, Honoré E. (2009) Polycystin-1 and -2 dosage regulates pressure sensing. *Cell*, **139**, 587-596.
- [138] Woudenberg-Vrenken TE, Bindels RJ, Hoenderop JG. (2009) The role of transient receptor potential channels in kidney disease. *Nature Reviews Nephrology*, **5**, 441-449.
- [139] Xiao Z, Zhang S, Magenheimer BS, Luo J, Quarles LD. (2008) Polycystin-1 regulates skeletogenesis through stimulation of the osteoblast-specific transcription factor RUNX2-II. *Journal of Biological Chemistry*, **283**, 12624-12634.
- [140] Sandford RN. (2009) The diversity of PKD1 alleles: implications for disease pathogenesis and genetic counseling. *Kidney International*, **75**, 765-767.

- [141] Barr MM, DeModena J, Braun D, Nguyen CQ, Hall DH, Sternberg PW. (2001) The *Caenorhabditis elegans* autosomal dominant polycystic kidney disease gene homologs lov-1 and pkd-2 act in the same pathway. *Current Biology*, **11**, 1341-1346.
- [142] Pazour GJ, San Agustin JT, Follit JA, Rosenbaum JL, Witman GB. (2002) Polycystin-2 localises to kidney cilia and the ciliary level is elevated in orpk mice with polycystic kidney disease. *Current Biology*, **12**, R378-R380.
- [143] Tsiokas L, Arnould T, Zhu C, Kim E, Walz G, Sukhatme VP. (1999) Specific association of the gene product of PKD2 with the TRPC1 channel. *Proceedings of the National Academy of Sciences, USA*, **96**, 3934-3939.
- [144] Bai CX, Giamarchi A, Rodat-Despoix L, Padilla F, Downs T, Tsiokas L, Delmas P. (2008) Formation of a new receptor-operated channel by heteromeric assembly of TRPP2 and TRPC1 subunits. *EMBO Reports*, **9**, 472-479.
- [145] Nilius B. (2009) Polycystins under pressure. *Cell*, **139**, 466-467.
- [146] Köttgen M, Buchholz B, Garcia-Gonzalez MA, Kotsis F, Fu X, Doerken M, Boehlke C, Steffl D, Tauber R, Wegierski T, Nitschke R, Suzuki M, Kramer-Zucker A, Germino GG, Watnick T, Prenen J, Nilius B, Kuehn EW, Walz G. (2008) TRPP2 and TRPV4 form a polymodal sensory channel complex. *Journal of Cell Biology*, **182**, 437-447.
- [147] Qian F, Noben-Trauth K. (2005) Cellular and molecular function of mucolipins (TRPML) and polycystin 2 (TRPP2). *European Journal of Physiology*, **451**, 277-285.
- [148] Kim D, Baraniuk JN. (2007) Sensing the air around us: the voltage-gated-like ion channel family. *Current Allergy and Asthma Reports*, **2**, 85-92.
- [149] Nilius B, Owsianik G, Voets T, Peters JA. (2007) Transient receptor potential cation channels in disease. *Physiological Reviews*, **87**, 165-217.
- [150] Wang Q, Dai X, Li Q, Wang Z, Cantero M, Li S, Shen J, Tu J, Cantiello H, Chen X. (2012) Structural interaction and functional regulation of polycystin-2 by filamin. *PLoS One*, **7**(7):e40448.
- [151] Ishimaru Y, Inada H, Kubota M, Zhuang H, Tominaga M, and Matsunami H (2006) Transient receptor potential family members PKD1L3 and PKD2L1 form a candidate sour taste receptor. *Proceedings of the National Academy of Sciences, USA*, **103**, 12569-12574.
- [152] Dai XQ, Ramji A, Liu Y, Li Q, Karpinski E, Chen XZ. (2007) Inhibition of TRPP3 channel by amiloride and analogs. *Molecular Pharmacology*, **72**, 1576-1585.
- [153] Hofmann T, Schaefer M, Schultz G, Gudermann T. (2002) Subunit composition of mammalian transient receptor potential channels in living cells. *Proceedings of the National Academy of Sciences, USA*, **99**, 7461-7466.
- [154] Tsiokas L, Arnould T, Zhu C, Kim E, Walz G, Sukhatme VP. (1999) Specific association of the gene product of PKD2 with the TRPC1 channel. *Proceedings of the National Academy of Sciences, USA*, **96**, 3934-3939.
- [155] Kobori T, Smith GD, Sandford R, Edwardson JM. (2009) The transient receptor potential channels TRPP2 and TRPC1 form a heterotetramer with a 2:2 stoichiometry and an alternating subunit arrangement. *Journal of Biological Chemistry*, **284**, 35507-35513.

- [156] Cheung KK, Yeung SS, Au SW, Lam LS, Dai ZQ, Li YH, Yeung EW. (2011) Expression and association of TRPC1 with TRPC3 during skeletal myogenesis. *Muscle and Nerve*, **44**, 358-365.
- [157] Mehta D, Ahmmed GU, Paria BC, Holinstat M, Voyno-Yasenetskaya T, Tirupathi C, Minshall RD, Malik AB. (2003) RhoA interaction with inositol 1,4,5-trisphosphate receptor and transient receptor potential channel-1 regulates Ca²⁺ entry. Role in signalling increased endothelial permeability. *Journal of Biological Chemistry*, **278**, 33492-33500.
- [158] Tu JC, Xiao B, Yuan JP, Lanahan AA, Leoffert K, Li M, Linden DJ, Worley PF (1998) Homer binds a novel proline-rich motif and links group 1 metabotropic glutamate receptors with IP3 receptors. *Neuron*, **21**, 717-726.
- [159] Clapham DE. (2007) SnapShot: mammalian TRP channels. *Cell*, **129**, 220.
- [160] Chu X, Tong Q, Cheung JY, Wozney J, Conrad K, Mazack V, Zhang W, Stahl R, Barber DL, Miller BA. (2004) Interaction of TRPC2 and TRPC6 in erythropoietin modulation of calcium influx. *Journal of Biological Chemistry*, **279**, 10514-10522.
- [161] Sutton KA, Jungnickel MK, Wang Y, Cullen K, Lambert S, Florman HM (2004) Enkurin is a novel calmodulin and TRPC channel binding protein in sperm. *Developmental Biology*, **274**, 426-435.
- [162] Mast TG, Brann JH, Fadool DA. (2010) The TRPC2 channel forms protein-protein interactions with Homer and RTP in the rat vomeronasal organ. *BMC Neuroscience*, **11**, 61.
- [163] Alexander SPH, Mathie A, Peters JA. (2007) Guide to Receptors and Channels (GRAC), 2nd edn, *British Journal of Pharmacology*, **150** (Suppl. 1), S1-S168.
- [164] Hirschler-Laszkiewicz I, Tong Q, Conrad K, Zhang W, Flint WW, Barber AJ, Barber DL, Cheung JY, Miller BA. (2009) TRPC3 activation by erythropoietin is modulated by TRPC6. *Journal of Biological Chemistry*, **284**, 4567-4581.
- [165] Tong Q, Hirschler-Laszkiewicz I, Zhang W, Conrad K, Neagley DW, Barber DL, Cheung JY, Miller BA. (2008) TRPC3 is the erythropoietin-regulated calcium channel in human erythroid cells. *Journal of Biological Chemistry*, **283**, 10385-10395.
- [166] Ramsey IS, Delling M, Clapham DE. (2006) An introduction to TRP channels. *Annual Review of Physiology*, **68**, 619-647.
- [167] Kwan HY, Huang Y, Yao X. (2006) Protein kinase C can inhibit TRPC3 channels indirectly via stimulating protein kinase G. *Journal of Cell Physiology*, **207**, 315-321.
- [168] Quick K, Zhao J, Eijkelkamp N, Linley JE, Rugiero F, Cox JJ, Raouf R, Gringhuis M, Sexton JE, Abramowitz J, Taylor R, Forge A, Ashmore J, Kirkwood N, Kros CJ, Richardson GP, Freichel M, Flockerzi V, Birnbaumer L, Wood JN. (2012) TRPC3 and TRPC6 are essential for normal mechanotransduction in subsets of sensory neurons and cochlear hair cells. *Open Biology*, **2**, 120068.
- [169] Chen Y, Hu C, Hsu CK, Zhang Q, Bi C, Asnicar M, Hsiung HM, Fox N, Sliker LJ, Yang DD, Heiman ML, Shi Y. (2002) Targeted disruption of the melanin-concentrating hormone receptor-1 results in hyperphagia and resistance to diet-induced obesity. *Endocrinology*, **143**, 2469-2477.
- [170] Shimada M, Tritos NA, Lowell BB, Flier JS, Maratos-Flier E. (1998) Mice lacking melanin-concentrating hormone are hypophagic and lean. *Nature*, **396**, 670-674.
- [171] Bellone RR, Brooks SA, Sandmeyer L, Murphy BA, Forsyth G, Archer S, Bailey E, Grahn B. (2008) Differential gene expression of TRPM1, the potential cause of congenital stationary night

blindness and coat spotting patterns (LP) in the Appaloosa horse (*Equus caballus*). *Genetics*, **179**, 1861-1870.

[172] Morgans CW, Zhang J, Jeffrey BG, Nelson SM, Burke NS, Duvoisin RM, Brown RL. (2009) TRPM1 is required for the depolarizing light response in retinal ON-bipolar cells. *Proceedings of the National Academy of Sciences, USA*, **106**, 19174-19178.

[173] Uchida K, Tominaga M. (2011) TRPM2 modulates insulin secretion in pancreatic β -cells. *Islets*, **3**, 209-211.

[174] Xu C, Macciardi F, Li PP, Yoon IS, Cooke RG, Hughes B, Parikh SV, McIntyre RS, Kennedy JL, Warsh JJ. (2006) Association of the putative susceptibility gene, transient receptor potential protein melastatin type 2, with bipolar disorder. *American Journal of Medical Genetics Part B*, **141**, 36-43.

[175] Miller BA. (2006) The role of TRP channels in oxidative stress-induced cell death. *Journal of Membrane Biology*, **209**, 31-41.

[176] Yamamoto S, Takahashi N, Mori Y. (2010) Chemical physiology of oxidative stress-activated TRPM2 and TRPC5 channels. *Progress in Biophysics and Molecular Biology*, **103**, 18-27.

[177] Thiel G, Müller I, Rössler OG. (2013) Signal transduction via TRPM3 channels in pancreatic β -cells. *Journal of Molecular Endocrinology*, **50**, R75-R83.

[178] Mayer SI, Müller I, Mannebach S, Endo T, Thiel G. (2011) Signal transduction of pregnenolone sulfate in insulinoma cells: activation of Egr-1 expression involving TRPM3, voltage-gated calcium channels, ERK, and ternary complex factors. *Journal of Biological Chemistry*, **286**, 10084-10096.

[179] Harteneck C, Schultz G. (2007) TRPV4 and TRPM3 as volume-regulated cation channels. *Frontiers in Neuroscience*, Liedtke WB, Heller S, ed., *TRP Ion Channel Function in Sensory Transduction and Cellular Signalling Cascades*. CRC Press, Boca Raton.

[180] Vennekens R, Nilius B. (2007) Insights into TRPM4 function, regulation and physiological role. *Handbook of Experimental Pharmacology*, **179**, 269-285.

[181] Vennekens R, Olausson J, Meissner M, Bloch W, Mathar I, Philipp SE, Schmitz F, Weissgerber P, Nilius B, Flockerzi V, Freichel M (2007) Increased IgE-dependent mast cell activation and anaphylactic responses in mice lacking the calcium-activated nonselective cation channel TRPM4. *Nature Immunology*, **8**, 312-320.

[182] Shimizu T, Owsianik G, Freichel M, Flockerzi V, Nilius B, Vennekens R. (2009) TRPM4 regulates migration of mast cells in mice. *Cell Calcium*, **45**, 226-232.

[183] Wu LJ, Sweet TB, Clapham DE. (2010) International Union of Basic and Clinical Pharmacology. LXXVI. Current progress in the mammalian TRP ion channel family. *Pharmacology Reviews*, **62**, 381-404.

[184] Harteneck C, Reiter B. (2007) TRP channels activated by extracellular hypo-osmoticity in epithelia. *Biochemical Society Transactions*, **35**, 91-95.

[185] Liu D, Liman ER. (2003) Intracellular Ca^{2+} and the phospholipid PIP2 regulate the taste transduction ion channel TRPM5. *Proceedings of the National Academy of Sciences, USA*, **100**, 15160-15165.

- [186] Nakashimo Y, Takumida M, Fukuiri T, Anniko M, Hirakawa K. (2010) Expression of transient receptor potential channel vanilloid (TRPV1-4), melastatin (TRPM) 5 and 8, and ankyrin (TRPA1) in the normal and methimazole-treated mouse olfactory epithelium. *Acta Otolaryngologia*, **130**, 1278-1286.
- [187] Mitrovic S, Nogueira C, Cantero-Recasens G, Kiefer K, Fernández-Fernández JM, Popoff JF, Casano L, Bard FA, Gomez R, Valverde MA, Malhotra V. (2013) TRPM5-mediated calcium uptake regulates mucin secretion from human colon goblet cells. *Elife*, **2**:e00658.
- [188] Chubanov V, Gudermann T, Schlingmann KP (2006) Essential role for TRPM6 in epithelial magnesium transport and body magnesium homeostasis. *European Journal of Physiology*, **451**, 228-234.
- [189] Li M, Du J, Jiang J, Ratzan W, Su LT, Runnels LW, Yue L. (2007) Molecular determinants of Mg²⁺ and Ca²⁺ permeability and pH sensitivity in TRPM6 and TRPM7. *Journal of Biological Chemistry*, **282**, 25817-25830.
- [190] Xie J, Sun B, Du J, Yang W, Chen HC, Overton JD, Runnels LW, Yue L. (2011) Phosphatidylinositol 4,5-bisphosphate (PIP(2)) controls magnesium gatekeeper TRPM6 activity. *Science Reports*, **1**, 146.
- [191] Perraud AL, Zhao X, Ryazanov AG, Schmitz C. (2011) The channel-kinase TRPM7 regulates phosphorylation of the translational factor eEF2 via eEF2-k. *Cell Signalling*, **23**, 586-593.
- [192] Yogi A, Callera GE, Antunes TT, Tostes RC, Touyz RM. (2010) Transient receptor potential melastatin 7 (TRPM7) cation channels, magnesium and the vascular system in hypertension. *Circulation Journal*, **75**, 237-245.
- [193] Harrington AM, Hughes PA, Martin CM, Yang J, Castro J, Isaacs NJ, Blackshaw LA, Brierley SM. (2011) A novel role for TRPM8 in visceral afferent function. *Pain*, **152**, 1459-1468.
- [194] van Aken AF, Atiba-Davies M, Marcotti W, Goodyear RJ, Bryant JE, Richardson GP, Noben-Trauth K, Kros CJ. (2008) TRPML3 mutations cause impaired mechano-electrical transduction and depolarization by an inward-rectifier cation current in auditory hair cells of varitint-waddler mice. *Journal of Physiology*, **586**, 5403-5418.
- [195] HKim HJ, Li Q, Tjon-Kon-Sang S, So I, Kiselyov K, Soyombo AA, Muallem S. (2008) A novel mode of TRPML3 regulation by extracytosolic pH absent in the varitint-waddler phenotype. *EMBO Journal*, **27**, 1197-1205.
- [196] Gavva NR, Bannon AW, Surapaneni S, Hovland DN, Lehto SG, Gore A, Juan T, Deng H, Han B, Klionsky L, Kuang R, Le A, Tamir R, Wang J, Youngblood B, Zhu D, Norman MH, Magal E, Treanor JJ, Louis JC. (2007) The vanilloid receptor TRPV1 is tonically activated *in vivo* and involved in body temperature regulation. *Journal of Neuroscience*, **27**, 3366-3374.
- [197] Rosenbaum T, Gordon-Shaag A, Munari M, Gordon SE. (2004) Ca²⁺/calmodulin modulates TRPV1 activation by capsaicin. *Journal of General Physiology*, **123**, 53-62.
- [198] Goswami C, Hucho TB, Hucho F. (2007) Identification and characterisation of novel tubulin-binding motifs located within the C-terminus of TRPV1. *Journal of Neurochemistry*, **101**, 250-262.
- [199] Steiner AA, Turek VF, Almeida MC, Burmeister JJ, Oliveira DL, Roberts JL, Bannon AW, Norman MH, Louis JC, Treanor JJ, Gavva NR, Romanovsky AA. (2007) Nonthermal activation of transient receptor potential vanilloid-1 channels in abdominal viscera tonically inhibits autonomic cold-defense effectors. *Journal of Neuroscience*, **27**, 7459-7468.

- [200] Gracheva EO, Cordero-Morales JF, González-Carcacia JA, Ingolia NT, Manno C, Aranguren CI, Weissman JS, Julius D. (2011) Ganglion-specific splicing of TRPV1 underlies infrared sensation in vampire bats. *Nature*, **476**, 88-91.
- [201] Perálvarez-Marín A, Doñate-Macian P, Gaudet R. (2013) What do we know about the transient receptor potential vanilloid 2 (TRPV2) ion channel? *FEBS Journal*, **280**, 5471-5487.
- [202] Hisanaga E, Nagasawa M, Ueki K, Kulkarni RN, Mori M, Kojima I. (2009) Regulation of calcium-permeable TRPV2 channel by insulin in pancreatic beta-cells. *Diabetes*, **58**, 174-184.
- [203] Qin N, Nepper MP, Liu Y, Hutchinson TL, Lubin ML, Flores CM. (2008) TRPV2 is activated by cannabidiol and mediates CGRP release in cultured rat dorsal root ganglion neurons. *Journal of Neuroscience*, **28**, 6231-6238.
- [204] Peier AM, Reeve AJ, Andersson DA, Moqrich A, Earley TJ, Hergarden AC, Story GM, Colley S, Hogenesch JB, McIntyre P, Bevan S, Patapoutian A. (2002) A heat-sensitive TRP channel expressed in keratinocytes. *Science*, **296** (5575), 2046-2049.
- [205] Cohen DM. (2007) The Role of TRPV4 in the Kidney. In: Liedtke WB, Heller S, eds, *TRP Ion Channel Function in Sensory Transduction and Cellular Signaling Cascades*. CRC Press, Boca Raton.
- [206] Goswami C, Kuhn J, Heptall PA, Hucho T. (2010) Importance of non-selective cation channel TRPV4 interaction with cytoskeleton and their reciprocal regulations in cultured cells. *PLoS One*, **5**(7):e11654.
- [207] Vriens J, Appendino G, Nilius B. (2009) Pharmacology of vanilloid transient receptor potential cation channels. *Molecular Pharmacology*, **75**, 1262-1279.
- [208] Gradilone SA, Masyuk AI, Splinter PL, Banales JM, Huang BQ, Tietz PS, Masyuk TV, Larusso NF. (2007) Cholangiocyte cilia express TRPV4 and detect changes in luminal tonicity inducing bicarbonate secretion. *Proceedings of the National Academy of Sciences, USA*, **104**, 19138-19143.
- [209] Kwon RY, Hoey DA, Jacobs CR. (2011) Mechanobiology of primary cilia. *Cellular and Biomolecular Mechanics and Mechanobiology*, ed A. Gefen, **4**, SpringerLink, Heidelberg, 99-124.
- [210] Suzuki M, Hirao A, Mizuno A (2003) Microtubule-associated protein 7 increases the membrane expression of transient receptor potential vanilloid 4 (TRPV4). *Journal of Biological Chemistry*, **278**, 51448-51453.
- [211] Sidhaye VK, Güler AD, Schweitzer KS, D'Alessio F, Caterina MJ, King LS. (2006) Transient receptor potential vanilloid 4 regulates aquaporin-5 abundance under hypotonic conditions. *Proceedings of the National Academy of Sciences, USA*, **103**, 4747-4752.
- [212] Modregger J, Ritter B, Witter B, Paulsson M, Plomann M. (2000) All three PACSIN isoforms bind to endocytic proteins and inhibit endocytosis. *Journal of Cell Science*, **113**, 4511-4521.
- [213] Suzuki M, Mizuno A, Kodaira K, Imai M. (2003) Impaired pressure sensation in mice lacking TRPV4. *Journal of Biological Chemistry*, **278**, 22664-22668.
- [214] Phan MN, Leddy HA, Votta BJ, Kumar S, Levy DS, Lipshutz DB, Lee SH, Liedtke W, Guilak F. (2009) Functional characterization of TRPV4 as an osmotically sensitive ion channel in porcine articular chondrocytes. *Arthritis and Rheumatology*, **60**, 3028-3037.

- [215] van de Graaf SFJ, Hoenderop JGJ, Gkika D, Lamers D, Prenen J, Rescher U, Gerke V, Staub O, Nilius B, Bindels RJM. (2003) Functional expression of the epithelial Ca(2+) channels (TRPV5 and TRPV6) requires association of the S100A10-annexin 2 complex. *EMBO Reports*, **22**, 1478-1487.
- [216] Hoenderop JG, Nilius B, Bindels RJ. (2002) Transient Receptor Potential Cation Channel. Molecular mechanism of active Ca²⁺ reabsorption in the distal nephron. *Annual Review of Physiology*, **64**, 529-549.
- [217] Hoenderop JG, van Leeuwen JP, van der Eerden BC, Kersten FF, van der Kemp AW, Merillat AM, Waarsing JH, Rossier BC, Vallon V, Hummler E, Bindels RJ. (2003) Renal Ca²⁺ wasting, hyperabsorption, and reduced bone thickness in mice lacking TRPV5. *Journal of Clinical Investigation*, **112**, 1906-1914.
- [218] Barley NF, Howard A, O'Callaghan D, Legon S, Walters JR. (2001) Epithelial calcium transporter expression in human duodenum. *American Journal of Physiology*, **280**, G285-G290.
- [219] Bolanz KA, Hediger MA, Landowski CP. (2008) The role of TRPV6 in breast carcinogenesis. *Molecular Cancer Therapeutics*, **7**, 271-279.
- [220] Gerhold KA, Bautista DM. (2008) TRPA1: irritant detector of the airways. *Journal of Physiology*, **586**, 3303.
- [221] Baraldi PG, Preti D, Materazzi S, Geppetti P. (2010) Transient receptor potential ankyrin 1 (TRPA1) channel as emerging target for novel analgesics and anti-inflammatory agents. *Journal of Medical Chemistry*, **53**, 5085-5107.
- [222] Brône B, Peeters PJ, Marrannes R, Mercken M, Nuydens R, Meert T, Gijssen HJ. (2008) Tear gasses CN, CR, and CS are potent activators of the human TRPA1 receptor. *Toxicology and Applied Pharmacology*, **231**, 150-156.
- [223] Nagata K, Duggan A, Kumar G, García-Añoveros J. (2005) Nociceptor and hair cell transducer properties of TRPA1, a channel for pain and hearing. *Journal of Neuroscience*, **25**, 4052-4061.
- [224] Geng J, Liang D, Jiang K, Zhang P. (2011) Molecular evolution of the infrared sensory gene TRPA1 in snakes and implications for functional studies. *PLoS One*, **6**(12):e28644.
- [225] Story GM, Gereau RW. (2006) Numbing the senses: role of TRPA1 in mechanical and cold sensation. *Neuron*, **50**, 177-180.
- [226] Clapham DE, Julius D, Montell C, Schultz G. (2005) International Union of Pharmacology. XLIX. Nomenclature and structure-function relationships of transient receptor potential channels. *Pharmacological Reviews*, **57**, 427-450.
- [227] Christensen ST, Voss JW, Teilmann SC, Lambert IH. (2005) High expression of the taurine transporter TauT in primary cilia of NIH3T3 fibroblasts. *Cell Biology International*, **29**, 347-351.
- [228] Saito S, Shingai R. (2006) Evolution of thermo TRP ion channel homologs in vertebrates. *Physiological Genomics*, **27**, 219-230.
- [229] Shichida Y, Matsuyama T. (2009) Evolution of opsins and phototransduction. *Philosophical Transactions of the Royal Society, series B, Biological Sciences*, **364**, 2881-2895.
- [230] Trivedi D, Williams DS. (2010) Ciliary transport of opsin. *Advances in Experimental Medicine and Biology*, **664**, 185-191.

- [231] Arendt D, Tessmar-Raible K, Snyman H, Dorresteijn AW, Wittbrodt J. (2004) Ciliary photoreceptors with a vertebrate-type opsin in an invertebrate brain. *Science*, **306**(5697), 869-871.
- [232] Raychowdhury MK, McLaughlin M, Ramos AJ, Montalbetti N, Bouley R, Ausiello DA, Cantiello HF. (2005) Characterization of single channel currents from primary cilia of renal epithelial cells. *Journal of Biological Chemistry*, **280**, 34718-34722.
- [233] Enuka Y, Hanukoglu I, Edelheit O, Vaknine H, Hanukoglu A. (2012) Epithelial sodium channels (ENaC) are uniformly distributed on motile cilia in the oviduct and the respiratory airways. *Histochemistry and Cell Biology*, **37**, 339-353.
- [234] Hu J, Barr MM. (2005) ATP-2 interacts with the PLAT domain of LOV-1 and is involved in *Caenorhabditis elegans* polycystin signalling. *Molecular Biology of the Cell*, **16**, 458-469.
- [235] DeCaen PG, Dellling M, Vien TN, Clapham DE. (2013) Direct recording and molecular identification of the calcium channel of primary cilia. *Nature*, **504**, 315-318.
- [236] Korngreen A, Ma W, Priel Z, Silberberg SD. (1998) Extracellular ATP directly gates a cation-selective channel in rabbit airway ciliated epithelial cells. *Journal of Physiology*, **508**, 703-720.
- [237] Ou Y, Ruan Y, Cheng M, Moser JJ, Rattner JB, van der Hoorn FA. (2009) Adenylate cyclase regulates elongation of mammalian primary cilia. *Experimental Cell Research*, **315**, 2802-2817.
- [238] Kwon RY, Temiyasathit S, Tummala P, Quah CC, Jacobs CR. (2010) Primary cilium-dependent mechanosensing is mediated by adenylyl cyclase 6 and cyclic AMP in bone cells. *FASEB Journal*, **24**, 2859-2868.
- [239] Liu F, Patterson RJ, Wang JL. (2002) Intracellular function of galectins. *Biochimica et Biophysica Acta*, **1572**, 263-273.
- [240] Valkova N, Yunis R, Mak SK, Kang K, Kültz D. (2005) Nek8 mutation causes overexpression of galectin-1, sorcin, and vimentin and accumulation of the major urinary protein in renal cysts of jck mice. *Molecular and Cellular Proteomics*, **4**, 1009-1018.
- [241] Chiu MG, Johnson TM, Woolf AS, Dahm-Vicker EM, Long DA, Guay-Woodford L, Hillman KA, Bawumia S, Venner K, Hughes RC, Poirier F, Winyard PJ. (2006) Galectin-3 associates with the primary cilium and modulates cyst growth in congenital polycystic kidney disease. *American Journal of Pathology*, **169**, 1925-1938.
- [242] Domic J, Dabelic S, Flögel M. (2006) Galectin-3: an open-ended story. *Biochimica et Biophysica Acta*, **1760**, 616-635.
- [243] Rondanino C, Poland PA, Kinlough CL, Li H, Rbaibi Y, Myerburg MM, Al-Bataineh MM, Kashlan OB, Pastor-Soler NM, Hallows KR, Weisz OA, Apodaca G, Hughey RP. (2011) Galectin-7 modulates the length of the primary cilia and wound repair in polarised kidney epithelial cells. *American Journal of Physiology*, **301**, F622-F633.
- [244] Hadari YR, Arbel-Goren R, Levy Y, Amsterdam A, Alon R, Zakut R, Zick Y. (2000) Galectin-8 binding to integrins inhibits cell adhesion and induces apoptosis. *Journal of Cell Science*, **113**, 2385-2397.
- [245] Hori Y, Kobayashi T, Kikko Y, Kontani K, Katada T. (2008) Domain architecture of the atypical Arf-family GTPase Arl13b involved in cilia formation. *Biochemical and Biophysical Research Communications*, **373**, 119-124.

- [245] Cevik S, Hori Y, Kaplan OI, Kida K, Toivenon T, Foley-Fisher C, Cottell D, Katada T, Kontani K, Blacque OE (2010) Joubert syndrome Arl13b functions at ciliary membranes and stabilizes protein transport in *Caenorhabditis elegans*. *Journal of Cell Biology*, **188**, 953-969.
- [246] Larkins CE, Aviles GD, East MP, Kahn RA, Caspary T. (2011) Arl13b regulates ciliogenesis and the dynamic localization of Shh signaling proteins. *Molecular Biology of the Cell*, **22**, 4694-4703.
- [247] Horner VL, Caspary T. (2011) Disrupted dorsal neural tube BMP signalling in the cilia mutant Arl13b hnn stems from abnormal Shh signalling. *Developmental Biology*, **355**, 43-54.
- [248] Jacoby M, Cox JJ, Gayral S, Hampshire DJ, Ayub M, Blockmans M, Pernot E, Kisseleva MV, Compère P, Schiffmann SN, Gergely F, Riley JH, Pérez-Morga D, Woods CG, Schurmans S. (2009) INPP5E mutations cause primary cilium signalling defects, ciliary instability and ciliopathies in human and mouse *Nature Genetics*, **41**, 1027-1031.
- [249] Bielas SL, Silhavy JL, Brancati F, Kisseleva MV, Al-Gazali L, Sztriha L, Bayoumi RA, Zaki MS, Abdel-Aleem A, Rosti RO, Kayserili H, Swistun D, Scott LC, Bertini E, Boltshauser E, Fazzi E, Travaglini L, Field SJ, Gayral S, Jacoby M, Schurmans S, Dallapiccola B, Majerus PW, Valente EM, Gleeson JG. (2009) Mutations in INPP5E, encoding inositol polyphosphate-5-phosphatase E, link phosphatidyl inositol signalling to the ciliopathies. *Nature Genetics*, **41**, 1032-1036.
- [250] Luo N, Lu J, Sun Y. (2012) Evidence of a role of inositol polyphosphate 5-phosphatase INPP5E in cilia formation in zebrafish. *Vision Research*, **75**, 98-107.
- [251] Humbert MC, Weihbrecht K, Searby CC, Li Y, Pope RM, Sheffield VC, Seo S. (2012) ARL13B, PDE6D, and CEP164 form a functional network for INPP5E ciliary targeting. *Proceedings of the National Academy of Sciences, USA*, **109**, 19691-19696.
- [252] Eley L, Gabrielides C, Adams M, Johnson CA, Hildebrandt F, Sayer JA. (2008) Joubertin localises to collecting ducts and interacts with nephrocystin-1. *Kidney International*, **74**, 1139-1149.
- [253] Amann-Zalcenstein D, Avidan N, Kanyas K, Ebstein RP, Kohn Y, Hamdan A, Ben-Asher E, Karni O, Mujaheed M, Segman RH, Maier W, Macciardi F, Beckmann JS, Lancet D, Lerer B. (2006) AH11, a pivotal neurodevelopmental gene, and C6orf217 are associated with susceptibility to schizophrenia. *European Journal of Human Genetics*, **14**, 1111-1119.
- [254] Utsch, B, Sayer JA, Attanasio M, Pereira RR, Eccles M, Hennies HC, Otto EA, Hildebrandt F. (2006) Identification of the first AH11 gene mutations in nephronophthisis-associated Joubert syndrome. *Pediatric Nephrology*, **21**, 32-35.
- [255] Ou Y, Zhang Y, Cheng M, Rattner JB, Dobrinski I, van der Hoorn FA. (2012) Targeting of CRMP-2 to the primary cilium is modulated by GSK-3b. *PLoS One*, **7**(11):e48773.
- [256] Fan S, Hurd TW, Liu CJ, Straight SW, Weimbs T, Hurd EA, Domino SE, Margolis B. (2004) Polarity proteins control ciliogenesis via kinesin motor interactions. *Current Biology*, **14**, 1451-1461.
- [257] Fan S, Fogg V, Wang Q, Chen XW, Liu CJ, Margolis B (2007) A novel Crumbs3 isoform regulates cell division and ciliogenesis via importin beta interactions. *Journal of Cell Biology*, **178**, 387-398.
- [258] Andersen NJ, Yeaman C. (2010) Sec3-containing exocyst complex is required for desmosome assembly in mammalian epithelial cells. *Molecular Biology of the Cell*, **21**, 152-164.
- [259] Babbey CM, Bacallao RL, Dunn KW. (2010) Rab10 associates with primary cilia and the exocyst complex in renal epithelial cells. *American Journal of Physiology*, **299**, F495-F506.

- [260] Inoue M, Chiang SH, Chang L, Chen XW, Saltiel AR (2006) Compartmentalization of the exocyst complex in lipid rafts controls glut4 vesicle tethering. *Molecular Biology of the Cell*, **17**, 2303-2311.
- [261] Sjölander M, Uhlmann J, Ponstingl H. (2002) DelGEF, a homologue of the Ran guanine nucleotide exchange factor RanGEF, binds to the exocyst component Sec5 and modulates secretion. *FEBS Letters*, **532**, 211-215.
- [262] Chien Y, Kim S, Bumeister R, Loo YM, Kwon SW, Johnson CL, Balakireva MG, Romeo Y, Kopelovich L, Gale M, Yeaman C, Camonis JH, Zhao Y, White MA. (2006) RalB GTPase-mediated activation of the IkkappaB family kinase TBK1 couples innate immune signalling to tumour cell survival. *Cell*, **127**, 157-170.
- [263] Whalen DM, Malinauskas T, Gilbert RJ, Siebold C. (2013) Structural insights into proteoglycan-shaped Hedgehog signaling. *Proceedings of the National Academy of Sciences, USA*, **110**, 16420-16425.
- [264] Ribes V, Briscoe J. (2009) Establishing and interpreting graded Sonic Hedgehog during vertebrate neural tube patterning: the role of negative feedback. *Cold Spring Harbor Perspectives in Biology*, **1**(2): a002014.
- [265] Breunig JJ, Sarkisian MR, Arellano JI, Morozov YM, Ayoub AE, Sojitra S, Wang B, Flavell RA, Rakic P, Town T. (2008) Primary cilia regulate hippocampal neurogenesis by mediating sonic Hedgehog signalling. *Proceedings of the National Academy of Sciences, USA*, **105**, 13127-13132.
- [266] Ruiz I, Altaba A. (1999) Gli proteins encode context-dependent positive and negative functions: implications for development and disease. *Development*, **126**, 3205-3216.
- [267] Stecca B, Mas C, Ruiz i Altaba A. (2005) Interference with HH-GLI signaling inhibits prostate cancer. *Trends in Molecular Biology*, **11**, 199-203.
- [268] Huntzicker EG, Estay IS, Zhen H, Lokteva LA, Jackson PK, Oro AE. (2006) Dual degradation signals control Gli protein stability and tumour formation. *Genes and Development*, **20**, 276-281.
- [269] Qin J, Lin Y, Norman RX, Ko HW, Eggenschwiler JT. (2011) Intraflagellar transport protein 122 antagonizes Sonic Hedgehog signalling and controls ciliary localisation of pathway components. *Proceedings of the National Academy of Sciences, USA*, **108**, 1456-1461.
- [270] Bishop CL, Bergin AM, Fessart D, Borgdorff V, Hatzimasoura E, Garbe JC, Stampfer MR, Koh J, Beach DH. (2010) Primary cilium-dependent and independent Hedgehog signalling inhibits p16(INK4A). *Molecular Cell*, **40**, 533-547.
- [271] Hopyan S, Nadesan P, Yu C, Wunder J, Alman BA. (2005) Dysregulation of Hedgehog signalling predisposes to synovial chondromatosis. *Journal of Pathology*, **206**, 143-150.
- [272] Liu H, Gu D, Xie J. (2011) Clinical implications of Hedgehog signalling pathway inhibitors. *Chinese Journal of Cancer*, **30**, 13-26.
- [273] Apionishev S, Katanayeva NM, Marks SA, Kalderon D, Tomlinson A. (2005) *Drosophila* smoothed phosphorylation sites essential for Hedgehog signal transduction. *Nature Cell Biology*, **7**, 86-92.
- [274] Ruiz-Gómez A, Molnar C, Holguín H, Mayor F, de Celis JF. (2007) The cell biology of Smo signalling and its relationships with GPCRs. *Biochimica et Biophysica Acta*, **1768**, 901-1012.

- [275] Lum L, Zhang C, Oh S, Mann RK, von Kessler DP, Taipale J, Weis-Garcia F, Gong R, Wang B, Beachy PA. (2003) Hedgehog signal transduction via Smoothed association with a cytoplasmic complex scaffolded by the atypical kinesin, Costal-2. *Molecular Cell*, **12**, 1261-1274.
- [276] Corbit KC, Aanstad P, Singla V, Norman AR, Stainier DY, Reiter JF. (2005) Vertebrate smoothed functions at the primary cilium. *Nature*, **437**, 1018-1021.
- [277] Zhang C, Williams EH, Guo Y, Lum L, Beachy PA. (2004) Extensive phosphorylation of smoothed in Hedgehog pathway activation. *Proceedings of the National Academy of Sciences, USA*, **101**, 17900-17907.
- [278] Strutt H, Thomas C, Nakano Y, Stark D, Neave B, Taylor AM, Ingham PW. (2001) Mutations in the sterol-sensing domain of Patched suggest a role for vesicular trafficking in Smoothed regulation. *Current Biology*, **11**, 608-613.
- [279] May SR, Ashique AM, Karlen M, Wang B, Shen Y, Zarbalis K, Reiter J, Ericson J, Peterson AS. (2005) Loss of the retrograde motor for IFT disrupts localisation of Smo to cilia and prevents the expression of both activator and repressor functions of Gli. *Developmental Biology*, **287**, 378-389.
- [280] Deneff N, Neubüser D, Perez L, Cohen SM. (2000) Hedgehog induces opposite changes in turnover and subcellular localisation of patched and smoothed. *Cell*, **102**, 521-531.
- [281] Chen Y, Struhl G. (1998) In vivo evidence that Patched and Smoothed constitute distinct binding and transducing components of a Hedgehog receptor complex. *Development*, **125**, 4943-4948.
- [282] Taipale J, Chen JK, Cooper MK, Wang B, Mann RK, Milenkovic L, Scott MP, Beachy PA. (2000) Effects of oncogenic mutations in Smoothed and Patched can be reversed by cyclopamine. *Nature*, **406**, 1005-1009.
- [283] Merchant M, Vajdos FF, Ultsch M, Maun HR, Wendt U, Cannon J, Desmarais W, Lazarus RA, de Vos AM, de Sauvage FJ. (2004) Suppressor of fused regulates Gli activity through a dual binding mechanism. *Molecular Cell Biology*, **24**, 8627-8641.
- [284] Tukachinsky H, Lopez LV, Salic A. (2010) A mechanism for vertebrate Hedgehog signalling: recruitment to cilia and dissociation of SuFu-Gli protein complexes. *Journal of Cell Biology*, **191**, 415-428.
- [285] Kogerman P, Grimm T, Kogerman L, Krause D, Undén AB, Sandstedt B, Toftgård R, Zaphiropoulos PG. (1999) Mammalian suppressor-of-fused modulates nuclear-cytoplasmic shuttling of Gli-1. *Nature Cell Biology*, **1**, 312-319.
- [286] Kise Y, Morinaka A, Teglund S, Miki H. (2009) SuFu recruits GSK3beta for efficient processing of Gli3. *Biochemical and Biophysical Research Communications*, **387**, 569-574.
- [287] Wong SY, Seol AD, So PL, Ermilov AN, Bichakjian CK, Epstein EH, Dlugosz AA, Reiter JF. (2009) Primary cilia can both mediate and suppress Hedgehog pathway-dependent tumorigenesis. *Nature Medicine*, **15**, 1055-1061.
- [288] Karpen HE, Bukowski JT, Hughes T, Gratton JP, Sessa WC, Gailani MR. (2001) The sonic Hedgehog receptor patched associates with caveolin-1 in cholesterol-rich microdomains of the plasma membrane. *Journal of Biological Chemistry*, **276**, 19503-19511.
- [289] Rohatgi R, Milenkovic L, Scott MP. (2007) Patched1 regulates Hedgehog signalling at the primary cilium. *Science*, **317**, 372-376.

- [290] Liu A, Wang B, Niswander LA. (2005) Mouse intraflagellar transport proteins regulate both the activator and repressor functions of Gli transcription factors. *Development*, **132**, 3103-3111.
- [291] Dai P, Akimaru H, Tanaka Y, Maekawa T, Nakafuku M, Ishii S. (1999) Sonic Hedgehog-induced activation of the Gli1 promoter is mediated by GLI3. *Journal of Biological Chemistry*, **274**, 8143-8152.
- [292] Stone DM, Murone M, Luoh S, Ye W, Armanini MP, Gurney A, Phillips H, Brush J, Goddard A, de Sauvage FJ, Rosenthal A. (1999) Characterization of the human suppressor of fused, a negative regulator of the zinc-finger transcription factor Gli. *Journal of Cell Science*, **112**, 4437-4448.
- [293] Dunaeva M, Michelson P, Kogerman P, Toftgard R. (2003) Characterization of the physical interaction of Gli proteins with SUFU proteins. *Journal of Biological Chemistry*, **278**, 5116-5122.
- [294] Cheung HO, Zhang X, Ribeiro A, Mo R, Makino S, Puviindran V, Law KK, Briscoe J, Hui CC. (2009) The kinesin protein Kif7 is a critical regulator of Gli transcription factors in mammalian hedgehog signaling. *Science Signalling*, **2**(76):ra29.
- [295] Law KKL, Makino S, Mo R, Zhang X, Puviindran V, Hui C. (2012) Antagonistic and cooperative actions of Kif7 and Sufu define graded intracellular Gli activities in Hedgehog signaling. *PLoS One*, **7**(11):e50193.
- [296] Nolan-Stevaux O, Lau J, Truitt ML, Chu GC, Hebrok M, Fernández-Zapico ME, Hanahan D. (2009) GLI1 is regulated through Smoothed-independent mechanisms in neoplastic pancreatic ducts and mediates PDAC cell survival and transformation. *Genes and Development*, **23**, 24-36.
- [297] Hopyan S, Nadesan P, Yu C, Wunder J, Alman BA. (2005) Dysregulation of hedgehog signalling predisposes to synovial chondromatosis. *Journal of Pathology*, **206**, 143-150.
- [298] Haycraft CJ, Banizs B, Aydin-Son Y, Zhang Q, Michaud EJ, Yoder BK. (2005) Gli2 and Gli3 localize to cilia and require the intraflagellar transport protein polaris for processing and function. *PLoS Genetics*, **1**, e53.
- [299] Regl G, Kasper M, Schnidar H, Eichberger T, Neill GW, Ikram MS, Quinn AG, Philpott MP, Frischauf AM, Aberger F. (2004) The zinc-finger transcription factor GLI2 antagonizes contact inhibition and differentiation of human epidermal cells. *Oncogene*, **23**, 1263-1274.
- [300] Tojo M, Kiyosawa H, Iwatsuki K, Nakamura K, Kaneko F. (2003) Expression of the GLI2 oncogene and its isoforms in human basal cell carcinoma. *British Journal of Dermatology*, **148**, 892-897.
- [301] Sheng H, Goich S, Wang A, Grachtchouk M, Lowe L, Mo R, Lin K, de Sauvage FJ, Sasaki H, Hui CC, Dlugosz AA. (2002) Dissecting the oncogenic potential of Gli2: deletion of an NH(2)-terminal fragment alters skin tumour phenotype. *Cancer Research*, **62**, 5308-5316.
- [302] Bishop CL, Bergin AM, Fessart D, Borgdorff V, Hatzimasoura E, Garbe JC, Stampfer MR, Koh J, Beach DH. (2010) Primary cilium-dependent and -independent Hedgehog signalling inhibits p16(INK4A). *Biology of the Cell*, **240**, 533-547.
- [303] França MM, Jorge AA, Carvalho LR, Costalonga EF, Vasques GA, Leite CC, Mendonca BB, Arnhold IJ. (2010) Novel heterozygous nonsense GLI2 mutations in patients with lobe without holoprosencephaly. *Journal of Clinical Endocrinology and Metabolism*, **95**, E384-E391.

- [304] Regl G, Neill GW, Eichberger T, Kasper M, Ikram MS, Koller J, Hintner H, Quinn AG, Frischauf AM, Aberger F. (2002) Human GLI2 and GLI1 are part of a positive feedback mechanism in basal cell carcinoma. *Oncogene*, **21**, 5529-5539.
- [305] Wen X, Lai CK, Evangelista M, Hongo JA, de Sauvage FJ, Scales SJ. (2010) Kinetics of Hedgehog-dependent full-length Gli3 accumulation in primary cilia and subsequent degradation. *Molecular Cell Biology*, **30**, 1910-1922.
- [306] Bai CB, Stephen D, Joyner AL. (2004) All mouse ventral spinal cord patterning by Hedgehog is Gli dependent and involves an activator function of Gli3. *Developmental Cell*, **6**, 103-115.
- [307] Humke EW, Dorn KV, Milenkovic L, Scott MP, Rohatgi R. (2010) The output of Hedgehog signalling is controlled by the dynamic association between suppressor of fused and the Gli proteins. *Genes and Development*, **24**, 670-682.
- [308] Kang S, Graham JM, Olney AH, Biesecker LG. (1997) GLI3 frameshift mutations cause autosomal dominant Pallister-Hall syndrome. *Nature Genetics*, **15**, 266-268.
- [309] Park TJ, Mitchell BJ, Abitua PB, Kintner C, Wallingford JB. (2008) Dishevelled controls apical docking and planar polarization of basal bodies in ciliated epithelial cells. *Nature Genetics*, **40**, 871-879.
- [310] Wallingford JB, Mitchell B. (2011) Strange as it may seem: the many links between Wnt signaling, planar cell polarity, and cilia. *Genes and Development*, **25**, 201-213.
- [311] Barker N. (2008) The canonical Wnt/beta-catenin signalling pathway. *Methods in Molecular Biology*, **468**, 5-15.
- [312] Karasawa T, Yokokura H, Kitajewski J, Lombroso PJ. (2002) Frizzled-9 is activated by Wnt-2 and functions in Wnt/beta -catenin signalling. *Journal of Biological Chemistry*, **277**, 37479-37486.
- [313] Katoh M. (2008) WNT signalling in stem cell biology and regenerative medicine. *Current Drug Targets*, **9**, 565-570.
- [314] Katoh M, Katoh M. (2007) WNT signalling pathway and stem cell signalling network. *Clinical Cancer Research*, **13**, 4042-4045.
- [315] Sugiyama Y, Stump RJ, Nguyen A, Wen L, Chen Y, Wang Y, Murdoch JN, Lovicu FJ, McAvoy JW. (2010) Secreted frizzled-related protein disrupts PCP in eye lens fiber cells that have polarised primary cilia. *Developmental Biology*, **338**, 193-201.
- [316] Penton A, Wodarz A, Nusse R (2002) A mutational analysis of Disheveled in Drosophila defines novel domains in the Disheveled protein as well as novel suppressing alleles of axin. *Genetics*, **161**, 747-762.
- [317] Vladar EK, Axelrod JD. (2008) Disheveled links basal body docking and orientation in ciliated epithelial cells. *Trends in Cell Biology*, **18**, 517-520.
- [318] Park TJ, Mitchell BJ, Abitua PB, Kintner C, Wallingford JB. (2008) Disheveled controls apical docking and planar polarization of basal bodies in ciliated epithelial cells. *Nature Genetics*, **40**, 871-879.
- [319] Steere N, Chae V, Burke M, Li F-Q, Takemaru K-I, Kuriyama, R. (2012) A Wnt/beta-catenin pathway antagonist Chibby binds Cenexin at the distal end of mother centrioles and functions in primary cilia formation. *PLoS One*, **7**(7):e41077.

- [320] Enjolras C, Thomas J, Chhin B, Cortier E, Duteyrat JL, Soulavie F, Kernan MJ, Laurençon A, Durand B. (2012) *Drosophila* chibby is required for basal body formation and ciliogenesis but not for Wg signalling. *Journal of Cell Biology*, **197**, 313-325.
- [321] Shiba D, Manning DK, Koga H, Beier DR, Yokoyama T. (2010) Inv acts as a molecular anchor for Nphp3 and Nek8 in the proximal segment of primary cilia. *Cytoskeleton*, **67**, 112-119.
- [322] Ezratty EJ, Stokes N, Chai S, Shah AS, Williams SE, Fuchs E. (2011) A role for the primary cilium in Notch signalling and epidermal differentiation during skin development. *Cell*, **145**, 1129-1141.
- [323] Hosaka Y, Saito T, Sugita S, Hikata T, Kobayashi H, Fukai A, Taniguchi Y, Hirata M, Akiyama H, Chung UI, Kawaguchi H, Chen S, Tao J, Bae Y, Jiang MM, Bertin T, Chen Y, Yang T, Lee B. (2013) Notch signalling in chondrocytes modulates endochondral ossification and osteoarthritis development. *Proceedings of the National Academy of Sciences, USA*, **110**, 1875-1880.
- [324] Chen S, Tao J, Bae Y, Jiang MM, Bertin T, Chen Y, Yang T, Lee B. (2013) Notch gain of function inhibits chondrocyte differentiation via Rbpj-dependent suppression of Sox9. *Journal of Bone and Mineral Research*, **28**, 649-659.
- [325] Lopes SS, Lourenço R, Pacheco L, Moreno N, Kreiling J, Saúde L. (2010) Notch signalling regulates left-right asymmetry through ciliary length control. *Development*, **137**, 3625-3632.
- [326] Zanotti S, Canalis E. (2013) Notch suppresses nuclear factor of activated T cells (NFAT) transactivation and Nfatc1 expression in chondrocytes. *Endocrinology*, **154**, 762-772.

1.2 Axoneme Associated Proteins

Chaperones	Interaction, Localisation and Signalling Cascade	Disease Implication / Ancillary Information
TCP1 (TCP1 ring complex (TRiC))	Chaperone protein localised to motile cilia[1]. Required for actin and tubulin function[2]. Interacts with histone deacetylase 3 (HDAC3) [3].	
NDE1	Partner of dynein of LC8 light chain which controls ciliary length, influences G1-S phase transition[4].	
Y-Shaped Linkers	Y-shaped linkers are believed to be comprised of a microtubule binding NPHP1, 4 , longer coiled domains of CEP290 and NPHP8 (making up the filament) and ciliary membrane (transmembrane components of TMEMs) and TCTN2, 3 , with TCTN1 (providing an extracellular membrane domain)[5].	Proteins MKS-1 , (MKSR-1 , and MKSR-2), MKS3/TMEM67 , MKS-5/RPGRI1L , MKS-6/CC2D2A , NPHP-1 , and NPHP-4 are located within the transition zone[6].
Tektins	Found attached to axonemal microtubules. Involved in the assembly of centrioles [7].	Involved in determining microtubule spacings in the axoneme[8]
TEKT1	Important in development of the sperm-tail basal body and axoneme[7, 9].	
TEKT2	Expressed pro-metaphase/late anaphase . Similar to tektins in sperm flagella and has an association with the centrosome and centrioles[10].	
TEKT3	Expressed in sperm producing cells, associated with axoneme sperm tail[11].	
TEKT4	Outer fibre component of sperm flagella[12], absence causes sub-fertility[13].	
TEKT5	Forms a component of the middle piece of the sperm flagella[14].	
ODF1 (Outer dense fibers-1)	Outer dense fibers of the axonemes of motile cilia. Phosphorylated by CDK5 enhancing ODF1-OIP1 function[15].	
Rabin	Ciliary membrane assembly is initiated by Rab11 and TRAPP1 by transport to the centrosome[16]. Rabin interacts with the GTP 'locked' form of RAB11 [17].	Involved in ciliogenesis, where Rab8 and RAB11 are required[17].
I2-Inhibitor	Phosphatase-Inhibitor-2 promotes acetylation of tubulin within the primary cilium[18].	
PACRG	PACRG is required for correct development of the (9+2) cilium , and defects affect beat frequency. Interacts with Rib72 (outer doublet proto-filament ribbon) and they localise together. PACRG localises along the full length of the basal body and axoneme, where it is located on the outer sub-fibre doublets , and possibly links between MT doublets [19, 20].	Expression is co-regulated with the Parkinson's Disease gene Parkin . Suspected involvement in human ciliopathies Asthenospermia and Primary Ciliary Dyskinesia . Evolutionarily conserved axonemal protein[21].
TCTEX-1	The TCTEX-1 binding protein is phosphorylated before the S-phase and recruited to the ciliary transition zone , where it has a role in ciliary disassembly and re-sorption [22]. It may modulate ciliary length and G1-S progression. Interacts with NDE1 (partner of LC8) and controls ciliary length[4, 23].	Localisation to the transition zone. Required for Rhodopsin transport by association with dynein light chain[24].
Nephrocystin Family		
NPHP1/JBTS4	NPHP1 localises to the transition zone [25] with PLK1 [26] where it interacts with the inversin	See INV and NPHP2.

	compartment (NPHP2)[27] and NPHP4 [28].	
NPHP2 Inversin / INVS (Nephrocystin2)	Localises to the axonemal shaft and transition zone [29]. Contains Ankyrin domains, which act as an anchor for NPHP3 and NEK8 in the proximal region of the cilium[30]. Interacts with Aurora-A and HDAC6 in ciliary assembly[31]. INVS is an essential intra-ciliary anchor of NPHP8/NEK8 and NPHP3 [30]. NPHP1 and NPHP4 localise to the proximal end of ciliary compartment[30]. NPHP2 interacts with NPHP1 [33] and functions as a molecular switch between WNT pathways[34].	Acts as a molecular switch between Wnt signaling pathways[34].
NPHP3	Part of the STAND NTPase family [35]. Interacts with NPHP1 and NPHP2 , inhibiting canonical Wnt signalling[36]. Depletion or inhibition of NPHP3 leads to planar cell polarity defects[36].	Localises to primary and retinal cilia[36]. Found attached with NEK8 to Inversin [37].
NPHP4	Interacts with NPHP1 and RPGRIP1L [28](Hippo signalling regulating cell proliferation)[28-40], p130Cas and Pyk2 are found with the NPHP4 complex in actin- and microtubule- based structures[40].	Localises to the transition zone, basal body and the centrosome[40, 41].
NPHP5 (IQCB1)	Interacts with NPHP1 , NPHP6 , Calmodulin and RPGR [42 43]. Localised to the centrosome, where it binds NPHP6/CEP290 . Depletion prevents centrosomal binding and inhibits ciliogenesis[44].	Localised to cilia. Retinal cilia defects share a similar pathology to those of NPHP6 [37, 43, 45]. Localised to the centrosome[44].
NPHP6	See MKS4/JBTS5.	
NPHP7/GLIS2	Interacts with CTBP1 as a transcriptional repressor [46] and with p120 [47]. BBS1 and NPHP7 are required for ciliary motility[48].	Defects/mutations associated with nephronophthisis [49].
NPHP8/RPGRIP1L/MKS5 RPGRIP1-Ligand *See also MKS5/JBTS7/RPGRIP1L/NPHP8	Localises to the primary cilium and basal body in the centrosome where it is proposed that RPGRIP1 and RPGRIP1L function as cilium-specific scaffolds that recruit a NEK4 serine/threonine kinase (signalling network) which regulates cilium stability[50]. Interacts with NPHP4 [28].	Localises to basal bodies and the axoneme[28]. RPGRIP1L is mutated in Joubert Syndrome and in nephronophthisis[28, 51].
NPHP9/NEK8	Serine-threonine protein kinase involved in ciliogenesis and the cell cycle (G2 to M phase)[52]. Localised to the proximal region of primary cilium and expressed weakly in the cytosol. May interact with expression, localisation and signalling of Polycystin-1 and 2 [53]. Mutation results in over expression of Gal-1 , Sorcin and Vimentin [54]. Localises to the proximal region of the cilium[52] although reported along the full length[53].	Involved in PKD1 cystogenesis and cell-cell adhesions [55]. Involved in nephronophthisis [56] and cyst formation [57]. Linked to PCD [58].
NEK Family		
NEK1	Involved with PRKA in ciliogenesis and Shh signalling [59 60]. Regulates VDAC1 opening and closing of anion channels and is involved in apoptosis[61]. Silencing NEK1 mitigates or slows down DNA repair and blocks phase arrest [62]. Localises to the centrosome[52].	Involved in short ribbed polydactyly [63], linked to PCD [58] and polycystic kidney disease [52]
NEK2	Involved in G2-M transition. Regulates centrosome structure and promotes centrosome mitotic fissioning by phosphorylating centrosomal proteins[31, 64]. NEK2/NIMA proteins are involved in nuclear membrane breakdown and are responsible for centromere separation [52, 65]. Involved in	NEK2A targets nucleolar NEK11 in G1/S arrested cells via a nuclear targeting motif suggesting nuclear function[66]. Located in the distal (-) ends of both centrioles at the beginning of S-phase [67]. Required for G2/M-phase

	regulating the mitotic spindle [52].	ciliary disassembly[68].
NEK3 (Might be in the cilium)	Localises to the centrosome[69]and in the cytoplasm where it regulates microtubule acetylation[70].	Prolactin receptor signaling and cytoskeletal reorganisation , but little known about its role[70, 71].
NEK4	Regulates ciliary assembly and stability. Is recruited to scaffolds of RPGRIP1 and RPGRIP1L and also localises to the ciliary rootlet [50].	Involved in Joubert and Meckel-Gruber syndromes[50]
NEK5	Nuclear protein, localises to the proximal ends of centrioles during Interphase. Loss of NEK5 results in loss of γ-tubulin and premature centrosome fissioning[69].	Negative centrosomal regulator[69].
NEK6	Involved in mitosis[58]. NEK9 activates the NEK6 and NEK7 kinases[72, 73]. NEK6/NEK9 forms a signal transduction module in which binding of NEK6 to NEK9 is regulated by DYNLL/LC8 [74].	Depletion of NEK6 results in defective mitosis[73]. Regulates the mitotic spindle[58, 69].
NEK7	Regulator of mitosis and cytokinesis[58, 73, 868]. Interacts with NEK9 [72] where NEK9 activates NEK6 and NEK7 kinases[72]. Localises to the centrosome[73, 75].	Depletion of NEK7 results in defective mitosis [73] and is involved in polyploidy and cancer [76].
NEK8 (see NPHP9)	Common to both families.	
NEK9	Regulates mitotic G1-S progression[58] and interphase progression[78]. Interacts with NEK6 [72, 77], PLK1 [72], SSRP1 [78], Eg5 [72] and Ran (Interphase nuclear pore transporter)[77]. NEK9 is activated by PLK1 and controls early centrosome separation through a complex of NEK6/7 kinases and EG5 [67, 72]	Regulates mitotic spindle[561]. Forms part of a signalling module in which NEK6/NEK9 binding is regulated by DYNLL/LC8 [74]. Eg5 is also known as KIF7 .
NEK10	Mediates G2/M cell cycle arrest and response to ultra-violet radiation [79].	
NEK11	Interacts with NEK2A in the nucleus during G1-S arrest[66].	
RP1 (Retinitis Pigmentosa Protein-1)	Oxygen Regulated Protein-1 . Role in outer segments of photoreceptors[80].	
RP2 (Retinitis Pigmentosa Protein-2)	Ciliary localisation controlled by importin-β2 [81].	
RPGR Retinitis Pigmentosa Guanosine Triphosphatase (GTPase) Regulator (RPGR)[82].	Interacts with novel transport proteins in outer rod photoreceptor segments and rods[82]. Interacts with RPGRIP-1 , CEP290 , NPM , SMC1 , SMC3 , and IFT88 [83]. Co-localises to centrioles and basal bodies[84], with isoforms found in photoreceptors and the transition zone of motile cilia[85].	There is no consensus as yet to localisation of RPGR. Isoforms have been found in the retina and mutations are involved with defects in photoreceptors and in ciliopathies [82, 86].
RPGRIP1 Retinitis Pigmentosa GTPase Regulator Interacting Protein	NPHP4 and RPGR form components of the RPGRIP1 interactome complex[87], RPGRIP1 and RPGRIP1L are involved ciliary integrity via the serine/threonine kinase NEK4 via interactions with NEK4 [50]. See MKS5/NPHP8 .	Mutated in Leber Congenital Amaurosis [88, 89].
DCDC2	A protein involved in binding to microtubules, localises to the primary cilium where it interacts with KIF3A . Increased expression increases ciliary length by activating Shh signalling , whilst decreased expression enhances Wnt signalling[90].	Associated with Dyslexia [90].
TCTN1/TCTN2/TCTN3 (Tectonics)	Tectonics are glycoprotein activators and regulators of Shh [91]. Interacts with Smo and RAB23 where they form complexes with membrane associated cilium proteins. Associated	The loss of TCTN1 (or TCTN2), TMEM67 or CC2D2A causes phenotypical specific defects in ciliogenesis and in membrane

	components within the transition zone include ARL13b, AC3, Smo, and PKD2 [92]. Components of MKS1, TMEM216, TMEM67, CEP290, B9D1, TCTN2 and CC2D2A which are localised to the transition zone[92]. TCTN2 plays a role in Hh signalling downstream of Smo and RAB23 where it acts as a repressor[91, 93].	composition[92].
LCA5 (Lebercilin)	Localises to axoneme microtubules and basal body of photoreceptors[94].	Associated with retinal defects.
PKA (Protein Kinase-A)	Dependent on cAMP concentration for function in binding to R-PKA activating C-PKA [95]. A subunit of PKA binds it to the cilium base via A-kinase anchoring proteins (AKAPs) where it is involved in Shh regulation [95].	
Importin-β2 (Ciliary Trafficking)	Importin contains α-subunit components which bind the nuclear localization sequences (NLS) , and β-subunits which dock and pass through nuclear pore complexes [96]. It has been found that importin-β2 regulates import of KIF17 and RAN-GTP [97], along with Retinitis Pigmentosa-2 [81]. The KIF17 motor tail contains a ciliary localisation sequence (CLS) which is similar to NLS indicating a possible similar regulatory mechanism[97].	Similarity of the pore complex with the primary cilium has been noted. KIF17 function is regulated by a ciliary gradient of the GTPase RAN [97].
Suspected in the Cilium		
MEK-1 / MAPK1 (suspected to be in the cilium/centrosome)	Mitogen-activated Protein Kinase-1. Interacts with HOP1 during meiosis[98].	
XPNPEP3 (Aminopeptidase-P3) (Suspected to be in the cilium)	Xaa-Pro aminopeptidase-3. Also known as aminopeptidase P3, is involved in a ciliopathic condition (although any role in cilium is still unknown), localises to mitochondria , and has cilium related function as several ciliary cystogenic proteins were found to be substrates of XPNPEP3 [99, 100].	Involved in a nephronophthisis like nephropathy[99, 100].

[1] Stephens RE, Lemieux NA. (1999) Molecular chaperones in cilia and flagella: implications for protein turnover. *Cell Motility and Cytoskeleton*, **44**, 274-283.

[2] Ursic D, Sedbrook JC, Himmel KL, Culbertson MR. (1994) The essential yeast Tcp1 protein affects actin and microtubules. *Molecular Biology of the Cell*, **5**, 1065-1080.

[3] Guenther MG, Yu J, Kao GD, Yen TJ, Lazar MA. (2002) Assembly of the SMRT-histone deacetylase 3 repression complex requires the TCP-1 ring complex. *Genes and Development*, **16**, 3130-3135.

[4] Jackson JK. (2011) Do cilia put brakes on the cell cycle? *Nature Cell Biology*, **13**, 340-342.

[5] Garcia-Gonzalom FR, Reiterm, F. (2012) Scoring a backstage pass: mechanisms of ciliogenesis and ciliary access. *Journal of Cell Biology*, **197**, 697-709.

[6] Williams CL, Li C, Kida K, Inglis PN, Mohan S, Semenec L, Bialas NJ, Stupay RM, Chen N, Blacque OE, Yoder BK, Leroux MR. (2011) MKS and NPHP modules cooperate to establish basal body/transition zone membrane associations and ciliary gate function during ciliogenesis. *Journal of Cell Biology*, **192**, 1023-1041.

- [7] Larsson M, Norrander J, Gräslund S, Brundell E, Linck R, Ståhl S, Höög C. (2000) The spatial and temporal expression of Tekt1, a mouse tektin C homologue, during c of the sperm tail basal body and axoneme. *European Journal of Cell Biology*, **79**, 718-725.
- [8] Amos LA, Norrander JM, Perrone CA, Linck RW. (1996) Structural comparison of tektins and evidence for their determination of complex spacings in flagellar microtubules. *Journal of Molecular Biology*, **257**, 385-397.
- [9] Norrander JM, Amos LA, Linck RW. (1992) Primary structure of tektin A1: comparison with intermediate-filament proteins and a model for its association with tubulin. *Proceedings of the National Academy of Sciences, USA*, **89**, 8567-8571.
- [10] Steffen W, Fajer EA, Linck RW. (1994) Centrosomal components immunologically related to tektins from ciliary and flagellar microtubules. *Journal of Cell Science*, **107**, 2095-2105.
- [11] Roy A, Yan W, Burns KH, Matzuk MM. (2004) Tektin3 encodes an evolutionarily conserved putative testicular microtubules-related protein expressed preferentially in male germ cells. *Molecular and Reproductive Development*, **67**, 295-302.
- [12] Iida H, Honda Y, Matsuyama T, Shibata Y, Inai T. (2006) Tektin 4 is located on outer dense fibers, not associated with axonemal tubulins of flagella in rodent spermatozoa. *Molecular and Reproductive Development*, **73**, 929-936.
- [13] Roy A, Lin YN, Agno JE, DeMayo FJ, Matzuk MM. (2007) Absence of tektin 4 causes asthenozoospermia and subfertility in male mice. *FASEB Journal*, **21**, 1013-1025.
- [14] Murayama E, Yamamoto E, Kaneko T, Shibata Y, Inai T, Iida H. (2008) Tektin5, a new Tektin family member, is a component of the middle piece of flagella in rat spermatozoa. *Molecular and Reproductive Development*, **75**, 650-658.
- [15] Rosales JL, Sarker K, Ho N, Broniewska M, Wong P, Cheng M, van der Hoorn FA, Lee KY. (2007) ODF1 phosphorylation by Cdk5/p35 enhances ODF1-OIP1 interaction. *Cell Physiology and Biochemistry*, **20**, 311-318.
- [16] Westlake CJ, Baye LM, Nachury MV, Wright KJ, Ervin KE, Phu L, Chalouni C, Beck JS, Kirkpatrick DS, Slusarski DC, Sheffield VC, Scheller RH, Jackson PK. (2011) Primary cilia membrane assembly is initiated by Rab11 and transport protein particle II (TRAPP2) complex-dependent trafficking of Rabin8 to the centrosome. *Proceedings of the National Academy of Sciences, USA*, **108**, 2759-2764.
- [17] Knödler A, Feng S, Zhang J, Zhang X, Das A, Peränen J, Guo W. (2010) Coordination of Rab8 and Rab11 in primary ciliogenesis. *Proceedings of the National Academy of Sciences, USA*, **107**, 6346-6351.
- [18] Wang W, Brautigan DL. (2008) Phosphatase inhibitor 2 promotes acetylation of tubulin in the primary cilium of human retinal epithelial cells. *BMC Cell Biology*, **9**, 62.
- [19] Wilson GR, Wang HX, Egan GF, Robinson PJ, Delatycki MB, O'Bryan MK, Lockhart PJ. (2010) Deletion of the Parkin co-regulated gene causes defects in ependymal ciliary motility and hydrocephalus in the quaking viable mutant mouse. *Human Molecular Genetics*, **19**, 1593-1602.
- [20] Ikeda K, Ikeda T, Morikawa K, Kamiya R. (2007) Axonemal localisation of *Chlamydomonas* PACRG, a homologue of the human Parkin-coregulated gene product. *Cell Motility and Cytoskeleton*, **64**, 814-821.

- [21] Dawe HR, Farr H, Portman N, Shaw MK, Gull K. (2005) The Parkin co-regulated gene product, PACRG, is an evolutionarily conserved axonemal protein that functions in outer-doublet microtubule morphogenesis. *Journal of Cell Science*, **118**, 5421-5430.
- [22] Li A, Saito M, Chuang JZ, Tseng YY, Dedesma C, Tomizawa K, Kaitsuka T, Sung CH. (2011) Ciliary transition zone activation of phosphorylated Tctex-1 controls ciliary resorption, S-phase entry and fate of neural progenitors. *Nature Cell Biology*, **13**, 402-411.
- [23] Palmer KJ, MacCarthy-Morrogh L, Smyllie N, Stephens DJ. (2011) A role for Tctex-1 (DYNLT1) in controlling primary cilium length. *European Journal of Cell Biology*, **90**, 865-871.
- [24] Williams JC, Xie H, Hendrickson WA. (2005) Crystal structure of dynein light chain TcTex-1. *Journal of Biological Chemistry*, **280**, 21981-21986.
- [25] Fliegau M, Horvath J, von Schnakenburg C, Olbrich H, Müller D, Thumfart J, Schermer B, Pazour GJ, Neumann HP, Zentgraf H, Benzing T, Omran H. (2006) Nephrocystin specifically localizes to the transition zone of renal and respiratory cilia and photoreceptor connecting cilia. *Journal of the American Society of Nephrology*, **17**, 2424-2433.
- [26] Seeger-Nukpezah T, Liebau MC, Höpker K, Lamkemeyer T, Benzing T, Golemis EA, Schermer B. (2012) The centrosomal kinase Plk1 localizes to the transition zone of primary cilia and induces phosphorylation of nephrocystin-1. *PLoS One*, **7**(6):e38838.
- [27] Szymanska K, Johnson CA. (2011) The transition zone: an essential functional compartment of cilia. *Cilia*, **1**, 10.
- [28] Arts HH, Doherty D, van Beersum SE, Parisi MA, Letteboer SJ, Gorden NT, Peters TA, Märker T, Voeselek K, Kartono A, Ozyurek H, Farin FM, Kroes HY, Wolfrum U, Brunner HG, Cremers FP, Glass IA, Knoers NV, Roepman R. (2007) Mutations in the gene encoding the basal body protein RPGRIP1L, a nephrocystin-4 interactor, cause Joubert syndrome. *Nature Genetics*, **39**, 882-888.
- [29] Shiba D, Yamaoka Y, Hagiwara H, Takamatsu T, Hamada H, Yokoyama T. (2009) Localisation of Inv in a distinctive intraciliary compartment requires the C-terminal ninein-homolog-containing region. *Journal of Cell Science*, **122**, 44-54.
- [30] Shiba D, Manning DK, Koga H, Beier DR, Yokoyama T. (2010) Inv acts as a molecular anchor for Nphp3 and Nek8 in the proximal segment of primary cilia. *Cytoskeleton*, **67**, 112-119.
- [31] Fry AM. (2002) The Nek2 protein kinase: a novel regulator of centrosome structure. *Oncogene*, **21**, 6184-6194.
- [32] Mergen M, Engel C, Müller B, Follo M, Schäfer T, Jung M, Walz G. (2013) The nephronophthisis gene product NPHP2/Inversin interacts with Aurora A and interferes with HDAC6-mediated cilia disassembly. *Nephrology, Dialysis and Transplantation*, **28**, 2744-2753.
- [33] Otto EA, Schermer B, Obara T, O'Toole JF, Hiller KS, Mueller AM, Ruf RG, Hoefele J, Beekmann F, Landau D, Foreman JW, Goodship JA, Strachan T, Kispert A, Wolf MT, Gagnadoux MF, Nivet H, Antignac C, Walz G, Drummond IA, Benzing T, Hildebrandt F. (2003) Mutations in INVS encoding inversin cause nephronophthisis type 2, linking renal cystic disease to the function of primary cilia and left-right axis determination. *Nature Genetics*, **34**, 413-420.
- [34] Lienkamp S, Ganner A, Walz G. (2012) Inversin, Wnt signaling and primary cilia. *Differentiation*, **283**, S49-S55.

- [35] Leipe DD, Koonin EV, Aravind L (2004) STAND, a class of P-loop NTPases including animal and plant regulators of programmed cell death: multiple, complex domain architectures, unusual phyletic patterns, and evolution by horizontal gene transfer. *Journal of Molecular Biology*, **343**, 1-28.
- [36] Bergmann C, Fliegau M, Bröchle NO, Frank V, Olbrich H, Kirschner J, Schermer B, Schmedding I, Kispert A, Kränzlin B, Nürnberg G, Becker C, Grimm T, Girschick G, Lynch SA, Kelehan P, Senderek J, Neuhaus TJ, Stallmach T, Zentgraf H, Nürnberg P, Gretz N, Lo C, Lienkamp S, Schäfer T, Walz G, Benzing T, Zerres K, Omran H. (2008) Loss of nephrocystin-3 function can cause embryonic lethality, Meckel-Gruber-like syndrome, situs inversus, and renal-hepatic-pancreatic dysplasia. *American Journal of Human Genetics*, **82**, 959-970.
- [37] Avner ED, Harmon WE, Niaudet P. (2009) *Paediatric Nephrology*. Springer, Berlin, Heidelberg.
- [38] Habbig S, Bartram MP, Müller RU, Schwarz R, Andriopoulos N, Chen S, Sägmüller JG, Hoehne M, Burst V, Liebau MC, Reinhardt HC, Benzing T, Schermer B. (2011) NPHP4, a cilia-associated protein, negatively regulates the Hippo pathway. *Journal of Cell Biology*, **193**, 633-642.
- [39] Schuermann MJ, Otto E, Becker A, Saar K, Ruschendorf F, Polak BC, Ala-Mello S, Hoefele J, Wiedensohler A, Haller M, Omran H, Nürnberg P, Hildebrandt F (2002) Mapping of gene loci for nephronophthisis type 4 and Senior-Loken syndrome, to chromosome 1p36. *American Journal of Human Genetics*, **70**, 1240-1246.
- [40] Mollet G, Silbermann F, Delous M, Salomon R, Antignac C, Saunier S. (2005) Characterization of the nephrocystin/nephrocystin-4 complex and subcellular localisation of nephrocystin-4 to primary cilia and centrosomes. *Human Molecular Genetics*, **14**, 645-656.
- [41] Winklebauer ME, Schafer JC, Haycraft CJ, Swoboda P, Yoder BK. (2005) The *C. elegans* homologs of nephrocystin-1 and nephrocystin-4 are cilia transition zone proteins involved in chemosensory perception. *Journal of Cell Science*, **118**, 5575-5587.
- [42] Schäfer T, Pütz M, Lienkamp S, Ganner A, Bergbreiter A, Ramachandran H, Gieloff V, Gerner M, Mattonet C, Czarnecki PG, Sayer JA, Otto EA, Hildebrandt F, Kramer-Zucker A, Walz G. (2008) Genetic and physical interaction between the NPHP5 and NPHP6 gene products. *Human Molecular Genetics*, **17**, 3655-3662.
- [43] Murga-Zamalloa CA, Swaroop A, Khanna H. (2009) RPGR-containing protein complexes in syndromic and non-syndromic retinal degeneration due to ciliary dysfunction. *Journal of Genetics*, **88**, 399-407.
- [44] Barbelanne M, Song J, Ahmadzai M, Tsang WY. (2013) Pathogenic NPHP5 mutations impair protein interaction with Cep290, a prerequisite for ciliogenesis. *Human Molecular Genetics*, **22**, 2482-2494.
- [45] Cideciyan AV, Rachel RA, Aleman TS, Swider M, Schwartz SB, Sumaroka A, Roman AJ, Stone EM, Jacobson SG, Swaroop A. (2011) Cone photoreceptors are the main targets for gene therapy of NPHP5 (IQCB1) or NPHP6 (CEP290) blindness: generation of an all-cone Nphp6 hypomorph mouse that mimics the human retinal ciliopathy. *Human Molecular Genetics*, **20**, 1411-1423.
- [46] Kim SC, Kim YS, Jetten AM. (2005) Krüppel-like zinc finger protein Gli-similar 2 (Glis2) represses transcription through interaction with C-terminal binding protein 1 (CtBP1) *Nucleic Acids Research*, **33**, 6805-6815.
- [47] Hosking CR, Ulloa F, Hogan C, Ferber EC, Figueroa A, Gevaert K, Birchmeier W, Briscoe J, Fujita Y. (2007) The transcriptional repressor Glis2 is a novel binding partner for p120 catenin. *Molecular Biology of the Cell*, **18**, 1918-1927.

- [48] Kim YH, Epting D, Slanchev K, Engel C, Walz G, Kramer-Zucker, A. (2013) A complex of BBS1 and NPHP7 is required for cilia motility in zebrafish. *PLoS One*, **8**(9):e72549.
- [49] Attanasio M, Uhlenhaut NH, Sousa VH, O'Toole JF, Otto E, Anlag K, Klugmann C, Treier AC, Helou J, Sayer JA, Seelow D, Nürnberg G, Becker C, Chudley AE, Nürnberg P, Hildebrandt F, Treier M. (2007) Loss of GLIS2 causes nephronophthisis in humans and mice by increased apoptosis and fibrosis. *Nature Genetics*, **39**, 1018-1024.
- [50] Coene KL, Mans DA, Boldt K, Gloeckner CJ, van Reeuwijk J, Bolat E, Roosing S, Letteboer SJ, Peters TA, Cremers FP, Ueffing M, Roepman R. (2011) The ciliopathy-associated protein homologs RPGRIP1 and RPGRIP1L are linked to cilium integrity through interaction with Nek4 serine/threonine kinase. *Human Molecular Genetics*, **20**, 3592-3605.
- [51] Wolf MT, Saunier S, O'Toole JF, Wanner N, Groshong T, Attanasio M, Salomon R, Stallmach T, Sayer JA, Waldherr R, Griebel M, Oh J, Neuhaus TJ, Josefiak U, Antignac C, Otto EA, Hildebrandt F. (2007) Mutational analysis of the RPGRIP1L gene in patients with Joubert syndrome and nephronophthisis. *Kidney International*, **72**, 1520-1526.
- [52] Mahjoub MR, Trapp ML, Quarmby LM. (2005) NIMA related kinases defective in murine models of polycystic kidney diseases localize to primary cilia and centrosomes. *Journal of the American Society of Nephrology*, **16**, 3485-3489.
- [53] Sohara E, Luo Y, Zhang J, Manning DK, Beier DR, Zhou J. (2008) Nek8 regulates the expression and localisation of polycystin-1 and polycystin-2. *Journal of the American Society of Nephrology*, **19**, 469-476.
- [54] Valkova N, Yunis R, Mak SK, Kang K, Kültz D. (2005) Nek8 mutation causes overexpression of galectin-1, sorcin, and vimentin and accumulation of the major urinary protein in renal cysts of jck mice. *Molecular and Cellular Proteomics*, **4**, 1009-1018.
- [55] Natoli TA, Gareski TC, Dackowski WR, Smith L, Bukanov NO, Russo RJ, Husson H, Matthews D, Piepenhagen P, Ibraghimov-Beskrovnaya O. (2008) Pkd1 and Nek8 mutations affect cell-cell adhesion and cilia in cysts formed in kidney organ cultures. *American Journal of Physiology*, **294**, F73-F83.
- [56] Otto EA, Trapp ML, Schultheiss UT, Helou J, Quarmby LM, Hildebrandt F (2008) NEK8 mutations affect ciliary and centrosomal localisation and may cause nephronophthisis. *Journal of the American Society of Nephrology*, **19**, 587-592.
- [57] Trapp ML, Galtseva A, Manning DK, Beier DR, Rosenblum ND, Quarmby LM. (2008) Defects in ciliary localisation of Nek8 is associated with cystogenesis. *Pediatric Nephrology*, **23**, 377-387.
- [58] Quarmby LM, Mahjoub MR. (2005) Caught Nek-ing: cilia and centrioles. *Journal of Cell Science*, **118**, 5161-5169.
- [59] Shalom O, Shalva N, Alschuler Y, Motro B. (2008) The mammalian Nek1 kinase is involved in primary cilium formation. *FEBS Letters*, **582**, 1465-1470.
- [60] Evangelista M, Lim TY, Lee J, Parker L, Ashique A, Peterson AS, Ye W, Davis DP, de Sauvage FJ. (2008) Kinome siRNA screen identifies regulators of ciliogenesis and Hedgehog signal transduction. *Science Signalling*, **1**, ra7.

- [61] Chen Y, Gaczynska M, Osmulski P, Polci R, Riley DJ. (2010) Phosphorylation by Nek1 regulates opening and closing of voltage dependent anion channel 1. *Biochemical and Biophysical Research Communications*, **394**, 798-803.
- [62] Pelegrini AL, Moura DJ, Brenner BL, Ledur PF, Maques GP, Henriques JA, Saffi J, Lenz G. (2010) Nek1 silencing slows down DNA repair and blocks DNA damage-induced cell cycle arrest. *Mutagenesis*, **25**, 447-454.
- [63] Thiel C, Kessler K, Giessl A, Dimmler A, Shalev SA, von der Haar S, Zenker M, Zahnleiter D, Stöss H, Beinder E, Abou Jamra R, Ekici AB, Schröder-Kress N, Aigner T, Kirchner T, Reis A, Brandstätter JH, Rauch A. (2011) NEK1 mutations cause short-rib polydactyly syndrome type majewski. *American Journal of Human Genetics*, **88**, 106-114.
- [64] Jeong Y, Lee J, Kim K, Yoo JC, Rhee K. (2007) Characterization of NIP2/centrobin, a novel substrate of Nek2, and its potential role in microtubule stabilization. *Journal of Cell Science*, **120**, 2106-2116.
- [65] Faragher AJ, Fry AM. (2003) Nek2A kinase stimulates centrosome disjunction and is required for formation of bipolar mitotic spindles. *Molecular Biology of the Cell*, **14**, 2876-2889.
- [66] Noguchi K, Fukazawa H, Murakami Y, Uehara Y. (2004) Nucleolar Nek11 is a novel target of Nek2A in G1/S-arrested cells. *Journal of Biological Chemistry*, **279**, 32716-32727.
- [67] Alieva IB, Uzbekov RE. (2008) The centrosome is a polyfunctional multiprotein cell complex. *Biochemistry*, **73**, 626-643.
- [68] Spalluto C, Wilson DI, Hearn T. (2012) Nek2 localises to the distal portion of the mother centriole/basal body and is required for timely cilium disassembly at the G2/M transition. *European Journal of Cell Biology*, **91**, 675-686.
- [69] Sahota NK. (2011) *Cell Cycle Studies on the Human Nek3, Nek5 and Nek11 Protein Kinases*. University of Leicester Thesis.
- [70] Chang J, Baloh RH, Milbrandt J. (2009) The NIMA-family kinase Nek3 regulates microtubule acetylation in neurons. *Journal of Cell Science*, **122**, 2274-2282.
- [71] Miller SL, Antico G, Raghunath PN, Tomaszewski JE, Clevenger CV. (2007) Nek3 kinase regulates prolactin-mediated cytoskeletal reorganization and motility of breast cancer cells. *Oncogene*, **26**, 4668-4678.
- [72] Bertran MT, Sdelci S, Regué L, Avruch J, Caelles C, Roig J. (2011) Nek9 is a Plk1-activated kinase that controls early centrosome separation through Nek6/7 and Eg5. *EMBO Journal*, **30**, 2634-2647.
- [73] O'Regan L, Fry AM. (2009) The Nek6 and Nek7 protein kinases are required for robust mitotic spindle formation and cytokinesis. *Molecular and Cellular Biology*, **29**, 3975-3990.
- [74] Regué L, Sdelci S, Bertran MT, Caelles C, Reverter D, Roig J. (2011) DYNLL/LC8 controls signal transduction through the Nek9/Nek6 signalling module by regulating Nek6 binding to Nek9. *Journal of Biological Chemistry*, **286**, 18118-18129.
- [75] Yissachar N, Salem H, Tennenbaum T, Motro B. (2006) Nek7 kinase is enriched at the centrosome, and is required for proper spindle assembly and mitotic progression. *FEBS Letters*, **580**, 6489-6495.

- [76] Salem H, Rachmin I, Yissachar N, Cohen S, Amiel A, Haffner R, Lavi L, Motro B. (2010) Nek7 kinase targeting leads to early mortality, cytokinesis disturbance and polyploidy. *Oncogene*, **29**, 4046-4057.
- [77] Roig J, Mikhailov A, Belham C, Avruch J. (2002) Nercc1, a mammalian NIMA-family kinase, binds the Ran GTPase and regulates mitotic progression. *Genes and Development*, **16**, 1640-1658.
- [78] Tan BCM, Sheng-Chung L. (2004) Nek9, a novel FACT-associated protein, modulates interphase progression. *Journal of Biological Chemistry*, **279**, 9321-9330.
- [79] Moniz LS, Stambolic V. (2011) Nek10 mediates G2/M cell cycle arrest and MEK autoactivation in response to UV irradiation. *Molecular and Cellular Biology*, **31**, 30-42.
- [80] Roepman R, Bernoud-Hubac N, Schick DE, Maugeri A, Berger W, Ropers HH, Cremers FP, Ferreira PA. (2000) The retinitis pigmentosa GTPase regulator (RPGR) interacts with novel transport-like proteins in the outer segments of rod photoreceptors. *Human Molecular Genetics*, **9**, 2095-2105.
- [81] Hurd TW, Fan S, Margolis BL. (2011) Localization of retinitis pigmentosa 2 to cilia is regulated by Importin beta2. *Journal of Cell Science*, **124**, 718-726.
- [82] He S, Parapuram SK, Hurd TW, Behnam B, Margolis B, Swaroop A, Khanna H. (2008) Retinitis Pigmentosa GTPase Regulator (RPGR) protein isoforms in mammalian retina: insights into X-linked Retinitis Pigmentosa and associated ciliopathies. *Vision Research*, **48**, 366-376.
- [83] Hosch J, Lorenz B, Stieger K. (2011) RPGR: role in the photoreceptor cilium, human retinal disease, and gene therapy. *Ophthalmic Genetics*, **32**, 1-11.
- [84] Shu X, Fry AM, Tulloch B, Manson FD, Crabb JW, Khanna H, Faragher AJ, Lennon A, He S, Trojan P, Giessl A, Wolfrum U, Vervoort R, Swaroop A, Wright AF. (2005) RPGR ORF15 isoform co-localises with RPGRIP1 at centrioles and basal bodies and interacts with nucleophosmin. *Human Molecular Genetics*, **14**, 1193-1197.
- [85] Hong DH, Pawlyk B, Sokolov M, Strissel KJ, Yang J, Tulloch B, Wright AF, Arshavsky VY, Li T. (2003) RPGR isoforms in photoreceptor connecting cilia and the transitional zone of motile cilia. *Investigative Ophthalmology and Vision Science*, **44**, 2413-2421.
- [86] Chang B, Khanna H, Hawes N, Jimeno D, He S, Lillo C, Parapuram SK, Cheng H, Scott A, Hurd RE, Sayer JA, Otto EA, Attanasio M, O'Toole JF, Jin G, Shou C, Hildebrandt F, Williams DS, Heckenlively JR, Swaroop A. (2006) In-frame deletion in a novel centrosomal/ciliary protein CEP290/NPHP6 perturbs its interaction with RPGR and results in early-onset retinal degeneration in the rd16 mouse. *Human Molecular Genetics*, **15**, 1847-1857.
- [87] Patil H, Tserentsoodol N, Saha A, Hao Y, Webb M, Ferreira PA. (2012) Selective loss of RPGRIP1-dependent ciliary targeting of NPHP4, RPGR and SDCCAG8 underlies the degeneration of photoreceptor neurons. *Cell Death and Disease*, **3**, 355.
- [88] Dryja TP, Adams SM, Grimsby JL, McGee TL, Hong DH, Li T, Andréasson S, Berson EL. (2001) Null RPGRIP1 alleles in patients with Leber congenital amaurosis. *American Journal of Human Genetics*, **68**, 1295-1298.
- [89] Koenekoop RK. (2005) RPGRIP1 is mutated in Leber congenital amaurosis: a mini-review. *Ophthalmic Genetics*, **26**, 175-179.
- [90] Massinen S, Hokkanen ME, Matsson H, Tammimies K, Tapia-Páez I, Dahlström-Heuser V, Kuja-Panula J, Burghoorn J, Jeppsson KE, Swoboda P, Peyrard-Janvid M, Toftgård R, Castrén E,

- Kere J. (2011) Increased expression of the dyslexia candidate gene DCDC2 affects length and signalling of primary cilia in neurons. *PLoS One*, **6**(6):e20580.
- [91] Reiter JF, Skarnes WC. (2006) Tectonic, a novel regulator of the Hedgehog pathway required for both activation and inhibition. *Genes and Development*, **20**, 22-27.
- [92] Garcia-Gonzalo FR, Corbit KC, Sirerol-Piquer MS, Ramaswami G, Otto EA, Noriega TR, Seol AD, Robinson JF, Bennett CL, Josifova DJ, García-Verdugo JM, Katsanis N, Hildebrandt F, Reiter JF. (2011) A transition zone complex regulates mammalian ciliogenesis and ciliary membrane composition. *Nature Genetics*, **43**, 776-784.
- [93] Shaheen R, Faqeih E, Seidahmed MZ, Sunker A, Alali FE, AlQahtani K, Alkuraya FS. (2011) A TCTN2 mutation defines a novel Meckel Gruber syndrome locus. *Human Mutations*, **32**, 573-578.
- [94] den Hollander AI, Koenekoop RK, Mohamed MD, Arts HH, Boldt K, Towns KV, Sedmak T, Beer M, Nagel-Wolfrum K, McKibbin M, Dharmaraj S, Lopez I, Ivings L, Williams GA, Springell K, Woods CG, Jafri H, Rashid Y, Strom TM, van der Zwaag B, Gosens I, Kersten FF, van Wijk E, Veltman JA, Zonneveld MN, van Beersum SE, Maumenee IH, Wolfrum U, Cheetham ME, Ueffing M, Cremers FP, Inglehearn CF, Roepman R. (2007) Mutations in LCA5, encoding the ciliary protein lebercilin, cause Leber congenital amaurosis. *Nature Genetics*, **39**, 889-895.
- [95] Barzi M, Berenguer J, Menendez A, Alvarez-Rodriguez R, Pons S. (2010) Sonic-Hedgehog-mediated proliferation requires the localisation of PKA to the cilium base. *Journal of Cell Science*, **123**, 62-69.
- [96] Forwood JK, Lange A, Zachariae U, Marfori M, Preast C, Grubmüller H, Stewart M, Corbett AH, Kobe B. (2010) Quantitative structural analysis of importin- β flexibility: paradigm for solenoid protein structures. *Structure*, **18**, 1171-1178.
- [97] Dishinger JF, Kee HL, Jenkins PM, Fan S, Hurd TW, Hammond JW, Truong YN, Margolis B, Martens JR, Verhey KJ. (2010) Ciliary entry of the kinesin-2 motor KIF17 is regulated by importin- β 2 and Ran-GTP. *Nature Cell Biology*, **12**, 703-710.
- [98] de los Santos T, Hollingsworth NM. (1999) Red1p, a MEK1-dependent phosphoprotein that physically interacts with Hop1p during meiosis in yeast. *Journal of Biological Chemistry*, **274**, 1783-1790.
- [99] O'Toole JF, Liu Y, Davis EE, Westlake CJ, Attanasio M, Otto EA, Seelow D, Nurnberg G, Becker C, Nuutinen M, Kärppä M, Ignatius J, Uusimaa J, Pakanen S, Jaakkola E, van den Heuvel LP, Fehrenbach H, Wiggins R, Goyal M, Zhou W, Wolf MT, Wise E, Helou J, Allen SJ, Murga-Zamalloa CA, Ashraf S, Chaki M, Heeringa S, Chernin G, Hoskins BE, Chaib H, Gleeson J, Kusakabe T, Suzuki T, Isaac RE, Quarmby LM, Tennant B, Fujioka H, Tuominen H, Hassinen I, Lohi H, van Houten JL, Rotig A, Sayer JA, Rolinski B, Freisinger P, Madhavan SM, Herzer M, Madignier F, Prokisch H, Nurnberg P, Jackson PK, Khanna H, Katsanis N, Hildebrandt F. (2010) Individuals with mutations in XPNPEP3, which encodes a mitochondrial protein, develop a nephronophthisis-like nephropathy. *Journal of Clinical Investigation*, **120**, 791-802.
- [100] Otto EA, Ramaswami G, Janssen S, Chaki M, Allen SJ, Zhou W, Airik R, Hurd TW, Ghosh AK, Wolf MT, Hoppe B, Neuhaus TJ, Bockenbauer D, Milford DV, Soliman NA, Antignac C, Saunier S, Johnson CA, Hildebrandt F; GPN Study Group. (2011) Mutation analysis of 18 nephronophthisis associated ciliopathy disease genes using a DNA pooling and next generation sequencing strategy. *Journal of Medical Genetics*, **48**, 105-116.

1.3 Centrosome Associated Proteins

Associated Protein	Interaction, Localisation and Signalling Cascade	Disease Implication / Ancillary Information
Centriole Duplication Complex	SAS-4, SAS-5, SPD-2 and ZYG-1 are required for centriole formation[1, 2].	
SAS2	Complexes with SAS-4 , and SAS-5 [3], are responsible for histone acetyl-transferase activity of SAS-2 [3].	
SAS3	Multi-subunit histone acetyl-transferase .	Involved in stem cell population self renew and cancer[4].
SAS4/CPAP	Controls centriole size[5]. SAS-4 and SAS-5 complex is silenced by SAS-2 [3] SAS-4 determines the centrosome size and centriole stability[5].	
SAS5	Forms a complex with SAS-6 [2, 3]. Required for centrosome duplication[6].	
SAS6	SAS-6 is a cartwheel protein that is responsible for creating the 9-fold centriole symmetry [7]. Required for centrosome duplication. SAS-6 and SAS-5 associate, and interact with SAS-4, SPD-2 and ZYG-1 [1]. Involved in ciliogenesis and localises to the basal body and axoneme[1, 2, 8]	
SPD2 (Spindle defective protein-2)	SPD2 appears on the maternal centriole post-fertilisation recruiting ZYG1 kinase, which in turn recruits the SAS-5/SAS-6 complex forming a procentriole 'central-hub' template upon which microtubule triplets are formed[5, 9, 10].	
ZYG1 (Zygote defective protein-1)	Regulates meiotic and mitotic centriole duplication [11, 12]. Curiously, truncation of ZYG-1 blocks centrosome duplication during the mitotic cycle, and results in centrosome amplification during the meiotic cycle[13]. Related to PLK4 [13].	
PLK4/SAK (Polo Like Kinase)	Initiates centriole assembly (involving SAS6 and SAS4)[14] via recruitment with, and phosphorylation of, CEP152 in the centrosome[15, 16]. Insufficient or aberrant PLK4 causes abnormal centriole induction containing γ - tubulin [17] and produces multiple centrioles through controlling β - TrCP mediated degradation[15, 18, 19]. Down regulated by p53 [637] and CUL1 , which function as tumour suppressors/regulators[18].	
CEP135	Involved in basal body maturation and stabilises against ciliary forces [19]. CEP135 is believed to stabilise the basal body by interacting with the A-C-subfibre linkages[19]. Required for centrosomal localisation of C-NAP1 [20].	Part of the PCM involved in microtubule organization [21]. Controls formation of motile cilia central microtubule pair[22].
Assembly Co-Factors		
CP110	Cell cycle dependent kinase (G1 - S) co-inciding with chromosome replication[23]. Regulates centriole duplication, cytokinesis and suppresses the ciliogenesis program through unknown mechanisms[23-25]. CP110 interacts with CEP290 and RAB8 for ciliogenesis. Interactions between CEP290 and CP110 are required for CP110 to suppress primary cilium formation[24], while CP110 and CEP97 inhibits centriole to basal body conversion [26, 27]. CEP290 and CP110 interact with Rab8 GTPase , since depletion of CEP290 interferes with localisation of RAB8A to the centrosome and cilium. Interacts with CEP97 and KIF24 to remodel microtubules[28], and also with two Ca^{2+} binding domain proteins, Calmodulin (CaM) and	Involved in ciliogenesis. Loss of CEP97 or CP110 promotes ciliary formation[26]. CEP97 depletion results in missing CP110 causing polyploidy and spindle defects/inhibition . Longer-term interruption of CP110 phosphorylation leads to improper centrosome separation and overt polyploidy [23]. Degraded by Cyclin-F [30]. CP110 suppresses primary cilium formation by interacting with CEP290 [24]. CEP97 recruits CP110 to the centriole, where it caps the end of the distal centriole microtubules[26]. Involved with centriole length through

	Centrin [25]. Interacts with Neurl4 on the daughter centriole [29].	CPAP [31]
NLP (Ninein Like Protein)	Localises to the mother centriole, binds to γ-tubulin , and is the G(2)/M target of NEK2 and PLK1 protein kinases[32]. Localisation and stability controlled by PLK1, NEK2, CDC2 and Aurora-B [33].	Involved in mitotic progression and tumorigenesis[33].
CEP120	Required for centriole assembly [34]. Interacts with TACCs to control nuclear migration and is also involved in neural progenitor pool in neurogenesis [35]. Localises asymmetrically to the daughter centriole [34].	Involved in centriole elongation [36].
CEP152	Required for centriole duplication , interacts with PLK4 [16].	CEP152 and CEP63 are involved in centriole duplication [37].
MEC-17 (K40 acetyl-transferase)	MEC-17 exclusively acetylates K40 on α-tubulin [38]. Associated with axonemal stabilised microtubules α-tubulin promotes rapid ciliogenesis and efficient mechano-transduction [39]. Not catalytic for free tubulin. α-TAT1 is required for axonemal microtubules and primary cilium kinetics[39].	Acetylation site on luminal side of MT. So far α-TAT1 is the only α-tubulin K40 acetyltransferase found in mammals and nematodes , and is highly conserved[39]. Controls axis of ciliogenesis with myosin-II [40].
Centrosomal Transport Particles		
TRAPII	Involved in complex trafficking of Rabin8 to the centrosome. Initiated by RAB11 [41].	Involved in Golgi derived transport .
Basal Body Appendages		
Basal Feet Basal Appendages	Composed of Centriolin/CEP110 [42], Pericentrin, Ninein [43], CEP170 [44], ODF2/Cenexin [45], PLK1 [46] and ϵ-tubulin [47].	KIF3A interacts with dynein (p150^{Glu}) to organize subdistal appendages[48].
Cenexin/ODF2	Outer Dense Fiber Protein-2 . Contains three splice variants[49]. ODF2 and Cenexin are formed from alternative splice sites of the same gene[50]. Localises to the mother centriole in G0/G1-Phase [45, 51], however is acquired by the immature centriole at G2/M transition in prophase [45]. Component of sperm-tail outer dense fibers [49] and scaffold component of the centrosome and distal appendages . Interacts with PLK1 [52], binds with Rab8a but not other Rabs[24, 53]. Variations in tubulin tyrosination, detyrosination (Glu-tubulin) may interfere with the substrate function of MTs, influencing G1-phase [54].	Loss of ODF2 results in lack of distal/sub-distal appendages and inability to carry out ciliogenesis [55]. Localises to the distal (+) end of the Basal Body at the beginning of S-phase [9]. Marker for the 'mature' centriole[9].
Ninein (Ninein GSK3B interacting protein)	Forms part of the centrosomal anchoring complex of the PCM , associated with microtubules where it is involved in stability, distribution and attachment of microtubules. Localises around distal end of maternal centriole[9, 56, 57]. At the open end of the PCM tube , CEP110 and Ninein colocalise with CEP250/C-NAP1 [58, 59]. This is associated with maturation of the daughter centrosome at G1 transition[58].	Localises to the distal (+) end of the Basal Body and basal feet . Also coats the proximal (-) ends of both the Basal Body and the Proximal Centrioles at the beginning of S-phase [9].
CEP170	Part of the microtubule anchoring complex . CEP170 regulates KIF2 [60]. Interacts with Centriolin, Cenexin/ODF-2 forming part of an anchoring complex and peri-centriolar satellites [9, 61]. Presence discriminates centriole over-duplication from amplification[46].	Associates with mother centriole during G1, S, and early G2 , but two centrioles during late G2-phase [46].
CEP110/CNTRL/Centriolin	In G1-phase it is only present upon the mature centriole distal end and peri-centriolar satellites. During replication it appears first on the proximal end of the daughter centriole , but on the distal end after mitosis . It appears on the second centrosome in Prophase-Metaphase[9, 58]. After duplication and	Cancer implications with CEP110. Involved in stem cell Myelo-Proliferation Disorder (MPD) where the tyrosine receptor kinase for FGFR1 is found fused to CEP110 [58, 62, 63].

	disjunction it appears on the proximal end of the daughter centriole , and then the distal end after mitosis[9, 58]. Interacts with Ninein and associated with centrosome maturation . CEP110 and Ninein are located in specific domains upon mature centrosomes[58].	CEP110 and Ninein are associated with the centrioles in both mother and daughter centrosomes[58, 59].
Pericentrin-A / Pericentrin-B / (Kendrin)[67]	Proteins formed from alternative splicing of same gene[64, 65]. Kendrin interacts with PCM-1 [64, 66], CG-NAP [67], CEP215 [68], and possibly calmodulin [69]; binds to DISC1 (localising it to the centrosome[70]); Over-expression disrupts MT organisation[71]. Interacts with the nucleating component of γ-tubulin [72] and GCP2 providing a physical role for structural support within the centrosome for the nucleating component of γ-tubulin [73]. Required for ciliogenesis, complexes with IFT transport proteins and Polycystin-2 [74, 75].	Microcephalin and pericentrin control mitotic entry through Chk-1 [76]. Implicated in cancer , as target of membrane type-1 Matrix Metallo-Proteinase [77]. Involved in anchoring γ-TuRC of microtubules to the centrosome and basal feet [78], with roles in cancer , bipolar disorder , schizophrenia [64]. For review of Pericentrin role in cellular function and disease see Delaval et al., (2010)[64].
Given the size of the basal appendages, they most likely consist of hundreds of as yet unclassified proteins and their interaction partners.		
Associated Proteins		
BBS1-BBS12 Bardet-Biedel Proteins BBSome	The BBSome (BBS1-12) [79] complex localises to the basal body , centriolar satellites and also to the membrane of the cilium [80]. It is required for ciliogenesis during which the BBSome associates with Rabin8 (BBS1 enabling RAB8 GTPase) [81]. BBS4 interacts with DCTN1 [82] and also functions as an adaptor between PCM and p150^{Glued} [9, 61]. Loss of BBS4 disrupts the PCM , de-anchoring microtubules [9, 61]. BBS5 -binds phosphoinositidyl 3-phosphate and is thus involved in endosomal trafficking [83]. BBS6 interacts with CEP55 , CEP110 and Centriolin which are involved in cytokinesis [9, 84]. BBS7 and BBS8 are required for stabilising IFT complexes [85] with BBS8 being found localised to basal bodies [86] where it associates with BBS1 , BBS2 BBS4 and PCM-1 [9, 88]. BBS11 interacts with actin [88].	Common defects (which were usually in BBS1 , BBS2 [90], BBS4 [91], BBS5 [92], BBS6 , or BBS8 [91, 93]) include obesity, retinopathy, motile ciliary function[94], and cognitive impairments[79, 95]. Disruption of BBS proteins results in loss of Planar Cell Polarity [96]. Articular cartilage changes indicative of osteoarthritis have been observed in BBS mutants [95]. BBS8 is involved in planar cell polarity with Vangl2 [97]
Centrosomal MT Anchoring Complex	Involved in attaching γ-TuRC to the centrosome through docking stations upon the heads of the basal feet. The pericentriolar complex itself is suspected to comprise of Pericentrin bound PCM-1/BBS4 to Ninein [98], Ninein-Like-Protein (NLP) [99], CG-NAP [100] and Centrin , while BBS4 functions as a link between PCM-1 and p150^{Glued} [9, 61]. The anchoring complex itself is believed to be comprised of Ninein [101], ODF-2/Cenexin [45, 46], Centriolin and ϵ-tubulin [9, 47] which comprises the pericentriolar satellite heads[102]. Ninein acts as a molecular link for the anchoring of γ-TuRC complexes at the centrosome[101].	Alieva et al., (2008)[9] points out that different proteins complexes can anchor MTs to the centrosome. As they are comprised of different anchoring base structures, it is reasonable to conclude that they may individually have different transport functions.
Centriolar Satellites	Satellites are assembly points for proteins, where it has been proposed that ciliopathic proteins are components[103]. PCM1 , ODF1 , BBS4 and CEP290 are the primary components of the satellites which are responsible for satellite integrity [103-105, stow], where CEP72 is a PCM1 interacting protein needed for CEP290 recruitment[106]. At Interphase they form poly-protein complexes of 70-100 nm sized granules which are observed[61], around the basal body[9, 105, 107]. Loss of Cenexin prevents	CEP72 and CEP290 recruit BBS proteins to the cilium [106]. For review see Kubo et al., (1999)[107] and Tateishi et al., (2013)[44].

	centriolar satellites from forming. CEP110 has been proposed as having a role as a binding protein[9].	
Alar Sheet Components (Alar Sheets)	ODF1 , ODF2 [44, 55], CEP164 [108], CCDC123/CEP123 [109, 110] and HYLS1 [111] are known components of the Alar Sheets . Docking of the mother centriole to the cell membrane requires ODF1 , ODF2 , Ninein , MKS1 , MKS3 , CEP164 , POCS and CEP123 [112, 113].	ODF2 is required for distal appendage formation[55].
CEP164	Needed for cilium formation, localises to the distal appendages of mature centrioles with Ninein and CEP170 [114]. CEP164 plays a role in transition-fiber assembly, where it localises to the distal (+) end of the basal body. Depletion prevents cilium assembly [114]. Centriole appendage protein is required for primary cilium formation and It mediates vesicle docking to the mother centriole[115].	Part of the DNA repair response to UV light[116].
OFD1/ CXORF5 (Oro Facial Digital Syndrome)	Required for primary cilia formation[117] and expressed during mesenchymal to epithelial transition , with a suspected role in mechanosensory renal signal transduction [118]. Interacts with RuvB1 and localises to the primary cilium, to the nucleus[119] and to the basal body, where it is involved in centriole elongation, distal appendage formation, and recruitment of IFT88 [120]. Co-localises with PCM-1 , BB4 and CEP290 . Co-localises with PCM1 , BBS4 and CEP290 as principal components of centriolar satellites which are the assembly points for proteins involved in many ciliopathies. Upon break-down of satellite granules, only OFD1 and CEP290 are reported to remain[121].	Involved with human oral-facial-digital type-1 syndrome . Localises with PCM1 , BBS4 and CEP290 as main components of centriolar satellites. Upon breakdown of satellite granules, only OFD1 and CEP290 remain[121].
CEP123 (Cep89/CCDC123)	Required for ciliogenesis at the distal end of the mother centriole, interacts with the centriolar satellite proteins PCM-1 , OFD1 and CEP290 [122].	
Centriole Anchoring Complexes	Known proteins associated with anchoring at the centriole	Knowledge of these components is presently incomplete
Centrobilin (BRCA2 interacting protein)	Daughter centriole specific [9], asymmetrically localises to the daughter centriole before replication[123], where between G and S phase it is only detectable on new procentrioles [9]. Involved in microtubule formation and stability[124]. Interacts with PLK1 [125], SNARES [126] and tubulin where it is involved in centriole elongation [127]. Depletion induced G1-S phase arrest , leading to p38-p53 mediated cell-cycle arrest [128].	Associated with Chediak-Higashi Syndrome , involving impaired phagolysosome formation through microtubule defects[126]. Localises exclusively to the (+) end of the Basal Body and parts of the basal feet [9].
SGO1	SGO1 functions for centriole cohesion , where it is suspected to act as the 'glue' holding centrioles together. Disengages in late mitosis[129].	
CG-NAP/ACAP450	CG-NAP and Pericentrin/Kendrin anchor microtubule nucleation sites in the centrosome by anchoring the γ -TuRC complex[130]. Interacts with CDC42 at the Golgi apparatus [131]. Binds to the dynactin [61, 132] complex via p150^{Glued} interacting with γ -tubulin, CEP55 [133], and Calmodulin [75]. CG-NAP is recruited to the Golgi through interaction with the dynein/dynactin complex[134].	
CEP55	CEP55 associates with γ -TuRC anchors, CG-NAP and Kendrin . At mitotic entry CEP55 is activated by ERK2/CDK1 phosphorylation (allowing interaction with PLK1) where it localises for a role in cytokinesis[133].	

Centrosomin-A /Centrosomin-B	Centrosomin A and B forms are derived from one gene[135, 136]. A forms a centrosomal protein (interacts with γ - tubulin , Aurora-A [137]) while the B isoform has a nuclear association [136].	Interacts with a vast number of proteins.
PCM1	Cell cycle association with the centrosome[138, 139], centriolar satellites and microtubules[102]. Interacts with Pericentrin [140], BBS4 (localises to satellites and basal body, and acts as an adaptor of p150^{Glued} [61]), BBS9 [93] binds to Centrin , Ninein and Pericentrin [141] where it interacts with pericentrin-B [93].	PCM1 recruits PLK1 to the centrosome for disassembly of the primary cilium[142]. Mutations associated with Schizophrenia (DISC1 results in BBS4 disruption)[143].
Rabin8	Primary cilium membrane assembly is initiated by a RAB11 and TRAPP II complex involved in transport of Rabin8 to the centrosome[41].	
CP190	CP190 and CP60 cycle asynchronously between the nucleus and centrosome[144, 145]. Regulates myosin function [146] and interacts with the γ - tubulin ring complex [147].	
CEP250/C-NAP1	C-NAP1 and Rootletin regulate centrosome cohesion[148] and fissioning via phosphorylation, balancing the actions of NEK2 and PP1 [149].	
CP60	The maximum concentration of CP60 is expressed at anaphase and telophase , falling at entry to Interphase where it localises to the nucleus [9, 150]. Required for CP190 to form a complex with γ - tubulin [144, 151].	
Rootletin	Forms long striated rootlets associated with the proximal end of ciliary basal bodies and they are also found radiating from centrosomes , nominally expressing primary cilia[152, 156]. Rootletin is believed to be localised with β-catenin between the C-NAP1 striates of the rootlet where it is involved in ciliogenesis[154, 155].	Indicates a role for NEK2 kinase (and substrate C-NAP1) with Rootletin as a dynamic controller of centrosome cohesion [154].
CEP68	Required for centrosome cohesion of the striated rootlet . CEP68 interacts with C-NAP1 and Rootletin (collects on fibres)[68].	Confusing information in literature.
CEP76	Involved in regulating centriole and centrosome duplication. Interacts with CEP110 [156].	
NB: CP110 and OFD1 have as yet undefined roles in the transition from centriole to basal body as well as in ciliogenesis[157].		

[1] Leidel S, Delattre M, Cerutti L, Baumer K, Gönczy P. (2005) SAS-6 defines a protein family required for centrosome duplication in *C. elegans* and in human cells. *Nature Cell Biology*, **7**, 115-125.

[2] Vladar EK, Stearns T. (2007) Molecular characterization of centriole assembly in ciliated epithelial cells. *Journal of Cell Biology*, **178**, 31-42.

[3] Sutton A, Shia WJ, Band D, Kaufman PD, Osada S, Workman JL, Sternglanz R. (2003) Sas4 and Sas5 are required for the histone acetyltransferase activity of Sas2 in the SAS complex. *Journal of Biological Chemistry*, **278**, 16887-16892

[4] Voss AK, Thomas T. (2009) MYST family histone acetyltransferases take center stage in stem cells and development. *Bioessays*, **31**, 1050-1061.

[5] Kirkham M, Muller-Reichert T, Oegema K, Grill S, Hyman AA. (2003) SAS-4 is a *C. elegans* centriolar protein that controls centrosome size. *Cell*, **112**, 575-587.

- [6] Delattre M, Leidel S, Wani K, Baumer K, Bamat J, Schnabel H, Feichtinger R, Schnabel R, Gönczy P. (2004) Centriolar SAS-5 is required for centrosome duplication in *C. elegans*. *Nature Cell Biology*, **6**, 656-664.
- [7] Nakazawa Y, Hiraki M, Kamiya R, Hirono M. (2007) SAS-6 is a cartwheel protein that establishes the 9-fold symmetry of the centriole. *Current Biology*, **17**, 2169-2174.
- [8] Dammermann A, Müller-Reichert T, Pelletier L, Habermann B, Desai A, Oegema K. (2004) Centriole assembly requires both centriolar and pericentriolar material proteins. *Developmental Cell*, **7**, 815-829.
- [9] Alieva IB, Uzbekov RE. (2008) The centrosome is a polyfunctional multiprotein cell complex. *Biochemistry*, **73**, 626-643.
- [10] Delattr M, Canard C, Gönczy P. (2006) Sequential protein recruitment in *C. elegans* centriole formation. *Current Biology*, **16**, 1844-1849.
- [11] O'Connell KF. (2002) The ZYG-1 kinase, a mitotic and meiotic regulator of centriole replication. *Oncogene*, **21**, 6201-6208.
- [12] O'Connell KF, Caron C, Kopish KR, Hurd DD, Kempfues KJ, Li Y, White JG (2001) The *C. elegans* *zyg-1* gene encodes a regulator of centrosome duplication with distinct maternal and paternal roles in the embryo. *Cell*, **105**, 547-558.
- [13] Peters N, Perez DE, Song MH, Liu Y, Müller-Reichert T, Caron C, Kempfues KJ, O'Connell KF. (2010) Control of mitotic and meiotic centriole duplication by the Plk4-related kinase ZYG-1. *Journal of Cell Science*, **123**, 795-805.
- [14] Kuriyama R. (2009) Centriole assembly in CHO cells expressing Plk4/SAS6/SAS4 is similar to centriogenesis in ciliated epithelial cells. *Cell Motility and Cytoskeleton*, **66**, 588-596.
- [15] Cizmecioglu O, Arnold M, Bahtz R, Settele F, Ehret L, Haselmann-Weiss U, Antony C, Hoffmann I. (2010) Cep152 acts as a scaffold for recruitment of Plk4 and CPAP to the centrosome. *Journal of Cell Biology*, **191**, 731-739.
- [16] Hatch EM, Kulukian A, Holland AJ, Cleveland DW, Stearns T. (2010) Cep152 interacts with Plk4 and is required for centriole duplication. *Journal of Cell Biology*, **191**, 721-729.
- [17] Kuriyama R, Bettencourt-Dias M, Hoffmann I, Arnold M, Sandvig L. (2009) Gamma-tubulin-containing abnormal centrioles are induced by insufficient Plk4 in human HCT116 colorectal cancer cells. *Journal of Cell Science*, **122**, 2014-2023.
- [18] Korzeniewski N, Zheng L, Cuevas R, Parry J, Chatterjee P, Anderton B, Duensing A, Münger K, Duensing S. (2009) Cullin 1 functions as a centrosomal suppressor of centriole multiplication by regulating polo-like kinase 4 protein levels. *Cancer Research*, **69**, 6668-6675.
- [19] Guderian G, Westendorf J, Uldschmid A, Nigg EA. (2010) Plk4 trans-autophosphorylation regulates centriole number by controlling betaTrCP-mediated degradation. *Journal of Cell Science*, **123**, 2163-2169.
- [19] Bayless BA, Giddings TH, Winey M, Pearson CG. (2012) Bld10/Cep135 stabilizes basal bodies to resist cilia-generated forces. *Molecular Biology of the Cell*, **23**, 4820-4832.
- [20] Kim K, Lee S, Chang J, Rhee K. (2008) A novel function of CEP135 as a platform protein of C-NAP1 for its centriolar localisation. *Experimental Cell Research*, **314**, 3692-3700.

- [21] Ohta T, Essner R, Ryu JH, Palazzo RE, Uetake Y, Kuriyama R. (2002) Characterization of Cep135, a novel coiled-coil centrosomal protein involved in microtubule organization in mammalian cells. *Journal of Cell Biology*, **156**, 87-99.
- [22] Carvalho-Santos Z, Machado P, Alvarez-Martins I, Gouveia SM, Jana SC, Duarte P, Amado T, Branco P, Freitas MC, Silva ST, Antony C, Bandeiras TM, Bettencourt-Dias M. (2012) BLD10/CEP135 is a microtubule-associated protein that controls the formation of the flagellum central microtubule pair. *Developmental Cell*, **23**, 412-424.
- [23] Chen Z, Indjeian VB, McManus M, Wang L, Dynlacht BD. (2002) CP110, a cell cycle-dependent CDK substrate, regulates centrosome duplication in human cells. *Developmental Cell*, **3**, 339-350.
- [24] Tsang WY, Bossard C, Khanna H, Peränen J, Swaroop A, Malhotra V, Dynlacht BD. (2008) CP110 suppresses primary cilia formation through its interaction with CEP290, a protein deficient in human ciliary disease. *Developmental Cell*, **15**, 187-197.
- [25] Tsang WY, Spektor A, Luciano DJ, Indjeian VB, Chen Z, Salisbury JL, Sánchez I, Dynlacht BD. (2006) CP110 cooperates with two calcium-binding proteins to regulate cytokinesis and genome stability. *Molecular Biology of the Cell*, **17**, 3423-3434.
- [26] Spektor A, Tsang WY, Khoo D, Dynlacht BD. (2007) Cep97 and CP110 suppress a cilia assembly program. *Cell*, **130**, 678-690.
- [27] Bettencourt-Dias M, Carvalho-Santos Z. (2007) Double life of centrioles: CP110 in the spotlight. *Trends in Cell Biology*, **18**, 8-11.
- [28] Kobayashi T, Tsang WY, Li J, Lane W, Dynlacht BD. (2011) Centriolar Kinesin Kif24 Interacts with CP110 to Remodel Microtubules and Regulate Ciliogenesis. *Cell*, **145**, 914-925.
- [29] Li J, Kim S, Kobayashi T, Liang FX, Korzeniewski N, Duensing S, Dynlacht BD. (2012) Neurl4, a novel daughter centriole protein, prevents formation of ectopic microtubule organizing centres. *EMBO Reports*, **13**, 547-553.
- [30] D'Angiolella V, Donato V, Vijayakumar S, Saraf A, Florens L, Washburn MP, Dynlacht B, Pagano M. (2010) SCF(Cyclin F) controls centrosome homeostasis and mitotic fidelity through CP110 degradation. *Nature*, **466**, 138-142.
- [31] Schmidt TI, Kleylein-Sohn J, Westendorf J, Le Clech M, Lavoie SB, Stierhof YD, Nigg EA. (2009) Control of centriole length by CPAP and CP110. *Current Biology*, **19**, 1005-1011.
- [32] Rapley J, Baxter JE, Blot J, Wattam SL, Casenghi M, Meraldi P, Nigg EA, Fry AM. (2005) Coordinate regulation of the mother centriole component nlp by nek2 and plk1 protein kinases. *Molecular and Cellular Biology*, **25**, 1309-1324.
- [33] Li J, Zhan Q. (2011) The role of centrosomal Nlp in the control of mitotic progression and tumorigenesis. *British Journal of Cancer*, **104**, 1523-1528.
- [34] Mahjoub MR, Xie Z, Stearns T. (2010) Cep120 is asymmetrically localized to the daughter centriole and is essential for centriole assembly. *Journal of Cell Biology*, **191**, 331-346.
- [35] Xie Z, Moy LY, Sanada K, Zhou Y, Buchman JJ, Tsai LH (2007) Cep120 and TACCs control interkinetic nuclear migration and the neural progenitor pool. *Neuron*, **56**, 79-93.

- [36] Lin YN, Wu CT, Lin YC, Hsu WB, Tang CJ, Chang CW, Tang TK. (2013) CEP120 interacts with CPAP and positively regulates centriole elongation. *Journal of Cell Biology*, **202**, 211-219.
- [37] Brown NJ, Marjanović M, Lüders J, Stracker TH, Costanzo V (2013) Cep63 and Cep152 Cooperate to Ensure Centriole Duplication. *PLoS ONE*, **8**(7):e69986.
- [38] Akella JS, Wloga D, Kim J, Starostina NG, Lyons-Abbott S, Morrisette NS, Dougan ST, Kipreos ET, Gaertig J. (2009) MEC-17 is an alpha-tubulin acetyltransferase. *Nature*, **467**, 218-222.
- [39] Shida T, Cueva JG, Xu Z, Goodman MB, Nachury MV. (2010) The major alpha-tubulin K40 acetyltransferase alphaTAT1 promotes rapid ciliogenesis and efficient mechanosensation. *Proceedings of the National Academy of Sciences, USA*, **107**, 21517-21522.
- [40] Rao Y. (2013) *An Atat1/Mec-17-Myosin II axis controls ciliogenesis*. Dissertation. <http://hdl.handle.net/10161/7224>
- [41] Westlake CJ, Baye LM, Nachury MV, Wright KJ, Ervin KE, Phu L, Chalouni C, Beck JS, Kirkpatrick DS, Slusarski DC, Sheffield VC, Scheller RH, Jackson PK. (2011) Primary cilia membrane assembly is initiated by Rab11 and transport protein particle II (TRAPP II) complex-dependent trafficking of Rabin8 to the centrosome. *Proceedings of the National Academy of Sciences, USA*, **108**, 2759-2764.
- [42] Gromley A, Jurczyk A, Sillibourne J, Halilovic E, Mogensen M, Groisman I, Blomberg M, Doxsey S. (2003) A novel human protein of the maternal centriole is required for the final stages of cytokinesis and entry into S phase. *Journal of Cell Biology*, **161**, 535-545.
- [43] Mogensen MM, Malik A, Piel M, Bouckson-Castaing V, Bornens M. (2000) Microtubule minus-end anchorage at centrosomal and non-centrosomal sites: the role of ninein. *Journal of Cell Science*, **113**, 3013-3023.
- [44] Tateishi K, Yamazaki Y, Nishida T, Watanabe S, Kunimoto K, Ishikawa H, Tsukita S. (2013) Two appendages homologous between basal bodies and centrioles are formed using distinct Odf2 domains. *Journal of Cell Biology*, **203**, 417-425.
- [45] Lange BM, Gull K. (1995) A molecular marker for centriole maturation in the mammalian cell cycle. *Journal of Cell Biology*, **130**, 919-927.
- [46] Guarguaglini G, Duncan PI, Stierhof YD, Holmström T, Duensing S, Nigg EA (2005) The forkhead-associated domain protein Cep170 interacts with Polo-like kinase 1 and serves as a marker for mature centrioles. *Molecular Biology of the Cell*, **16**, 1095-1107.
- [47] Chang P, Giddings TM, Winey M, Stearns T. (2003) ϵ -Tubulin is required for centriole duplication and microtubule organization. *Nature Cell Biology*, **5**, 71-76.
- [48] Kodani A, Salomé Sirerol-Piquer M, Seol A, Garcia-Verdugo JM, Reiter JF. (2013) Kif3a interacts with dynactin subunit p150 glued to organize centriole subdistal appendages. *EMBO Journal*, **32**, 597-607.
- [49] Hüber D, Geisler S, Monecke S, Hoyer-Fender S. (2008) Molecular dissection of ODF2/Cenexin revealed a short stretch of amino acids necessary for targeting to the centrosome and the primary cilium. *European Journal of Cell Biology*, **87**, 137-146.
- [50] Huber D, Hoyer-Fender S. (2007) Alternative splicing of exon 3b gives rise to ODF2 and cenexin. *Cytogenetics and Genome Research*, **119**, 68-73.

- [51] Nakagawa Y, Yamane Y, Okanou T, Tsukita S, Tsukita S. (2001) Outer dense fiber 2 is a widespread centrosome scaffold component preferentially associated with mother centrioles: its identification from isolated centrosomes. *Molecular Biology of the Cell*, **12**, 1687-1697.
- [52] Soung NK, Kang YH, Kim K, Kamijo K, Yoon H, Seong YS, Kuo YL, Miki T, Kim SR, Kuriyama R, Giam CZ, Ahn CH, Lee KS. (2006) Requirement of cenexin for proper mitotic functions of polo-like kinase 1 at the centrosomes. *Molecular and Cellular Biology*, **26**, 8316-8335.
- [53] Yoshimura S, Egerer J, Fuchs E, Haas AK, Barr FA. (2007) Functional dissection of Rab GTPases involved in primary cilium formation. *Journal of Cell Biology*, **178**, 363-369.
- [54] Chen Y, Kong Q. (2006) Cell brain: Insight into hepatocarcinogenesis. *Medical Hypotheses*, **67**, 44-52.
- [55] Ishikawa H, Kubo A, Tsukita S, Tsukita S. (2005) Odf2-deficient mother centrioles lack distal/subdistal appendages and the ability to generate primary cilia. *Nature Cell Biology*, **7**, 517-524.
- [56] Mogensen MM, Malik A, Piel M, Bouckson Castaing V, Bornens M. (2000) Microtubule minus end anchorage at centrosomal and non centrosomal sites: the role of ninein. *Journal of Cell Science*, **113**, 3013-3023.
- [57] Mogensen M M. (2004) *Centrosomes in Development and Disease*, (Nigg EA, ed.) Wiley-VCH Verlag GmbH and Co, KGaA, Weinheim.
- [58] Ou YY, Mack GJ, Zhang M, Rattner JB. (2002) CEP110 and ninein are located in a specific domain of the centrosome associated with centrosome maturation. *Journal of Cell Science*, **115**, 1825-1835.
- [59] Mack GJ, Rees J, Sandblom O, Balczon R, Fritzler MJ, Rattner JB. (1998) Autoantibodies to a group of centrosomal proteins in human autoimmune sera reactive with the centrosome. *Arthritis and Rheumatology*, **41**, 551-558.
- [60] Welburn JP, Cheeseman IM. (2012) The microtubule-binding protein Cep170 promotes the targeting of the kinesin-13 depolymerase Kif2b to the mitotic spindle. *Molecular Biology of the Cell*, **23**, 4786-4795.
- [61] Kim JC, Badano J L, Sibold S, Esmail MA, Hill J, Hoskins BE, Leitch CC, Venner K, Ansley SJ, Ross AJ, Leroux MR, Katsanis N, Beales PL. (2004) The Bardet-Biedl protein BBS4 targets cargo to the pericentriolar region and is required for microtubule anchoring and cell cycle progression. *Nature Genetics*, **36**, 462-470.
- [62] Guasch G, Mack GJ, Popovici C, Dastugue N, Birnbaum D, Rattner JB, Pebusque MJ. (2000) FGFR1 is fused to the centrosome-associated protein CEP110 in the 8p12 stem cell myeloproliferative disorder with t(8;9)(p12;q33) *Blood*, **95**, 1788-1796.
- [63] Vizmanos JL, Novo FJ, Román JP, Baxter EJ, Lahortiga I, Larráyoiz MJ, Odero MD, Giraldo P, Calasanz MJ, Cross NC. (2006) NIN, a gene encoding a CEP110-like centrosomal protein, is fused to PDGFRB in a patient with a t(5;14)(q33;q24) and an Imatinib-Responsive myeloproliferative disorder1. *Cancer Research*, **64**, 2673-2676.
- [64] Delaval B, Doxsey SJ. (2010) Pericentrin in cellular function and disease. *Journal of Cell Biology*, **188**, 181-190.

- [65] Purohit A, Tynan SH, Vallee R, Doxsey SJ. (1999) Direct interaction of pericentrin with cytoplasmic dynein light intermediate chain contributes to mitotic spindle organization. *Journal of Cell Biology*, **147**, 481-492.
- [66] Li Q, Hansen D, Killilea A, Joshi HC, Palazzo RE, Balczon R. (2001) Kendrin/pericentrin-B, a centrosome protein with homology to pericentrin that complexes with PCM-1. *Journal of Cell Science*, **114**, 797-809.
- [67] Takahashi M, Yamagiwa A, Nishimura T, Mukai H, Ono Y. (2002) Centrosomal proteins CG-NAP and kendrin provide microtubule nucleation sites by anchoring gamma-tubulin ring complex. *Molecular Biology of the Cell*, **13**, 3235-3234.
- [68] Graser S, Stierhof YD, Nigg EA. (2007) Cep68 and Cep215 (Cdk5rap2) are required for centrosome cohesion is required for the final stages of cytokinesis and entry into S phase. *Journal of Cell Biology*, **161**, 535-545.
- [69] Flory MR, Moser MJ, Monnat RJ Jr, Davis TN. (200) Identification of a human centrosomal calmodulin-binding protein that shares homology with pericentrin. *Proceedings of the National Academy of Sciences USA*, **97**, 5919-5923.
- [70] Miyoshi K, Asanuma M, Miyazaki I, Diaz-Corrales FJ, Katayama T, Tohyama M, Ogawa N. (2004) DISC1 localises to the centrosome by binding to kendrin. *Biochemical and Biophysical Research Communications*, **317**, 1195-1199.
- [71] Shimizu S, Matsuzaki S, Hattori T, Kumamoto N, Miyoshi K, Katayama T, Tohyama M. (2008) DISC1-kendrin interaction is involved in centrosomal microtubule network formation. *Biochemical and Biophysical Research Communications*, **377**, 1051-1056.
- [72] Dichtenberg JB, Zimmerman W, Sparks CA, Young A, Vidar C, Zheng Y, Carrington W, Fay FS, Doxsey SJ. (1998) Pericentrin and gamma-tubulin form a protein complex and are organized into a novel lattice at the centrosome. *Journal of Cell Biology*, **141**, 163-174.
- [73] Takahashi M, Yamagiwa A, Nishimura T, Mukai H, Ono Y. (2002) Centrosomal proteins CG-NAP and kendrin provide microtubule nucleation sites by anchoring gamma-tubulin ring complex. *Molecular Biology of the Cell*, **13**, 3235-3245.
- [74] Jurczyk A, Gromley A, Redick S, San Agustin J, Witman G, Pazour GJ, Peters DJ, Doxsey S. (2004) Pericentrin forms a complex with intraflagellar transport proteins and polycystin-2 and is required for primary cilia assembly. *Journal of Cell Biology*, **166**, 637-643.
- [75] Gillingham A, Munro S. (2000) The PACT domain, a conserved centrosomal targeting motif in the coiled-coil proteins AKAP450 and pericentrin. *EMBO Reports*, **1**, 524-529.
- [76] Tibelius A, Marhold J, Zentgraf H, Heilig CE, Neitzel H, Ducommun B, Rauch A, Ho AD, Bartek J, Krämer A. (2009) Microcephalin and pericentrin regulate mitotic entry via centrosome-associated Chk1. *Journal of Cell Biology*, **185**, 1149-1157.
- [77] Golubkov VS, Chekanov AV, Doxsey SJ, Strongin AY. (2005) Centrosomal pericentrin is a direct cleavage target of membrane type-1 matrix metalloproteinase in humans but not in mice: potential implications for tumorigenesis. *Journal of Biological Chemistry*, **280**, 42237-42241.
- [78] Zimmerman WC, Sillibourne J, Rosa J, Doxsey SJ (2004) Mitosis-specific anchoring of gamma tubulin complexes by pericentrin controls spindle organization and mitotic entry. *Molecular Biology of the Cell*, **15**, 3642-3657.

- [79] Rooryck C, Lacombe D. (2008) Bardet-Biedl syndrome. *Annals of Endocrinology*, **69**, 463-471.
- [80] Nachury MV, Loktev AV, Zhang Q, Westlake CJ, Peränen J, Merdes A, Slusarski DC, Scheller RH, Bazan JF, Sheffield VC, Jackson PK. (2007) A core complex of BBS proteins cooperates with the GTPase Rab8 to promote ciliary membrane biogenesis. *Cell*, **129**, 1201-1213.
- [81] Nachury MV. (2008) Tandem affinity purification of the BBSome, a critical regulator of Rab8 in ciliogenesis. *Methods in Enzymology*, **439**, 501-513.
- [82] Carmi R, Rokhlina T, Kwitek-Black AE, Elbedour K, Nishimura D, Stone EM, Sheffield VC (1995) Use of a DNA pooling strategy to identify a human obesity syndrome locus on chromosome 15. *Human Molecular Genetics*, **4**, 9-13.
- [83] Takai Y, Sasaki T, Matozaki T. (2001) Small GTP-binding proteins. *Physiology Reviews*, **81**, 153-208.
- [84] Kim JC, Ou YY, Badano JL, Esmail MA, Leitch CC, Fiedrich E, Beales PL, Archibald JM, Katsanis N, Rattner JB, Leroux MR. (2005) MKKS/BBS6, a divergent chaperonin-like protein linked to the obesity disorder Bardet-Biedl syndrome, is a novel centrosomal component required for cytokinesis. *Journal of Cell Science*, **118**, 1007-1020.
- [85] Ou G, Blacque OE, Snow JJ, Leroux MR, Scholey JM. (2005) Functional coordination of intraflagellar transport motors. *Nature*, **436**, 583-587.
- [86] Mykytyn K, Sheffield VC. (2004) Establishing a connection between cilia and Bardet-Biedl Syndrome. *Trends in Molecular Medicine*, **10**, 106-109.
- [87] Chang B, Khanna H, Hawes N, Jimeno D, He S, Lillo C, Parapuram SK, Cheng H, Scott A, Hurd RE, Sayer JA, Otto EA, Attanasio M, O'Toole JF, Jin G, Shou C, Hildebrandt F, Williams DS, Heckenlively JR, Swaroop A. (2006) In-frame deletion in a novel centrosomal/ciliary protein CEP290/NPHP6 perturbs its interaction with RPGR and results in early-onset retinal degeneration in the rd16 mouse. *Human Molecular Genetics*, **15**, 1847-1857.
- [88] Kudryashova E, Kudryashov D, Kramerova I, Spencer MJ. (2005) Trim32 is a ubiquitin ligase mutated in limb girdle muscular dystrophy type 2H that binds to skeletal muscle myosin and ubiquitinates actin. *Journal of Molecular Biology*, **354**, 413-424.
- [89] Kudryashova E, Wu J, Havton LA, Spencer MJ. (2009) Deficiency of the E3 ubiquitin ligase TRIM32 in mice leads to a myopathy with a neurogenic component. *Human Molecular Genetics*, **18**, 1353-1367.
- [90] Nishimura DY, Fath M, Mullins RF, Searby C, Andrews M, Davis R, Andorf JL, Mykytyn K, Swiderski RE, Yang B, Carmi R, Stone EM, Sheffield VC. (2004) Bbs2-null mice have neurosensory deficits, a defect in social dominance, and retinopathy associated with mislocalisation of rhodopsin. *Proceedings of the National Academy of Sciences, USA*, **101**, 16588-16593.
- [91] Mykytyn K, Mullins RF, Andrews M, Chiang AP, Swiderski RE, Yang B, Braun T, Casavant T, Stone EM, Sheffield VC. (2004) Bardet-Biedl syndrome type 4 (BBS4)-null mice implicate Bbs4 in flagella formation but not global cilia assembly. *Proceedings of the National Academy of Sciences, USA*, **101**, 8664-8669.
- [92] Li JB, Gerdes JM, Haycraft CJ, Fan Y, Teslovich TM, May-Simera H, Li H, Blacque OE, Li L, Leitch CC, Lewis RA, Green JS, Parfrey PS, Leroux MR, Davidson WS, Beales PL, Guay-Woodford LM, Yoder BK, Stormo GD, Katsanis N, Dutcher SK. (2004) Comparative genomics identifies a flagellar and basal body proteome that includes the BBS5 human disease gene. *Cell*, **117**, 541-552.

- [93] Ansley SJ, Badano JL, Blacque OE, Hill J, Hoskins BE, Leitch CC, Kim JC, Ross AJ, Eichers ER, Teslovich TM, Mah AK, Johnsen RC, Cavender JC, Lewis RA, Leroux MR, Beales PL, Katsanis N. (2003) Basal body dysfunction is a likely cause of pleiotropic Bardet-Biedl syndrome. *Nature*, **425**, 628-633.
- [94] Shah AS, Farmen SL, Moninger TO, Businga TR, Andrews MP, Bugge K, Searby CC, Nishimura D, Brogden KA, Kline JN, Sheffield VC, Welsh MJ. (2008) Loss of Bardet-Biedl syndrome proteins alters the morphology and function of motile cilia in airway epithelia. *Proceedings of the National Academy of Sciences, USA*, **105**, 3380-3385.
- [95] Kaushik AP, Martin JA, Zhang Q, Sheffield VC, Morcuende JA. (2009) Cartilage abnormalities associated with defects of chondrocytic primary cilia in Bardet-Biedl syndrome mutant mice. *Journal of Orthopaedic Research*, **27**, 1093-1099.
- [96] Ross AJ, May-Simera H, Eichers ER, Kai M, Hill J, Jagger DJ, Leitch CC, Chapple JP, Munro PM, Fisher S, Tan PL, Phillips HM, Leroux MR, Henderson DJ, Murdoch JN, Copp AJ, Eliot MM, Lupski JR, Kemp DT, Dollfus H, Tada M, Katsanis N, Forge A, Beales PL. (2005) Disruption of Bardet-Biedl syndrome ciliary proteins perturbs planar cell polarity in vertebrates. *Nature Genetics*, **37**, 1135-1140.
- [97] May-Simera HL, Kai M, Hernandez V, Osborn DP, Tada M, Beales PL. (2010) Bbs8, together with the planar cell polarity protein Vangl2, is required to establish left-right asymmetry in zebrafish. *Developmental Biology*, **345**, 215-225.
- [98] Delgehyr N, Sillibourne J, Bornens M. (2005) Microtubule nucleation and anchoring at the centrosome are independent processes linked by ninein function. *Journal of Cell Science*, **118**, 1565-1575.
- [99] Casenghi M, Meraldi P, Weinhart U, Duncan PI, Körner R, Nigg EA. (2003) Polo-like kinase 1 regulates Nlp, a centrosome protein involved in microtubule nucleation. *Developmental Cell*, **5**, 113-125.
- [100] Takahashi, M, Yamagiwa, A, Nishimura, T, Mukai, H, Ono, Y. (2002) Centrosomal proteins CG-NAP and kendrin provide microtubule nucleation sites by anchoring γ -tubulin ring complex. *Molecular Biology of the Cell*, **13**, 3235-3245.
- [101] Delgehyr N, Sillibourne J, Bornens M. (2005) Microtubule nucleation and anchoring at the centrosome are independent processes linked by ninein function. *Journal of Cell Science*, **118**, 1565-1575.
- [102] Dammermann A, Merdes A. (2002) Assembly of centrosomal proteins and microtubule organization depends on PCM-1. *Journal of Cell Biology*, **159**, 255-266.
- [103] Lopes CAM, Prosser SL, Romio L, Hirst RA, O'Callaghan C, Woolf AS, Fry AM. (2011) Centriolar satellites are assembly points for proteins implicated in human ciliopathies, including oral-facial-digital syndrome 1. *Journal of Cell Science*, **124**, 600-612.
- [104] Kim J, Krishnaswami SR, Gleeson JG. (2008) CEP290 interacts with the centriolar satellite component PCM-1 and is required for Rab8 localisation to the primary cilium. *Human Molecular Genetics*, **17**, 3796-3805.
- [105] Li Q, Hansen D, Killilea A, Joshi HC, Palazzo RE, Balczon R. (2001) Kendrin/pericentrin-B, a centrosome protein with homology to pericentrin that complexes with PCM-1. *Journal of Cell Science*, **114**, 797-809.

- [106] Stowe TR, Wilkinson CJ, Iqbal A, Stearns T. (2012) The centriolar satellite proteins Cep72 and Cep290 interact and are required for recruitment of BBS proteins to the cilium. *Molecular Biology of the Cell*, **23**, 3322-3335.
- [107] Kubo A, Sasaki H, Yuba Kudo A, Tsukita S, Shiina N. (1999) Centriolar satellites: molecular characterization, ATP-dependent movement toward centrioles and possible involvement in ciliogenesis. *Journal of Cell Biology*, **147**, 969-980.
- [108] Schmidt KN, Kuhns S, Neuner A, Hub B, Zentgraf H, Pereira G. (2012) Cep164 mediates vesicular docking to the mother centriole during early steps of ciliogenesis. *Journal of Cell Biology*, **199**, 1083-1101.
- [109] Sillibourne JE, Specht CG, Izeddin I, Hurbain I, Tran P, Triller A, Darzacq X, Dahan M, Bornens M (2011) Assessing the localisation of centrosomal proteins by PALM/STORM nanoscopy. *Cytoskeleton*, **68**, 619-627.
- [110] Reiter JF, Blacque OE, Leroux MR. (2012) The base of the cilium: roles for transition fibres and the transition zone in ciliary formation, maintenance and compartmentalization. *EMBO Reports*, **13**, 608-618.
- [111] Garcia-Gonzalo FR, Corbit KC, Sirerol-Piquer MS, Ramaswami G, Otto EA, Noriega TR, Seol AD, Robinson JF, Bennett CL, Josifova DJ, García-Verdugo JM, Katsanis N, Hildebrandt F, Reiter JF. (2011) A transition zone complex regulates mammalian ciliogenesis and ciliary membrane composition. *Nature Genetics*, **43**, 776-784.
- [112] Reiter JF, Blacque OE, Leroux MR. (2012) The base of the cilium: roles for transition fibres and the transition zone in ciliary formation, maintenance and compartmentalization. *EMBO Reports*, **13**, 608-618.
- [113] Basten SG, Giles RH. (2013) Functional aspects of primary cilia in signaling, cell cycle and tumorigenesis. *Cilia*, **2**, 6.
- [114] Graser S, Stierhof YD, Lavoie SB, Gassner OS, Lamla S, Le Clech M, Nigg EA. (2007) Cep164, a novel centriole appendage protein required for primary cilium formation. *Journal of Cell Biology*, **179**, 321-230.
- [115] Schmidt KN, Kuhns S, Neuner A, Hub B, Zentgraf H, Pereira G. (2012) Cep164 mediates vesicular docking to the mother centriole during early steps of ciliogenesis. *Journal of Cell Biology*, **199**, 1083-1101.
- [116] Pan YR, Lee, EY (2009) UV-dependent interaction between Cep164 and XPA mediates localisation of Cep164 at sites of DNA damage and UV sensitivity. *Cell Cycle*, **8**, 655-664.
- [117] Ferrante MI, Zullo A, Barra A, Bimonte S, Messaddeq N, Studer M, Dollé P, Franco B. (2006) Oral-facial-digital type protein is required for primary cilia formation and left-right axis specification. *Nature Genetics*, **38**, 112-117.
- [118] Romio L, Fry AM, Winyard PJ, Malcolm S, Woolf AS, Feather SA. (2004) OFD1 is a centrosomal/basal body protein expressed during mesenchymal-epithelial transition in human nephrogenesis. *Journal of the American Society of Nephrology*, **15**, 2556-2568.
- [119] Giorgio G, Alfieri M, Prattichizzo C, Zullo A, Cairo S, Franco B. (2007) Functional characterization of the OFD1 protein reveals a nuclear localisation and physical interaction with subunits of a chromatin remodeling complex. *Molecular Biology of the Cell*, **18**, 4397-4404.

- [120] Singla V, Romaguera-Ros M, Garcia-Verdugo JM, Reiter JF. (2010) Odf1, a human disease gene, regulates the length and distal structure of centrioles. *Developmental Cell*, **18**, 410-424.
- [121] Lopes CA, Prosser SL, Romio L, Hirst RA, O'Callaghan C, Woolf AS, Fry AM. (2011) Centriolar satellites are assembly points for proteins implicated in human ciliopathies, including oral-facial-digital syndrome 1. *Journal of Cell Science* **124**, 600-612.
- [122] Sillibourne JE, Hurbain I, Grand-Perret T, Goud B, Tran P, Bornens M. (2013) Primary ciliogenesis requires the distal appendage component Cep123. *Biology Open*, **2**, 535-545.
- [123] Zou, C, Li, J, Bai, Y, Gunning, W, Wazer, D, Band, V, Gao, Q. (2005) Centrobin: a novel daughter centriole-associated protein that is required for centriole duplication. *Journal of Cell Biology*, **171**, 437-445.
- [124] Jeong Y, Lee J, Kim K, Yoo JC, Rhee K. (2007) Characterization of NIP2/centrobin, a novel substrate of Nek2, and its potential role in microtubule stabilization. *Journal of Cell Science*, **120**, 2106-2116.
- [125] Lee J, Jeong Y, Jeong S, Rhee K. (2010) Centrobin/NIP2 is a microtubule stabilizer whose activity is enhanced by PLK1 phosphorylation during mitosis. *Journal of Biological Chemistry*, **285**, 25476-25484.
- [126] Tchernev VT, Mansfield TA, Giot L, Kumar AM, Nandabalan K, Li Y, Mishra, VS, Detter JC, Rothberg JM, Wallace MR, Southwick FS, Kingsmore SF. (2002) The Chediak-Higashi protein interacts with SNARE complex and signal transduction proteins. *Molecular Medicine*, **8**, 56-64.
- [127] Gudi R, Zou C, Li J, Gao Q. (2011) Centrobin-tubulin interaction is required for centriole elongation and stability. *Journal of Cell Biology*, **193**, 711-725.
- [128] Song L, Dai T, Xiong H, Lin C, Lin H, Shi T, Li J. (2010) Inhibition of centriole duplication by centrobin depletion leads to p38-p53 mediated cell-cycle arrest. *Cell Signalling*, **22**, 857-864.
- [129] Tsang WY, Dynlacht BD. (2008) Sgo1, a guardian of centriole cohesion. *Developmental Cell*, **14**, 320-322.
- [130] Takahashi M, Yamagiwa A, Nishimura T, Mukai H, Ono Y. (2002) Centrosomal proteins CG-NAP and kendrin provide microtubule nucleation sites by anchoring gamma-tubulin ring complex. *Molecular Biology of the Cell*, **13**, 3235-3245.
- [131] Larocca MC, Shanks RA, Tian L, Nelson DL, Stewart DM, Goldenring JR. (2004) AKAP350 interaction with cdc42 interacting protein 4 at the Golgi apparatus. *Molecular Biology of the Cell*, **15**, 2771-2781.
- [132] Kim HS, Takahashi M, Matsuo K, Ono Y. (2007) Recruitment of CG-NAP to the Golgi apparatus through interaction with dynein-dynactin complex. *Genes and Cells*, **12**, 421-434.
- [133] Fabbro M, Zhou BB, Takahashi M, Sarcevic B, Lal P, Graham ME, Gabrielli BG, Robinson PJ, Nigg EA, Ono Y, Khanna KK. (2005) Cdk1/Erk2- and Plk1-dependent phosphorylation of a centrosome protein, Cep55, is required for its recruitment to midbody and cytokinesis. *Developmental Cell*, **9**, 477-488.
- [134] Gillingham AK, Munro S. (2000) The PACT domain, a conserved centrosomal targeting motif in the coiled-coil proteins akap450 and pericentrin. *EMBO Reports*, **1**, 524-529.

- [135] Li K, Kaufman TC. (1996) The homeotic target gene centrosomin encodes an essential centrosomal component. *Cell*, **85**, 585-596.
- [136] Petzelt C, Joswig G, Mincheva A, Lichter P, Stammer H, Werner D. (1997) The centrosomal protein centrosomin A and the nuclear protein centrosomin B derive from one gene by post-transcriptional processes involving RNA editing. *Journal of Cell Science*, **110**, 2573-2578.
- [137] Terada Y, Uetake Y, Kuriyama R. (2003) Interaction of Aurora-A and centrosomin at the microtubule-nucleating site in *Drosophila* and mammalian cells. *Journal of Cell Biology*, **162**, 757-763.
- [138] Calarco-Gillam PD, Siebert MC, Hubble R, Mitchison T, Kirschner M. Cell (1983) Centrosome development in early mouse embryos as defined by an autoantibody against pericentriolar material. *Cell*, **35**, 621-629.
- [139] Balczon R, Bao L, Zimmer WE, Brown K, Zinkowski RP, Brinkley BR. (1995) Dissociation of centrosome replication events from cycles of DNA synthesis and mitotic division in hydroxyurea-arrested Chinese hamster ovary cells. *Journal of Cell Biology*, **130**, 105-115.
- [140] Li Q, Hansen D, Killilea A, Joshi H C, Palazzo R E, Balczon R (2001) Kendrin/pericentrin-B, a centrosome protein with homology to pericentrin that complexes with PCM-1. *Journal of Cell Science*, **114**, 797-809.
- [141] Azimzadeh J, Bornens M. (2007) Structure and duplication of the centrosome. *Journal of Cell Science*, **120**, 2139-2142.
- [142] Wang G, Chen Q, Zhang X, Zhang B, Zhuo X, Liu J, Jiang Q, Zhang C. (2013) PCM1 recruits Plk1 to the pericentriolar matrix to promote primary cilia disassembly before mitotic entry. *Journal of Cell Science*, **126**, 1355-1365.
- [143] Kamiya A, Tan PL, Kubo K, Engelhard C, Ishizuka K, Kubo A, Tsukita S, Pulver AE, Nakajima K, Cascella NG, Katsanis N, Sawa A (2008) PCM1 is recruited to the centrosome by the cooperative action of DISC1 and BBS4 and is a candidate for psychiatric illness. *Archives of General Psychiatry*, **65**, 996-1006.
- [144] Oegema K, Marshall WF, Sedat JW, Alberts BM. (1997) Two proteins that cycle asynchronously between centrosomes and nuclear structures: *Drosophila* CP60 and CP190. *Journal of Cell Science*, **110**, 1573-1583.
- [145] Oegema K, Whitfield WG, Alberts B. (1995) The cell cycle-dependent localisation of the CP190 centrosomal protein is determined by the coordinate action of two separable domains. *Journal of Cell Biology*, **131**, 1261-1273.
- [146] Chodagam S, Royou A, Whitfield W, Karess R, Raff JW. (2005) The centrosomal protein CP190 regulates myosin function during early *Drosophila* development. *Current Biology*, **15**, 1308-1313.
- [147] Moritz M, Zheng Y, Alberts BM, Oegema K. (1998) Recruitment of the gamma-tubulin ring complex to *Drosophila* salt-stripped centrosome scaffolds. *Journal of Cell Biology*, **142**, 775-786.
- [148] Ou YY, Mack GJ, Zhang M, Rattner JB. (2002) CEP110 and ninein are located in a specific domain of the centrosome associated with centrosome maturation. *Journal of Cell Science*, **115**, 1825-1835.

- [149] Mi J, Guo C, Brautigan DL, Larner JM. (2007) Protein phosphatase-1alpha regulates centrosome splitting through Nek2. *Cancer Research*, **67**, 1082-1089.
- [150] Kellogg DR, Oegema K, RaffJ, Schneider K, Alberts BM. (1995) CP60: a microtubule-associated protein that is localized to the centrosome in a cell cycle-specific manner. *Molecular Biology of the Cell*, **6**, 1673-1684.
- [151] Oegema K, Whitfield WG, Alberts B. (1995) The cell cycle-dependent localisation of the CP190 centrosomal protein is determined by the coordinate action of two separable domains. *Journal of Cell Biology*, **131**, 1261-1273.
- [152] Yang J, Liu X, Yue G, Adamian M, Bulgakov O, Li T (2002) Rootletin, a novel coiled-coil protein, is a structural component of the ciliary rootlet. *Journal of Cell Biology*, **159**, 431-440.
- [153] Conroy PC, Saladino C, Dantas TJ, Lalor P, Dockery P, Morrison CG. (2012) C-NAP1 and rootletin restrain DNA damage-induced centriole splitting and facilitate ciliogenesis. *Cell Cycle*, **11**, 3769-3778.
- [154] Bahmanyar S, Kaplan DD, Deluca JG, Giddings TH Jr, O'Toole ET, Winey M, Salmon ED, Casey PJ, Nelson WJ, Barth AI. (2008) beta-Catenin is a Nek2 substrate involved in centrosome separation. *Genes and Development*, **22**, 91-105.
- [155] Klotz C, Bordes N, Laine CM, Sandoz D, Bornens M. (2005) A protein of 175,000 daltons associated with striated rootlets in ciliated epithelia, as revealed by a monoclonal antibody. *Cell Motility and the Cytoskeleton*, **6**, 56-67.
- [156] Tsang WY, Spektor A, Vijayakumar S, Bista BR, Li J, Sanchez I, Duensing S, Dynlacht BD. (2009) Cep76, a centrosomal protein that specifically restrains centriole reduplication. *Developmental Cell*, **16**, 649-660.
- [157] Kobayashi T, Dynlacht BD. (2011) Regulating the transition from centriole to basal body. *Journal of Cell Biology*, **193**, 435-444.

1.4 Cell-Cycle Regulatory Kinases

Cyclin Dependent Kinases	Interaction, Localisation and Signalling Cascade	Disease Implication / Ancillary Information
CDK1	Cyclin Dependent Kinase, regulates G2/M phase. Involved with NEK6/7 and EG5 contributing to the accumulation of EG5 at the centrosome[1]. NEK9 is phosphorylated by CDK1 [1]. CDK1 is proposed to trigger centrosome separation in late G2 phase through phosphorylation of motor protein EG5 [2], although PLK1 can also act in this way, slowly through CDK2 compensation[2]. Interacts with CEP55 [3], CEP63 (recruits CDK1 to the centrosome)[4, 5]. CDK1 is involved in mitotic spindle symmetry and alignment for cell division [6].	Implications of CDKs in mitotic entry, centrosome replication and cancer[4].
CDK2	Cyclin Dependent Kinase. Regulates and essential for G1/S transition[7, 8]. Interacts with subunits of Cyclins-A and E [9].	Cyclin-A and Cyclin-E complex with CDK2 to initiate centrosome duplication[9].
CDK20/p42 Mitogen Activated Kinase (MAPK1)	Cyclin associated kinase[10] involved in cilium formation , Hedgehog and Wnt signalling[11, 12]. Activates CDK2 (and others). And is also found in nucleus and mitochondria . Stabilised by binding to the Bromi protein [13] and is implicated in G1-to-S phase transition[11].	Implicated in cancer [14].
Associated Cyclins		
Cyclin-A1/Cyclin-A2	Required for progression through S-phase and G2/M transition. Complexes with CDK2 [15] involved in cellular activity and proliferation[16]. Is repressed in oncogenic signalling[17].	Required for centrosome duplication which requires E2F and a Cyclin-A/CDK2 complex[18].
Cyclin-B	Cyclin-B1 localises with microtubules and is found in the cilium in G1-phase [19], whilst Cyclin-B2 is found localised to the Golgi region [20]. Cyclin-B1 nuclear localisation appears to be controlled by Cyclin-F [21].	
Cyclin-C	Interacts with CDK-8 . Responsible for phosphorylating RNA polymerase-II [22].	Involved in G0/G1 transition and Rb dependent G0-exit [23, 24].
Cyclin-D	Involved in G1/S transition and integrin mediated cell attachment to the extracellular matrix through regulation of cell cycle[25]. Interacts with FAK , Rho GTPases and ERK controlling intracellular tension and extracellular stiffness [25]. Involved in extracellular signalling through Kinase Kinase-½ and NF-kappa-β signalling pathways. Cyclin-D2 induces maturity in B-cells[26].	G2/M protein p58 interacts with Cyclin-D3[27].
Cyclin-E	Cyclin-E binds CDK2 in G1-phase , and is required during S-phase for progression. Localises to the centrosome with Wts/Lats kinase[28]. Identified in the cilium where the CDK2-cyclin E complex associates with the centrosome during cell cycle progression[29].	
Cyclin-F (Fbox1)	CP110 and Cyclin-F are physically associated on the centrioles during the G2 phase of the cell cycle. Depletion of Cyclin-F leads to centrosomal and mitotic abnormalities [30]. The genomic location of Cyclin-F gene is located close to PKD1 [31].	Much about Cyclin-F is still unknown. Controls centrosome homeostasis and mitotic fidelity through CP110 degradation[30].
Aurora-Kinases	Peaks during G2 to M phase transition in the cell cycle[32]. Interacts with c-terminal of Centrosomin (whose N-terminal binds to γ-tubulin [33]). Phosphorylation of Aurora-A causes Mdm2 mediated destabilisation of p53 [34], and G2-M cell cycle arrest [34]. Aurora-A interacts with basal body scaffolding proteins HEF1 and NEDD9 [35] which	Auroras A, B and C kinases have roles in cycle-cycle regulation and mitosis/meiosis[39, 40-43]. Aurora-A is involved in early and late mitotic events[43]. Involved in mitosis with organisation of the kinetochore at metaphase, chromosomes at

	complexes and localises to the ciliary base, phosphorylating and activating tubulin de-acetylase (HDAC6) , promoting ciliary disassembly [35-37]. Stabilisation of Aurora-A and HDAC6 may prevent cilium resorption [37]. Cofactors with CEP192 for MTOC function and spindle assembly [38]. Aurora-A activation initiates ciliary disassembly[37].	prometaphase[40]. Aurora-B is a regulator of mitotic chromosome segregation and required for chromatid orientation[41]. Binds to microtubules and KIF4 [44]. Aurora-C is required for cytokinesis and meiosis [45].
CDC2L1 (p58)	Protein kinase involved in the Hedgehog signaling pathway[46] and interacts with Cyclin-D3 [27].	
EF2 (Suspected in cilium) Elongation Factor 2 Kinase	Promotes G0 to S phase transition. E2F targets gene expression during the progression of cell cycle. EF2 with pRB involves accretion of inhibitory histone modifications invoking chromatin compaction[47].	

[1] Bertran MT, Sdelci S, Regué L, Avruch J, Caelles C, Roig J. (2011) Nek9 is a Plk1-activated kinase that controls early centrosome separation through Nek6/7 and Eg5. *EMBO Report*, **30**, 2634-2647.

[2] Smith E, Hégarat N, Vesely C, Roseboom I, Larch C, Streicher H, Straatman K, Flynn H, Skehel M, Hirota T, Kuriyama R, Hochegger H. (2010) Differential control of Eg5-dependent centrosome separation by Plk1 and Cdk1. *EMBO Report*, **30**, 2233-2245.

[3] Fabbro M, Zhou BB, Takahashi M, Sarcevic B, Lal P, Graham ME, Gabrielli BG, Robinson PJ, Nigg EA, Ono Y, Khanna KK. (2005) Cdk1/Erk2- and Plk1-dependent phosphorylation of a centrosome protein, Cep55, is required for its recruitment to midbody and cytokinesis. *Developmental Cell*, **9**, 477-488.

[4] Löffler H, Fechter A, Matuszewska M, Saffrich R, Mistrik M, Marhold J, Hornung C, Westermann F, Bartek J, Krämer A. (2011) Cep63 recruits Cdk1 to the centrosome: implications for regulation of mitotic entry, centrosome amplification, and genome maintenance. *Cancer Research*, **71**, 2129-2139.

[5] Smith E, Dejsuphong D, Balestrini A, Hampel M, Lenz C, Takeda S, Vindigni A, Costanzo V. (2009) An ATM- and ATR-dependent checkpoint inactivates spindle assembly by targeting CEP63. *Nature Cell Biology*, **11**, 278-285.

[6] Liakopoulos D, Kusch J, Grava S, Vogel J, Barral Y. (2003) Asymmetric loading of Kar9 onto spindle poles and microtubules ensures proper spindle alignment. *Cell*, **112**, 561-574.

[7] Morgan DL. (2007) *The Cell Cycle: Principles of Control*. New Science Press, London, 30-31.

[8] Koff A, Giordano A, Desai D, Yamashita K, Harper JW, Elledge S, Nishimoto T, Morgan DO, Franza BR, Roberts JM. (1992) Formation and activation of a cyclin E-cdk2 complex during the G1 phase of the human cell cycle. *Science*, **257**, 1689-1694.

[9] Jackman M, Kubota Y, den Elzen N, Hagting A, Pines J. (2002) Cyclin A- and cyclin E-Cdk complexes shuttle between the nucleus and the cytoplasm. *Molecular Biology of the Cell*, **13**, 1030-1045.

[10] Liu Y, Wu C, Galaktionov K. (2004) p42, a novel cyclin-dependent kinase-activating kinase in mammalian cells. *Journal of Biological Chemistry*, **279**, 4507-4514.

[11] Feng H, Cheng AS, Tsang DP, Li MS, Go MY, Cheung YS, Zhao GJ, Ng SS, Lin MC, Yu J, Lai PB, To KF, Sung JJ. (2011) Cell cycle-related kinase is a direct androgen receptor-regulated gene that drives β -catenin/T cell factor-dependent hepatocarcinogenesis. *Journal of Clinical Investigation*, **121**, 3159-3175

- [12] Pirke P, Efimenko E, Mohan S, Burghoorn J, Crona F, Bakhoun MW, Trieb M, Schuske K, Jorgensen EM, Piasecki BP, Leroux MR, Swoboda P. (2011) Transcriptional profiling of *C. elegans* DAF-19 uncovers a ciliary base-associated protein and a CDK/CCRK/LF2p-related kinase required for intraflagellar transport. *Developmental Biology*, **357**, 235-247.
- [13] Ko HW, Norman RX, Tran J, Fuller KP, Fukuda M, Eggenschwiler JT. (2010) Broad-minded links cell cycle-related kinase to cilia assembly and Hedgehog signal transduction. *Developmental Cell*, **18**, 237-247.
- [14] An X, Ng SS, Xie D, Zeng YX, Sze J, Wang J, Chen YC, Chow BK, Lu G, Poon WS, Kung HF, Wong BC, Lin MC. (2010) Functional characterisation of cell cycle-related kinase (CCRK) in colorectal cancer carcinogenesis. *European Journal of Cancer*, **46**, 1752-1761.
- [15] Diederichs S, Bäumer N, Ji P, Metzelder SK, Idos GE, Cauvet T, Wang W, Möller M, Pierschalski S, Gromoll J, Schrader MG, Koeffler HP, Berdel WE, Serve H, Müller-Tidow C. (2004) Identification of interaction partners and substrates of the cyclin A1-CDK2 complex. *Journal of Biological Chemistry*, **279**, 33727-33741.
- [16] Tsang WY, Wang L, Chen Z, Sánchez I, Dynlacht BD. (2007) SCAPER, a novel cyclin A interacting protein that regulates cell cycle progression. *Journal of Cell Biology*, **178**, 621-633.
- [17] Bäumer N, Tickenbrock L, Tschanter P, Lohmeyer L, Diederichs S, Bäumer S, Skryabin BV, Zhang F, Agrawal-Singh S, Köhler G, Berdel WE, Serve H, Koschmieder S, Müller-Tidow C. (2011) Inhibitor of cyclin-dependent kinase (CDK) interacting with cyclin A1 (INCA1) regulates proliferation and is repressed by oncogenic signalling. *Journal of Biological Chemistry*, **286**, 28210-28222.
- [18] Meraldi P, Lukas J, Fry AM, Bartek J, Nigg EA. (1999) Centrosome duplication in mammalian somatic cells requires E2F and Cdk2-cyclin A. *Nature Cell Biology*, **1**, 88-93.
- [19] Spalluto C, Wilson DI, Hearn T. (2013) Evidence for re-liciation of RPE1 cells in late G1 phase, and ciliary localisation of cyclin B1. *FEBS Open Biology*, **3**, 334-340.
- [20] Jackman M, Firth M, Pines J. (1995) Human cyclins B1 and B2 are localized to strikingly different structures: B1 to microtubules, B2 primarily to the Golgi apparatus. *EMBO Journal*, **14**, 1646-1654.
- [21] Kong M, Barnes EA, Ollendorff V, Donoghue DJ (2000) Cyclin F regulates the nuclear localisation of cyclin B1 through a cyclin-cyclin interaction. *EMBO Journal*, **19**, 1378-1388.
- [22] Kang YK, Guermah M, Yuan CX, Roeder RG (2002) The TRAP/Mediator coactivator complex interacts directly with estrogen receptors α and β through the TRAP220 subunit and directly enhances estrogen receptor function *in vitro*. *Proceedings of the National Academy of Sciences, USA*, **99**, 2642-2647.
- [23] Ren S, Rollins BJ. (2004) Cyclin C/cdk3 promotes Rb-dependent G0 exit. *Cell*, **117**, 239-251.
- [24] Sage J. (2004) Cyclin C makes an entry into the cell cycle. *Developmental Cell*, **6**, 607-608.
- [25] Assoian RK, Klein EA. (2008) Growth control by intracellular tension and extracellular stiffness. *Trends in Cell Biology*, **18**, 347-352.
- [26] Piatelli MJ, Wardle C, Blois J, Doughty C, Schram BR, Rothstein TL, Chiles TC. (2004) Phosphatidylinositol 3-kinase-dependent mitogen-activated protein/extracellular signal-regulated

kinase kinase 1/2 and NF-kappa B signalling pathways are required for B cell antigen receptor-mediated cyclin D2 induction in mature B cells. *Journal of Immunology*, **172**, 2753-2762.

[27] Zhang S, Cai M, Zhang S, Xu S, Chen S, Chen X, Chen C, Gu J. (2002) Interaction of p58(PITSLRE), a G2/M-specific protein kinase, with cyclin D3. *Journal of Biological Chemistry*, **277**, 35314-35322.

[28] Shimizu T, Ho LL, Lai ZC. (2008) The mob as tumour suppressor gene is essential for early development and regulates tissue growth in *Drosophila*. *Genetics*, **178**, 957-965.

[29] Plotnikova OV, Golemis EA, Pugacheva EN. (2008) Cell cycle-dependent ciliogenesis and cancer. *Cancer Research*, **68**, 2058-2061.

[30] D'Angiolella V, Donato V, Vijayakumar S, Saraf A, Florens L, Washburn MP, Dynlacht B, Pagano M. (2010) SCF (Cyclin F) controls centrosome homeostasis and mitotic fidelity through CP110 degradation. *Nature*, **466**, 138-142.

[31] Kraus B, Pohlschmidt M, Leung AL, Germino GG, Snarey A, Schneider MC, Reeders ST, Frischauf AM. (1994) A novel cyclin gene (CCNF) in the region of the polycystic kidney disease gene (PKD1). *Genomics*, **24**, 27-33.

[32] Lukasiewicz KB, Lingle WL. (2009) Aurora A, centrosome structure, and the centrosome cycle. *Environmental and Molecular Mutagenesis*, **50**, 602-619.

[33] Terada Y, Uetake Y, Kuriyama R. (2003) Interaction of Aurora-A and centrosomin at the microtubule-nucleating site in *Drosophila* and mammalian cells. *Journal of Cell Biology*, **162**, 757-763.

[34] Katayama H, Sasai K, Kawai H, Yuan ZM, Bondaruk J, Suzuki F, Fujii S, Arlinghaus RB, Czerniak BA, Sen S. (2004) Phosphorylation by aurora kinase A induces Mdm2-mediated destabilization and inhibition of p53. *Nature Genetics*, **36**, 55-62.

[35] Alieva IB, Uzbekov RE. (2008) The centrosome is a polyfunctional multiprotein cell complex. *Biochemistry*, **73**, 626-643.

[36] Pugacheva E, Golemis E. (2005) The focal adhesion scaffolding protein HEF1 regulates activation of the Aurora-A and Nek2 kinases at the centrosome. *Nature Cell Biology*, **7**, 937-946.

[37] Pugacheva EN, Jablonski SA, Hartman TR, Henske EP, Golemis EA. (2007) HEF1-dependent Aurora A activation induces disassembly of the primary cilium. *Cell*, **129**, 1351-1363.

[38] Joukov V, De Nicolo A, Rodriguez A, Walter JC, Livingston DM. (2010) Centrosomal protein of 192 kDa (Cep192) promotes centrosome-driven spindle assembly by engaging in organelle-specific Aurora A activation. *Proceedings of the National Academy of Sciences, USA*, **107**, 21022-21027.

[39] Sabino D, Brown NH, Basto R. (2011) *Drosophila* Ajuba is not an Aurora-A activator but is required to maintain Aurora-A at the centrosome. *Journal of Cell Science*, **124**, 1156-1166.

[40] Ma C, Cummings C, Liu XJ. (2003) Biphasic activation of Aurora-A kinase during the meiosis I-meiosis II transition in *Xenopus* oocytes. *Molecular and Cellular Biology*, **23**, 1703-1716.

[41] Hauf S, Biswas A, Langeegger M, Kawashima SA, Tsukahara T, Watanabe Y. (2007) Aurora controls sister kinetochore mono-orientation and homolog bi-orientation in meiosis-I. *EMBO Journal*, **26**, 4475-4486.

- [42] Nigg EA. (2001) Mitotic kinases as regulators of cell division and its checkpoints. *Nature Reviews Molecular and Cellular Biology*, **2**, 21-32.
- [43] Marumoto T, Honda S, Hara T, Nitta M, Hirota T, Kohmura E, Saya H (2003) Aurora-A kinase maintains the fidelity of early and late mitotic events in HeLa cells. *Journal of Biological Chemistry*, **278**, 51786-51795.
- [44] Ozlü N, Monigatti F, Renard BY, Field CM, Steen H, Mitchison TJ, Steen JJ. (2010) Binding partner switching on microtubules and aurora-B in the mitosis to cytokinesis transition. *Molecular and Cellular Proteomics*, **9**,336-350.
- [45] Yang KT, Li SK, Chang CC, Tang CJ, Lin YN, Lee SC, Tang TK. (2010) Aurora-C kinase deficiency causes cytokinesis failure in meiosis I and production of large polyploid oocytes in mice. *Molecular Biology of the Cell*, **21**, 2371-2383.
- [46] Evangelista M, Lim TY, Lee J, Parker L, Ashique A, Peterson AS, Ye W, Davis DP, de Sauvage FJ. (2008) Kinome siRNA screen identifies regulators of ciliogenesis and hedgehog signal transduction. *Science Signalling*, **1**, ra7.
- [47] Blais A, Dynlacht BD. (2007) E2F-associated chromatin modifiers and cell cycle control. *Current Opinion in Cell Biology*, **19**, 658-662.

1.5 Regulatory Components

Centrosome Localisation	Interaction, Localisation and Signalling Cascade	Disease Implication / Ancillary Information
Nesprin	Required for centrosomal positioning, cell polarity and ciliogenesis. Interacts with Meckelin for ciliogenesis via remodeling actin [1].	
Gimap5	GTPase IMAP family member. Localises to the ER , Golgi and the centrosome . Interacts with CHOP for mediating endoplasmic reticulum stress induced apoptosis[2].	
PLK1(Polo-Like-Kinase-1)	Associated with G2/M transition in early prophase[3]. Localises to the transition zone, where it phosphorylates NPHP1 [4], and activates histone deacetylase 6 (HDAC6) is recruited to the pericentriolar matrix by PCM1 in a dynactin dependent manner[5]. Interaction between PCM1 and PLK1 is phosphorylation dependent, a process in which CDK1 acts as the priming kinase[5]. PLK1 interacts with many pathways, is associated with aneuploidy and centrosome abnormality, as well as in p53 inactivation [6, 7]. PLK1 prevents centrosome separation from ionizing radiation exposure[8] while PLK1 phosphorylation inhibits ATM/ATR -dependent activation[9] in response to DNA damage[10]. PLK phosphorylates Cyclin-B1 allowing nuclear targetting [11].	
CEP215 (CDK5RAP2)	Localises to the centrosome through-out the cell cycle where CEP215 and CEP68 are involved in centrosome cohesion[12]. Interacts with Pericentrin and CDK5R1 [13].	
CEP97	CEP97 and CP110 suppress ciliary assembly[14]. Depletion of CEP97 results in loss of CP110 giving rise to polyploidy and spindle defects [15].	Involved in the transition from centriole to basal body [16].
CEP63 (Tumour Suppressor)	Acts as an ATM/ATR -dependent checkpoint for Double Strand DNA breaks halting spindle assembly[9]. Involved as an ATM/ATR -dependent checkpoint for DSBs halting spindle assembly[9]. CEP63 and CEP152 are involved in centriole duplication[17].	Mitotic checkpoint . Interacts with Disrupted-In-Schizophrenia 1 (DISC1)[18]. Recruits CDK-1 to the centrosome[19].
TRAF7 (Suspected in the centrosome)	MoD1 transcription target, where ubiquitylation of NF-kappa-β is regulated exclusively by TRAF7 [20].	Also Cytoplasmic.
HSP73 (Heat Shock Protein)	Centrosomally co-localised with Pericentrin and TCP1 [21] with a role as a molecular chaperone [22]. Interacts with Cyclin-D (promotes stability for interaction with CDK4 [23]).	
Centrin (CETN1/2/3)	Centrins are localised to the centriole/pericentriolar material[24, 25] and are involved in microtubule severing [26]. Centrins have a variety of roles within the cell[27]. CETN2 is required for centriole/centrosome duplication and plays a role in organising the microtubule network around the centrosome[28]. Involved in photoreceptors where it interacts with Transducin , CDK2 and in the assembly of Centrin and G-protein complexes[29], Involved in DNA damage recognition and repair [30]. Interacts with CP110 [31] and localises to fibrous striated rootlets connected to basal bodies[32].	Localises to the distal (+) end of the basal body , and proximal centriole coating the outer surface and inner (+) end surfaces at the beginning of S-phase [22]. Centrin-2 is involved in the nuclear pore where it plays a role in mRNA and protein export[33].
CEP152	Depletion of CEP152 prevents centriole replication and leads to loss of SAS6 . Co-localises with and is phosphorylated by PLK4 [34]. Scaffolds PLK4 and	

	CPAP to regulate centrosome duplication [35].	
CEP192	Regulates peri-centriolar material recruitment, where it may act as a γ - TuRC scaffold for MT nucleation and spindle formation[36]. Interacts with Aurora-A for spindle assembly[37]	
NEDD1	NEDD1 is responsible for targeting the γ - TuRC complex to the centrosome, is involved in centriole replication and spindle assembly[38].	
NEDD8 (Suspected in the centrosome)	Responsible for Katanin degradation[39] and p53 localisation[40].	
NEDD9	Interacts with Aurora-A [22], involved in integrin signalling [41].	Involved with Alzheimer's disease[42].
p53	Functions as a regulator of cell cycle and tumour suppressor. Loss of centrosome integrity causes p38-p53-p21 dependent G1-S-phase arrest [43]. Some p53 localised to the centrosome[22].	Interacts with a large number of complexes.
HEF-1	Focal adhesion scaffolding protein involved with activation of Aurora-A and NEK2 [44], where HEF1 dependent Aurora-A activation induces ciliary disassembly [45].	
CDC14B	Phosphatase involved in ciliary length control [46].	
FOR20	Contains a LIS-1 domain , identified in centrosomes and pericentriolar satellites where it is involved in ciliogenesis. Possibly involved with the interaction of PCM1 satellites with microtubules and their motor proteins[47].	
FOP	Similar in homology to OFD1 and FOR20 , FOP co-localises with PCM1 in cell cycle, and might be a satellite cargo protein. Inhibition of FOP inhibits primary cilium formation [48].	FOP-FGFR1 involved in myeloproliferation disorder[48, 49].
CEP37	Localises to distal tip of axoneme and distal end of basal body[50]	
CEP128	Localises subdistally to the basal body and possibly to the satellites[50]	
Golgi Complexes		
MT Anchoring	GMAP210 targets the γ - TuRC to the cis-Golgi membranes functioning as a secondary MTOC , nominally to the cytoplasmic Golgi face, and is also required for Golgi ribbon formation[51].	

[1] Dawe HR, Adams M, Wheway G, Szymanska K, Logan CV, Noegel AA, Gull K, Johnson CA. (2009) Nesprin-2 interacts with meckelin and mediates ciliogenesis via remodelling of the actin cytoskeleton. *Journal of Cell Science*, **122**, 2716-2726.

[2] Pino SC, O'Sullivan-Murphy B, Lidstone EA, Yang C, Lipson KL, Jurczyk A, diIorio P, Brehm MA, Mordes JP, Greiner DL, Rossini AA, Bortell R. (2009) CHOP mediates endoplasmic reticulum stress-induced apoptosis in Gimap5-deficient T cells. *PLoS One*, **4**(5):e5468.

[3] Niiya F, Tatsumoto T, Lee KS, Miki T. (2006) Phosphorylation of the cytokinesis regulator ECT2 at G2/M phase stimulates association of the mitotic kinase Plk1 and accumulation of GTP-bound RhoA. *Oncogene*, **25**, 827-837.

[4] Seeger-Nukpezah T, Liebau MC, Höpker K, Lamkemeyer T, Benzing T, Golemis EA, Schermer B. (2012) The centrosomal kinase Plk1 localizes to the transition zone of primary cilia and induces phosphorylation of nephrocystin-1. *PLoS One*, **7**(6):e38838.

- [5] Wang G, Chen Q, Zhang X, Zhang B, Zhuo X, Liu J, Jiang Q, Zhang C. (2013) PCM1 recruits Plk1 to the pericentriolar matrix to promote primary cilia disassembly before mitotic entry. *Journal of Cell Science*, **126**, 1355-1365.
- [6] Liu XS, Li H, Song B, Liu X. (2010) Polo-like kinase 1 phosphorylation of G2 and S-phase-expressed 1 protein is essential for p53 inactivation during G2 checkpoint recovery. *EMBO Reports*, **11**, 626-632.
- [7] McKenzie L, King S, Marcar L, Nicol S, Dias SS, Schumm K, Robertson P, Bourdon JC, Perkins N, Fuller-Pace F, Meek DW. (2010) p53-dependent repression of polo-like kinase-1 (PLK1). *Cell Cycle*, **9**, 4200-4212.
- [8] Zhang W, Fletcher L, Muschel RJ. (2005) The role of Polo-like kinase 1 in the inhibition of centrosome separation after ionizing radiation. *Journal of Biological Chemistry*, **280**, 42994-42999.
- [9] Smith E, Dejsuphong D, Balestrini A, Hampel M, Lenz C, Takeda S, Vindigni A, Costanzo V. (2009) An ATM- and ATR-dependent checkpoint inactivates spindle assembly by targeting CEP63. *Nature Cell Biology*, **11**, 278-285.
- [10] Tsvetkov L, Stern DF. (2005) Phosphorylation of Plk1 at S137 and T210 is inhibited in response to DNA damage. *Cell Cycle*, **4**, 166-171
- [11] Toyoshima-Morimoto F, Taniguchi E, Shinya N, Iwamatsu A, Nishida E. (2001) Polo-like kinase 1 phosphorylates cyclin B1 and targets it to the nucleus during prophase. *Nature*, **410**, 215-220.
- [12] Graser S, Stierhof YD, Nigg EA. (2007) Cep68 and Cep215 (Cdk5rap2) are required for centrosome cohesion. *Journal of Cell Science*, **120**, 4321-4331.
- [13] Wang X, Ching YP, Lam WH, Qi Z, Zhang M, Wang JH. (2000) Identification of a common protein association region in the neuronal Cdk5 activator. *Journal of Biological Chemistry*, **275**, 31763-31769.
- [14] Spektor A, Tsang WY, Khoo D, Dynlacht BD. (2007) Cep97 and CP110 suppress a cilia assembly program. *Cell*, **130**, 678-690.
- [15] Chen Z, Indjeian VB, McManus M, Wang L, Dynlacht BD. (2002) CP110, a cell cycle-dependent CDK substrate, regulates centrosome duplication in human cells. *Developmental Cell*, **3**, 339-350.
- [16] Kobayashi T, Dynlacht BD. (2011) Regulating the transition from centriole to basal body. *Journal of Cell Biology*, **193**, 435-444.
- [17] Brown NJ, Marjanović M, Lüders J, Stracker TH, Costanzo V. (2013) Cep63 and Cep152 cooperate to ensure centriole duplication. *PLoS One*, **8**(7):e69986.
- [18] Morris JA, Kandpal G, MaL, Austin CP. (2003) DISC1 (Disrupted-In-Schizophrenia 1) is a centrosome-associated protein that interacts with MAP1A, MIPT3, ATF4/5 and NUDEL: regulation and loss of interaction with mutation. *Human Molecular Genetics*, **12**, 1591-1608.
- [19] Tsikitis M, Acosta-Alvear D, Blais A, Campos EI, Lane WS, Sánchez I, Dynlacht BD (2010) Traf7, a MyoD1 transcriptional target, regulates nuclear factor-kappaB activity during myogenesis. *EMBO Reports*, **11**, 969-976.
- [20] Xu LG, Li LY, Shu HB. (2004) TRAF7 potentiates MEKK3-induced AP1 and CHOP activation and induces apoptosis. *Journal of Biological Chemistry*, **279**, 17278-17282.

- [21] Brown CR, Hong-Brown LQ, Doxsey SJ, Welch WJ. (1996) Molecular chaperones and the centrosome. A role for HSP 73 in centrosomal repair following heat shock treatment. *Journal of Biological Chemistry*, **271**, 833-840.
- [22] Alieva IB, Uzbekov RE. (2008) The centrosome is a polyfunctional multiprotein cell complex. *Biochemistry*, **73**, 626-643.
- [23] Diehl JA, Yang W, Rimerman RA, Xiao H, Emili A. (2003) Hsc70 regulates accumulation of cyclin D1 and cyclin D1-dependent protein kinase. *Molecular and Cellular Biology*, **23**, 1764-1774.
- [24] Errabolu R, Sanders MA, Salisbury JL. (1994) Cloning of a cDNA encoding human centrin, an EF-hand protein of centrosomes and mitotic spindle poles. *Journal of Cell Science*, **107**, 9-16.
- [25] Baron AT, Greenwood TM, Bazinet CW, Salisbury JL. (1992) Centrin is a component of the pericentriolar lattice. *Biology of the Cell / under the auspices of the European Cell Biology Organization*, **76**, 383-388.
- [26] Sanders MA, Salisbury JL. (1994) Centrin plays an essential role in microtubule severing during flagellar excision in *Chlamydomonas reinhardtii*. *Journal of Cell Biology*, **124**, 795-805.
- [27] Vonderfecht T, Stemm-Wolf AJ, Hendershott M, Giddings TH Jr, Meehl JB, Winey M. (2011) The two domains of centrin have distinct basal body functions in *Tetrahymena*. *Molecular Biology of the Cell*, **22**, 2221-2234.
- [28] Salisbury JL, Suino KM, Busby R, Springett M. (2002) Centrin-2 is required for centriole duplication in mammalian cells. *Current Biology*, **12**, 1287-1292.
- [29] Trojan P, Krauss N, Choe HW, Giessl A, Pulvermüller A, Wolfrum U. (2008) Centrin in retinal photoreceptor cells: regulators in the connecting cilium. *Progress in Retinal Eye Research*, **27**, 237-259.
- [30] Krasikova YS, Rechkunova NI, Maltseva EA, Craescu CT, Petrusseva IO, Lavrik OI. (2012) Influence of centrin 2 on the interaction of nucleotide excision repair factors with damaged DNA. *Biochemistry*, **77**, 346-353.
- [31] Tsang WY, Spektor A, Luciano DJ, Indjeian VB, Chen Z, Salisbury JL, Sánchez I, Dynlacht BD. (2006) CP110 cooperates with two calcium-binding proteins to regulate cytokinesis and genome stability. *Molecular Biology of the Cell*, **17**, 3423-3434.
- [32] Lemullois M, Fryd-Versavel G, Fleury-Aubusson A. (2004) Localisation of centrin in the hypotrich ciliate *Paraurostyla weissei*. *Protist*, **155**, 331-346.
- [33] Resendes KK, Rasala BA, Forbes DJ. (2008) Centrin 2 localises to the vertebrate nuclear pore and plays a role in mRNA and protein export. *Molecular and Cellular Biology*, **28**, 1755-1769.
- [34] Hatch EM, Kulukian A, Holland AJ, Cleveland DW, Stearns T. (2010) Cep152 interacts with Plk4 and is required for centriole duplication. *Journal of Cell Biology*, **191**, 721-729.
- [35] Cizmecioglu O, Arnold M, Bahtz R, Settele F, Ehret L, Haselmann-Weiss U, Antony C, Hoffmann I. (2010) Cep152 acts as a scaffold for recruitment of Plk4 and CPAP to the centrosome. *Journal of Cell Biology*, **191**, 731-739.
- [36] Gomez-Ferreria M, Rath U, Buster D, Chanda S, Caldwell J, Rines D, Sharp D. (2007) Human Cep192 is required for mitotic centrosome and spindle assembly. *Current Biology*, **17**, 1960-1966.

- [37] Joukov V, De Nicolo A, Rodriguez A, Walter JC, Livingston DM. (2010) Centrosomal protein of 192 kDa (Cep192) promotes centrosome-driven spindle assembly by engaging in organelle-specific Aurora A activation. *Proceedings of the National Academy of Sciences, USA*, **107**, 21022-21027.
- [38] Haren L, Remy MH, Bazin I, Callebaut I, Wright M, Merdes AJ. (2006) NEDD1-dependent recruitment of the gamma-tubulin ring complex to the centrosome is necessary for centriole duplication and spindle assembly. *Journal of Cell Biology*, **172**, 505-515.
- [39] Kurz T, Pintard L, Willis JH, Hamill DR, Gonczy P, Peter M, Bowerman B. (2002) Cytoskeletal regulation by the Nedd8 ubiquitin-like protein modification pathway. *Science*, **295**, 1294-1298.
- [40] Liu G, Xirodimas DP. (2010) NUB1 promotes cytoplasmic localisation of p53 through cooperation of the NEDD8 and ubiquitin pathways. *Oncogene*, **29**, 2252-2261.
- [41] Kondo S, Iwata S, Yamada T, Inoue Y, Ichihara H, Kichikawa Y, Katayose T, Souta-Kuribara A, Yamazaki H, Hosono O, Kawasaki H, Tanaka H, Hayashi Y, Sakamoto M, Kamiya K, Dang NH, Morimoto C. (2012) Impact of the integrin signaling adaptor protein NEDD9 on prognosis and metastatic behavior of human lung cancer. *Clinical Cancer Research*, **18**, 6326-6338.
- [42] Xing YY, Yu JT, Yan WJ, Chen W, Zhong XL, Jiang H, Wang P, Tan L. (2011) NEDD9 is genetically associated with Alzheimer's disease in a Han Chinese population. *Brain Research*, **1369**, 230-234.
- [43] Mikule K, Delaval B, Kaldis P, Jurczyk A, Hergert P, Doxsey S. (2007) Loss of centrosome integrity causes p38-p53-p21-dependent G1-S arrest. *Nature Cell Biology*, **9**, 160-170.
- [44] Pugacheva E, Golemis E. (2005) The focal adhesion scaffolding protein HEF1 regulates activation of the Aurora-A and Nek2 kinases at the centrosome. *Nature Cell Biology*, **7**, 937-946.
- [45] Pugacheva EN, Jablonski SA, Hartman TR, Henske EP, Golemis EA. (2007) HEF1-dependent Aurora A activation induces disassembly of the primary cilium. *Cell*, **129**, 1351-1363.
- [46] Clement A, Solnica-Krezel L, Gould KL. (2011) The Cdc14B phosphatase contributes to ciliogenesis in zebrafish. *Development*, **138**, 291-302.
- [47] Sedjaj F, Acquaviva C, Chevrier V, Chauvin JP, Coppin E, Aouane A, Coulier F, Tolun A, Pierres M, Birnbaum D, Rosnet O. (2010) Control of ciliogenesis by FOR20, a novel centrosome and pericentriolar satellite protein. *Journal of Cell Science*, **123**, 2391-2401.
- [48] Lee JY, Stearns T. (2013) FOP is a centriolar satellite protein involved in ciliogenesis. *PLoS One*, **8**(3):e58589.
- [49] Guasch G1, Delaval B, Arnoulet C, Xie MJ, Xerri L, Sainty D, Birnbaum D, Pébusque MJ. (2004) FOP-FGFR1 tyrosine kinase, the product of a t(6;8) translocation, induces a fatal myeloproliferative disease in mice. *Blood*, **103**, 309-312.
- [50] Schröder JM, Rogowski M, Jakobsen K, Vanselow K, Geimer S, Pedersen LB, Andersen JS. (2012) Identification and characterization of two novel centriolar appendage component proteins. *Cilia*, **1**, P44.
- [51] Rios RM, Sanchis A, Tassin AM, Fedriani C, Bornens M. (2004) GMAP-210 recruits γ -tubulin complexes to cis-Golgi membranes and is required for Golgi ribbon formation. *Cell*, **118**, 323-335.

Appendix II: Rab-GTPases - Ciliary and Golgi Function

RAB Member	Cellular Location	Interactions
RAB1	Endoplasmic Reticulum/Golgi	Required for transport between ER and Golgi[1, 2, 3] involved in pre-Golgi endoplasmic to Golgi Intermediate compartment ERGIC [4, 5]. Regulates calcium signalling receptor (hCaR)[6]. RAB1A is involved in microtubule anterograde melanosome transport [7]. Interacts with the GM130 effector complex regulating COPII vesicle cis-Golgi tethering [8].
RAB2	Endoplasmic Reticulum/Golgi	Essential for the maturation of pre-Golgi intermediates [9], regulates vesicle trafficking between the endoplasmic reticulum and cis-Golgi network [10, 11]. Involved with the endoplasmic reticulum and the Golgi[5] where it is required for pre-Golgi maturation [9] and Endoplasmic Reticulum-to-Golgi Intermediate compartment ERGIC [4].
RAB3A	Secretory vesicles	RAB3 modulates the activity of the fusion machinery by controlling the formation or the stability of the SNARE complex[12] and regulates vesicle fusion [13-15]. Involved with KIF1 motors[16].
RAB3D	<i>trans</i> -Golgi vesicles	Associated with a subset of post- <i>trans</i> -Golgi network vesicles not involved with the endosome or lysosome[17].
RAB4	Endosome (early)[20]	Rab4 and Rab11 regulate the recycling of angiotensin [18, 19]. Rab4 regulates KIFC2 activity[20], interacts with KIF3 [20-22] and interacts with KIF3B [22, 23]. Involved in plasma membrane recycling[24]. Rab4 , and Rab5 are important in early regulation of endosome trafficking while Rab7 is involved with the late endosome[25]. Interacts with DYNC1L1 [22].
RAB5A*[39]	Clathrin coated pits/membrane	Functions for internalisation. Rab5A and Rab7 are lysosomal co-regulators and catalysts[26]. Rab4 , and Rab5 are important in early regulation of endosomal trafficking while Rab7 is involved with the late endosome[27]. Rab5 is vital for endosomal biogenesis [27], while clathrin and Rab5 are required for endocytosis[28, 29].
RAB5C*[39]	Endosome (early)	Wnt11 mediates cell adhesion through Rab5C and E-cadherin , a key regulator of early endocytosis [30].
RAB6*[39]	<i>medial</i> to <i>trans</i> -Golgi[31], Golgi to plasma membrane and Golgi to endoplasmic reticulum retrograde transport[24, 32].	Regulates recruitment of the dynactin complex to Golgi membranes[33]. KIF20A interacts with Rab6 at the Golgi , transformation to GDP form releases KIF20A [34] required for cytokinesis [35]. Rab6 family members interact with dynein light chain [36], and target exocytotic carriers [37]. Rab6 effectors may include dynactin , myosin , KIF5A/KIF5B , KIF1C , and KIF20 [22, 38]. Rab6 and Rab8 are involved in vesicle docking and fusion for exocytosis[39]. Rab6 is involved with p150^{GLUED} , p50^{Dynamitin} in the Golgi [23].
RAB7	Endosomes (late), Lysosomes and Phagosome[24]	Rab7 effector protein RILP controls trafficking through late endosomes to lysosomes [19, 24]. Transported by the dynein-dynactin-complex [36, 37] and are required for lysosome biogenesis [41, 42]. Rab4 , and Rab5 are important in early regulation of endosomal trafficking while Rab7 is involved with the late endosome[21]. Interacts with dynactin [23]. Interacts with RILP [41, 45], CHM [46, 47] and AP-1-Clathrin adaptor.
RAB8*[43] RAB8A*[44]	<i>trans</i> -Golgi[20], secretory vesicles, Modulators of ciliary protein trafficking [39].	Rab8 interacts with Rabin and Rab11 for transport of vesicles (with IFT20) containing Golgi derived materials to the ciliary membrane[43]. Rab8a localises to the cilium and interacts with Centxin/ODF2 [44, 49] and CEP290 and the PCM [48]. Involved in macropinosome membrane trafficking and Cholera-B toxin trafficking to the Golgi [50]. Rab8 and Rab11 are involved in ciliogenesis[51]. Interacts with myosin in the Golgi [23].
RAB9	Late Endosome and the <i>trans</i> -Golgi [24]	Regulates late Endosome size[52] and transport of vesicles to the trans-Golgi [53]. Required for viral replication [54].
RAB10*[43]	Golgi sorting and endosomes[24]. Associates with the primary cilium in renal epithelium[55].	RAB10 co-localises with Exocyst proteins at the base of the cilium[55]. Involved with transport of TLR4 to the cell membrane[56]. Regulates glutamate receptor recycling in

		endocytosis[57] and endoplasmic reticulum morphology [58].
RAB11*[43]	<i>trans</i> -Golgi network[24], Endosome (early), regulates recycling[60, 61]. Stretch activated exocytosis[61].	Regulates compartmentalisation of early endosomes required for efficient transport from early endosomes to the trans-Golgi network [62]. Rab11-FIP3 links Rab11-GTPase and cytoplasmic dynein DYNC1LI1 mediating transport to the endosomal-recycling compartment[63]. Rab4 and Rab11 together regulate the recycling of angiotensin [18]. Interacts with myosin in the recycling compartment[23]. Interacts with KIF3B [22].
RAB12	Secretory granules[64].	Regulates mTORC1 activity through degradation of the amino acid transporter PAT4 [65].
RAB13	Cytoplasmic vesicles, and tight Junctions[66].	Mediates recycling of occludin [67], interacts with Kinase-A [68]. Involved in regulation of membrane trafficking between the endosome and the TGN in epithelial cells[69].
RAB14	Endosome (early) and the <i>trans</i> -Golgi network[70]	Involved in trans-Golgi to plasma membrane transport[24] as well as Golgi and endosome membrane trafficking[71]. Interacts with KIF16B [22].
RAB15	Endosome (early and recycling)[32]	Inhibitor of endocytic internalisation[53]. Recycles receptors from the recycling endosome[72].
RAB17*[44]	Endosome (apical recycling)	Involved in recycling transport[53]. Regulates receptor mediated endocytosis in epithelial cells and localises to the recycling endosome[73].
RAB18	Endoplasmic reticulum, Golgi and Endosome[73-77], lipid droplets[78], synaptic granule[78] and secretory granules[79].	Rab18 and Rab43 are involved in ER-Golgi trafficking, Rab43-T32N redistributes Golgi elements to ER exit sites . Rab43 redistributes the p150(Glued) subunit of dynactin , consistent with a specific role in regulating association of pre-Golgi intermediates with microtubules[74, 4]. Loss of Rab18 function causes Warburg-micro syndrome [81].
RAB20	Epithelial specific	Associated with dense apical tubules[53]. Regulates phagosome maturation in macrophages[82].
RAB21	Early endosome[83].	Involved in cell adhesion and endosomal recycling of integrin receptors [84]. Regulates cell adhesion and controls trafficking of β1-integrins [84].
RAB22	Endosomes (late and early)[85], Rab22B involved in <i>trans</i> -Golgi membranes[86].	Affects the morphology and function of endosomes[85], with Rab22B being involved in <i>trans</i> -Golgi membranes[86].
RAB23*[43, 44]	Cilium, also locates to the Plasma Membrane, Endosome (early) and Endocytic pathways[24].	GTPase [87] involved in signal transduction, essential negative regulator of Sonic Hedgehog [88, 89]; involved in organogenesis[90]. Rab23 regulates Smoothed levels[91] and has a role in planar polarisation[92].
RAB24	<i>cis</i> -Golgi[93], Endoplasmic Reticulum and Endosome (late), and the Autophagosome[86].	Involved in protein trafficking pathways and may function in vesicle transport [94]. Involved in cell division[95]. Involved with Rab7 and Rab23 in the autophagosome [86].
RAB25	Endosome(late), recycling endosome[24, 86].	Apical re-cycling [24, 53, 96]. Regulates metastasis and invasion in gastric, head and neck cancers[95, 98]. Rab25 is associated with α5β1-integrin in invasive migration [99].
RAB26	Golgi derived trafficking, secretory vesicles	Involved in transport of G-coupled α2-adrenergic receptors from the Golgi[86, 100].
RAB27	Melanosomes, apical plasma membrane vesicles and secretory granules[86, 101]	Involved in regulated secretion and membrane trafficking[88]. Interacts with Slac2 and myosin-Va for transport[24, 101]. Rab27A and Rab27B control components of the secretory exosome pathway [102, 103]. Prenylation of Rab27A may play a role in degeneration of photoreceptors[104]. Interacts with myosins and Rab27A [105] in the melanosome [23]. Interacts with KIF5 [22].
RAB28	Basal body and ciliary rootlet	Involved in autosomal recessive cone-rod dystrophy and macular degeneration. Localises to basal body and ciliary rootlet[106].
RAB30	Golgi	Localises to the Golgi where it is required for Golgi integrity and is involved in control of morphology[107].
RAB31	<i>trans</i> -Golgi network[20]	Rab31 levels possibly modulate breast cancer cell matrix adhesion and invasive capacity[108].
RAB32	Mitochondria and melanosome[81].	Involved in apoptosis , and targeting PKA to endoplasmic reticulum and mitochondrial membranes[109]. Rab32 and Rab38 are involved in melanosome biogenesis[110] and post Golgi

		sorting[111].
RAB33	Golgi[27], Autophagosome[83].	Involved in retrograde transport to the Endoplasmic Reticulum[32], and with autophagy [24]. Localised to <i>medial</i> -Golgi cisternae[111, 112]; involved with Rab5 in the Macropinosome [86].
RAB34	Golgi, macropinosomes[86]	RAB34 controls intra-Golgi and lysosome positioning[24, 113], involved in response to hyperglycemia[114].
RAB35	Plasma membrane, Endosomes[32], recycling endosome[86]	Involved in membrane and endosomal recycling[115].
RAB36	Endosome/Lysosome	Regulates distribution of endosomes and lysosomes[116].
RAB37	Secretory granules/vesicles [24]	Involved with secretory granules and insulin exocytosis[117, 118].
RAB38	Melanosome[86]	Rab32 and Rab38 control post Golgi sorting of melanocytic enzymes[111] Associated with proteinuria and hypertension in renal disease[119] and poor outcome in glioma progression[120].
RAB39A	Golgi association, and Caspase-1 involvement.	Involved with binding caspase-1 secretion of interleukin-1 β [121]. Golgi associated and also involved in endocytosis[122].
RAB39B	Golgi	Unknown but associated with autism, epilepsy and retardation[24, 123].
RAB40	Golgi	Mediates intra-Golgi trafficking with Rab6 and Rab33 [83].
RAB41	Golgi	Required for Golgi organisation and ER-to-Golgi trafficking[124]
RAB43	Secretory packaging, <i>trans</i> -Golgi network [125]	RAB1A/B and RAB43 respectively, are important for viron assembly[2]. Retrograde transport from plasma membrane to the trans-Golgi Network [126].
* Involved with the cilium or periciliary environment[44, 127]. For a review of pathological significance see Kelly et al., (2012) [24]. For a review of Rab-GTPase proteins see Klöpper et al., (2012) [128], Schwartz et al., (2008)[3] and Jordan et al., (2005)[23].		

[1] Batoko H, Zheng H, Hawes, Moore I. (2000) Rab1 GTPase is required for transport between the endoplasmic reticulum and Golgi apparatus and for normal Golgi movement in plants. *Plant Cell*, **12**, 2201-2218.

[2] Zenner HL, Yoshimura S, Barr FA, Crump CM. (2011) Analysis of RabGTPase-activating proteins indicates that Rab1a/b and Rab43 are important for HSV-1 secondary envelopment. *Journal of Virology*, 21680502.

[3] Schwartz SL, Cao C, Pylypenko O, Rak,A, Wandinger-Ness A. (2007) Rab GTPases at a glance. *Journal of Cell Science*, **120**, 3905-3910.

[4] Yadav S, Linstedt AD. (2011) Golgi positioning. *Cold Spring Harbour Perspectives in Biology*, **3**(5), pii: a005322.

[5] Sannerud R, Marie M, Nizak C, Dale HA, Pernet-Gallay K, Perez F, Goud B, Saraste J. (2006) Rab1 defines a novel pathway connecting the pre-Golgi intermediate compartment with the cell periphery. *Molecular Biology of the Cell*, **17**, 1514-1526.

[6] Zhuang X, Adipietro KA, Datta S, Northup JK, Ray K. (2010) Rab1 small GTP-binding protein regulates cell surface trafficking of the human calcium-sensing receptor. *Endocrinology*, **151**, 5114-5123.

[7] Ishida M, Ohbayashi N, Maruta Y, Ebata Y, Fukuda M. (2012) Functional involvement of Rab1A in microtubule-dependent anterograde melanosome transport in melanocytes. *Journal of Cell Science*, **125**, 5177-5187.

[8] Moyer BD, Allan BB, Balch WE. (2001) Rab1 interaction with a GM130 effector complex regulates COPII vesicle cis-Golgi tethering. *Traffic*, **2**, 268-276.

- [9] Tisdale EJ, Balch WE. (1996) Rab2 is essential for the maturation of pre-Golgi intermediates. *Journal of Biological Chemistry*, **271**, 29372-29379.
- [10] Cheung AY, Chen CY, Glaven RH, de Graaf BH, Vidali L, Hepler PK, Wu HM. (2002) Rab2 GTPase regulates vesicle trafficking between the endoplasmic reticulum and the Golgi bodies and is important to pollen tube growth. *Plant Cell*, **14**, 945-962.
- [11] Alberts B, Bray D, Lewis J, Raff M, Roberts K, Walter P. (2002) *Molecular Biology of the Cell*, Garland Publishing New York.
- [12] Han JH, Lee C, Cheang Y, Kaang BK. (2005) Suppression of long-term facilitation by Rab3-effector protein interaction. *Brain Research, Molecular Brain Research*, **139**, 13-22.
- [13] Geppert M, Goda Y, Stevens CF, Südhof TC. (1997) The small GTP-binding protein Rab3A regulates a late step in synaptic vesicle fusion. *Nature*, **387**, 810-814.
- [14] Nonet ML, Staunton JE, Kilgard MP, Fergestad T, Hartweg E, Horvitz HR, Jorgensen EM, Meyer BJ. (2006) *Caenorhabditis elegans* Rab-3 mutant synapses exhibit impaired function and are partially depleted of vesicles. *Journal of Neuroscience*, **17**, 8061-8073.
- [15] Mahoney TR, Liu Q, Itoh T, Luo S, Hadwiger G, Vincent R, Wang ZW, Fukuda M, Nonet ML. (2006) Regulation of synaptic transmission by RAB-3 and RAB-27 in *Caenorhabditis elegans*. *Molecular Biology of the Cell*, **17**, 2617-2625.
- [16] Niwa S, Tanaka Y, Hirokawa N. (2008) KIF1B β - and KIF1A mediated axonal transport of presynaptic regulator Rab3 occurs in a GTP-dependent manner through DENN/MADD. *Nature Cell Biology*, **10**, 1269-1279.
- [17] Pavlos NJ, Xu J, Riedel D, Yeoh JS, Teitelbaum SL, Papadimitriou JM, Jahn R, Ross FP, Zheng MH. (2005) Rab3D regulates a novel vesicular trafficking pathway that is required for osteoclastic bone resorption. *Molecular Biology of the Cell*, **25**, 5253-5269.
- [18] Li H, Li HF, Felder RA, Periasamy A, Jose PA. (2008) Rab4 and Rab11 coordinately regulate the recycling of angiotensin II type I receptor as demonstrated by fluorescence resonance energy transfer microscopy. *Journal of Biomedical Optics*, **13**(3):031206.
- [19] Ward ES, Martinez C, Vaccaro C, Zhou J, Tang Q, Ober RJ. (2005) From sorting endosomes to exocytosis: association of Rab4 and Rab11 GTPases with the Fc receptor, FcRn, during recycling. *Molecular Biology of the Cell*, **16**, 2028-2038.
- [20] Bananis E, Nath S, Gordon K, Satir P, Stockert RJ, Murray JW, Wolkoff AW. (2004) Microtubule-dependent movement of late endocytic vesicles *in vitro*: requirements for dynein and kinesin. *Molecular Biology of the Cell*, **15**, 3688-3697.
- [21] Imamura T, Huang J, Usui I, Satoh H, Bever J, Olefsky JM. (2003) Insulin-induced GLUT4 translocation involves protein kinase C λ -mediated functional coupling between Rab4 and the motor protein kinesin. *Molecular Biology of the Cell*, **23**, 4892-4900.
- [22] Horgan CP, McCaffrey MW. (2011) Rab GTPases and microtubule motors. *Biochemical Society Transactions*, **39**, 1202-1206.
- [23] Jordens I, Marsman M, Kuijl C, Neefjes J. (2005) Rab proteins, connecting transport and vesicle fusion. *Traffic*, **6**, 1070-1077.

- [24] Kelly EE, Horgan CP, Goud B, McCaffrey MW. (2012) The Rab family of proteins: 25 years on. *Biochemical Society Transactions*, **40**, 1337-1347.
- [25] McCaffrey MW, Bielli A, Cantalupo G, Mora S, Roberti V, Santillo M, Drummond F, Bucci C. (2001) Rab4 affects both recycling and degradative endosomal trafficking. *FEBS Letters*, **495**, 21-30.
- [26] Croizet-Berger K, Daumerie C, Couvreur M, Courtoy PJ, van den Hove MF. (2002) The endocytic catalysts, Rab5a and Rab7, are tandem regulators of thyroid hormone production. *Proceedings of the National Academy of Sciences, USA*, **99**, 8277-8282.
- [27] Zeigerer A, Gilleron J, Bogorad RL, Marsico G, Nonaka H, Seifert S, Epstein-Barash H, Kuchimanchi S, Peng CG, Ruda VM, del Conte-Zerial P, Hengstler JG, Kalaidzidis Y, Koteliensky V, Zerial M. (2012) Rab5 is necessary for the biogenesis of the endolysosomal system *in vivo*. *Nature*, **485**, 465-470.
- [28] Nielsen E, Severin F, Backer JM, Hyman AA, Zerial M. (1999) Rab5 regulates motility of early endosomes on microtubules. *Nature Cell Biology*, **1**, 376-382.
- [29] Ding Q, Wang Z, Chen Y. (2009) Endocytosis of adiponectin receptor 1 through a clathrin- and Rab5-dependent pathway. *Cell Research*, **19**, 317-327.
- [30] Ulrich F, Krieg M, Schötz EM, Link V, Castanon I, Schnabel V, Taubenberger A, Mueller D, Puech PH, Heisenberg CP. (2005) Wnt11 functions in gastrulation by controlling cell cohesion through Rab5c and E-cadherin. *Developmental Cell*, **9**, 555-564.
- [31] Goud B, Zahraoui A, Tavitian A, Saraste J. (1990) Small GTP-binding protein associated with Golgi cisternae. *Nature*, **345**, 553-556.
- [32] Hayes GL, Brown FC, Haas AK, Nottingham RM, Barr FA, Pfeffer SR. (2009) Multiple Rab GTPase binding sites in GCC185 suggest a model for vesicle tethering at the trans-Golgi. *Molecular Biology of the Cell*, **20**, 209-217.
- [33] Short B, Preisinger C, Schaletzky J, Kopajtich R, Barr FA. (2002) The Rab6 GTPase regulates recruitment of the dynactin complex to Golgi membranes. *Current Biology*, **12**, 1792-1795.
- [34] Echard A, Jollivet F, Martinez O, Lacapère JJ, Rousselet A, Janoueix-Lerosey I, Goud B. (1998) Interaction of a Golgi-associated kinesin-like protein with Rab6. *Science*, **279**, 580-585.
- [35] Fontijn RD, Goud B, Echard A, Jollivet F, van Marle J, Pannekoek H, Horrevoets AJ. (2001) The human kinesin-like protein RB6K is under tight cell cycle control and is essential for cytokinesis. *Molecular Biology of the Cell*, **21**, 2944-2955.
- [36] Wanschers B, van de Vorstenbosch R, Wijers M, Wieringa B, King SM, Fransen J. (2008) Rab6 family proteins interact with the dynein light chain protein DYNLRB1. *Cell Motility and Cytoskeleton*, **65**, 183-196.
- [37] Zerial M, McBride H. (2001) Rab proteins as membrane organizers. *Nature Reviews Molecular and Cellular Biology*, **2**, 107-117.
- [38] Storrie B, Micaroni M, Morgan GP, Jones N, Kamykowski JA, Wilkins N, Pan TH, Marsh BJ. (2012) Electron tomography reveals Rab6 is essential to the trafficking of trans-Golgi clathrin and COPI-coated vesicles and the maintenance of Golgi cisternal number. *Traffic*, **13**, 727-744.
- [39] Grigoriev I, Yu KL, Martinez-Sanchez E, Serra-Marques A, Smal I, Meijering E, Demmers J, Peränen J, Pasterkamp RJ, van der Sluijs P, Hoogenraad CC, Akhmanova A. (2011) Rab6, Rab8, and

MICAL3 cooperate in controlling docking and fusion of exocytotic carriers. *Current Biology*, **21**, 967-974.

[40] Jordens I, Fernandez-Borja M, Marsman M, Dusseljee S, Janssen L, Calafat J, Janssen H, Wubbolts R, Neefjes J. (2001) The Rab7 effector protein RILP controls lysosomal transport by inducing the recruitment of dynein-dynactin motors. *Current Biology*, **11**, 1680-1685.

[41] Cantalupo G, Alifano P, Roberti V, Bruni CB, Bucci C. (2001) Rab-interacting lysosomal protein (RILP): the Rab7 effector required for transport to lysosomes. *EMBO Journal*, **20**, 683-693.

[42] Bucci C, Thomsen P, Nicoziani P, McCarthy J, van Deurs B. (2000) Rab7: a key to lysosome biogenesis. *Molecular Biology of the Cell*, **11**, 467-480.

[43] Hsiao Y, Tuz K, Ferland RJ. (2012) Trafficking in and to the primary cilium. *Cilia*, **1**, 4.

[44] Yoshimura S, Egerer J, Fuchs E, Haas AK, Barr FA. (2007) Functional dissection of RabGTPases involved in primary cilium formation. *Journal of Cell Biology*, **178**, 363-369.

[45] Caplan S, Hartnell LM, Aguilar RC, Naslavsky N, Bonifacino JS. (2001) Human Vam6p promotes lysosome clustering and fusion *in vivo*. *Journal of Cell Biology*, **154**, 109-122.

[46] Rak A, Pylypenko O, Niculae A, Goody RS, Alexandrov K. (2003) Crystallization and preliminary X-ray diffraction analysis of monoprenylated Rab7 GTPase in complex with Rab escort protein 1. *Journal of Structural Biology*, **141**, 93-95.

[47] Alexandrov K, Simon I, Iakovenko A, Holz B, Goody RS, Scheidig AJ. (1998) Moderate discrimination of REP-1 between Rab7 x GDP and Rab7 x GTP arises from a difference of an order of magnitude in dissociation rates. *FEBS Letters*, **425**, 460-464.

[48] Kim J, Krishnaswami SR, Gleeson JG. (2008) CEP290 interacts with the centriolar satellite component PCM-1 and is required for Rab8 localization to the primary cilium. *Human Molecular Genetics*, **17**, 3796-3805.

[49] Yoshimura S, Haas AK, Barr FA. (2008) Analysis of RabGTPase and GTPase-activating protein function at primary cilia. *Methods in Enzymology*, **439**, 353-364.

[50] Hattula K, Furuholm J, Tikkanen J, Tanhuanpää K, Laakkonen P, Peränen J. (2006) Characterization of the Rab8-specific membrane traffic route linked to protrusion formation. *Journal of Cell Science*, **119**, 4866-4877.

[51] Knödler A, Feng S, Zhang J, Zhang X, Das A, Peränen J, Guo W. (2010) Coordination of Rab8 and Rab11 in primary ciliogenesis. *Proceedings of the National Academy of Sciences, USA*, **107**, 6346-6351.

[52] Ganley IG, Carroll K, Bittova L, Pfeffer S. (2004) Rab9 GTPase regulates late endosome size and requires effector interaction for its stability. *Molecular Biology of the Cell*, **15**, 5420-5430.

[53] Rodman JS, Wandinger-Ness A. (2000) Rab GTPases coordinate endocytosis. *Journal of Cell Science*, **113**, 183-192.

[54] Murray JL, Mavrikis M, McDonald NJ, Yilla M, Sheng J, Bellini WJ, Zhao L, Le Doux JM, Shaw MW, Luo CC, Lippincott-Schwartz J, Sanchez A, Rubin DH, Hodge TW. (2005) Rab9 GTPase is required for replication of human immunodeficiency virus type 1, filoviruses, and measles virus. *Journal of Virology*, **79**, 11742-11751.

- [55] Babbey CM, Bacallao RL, Dunn KW. (2010) Rab10 associates with primary cilia and the exocyst complex in renal epithelial cells. *American Journal of Physiology*, **299**, F495-F506.
- [56] Wang D, Lou J, Ouyang C, Chen W, Liu Y, Liu X, Cao X, Wang J, Lu L. (2010) Ras-related protein Rab10 facilitates TLR4 signaling by promoting replenishment of TLR4 onto the plasma membrane. *Proceedings of the National Academy of Sciences, USA*, **107**, 13806-13811.
- [57] Glodowski DR, Chen CC, Schaefer H, Grant BD, Rongo C. (2007) RAB-10 regulates glutamate receptor recycling in a cholesterol-dependent endocytosis pathway. *Molecular Biology of the Cell*, **18**, 4387-4396.
- [58] English AR, Voeltz GK. (2013) Rab10 GTPase regulates ER dynamics and morphology. *Nature Cell Biology*, **15**, 169-178.
- [59] Ullrich O, Reinsch S, Urbé S, Zerial M, Parton RG. (1996) Rab11 regulates recycling through the pericentriolar recycling endosome. *Journal of Cell Biology*, **135**, 913-924.
- [60] Jeffries TR, Morgan GW, Field MC. (2001) A developmentally regulated Rab11 homologue in *Trypanosoma brucei* is involved in recycling processes. *Journal of Cell Science*, **114**, 2617-2626.
- [61] Khandelwal P, Prakasam HS, Clayton DR, Ruiz WG, Gallo LI, van Roekel D, Lukianov S, Peränen J, Goldenring JR, Apodaca G. (2013) A Rab11a-Rab8a-Myo5B network promotes stretch-regulated exocytosis in bladder umbrella cells. *Molecular Biology of the Cell*, **24**, 1007-1019.
- [62] Wilcke M, Johannes L, Galli T, Mayau V, Goud B, Salamero J. (2000) Rab11 regulates the compartmentalization of early endosomes required for efficient transport from early endosomes to the trans-golgi network. *Journal of Cell Biology*, **151**, 1207-1220.
- [63] Horgan CP, Hanscom SR, Jolly RS, Futter CE, McCaffrey MW. (2010) Rab11-FIP3 links the Rab11 GTPase and cytoplasmic dynein to mediate transport to the endosomal-recycling compartment. *Journal of Cell Science*, **123**, 181-191.
- [64] Iida H, Wang L, Nishii K, Ookuma A, Shibata Y. (1996) Identification of rab12 as a secretory granule-associated small GTP-binding protein in atrial myocytes. *Circulation Research*, **78**, 343-347.
- [65] Matsui T, Fukuda M. (2013) Rab12 regulates mTORC1 activity and autophagy through controlling the degradation of amino-acid transporter PAT4. *EMBO Report*, **14**, 450-457.
- [66] Zahraoui A, Joberty G, Arpin M, Fontaine JJ, Hellio R, Tavitian A, Louvard D. (1994) A small rabGTPase is distributed in cytoplasmic vesicles in non polarized cells but colocalizes with the tight junction marker ZO-1 in polarized epithelial cells. *Journal of Cell Biology*, **124**, 101-115.
- [67] Morimoto S, Nishimura N, Terai T, Manabe S, Yamamoto Y, Shinahara W, Miyake H, Tashiro S, Shimada M, Sasaki T. (2005) Rab13 mediates the continuous endocytic recycling of occludin to the cell surface. *Journal of Biological Chemistry*, **280**, 2220-2228.
- [68] Zahraoui A. (2005) Properties of Rab13 interaction with protein kinase A. *Methods in Enzymology*, **403**, 723-732.
- [69] Nokes RL, Fields IC, Collins RN, Fölsch H. (2008) Rab13 regulates membrane trafficking between TGN and recycling endosomes in polarized epithelial cells. *Journal of Cell Biology*, **182**, 845-853.
- [70] Hutagalung AH, Novick PJ. (2011) Role of Rab GTPases in membrane traffic and cell physiology. *Physiological Reviews*, **91**, 119-149.

- [71] Junutula JR, De Mazière AM, Peden AA, Ervin KE, Advani RJ, van Dijk SM, Klumperman J, Scheller RH. (2004) Rab14 is involved in membrane trafficking between the Golgi complex and endosomes. *Molecular Biology of the Cell*, **15**, 2218-2229.
- [72] Strick DJ, Elferink LA. (2005) Rab15 effector protein: a novel protein for receptor recycling from the endocytic recycling compartment. *Molecular Biology of the Cell*, **16**, 5699-5709.
- [73] Hunziker W, Peters PJ. (1998) Rab17 localizes to recycling endosomes and regulates receptor-mediated transcytosis in epithelial cells. *Journal of Biological Chemistry*, **273**, 15734-15741.
- [74] Schafer U, Seibold S, Schneider A, Neugebauer E. (2000) Isolation and characterisation of the human rab18 gene after stimulation of endothelial cells with histamine. *FEBS Letters*, **466**, 148-154.
- [75] Dejgaard SY, Murshid A, Erman A, Kizilay O, Verbich D, Lodge R, Dejgaard K, Ly-Hartig TBN, Pepperkok R, Simpson JC, Presley JF. (2008) Rab18 and Rab43 have key roles in ER-Golgi trafficking. *Journal of Cell Science*, **121**, 2768-2781.
- [76] Martin S, Driessen K, Nixon SJ, Zerial M, Parton RG. (2005) Regulated localization of Rab18 to lipid droplets: effects of lipolytic stimulation and inhibition of lipid droplet catabolism. *Journal of Biological Chemistry*, **280**, 42325-42335.
- [77] Ozeki S, Cheng J, Tauchi-Sato K, Hatano N, Taniguchi H, Fujimoto T. (2005) Rab18 localizes to lipid droplets and induces their close apposition to the endoplasmic reticulum-derived membrane. *Journal of Cell Science*, **118**, 2601-2611.
- [78] Burré J, Beckhaus T, Corvey C, Karas M, Zimmermann H, Volkandt W. (2006) Synaptic vesicle proteins under conditions of rest and activation: analysis by 2-D difference gel electrophoresis. *Electrophoresis*, **27**, 3488-3496.
- [79] Takamori S, Holt M, Stenius K, Lemke EA, Grønborg M, Riedel D, Urlaub H, Schenck S, Brügger B, Ringler P, Müller SA, Rammner B, Gräter F, Hub JS, De Groot BL, Mieskes G, Moriyama Y, Klingauf J, Grubmüller H, Heuser J, Wieland F, Jahn R. (2006) Molecular anatomy of a trafficking organelle. *Cell*, **127**, 831-846.
- [80] Vazquez-Martinez R, Cruz-Garcia D, Duran-Prado M, Peinado JR, Castaño JP, Malagon MM. (2007) Rab18 inhibits secretory activity in neuroendocrine cells by interacting with secretory granules. *Traffic*, **8**, 867-882.
- [81] Bem D, Yoshimura S, Nunes-Bastos R, Bond FC, Kurian MA, Rahman F, Handley MT, Hadzhiev Y, Masood I, Straatman-Iwanowska AA, Cullinane AR, McNeill A, Pasha SS, Kirby GA, Foster K, Ahmed Z, Morton JE, Williams D, Graham JM, Dobyns WB, Burglen L, Ainsworth JR, Gissen P, Müller F, Maher ER, Barr FA, Aligianis IA. (2011) Loss-of-function mutations in RAB18 cause Warburg micro syndrome. *American Journal of Human Genetics*, **88**, 499-507.
- [82] Egami Y, Araki N. (2012) Rab20 regulates phagosome maturation in RAW264 macrophages during Fc gamma receptor-mediated phagocytosis. *PLoS One*, **7**(4):e35663.
- [83] Stenmark H. (2009) Rab GTPases as coordinators of vesicle traffic. *Nature Reviews Molecular and Cellular Biology*, **10**, 513-525.
- [84] Pellinen T, Arjonen A, Vuoriluoto K, Kallio K, Fransén JA, Ivaska J. (2006) Small GTPase Rab21 regulates cell adhesion and controls endosomal traffic of beta1-integrins. *Journal of Cell Biology*, **173**, 767-780.

- [85] Mesa R, Salomón C, Roggero M, Stahl PD, Mayorga LS. (2001) Rab22a affects the morphology and function of the endocytic pathway. *Journal of Cell Science*, **114**, 4041-4049.
- [86] Ng EL, Wang Y, Tang BL. (2007) Rab22B's role in trans-Golgi network membrane dynamics. *Biochemical and Biophysical Research Communications*, **361**, 751-757.
- [87] Zhang, QH, Ye M, Wu XY, Ren SX, Zhao M, Zhao CJ, Fu G, Shen Y, Fan HY, Lu G, Zhong M, Xu XR, Han ZG, Zhang JW, Tao J, Huang QH, Zhou J, Hu GX, Gu J, Chen SJ, Chen Z. (2000) Cloning and functional analysis of cDNAs with open reading frames for 300 previously undefined genes expressed in CD34⁺ hematopoietic stem/progenitor cells. *Genome Research*, **10**, 1546-1560.
- [88] Eggenschwiler JT, Espinoza E, Anderson KV. (2001) Rab23 is an essential negative regulator of the mouse Sonic hedgehog signalling pathway. *Nature*, **412**, 194-198.
- [89] Evans TM, Ferguson C, Wainwright BJ, Parton RG, Wicking C. (2004) Rab23, a negative regulator of hedgehog signaling, localizes to the plasma membrane and the endocytic pathway. *Traffic*, **4**, 869-884
- [90] Günther T, Struwe M, Aguzzi A, Schughart K. (1994) Open brain, a new mouse mutant with severe neural tube defects, shows altered gene expression patterns in the developing spinal cord. *Development*, **120**, 3119-3130.
- [91] Boehlke C, Bashkurov M, Buescher A, Krick T, John AK, Nitschke R, Walz G, Kuehn EW. (2010) Differential role of Rab proteins in ciliary trafficking: Rab23 regulates smoothed levels. *Journal of Cell Science*, **123**, 1460-1467.
- [92] Pataki C, Matussek T, Kurucz E, Andó I, Jenny A, Mihály J. (2010) Drosophila Rab23 is involved in the regulation of the number and planar polarization of the adult cuticular hairs. *Genetics*, **184**, 1051-1065.
- [93] Martinez O, Goud B. (1998) Rab proteins. *Biochimica Biophysica Acta*, **1404**, 101-112.
- [94] Erdman RA, Shellenberger KE, Overmeyer JH, Maltese WA. (2000) Rab24 is an atypical member of the Rab GTPase family. Deficient GTPase activity, GDP dissociation inhibitor interaction, and prenylation of Rab24 expressed in cultured cells. *Journal of Biological Chemistry*, **275**, 3848-3856.
- [95] Militello RD, Munafó DB, Berón W, López LA, Monier S, Goud B, Colombo MI. (2013) Rab24 is required for normal cell division. *Traffic*, **14**, 502-518.
- [96] Hales CM, Griner R, Hobdy-Henderson KC, Dorn MC, Hardy D, Kumar R, Navarre J, Chan EK, Lapierre LA, Goldenring JR. (2001) Identification and characterization of a family of Rab11-interacting proteins. *Journal of Biological Chemistry*, **276**, 39067-39075.
- [97] Amornphimoltham P, Rechache K, Thompson J, Masedunskas A, Leelahavanichkul K, Patel V, Molinolo A, Gutkind JS, Weigert R. (2013) Rab25 regulates invasion and metastasis in head and neck cancer. *Clinical Cancer Research*, **19**, 1375-1388.
- [98] Cao C, Lu C, Xu J, Zhang J, Zhang J, Li M. (2013) Expression of Rab25 correlates with the invasion and metastasis of gastric cancer. *Chinese Journal of Cancer Research*, **25**, 192-199.
- [99] Caswell PT, Spence HJ, Parsons M, White DP, Clark K, Cheng KW, Mills GB, Humphries MJ, Messent AJ, Anderson KI, McCaffrey MW, Ozanne BW, Norman JC. (2007) Rab25 associates with $\alpha 5\beta 1$ integrin to promote invasive migration in 3D microenvironments. *Developmental Cell*, **13**, 496-510.

- [100] Li C, Fan Y, Lan TH, Lambert NA, Wu G. (2012) Rab26 modulates the cell surface transport of α_2 -adrenergic receptors from the Golgi. *Journal of Biological Chemistry*, **287**, 42784-42794.
- [101] Imai A, Yoshie S, Nashida T, Shimomura H, Fukuda M. (2006) Functional involvement of Noc2, a Rab27 effector, in rat parotid acinar cells. *Archives of Biochemistry and Biophysics*, **455**, 127-135.
- [102] Fukuda M. (2005) Versatile role of Rab27 in membrane trafficking: focus on the Rab27 effector families. *Journal of Biochemistry*, **137**, 9-16.
- [103] Tolmachova T, Anders R, Abrink M, Bugeon L, Dallman MJ, Futter CE, Ramalho JS, Tonagel F, Tanimoto N, Seeliger MW, Huxley C, Seabra MC. (2006) Independent degeneration of photoreceptors and retinal pigment epithelium in conditional knockout mouse models of choroideremia. *Journal of Clinical Investigation*, **116**, 386-394.
- [104] Ostrowski M, Carmo NB, Krumeich S, Fanget I, Raposo G, Savina A, Moita CF, Schauer K, Hume AN, Freitas RP, Goud B, Benaroch P, Hacohen N, Fukuda M, Desnos C, Seabra MC, Darchen F, Amigorena S, Moita LF, Thery C. (2010) Rab27a and Rab27b control different steps of the exosome secretion pathway. *Nature Cell Biology*, **12**, 19-30.
- [105] Hammer JA, Wu XS. (2002) Rabs grab motors: defining the connections between Rab GTPases and motor proteins. *Current Opinion in Cell Biology*, **14**, 69-75.
- [106] Roosing S, Rohrschneider K, Beryozkin A, Sharon D, Weisschuh N, Staller J, Kohl S, Zelinger L, Peters TA, Neveling K, Strom TM; European Retinal Disease Consortium, van den Born LI, Hoyng CB, Klaver CC, Roepman R, Wissinger B, Banin E, Cremers FP, den Hollander AI. (2013) Mutations in RAB28, encoding a farnesylated small GTPase, are associated with autosomal-recessive cone-rod dystrophy. *American Journal Human Genetics*, **93**, 110-117.
- [107] Kelly EE, Giordano F, Horgan CP, Jollivet F, Raposo G, McCaffrey MW. (2012) Rab30 is required for the morphological integrity of the Golgi apparatus. *Biology of the Cell*, **104**, 84-101.
- [108] Grismayer B, Sölch S, Seubert B, Kirchner T, Schäfer S, Baretton G, Schmitt M, Luther T, Krüger A, Kotzsch M, Magdolen V. (2010) Rab31 expression levels modulate tumor-relevant characteristics of breast cancer cells. *Molecular Cancer*, **11**, 62.
- [109] Bui M, Gilady SY, Fitzsimmons RE, Benson MD, Lynes EM, Gesson K, Alto NM, Strack S, Scott JD, Simmen T. (2010) Rab32 modulates apoptosis onset and mitochondria-associated membrane (MAM) properties. *Journal of Biological Chemistry*, **285**, 31590-315602.
- [110] Bultema JJ, Di Pietro SM. (2013) Cell type-specific Rab32 and Rab38 cooperate with the ubiquitous lysosome biogenesis machinery to synthesize specialized lysosome-related organelles. *Small GTPases*, **4**, 16-21.
- [111] Wasmeier C, Romao M, Plowright L, Bennett DC, Raposo G, Seabra MC. (2006) Rab38 and Rab32 control post-Golgi trafficking of melanogenic enzymes. *Journal of Cell Biology*, **175**, 271-281.
- [112] Zheng JY, Koda T, Fujiwara T, Kishi M, Ikehara Y, Kakinuma M. (1998) A novel RabGTPase, Rab33B, is ubiquitously expressed and localized to the medial Golgi cisternae. *Journal of Cell Science*, **111**, 1061-1069.
- [113] Wang T, Hong W. (2002) Interorganellar regulation of lysosome positioning by the Golgi apparatus through Rab34 interaction with Rab-interacting lysosomal protein. *Molecular Biology of the Cell*, **13**, 4317-4332.

- [114] Goldenberg NM, Silverman M. (2009) Rab34 and its effector munc13-2 constitute a new pathway modulating protein secretion in the cellular response to hyperglycemia. *American Journal of Physiology*, **297**, C1053-C1058.
- [115] Grant BD, Donaldson JG. (2009) Pathways and mechanisms of endocytic recycling. *Nature Reviews Molecular and Cellular Biology*, **10**, 597-608.
- [116] Chen L, Hu J, Yun Y, Wang T. (2010) Rab36 regulates the spatial distribution of late endosomes and lysosomes through a similar mechanism to Rab34. *Molecular Membrane Biology*, **27**, 24-31.
- [117] Ljubici, S, Bezzi P, Brajkovic S, Nesca V, Guay C, Ohbayashi N, Fukuda M, Abderrhamani A, Regazzi R. (2013) The GTPase Rab37 participates in the control of insulin exocytosis. *PLoS One*, **8**(6):e68255.
- [118] Masuda ES, Luo Y, Young C, Shen M, Rossi AB, Huang BC, Yu S, Bennett MK, Payan DG, Scheller RH. (2000) Rab37 is a novel mast cell specific GTPase localized to secretory granules. *FEBS Letters*, **470**, 61-64.
- [119] Rangel-Filho A, Lazar J, Moreno C, Geurts A, Jacob HJ. (2013) Rab38 modulates proteinuria in model of hypertension-associated renal disease. *Journal of the American Society of Nephrology*, **24**, 283-292.
- [120] Wang H, Jiang C. (2013) RAB38 confers a poor prognosis, associated with malignant progression and subtype preference in glioma. *Oncology Report*, **30**, 2350-2356.
- [121] Becker CE, Creagh EM, O'Neill LA. (2009) Rab39a binds caspase-1 and is required for caspase-1-dependent interleukin-1beta secretion. *Journal of Biological Chemistry*, **284**, 34531-34537.
- [122] Chen T, Han Y, Yang M, Zhang W, Li N, Wan T, Guo J, Cao X. (2003) Rab39, a novel Golgi-associated Rab GTPase from human dendritic cells involved in cellular endocytosis. *Biochemical and Biophysical Research Communications*, **303**, 1114-1120.
- [123] Giannandrea M, Bianchi V, Mignogna ML, Sirri A, Carrabino S, D'Elia E, Vecellio M, Russo S, Cogliati F, Larizza L, Ropers HH, Tzschach A, Kalscheuer V, Oehl-Jaschkowitz B, Skinner C, Schwartz CE, Gez J, van Esch H, Raynaud M, Chelly J, de Brouwer AP, Toniolo D, D'Adamo P. (2010) Mutations in the small GTPase gene RAB39B are responsible for X-linked mental retardation associated with autism, epilepsy, and macrocephaly. *American Journal of Human Genetics*, **86**, 185-195.
- [124] Liu S, Hunt L, Storie B. (2013) Rab41 is a novel regulator of Golgi apparatus organization that is needed for ER-to-Golgi trafficking and cell growth. *PLoS One*, **8**(8):e71886.
- [125] Alexander K, Haas AK, Yoshimura S, Stephens DJ, Preisinger C, Fuchs E, Francis A, Barr FA. (2007) Analysis of GTPase-activating proteins: Rab1 and Rab43 are key Rabs required to maintain a functional Golgi complex in human cells. *Journal of Cell Science*, **120**, 2997-3010.
- [126] Fuchs E, Haas AK, Spooner RA, Yoshimura S, Lord JM, Barr FA. (2007) Specific Rab GTPase-activating proteins define the Shiga toxin and epidermal growth factor uptake pathways. *Journal of Cell Biology*, **177**, 1133-1143.
- [127] Hsiao Y, Tuz K, Ferland RJ. (2012) Trafficking in and to the primary cilium. *Cilia*, **1**, 4.

[128] Klöpper TH, Kienle N, Fasshauer D, Munro S. (2012) Untangling the evolution of Rab G proteins: implications of a comprehensive genomic analysis. *BMC Biology*, **10**, 71.

Appendix III: Kinesin and Dynein Microtubule Motors

3.1 Kinesin Motor Proteins

Kinesin	Kinesin-like protein KIF Interacts with/function	Importance/Known Disease(s)
KIF1A	Axonal vesicle transporter[1], synaptic vesicle transport and binding[2]. Anterograde motor, one of the faster, with a velocity of 1.2 microns/second[1]. Interacts with synaptic vesicles [3], Rab3A [1] and Liprin-α (integrin matrix interactions/focal adhesions)[4, 5].	Hereditary spastic paraparesis [6], neuropathies and neuroblastoma [7]. KIF1A and KIF1B mediated transport of the Rab3A [8] regulator DENN/MADD [9].
KIF1B	Interacts with glucose transporter binding protein[10], and is involved in synaptic vesicle precursor transport[12]. KIF1Bα involved with mitochondria localisation[13] scaffolding proteins S-Scam [14] and PSD-95/97 [12].	Charcot–Marie–Tooth disease (type CMT2A)[12].
KIF1C	Involved in the transport of $\alpha 5\beta 1$ integrins and in cell migration[15].	Possible effector of Rab6 [16], Rab6A and Rab6B [9].
KIF2A	Kinesin-13 members are involved in interphase microtubule depolymerisation[19]. Role in mitosis[11], a vaccinia viral target [18], KIF2A, B and C proteins have distinct roles in mitosis [19].	KIF2 role in Schizophrenia [20].
KIF2B	Required for successful chromosome segregation [21].	KIF2A-C assist in destabilising microtubules[12, 19].
KIF2C	Anaphase centromere association, microtubule depolymerisation [12, 19, 22, 23]. A critical regulator of microtubule activity[22].	Found in the centrosome , involved in Wnt signalling [22].
KIF3A*	KIF3A and KIF3B are part of the IFT Complex . KIF3A and KIF3C form a novel neuronal heteromeric kinesin that associates with membrane vesicles [24, 25] and retinal transport [26]. Interacts with dynactin sununit p150^{Glued} organising sub-distal appendages [29].	Form part of the IFT complex for ciliary transport . Transports Fodrin [28] and interacts with KDEL receptor in ER [29]. KIF3 interacts with Rab7 [30, 31].
KIF3B*	Interacts with the RAB4A [32] cascade, also intereacts with polycystin-2 and fibrocystin [33] and the SMC3 subunit of the cohesin complex. Intracellular movement of organelles and vesicles. During mitosis/meiosis moves chromosomes[25, 34, 35]; vertebrate retinal transport[28]. Mediates interaction and functionality between polycystin and fibrocystin [33].	Lack of KIF3B results in randomised left-right asymmetry due to loss of nodal cilia generating leftward flow[36]. KIF3B is involved with APC tumour suppressor gene[37] and is also involved with β-catenin [12]. Interacts with Rab4 [8, 38] and Rab11A [8].
KIF3C*	Association with RNA granules [39], membrane vesicles [24].	Fragile X and mental retardation [39].
KIF4A	Known to interact with BRAC2 [41]; associated with chromosomes during mitosis[40, 42]; involved in mid-zone formation [43]. Localises to the nucleus during interphase where it associates with the DNA damage response [41].	KIF4 is involved in neuronal survival[44].
KIF4B	Organises central spindle mid-zone [43] and mid-body and is necessary for successful cytokinesis [42-48].	Involved in suppression of PARP-1 [49].
KIF5A	Known to interact with the kinesin light chain and glutamate receptor protein GRIP1 [50]. Involved in cargo transport through GRIP1 binding GLuR2 of the AMPA receptor[50]. Interacts with Rab6A [8], Rab27A and Rab27B [8]. KIF5 functions in dendrites for axon vesicle transport[12].	Spastic paraplegia [51] and retroviral budding[52]. KIF5 and DISC2 form a cargo complex with LIS2 , NUDEL and 14-3-3ϵ [53]. Interacts with p115 [54]. Involved in vaccinia virus transport to apical membrane [55].
KIF5B	KIF5B is known to interact with SNARE proteins SNAP-23 and SNAP-25 [56], YWHAH [57] and the kinesin light chain [56, 58]. Associated with transport of mitochondria [59] and the ribosome receptor [60]. KIF5 and the kinesin light chain transports Rab4 for endosomal function[62], also tubulin , APP and ApoER2 and JIP1 [12]. KIF5 shows preferential binding to GTP-tubulin rich microtubules[63]. For a review see Hirokawa et al., (2008)[12].	KIF5 Family [62]: Involved in AMPA receptor transport, mRNA transport (KIF5A, B and C)[64], SNAP25 , syntaxin , GLuR2 , GRIP1 , Kinectin and mitochondria [65]. Involved in perinuclear autophagosome localisation in cancer cells[66]. Possible effector of Rab6 [16].
KIF5C	Found in neurons[67], specifically motor neurons[68, 69], associated with (GABAA) receptor interacting factor-1 as an anterograde adaptor[70]. KIF5B and KIF5C bind to Ran binding protein two (RBP-2)[71].	Carries M6PR and Clathrin AP1 [12].

KIF7*	Cilia associated. Involved with and mediates Sonic Hedgehog signalling[72, 73]. Interacts with Gli2 and Gli3 and is responsible for Gli3 localisation[74, 75].	Cancer association[72] and involvement with Hedgehog signalling[72, 75].
KIF9	Involved in maintaining cytoskeletal cell shape through interacting with Ras-like GTPase Gem [76].	
KIF10	Attaches to kinetochore [77], probably a kinetochore motor.	
KIF11	Required for RanBP1 dependent centrosome fissioning , microtubule integrity[78]. Inhibition blocks cell cycle and can induce apoptosis [79].	
KIF12	Expressed in the foetal liver, adult brain and in pancreatic islets[80].	Kidney , uterine, pancreatic tumour expression[80].
KIF13A	Associated with the Golgi[81], transports mannose-6-phosphate receptor from TGN to plasma membrane through AP-1 complex[81].	Associated with predisposition to Schizophrenia [83] and RB oncogenesis [84].
KIF13B	Involved with ARF6 modulation, where KIF13B binding suppresses activity[85].	Carries PIP3 and Centaurin-1α [12].
KIF14	Cytokinesis and mid-body formation[86], associated with forming spindle poles [87]; silencing disrupts cytokinesis and cell cycle [86].	Poor prognosis marker, over-expressed in lung tumours[87], and retinoblastoma [88].
KIF15	Mitotic processes and neuronal migration[88]. KIF15 cooperates with Eg5 for bipolar spindle assembly [89].	
KIF16B	Unique PX domain involved in endosomal anchoring and membrane trafficking [91]. Interacts with PIP3 , EGF (and receptor modulating recycling) and Rab5 [92].	Binds PIP3 containing vesicles[12]. Interacts with Rab5 [40] and Rab14 [8].
KIF17*	Dendritic vesicle transport for receptors (NMDA [93] and glutamate [94]), KIF17B and RNA-binding protein TB-RBP transport cAMP responsive element[95], regulation of N-methyl-D-aspartate (NMDA) receptor subunit NR2B transport[96, 97]. Involved in processes in the distal axoneme [98], has a role in learning [99] and is vital for outer photoreceptor development [98].	KIF17 may have a role in Catalepsy [100], opiate dependency [101], and Huntington's disease [102]. Targets cyclic nucleotide-gated (CNG) channel CNGB1B to the primary cilium in olfaction sensory neurons[103].
KIF18A	Reported interaction with oestrogen and endoplasmic reticulum [104-105], involved in kinetochores [106].	
KIF19A*	Regulates ciliary length through depolymerisation at microtubule tips in the cilium[107].	
KIF20A	Interacts with RAB6A and the Golgi [16, 108, 112]. Required for cytokinesis and nuclear control [109-111]. RAB6-KIFL reported to have tissue specific expression[112]. Also known as Rabkinesin-6 , Rab6-kinesin and RAB6KIFL [62].	Involved in pancreatic cancer [113]. Possible effector of Rab6 [16], Rab6A and Rab6B [8].
KIF21A	Neuronal association[114].	Congenital fibrosis [114].
KIF21B	Neuronal dendritic association[114].	Little known.
KIF22	Known to interact with SIAH1 (ubiquitin-protein ligase E3) as part of the β-catenin degradation pathway involving p53-mediated apoptosis[116, 117]. Interacts with α-tubulin and degrades kinesin Kid [116].	Parkinson's disease association.
KIF23	Involved in cytokinesis and mid-body bridging of anti-parallel micro-tubules, exists in two isoforms known to interact with BIRC6 [118] and ARF3 [119, 120].	
KIF24*	Binds to microtubules , interacts with centrosomal CEP110 and CEP97 centrosomal proteins which regulate centriole length and ciliogenesis. KIF24 localises to the basal body (mother centriole) where loss of KIF24 produces aberrant cilia , and loss of CP110 from the mother centriole. KIF24 binds to, depolymerises and remodels centriolar microtubules without significantly altering cytoplasmic microtubules[121].	Localises preferentially to the basal body/mother centriole . Possible risk factor for Fronto-temporal Lobe Degeneration [122].
KIF27	Expressed in embryogenesis. Sonic Hedgehog involvement[73, 118].	Expressed in melanoma .
KIFC1	Involved in mitotic spindle [120]; associated with the nuclear membrane and acrosome in spermatids, as well as nucleoporin NUP62 and RAN-GTPase [123]. Transports dsDNA in the cytoplasm[124].	Found in the centrosome. Possible effector of Rab6 [16].
KIFC2[132]	Cell division , localises with some axon transport vesicles and	Multi-vesicular bodies[127], regulated

	organelles [125], accumulates at the proximal and distal ends of the ligature[126, 127].	by RAB4 [31].
KIFC3[131]	Minus-end directed, Golgi association in positioning and integration[128, 129], co-localisation with Annexin XIIIb [130] involved in apical transport of trans-Golgi-Network derived vesicles [131], expressed in morphogenesis of retina and RPE [129]. Involved in apical transport of Annexin XIIb where it localises to apical membrane processes [131].	Potentially involved in human retinal degeneration [129, 132], and Bardet-Biedl syndrome [132].
KIFC4[132]	Identified but role uncertain[133].	
KIFC5A?	Similar in genetic coding to KIFC1 . Localised to male germ cells suggesting role with microtubule complexes, meiotic spindle, manchette and flagella [134].	
Kinesin13	Novel kinesin involved in length control of the flagellum[135].	
XKLP2	Kinesin like protein which binds to the centrosome and is detected upon microtubules in mitosis and during Interphase [136].	XKLP2 is associated with malignant transformation and squamous cell carcinoma of the lung[136].
[*] Primary cilium associated[137, 138]		

[1] Okada Y, Yamazaki H, Sekine-Aizawa Y, Hirokawa N. (1995) The neuron-specific kinesin superfamily protein KIF1A is a unique monomeric motor for anterograde axonal transport of synaptic vesicle precursors. *Cell*, **81**, 769-780.

[2] Kikkawa M, Hirokawa N. (2006) High-resolution cryo-EM maps show the nucleotide binding pocket of KIF1A in open and closed conformations. *EMBO Journal*, **25**, 4187-4194.

[3] Rivière JB, Ramalingam S, Lavastre V, Shekarabi M, Holbert S, Lafontaine J, Srour M, Merner N, Rochefort D, Hince P, Gaudet R, Mes-Masson AM, Baets J, Houlden H, Brais B, Nicholson GA, Van Esch H, Nafissi S, De Jonghe P, Reilly MM, Timmerman V, Dion PA, Rouleau GA. (2011) KIF1A, an axonal transporter of synaptic vesicles, is mutated in hereditary sensory and autonomic neuropathy type 2. *American Journal of Human Genetics*, **89**, 219-230.

[4] Asperti C, Pettinato E, de Curtis I. (2010) Liprin-alpha1 affects the distribution of low-affinity beta1 integrins and stabilizes their permanence at the cell surface. *Experimental Cell Research*, **316**, 915-926.

[5] Shin H, Wyszynski M, Huh KH, Valtschanoff JG, Lee JR, Ko J, Streuli M, Weinberg RJ, Sheng M, Kim E. (2003) Association of the kinesin motor KIF1A with the multimodular protein liprin-alpha. *Journal of Biological Chemistry*, **278**, 11393-11401.

[6] Erlich Y, Edvardson S, Hodges E, Zenvirt S, Thekkat P, Shaag A, Dor T, Hannon GJ, Elpeleg O. (2011) Exome sequencing and disease-network analysis of a single family implicate a mutation in KIF1A in hereditary spastic paraparesis. *Genome Research*, **21**, 658-664.

[7] Nagai M, Ichimiya S, Ozaki T, Seki N, Mihara M, Furuta S, Ohira M, Tomioka N, Nomura N, Sakiyama S, Kubo O, Takakura K, Hori T, Nakagawara A. (2000) Identification of the full-length KIAA0591 gene encoding a novel kinesin-related protein which is mapped to the neuroblastoma suppressor gene locus at 1p36.2. *International Journal of Oncology*, **16**, 907-916.

[8] Horgan CP, McCaffrey MW. (2011) Rab GTPases and microtubule motors. *Biochemical Society Transactions*, **39**, 1202-1206.

[9] Niwa S, Tanaka Y, Hirokawa N. (2008) KIF1B- β and KIF1A mediated axonal transport of presynaptic regulator Rab3 occurs in a GTP-dependent manner through DENN/MADD. *Nature Cell Biology*, **10**, 1269-1279.

- [10] Bunn RC, Jensen MA, Reed BC. (1999) Protein interactions with the glucose transporter binding protein GLUT1CBP that provide a link between GLUT1 and the cytoskeleton. *Molecular Biology of the Cell*, **10**, 819-932.
- [12] Hirokawa N, Noda Y. (2008) Intracellular transport and kinesin superfamily proteins, KIFs: structure, function, and dynamics. *Physiological Reviews*, **88**, 1089-1118.
- [13] Wozniak MJ, Melzer M, Dorner C, Haring HU, Lammers R. (2005) The novel protein KBP regulates mitochondria localization by interaction with a kinesin-like protein. *BMC Cell Biology*, **6**, 35.
- [14] Mok H, Shin H, Kim S, Lee JR, Yoon J, Kim E. (2002) Association of the kinesin superfamily motor protein KIF1B α with postsynaptic density-95 (PSD-95), synapse-associated protein-97, synaptic scaffolding molecule PSD-95/discs large/zona occludens-1 proteins. *Journal of Neuroscience*, **22**, 5253-5258.
- [15] Theisen U, Straube E, Straube A. (2012) Directional persistence of migrating cells requires Kif1C-mediated stabilization of trailing adhesions. *Developmental Cell*, **23**, 1153-1166.
- [16] Storrie B, Micaroni M, Morgan GP, Jones N, Kamykowski JA, Wilkins N, Pan TH, Marsh BJ. (2012) Electron tomography reveals Rab6 is essential to the trafficking of trans-Golgi clathrin and COPI-coated vesicles and the maintenance of Golgi cisternal number. *Traffic*, **13**, 727-744.
- [17] Mennella V, Rogers GC, Rogers SL, Buster DW, Vale RD, Sharp DJ. (2005) Functionally distinct kinesin-13 family members cooperate to regulate microtubule dynamics during interphase. *Nature Cell Biology*, **7**, 235-245.
- [18] Schepis A, Stauber T, Krijnse Locker J. (2008) Kinesin-1 plays multiple roles during the vaccinia virus life cycle. *Cellular Microbiology*, **9**, 1960-1973.
- [19] Manning AL, Ganem NJ, Bakhoun SF, Wagenbach M, Wordeman L, Compton DA. (2007) The kinesin-13 proteins Kif2a, Kif2b, and Kif2c/MCAK have distinct roles during mitosis in human cells. *Molecular Biology of the Cell*, **18**, 2970-2979.
- [20] Li C, Zheng Y, Qin W, Tao R, Pan Y, Xu Y, Li X, Gu N, Feng G, He L. (2006) A family-based association study of kinesin heavy chain member 2 gene (KIF2) and schizophrenia. *Neuroscience Letters*, **407**, 151-155.
- [21] Hood EA, Kettenbach AN, Gerber SA, Compton DA. (2012) Plk1 regulates the kinesin-13 protein Kif2b to promote faithful chromosome segregation. *Molecular Biology of the Cell*, **23**, 2264-2274.
- [22] May-Simera HL, Kelley MW. (2012) Cilia, Wnt signaling, and the cytoskeleton. *Cilia*, **1**, 7.
- [23] Moore AT, Rankin KE, von Dassow G, Peris L, Wagenbach M, Ovechkina Y, Andrieux A, Job D, Wordeman L. (2005) MCAK associates with the tips of polymerizing microtubules. *Journal of Cell Biology*, **169**, 391-397.
- [24] Muresan V, Abramson T, Lyass A, Winter D, Porro E, Hong F, Chamberlin NL, Schnapp BJ. (1998) KIF3C and KIF3A form a novel neuronal heteromeric kinesin that associates with membrane vesicles. *Molecular Biology of the Cell*, **9**, 637-652.
- [25] Yamazaki H, Nakata T, Okada Y, Hirokawa N. (1995) KIF3A/B: a heterodimeric kinesin superfamily protein that works as a microtubule plus end-directed motor for membrane organelle transport. *Journal of Cell Biology*, **130**, 1387-1399.

- [26] Whitehead JL, Wang SY, Bost-Usinger L, Hoang E, Frazer KA, Burnside B. (1999) Photoreceptor localization of the KIF3A and KIF3B subunits of the heterotrimeric microtubule motor kinesin II in vertebrate retina. *Experimental Eye Research*, **69**, 491-503.
- [27] Kodani A, Salomé Sirerol-Piquer M, Seol A, Garcia-Verdugo JM, Reiter JF. (2013) Kif3a interacts with dynactin subunit p150 glued to organize centriole subdistal appendages. *EMBO Journal*, **32**, 597-607.
- [28] Takeda S, Yamazaki H, Seog DH, Kanai Y, Terada S, Hirokawa N. (2000) Kinesin superfamily protein 3 (KIF3) motor transports fodrin associating vesicles important for neurite building. *Journal of Cell Biology*, **148**, 1255-1265.
- [29] Stauber T, Simpson JC, Pepperkok R, Vernos I. (2006) A role for kinesin-2 in COPI-dependent recycling between the ER and the Golgi complex. *Current Biology*, **16**, 2245-2251.
- [30] Bananis E, Murray JW, Stockert RJ, Satir P, Wolkoff A.W. (2003) Regulation of early endocytic vesicle motility and fission in are constituted system. *Journal of Cell Science*, **116**, 2749-2761.
- [31] Bananis E, Nath S, Gordon K, Satir P, Stockert RJ, Murray JW, Wolkoff AW. (2004) Microtubule-dependent movement of late endocytic vesicles in vitro: requirements for Dynein and Kinesin. *Molecular Biology of the Cell*, **15**, 3688-3697.
- [32] Imamura T, Huang J, Usui I, Satoh H, Bever J, Olefsky JM. (2003) Insulin-induced GLUT4 translocation involves protein kinase C-lambda-mediated functional coupling between Rab4 and the motor protein kinesin. *Molecular Biology of the Cell*, **23**, 4892-4900.
- [33] Wu Y, Dai X, Li Q, Chen CX, Mai W, Hussain Z, Long W, Montalbetti N, Li G, Glynne R, Wang S, Cantiello HF, Wu G, Chen X. (2006) Kinesin-2 mediates physical and functional interactions between polycystin-2 and fibrocystin. *Human Molecular Genetics*, **15**, 3280-3292.
- [34] Haraguchi K, Hayashi T, Jimbo T, Yamamoto T, Akiyama T. (2006) Role of the kinesin-2 family protein, KIF3, during mitosis. *Journal of Biological Chemistry*, **281**, 4094-4099.
- [35] Shimizu K, Shirataki H, Honda T, Minami S, Takai Y. (1998) Complex formation of SMAP/KAP3, a KIF3A/B ATPase motor-associated protein, with a human chromosome-associated polypeptide. *Journal of Biological Chemistry*, **273**, 6591-6594.
- [36] Nonaka S, Tanaka Y, Okada Y, Takeda S, Harada A, Kanai Y, Kido M, Hirokawa N. (1999) Randomization of left-right asymmetry due to loss of nodal cilia generating leftward flow of extraembryonic fluid in mice lacking KIF3B motor protein. *Cell*, **95**, 829-837.
- [37] Jimbo T, Kawasaki Y, Koyama R, Sato R, Takada S, Haraguchi K, Akiyama T. (2002) Identification of a link between the tumour suppressor APC and the kinesin superfamily. *Nature Cell Biology*, **4**, 323-327.
- [38] Jordens I, Marsman M, Kuijl C, Neefjes J. (2005) Rab proteins, connecting transport and vesicle fusion. *Traffic*, **6**, 1070-1077.
- [39] Davidovic L, Jaglin XH, Lepagnol-Bestel AM, Tremblay S, Simonneau M, Bardoni B, Khandjian EW. (2008) The fragile X mental retardation protein is a molecular adaptor between the neurospecific KIF3C kinesin and dendritic RNA granules. *Human Molecular Genetics*, **16**, 3047-3058.

- [40] Geiman TM, Sankpal UT, Robertson AK, Chen Y, Mazumdar M, Heale JT, Schmiesing JA, Kim W, Yokomori K, Zhao Y, Robertson K D. (2004) Isolation and characterization of a novel DNA methyltransferase complex linking DNMT3B with components of the mitotic chromosome condensation machinery. *Nucleic Acids Research*, **32**, 2716-2729.
- [41] Wu G, Zhou L, Khidr L, Guo XE, Kim W, Lee YM, Krasieva T, Chen PL. (2008) A novel role of the chromokinesin Kif4A in DNA damage response. *Cell Cycle*, **7**, 2013-2020.
- [42] Mazumdar M, Sundareshan S, Misteli T. (2004) Human chromokinesin KIF4A functions in chromosome condensation and segregation. *Journal of Cell Biology*, **166**, 613-620.
- [43] Zhu C, Jiang W. (2005) Cell cycle-dependent translocation of PRC1 on the spindle by Kif4 is essential for midzone formation and cytokinesis. *Proceedings of the National Academy of Sciences, USA*, **102**, 343-348.
- [44] Peretti D, Peris L, Rosso S, Quiroga S, Caceres A. (2000) Evidence for the involvement of KIF4 in the anterograde transport of L1-containing vesicles. *Journal of Cell Biology*, **149**, 141-152.
- [45] Hanada T, Lin L, Tibaldi EV, Reinherz EL, Chishti AH. (2000) GAKIN, a novel kinesin-like protein associates with the human homologue of the Drosophila discs large tumor suppressor in T lymphocytes. *Journal of Biological Chemistry*, **275**, 28774-28784.
- [46] Ha MJ, Yoon J, Moon E, Lee YM, Kim HJ, Kim W. (2000) Assignment of the kinesin family member 4 genes (KIF4A and KIF4B) to human chromosome bands Xq13.1 and 5q33.1 by *in situ* hybridization. *Cytogenetics and Cellular Genetics*, **88**, 41-42.
- [47] Kurasawa Y, Earnshaw WC, Mochizuki Y, Dohmae N, Todokoro K. (2005) Essential roles of KIF4 and its binding partner PRC1 in organized central spindle midzone formation. *EMBO Journal*, **23**, 3237-3248.
- [48] Lee YM, Lee S, Lee E, Shin H, Hahn H, Choi W, Kim W. (2002) Human kinesin superfamily member 4 is dominantly localized in the nuclear matrix and is associated with chromosomes during mitosis. *Biochemical Journal*, **360**, 549-556.
- [49] Midorikawa R, Takei Y, Hirokawa N. (2006) KIF4 motor regulates activity-dependent neuronal survival by suppressing PARP-1 enzymatic activity. *Cell*, **125**, 371-383.
- [50] Setou M, Seog DH, Tanaka Y, Yoshimitsu KY, Takei Y, Kawagishi M, Hirokawa N. (2002) Glutamate-receptor-interacting protein GRIP1 directly steers kinesin to dendrites. *Nature*, **417**, 83-87.
- [51] Fichera M, Lo Giudice M, Falco M, Sturnio M, Amata S, Calabrese O, Bigoni S, Calzolari E, Neri M. (2005) Evidence of kinesin heavy chain (KIF5A) involvement in pure hereditary spastic paraplegia. *Neurology*, **63**, 1108-1110.
- [52] Amit I, Yakir L, Katz M, Zwang Y, Marmor MD, Citri A, Shtiegman K, Alroy I, Tuvia S, Reiss , Roubini E, Cohen M, Wides R, Bacharach E, Schubert U, Yarden Y. (2004) Tal, a Tsg101-specific E3 ubiquitin ligase, regulates receptor endocytosis and retrovirus budding. *Genes and Development*, **18**, 1737-1752.
- [53] Taya S, Shinoda T, Tsuboi D, Asaki J, Nagai K, Hikita T, Kuroda S, Kuroda K, Shimizu M, Hirotsune S, Iwamatsu A, Kaibuchi K. (2007) DISC1 regulates the transport of the NUDEL/LIS1/14-3-3epsilon complex through kinesin-1. *Journal of Neuroscience*, **27**, 15-26.
- [54] Wozniak MJ, Allan VJ. (2006) Cargo selection by specific kinesin light chain 1 isoforms. *EMBO Journal*, **25**, 5457-5468.

- [55] Rietdorf J, Ploubidou A, Reckmann I, Holmstrom A, Frischknecht F, Zettl M, Zimmermann T, Way M. (2001) Kinesin-dependent movement on microtubules precedes actin-based motility of vaccinia virus. *Nature Cell Biology*, **3**, 992-1000.
- [56] Diefenbach RJ, Diefenbach E, Douglas MW, Cunningham AL. (2002) The heavy chain of conventional kinesin interacts with the SNARE proteins SNAP25 and SNAP23. *Biochemistry*, **41**, 14906-14915.
- [57] Ichimura T, Wakamiya-Tsuruta A, Itagaki C, Taoka M, Hayano T, Natsume T, Isobe T. (2002) Phosphorylation-dependent interaction of kinesin light chain 2 and the 14-3-3 protein. *Biochemistry*, **41**, 5566-5572.
- [58] Rahman A, Kamal A, Roberts EA, Goldstein LS. (1999) Defective kinesin heavy chain behavior in mouse kinesin light chain mutants. *Journal of Cell Biology*, **146**, 1277-1288.
- [59] Tanaka Y, Kanai Y, Okada Y, Nonaka S, Takeda S, Harada A, Hirokawa N. (1998) Targeted disruption of mouse conventional kinesin heavy chain, kif5B, results in abnormal perinuclear clustering of mitochondria. *Cell*, **93**, 1147-1158.
- [60] Diefenbach RJ, Diefenbach E, Douglas MW, Cunningham AL. (2004) The ribosome receptor, p180, interacts with kinesin heavy chain, KIF5B. *Biochemical and Biophysical Research Communications*, **319**, 987-992.
- [61] Hirokawa N, Noda Y, Okada Y. (1998) Kinesin and dynein superfamily proteins in organelle transport and cell division. *Current Opinion in Cell Biology*, **10**, 60-73.
- [62] Hirokawa N, Noda Y, Tanaka Y, Niwa S. (2009) Kinesin superfamily motor proteins and intracellular transport. *Nature Reviews Molecular and Cellular Biology*, **10**, 682-696.
- [63] Nakata T, Niwa S, Okada Y, Perez F, Hirokawa N. (2011) Preferential binding of a kinesin-1 motor to GTP-tubulin-rich microtubules underlies polarized vesicle transport. *Journal of Cell Biology*, **194**, 245-255.
- [64] Hirokawa N. (2006) mRNA transport in dendrites: RNA granules, motors, and tracks. *Journal of Neuroscience*, **26**, 7139-7142.
- [65] Sheng Z, Cai Q (2012) Mitochondrial transport in neurons: impact on synaptic homeostasis and neurodegeneration. *Nature Reviews Neuroscience*, **13**, 77-93.
- [66] Cardoso CMP, Groth-Pedersen L, Høyer-Hansen M, Kirkegaard T, Corcelle E, Andersen JS, Jäättelä M, Nylandsted J. (2009) Depletion of kinesin 5B affects lysosomal distribution and stability and induces peri-nuclear accumulation of autophagosomes in cancer cells. *PLoS One*, **4**(2):e4424.
- [67] Niclas J, Navone F, Hom-Booher N, Vale RD. (1994) Cloning and localization of a conventional kinesin motor expressed exclusively in neurons. *Neuron*, **12**, 1059-1072.
- [68] Kanai Y, Okada Y, Tanaka Y, Harada A, Terada S, Hirokawa N. (2000) KIF5C, a novel neuronal kinesin enriched in motor neurons. *Journal of Neuroscience*, **20**, 6374-6384;
- [69] Goldstein LS. (1991) The kinesin superfamily: tails of functional redundancy. *Trends in Cell Biology*, **1**, 93-98.

- [70] Smith MJ, Pozo K, Brickley K, Stephenson FA. (2006) Mapping the GRIF-1 binding domain of the kinesin, KIF5C, substantiates a role for GRIF-1 as an adaptor protein in the anterograde trafficking of cargoes. *Journal of Biological Chemistry*, **281**, 27216-27228.
- [71] Cai Y, Singh BB, Aslanukov A, Zhao H, Ferreira PA. (2001) The docking of kinesins, KIF5B and KIF5C, to Ran-binding protein 2 (RanBP2) is mediated via a novel RanBP2 domain. *Journal of Biological Chemistry*, **276**, 41594-41602.
- [72] Katoh Y, Katoh M. (2004) Characterization of KIF7 gene in silico. *International Journal of Oncology*, **25**, 1881-1886.
- [73] Katoh Y, Katoh M. (2006) Hedgehog signaling pathway and gastrointestinal stem cell signaling network. *International Journal of Molecular Medicine*, **18**, 1019-1023.
- [74] Endoh-Yamagami S, Evangelista M, Wilson D, Wen X, Theunissen JW, Phamluong K, Davis M, Scales SJ, Solloway MJ, de Sauvage FJ, Peterson AS. (2009) The mammalian Cos2 homolog Kif7 plays an essential role in modulating Hh signal transduction during development. *Current Biology*, **19**, 1320-1326.
- [75] Cheung HO, Zhang X, Ribeiro A, Mo R, Makino S, Puvindran V, Law KK, Briscoe J, Hui CC. (2009) The kinesin protein Kif7 is a critical regulator of Gli transcription factors in mammalian hedgehog signaling. *Science Signaling*, **2**, ra29.
- [76] Piddini E, Schmid JA, de Martin R, Dotti CG. (2001) The Ras-like GTPase Gem is involved in cell shape remodelling and interacts with the novel kinesin-like protein KIF9. *EMBO Journal*, **20**, 4076 - 4087.
- [77] Wood KW, Sakowicz R, Goldstein LS, Cleveland DW (1997) CENP-E is a plus end-directed kinetochore motor required for metaphase chromosome alignment. *Cell*, **91**, 357-366.
- [78] Di Fiore B, Ciciarello M, Mangiacasale R, Palena A, Tassin AM, Cundari E, Lavia P. (2003) Mammalian RanBP1 regulates centrosome cohesion during mitosis. *Journal of Cell Science*, **116**, 3399-3411.
- [79] Carter BZ, Mak DH, Shi Y, Schober WD, Wang RY, Konopleva M, Koller E, Dean NM, Andreeff M. (2006) Regulation and targeting of Eg5, a mitotic motor protein in blast crisis CML: overcoming imatinib resistance. *Cell Cycle*, **5**, 2223-2229.
- [80] Katoh M, Katoh M. (2005) Characterization of KIF12 gene in silico. *Oncology Reports*, **13**, 367-370.
- [81] Nakagawa T, Setou M, Seog D, Ogasawara K, Dohmae N, Takio K, Hirokawa N. (2001) A novel motor, KIF13A, transports mannose-6-phosphate receptor to plasma membrane through direct interaction with AP-1 complex. *Cell*, **103**, 569-581.
- [82] Lu L, Lee YR, Pan R, Maloof JN, Liu B. (2004) An internal motor kinesin is associated with the Golgi apparatus and plays a role in trichome morphogenesis in *Arabidopsis*. *Molecular Biology of the Cell*, **16**, 811-823.
- [83] Jamain S, Quach H, Fellous M, Bourgeron T. (2001) Identification of the human KIF13A gene homologous to *Drosophila* kinesin-73 and candidate for schizophrenia. *Genomics*, **74**, 36-44.
- [84] Chen D, Pajovic S, Duckett A, Brown VD, Squire JA, Gallie BL. (2002) Genomic amplification in retinoblastoma narrowed to 0.6 megabase on chromosome 6p containing a kinesin-like gene, RBKIN. *Cancer Research*, **62**, 967-971.

- [85] Venkateswarlu K, Hanada T, Chishti AH. (2005) Centaurin- α 1 interacts directly with kinesin motor protein KIF13B. *Journal of Cell Science*, **118**, 2471-2484.
- [86] Carleton M, Mao M, Biery M, Warren P, Kim S, Buser C, Marshall CG, Fernandes C, Annis J, Linsley PS (2006) RNA interference-mediated silencing of mitotic kinesin KIF14 disrupts cell cycle progression and induces cytokinesis failure. *Molecular Biology of the Cell*, **26**, 3853-3863.
- [87] Corson TW, Huang A, Tsao MS, Gallie BL. (2005) KIF14 is a candidate oncogene in the 1q minimal region of genomic gain in multiple cancers. *Oncogene*, **24**, 4741-4753.
- [87] Corson TW, Zhu CQ, Lau SK, Shepherd FA, Tsao M, Gallie BL. (2007) KIF14 messenger RNA expression is independently prognostic for outcome in lung cancer. *Clinical Cancer Research*, **13**, 3229-3234.
- [88] Buster DW, Baird DH, Yu W, Solowska JM, Chauvière M, Mazurek A, Kress M, Baas PW. (2003) Expression of the mitotic kinesin Kif15 in postmitotic neurons: implications for neuronal migration and development. *Journal of Neurocytology*, **32**, 79-96.
- [89] Tanenbaum ME, Macůrek L, Janssen A, Geers EF, Alvarez-Fernández M, Medema RH. (2009) Kif15 cooperates with Eg5 to promote bipolar spindle assembly. *Current Biology*, **19**, 1703-1711.
- [91] Blatner NR, Wilson MI, Lei C, Hong W, Murray D, Williams RL, Cho W. (2007) The structural basis of novel endosome anchoring activity of KIF16B kinesin. *EMBO Journal*, **26**, 3709-3719.
- [92] Hoepfner S, Severin F, Cabezas A, Habermann B, Runge A, Gillooly D, Stenmark H, Zerial M. (2005) Modulation of receptor recycling and degradation by the endosomal kinesin KIF16B. *Cell*, **121**, 437-450.
- [93] Setou M, Nakagawa T, Seog DH, Hirokawa N. (2000) Kinesin superfamily motor protein KIF17 and mLin-10 in NMDA receptor-containing vesicle transport. *Science*, **288**, 1796-1802.
- [94] Kayadjanian N, Lee HS, Piña-Crespo J, Heinemann SF. (2007) Localization of glutamate receptors to distal dendrites depends on subunit composition and the kinesin motor protein KIF17. *Molecular and Cellular Neuroscience*, **34**, 219-230.
- [95] Chennathukuzhi V, Morales CR, El-Alfy M, Hecht NB. (2004) The kinesin KIF17b and RNA-binding protein TB-RBP transport specific cAMP-responsive element modulator-regulated mRNAs in male germ cells. *Proceedings of the National Academy of Sciences, USA*, **100**, 15566-15571.
- [96] Guillaud L, Setou M, Hirokawa N. (2003) KIF17 dynamics and regulation of NR2B trafficking in hippocampal neurons. *Journal of Neuroscience*, **23**, 131-140.
- [97] Dhar SS, Wong-Riley MT. (2011) *Biochim Biophys Acta*. The kinesin superfamily protein KIF17 is regulated by the same transcription factor (NRF-1) as its cargo NR2B in neurons. *Biochimica Biophysica Acta*, **1813**, 403-411.
- [98] Insinna C, Pathak N, Perkins B, Drummond I, Besharse JC. (2008) The homodimeric kinesin, Kif17, is essential for vertebrate photoreceptor sensory outer segment development. *Developmental Biology*, **316**, 160-170.
- [99] Yin X, Takei Y, Kido MA, Hirokawa N. (2011) Molecular motor KIF17 is fundamental for memory and learning via differential support of synaptic NR2A/2B levels. *Neuron*, **70**, 310-325.

- [100] Yanahashi S, Hashimoto K, Hattori K, Yuasa S, Iyo M. (2004) Role of NMDA receptor subtypes in the induction of catalepsy and increase in Fos protein expression after administration of haloperidol. *Brain Research*, **1011**, 84-93.
- [101] Wei J, Dong M, Xiao C, Jiang F, Castellino FJ, Prorok M, Dai Q. (2006) Conantokins and variants derived from cone snail venom inhibit naloxone-induced withdrawal jumping in morphine-dependent mice. *Neuroscience Letters*, **405**, 137-141.
- [102] Li L, Fan M, Icton CD, Chen N, Leavitt BR, Hayden MR, Murphy TH, Raymond LA. (2003) Role of NR2B-type NMDA receptors in selective neurodegeneration in Huntington disease. *Neurobiology Aging*, **24**, 1113-1121.
- [103] Jenkins PM, Hurd TW, Zhang L, McEwen DP, Brown RL, Margolis B, Verhey KJ, Martens JR. (2006) Ciliary targeting of olfactory CNG channels requires the CNGB1b subunit and the kinesin-2 motor protein, KIF17. *Current Biology*, **16**, 1211-1216.
- [104] Luboshits G, Benayahu D. (2005) MS-KIF18A, new kinesin; structure and cellular expression. *Gene*, **351**, 19-28.
- [105] Luboshits G, Benayahu DJ. (2007) MS-KIF18A, a kinesin, is associated with estrogen receptor. *Journal of Cellular Biochemistry*, **100**, 693-702.
- [106] Stumpff J, von Dassow G, Wagenbach M, Asbury C, Wordeman L. (2008) The kinesin-8 motor Kif18A suppresses kinetochore movements to control mitotic chromosome alignment. *Developmental Cell*, **14**, 252-262.
- [107] Niwa S, Nakajima K, Miki H, Minato Y, Wang D, Hirokawa N. (2012) KIF19A Is a microtubule-depolymerizing kinesin for ciliary length control. *Developmental Cell*, **23**, 1167-1175.
- [108] Echard A, Jollivet F, Martinez O, Lacapère JJ, Rousselet A, Janoueix-Lerosey I, Goud B. (1998) Interaction of a Golgi-associated kinesin-like protein with Rab6. *Science*, **279**, 580-585.
- [109] Hill E, Clarke M, Barr FA. (2000) The Rab6-binding kinesin, Rab6-KIFL, is required for cytokinesis. *EMBO Journal*, **19**, 5711-5719.
- [110] Fontijn RD, Goud B, Echard A, Jollivet F, van Marle J, Pannekoek H, Horrevoets AJ. (2001) The human kinesin-like protein RB6K is under tight cell cycle control and is essential for cytokinesis. *Molecular Biology of the Cell*, **21**, 2944-2955.
- [111] Miki H, Setou M, Kaneshiro, K, Hirokawa N. (2001) All kinesin superfamily protein, KIF, genes in mouse and human. *Proceedings of the National Academy of Sciences, USA*, **98**, 7004-7011.
- [112] Lai F, Fernald AA, Zhao N, Le Beau MM. (2000) cDNA cloning, expression pattern, genomic structure and chromosomal location of RAB6KIFL, a human kinesin-like gene. *Gene*, **248**, 117-125.
- [113] Taniuchi K, Nakagawa H, Nakamura T, Eguchi H, Ohigashi H, Ishikawa O, Katagiri T, Nakamura Y. (2005) Down-regulation of RAB6KIFL/KIF20A, a kinesin involved with membrane trafficking of discs large homologue 5, can attenuate growth of pancreatic cancer cell. *Cancer Research*, **65**, 105-112.
- [114] Marszalek JR, Weiner JA, Farlow SJ, Chun J, Goldstein LS. (1999) Novel dendritic kinesin sorting identified by different process targeting of two related kinesins: KIF21A and KIF21B. *Journal of Cell Biology*, **145**, 469-479.

- [115] Yamada K, Hunter DG, Andrews C, Engle EC. (2005) A novel KIF21A mutation in a patient with congenital fibrosis of the extraocular muscles and Marcus Gunn jaw-winking phenomenon. *Archives in Ophthalmology*, **123**, 1254-1259.
- [116] Germani A, Bruzzoni-Giovanelli H, Fellous A, Gisselbrecht S, Varin-Blank N, Calvo F. (2000) SIAH-1 interacts with alpha-tubulin and degrades the kinesin Kid by the proteasome pathway during mitosis. *Oncogene*, **19**, 5997-6006.
- [117] Liu J, Stevens J, Rote CA, Yost HJ, Hu Y, Neufeld KL, White RL, Matsunami N. (2001) Siah-1 mediates a novel beta-catenin degradation pathway linking p53 to the adenomatous polyposis coli protein. *Molecular Cell*, **7**, 927-936.
- [118] Katoh Y, Katoh M. (2004) KIF27 is one of orthologs for *Drosophila* Costal-2. *International Journal of Oncology*, **25**, 1875-1880.
- [119] Boman AL, Kuai J, Zhu X, Chen J, Kuriyama R, Kahn RA (October) Arf proteins bind to mitotic kinesin-like protein 1 (MKLP1) in a GTP-dependent fashion. *Cell Motility and Cytoskeleton*, **44**, 119-32.
- [120] Neef R, Preisinger C, Sutcliffe J, Kopajtich R, Nigg EA, Mayer TU, Barr FA. (2003) Phosphorylation of mitotic kinesin-like protein 2 by polo-like kinase 1 is required for cytokinesis. *Journal of Cell Biology*, **162**, 863-875.
- [121] Kobayashi T, Tsang WY, Li J, Lane W, Dynlacht BD. (2011) Centriolar kinesin Kif24 interacts with CP110 to remodel microtubules and regulate ciliogenesis. *Cell*, **145**, 914-925.
- [122] Venturelli E, Villa C, Fenoglio C, Clerici F, Marcone A, Benussi L, Ghidoni R, Gallone S, Scalabrini D, Cortini F, Fumagalli G, Cappa S, Binetti G, Franceschi M, Rainero I, Giordana MT, Mariani C, Bresolin N, Scarpini E, Galimberti D. (2011) Is KIF24 a genetic risk factor for frontotemporal lobar degeneration? *Neuroscience Letters*, **482**, 240-244.
- [123] Yang WX, Jefferson H, Sperry AO. (2006) The molecular motor KIFC1 associates with a complex containing nucleoporin NUP62 that is regulated during development and by the small GTPase RAN. *Biology and Reproduction*, **74**, 684-690.
- [124] Farina F, Pierobon P, Delevoye C, Monnet J, Dingli F, Loew D, Quanz M, Dutreix M, Cappello G. (2013) Kinesin KIFC1 actively transports bare double-stranded DNA. *Nucleic Acids Research*, **41**, 4926-4937.
- [125] Hanlon DW, Yang Z, Goldstein LS. (1997) Characterization of KIFC2, a neuronal kinesin superfamily member in mouse. *Neuron*, **8**, 439-451.
- [126] Hunter AW, Caplow M, Coy DL, Hancock WO, Diez S, Wordeman L, Howard J. (2003) The kinesin-related protein MCAK is a microtubule depolymerase that forms an ATP-hydrolyzing complex at microtubule ends. *Molecular Cell*, **11**, 445-457.
- [127] Saito N, Okada Y, Noda Y, Kinoshita Y, Kondo S, Hirokawa N. (1997) KIFC2 is a novel neuron-specific C-terminal type kinesin superfamily motor for dendritic transport of multivesicular body-like organelles. *Neuron*, **18**, 425-438.
- [128] Xu Y, Takeda S, Nakata T, Noda Y, Tanaka Y, Hirokawa N. (2002) Role of KIFC3 motor protein in Golgi positioning and integration. *Journal of Cell Biology*, **158**, 293-303.
- [129] Hoang E, Bost-Usinger L, Burnside B. (1999) Characterization of a novel C-kinesin (KIFC3) abundantly expressed in vertebrate retina and RPE. *Experimental Eye Research*, **69**, 57-68.

- [130] Lafont F, Lecat S, Verkade P, Simons K. (1998) Annexin XIIIb associates with lipid microdomains to function in apical delivery. *Journal of Cell Biology*, **142**, 1413-1427.
- [131] Noda Y, Okada Y, Saito N, Setou M, Xu Y, Zhang Z, Hirokawa NJ. (2001) KIFC3, a microtubule minus end-directed motor for the apical transport of annexin XIIIb-associated Triton-insoluble membranes. *Cell Biology*, **155**, 77-88.
- [132] Hoang EH, Whitehead JL, Dosé AC, Burnside B. (1998) Cloning of a novel C-terminal kinesin (KIFC3) that maps to human chromosome 16q13-q21 and thus is a candidate gene for Bardet-Biedl syndrome. *Genomics*, **52**, 219-222.
- [133] Yang Z, Hanlon DW, Marszalek JR, Goldstein LS. (1997) Identification, partial characterization, and genetic mapping of kinesin-like protein genes in mouse. *Genomics*, **45**, 123-131.
- [134] Navolanic PM, Sperry AO. (2000) Identification of isoforms of a mitotic motor in mammalian spermatogenesis. *Biology and Reproduction*, **62**, 1360-1369.
- [135] Blaineau C, Tessier M, Dubessay P, Tasse L, Crobu L, Pagès M, Bastien P. (2007) A novel microtubule-depolymerizing kinesin involved in length control of a eukaryotic flagellum. *Current Biology*, **17**, 778-782.
- [136] Boleti H, Karsenti E, Vernos I. (1996) Xklp2, a novel *Xenopus* centrosomal kinesin-like protein required for centrosome separation during mitosis. *Cell*, **84**, 49-59.
- [137] Ma Y, Lin D, Sun W, Xiao T, Yuan J, Han N, Guo S, Feng X, Su K, Mao Y, Cheng S, Gao Y. (2006) Expression of targeting protein for xklp2 associated with both malignant transformation of respiratory epithelium and progression of squamous cell lung cancer. *Clinical Cancer Research*, **12**, 1121-1127.
- [138] Rosenbaum JL, Witman GB. (2002) Intraflagellar transport. *Nature Reviews Molecular and Cellular Biology*, **3**, 813-825.
- [139] Hirokawa N, Takemura R. (2004) Molecular motors in neuronal development, intracellular transport and diseases. *Current Opinion in Neurobiology*, **14**, 564-557.

3.2 Axonemal Dynein Proteins

Axonemal Dynein	Dynein-like protein Interacts with/function	Importance/Known Disease(s)
DNAH1-4	Heavy Chain ; Little information	
DNAH5	Heavy Chain ; Involved in sperm and motile cilia movement[1-3] outer dynein arm protein .	Primary Ciliary Dyskinesia-3 (also known as PCD3) and defects in left-right asymmetry[1, 4-6].
DNAH6-8	Heavy Chain ;	
DNAH9	Heavy Chain ; involved in ciliary movement [3, 7]	PCD12 [4, 8].
DNAH10	Heavy Chain ;	
DNAH11	Heavy Chain ; ATP based motor involved in respiratory cilia[9] regulates the sub-cellular distribution of mitochondria[10] required for activation of MKK3/6 and p38 MAPKs [11].	PCD7 . Mutations responsible for minority of cases of PCD[6, 12] and situs inversus, Kartagener syndrome and association with uniparental disomy [13], involvement in ectopic pregnancy [14].
DNAH12-14, 17	Heavy Chain ; little information.	
DNALI1	Light Intermediate Inner dynein arm chain ; associated with cilia in the trachea and in flagella of mature sperm (active dynein), in spermatids and spermatocytes [15, 16].	Asthenozoospermia [6], PCD and situs inversus totalis [19].
DNAHL1	Intermediate Chain ;	
DNAI1	Intermediate chain ; Dynein chain bridges between microtubule doublets and responsible for motion of the axoneme[17].	PCD1 . Mutations resulting in PCD [18] also result in solitus or situs inversus (Kartagener Syndrome) [19] Links with neuroblastoma [19].
DNAI2	Intermediate Chain ; composed of 14 exons located at 17q25, is highly expressed in trachea, testis, respiratory cilia and sperm flagella [20].	PCD9 [20, 21].
DNAL1	Dynein Light Chain ; Components for part of outer dynein arm provide ATP powered movement[22]	Mutations associated with PCD [23].
DNAL4	Dynein Light Chain	

3.3 Cytoplasmic Dynein Proteins

Cytoplasmic Dynein/Gene	Dynein-like protein Interacts with/function	Importance/Known Disease(s)
DYNC1H1	Heavy dynein-1 heavy chain-1 [24, 25]; Known to interact with PAFAH1B1 [26] and CDC5L [27]. Involved in nuclear pore complex and in mediating fertilisation nuclear union[28], peri-nuclear aggregation[29] and in localisation to Golgi apparatus [30, 31]. Interacts with light chain component and neuronal proteins[32].	
DYNC2H1*	Dynein-2 heavy chain-1 [33-35]; localises primarily to the Golgi apparatus[25] where it is involved in establishing Golgi organisation and identified in IFT transport[37]. Found in neuronal and ciliated cells [37]. For review of dynein IFT role see Krock et al., (2009)[38].	Associated with Short-Rib-Polydactyly [39]
DYNC1I1	Cytoplasmic dynein-1 intermediate chain-1 ; DYNC1I1 is known to interact with DYNLL1 [24]; interacts with SNARE proteins SNAP25 and 23 and is involved in actin cytoskeleton remodelling [40]. It is up regulated in senescent cells [41]. Microtubule ending binding protein one EB1 associates with components of the dynactin complex and the dynein intermediate cytoplasmic chain[42].	The Herpes Simplex Virus-1 U(L)34 binding of viral protein VP26 [44]. Protein binds with a cytoplasmic dynein intermediate chain and targets nuclear membrane pores [43, 44]. Binds viral protein VP26 [44].
DYNC1I2	Cytoplasmic dynein-1 intermediate chain-2 ; Acts as a scaffold and is involved in linking dynein to cargos and to adapter proteins that regulate dynein function[24, 45-46].	
DYNC1L1	Cytoplasmic dynein-1 light intermediate chain-1 ; important in linking dynein and adaptor proteins to cargoes which	Interacts with Rab4 and Rab11A [50].

	regulate dynein function. Binds to organelles and membranes and chromosomes . Involved in transport of pericentrin [47]; required as a check point for spindle assembly , and involved in removal of MAD1L1 and MAD1L2 from kinetochores [24, 47-49].	
DYNC1L12	Cytoplasmic dynein-1 light intermediate chain-2 ; confusion exists with at least two isoforms known[49, 51], interacts with many transcription factors .	Interacts with Rab11A [50].
DYNC2L11*	Cytoplasmic dynein-1 light intermediate chain-2 [52]	Involved in intraflagellar transport[36, 53, 54].
DYNLL1	Cytoplasmic dynein light chain-1 ; Involved in intracellular transport , kinetochore and motility [24, 55, 56]. Components have been found to interact with myosin-Va [57, 58], IκBα [77], p21 [10, 60], neuronal nitric oxidasesynthase (nNOS)[66] and nuclear respiratory factor-1 [62, 63]. Co-localises with TRPS1 in the cell nucleus[64]. Involved in the nuclear accumulation of p53 from DNA damage [65]. Down regulated in chondrocytes in response to hydrostatic pressure through mechanotransduction [66].	A viral target in retrograde transport from the plasma membrane to the nucleus and also involved in apoptosis [56].
DYNLL2	Cytoplasmic dynein light chain-2 ; Interacts with myosin Va [58, 67], Bcl-2 modification factor[57, 59, 68] and localises to mitochondria [69].	Low expression in certain cancers[59, 71, 72].
DYNLRB1	Dynein light chain Roadblock-Type-1 :[24, 72, 73].	Interacts with Rab6A and Rab6B [50, 72].
DYNLRB2	Little information	
DYNLT1	Dynein light chain Tctex-type 1 ; Involved in cargo binding[40, 74, 75], vesicle transport[76], apical delivery of rhodopsin [77] (potential for ciliary transport), voltage dependent anion-selective channel (VDAC) ion channel and heat-shock protein PBP74 interaction with light chain Tctex-1 [78], involved with neural progenitor cells where Tctex-1 is involved in actin remodelling during neurite growth[40].	Mutation involved in pulmonary hypertension through BMPR-11 and Tctex-1 [79], Interacts with CD155 receptor in Polio virus endocytosis[80] and pathogenesis[81], binds herpes viral capsid VP26 dynein light chains RP3 and Tctex-1 [75].
DYNLT3	Dynein, light chain, Tctex type-3 ; cytoplasmic transport, binds with BUB3 (spindle checkpoint at prometophase on kinetochores)[82, 83], functions as a transcription regulator of Bcl-2 through binding to SATB1 (chromatin organiser and transcription organiser[84, 85]) in a dynein-independent manner[86], interacts with voltage dependent anion selective channels [78].	Bcl-2 implicated in number of diseases; melanoma , breast , prostate , lung cancer , schizophrenia and in apoptosis through cytochrome-c [87, 88].
For review of cytoplasmic dynein naming nomenclature see Pfister et al., (2005)[24].		

[1] Olbrich H, Haffner K, Kispert A, Volkel A, Volz A, Sasmaz G, Reinhardt R, Hennig S, Lehrach H, Konietzko N, Zariwala M, Noone PG, Knowles M, Mitchison HM, Meeks M, Chung EM, Hildebrandt F, Sudbrak R, Omran H. (2002) Mutations in DNAH5 cause primary ciliary dyskinesia and randomization of left-right asymmetry. *Nature Genetics*, **30**, 143-144.

[2] Maiti AK, Mattéi MG, Jorissen M, Volz A, Zeigler A, Bouvagnet P. (2000) Identification, tissue specific expression, and chromosomal localisation of several human dynein heavy chain genes. *European Journal of Human Genetics*, **8**, 923-932.

[3] Fliegauf M, Olbrich H, Horvath J, Wildhaber JH, Zariwala MA, Kennedy M, Knowles MR, Omran H. (2005) Mislocalization of DNAH5 and DNAH9 in respiratory cells from patients with primary ciliary dyskinesia. *American Journal of Respiratory and Critical Care Medicine*, **171**, 1343-1349.

[4] Olbrich H, Horváth J, Fekete A, Loges NT, van's Gravesande KS, Blum A, Hörmann K, Omran H. (2006) Axonemal localization of the dynein component DNAH5 is not altered in secondary ciliary dyskinesia. *Pediatric Research*, **59**, 418-422.

- [5] Thai CH, Gambling TM, Carson JL. (2002) Freeze fracture study of airway epithelium from patients with primary ciliary dyskinesia. *Thorax*, **57**, 363-365.
- [6] Zuccarello D, Ferlin A, Cazzadore C, Pepe A, Garolla A, Moretti A, Cordeschi G, Francavilla S, Foresta C. (2008) Mutations in dynein genes in patients affected by isolated non-syndromic asthenozoospermia. *Human Reproduction*, **23**, 1957-1962.
- [7] Milisav I, Jones MH, Affara NA. (1996) Characterization of a novel human dynein-related gene that is specifically expressed in testis. *Mammalian Genome*, **7**, 667-672.
- [8] Bartoloni L, Blouin JL, Maiti AK, Sainsbury A, Rossier C, Gehrig C, She JX, Marron MP, Lander ES, Meeks M, Chung E, Armengot M, Jorissen M, Scott HS, Delozier-Blanchet CD, Gardiner RM, Antonarakis SE. (2001) Axonemal beta heavy chain dynein DNAH9: cDNA sequence, genomic structure, and investigation of its role in primary ciliary dyskinesia. *Genomics*, **72**, 21-33.
- [9] Chapelin C, Duriez B, Magnino F, Goossens M, Escudier E, Amselem S. (1997) Isolation of several human axonemal dynein heavy chain genes: genomic structure of the catalytic site, phylogenetic analysis and chromosomal assignment. *FEBS Letters*, **412**, 325-330.
- [10] Varadi A, Johnson-Cadwell LI, Cirulli V, Yoon Y, Allan VJ, Rutter GA. (2005) Cytoplasmic dynein regulates the subcellular distribution of mitochondria by controlling the recruitment of the fission factor dynamin-related protein-1. *Journal of Cell Science*, **117**, 4389-4400.
- [11] Cheung PY, Zhang Y, Long J, Lin S, Zhang M, Jiang Y, Wu Z. (2004) p150(Glued), Dynein, and microtubules are specifically required for activation of MKK3/6 and p38 MAPKs. *Journal of Biological Chemistry*, **279**, 45308-45311.
- [12] Schwabe GC, Hoffmann K, Loges NT, Birker D, Rossier C, de Santi MM, Olbrich H, Fliegauf M, Faily M, Liebers U, Collura M, Gaedicke G, Mundlos S, Wahn U, Blouin JL, Niggemann B, Omran H, Antonarakis SE, Bartoloni L. (2008) Primary ciliary dyskinesia associated with normal axoneme ultrastructure is caused by DNAH11 mutations. *Human Mutations*, **29**, 289-298.
- [13] Bartoloni L, Blouin JL, Pan Y, Gehrig C, Maiti AK, Scamuffa N, Rossier C, Jorissen M, Armengot M, Meeks M, Mitchison HM, Chung EM, Delozier-Blanchet CD, Craigen WJ, Antonarakis SE. (2002) Mutations in the DNAH11 (axonemal heavy chain dynein type 11) gene cause one form of situs inversus totalis and most likely primary ciliary dyskinesia. *Proceedings of the National Academy of Sciences, USA*, **99**, 10282-10286.
- [14] Blyth M, Wellesley D. (2008) Ectopic pregnancy in primary ciliary dyskinesia. *Journal of Obstetrics and Gynaecology*, **28**, 358.
- [15] Rashid S, Breckle R, Hupe M, Geisler S, Doerwald N, Neesen J. (2006) The murine Dnali1 gene encodes a flagellar protein that interacts with the cytoplasmic dynein heavy chain 1. *Molecular Reproduction and Development*, **73**, 784-794.
- [16] Zariwala M, Noone PG, Sannuti A, Minnix S, Zhou Z, Leigh MW, Hazucha M, Carson JL, Knowles MR. (2002) Germline mutations in an intermediate chain dynein cause primary ciliary dyskinesia. *American Journal of Respiratory Cell and Molecular Biology*, **25**, 577-583.
- [16] Pennarun G, Escudier E, Chapelin C, Bridoux AM, Cacheux V, Roger G, Clement A, Goossens M, Amselem S, Duriez B. (2000) Loss-of-function mutations in a human gene related to *Chlamydomonas reinhardtii* dynein IC78 result in primary ciliary dyskinesia. *American Journal of Human Genetics*, **65**, 1508-1519.

- [18] Zariwala MA, Leigh MW, Ceppa F, Kennedy MP, Noone PG, Carson JL, Hazucha MJ, Lori A, Horvath J, Olbrich H, Loges NT, Bridoux AM, Pennarun G, Duriez B, Escudier E, Mitchison HM, Chodhari R, Chung EM, Morgan LC, de Iongh RU, Rutland J, Pradal U, Omran H, Amselem S, Knowles MR. (2006) Mutations of DNAI1 in primary ciliary dyskinesia: evidence of founder effect in a common mutation. *American Journal of Respiratory and Critical Care Medicine*, **174**, 858-866.
- [19] Guichard C, Harricane MC, Lafitte JJ, Godard P, Zaegel M, Tack V, Lalau G, Bouvagnet P. (2001) Axonemal dynein intermediate-chain gene (DNAI1) mutations result in situs inversus and primary ciliary dyskinesia (Kartagener syndrome). *American Journal of Human Genetics*, **68**, 1030-1035.
- [20] Pennarun G, Chapelin C, Escudier E, Bridoux AM, Dastot F, Cacheux V, Goossens M, Amselem S, Duriez B. (2000) The human dynein intermediate chain 2 gene (DNAI2): cloning, mapping, expression pattern, and evaluation as a candidate for primary ciliary dyskinesia. *Human Genetics*, **107**, 642-649.
- [21] Loges NT, Olbrich H, Fenske L, Mussaffi H, Horvath J, Fliegau M, Kuhl H, Baktai G, Peterffy E, Chodhari R, Chung EM, Rutman A, O'Callaghan C, Blau H, Tiszlavicz L, Voelkel K, Witt M, Zietkiewicz E, Neesen J, Reinhardt R, Mitchison HM, Omran H. (2008) DNAI2 mutations cause primary ciliary dyskinesia with defects in the outer dynein arm. *American Journal of Human Genetics*, **83**, 547-558.
- [22] Horváth J, Fliegau M, Olbrich H, Kispert A, King SM, Mitchison H, Zariwala MA, Knowles MR, Sudbrak R, Fekete G, Neesen J, Reinhardt R, Omran H. (2005) Identification and analysis of axonemal dynein light chain 1 in primary ciliary dyskinesia patients. *American Journal of Respiratory Cell and Molecular Biology*, **33**, 41-47.
- [23] Lancaster MA, Gleeson JG. (2009) The primary cilium as a cellular signaling center: lessons from disease. *Current Opinion in Genetics and Development*, **19**, 220-229.
- [24] Pfister KK, Fisher EM, Gibbons IR, Hays TS, Holzbaur EL, McIntosh JR, Porter ME, Schroer TA, Vaughan KT, Witman GB, King SM, Vallee RB. (2005) Cytoplasmic dynein nomenclature. *Journal of Cell Biology*, **171**, 411-413.
- [25] Vaisberg EA, Grissom PM, McIntosh JR. (1996) Mammalian cells express three distinct dynein heavy chains that are localized to different cytoplasmic organelles. *Journal of Cell Biology*, **133**, 831-842.
- [26] Tai C, Dujardin DL, Faulkner NE, Vallee RB. (2002) Role of dynein, dynactin, and CLIP-170 interactions in LIS1 kinetochore function. *Journal of Cell Biology*, **156**, 959-968.
- [27] Ajuh P, Kuster B, Panov K, Zomerdijk JC, Mann M, Lamond AI. (2000) Functional analysis of the human CDC5L complex and identification of its components by mass spectrometry. *EMBO Journal*, **19**, 6569-6581.
- [28] Payne C, Rawe V, Ramalho-Santos J, Simerly C, Schatten G. (2004) Preferentially localized dynein and perinuclear dynactin associate with nuclear pore complex proteins to mediate genomic union during mammalian fertilization. *Journal of Cell Science*, **116**, 4727-4738.
- [29] Byers HR, Maheshwary S, Amodeo DM, Dykstra SG. (2003) Role of cytoplasmic dynein in perinuclear aggregation of phagocytosed melanosomes and supranuclear melanin cap formation in human keratinocytes. *Journal of Investigative Dermatology*, **121**, 813-820.
- [30] Roghi C, Allan VJ. (1999) Dynamic association of cytoplasmic dynein heavy chain 1a with the Golgi apparatus and intermediate compartment. *Journal of Cell Science*, **112**, 4673-4685.

- [31] Navarro-Lérida I, Martínez MM, Roncal F, Gavilanes F, Albar JP, Rodríguez-Crespo I. (2004) Proteomic identification of brain proteins that interact with dynein light chain LC8. *Proteomics*, **4**, 339-346.
- [32] Ito D, Murata M, Watanabe K, Yoshida T, Saito I, Tanahashi N, Fukuuchi Y. (2000) C242T polymorphism of NADPH oxidase p22 PHOX gene and ischemic cerebrovascular disease in the Japanese population. *Stroke*, **31**, 936.
- [33] Hirokawa N, Noda Y, Okada Y. (1998) Kinesin and dynein superfamily proteins in organelle transport and cell division. *Current Opinion in Cell Biology*, **10**, 60-73.
- [34] Grissom PM, Vaisberg EA, McIntosh JR. (2002) Identification of a novel light intermediate chain (D2LIC) for mammalian cytoplasmic dynein 2. *Molecular Biology of the Cell*, **13**, 817-829.
- [35] Neesen J, Koehler MR, Kirschner R, Steinlein C, Kreutzberger J, Engel W, Schmid M. (1997) Identification of dynein heavy chain genes expressed in human and mouse testis: chromosomal localization of an axonemal dynein gene. *Gene*, **200**, 193-202.
- [36] Hou Y, Pazour GJ, Witman G B. (2004) A dynein light intermediate chain, D1bLIC, is required for retrograde intraflagellar transport. *Molecular Biology of the Cell*, **15**, 4382-4394.
- [37] Mikami A, Tynan SH, Hama T, Luby-Phelps K, Saito T, Crandall JE, Besharse JC, Vallee RB. (2003) Molecular structure of cytoplasmic dynein 2 and its distribution in neuronal and ciliated cells. *Journal of Cell Science*, **115**, 4801-4808.
- [38] Krock BL, Mills-Henry I, Perkins BD. (2009) Retrograde intraflagellar transport by cytoplasmic dynein-2 is required for outer segment extension in vertebrate photoreceptors but not arrestin translocation. *Investigative Ophthalmology and Vision Science*, **50**, 5463-5471.
- [39] Merrill AE, Merriman B, Farrington-Rock C, Camacho N, Sebald ET, Funari VA, Schibler MJ, Firestein MH, Cohn ZA, Priore MA, Thompson AK, Rimoin DL, Nelson SF, Cohn DH, Krakow D. (2009) Ciliary abnormalities due to defects in the retrograde transport protein DYNC2H1 in short-rib polydactyly syndrome. *American Journal of Human Genetics*, **84**, 542-549.
- [40] Chuang JZ, Yeh TY, Bollati F, Conde C, Canavosio F, Caceres A, Sung C. (2005) The dynein light chain Tctex-1 has a dynein-independent role in actin remodeling during neurite outgrowth. *Developmental Cell*, **9**, 75-86.
- [41] Horikawa I, Parker ES, Solomon GG, Barrett JC. (2001) Upregulation of the gene encoding a cytoplasmic dynein intermediate chain in senescent human cells. *Journal of Cell. Biochemistry*, **82**, 415-421.
- [42] Berrueta L, Tirnauer JS, Schuyler SC, Pellman D, Bierer BE. (1999) The APC-associated protein EB1 associates with components of the dynactin complex and cytoplasmic dynein intermediate chain. *Current Biology*, **9**, 425-428.
- [43] Ye GJ, Vaughan KT, Vallee RB, Roizma, B. (2000) The herpes simplex virus 1 U(L)34 protein interacts with a cytoplasmic dynein intermediate chain and targets nuclear membrane. *Journal of Virology*, **74**, 1355-1363.
- [44] Döhner K, Wolfstein A, Prank U, Echeverri C, Dujardin D, Vallee R, Sodeik B. (2002) Function of dynein and dynactin in Herpes simplex virus capsid transport. *Molecular Biology of the Cell*, **13**, 2795-2809.

- [45] Vaughan KT, Vallee RB. (1996) Cytoplasmic dynein binds dynactin through a direct interaction between the intermediate chains and p150Glued. *Journal of Cell Biology*, **131**, 1507-1516.
- [46] Mayya V, Lundgren DH, Hwang SI, Rezaul K, Wu L, Eng JK, Rodionov V, Han DK. (2009) Quantitative phosphoproteomic analysis of T cell receptor signaling reveals system-wide modulation of protein-protein interactions. *Science Signaling*, **18**, ra46.
- [47] Tynan SH, Purohit A, Doxsey SJ, Vallee RB. (2000) Light intermediate chain 1 defines a functional subfraction of cytoplasmic dynein which binds to pericentrin. *Journal of Biological Chemistry*, **275**, 32763-32768.
- [48] Bielli A, Thörnqvist PO, Hendrick AG, Finn R, Fitzgerald K, McCaffrey MW. (2001) The small GTPase Rab4A interacts with the central region of cytoplasmic dynein light intermediate chain-1. *Biochemical and Biophysical Research Communications*, **281**, 1141-1153.
- [49] Olsen JV, Blagoev B, Gnäd F, Macek B, Kumar C, Mortensen P, Mann M. (2006) Global, *in vivo*, and site-specific phosphorylation dynamics in signaling networks. *Cell*, **127**, 635-648.
- [50] Horgan CP, McCaffrey MW. (2011) Rab GTPases and microtubule motors. *Biochemical Society Transactions*, **39**, 1202-1206.
- [51] Hughes SM, Vaughan KT, Herskovits JS, Vallee RB. (1995) Molecular analysis of a cytoplasmic dynein light intermediate chain reveals homology to a family of ATPases. *Journal of Cell Science*, **108**, 17-24.
- [52] Benison G, Nyarko A, Barbar E. (2006) Heteronuclear NMR identifies a nascent helix in intrinsically disordered Dynein intermediate chain: implications for folding and dimerization. *Journal of Molecular Biology*, **362**, 1082-1093.
- [53] Goetz SC, Anderson KV. (2010) The primary cilium: a signalling centre during vertebrate development. *Nature Reviews Genetics*, **11**, 331-344.
- [54] Signor D, Wedaman KP, Orozco JT, Dwyer ND, Bargmann CI, Rose LS, Scholey JM. (1999) Role of a class DHC1b dynein in retrograde transport of IFT motors and IFT raft particles along cilia, but not dendrites, in chemosensory neurons of living *Caenorhabditis elegans*. *Journal of Cell Biology*, **147**, 519-530.
- [55] Dick T, Ray K, Salz HK, Chia W. (1996) Cytoplasmic dynein (*ddlc1*) mutations cause morphogenetic defects and apoptotic cell death in *Drosophila melanogaster*. *Molecular and Cellular Biology*, **16**, 1966-1977.
- [56] Rodríguez-Crespo I, Yélamos B, Roncal F, Albar JP, Ortiz de Montellano PR, Gavilanes F. (2001) Identification of novel cellular proteins that bind to the LC8 dynein light chain using a pepscan technique. *FEBS Letters*, **503**, 135-141.
- [57] Naisbitt S, Valtschanoff J, Allison DW, Sala C, Kim E, Craig AM, Weinberg RJ, Sheng M. (2000) Interaction of the postsynaptic density-95/guanylate kinase domain-associated protein complex with a light chain of myosin-V and dynein. *Journal of Neuroscience*, **20**, 4524-4534.
- [58] Puthalakath H, Villunger A, O'Reilly LA, Beaumont JG, Coultas L, Cheney RE, Huang DC, Strasser A. (2001) Bmf: a proapoptotic BH3-only protein regulated by interaction with the myosin V actin motor complex, activated by anoikis. *Science*, **293**, 1829-1832.

- [59] Day CL, Puthalakath H, Skea G, Strasser A, Barsukov I, Lian L, Huang D, Hinds MG. (2004) Localization of dynein light chains 1 and 2 and their pro-apoptotic ligands. *Biochemical Journal*, **377**, 597-605.
- [60] Vadlamudi RK, Bagheri-Yarmand R, Yang Z, Balasenthil S, Nguyen D, Sahin Aysegul A, den Hollander P, Kumar R. (2004) Dynein light chain 1, a p21-activated kinase 1-interacting substrate, promotes cancerous phenotypes. *Cancer Cell*, **5**, 575-585.
- [61] Bekri S, Adelaide J, Merscher S, Grosgeorge J, Caroli-Bosc F, Perucca-Lostanlen D, Kelley PM, Pebusque MJ, Theillet C, Birnbaum D, Gaudray P. (1998) Detailed map of a region commonly amplified at 11q13-->q14 in human breast carcinoma. *Cytogenetics and Cell Genetics*, **79**, 125-131.
- [62] Herzig RP, Andersson U, Scarpulla RC. (2000) Dynein light chain interacts with NRF-1 and EWG, structurally and functionally related transcription factors from humans and drosophila. *Journal of Cell Science*, **113**, 4263-4273.
- [63] Biswas M, Chan JY. (2010) Role of Nrf1 in antioxidant response element-mediated gene expression and beyond. *Toxicology and Applied Pharmacology*, **244**, 16-20.
- [64] Kaiser FJ, Tavassoli K, Van den Bemd GJ, Chang GT, Horsthemke B, Möröy T, Lüdecke HJ (2003) Nuclear interaction of the dynein light chain LC8a with the TRPS1 transcription factor suppresses the transcriptional repression activity of TRPS1. *Human Molecular Genetics*, **12**, 1349-1358.
- [65] Lo K, Kan H, Chan L, Xu W, Wang K, Wu Z, Sheng M, Zhang M. (2005) The 8-kDa dynein light chain binds to p53-binding protein 1 and mediates DNA damage-induced p53 nuclear accumulation. *Journal of Biological Chemistry*, **280**, 8172-8179.
- [66] Sironen RK, Karjalainen HM, Elo MA, Kaarniranta K, Törrönen K, Takigawa M, Helminen HJ, Lammi MJ. (2002) cDNA array reveals mechanosensitive genes in chondrocytic cells under hydrostatic pressure. *Biochimica Biophysica Acta*, **1591**, 45-54.
- [67] Wagner W, Fodor E, Ginsburg A, Hammer JA. (2006) The binding of DYNLL2 to myosin Va requires alternatively spliced exon B and stabilizes a portion of the myosin's coiled-coil domain. *Biochemistry*, **45**, 11564-11577.
- [68] Ng DC, Chan SF, Kok KH, Yam JW, Ching YP, Ng IO, Jin DY. (2006) Mitochondrial targeting of growth suppressor protein DLC2 through the START domain. *FEBS Letters*, **580**, 191-198.
- [69] Hódi Z, Németh AL, Radnai L, Hetényi C, Schlett K, Bodor A, Perczel A, Nyitray L. (2006) Alternatively spliced exon B of Myosin va is essential for binding the tail-associated light chain shared by dynein. *Biochemistry*, **45**, 12582-12595.
- [70] Ullmannova V, Popescu NC. (2006) Expression profile of the tumor suppressor genes DLC-1 and DLC-2 in solid tumors. *International Journal of Oncology*, **29**, 1127-1132.
- [71] Morales AA, Olsson A, Celsing F, Osterborg A, Jondal M, Osorio LM (2004) Expression and transcriptional regulation of functionally distinct Bmf isoforms in B-chronic lymphocytic leukemia cells. *Leukemia*, **18**, 41-47.
- [72] Wanschers B, van de Vorstenbosch R, Wijers M, Wieringa B, King SM, Fransen J. (2008) Rab6 family proteins interact with the dynein light chain protein DYNLRB1. *Cell Motility and Cytoskeleton*, **65**, 183-196.

- [73] Jiang J, Yu L, Huang X, Chen X, Li D, Zhang Y, Tang L, Zhao S. (2001) Identification of two novel human dynein light chain genes, DNLC2A and DNLC2B, and their expression changes in hepatocellular carcinoma tissues from 68 Chinese patients. *Gene*, **281**, 103-113.
- [74] Dedesma C, Chuang JZ, Alfinito PD, Sung CH. (2006) Dynein light chain Tctex-1 identifies neural progenitors in adult brain. *Journal of Comparative Neurology*, **496**, 773-786.
- [75] Douglas MW, Diefenbach RJ, Homa FL, Miranda-Saksena M, Rixon FJ, Vittone V, Byth K, Cunningham AL. (2004) Herpes simplex virus type 1 capsid protein VP26 interacts with dynein light chains RP3 and Tctex1 and plays a role in retrograde cellular transport. *Journal of Biological Chemistry*, **279**, 28522-28530.
- [76] Nagano F, Orita S, Sasaki T, Naito A, Sakaguchi G, Maeda M, Watanabe T, Kominami E, Uchiyama Y, Takai Y. (1998) Interaction of Doc2 with tctex-1, a light chain of cytoplasmic dynein. Implication in dynein-dependent vesicle transport. *Journal of Biological Chemistry*, **273**, 30065-30068.
- [77] Yeh TY, Peretti D, Chuang JZ, Rodriguez-Boulan E, Sung CH. (2007) Regulatory dissociation of Tctex-1 light chain from dynein complex is essential for the apical delivery of rhodopsin. *Traffic*, **7**, 1495-1502.
- [78] Schwarzer C, Barnikol-Watanabe S, Thinnes FP, Hilschmann N. (2002) Voltage-dependent anion-selective channel (VDAC) interacts with the dynein light chain Tctex1 and the heat-shock protein PBP74. *International Journal of Biochemistry and Cell Biology*, **34**, 1059-1070.
- [79] Machado RD, Rudarakanchana N, Atkinson C, Flanagan JA, Harrison R, Morrell NW, Trembath RC. (2004) Functional interaction between BMPR-II and Tctex-1, a light chain of Dynein, is isoform-specific and disrupted by mutations underlying primary pulmonary hypertension. *Human Molecular Genetics*, **12**, 3277-3286.
- [80] Ohka S, Matsuda N, Tohyama K, Oda T, Morikawa M, Kuge S, Nomoto A. (2004) Receptor (CD155)-dependent endocytosis of poliovirus and retrograde axonal transport of the endosome. *Journal of Virology*, **78**, 7186-7198.
- [81] Mueller S, Cao X, Welker R, Wimmer E. (2002) Interaction of the poliovirus receptor CD155 with the dynein light chain Tctex-1 and its implication for poliovirus pathogenesis. *Journal of Biological Chemistry*, **277**, 7897-7904.
- [82] Logarinho E, Bousbaa H. (2008) Kinetochore-microtubule interactions "in check" by Bub1, Bub3 and BubR1: The dual task of attaching and signalling. *Cell Cycle*, **7**, 1763-1768.
- [83] Doncic A, Ben-Jacob E, Einav S, Barkai N. (2009) Reverse engineering of the spindle assembly checkpoint. *PLoS One*, **4**(8):e6495.
- [84] Yasui D, Miyano M, Cai S, Varga-Weisz P, Kohwi-Shigematsu T. (2002) SATB1 targets chromatin remodelling to regulate genes over long distances. *Nature*, **419**, 641-645.
- [85] Lo KW, Kogoy JM, Pfister KK. (2007) The DYNLT3 light chain directly links cytoplasmic dynein to a spindle checkpoint protein, Bub3. *Journal of Biological Chemistry*, **282**, 11205-11212.
- [86] Yeh TY, Chuang JZ, Sung CH. (2005) Dynein light chain rp3 acts as a nuclear matrix-associated transcriptional modulator in a dynein-independent pathway. *Journal of Cell Science*, **118**, 3431-3443.

[87] Shimizu S, Konishi A, Kodama T, Tsujimoto Y. (2000) BH4 domain of antiapoptotic Bcl-2 family members closes voltage-dependent anion channel and inhibits apoptotic mitochondrial changes and cell death. *Proceedings of the National Academy of Sciences, USA*, **97**, 3100-3105.

[88] Shimizu S, Narita M, Tsujimoto Y. (1999) Bcl-2 family proteins regulate the release of apoptogenic cytochrome c by the mitochondrial channel VDAC. *Nature*, **399**, 483-487.

Appendix IV: Intra-Flagellar Transport Complexes

General ICT Components	Human or Equivalent	Ancillary Information / Interacts with
Anterograde Motors		
Kinesin-2 Heterodimer	KIF3A	KIF3A constrains β-catenin/Wnt signalling through ciliary and cytosolic mechanisms[1].
	KIF3B	
	KAP, KIFAP3	
Kinesin-2 Homodimer	KIF17	Ciliary proteins are required to activate Kinesin-2 by docking the motor to the IFT complex [2, 3, 4, 5]. Involved in photoreceptor outer segment development, co-localises with IFT yet its full role is yet to be determined[6].
Kinesin13	KIF24	Depolymerises microtubules[7-9], role with IFT complexes unknown.
Retrograde Motors		
Dynein		
Heavy Chain	DYNC2H1	
Intermediate Chain	DYNC111-DYNC112 (WDR34)[5, 11]	TAK1-associated suppressor of the IL-1R/TLR3/TLR4 -induced NF-Kappa-β activation pathway[11].
Light Intermediate Chain	DYNC2LL1	
Light Chain	DYNLL1	
Retrograde Complex		
IFT Complex A		
		Involved in functionally distinct zones in mechano-sensory cilia[12, 13].
IFT144,	WDR19[14]	
IFT140	IFT140	
IFT139	THM1, TTC21B	Required to restrict Sonic Hedgehog (Shh) activity[15].
IFT122/IFT122A	IFT122, WDR10[16]	Antagonises Shh pathway in the cilium, and controls ciliary localisation of Shh +/- regulators. Disruption results in tip accumulation of Gli2/Gli3 while blocking functionality of TULP3 . SuFu also localises to the cilium through IFT122 [17].
IFT121/ IFT121B	WDR35	Involved in vesicle trafficking, mutations cause short-ribbed polydactyly [18], required for mammalian ciliogenesis [19].
IFT43	IFT43	
Anterograde Complex		
IFT Complex B		
		The complex has been shown to function through the direct interaction of the IFT81 and IFT74/72 subunits[20].
IFT172	IFT172	Encoded by FLA11 , Interacts with <i>Chlamydomonas</i> microtubule end binding protein (EB1), believed to regulate IFT at the ciliary tip [21, 22].
IFT88	IFT88 (Polaris, T737)[23]	Involved in G1-S -phase transition where over-expression induces apoptosis[24]. Involved in spindle orientation in mitosis[25]. Role in Sonic Hedgehog signalling[26].
IFT81	IFT81[27]	Expressed in sensory neurons, localises at the base of cilium, interacts and co-localises with IFT-74 [28]. Interacts with basal body components, and CEP170 , regulating disassembly of the cilium[20, 29].
IFT80	IFT80 (WDR56)	Required for ciliary assembly and osteogenesis[30].
IFT74/IFT72	IFT74 (CCDC2)	Involved in ciliary function[20, 28] and disassembly under shear stress[31].
IFT70		Core component of IFT-B complex . Required for flagellar assembly [32] regulator of ciliary tubulin polyglutamylation [33].
IFT57	IFT57	Required for ciliary maintenance and regulates IFT Kinesin-2 dissociation in photoreceptors and generally required for efficient IFT transport[34].
IFT54	IFT54	
IFT52	IFT52, NGDS	Involved in cyto-kinesis and hypoxic response[35].
IFT46	IFT46, C11orf60	Involved in chondrocytes, regulating BMP expression[36].
IFT27	IFT27, RABL4	RAB-like-GTPase - small G-protein involved in cell-cycle control[37, 38].

IFT25	IFT25, HSPB11	Phospho-protein component[39], interacts with IFT27 [38, 40].
IFT22	RABL5	Address label for vesicle trafficking . Regulates the cellular pool size and the number of IFT particles in the flagellar compartment[41].
IFT20	IFT20	Highly dynamic, localising between the cilium, the centrosome and the Golgi complex where it travels along microtubules[42, 43]. Required for opsin trafficking and development of photo-receptors[44].
*Mutations in IFT components are linked in many disease processes. Modified and adapted from Ishikawa et al., (2011)[5]. For review of IFT see Absalon et al., (2008)[45], Julkowska et al., (2009)[46], Ou et al., (2007)[47], Goetz et al., (2010)[26], and Bhogaraju et al., (2013)[48].		

- [1] Silverman MA, Leroux MR. (2009) Intraflagellar transport and the generation of dynamic, structurally and functionally diverse cilia. *Trends in Cell Biology*, **9**, 306-316.
- [2] Ou G, Blacque OE, Snow JJ, Leroux MR, Scholey JM. (2005) Functional coordination of intraflagellar transport motors. *Nature*, **436**, 583-587.
- [3] Snow JJ, Ou G, Gunnarson AL, Walker MR, Zhou HM, Brust-Mascher I, Scholey JM. (2004) Two anterograde intraflagellar transport motors cooperate to build sensory cilia on *C. elegans* neurons. *Nature Cell Biology*, **6**, 1109-1113.
- [4] Dishinger JF, Kee HL, Jenkins PM, Fan, S, Hurd, TW, Hammond JW, Truong, YN, Margolis B, Martens JR, Verhey KJ. (2010) Ciliary entry of the kinesin-2 motor KIF17 is regulated by importin-beta2 and RanGTP. *Nature Cell Biology*, **12**, 703-710.
- [5] Ishikawa H, Marshall WF. (2011) Ciliogenesis: building the cell's antenna. *Nature Reviews Molecular and Cellular Biology*, **12**, 222-234.
- [6] Insinna C, Pathak N, Perkins B, Drummond I, Besharse JC. (2008) The homodimeric kinesin, Kif17, is essential for vertebrate photoreceptor sensory outer segment development. *Developmental Biology*, **316**, 160-170.
- [7] Blaineau C, Tessier M, Dubessay P, Tasse L, Crobu L, Pagès M, Bastien P. (2007) A novel microtubule-depolymerizing kinesin involved in length control of a eukaryotic flagellum. *Current Biology*, **17**, 778-782.
- [8] Dawson SC, Sagolla MS, Mancuso JJ, Woessner DJ, House SA, Fritz-Laylin L, Cande WZ. (2007) Kinesin-13 regulates flagellar, interphase, and mitotic microtubule dynamics in *Giardia intestinalis*. *Eukaryotic Cell*, **6**, 2354-2364.
- [9] Piao T, Luo M, Wang L, Guo Y, Li D, Li P, Snell WJ, Pan J. (2009) A microtubule depolymerizing kinesin functions during both flagellar disassembly and flagellar assembly in *Chlamydomonas*. *Proceedings of the National Academy of Sciences, USA*, **106**, 4713-4718.
- [10] Moores CA, Milligan RA. (2006) Lucky 13 - microtubule depolymerisation by kinesin-13 motors. *Journal of Cell Science*, **119**, 3905-3913.
- [11] Gao D, Wang R, Li B, Yang Y, Zhai Z, Chen DY. (2009) WDR34 is a novel TAK1-associated suppressor of the IL-1R/TLR3/TLR4-induced NF-kappaB activation pathway. *Cellular and Molecular Life Science*, **66**, 2573-2584.
- [12] Iomini C, Li L, Esparza JM, Dutcher SK. (2009) Retrograde intraflagellar transport mutants identify complex A proteins with multiple genetic interactions in *Chlamydomonas reinhardtii*. *Genetics*, **183**, 885-896.

- [13] Lee E, Sivan-Loukianova E, Eberl DF, Kernan MJ. (2008) An IFT-A protein is required to delimit functionally distinct zones in mechanosensory cilia. *Current Biology*, **18**, 1899-1906.
- [14] Lin B, White JT, Utleg AG, Wang S, Ferguson C, True LD, Vessella R, Hood L, Nelson PS. (2003) Isolation and characterization of human and mouse WDR19, a novel WD-repeat protein exhibiting androgen-regulated expression in prostate epithelium. *Genomics*, **82**, 331-342.
- [15] Stottmanna RW, Trana PV, Turbe-Doana A, Beier DR. (2009) Ttc21b is required to restrict sonic hedgehog activity in the developing mouse forebrain. *Developmental Biology*, **335**, 166-178.
- [16] Gross C, De Baere E, Lo A, Chang W, Messiaen L. (2001) Cloning and characterization of human WDR10, a novel gene located at 3q21 encoding a WD-repeat protein that is highly expressed in pituitary and testis. *DNA and Cell Biology*, **20**, 41-52.
- [17] Qin J, Lin Y, Norman RX, Ko HW, Eggenschwiler JT. (2011) Intraflagellar transport protein 122 antagonizes sonic hedgehog signaling and controls ciliary localization of pathway components. *Proceedings of the National Academy of Sciences, USA*, **108**, 1456-1461.
- [18] Mill P, Lockhart PJ, Fitzpatrick E, Mountford HS, Hall EA, Reijns MA, Keighren M, Bahlo M, Bromhead CJ, Budd P, Aftimos S, Delatycki MB, Savarirayan R, Jackson IJ, Amor DJ. (2011) Human and mouse mutations in WDR35 cause short-rib polydactyly syndromes due to abnormal ciliogenesis. *American Journal of Human Genetics*, **88**, 508-515.
- [19] Mill P, Hall E, Keighren M, Lawson K, Jackson I. (2009) 16-P011 Wdr35 is required for mammalian ciliogenesis and Hh responsiveness. *Mechanisms of Development*, **126**, S265.
- [20] Lucker BF, Behal RH, Qin H, Siron LC, Taggart WD, Rosenbaum JL, Cole DG. (2005) Characterization of the intraflagellar transport complex B core: direct interaction of the IFT81 and IFT74/72 subunits. *Journal of Biological Chemistry*, **280**, 27688-27696.
- [21] Pedersen LB, Miller MS, Geimer S, Leitch JM, Rosenbaum JL, Cole DG. (2005) *Chlamydomonas* IFT172 is encoded by FLA11, interacts with CrEB1, and regulates IFT at the flagellar tip. *Current Biology*, **15**, 262-266.
- [22] Mukhopadhyay S, Wen X, Chih B, Nelson CD, Lane WS, Scales SJ, Jackson PK. (2010) TULP3 bridges the IFT-A complex and membrane phosphoinositides to promote trafficking of G protein-coupled receptors into primary cilia. *Genes and Development*, **24**, 2180-2193.
- [23] Schrick JJ, Onuchic LF, Reeders ST, Korenberg J, Chen XN, Moyer JH, Wilkinson JE, Woychik RP. (1995) Characterization of the human homologue of the mouse Tg737 candidate polycystic kidney disease gene. *Human and Molecular Genetics*, **4**, 559-567.
- [24] Robert A, Margall-Ducos G, Guidotti J, Br gerie O, Celati C, Br chet C, Desdouets C. (2007) The intraflagellar transport component IFT88/polaris is a centrosomal protein regulating G1-S transition in non-ciliated cells. *Journal of Cell Science*, **120**, 628-637.
- [25] Delaval B, Bright A, Lawson ND, Doxsey S. (2011) The cilia protein IFT88 is required for spindle orientation in mitosis. *Nature Cell Biology*, **13**, 461-468.
- [26] Goetz SC, Anderson KV. (2010) The primary cilium: a signalling centre during vertebrate development. *Nature Reviews Genetics*, **11**, 331-344.
- [27] Higashi M, Kobayashi K, Iijima M, Wakana S, Horiuchi M, Yasuda T, Yoshida G, Kanmura Y, Saheki T. (2000) Genomic organization and mapping of mouse CDV (carnitine deficiency-associated gene expressed in ventricle)-1 and its related CDV-1R gene. *Mammalian Genome*, **11**, 1053-1057.

- [28] Kobayashi T, Gengyo-Ando K, Ishihara T, Katsura I, Mitani S. (2007) IFT-81 and IFT-74 are required for intraflagellar transport in *C. elegans*. *Genes and Cells*, **12**, 593-602.
- [29] Lamla S. (2009) *Functional Characterisation of the Centrosomal Protein Cep170*. Dissertation, Faculty of Biology, LMU München, <http://edoc.ub.uni-muenchen.de/9783/>.
- [30] Yang S, Wang C. (2012) The intraflagellar transport protein IFT80 is required for cilia formation and osteogenesis. *Bone*, **51**, 407-417.
- [31] Iomini C, Tejada K, Mo W, Vaananen H, Piperno G. (2004) Primary cilia of human endothelial cells disassemble under laminar shear stress. *Journal of Cell Biology*, **164**, 811-817.
- [32] Fan Z, Behal RH, Geimer S, Wang Z, Williamson SM, Zhang H, Cole DG, Qin H. (2010) *Chlamydomonas* IFT70/CrDYF-1 is a core component of IFT particle complex B and is required for flagellar assembly. *Molecular Biology of the Cell*, **21**, 2696-2706.
- [33] Pathak N, Obara T, Mangos S, Liu Y, Drummond IA. (2007) The zebrafish fleer gene encodes an essential regulator of cilia tubulin polyglutamylation. *Molecular Biology of the Cell*, **18**, 4353-4364.
- [34] Krock BL, Perkins BD. (2008) The intraflagellar transport protein IFT57 is required for cilia maintenance and regulates IFT-particle-kinesin-II dissociation in vertebrate photoreceptors. *Journal of Cell Science*, **121**, 1907-1915.
- [35] Brown JM, Fine NA, Pandiyan G, Thazhath R, Gaertig J. (2003) Hypoxia regulates assembly of cilia in suppressors of *Tetrahymena* lacking an intraflagellar transport subunit gene. *Molecular Biology of the Cell*, **14**, 3192-3207.
- [36] Gouttenoire J, Valcourt U, Bougault C, Aubert-Foucher E, Arnaud E, Giraud L, Mallein-Gerin F. (2007) Knockdown of the intraflagellar transport protein IFT46 stimulates selective gene expression in mouse chondrocytes and affects early development in zebrafish. *Journal of Biological Chemistry*, **282**, 30960-30973.
- [37] Hou Y, Qin H, Follit JA, Pazour GJ, Rosenbaum JL, Witman GB. (2007) Functional analysis of an individual IFT protein: IFT46 is required for transport of outer dynein arms into flagella. *Journal of Cell Biology*, **176**, 653-665.
- [38] Qin H, Wang Z, Diener D, Rosenbaum J. (2007) Intraflagellar transport protein 27 is a small G protein involved in cell-cycle control. *Current Biology*, **17**, 193-202.
- [39] Wang Z, Fan ZC, Williamson SM, Qin H. (2009) Intraflagellar transport (IFT) protein IFT25 is a phosphoprotein component of IFT complex B and physically interacts with IFT27 in *Chlamydomonas*. *PLoS One*, **4**(5):e5384.
- [40] Lehtreck K, Luro S, Awata J, Witman GB. (2009) HA-tagging of putative flagellar proteins in *Chlamydomonas reinhardtii* identifies a novel protein of intraflagellar transport complex B. *Cell Motility and the Cytoskeleton*, **66**, 469-482.
- [41] Silva DA, Huang X, Behal RH, Cole DG, Qin H. (2012) The RABL5 homolog IFT22 regulates the cellular pool size and the amount of IFT particles partitioned to the flagellar compartment in *Chlamydomonas reinhardtii*. *Cytoskeleton*, **69**, 33-48.
- [42] Yin G, Dai J, Ji C, Ni X, Shu G, Ye X, Dai J, Wu Q, Gu S, Xie Y, Zhao RC, Mao Y. (2003) Cloning and characterization of the human IFT20 gene. *Molecular Biology Reports*, **30**, 255-260.

- [43] Follit JA, Tuft RA, Fogarty KE, Pazour GJ. (2006) The intraflagellar transport protein IFT20 is associated with the Golgi complex and is required for cilia assembly *Molecular Biology of the Cell*, **17**, 3781-3792.
- [44] Keady BT, Le YZ, Pazour GJ. (2011) IFT20 is required for opsin trafficking and photoreceptor outer segment development. *Molecular Biology of the Cell*, **22**, 921-930.
- [45] Absalon S, Blisnick T, Kohl L, Toutirais G, Doré G, Julkowska D, Tavenet A, Bastin P. (2008) Intraflagellar transport and functional analysis of genes required for flagellum formation in trypanosomes. *Molecular Biology of the Cell*, **19**, 929-944.
- [46] Julkowska D, Bastin, P. (2009) Tools for analyzing intraflagellar transport in trypanosomes. *Methods in Cell Biology*, **93**, 59-80.
- [47] Ou G, Koga M, Blacque OE, Murayama T, Ohshima Y, Schafer JC, Li C, Yoder BK, Leroux MR, Scholey JM. (2007) Sensory ciliogenesis in *Caenorhabditis elegans*: assignment of IFT components into distinct modules based on transport and phenotypic profiles. *Molecular Biology of the Cell*, **18**, 1554-1569.
- [48] Bhogaraju S, Engel BD, Lorentzen E. (2013) Intraflagellar transport complex structure and cargo interactions. *Cilia*, **2**, 10.

Appendix V:

Kinesin and Dynein Motors Responsible for Organelle Processes and Transport

Organelle	Transport Configuration	Ancillary Information
		Possible reaction components
Endoplasmic Reticulum	Positioning involves kinesin-light-chain (kinesin-1)[1]. Trafficking involves dynein and dynactin associating with vesicles[2, 3]. Kinesin light-chain-1B[1] may be involved in ER-tubular extension and motility[4].	Rab18 [5].
ER Sub Compartments	Kinesin [6] couples ER sub-compartments to microtubules through interaction of COPII vesicles with dynactin and dynein [7], as well as being involved in bi-directional vesicle transport in dendrite sub-compartments [6].	Rab18 [5].
ER Exit Sites to Golgi	Kinesin-2 , KIF5B and KIF1C [1, 6, 8, 9] are required for bi-directional motility of materials at ER exit sites and for efficient ER-to-Golgi transport. Dynein and dynactin are required for effective ER exit site transport and traffic to the Golgi [10, 11].	COPII transport processes[1]. The Xklp protein subunit is involved in ER-Golgi transport [1,10]. Rab1 [5].
Golgi to ER Transport	Involves KIF5 and dynein/dynactin [1]. Bicaudal-D regulate COPI-Golgi-ER transport by recruiting the dynein-dynactin motor complex[1, 2, 12].	COPI transport processes[1], where kinesin-2 is involved in recycling[13]. Rab2 [5].
Golgi Apparatus (Golgi Positioning)	Positioning of the Golgi requires mysosin II , VI [14], KIFC3 and dynein/dynactin [1, 15]. Transport processes require KIF5 , KIF20 and KIF24A [2, 16], KIFC3 (kinesin-14B)[17] and dynein heavy chain-1a [18, 19]. Golgi regulation through GTP binding CDC42 for regulating dynein recruitment to COP1 -coated vesicles[3]. KIF13A is associated with the Golgi stacks [20].	Rab1 , Rab6 , Rab8 [14], Rab33 , Rab40 [5, 16]. Rab34 is a novel component involved the Golgi secretory pathway[21].
Golgi Intermediate Compartment	Kinesin-2 (KIF3A and either KIF3B or KIF3C)[22] and dynein (heavy-chain-1a) are believed to move the endoplasmic-reticulum-Golgi complex towards the centrosome [19].	Dynein dependent viral transfer from ER to Golgi [23].
trans-Golgi Network to Plasma Membrane	Secretion pathways to the apical plasma membrane of epithelia involve myosin , KIF1A (kinesin-3), KIF1B (kinesin-3), KIFC3 (kinesin-14B)[24,25], KIF5C (kinesin-1), KIF13A [4], KIF17 (kinesin-2), dynein and dynactin , while basolateral membrane transport involves myosin I , KIF1A , KIF5B (kinesin-1), KIF5C , KIF17 , dynein and dynactin , with GTPase Rab8 [1, 2, 5, 26]. KIF17 is also involved in the cilium[26].	TGN to membrane trafficking and membrane fusion is still poorly understood. Rab3 , Rab8 , Rab26 , Rab27 and Rab37 are involved in vesicle trafficking[5].
trans-Golgi Network to Endosome	Secretory endosomal trafficking involves KIF5B (kinesin-1)[1], KIF13A (kinesin-3)[27] and mysosin Ib [1]. Recycling endosomes and the TGN utilise KIF3B and dynein/dynactin [1, 28]. Involves dynein , dynactin and Nexins (NX1-6) , with SNX5/SNX6 interacting with the p150^{Glued} component of dynactin [29].	SNX1 interacts with the proposed TGN-localised tether Rab6 interacting protein-1[29]. Rab22 [5].
Golgi to Endoplasmic Reticulum transport	Little is known about regulation of the ER to Golgi transport intermediates and their microtubule interactions[30, 31]. Involvement of KIF5B (kinesin-1)[31,32], kinesin-2, KIF1C (kinesin-3), dynein [8], myosin II and dynactin [1].	Rab2 [5].
Golgi Derived Vesicles	Kinesin-2 [26] with dynein and dynactin are associated with COPI vesicle transport[3].	Rab22 and Rab37 [5].
Lysosomes	KIF3A , KIF1B and KIF5B with dynein and dynactin are involved in positioning[1]. KIF2β [33], KIF3A [22], KIF5 [34], KIF5B (involved in Lysosome distribution)[35, 36], with kinesin-2 [22] and dynein [37]. Arl8 and SKIP link Lysosomes to kinesin-1 [38].	Huntington protein mediates dynein positioning of Endosomes and Lysosomes [39]. Rab7 [5].
Late Lysosomes	Involvement of kinesin-2 (KIF3A and either KIF3B or KIF3C)[29], and dynein [37]. Dynein transfers late	Interacts with spectrin , dynactin , and ORP1 . Activation by Rab7 [40].

	Endosomes after interaction with β-Spectrin which requires lysosomal protein Rab7-RILP and ORP1L [40].	
Endosomes	Endosome bidirectional microtubule transport involves kinesin-3 , with dynein , dynactin and Lis1 accumulating at the microtubule (+) ends as a reservoir of inactive retrograde motor complexes[41]. KIF1A [40], KIF5B and KIFC1 [41], KIFC2 [7] and cytoplasmic dynein have a role in signalling[42, 43] as well as KIF3A/kinesin-2 [1, 22] and are required for retrograde endosome motility[39]. Rab7 controls (-) end directed motor complex with dynein/dynactin[40].	Rab7 mediates fusion between Early and Late Endosomes, and the Late Endosomes with Lysosomes[44]. Involves Rab7-RILP-p150^{Glued} [40].
Early Endosomes	Positioning involves myosin 1b , KIF5B (kinesin-1) , kinesin-2 , KIF16B (kinesin-3) [45], dynein/dynactin[1], where dynein binding controls motility [46]. Involvement of KIFC2 [47, 48], KIF16B [45], KIF3A and dynein [46, 47]. Dynein and dynactin participate in the Early Endosome [50, 51] with dynein required for sorting and morphogenesis [51]. Early endosome endocytotic recycling in the TGN involves myosin , KIF3B , dynein/dynactin [1]. Early Endosome endocytotic dynamics involve KIF3A , KIFC1 , KIF5B , and myosin [1].	Rab4 controls entry into the endocytotic pathway [5, 52]. Involvement of Rab5 [1], Rab4 , Rab22 , Rab21 and Rab15 [5]. KIF16B is involved in endosomal anchoring[53].
Late Endosomes	Positioning involves KIF3A (kinesin-2), KIF1B (kinesin-3), KIF5B (kinesin-1) and dynein/dynactin[1] as well as Kinesin-1 , KIF2B and dynein/dynactin[1]. KIF3A is needed for both Late endosome and for Lysosomes, but not for Early or Recycling endosomes[7]. Kinesin-2 (KIF3A and either KIF3B or KIF3C)[22] and dynein [37] are involved in late endosomal trafficking and are required for receptor sorting and the morphogenesis of the early endosome[51]. Late endosome/lysosome dynamics require myosin VIIa , kinesin-1 , KIF2B and dynein/dynactin [1].	KIF2B involved in mitotic fidelity and progression[54]. Rab7 and Rab9 are located in the late endosomes[5, 49].
Endosomal Anchoring	KIF16B is involved in receptor recycling[43, 45], while dynein is also required for receptor sorting and morphogenesis[51].	
Endosome Recycling	KIF3 [36] is responsible for Endosome delivery while dynein and dynactin are involved in retrograde recycling[1, 55]. Dynein/dynactin activity is regulated by the IKK ε-Kinase and KIF5B (kinesin-1) [1]. Endosome to Golgi transport sorting occurs via Nexin-1 and phosphoinositides [29]. Positioning involves KIF5B and dynein/dynactin[1], and KIF2B , myosin V and dynein/dynactin are involved in endosomal and lysosomal dynamics [1].	Rab11-FIP3 , Rab15 and Rab35 are required in recycling endosomes while Rab15 , Rab17 and Rab25 are found in apical recycling [1, 5, 47].
Endocytotic Vesicles	Kinesin-1 (KIF1) and KIFC2 (regulated by Rab4) are involved in transfer and fissioning of endocytotic vesicles [47, 48]. Late stage vesicles require dynein and kinesin for transport[48] and are closely associated with dynein , dynactin , Rab7 , and KIF3A [48]. Ligand containing endocytotic vesicles interact with the microtubule cytoskeleton via dynein [56].	Involvement with Rab5 , Rab15 , Rab33 [5]
Vesicles	KIF3A , KIF3B and KAP3 have a role in dendritic vesicle transport[4], while KIF5B and KIFC1 are required for motility and fission of early endocytic vesicles [7]. KIF4 is implicated in anterograde vesicle transport[57].	GLUT4 [49] vesicles associated with Rab8 , Rab10 and Rab14 . Golgi vesicles with Rab3 , Rab26 , Rab27 , and Rab37 [5].
*For a review of the cytoskeletal pathways involved in organelle positioning, secretory and endocytic pathways and the cytoskeleton see Anitei et al., (2010)[1] and Hirokawa et al., (2010)[36].		
Melanosomes	Movement involves myosin V [14], kinesin [58], KIF5 , KIF3 [2], and dynein [59], which co-localises with the Melanosome[60].	Regulated by RAB1A [61], RAB27A [44, 62], RAB32 and RAB38 [5].
Pigment Granules	Kinesin-2 [63] with Dynein has a role in centrosome independent microtubule organisation for	

	transport[59], and also in dynein-dependent nucleation of microtubules and pigment transport[63].	
Podosomes	KIF1C (kinesin-3 family) and dynein[64]. Involvement with MMPs and Golgi derived vesicles [64]. KIF9 is involved in regulating matrix breakdown in macrophage podosomes[65].	KIF1C binds myosin providing linkage to the actin cytoskeleton [64].
Desmosomes	Kinesin-1 and -2 members are needed to assemble Desmosomes whereas cadherins require kinesins (KIF3A) , which are involved in their assembly[66]. Lis1 , Ndel1 , and CLIP170 are involved in microtubule organisation for cortical desmosomes [67] that are controlled by centrosomal proteins [68].	Lis involved with Nudel at mother centriole [69]. Lis1 regulates osteoclast formation and interactions with Plekhm1 and dynein/dynactin[70].
Nuclear Membrane / Nuclear Matrix	Bicaudal D2 , dynein , and kinesin-1 are associated with nuclear pore complexes [71] with kinesin-1 and dynein also being involved in nuclear transport [72] and the bi-directional migration of nuclei [73, 74]. KIF4 [75], kinesin-1-light-chain Klc1/2 also transport viral capsids [76].	Bicaudal-D2 is involved in regulating centrosome and nuclear positioning during mitotic entry[71, 77]. Viral targeting the nucleus with dynein[78].
Nuclear Processes	Dynein and kinesin-1 are involved in moving[79] and rotating[80] the nucleus, with kinesin-1 involved with the pore complex [71]. KIF9 is involved in centrosome-nucleus positioning [81].	UNC-83 coordinates kinesin-1 and dynein for nuclear migration [79].
Cell Membrane	Dynein is required to localise apical membrane protein Crumbs and is involved in apico-basal polarity [82]. Also involved in the immunological synapse [83]. Kinesin-5B is necessary for delivery of membrane and FcγR mediated phagocytosis [84]. Dynein regulates immune synapse formation in T-cells where the MTOC is involved in transport of membrane receptors [83, 85]	Macropinosome utilises Rab5 and Rab34 , the early phagosome Rab5 , Rab14 and Rab22 , with caveoli utilising Rab5 [5].
Focal Adhesions	KIF1A is associated with Liprin-α1 , which influences the distribution of β1-integrins , stabilising their presence at the cell surface[86, 87]. Kinesin-1 modulates substrate adhesion through microtubule targeting [88], while the dynein intermediate chain is involved in focal adhesion dynamics[89]. Osteocyte cilia respond to fluid flow by increasing focal adhesions and AKT signaling pathways [90].	Kinesin transport is associated with cell adhesion processes[91].
Matrix Interactions	KIF5B and KIF3A/KIF3B drive MT1-MMP surface expression, CD44 shedding and matrix degradation in macrophages[92].	
Cilium / Basal Body	KIF3 , KIF17 [26], KIF7 [93]) and KIF24 (Interacts with CP110 and CEP97)[94].	Rab8 , Rab17 and Rab23 [5].
Intra Flagellar Transport	KIF3A , KIF3B [26], DHC1b [95] are involved with the cilium [96], specifically the heavy chain DHC1B [97] and light intermediate chain D1BLIC [98].	See Appendix III for ciliary associated kinesin motors.
Sonic Hedgehog	KIF7 [99, 100] promotes HedgeHog signalling [101, 102] in growth plate chondrocytes by restricting the inhibitory function of SuFu [93] and interacts with Gli transcription factors controlling proteolysis and stability[103].	
RNA Transport	KIF5 is involved in mRNA transport[104-106] (KIF5B and KIF5C are part of the RAN-BP2 complex [107]). RAN-BP2 is reported to be an activator of KIF5B [108]. RNA granule traffic is reported to occur through KIF3C [109] and dynein [110], while multiple kinesins are reported to transfer RNA cargoes in Oocytes [111]. KIF17B and TB-RBP transport cAMP regulator-RNAs in male germ-cells[112]. RNA localisation sequences regulate dynein/dynactin copy number for transcription cargoes[113], where transport can be mediated by dynein[114].	RNA binding occurs selectively via Egalitarian to the dynein motor[110].

DNA transport	KIFC1 transports double-stranded DNA[115].	
Cell Cycle Related	Kinesins (KIF23 [116]), and dynein [117] have a role in cell division [118]. CLIP170 is transported by kinesin and controls dynein activity, including microtubule stability [119].	KIF23 implicated in glioma cell division[116].
Mitotic Processes	Many motors are involved in nuclear processes[120], including nuclear breakdown [74]. Kinesin KLP-18 is required for the mitotic spindle[121]. KIF4A is involved in chromosomal segregation [75]. Bicaudal-D2 , dynein , and kinesin-1 regulate the centrosome and nuclear positioning during mitotic entry [71].	
Centrosome		
Centrosome Tensegrity	Dynein is involved in centrosome dynamics [122], where it regulates dynamic positioning and provides the appropriate cytoskeletal forces for the centrosome in interphase cells[122,123]. Bicaudal-D2 , dynein , and kinesin-1 are additionally involved in centrosome positioning [71].	Forces may be transduced via the cytoskeleton to the nucleus[124,125].
Ciliogenesis	CRB3 and CRB1 are localised to the cilium end for formation. Crumbs -associated Par3/Par6/aPKC 'polarity cassette' localises to the cilium and regulates ciliogenesis. Both CRB3 and the 'cassette' polarity proteins associate with KIF3 (kinesin-II) [126].	
Peri-Centrosomal Vesicle Recycling	Recycling in the peri-centrosome compartment involves myosin Vb , whose tail interacts with Rab11A , Rab11B and Rab25 [127]. ARF GTPase protein ASAP1 interacts with Rabb11 and FIP3 regulating pericentrosomal of the recycling endosome [128].	
Others		
Mitochondria	KIF1B [130-132], KIF5 , KIF5B [129, 133], and dynein [129, 134].	Rab32 [133].
Multi-vesicular bodies	Involves KIFC2 [48, 135] and dynein which are required for maturity progression [136].	
Synaptic vesicles	KIF1B (Charcot-Marie-Tooth syndrome)[137] and dynein , where loss of function of dynein is implicated in Alzheimer's Disease [138].	Charcot-Marie [137] and Alzheimers disease [138].
Cyto-skeletal shape	KIF9 interacts with GTPase Gem is involved in cytoskeleton remodelling[139] and couples the centrosome to the nucleus[140].	

[1] Anitei M, Hoflack B. (2011) Bridging membrane and cytoskeleton dynamics in the secretory and endocytic pathways. *Nature Cell Biology*, **14**, 11-19.

[2] Hirokawa N, Noda Y, Tanaka Y, Niwa S. (2009) Kinesin superfamily motor proteins and intracellular transport. *Nature Reviews Molecular and Cellular Biology*, **10**, 682-696.

[3] Chen JL, Fucini RV, Lacomis L, Erdjument-Bromage H, Tempst P, Stamnes M. (2005) Coatamer-bound Cdc42 regulates dynein recruitment to COPI vesicles. *Journal of Cell Biology*, **169**, 383-389.

[4] Woźniak MJ, Bola B, Brownhill K, Yang YC, Levakova V, Allan VJ. (2009) Role of kinesin-1 and cytoplasmic dynein in endoplasmic reticulum movement in VERO cells. *Journal of Cell Science*, **122**, 1979-1989.

[5] Stenmark H. (2009) Rab GTPases as coordinators of vesicle traffic. *Nature Reviews Molecular and Cellular Biology*, **10**, 513-525.

[6] Bannai H, Inoue T, Nakayama T, Hattori M, Mikoshiba K. (2004) Kinesin dependent, rapid, bi-directional transport of ER sub-compartment in dendrites of hippocampal neurons. *Journal of Cell Science*, **117**, 163-175.

- [7] Nath S, Bananis E, Sarkar S, Stockert RJ, Sperry AO, Murray JW, Wolkoff AW. (2007) Kif5B and Kifc1 interact and are required for motility and fission of early endocytic vesicles in mouse liver. *Molecular Biology of the Cell*, **18**, 1839-1849.
- [8] Le Bot N, Antony C, White J, Karsenti E, Vernos I. (1998) Role of xklp3, a subunit of the *Xenopus* kinesin II heterotrimeric complex, in membrane transport between the endoplasmic reticulum and the Golgi apparatus. *Journal of Cell Biology*, **143**, 1559-1573.
- [9] Gupta V, Palmer KJ, Spence P, Hudson A, Stephens DJ. (2009) Kinesin-1 (uKHC/KIF5B) is required for bidirectional motility of ER exit sites and efficient ER-to-Golgi transport. *Traffic*, **9**, 1850-1866.
- [10] Watson P, Forster R, Palmer KJ, Pepperkok R, Stephens DJ. (2005) Coupling of ER exit to microtubules through direct interaction of COPII with dynactin. *Nature Cell Biology*, **7**, 48-55.
- [11] Barr A, Egerer J. (2005) Golgi positioning are we looking at the right MAP? *Journal of Cell Biology*, **168**, 993-998.
- [12] Matanis T, Akhmanova A, Wulf P, Del Nery E, Weide T, Stepanova T, Galjart N, Grosveld F, Goud B, De Zeeuw CI, Barnekow A, Hoogenraad CC. (2002) Bicaudal-D regulates COPI-independent Golgi-ER transport by recruiting the dynein-dynactin motor complex. *Nature Cell Biology*, **4**, 986-992.
- [13] Stauber T, Simpson JC, Pepperkok R, Vernos I. (2006) A role for kinesin-2 in COPI-dependent recycling between the ER and the Golgi complex. *Current Biology*, **16**, 2245-2251.
- [14] Jordens I, Marsman M, Kuijl C, Neefjes J. (2005) Rab proteins, connecting transport and vesicle fusion. *Traffic*, **6**, 1070-1077.
- [15] Corthésy-Theulaz I, Pauloin A, Pfeffer SR. (1992) Cytoplasmic dynein participates in the centrosomal localization of the Golgi complex. *Journal of Cell Biology*, **118**, 1333-1345.
- [16] Echard A, Jollivet F, Martinez O, Lacapere JJ, Rousselet A, Janoueix-Lerosey I, Goud B. (1998) Interaction of a Golgi-associated kinesin-like protein with Rab6. *Science*, **279**, 580-585.
- [17] Hirokawa N, Noda Y. (2008) Intracellular transport and kinesin superfamily proteins, KIFs: structure, function, and dynamics. *Physiological Reviews*, **88**, 1089-1118.
- [18] Vaisberg EA, Grissom PM, McIntosh JR. (1996) Mammalian cells express three distinct dynein heavy chains that are localized to different cytoplasmic organelles. *Journal of Cell Biology*, **133**, 831-842.
- [19] Roghi C, Allan VJ. (1999) Dynamic association of cytoplasmic dynein heavy chain 1a with the Golgi apparatus and intermediate compartment. *Journal of Cell Science*, **112**, 4673-4685.
- [20] Lu L, Lee YR, Pan R, Maloof JN, Liu B. (2005) An internal motor kinesin is associated with the Golgi apparatus and plays a role in trichome morphogenesis in *Arabidopsis*. *Molecular Biology of the Cell*, **16**, 811-823.
- [21] Goldenberg NM, Grinstein S, Silverman M. (2007) Golgi-bound Rab34 is a novel member of the secretory pathway. *Molecular Biology of the Cell*, **18**, 4762-4771.
- [22] Brown CL, Maier KC, Stauber T, Ginkel LM, Wordeman L, Vernos I, Schroer TA. (2005) Kinesin-2 is a motor for late endosomes and lysosomes. *Traffic*, **6**, 1114-1124.

- [23] Ramanathan HN, Chung DH, Plane SJ, Sztul E, Chu YK, Guttieri MC, McDowell M, Ali G, Jonsson CB. (2007) Dynein-dependent transport of the hantaan virus nucleocapsid protein to the endoplasmic reticulum-Golgi intermediate compartment. *Journal of Virology*, **81**, 8634-8647.
- [24] Noda Y, Okada Y, Saito N, Setou M, Xu Y, Zhang Z, Hirokawa N. (2001) KIFC3, a microtubule minus end-directed motor for the apical transport of annexinXIIIb-associated Triton-insoluble membranes. *Journal of Cell Biology*, **155**, 77-88.
- [25] Bard F, Malhotra V. (2006) The formation of TGN-to-plasma-membrane transport carriers. *Annual Review of Cellular and Developmental Biology*, **22**, 439-455
- [26] Dishinger JF, Kee HL, Jenkins PM, Fan S, Hurd TW, Hammond JW, Truong YN, Margolis B, Martens JR, Verhey KJ. (2010) Ciliary entry of the kinesin-2 motor KIF17 is regulated by importin-beta2 and RanGTP. *Nature Cell Biology*, **12**, 703-710.
- [27] Nakagawa T, Setou M, Seog D, Ogasawara K, Dohmae N, Takio K, Hirokawa N. (2000) A novel motor, KIF13A, transports mannose- 6-phosphate receptor to plasma membrane through direct interaction with AP-1 complex. *Cell*, **103**, 569-581.
- [28] Wassmer T, Attar N, Harterink M, van Weering JR, Traer CJ, Oakley J, Goud B, Stephens DJ, Verkade P, Korswagen HC, Cullen PJ. (2009) The retromer coat complex coordinates endosomal sorting and dynein-mediated transport, with carrier recognition by the trans-Golgi network. *Developmental Cell*, **17**, 110-122.
- [29] Carlton J, Bujny M, Peter BJ, Oorschot VM, Rutherford A, Mellor H, Klumperman J, McMahon HT, Cullen PJ. (2004) Sorting nexin-1 mediates tubular endosome-to-TGN transport through coincidence sensing of high- curvature membranes and 3-phosphoinositides. *Current Biology*, **14**, 1791-1800.
- [30] Tomás M, Martínez-Alonso E, Ballesta J, Martínez-Menárguez JA. (2010) Regulation of ER-Golgi intermediate compartment tubulation and mobility by COPI coats, motor proteins and microtubules. *Traffic*, **11**, 616-625.
- [31] Lippincott-Schwartz J, Cole NB, Marotta A, Conrad PA, Bloom GS. (1995) Kinesin is the motor for microtubule-mediated Golgi to-ER membrane traffic. *Journal of Cell Biology*, **128**, 293-306.
- [32] Wozniak MJ, Allan VJ. (2006) Cargo selection by specific kinesin light chain 1 isoforms. *EMBO Journal*, **25**, 5457-5468.
- [33] Santama N, Krijnse-Locker J, Griffiths G, Noda Y, Hirokawa N, Dotti CG. (1998) KIF2 β , a new kinesin superfamily protein in non-neuronal cells, is associated with lysosomes and may be implicated in their centrifugal translocation. *EMBO Journal*, **17**, 5855-5867.
- [34] Nakata T, Hirokawa N. (1995) Point mutation of adenosine triphosphate-binding motif generated rigor kinesin that selectively blocks anterograde lysosome membrane transport. *Journal of Cell Biology*, **131**, 1039-1053.
- [35] Cardoso CMP, Groth-Pedersen L, Høyer-Hansen M, Kirkegaard T, Corcelle E, Andersen JS, Jäättelä M, Nylandsted J. (2009) Depletion of kinesin 5B affects lysosomal distribution and stability and induces peri-nuclear accumulation of autophagosomes in cancer cells. *PLoS One*, **4**(2):e4424.
- [36] Hirokawa N, Niwa S, Tanaka Y. (2010) Molecular motors in neurons: transport mechanisms and roles in brain function, development, and disease. *Neuron*, **68**, 610-638.

- [37] Tan SC, Scherer J, Vallee RB. (2010) Recruitment of dynein to late endosomes and lysosomes through light intermediate chains. *Molecular Biology of the Cell*, **22**, 467-477.
- [38] Rosa-Ferreira C, Munro S. (2011) Arl8 and SKIP act together to link lysosomes to kinesin-1. *Developmental Cell*, **21**, 1171-1178.
- [39] Caviston JP, Zajac AL, Tokito M, Holzbaur EL. (2011) Huntingtin coordinates the dynein-mediated dynamic positioning of endosomes and lysosomes. *Molecular Biology of the Cell*, **22**, 478-492.
- [40] Johansson M, Rocha N, Zwart W, Jordens I, Janssen L, Kuijl C, Olkkonen VM, Neefjes J. (2007) Activation of endosomal dynein motors by stepwise assembly of Rab7-RILP-p150Glued, ORP1L, and the receptor β III spectrin. *Journal of Cell Biology*, **176**, 459-471.
- [41] Lenz JH, Schuchardt I, Straube A, Steinberg G. (2006) A dynein loading zone for retrograde endosome motility at microtubule plus-ends. *EMBO Journal*, **25**, 2275-2286.
- [42] Ha J, Lo KW, Myers KR, Carr TM, Humsi MK, Rasoul BA, Segal RA, Pfister KK. (2008) A neuron-specific cytoplasmic dynein isoform preferentially transports TrkB signaling endosomes. *Journal of Cell Biology*, **181**, 1027-1039.
- [43] Schuster M, Kilaru S, Ashwin P, Lin C, Severs NJ, Steinberg G. (2011) Controlled and stochastic retention concentrates dynein at microtubule ends to keep endosomes on track. *EMBO Journal*, **30**, 652-664.
- [44] Itzstein C, Coxon FP, Rogers MJ. (2011) The regulation of osteoclast function and bone resorption by small GTPases. *Small GTPases*, **2:3**, 117-130.
- [45] Hoepfner S, Severin F, Cabezas A, Habermann B, Runge A, Gillooly D, Stenmark H, Zerial M. (2005) Modulation of receptor recycling and degradation by the endosomal kinesin KIF16B. *Cell*, **121**, 437-450.
- [46] Schuster M, Lipowsky R, Assmann MA, Lenz P, Steinberg G. (2011) Transient binding of dynein controls bidirectional long-range motility of early endosomes. *Proceedings of the National Academy of Sciences, USA*, **108**, 3618-3623.
- [47] Bananis E, Murray JW, Stockert RJ, Satir P, Wolkoff AW. (2003) Regulation of early endocytic vesicle motility and fission in a reconstituted system. *Journal of Cell Science*, **116**, 2749-2761.
- [48] Bananis E, Nath S, Gordon K, Satir P, Stockert RJ, Murray JW, Wolkoff AW. (2004) Microtubule-dependent movement of late endocytic vesicles *in vitro*: requirements for dynein and kinesin. *Molecular Biology of the Cell*, **15**, 3688-3697.
- [49] Imamura T, Huang J, Usui I, Satoh H, Bever J, Olefsky JM. (2003) Insulin-induced GLUT4 translocation involves protein kinase C-mediated functional coupling between Rab4 and the motor protein kinesin. *Molecular Biology of the Cell*, **23**, 4892-4900.
- [50] Flores-Rodriguez N, Rogers SS, Kenwright DA, Waigh TA, Woodman PG, Allan VJ. (2011) Roles of dynein and dynactin in early endosome dynamics revealed using automated tracking and global analysis. *PLoS One*, **6(9)**:e24479.
- [51] Driskell OJ, Mironov A, Allan VJ, Woodman PG. (2007) Dynein is required for receptor sorting and the morphogenesis of early endosomes. *Nature Cell Biology*, **9**, 113-120.

- [52] van der Sluijs P, Hull M, Webster P, Mâle P, Goud B, Mellman I. (1992) The small GTP-binding protein rab4 controls an early sorting event on the endocytic pathway. *Cell*, **70**, 729-740.
- [53] Blatner NR, Wilson MI, Lei C, Hong W, Murray D, Williams RL, Cho W. (2007) The structural basis of novel endosome anchoring activity of KIF16B kinesin. *EMBO Journal*, **26**, 3709-3719.
- [54] Manning AL, Bakhom SF, Maffini S, Correia-Melo C, Maiato H, Compton DA. (2010) CLASP1, astrin and Kif2b form a molecular switch that regulates kinetochore-microtubule dynamics to promote mitotic progression and fidelity. *EMBO Journal*, **29**, 3531-3543.
- [55] Ai E, Skop AR. (2009) Endosomal recycling regulation during cytokinesis. *Communicative Integrative Biology*, **2**, 444-447.
- [56] Oda H, Stockert RJ, Collins C, Wang H, Novikoff PM, Satir P, Wolkoff AW. (1995) Interaction of the microtubule cytoskeleton with endocytic vesicles and cytoplasmic dynein in cultured rat hepatocytes. *Journal of Biological Chemistry*, **270**, 15242-15249.
- [57] Peretti D, Peris L, Rosso S, Quiroga S, Caceres A. (2000) Evidence for the involvement of KIF4 in the anterograde transport of L1-containing vesicles. *Journal of Cell Biology*, **149**, 141-152.
- [58] Hara M, Yaar M, Byers HR, Goukassian D, Fine RE, Gonsalves J, Gilchrest BA. (2000) Kinesin participates in melanosomal movement along melanocyte dendrites. *Journal of Investigative Dermatology*, **114**, 438-443.
- [59] Reilein AR, Serpinskaya AS, Karcher RL, Dujardin DL, Vallee R.B, Gelfand VI. (2003) Differential regulation of dynein-driven melanosome movement. *Biochemical and Biophysical Research Communications*, **309**, 652-658.
- [60] Vancoillie G, Lambert J, Mulder A, Koerten HK, Mommaas AM, Van Oostveldt P, Naeyaert JM. (2000) Cytoplasmic dynein colocalizes with melanosomes in normal human melanocytes. *British Journal of Dermatology*, **143**, 298-306.
- [61] Ishida M, Ohbayashi N, Maruta Y, Ebata Y, Fukuda M. (2012) Functional involvement of Rab1A in microtubule-dependent anterograde melanosome transport in melanocytes. *Journal of Cell Science*, **125**, 5177-5187.
- [62] Hume AN, Collinson LM, Rapak A, Gomes AQ, Hopkins CR, Seabra MC. (2001) Rab27a regulates the peripheral distribution of melanosomes in melanocytes. *Journal of Cell Biology*, **152**, 795-808.
- [63] Tuma MC, Zill A, Le Bot N, Vernos I, Gelfand V. (1998) Heterotrimeric kinesin II is the microtubule motor protein responsible for pigment dispersion in *Xenopus* melanophores. *Journal of Cell Biology*, **143**, 1547-1558.
- [64] Kopp P, Lammers R, Aepfelbacher M, Woehlke G, Rudel T, Machuy N, Steffen W, Linder S. (2006) The kinesin KIF1C and microtubule plus ends regulate podosome dynamics in macrophages. *Molecular Biology of the Cell*, **17**, 2811-2823.
- [65] Cornfine S, Himmel M, Kopp P, El Azzouzi K, Wiesner C, Kruger M, Rudel T, Linder S. (2011) The kinesin KIF9 and reggie/flotillin proteins regulate matrix degradation by macrophage podosomes. *Molecular Biology of the Cell*, **22**, 202-215.
- [66] Nekrasova OE, Amargo EV, Smith WO, Chen J, Kreitzer GE, Green KJ. (2011) Desmosomal cadherins utilize distinct kinesins for assembly into desmosomes. *Journal of Cell Biology*, **195**, 1185-1203.

- [67] Sumigray KD, Chen H, Lechler T. (2011) Lis1 is essential for cortical microtubule organization and desmosome stability in the epidermis. *Journal of Cell Biology*, **194**, 631-641.
- [68] Sumigray KD, Lechler T. (2011) Control of cortical microtubule organization and desmosome stability by centrosomal proteins. *Bioarchitecture*, **1**, 221-225.
- [69] Guo J, Yang Z, Song W, Chen Q, Wang F, Zhang Q, Zhu X. (2006) Nudel contributes to microtubule anchoring at the mother centriole and is involved in both dynein dependent and - independent centrosomal protein assembly. *Molecular Biology of the Cell*, **17**, 680-689.
- [70] Sumigray KD, Chen H, Lechler T. (2011) Lis1 regulates osteoclast formation and function through its interactions with dynein/dynactin and Plekha1. *PLoS One*, **6**(11):e27285.
- [71] Splinter D, Tanenbaum ME, Lindqvist A, Jaarsma D, Flotho A, Yu KL, Grigoriev I, Engelsma D, Haasdijk ED, Keijzer N, Demmers J, Fornerod M, Melchior F, Hoogenraad CC, Medema RH, Akhmanova A. (2010) Bicaudal D2, dynein, and kinesin-1 associate with nuclear pore complexes and regulate centrosome and nuclear positioning during mitotic entry. *PLoS Biology*, **8**(4):e1000350.
- [72] Starr DA. (2011) Watching nuclei move: Insights into how kinesin-1 and dynein function together. *Bioarchitecture*, **1**, 9-13.
- [73] Fridolfsson HN, Starr DA. (2010) Kinesin-1 and dynein at the nuclear envelope mediate the bidirectional migrations of nuclei. *Journal of Cell Biology*, **191**, 115-128.
- [74] Tanenbaum ME, Akhmanova A, Medema RH. (2010) Dynein at the nuclear envelope. *EMBO Report*, **11**, 649.
- [75] Mazumdar M, Sundareshan S, Misteli T. (2004) Human chromokinesin KIF4A functions in chromosome condensation and segregation. *Journal of Cell Biology*, **166**, 613-620.
- [76] Strunze S, Engelke MF, Wang IH, Puntener D, Boucke K, Schleich S, Way M, Schoenenberger P, Burckhardt CJ, Greber UF. (2011) Kinesin-1-mediated capsid disassembly and disruption of the nuclear pore complex promote virus infection. *Cell Host and Microbe*, **10**, 210-223.
- [77] Tanenbaum ME, Akhmanova A, Medema RH. (2011) Bi-directional transport of the nucleus by dynein and kinesin-1. *Communicative and Integrative Biology*, **4**, 21-25.
- [78] Suikkanen S, Aaltonen T, Nevalainen M, Välikehto O, Lindholm L, Vuento M, Vihinen-Ranta M. (2003) Exploitation of microtubule cytoskeleton and dynein during parvoviral traffic toward the nucleus. *Journal of Virology*, **77**, 10270-10279.
- [79] Fridolfsson HN, Ly N, Meyerzon M, Starr DA. (2010) UNC-83 coordinates kinesin-1 and dynein activities at the nuclear envelope during nuclear migration. *Developmental Biology*, **338**, 237-250.
- [80] Wu J, Lee KC, Dickinson RB, Lele TP. (2011) How dynein and microtubules rotate the nucleus. *Journal of Cell Physiology*, **226**, 2666-2674.
- [81] Tikhonenko I, Magidson V, Gräf R, Khodjakov A, Koonce MP. (2012) A kinesin-mediated mechanism that couples centrosomes to nuclei. *Cellular and Molecular Life Sciences*, **70**, 1285-1296.
- [82] Li Z, Wang L, Hays TS, Cai Y. (2008) Dynein-mediated apical localization of crumbs transcripts is required for Crumbs activity in epithelial polarity. *Journal of Cell Biology*, **180**, 31-38.

- [83] Hashimoto-Tane A, Yokosuka T, Sakata-Sogawa K, Sakuma M, Ishihara C, Tokunaga M, Saito T. (2011) Dynein-driven transport of T cell receptor microclusters regulates immune synapse formation and T cell activation. *Immunity*, **34**, 919-931.
- [84] Silver KE, Harrison RE. (2010) Kinesin 5B is necessary for delivery of membrane and receptors during Fc γ R-mediated phagocytosis. *Journal of Immunology*, **186**, 816-825.
- [85] Wubbolts R, Fernandez-Borja M, Jordens I, Reits E, Dusseljee S, Echeverri C, Vallee RB, Neefjes J. (1999) Opposing motor activities of dynein and kinesin determine retention and transport of MHC class II-containing compartments. *Cell Science*, **112**, 785-795.
- [86] Asperti C, Pettinato E, de Curtis I. (2010) Liprin-alpha1 affects the distribution of low-affinity β 1 integrins and stabilizes their permanence at the cell surface. *Experimental Cell Research*, **316**, 915-926.
- [87] Shin H, Wyszynski M, Huh KH, Valtschanoff JG, Lee JR, Ko J, Streuli M, Weinberg RJ, Sheng M, Kim E. (2003) Association of the kinesin motor KIF1A with the multimodular protein liprin-alpha. *Journal of Biological Chemistry*, **278**, 11393-11401.
- [88] Krylyshkina O, Kaverina I, Kranewitter W, Steffen W, Alonso MC, Cross RA, Small, J.V. (2002) Modulation of substrate adhesion dynamics via microtubule targeting requires kinesin-1. *Journal of Cell Biology*, **156**, 349-359.
- [89] Rosse C, Boeckeler K, Linch M, Radtke S, Frith D, Barnouin K, Morsi AS, Hafezparast M, Howell M, Parker PJ. (2012) Binding of dynein intermediate chain 2 to paxillin controls focal adhesion dynamics and migration. *Journal of Cell Science*, **125**, 3733-3738.
- [90] Jeon O, Yoo Y, Kim K, Jacobs C, Kim C. (2011) Primary cilia-mediated osteogenic response to fluid flow occurs via increases in focal adhesion and Akt Signaling pathway in MC3T3-E1 osteoblastic cells. *Cellular and Molecular Bioengineering*, 1-10.
- [91] Kaverina IN, Minin AA, Gyoeva FK, Vasiliev JM. (1997) Kinesin-associated transport is involved in the regulation of cell adhesion. *Cell Biology International*, **21**, 229-236.
- [92] Wiesner C, Faix J, Himmel M, Bentzien F, Linder S. (2010) KIF5B and KIF3A/KIF3B kinesins drive MT1-MMP surface exposure, CD44 shedding, and extracellular matrix degradation in primary macrophages. *Blood*, **2116**, 1559-1569.
- [93] Hsu SH, Zhang X, Yu C, Li ZJ, Wunder JS, Hui CC, Alman BA. (2011) Kif7 promotes hedgehog signalling in growth plate chondrocytes by restricting the inhibitory function of Sufu. *Development*, **138**, 3791-3801.
- [94] Kobayashi T, Tsang WY, Li J, Lane W, Dynlacht BD. (2011) Centriolar kinesin Kif24 interacts with CP110 to remodel microtubules and regulate ciliogenesis. *Cell*, **145**, 914-925.
- [95] Signor D, Wedaman KP, Orozco JT, Dwyer ND, Bargmann CI, Rose LS, Scholey JM. (1999) Role of a class DHC1b dynein in retrograde transport of IFT motors and IFT raft particles along cilia, but not dendrites, in chemosensory neurons of living *Caenorhabditis elegans*. *Journal of Cell Biology*, **147**, 519-530.
- [96] Goetz SC, Anderson KV. (2011) The Primary Cilium: A signaling center during vertebrate development. *Nature Reviews Genetics*, **11**, 331-344.

- [97] Qin H, Diener DR, Geimer S, Cole DG, Rosenbaum JL. (2004) Intraflagellar transport (IFT) cargo: IFT transports flagellar precursors to the tip and turnover products to the cell body. *Journal of Cell Biology*, **164**, 255-266.
- [98] Hou Y, Pazour GJ, Witman GB. (2004) A dynein light intermediate chain, D1bLIC, is required for retrograde intraflagellar transport. *Molecular Biology of the Cell*, **15**, 4382-4394.
- [99] Liem KF, He M, Ocbina PJ, Anderson KV. (2009) Mouse Kif7/Costal2 is a cilia-associated protein that regulates Sonic hedgehog signalling. *Proceedings of the National Academy of Sciences, USA*, **106**, 13377-13382.
- [100] Dafinger C, Liebau MC, Elsayed SM, Hellenbroich Y, Boltshauser E, Korenke GC, Fabretti F, Janecke AR, Ebermann I, Nürnberg G, Nürnberg P, Zentgraf H, Koerber F, Addicks K, Elsobky E, Benzing T, Schermer B, Bolz HJ. (2011) Mutations in KIF7 link Joubert syndrome with Sonic Hedgehog signalling and microtubule dynamics. *Journal of Clinical Investigation*, **121**, 2662-2667.
- [101] Klejnot M, Kozielski F. (2012) Structural insights into human Kif7, a kinesin involved in Hedgehog signalling. *Acta Crystallographica D Biological Crystallography*, **68**, 154-159.
- [102] Ingham PW, McMahon AP. (2009) Hedgehog signalling: Kif7 is not that fishy after all. *Current Biology*, **19**, R729-R731.
- [103] Cheung HO, Zhang X, Ribeiro A, Mo R, Makino S, Puvion-Randall V, Law KK, Briscoe J, Hui CC. (2009) The kinesin protein Kif7 is a critical regulator of Gli transcription factors in mammalian hedgehog signalling. *Science and Signalling*, **2**, ra29.
- [104] Kanai Y, Dohmae N, Hirokawa N. (2004) Kinesin transports RNA: isolation and characterization of an RNA-transporting granule. *Neuron*, **43**, 513-525.
- [105] Hirokawa N, Takemura R. (2005) Molecular motors and mechanisms of directional transport in neurons. *Nature Reviews Neuroscience*, **6**, 201-214.
- [106] Hirokawa N. (2006) mRNA transport in dendrites: RNA granules, motors, and tracks. *Journal of Neuroscience*, **26**, 7139-7142.
- [107] Cai Y, Singh BB, Aslanukov A, Zhao H, Ferreira PA. (2001) The docking of kinesins, KIF5B and KIF5C, to Ran-binding protein 2 (RanBP2) is mediated via a novel RanBP2 domain. *Journal of Biological Chemistry*, **276**, 41594-41602.
- [108] Cho KI, Yi H, Desai R, Hand AR, Haas AL, Ferreira PA. (2009) RANBP2 is an allosteric activator of the conventional kinesin-1 motor protein, KIF5B, in a minimal cell-free system. *EMBO Report*, **10**, 480-486.
- [109] Davidovic L, Jaglin XH, Lepagnol-Bestel AM, Tremblay S, Simonneau M, Bardoni B, Khandjian EW. (2007) The fragile X mental retardation protein is a molecular adaptor between the neurospecific KIF3C kinesin and dendritic RNA granules. *Human and Molecular Genetics*, **16**, 3047-3058.
- [110] Dienstbier M, Boehl F, Li X, Bullock SL. (2009) Egalitarian is a selective RNA-binding protein linking mRNA localization signals to the dynein motor. *Genes and Development*, **23**, 1546-1558.
- [111] Messitt TJ, Gagnon JA, Kreiling JA, Pratt CA, Yoon YJ, Mowry KL. (2008) Multiple kinesin motors coordinate cytoplasmic RNA transport on a subpopulation of microtubules in *Xenopus* oocytes. *Developmental Cell*, **15**, 426-436.

- [112] Chennathukuzhi V, Morales CR, El-Alfy M, Hecht NB. (2003) The kinesin KIF17b and RNA-binding protein TB-RBP transport specific cAMP-responsive element modulator-regulated mRNAs in male germ cells. *Proceedings of the National Academy of Sciences, USA*, **100**, 15566-15571.
- [113] Amrute-Nayak M, Bullock SL. (2012) Single-molecule assays reveal that RNA localization signals regulate dynein-dynactin copy number on individual transcript cargoes. *Nature Cell Biology*, **14**, 416-423.
- [114] Gagnon JA, Kreiling JA, Powrie EA, Wood TR, Mowry KL. (2013) Directional transport is mediated by a dynein-dependent step in an RNA localization pathway. *PLoS Biology*, **11**(4):e1001551.
- [115] Farina F, Pierobon P, Delevoye C, Monnet J, Dingli F, Loew D, Quanz M, Dutreix M, Cappello G. (2013) Kinesin KIFC1 actively transports bare double-stranded DNA. *Nucleic Acids Research*, **41**, 4926-4937.
- [116] Takahashi S, Fusaki N, Ohta S, Iwahori Y, Iizuka Y, Inagawa K, Kawakami Y, Yoshida K, Toda M. (2011) Down regulation of KIF23 suppresses glioma proliferation. *Journal of Neurooncology*, **106**, 519-529.
- [117] Niclas J, Allan VJ, Vale RD. (1996) Cell cycle regulation of dynein association with membranes modulates microtubule-based organelle transport. *Journal of Cell Biology*, **133**, 585-593.
- [118] Karki S, Holzbaur EL. (1999) Cytoplasmic dynein and dynactin in cell division and intracellular transport. *Current Opinion in Cell Biology*, **11**, 45-53.
- [119] Carvalho P, Gupta ML, Hoyt M.A, Pellman D. (2004) Cell cycle control of kinesin-mediated transport of Bik1 (CLIP-170) regulates microtubule stability and dynein activation. *Developmental Cell*, **6**, 815-829.
- [120] Hirokawa N, Noda Y, Okada Y. (1998) Kinesin and dynein superfamily proteins in organelle transport and cell division. *Current Opinion in Cell Biology*, **10**, 60-73.
- [121] Segbert C, Barkus R, Powers J, Strome S, Saxton WM, Bossinger O. (2003) KLP-18, a Klp2 kinesin, is required for assembly of acentrosomal meiotic spindles in *Caenorhabditis elegans*. *Molecular Biology of the Cell*, **14**, 4458-4469.
- [122] Wu J, Misra G, Russell RJ, Ladd AJ, Lele TP, Dickinson RB. (2011) Effects of dynein on microtubule mechanics and centrosome positioning. *Molecular Biology of the Cell*, **22**, 4834-4841.
- [123] Ueda M, Gräf R, MacWilliams HK, Schliwa M, Euteneuer U. (1997) Centrosome positioning and directionality of cell movements. *Proceedings of the National Academy of Sciences, USA*, **94**, 9674-9678.
- [124] De Santis G, Lennon AB, Boschetti F, Verheghe B, Verdonck P, Prendergast PJ. (2011) How can cells sense the elasticity of a substrate? An analysis using a cell tensegrity model. *European Cell Materials*, **22**, 202-213.
- [125] Wang N, Tytell JD, Ingber DE. (2009) Mechanotransduction at a distance: mechanically coupling the extracellular matrix with the nucleus. *Nature Reviews Molecular and Cellular Biology*, **10**, 75-82.
- [126] Fan S, Hurd TW, Liu CJ, Straight SW, Weimbs T, Hurd EA, Domino SE, Margolis B. (2004) Polarity proteins control ciliogenesis via kinesin motor interactions. *Current Biology*, **14**, 1451-1461.

- [127] Lapierre LA, Kumar R, Hales C, Navarre J, Bhartur SG, Burnette JO, Provance DW, Mercer JA, Bahler M, Goldenring, J.R. (2001) Myosin Vb is associated with the plasma membrane recycling systems. *Molecular Biology of the Cell*, **12**, 1843-1857.
- [128] Inoue H, Ha VL, Prekeris R, Randazzo PA. (2008) Arf GTPase-activating protein ASAP1 interacts with Rab11 effector FIP3 and regulates pericentrosomal localization of transferrin receptor-positive recycling endosome. *Molecular Biology of the Cell*, **19**, 4224-4237.
- [129] Glater EE, Megeath LJ, Stowers RS, Schwarz TL. (2006) Axonal transport of mitochondria requires Milton to recruit kinesin heavy chain and is light chain independent. *Journal of Cell Biology*, **173**, 545-557.
- [130] Nangaku M, Sato-Yoshitake R, Okada Y, Noda Y, Takemura R, Yamazaki H, Hirokawa N. (1994) KIF1B, a novel microtubule plus end-directed monomeric motor protein for transport of mitochondria. *Cell*, **79**, 1209-1220.
- [131] Xu Y, Takeda S, Nakata T, Noda Y, Tanaka Y, Hirokawa N. (2002) Role of KIF3C motor protein in Golgi positioning and integration. *Journal of Cell Biology*, **158**, 293-303.
- [132] Pilling AD, Horiuchi D, Lively CM, Saxton WM. (2006) Kinesin-1 and Dynein are the primary motors for fast transport of mitochondria in *Drosophila* motor axons. *Molecular Biology of the Cell*, **17**, 2057-2068.
- [133] Cai Q, Gerwin C, Sheng ZH. (2005) Syntrophin-mediated anterograde transport of mitochondria along neuronal processes. *Journal of Cell Biology*, **170**, 959-969.
- [134] Varadi A, Johnson-Cadwell LI, Cirulli V, Yoon Y, Allan VJ, Rutter GA. (2004) Cytoplasmic dynein regulates the subcellular distribution of mitochondria by controlling the recruitment of the fission factor dynamin-related protein-1. *Journal of Cell Science*, **117**, 4389-4400.
- [135] Saito N, Okada Y, Noda Y, Kinoshita Y, Kondo S, Hirokawa N. (1997) KIF2C is a novel neuron-specific C-terminal type kinesin superfamily motor for dendritic transport of multivesicular body-like organelles. *Neuron*, **18**, 425-438.
- [136] Woodman PG, Futter CE. (2008) Multivesicular bodies: co-ordinated progression to maturity. *Current Opinion in Cell Biology*, **20**, 408-414.
- [137] Zhao C, Takita J, Tanaka Y, Setou M, Nakagawa T, Takeda S, Yang HW, Terada S, Nakata T, Takei Y, Saito M, Tsuji S, Hayashi Y, Hirokawa N. (2001) Charcot-Marie-Tooth disease type 2A caused by mutation in a microtubule motor KIF1B β . *Cell*, **105**, 587-597.
- [138] Kimura N, Okabayashi S, Ono F. (2012) Dynein dysfunction disrupts intracellular vesicle trafficking bidirectionally and perturbs synaptic vesicle docking via endocytic disturbances a potential mechanism underlying age-dependent impairment of cognitive function. *American Journal of Pathology*, **180**, 550-561
- [139] Piddini E, Schmid JA, de Martin R, Dotti CG. (2001) The Ras-like GTPase Gem is involved in cell shape remodelling and interacts with the novel kinesin-like protein KIF9. *EMBO Journal*, **20**, 4076-4087.
- [140] Tikhonenko I, Magidson V, Gräf R, Khodjakov A, Koonce MP. (2013) A kinesin-mediated mechanism that couples centrosomes to nuclei. *Cellular and Molecular Life Sciences*, **70**, 1285-1296.

Appendix VI: A Select Review of Tomography and Modelling

6.1 Overview of Select Tomography Studies on Matrix, Cilia, Flagella, Cytoskeleton and Organelles

Structure	Tomography Investigation
Extracellular Matrix	Proteoglycan complexes and collagen architecture in Sly Syndrome, Young et al., (2011)[1]. Interactions between collagen and proteoglycans (2010) bovine cornea[2]. Imaging of extracellular matrix polymers of collagen fibrillin microfibrils, Baldcock et al., (2002)[3]. Reconstruction of collagen bundles, Starborg et al., (2008)[4].
The Primary Cilium	Tomography of the primary cilium, basal body and matrix in <i>Gallus gallus</i> chick sternal cartilage. Details of the matrix of proteoglycans and collagens interacting with the ciliary membrane. Jensen et al., (2004)[5].
Motile Axoneme Components	Structural analysis of cilia/flagella by cryo-electron tomography, Bui et al., (2013)[6]. <i>Chlamydomonas</i> (9+2) axoneme architecture in detail by Lin et al., (2012)[7]. Structural arrangement of dynein motors in the <i>Chlamydomonas</i> axoneme, Bui et al., (2012)[8]. <i>Chlamydomonas</i> microtubule doublet structure and dynein-11 interactions, Heuser et al., (2012)[9]. <i>Tetrahymena</i> cilia structure in comparison to <i>Chlamydomonas</i> and sea urchin sperm, Pigino et al., (2012)[10]. <i>Trypanosoma brucei</i> flagellum, Höög et al., (2012)[11]. Radial spokes of (9+2) cilia and flagella, Pigino et al., (2011)[12]. Microtubule doublets in flagellar, Nicastro et al., (2011)[13]. <i>Chlamydomonas reinhardtii</i> structure of flagellar inner and outer dynein arms, Movassagh et al., (2010)[14]. Tomography and model of <i>Leishmania mexicana</i> amastigote flagellum, demonstrating flagella tip interaction Gluenz et al., (2010)[15]. Asymmetry of <i>Chlamydomonas</i> flagella inner dynein arms, Bui et al., (2009)[16]. Molecular architecture of inner dynein arms of <i>Chlamydomonas reinhardtii</i> Bui et al., (2008)[17]. <i>Chlamydomonas</i> outer dynein arms, Iskikawa et al., (2007)[18]. <i>C. reinhardtii</i> microtubules and outer dynein arms, Oda et al., (2007)[19]. Axoneme microtubule architecture details, Nicastro et al., (2006)[20]. Microtubule doublets of sea urchin <i>Strongylocentrotus purpuratus</i> by Sui et al., (2006)[21]. Sea urchins flagella, <i>Arbacia lixula</i> by Nicastro et al., (2005)[22]. Outer dynein arms of the <i>Monarthopalpus flavus</i> sperm axoneme, Lupetti et al., (2005)[23]. Axoneme microtubules McEwen et al., (2002)[23]. Reconstruction of a (9+2) axoneme from thick sections McEwen et al., (1986)[25].
Intra Flagella Transport	Analysis of IFT particles <i>in situ</i> (2009) in <i>Chlamydomonas reinhardtii</i> , Pigino et al., (2009)[26].
Centrosome	Microtubule and γ -tubulin structure of the centrosome of <i>C. elegans</i> , O'Toole et al., (2012)[27]. Murine CD4+ T-cell synapse, with Golgi located in proximity to centrosome, Ueda et al., (2011)[28]. <i>Chlamydomonas reinhardtii</i> centrosome, basal body, transition zone, alar sheets, doublets, γ -shape linkers. O'Toole et al., (2007)[29]. Detailing structurally different microtubule ends of the centrosome of <i>Caenorhabditis elegans</i> , O'Toole et al., (2003)[30]. High-voltage electron tomography of spindle pole bodies and early mitotic spindles in the yeast <i>Saccharomyces cerevisia</i> , O'Toole et al., (1999)[31]. Centrosome of early <i>Drosophila</i> embryos, Mortiz et al., (1995)[32]
Peri Centrosomal Matrix	O'Toole et al., (2012)[26] and Moritz et al., (1995)[33].
Basal Body	<i>Chlamydomonas reinhardtii</i> basal body and triplets, Esparza et al., (2013)[34]. Motile basal body, basal foot structure and alar sheets in motile cilia, Kunimoto et al., (2012)[35]. Basal body and triplet architecture revealed by cryo-tomography, Li et al., (2011)[36]. <i>Tetrahymena thermophila</i> transition zone basal body, Giddings et al., (2010)[37]. Tomography of the human centriole detailing basal appendages, microtubule triplets and internal luminal components, Ibrahim et al., (2009) [38]. Structures of the microtubule axoneme, γ -shaped linkers, alar sheets and basal body in <i>Chlamydomonas</i> , O'Toole et al., (2003)[39].

Centriole	Human procentriole formation and assembly, Guichard et al., (2010)[40].
Transition zone	Basal bodies in <i>Tetrahymena thermophila</i> , Giddings et al., (2010)[37].
Alar Sheets	Transition zone fibres by Kunimoto et al., (2012)[35]. O'Toole et al., (2007)[30].
Basal Appendage	Structural detail of basal foot Kunimoto et al., (2012) [35].
Microtubules	Microtubule associated TIP proteins, Höög et al., (2013)[41]. Microtubule structure in <i>Ashbya gossypii</i> , Gibeaux et al., (2012)[42]. Growing microtubule ends in yeast, Höög et al., (2011) [43]. Microtubules in situ, review, Koning et al., (2010) [44]. Structural and molecular basis for microtubule mechanical properties, Sui et al., (2010)[45]. Lattice structure of microtubules, McIntosh et al., (2009)[46]. Visualization of cell microtubules in their native state, Bouchet-Marquis et al., (2007) [47]. Morphologically distinct microtubule ends in the mitotic centrosome O'Toole et al., (2003) [29]. Mitotic spindle microtubule of <i>Saccharomyces cerevisiae</i> , O'Toole et al., (1999)[31]. Microtubule model, Nogales et al., (1999)[48].
Microtubule Associated Proteins (MAP)	MAP in bovine tubulin, Cope et al., (2010)[49]. MAP interactions, Schwartz et al., (2010)[50].
γ -TuRC / γ -TuSC	Microtubule ends in <i>C. elegans</i> embryos, O'Toole et al., (2009)[52]. Structure of the γ -TuRC, Moritz et al., (2000)[52]. Microtubule nucleation by γ -tubulin within the centrosome, Moritz et al., (1995)[33].
Intermediate filaments	Keratin filament networks, Sailer et al., (2010)[53]. Vimentin and keratin intermediate filaments, Norlén et al., (2007)[56]. Vimentin intermediate filaments, Goldie et al., (2007)[57].
Actin	Baculovirus induced actin polymerisation, Mueller et al., (2014)[56]. Amellipodium actin filaments of migrating keratocytes, Weichsel et al., (2012)[57]. Networks of actin filaments in lamellipodia, Urban et al., (2010)[58]. Actin network in cytokinesis, Reichl et al., (2008)[59]. Actin filaments, Weber et al., (2005)[60]. Actin filaments, Grim et al., (1997)[61].
Golgi Apparatus	Golgi apparatus, Han et al., (2013)[62]. Cisternae <i>cis</i> -Golgi assembly, COPI and COPII vesicles, Donohoe et al., (2013)[63]. RabA4b and PI-4K β 1-labeled <i>trans</i> -Golgi network in <i>Arabidopsis</i> Kang et al., (2011)[64]. Golgi bodies, Hendersen et al., (2007)[65]. Tomography of ER exit sites and COPII transport vesicles, Zeuschner et al., (2006)[66]. Golgi structure, Review, Marsh et al., (2005)[67]. Continuities between cisternae at different levels of the Golgi complex in mouse β -islet cells, Marsh et al., (2004)[68]. Secretion induces the formation of tubular structures across Golgi sub-compartments, Trucco et al., (2004)[69]. Golgi structure and function, Mogelsvang et al., (2004)[70]. Evidence for continuous turnover of Golgi cisternae in <i>Pichia pastoris</i> , Mogelsvang et al., (2003)[71]. ERGIC, Golgi structure and ribbon in NRK cells, Ladinsky et al., (2002)[72]. Golgi region of pancreatic β -cell line, HIT-T15, Marsh et al., (2001)[73]. Multiple transport mechanisms through the Golgi in the pancreatic β -cells, Marsh et al., (2001)[74].
Polarisation of the Golgi	Golgi structure and ribbons in rat kidney Ladinsky et al., (1999)[75]. Tomography of the <i>trans</i> -Golgi and vesicle coats in NRK cells, Ladinsky et al., (1994)[76]. Polarised centrosome delivering secretory granules in the immunological synapse, Stinchcombe et al., (2006)[77].
Transport Motors	Kinesin-14 microtubule interaction, Gonzalez et al., (2013)[78] Kinesin microtubule motor complexes, Cope et al., (2010)[49]. Dynein regulatory complex, Heuser et al., (2009)[79].
Membranes	Clathrin coated pits, Milosevic et al., (2011)[81]. Synaptic vesicle tethers, Fernández-Busnadiego, et al., (2010)[82].

Membrane Receptors	Membrane protein structure, Bartesaghi et al., (2009)[83]. Synaptic membrane of rat hippocampal neurons, Chen et al., (2008)[84]. Membrane-bound cellular organelles, O'Toole et al., (2003)[30].
Vesicles	Chemoreceptor arrays in <i>Escherichia coli</i> , Liu et al., (2012)[85]. Process of endocytosis, Kukulski et al., (2012)[86].
Receptor Cytosis	Synaptic vesicles, Raimondi et al., (2011)[87]. Integrin-mediated focal adhesion sites, Patla et al., (2010)[88]. Membrane molecular arrangement of receptor arrays, Chen et al., (2008)[89].
Ciliary Pocket	FcRn mediated antibody transport, He et al., (2008)[80].
Endoplasmic Reticulum	Vesicles in the ciliary pocket, cobblestone HUVEV cells, Geerts et al., (2011)[90]. <i>Trypanosoma brucei</i> architecture, flagellum, basal body and flagella pocket, Lacombe et al., (2009)[91].
Endosomal Compartment	Connections between the phagophore and endoplasmic reticulum, Ylä-Anttila et al., (2009) [92]. Organisation of the endoplasmic reticulum, Lu et al., (2009)[93].
Nuclear Pore Complexes	Endosomal compartment, Murk et al., (2003)[94].
Vesicles	Metazoan nuclear pore complex, Maimon et al.,(2010)[95]. Nuclear pore complexes, Beck et al., (2007)[96]. Nuclear pore complexes of <i>Dictyostelium discoideum</i> , Beck et al., (2004)[97] Cryo-electron tomography, Stoffler et al., (2003)[98]. Nuclear pore complex, Winey et al., (1997)[99].
Cell Cycle	Clathrin coated vesicles and cargo, Heymann et al., (2013)[100] Clathrin vesicle polyhedral protein structure, Heyman et al., (2008)[101]. Clathrin coated vesicles, Cheng et al., (2007)[102]. Coated vesicle, Zampighi et al., (2005)[103].
Further papers can be found at the University of Utrecht website,	The Centrosome Cell Cycle, Chrétien et al., (1997) [104].
http://www.electronmicroscopy.nl/research/publications.html	

[1] Young RD, Liskova P, Pinali C, Palka P, Palos M, Jirsova K, Hrdlickova E, Tesarova M, Elleder M, Zeman J, Meek KM, Knupp C, Quantock AJ. (2011) Large proteoglycan complexes and disturbed collagen architecture in the corneal extracellular matrix of mucopolysaccharidosis type VII (Sly syndrome). *Investigative Ophthalmology and Vision Science*, **52**, 6720-6728.

[2] Lewis PN, Pinali C, Young RD, Meek KM, Quantock AJ, Knupp C. (2010) Structural interactions between collagen and proteoglycans are elucidated by three-dimensional electron tomography of bovine cornea. *Structure*, **18**, 239-245.

[3] Baldock C, Gilpin CJ, Koster AJ, Ziese U, Kadler KE, Kielty CM, Holmes DF. (2002) Three-dimensional reconstructions of extracellular matrix polymers using automated electron tomography. *Journal of Structural Biology*, **138**, 130-136.

[4] Starborg T, Lu Y, Kadler KE, Holmes DF. (2008) Electron microscopy of collagen fibril structure *in vitro* and *in vivo* including three-dimensional reconstruction. *Methods in Cell Biology*, **88**, 319-345.

[5] Jensen CG, Poole CA, McGlashan SR, Marko M, Issa ZI, Vujcich KV, Bowser SS. (2004) Ultrastructural, tomographic and confocal imaging of the chondrocyte primary cilium *in situ*. *Cell Biology International*, **28**, 101-110.

[6] Bui KH, Ishikawa T. (2013) 3D structural analysis of flagella/cilia by cryo-electron tomography. *Methods in Enzymology*, **524**, 305-323.

[7] Lin J, Heuser T, Song K, Fu X, Nicastro D. (2012) One of the nine doublet microtubules of eukaryotic flagella exhibits unique and partially conserved structures. *PLoS One*, **7**(10):e46494.

- [8] Bui KH, Toshiki Y, Yamamoto R, Kamiy, R, Ishikawa T. (2012) Polarity and asymmetry in the arrangement of dynein and related structures in the *Chlamydomonas* axoneme. *Journal of Cell Biology*, **198**, 913-925.
- [9] Heuser T, Barber CF, Lin J, Krell J, Rebesco M, Porter ME, Nicastro D. (2012) Cryoelectron tomography reveals doublet-specific structures and unique interactions in the II dynein. *Proceedings of the National Academy of Sciences, USA*, **109**, E2067-E2076.
- [10] Pigino G, Maheshwari A, Bui KH, Shingyoji C, Kamimura S, Ishikawa T. (2012) Comparative structural analysis of eukaryotic flagella and cilia from *Chlamydomonas*, *Tetrahymena*, and sea urchins. *Journal of Structural Biology*, **178**, 199-206.
- [11] Höög JL, Bouchet-Marquis C, McIntosh JR, Hoenger A, Gull K. (2012) Cryo-electron tomography and 3-D analysis of the intact flagellum in *Trypanosoma brucei*. *Journal of Structural Biology*, **178**, 189-198.
- [12] Pigino G, Bui KH, Maheshwari A, Lupetti P, Diener D, Ishikawa T. (2011) Cryoelectron tomography of radial spokes in cilia and flagella. *Journal of Cell Biology*, **195**, 673-687.
- [13] Nicastro D, Fu X, Heuser T, Tso A, Porter ME, Linck R.W. (2011) Cryo-electron tomography reveals conserved features of doublet microtubules in flagella. *Proceedings of the National Academy of Sciences, USA*, **108**, E845-E853.
- [14] Movassagh T, Bui KH, Sakakibara H, Oiwa K, Ishikawa T. (2010) Nucleotide-induced global conformational changes of flagellar dynein arms revealed by *in situ* analysis. *Nature Structural and Molecular Biology*, **17**, 761-767.
- [15] Gluenz E, Hoog J, Smith AE, Dawe HR, Shaw MK, Gull K. (2010) Beyond 9+0: noncanonical axoneme structures characterize sensory cilia from protists to humans. *FASEB Journal*, **24**, 3117-3121.
- [16] Bui KH, Sakakibara H, Movassagh T, Oiwa K, Ishikawa T. (2009) Asymmetry of inner dynein arms and inter-doublet links in *Chlamydomonas* flagella. *Journal of Cell Biology*, **186**, 437-46.
- [17] Bui KH, Sakakibara H, Movassagh T, Oiwa K, Ishikawa T. (2008) Molecular architecture of inner dynein arms *in situ* in *Chlamydomonas reinhardtii* flagella. *Journal of Cell Biology*, **183**, 923-932.
- [18] Ishikawa T, Sakakibara H, Oiwa K. (2007) The architecture of outer dynein arms *in situ*. *Journal of Molecular Biology*, **368**, 1249-1258.
- [19] Oda T, Hirokawa N, Kikkawa M. (2007) Three-dimensional structures of the flagellar dynein-microtubule complex by cryoelectron microscopy. *Journal of Cell Biology*, **177**, 243-252.
- [20] Nicastro D, Schwartz C, Pierson J, Gaudette R, Porter ME, McIntosh JR. (2006) The molecular architecture of axonemes revealed by cryoelectron tomography. *Science*, **313**, 944-948.
- [21] Sui H, Downing KH. (2006) Molecular architecture of axonemal microtubule doublets revealed by cryo-electron tomography. *Nature*, **442**, 475-478.
- [22] Nicastro D, McIntosh JR, Baumeister W. (2005) 3D structure of eukaryotic flagella in a quiescent state revealed by cryo-electron tomography. *Proceedings of the National Academy of Sciences, USA*, **102**, 15889-15894.

- [23] Lupetti P, Lanzavecchia S, Mercati D, Cantele F, Dallai R, Mencarelli C. (2005) Three-dimensional reconstruction of axonemal outer dynein arms *in situ* by electron tomography. *Cell Motility*, **62**, 69-83.
- [24] McEwen BF, Marko M, Hsieh CE, Mannella C. (2002) Use of frozen-hydrated axonemes to assess imaging parameters and resolution limits in cryoelectron tomography. *Journal of Structural Biology*, **138**, 47-57.
- [25] McEwen BF, Radermacher M, Rieder CL, Frank J. (1986) Tomographic three-dimensional reconstruction of cilia ultrastructure from thick sections. *Proceedings of the National Academy of Sciences, USA*, **83**, 9040-9044.
- [26] Pigino G, Geimer S, Lanzavecchia S, Paccagnini E, Cantele F, Diener DR, Rosenbaum JL, Lupetti P. (2009) Electron-tomographic analysis of intraflagellar transport particle trains *in situ*. *Journal Cell Biology*, **187**, 135-148.
- [27] O'Toole E, Greenan G, Lange KI, Srayko M, Müller-Reichert T. (2012) The role of γ -tubulin in centrosomal microtubule organization. *PLoS One*, **7**(1):e29795.
- [28] Ueda H, Morphew MK, McIntosh JR, Davis MM. (2011) CD4⁺ T-cell synapses involve multiple distinct stages. *Proceedings of the National Academy of Sciences, USA*, **2108**, 17099-17104.
- [29] O'Toole ET, Giddings TH, Dutcher SK. (2007) Understanding microtubule organizing centers by comparing mutant and wild-type structures with electron tomography. *Methods in Cell Biology*, **79**, 125-143.
- [30] O'Toole ET, McDonald KL, Mäntler J, McIntosh JR, Hyman AA, Müller-Reichert T. (2003) Morphologically distinct microtubule ends in the mitotic centrosome of *Caenorhabditis elegans*. *Journal Cell Biology*, **163**, 451-456.
- [31] O'Toole ET, Winey M, McIntosh JR. (1999) High-voltage electron tomography of spindle pole bodies and early mitotic spindles in the yeast *Saccharomyces cerevisiae*. *Molecular Biology of the Cell*, **10**, 2017-2031.
- [32] Moritz M, Braunfeld MB, Fung JC, Sedat JW, Alberts BM, Agard DA. (1995) Three-dimensional structural characterization of centrosomes from early *Drosophila* embryos. *Journal Cell Biology*, **130**, 1149-1159.
- [33] Moritz M, Braunfeld MB, Sedat JW, Alberts B, Agard DA. (1995) Microtubule nucleation by gamma-tubulin-containing rings in the centrosome. *Nature*, **378**, 638-640.
- [34] Esparza JM, O'Toole E, Li L, Giddings TH, Kozak B, Albee AJ, Dutcher SK. (2013) Katanin localization requires triplet microtubules in *Chlamydomonas reinhardtii*. *PLoS One*, **8**(1):e53940.
- [35] Kunimoto K, Yamazaki Y, Nishida T, Shinohara K, Ishikawa H, Hasegawa T, Okanou T, Hamada H, Noda T, Tamura A, Tsukita S, Tsukita S. (2012) Coordinated ciliary beating requires Odf2-mediated polarization of basal bodies via basal feet. *Cell*, **148**, 189-200.
- [36] Li S, Fernandez JJ, Marshall WF, Agard DA. (2011) Three-dimensional structure of basal body triplet revealed by electron cryo-tomography. *EMBO Journal*, **31**, 552-562.
- [37] Giddings TH, Meehl JB, Pearson CG, Winey M. (2010) Electron tomography and immunolabeling of *Tetrahymena thermophila* basal bodies. *Methods in Cell Biology*, **96**, 117-141.

- [38] Ibrahim R, Messaoudi C, Chichon FJ, Celati C, Marco S. (2009) Electron tomography study of isolated human centrioles. *Microscopic Research Techniques*, **72**, 42-48.
- [39] O'Toole ET, Giddings TH, McIntosh JR, Dutcher SK. (2003) Three-dimensional organization of basal bodies from wild type delta tubulin deletion strains of *Chlamydomonas reinhardtii*. *Molecular Biology of the Cell*, **14**, 2999-3012.
- [40] Guichard P, Chrétien D, Marco S, Tassin AM. (2010) Procentriole assembly revealed by cryo-electron tomography. *EMBO Journal*, **29**, 1565-1572.
- [41] Höög JL, Huisman SM, Brunner D, Antony C. (2013) Electron tomography reveals novel microtubule lattice and microtubule organizing centre defects in +TIP mutants. *PLoS One*, **8**(4):e61698.
- [42] Gibeaux R, Lang C, Politi AZ, Jaspersen SL, Philippsen P, Antony C. (2012) Electron tomography of the microtubule cytoskeleton in multinucleated hyphae of *Ashbya gossypii*. *Journal of Cell Science*, **125**, 5830-5839.
- [43] Höög JL, Huisman SM, Sebö-Lemke Z, Sandblad L, McIntosh JR, Antony C, Brunner D. (2011) Electron tomography reveals a flared morphology on growing microtubule ends *Journal of Cell Science*, **124**, 693-698.
- [44] Koningm RI. (2010) Cryo-electron tomography of cellular microtubules. *Methods in Cell Biology*, **97**, 455-473.
- [45] Sui H, Downing KH. (2010) Structural basis of interprotofilament interaction and lateral deformation of microtubules. *Structure*, **18**, 1022-1031.
- [46] McIntosh JR, Morphew MK, Grissom PM, Gilbert SP, Hoenger A. (2009) Lattice structure of cytoplasmic microtubules in a cultured Mammalian cell. *Journal of Molecular Biology*, **394**, 177-182.
- [47] Bouchet-Marquis C, Zuber B, Glynn AM, Eltsov M, Grabenbauer M, Goldie KN, Thomas D, Frangakis AS, Dubochet J, Chrétien D. (2007) Visualization of cell microtubules in their native state. *Biology of the Cell*, **99**, 45-53.
- [48] Nogales E, Whittaker M, Milligan RA, Downing KH. (1999) High-resolution model of the microtubule. *Cell*, **96**, 79-88.
- [49] Cope J, Gilbert S, Rayment I, Mastronarde D, Hoenger A. (2010) Cryo-electron tomography of microtubule-kinesin motor complexes. *Journal of Structural Biology*, **170**, 257-265.
- [50] Schwartz CL, Bouchet-Marquis C, Dawson SC, Hoenger A. (2010) 3D Cryo-electron tomography studies on microtubule - MAP interactions *in vitro* and *in situ*. *Microscopy and Microanalysis*, **16**, 994-995.
- [51] O'Toole E, Müller-Reichert T. (2009) Electron tomography of microtubule end-morphologies in *C. elegans* embryos. *Methods in Molecular Biology*, **545**, 135-144.
- [52] Moritz M, Braunfeld MB, Guenebaut V, Heuser J, Agard DA. (2000) Structure of the γ -tubulin ring complex: a template for microtubule nucleation. *Nature Cell Biology*, **2**, 365-370.
- [53] Sailer M, Höhn K, Lück S, Schmidt V, Beil M, Walther P. (2010) Novel electron tomographic methods to study the morphology of keratin filament networks. *Microscopy and Microanalysis*, **16**, 462-471.

- [54] Norlén L, Masich S, Goldie KN, Hoenger A. (2007) Structural analysis of vimentin and keratin intermediate filaments by cryo-electron tomography. *Experimental Cell Research*, **313**, 2217-2227.
- [55] Goldie KN, Wedig T, Mitra AK, Aebi U, Herrmann H, Hoenger A. (2007) Dissecting the 3-D structure of vimentin intermediate filaments by cryo-electron tomography. *Journal of Structural Biology*, **158**, 378-385.
- [56] Mueller J, Pfanzelter J, Winkler C, Narita A, Le Clainche C, Nemethova M, Carlier MF, Maeda Y, Weich MD, Ohkawa T, Schmeiser C, Resch GP, Small V. (2014) Electron tomography and simulation of Baculovirus actin comet tails support a tethered filament model of pathogen propulsion. *PLoS Biology*, **12**(1):e1001765.
- [57] Weichsel J, Urban E, Small JV, Schwarz.S. (2012) Reconstructing the orientation distribution of actin filaments in the lamellipodium of migrating keratocytes from electron microscopy tomography data. *Cytometry A*, **81**, 496-507.
- [58] Urban E, Jacob S, Nemethova M, Resch GP, Small JV. (2010) Electron tomography reveals unbranched networks of actin filaments in lamellipodia. *Nature Cell Biology*, **12**, 429-435.
- [59] Reichl, EM, Ren Y, Morphew MK, Delannoy M, Effler JC, Girard KD, Divi S, Iglesias PA, Kuo SC, Robinson DN. (2008) Interactions between myosin and actin crosslinkers control cytokinesis contractility dynamics and mechanics. *Current Biology*, **18**, 471-480.
- [60] Weber I. (2005) Cryoelectron tomography: implications for actin cytoskeleton research. *Croatia Chemica Acta*, **78**, 325-331.
- [61] Grimm R, Bärmann M, Häckl W, Typke D, Sackmann E, Baumeister, W. (1997) Energy filtered electron tomography of ice-embedded actin and vesicles. *Biophysical Journal*, **72**, 482-489.
- [62] Han HM, Bouchet-Marquis C, Huebinger J, Grabenbauer M. (2013) Golgi apparatus analyzed by cryo-electron microscopy. *Histochemistry and Cell Biology*, **140**, 369-381.
- [63] Donohoe BS, Kang BH, Gerl MJ, Gergely ZR, McMichael CM, Bednarek SY, Staehelin LA. (2013) Cis-Golgi cisternal assembly and biosynthetic activation occur sequentially in plants and algae. *Traffic*, **14**, 551-67.
- [64] Kang BH, Nielsen E, Preuss ML, Mastrorarde D, Staehelin LA. (2011) Electron tomography of RabA4b- and PI-4K β 1-labeled trans Golgi network compartments in Arabidopsis. *Traffic*, **12**, 313-329.
- [65] Henderson GP, Gan L, Jensen GJ. (2007) 3-D ultrastructure of *O. tauri*: electron cryotomography of an entire eukaryotic cell. *PLoS One*, **2**(8):e749.
- [66] Zeuschner D, Geerts WJ, van Donselaar E, Humbel BM, Slot JW, Koster AJ, Klumperman J. (2006) Immuno-electron tomography of ER exit sites reveals the existence of free COPII-coated transport carriers. *Nature Cell Biology*, **8**, 377-383.
- [67] Marsh B.J. (2005) Lessons from tomographic studies of the mammalian Golgi. *Biochimica et Biophysica Acta*, **1744**, 273-292.
- [68] Marsh BJ, Volkmann N, McIntosh JR, Howell KE. (2004) Direct continuities between cisternae at different levels of the Golgi complex in glucose-stimulated mouse islet beta cells. *Proceedings of the National Academy of Sciences, USA*, **101**, 5565-5570.

- [69] Trucco A, Polishchuk RS, Martella O, Di Pentima A, Fusella A, Di Giandomenico D, San Pietro E, Beznoussenko GV, Polishchuk EV, Baldassarre M, Buccione R, Geerts WJ, Koster AJ, Burger KN, Mironov AA, Luini A. (2004) Secretory traffic triggers the formation of tubular continuities across Golgi sub-compartments. *Nature Cell Biology*, **6**, 1071-1081.
- [70] Mogelsvang S, Marsh BJ, Ladinsky MS, Howell KE. (2004) Predicting function from structure: 3D structure studies of the mammalian Golgi complex. *Traffic*, **5**, 338-345.
- [71] Mogelsvang S, Gomez-Ospina N, Soderholm J, Glick BS, Staehelin LA. (2003) Tomographic evidence for continuous turnover of Golgi cisternae in *Pichia pastoris*. *Molecular Biology of the Cell*, **14**, 2277-2291.
- [72] Ladinsky MS, Wu CC, McIntosh S, McIntosh JR, Howell KE. (2002) Structure of the Golgi and distribution of reporter molecules at 20 degrees C reveals the complexity of the exit compartments. *Molecular Biology of the Cell*, **13**, 2810-2825.
- [73] Marsh BJ, Mastronarde DN, Buttle KF, Howell KE, McIntosh JR. (2001) Organellar relationships in the Golgi region of pancreatic beta cell line, HIT-T15, visualized by high resolution electron tomography. *Proceedings of the National Academy of Sciences, USA*, **98**, 2399-2406.
- [74] Marsh BJ, Mastronarde DN, McIntosh JR, Howell KE. (2001) Structural evidence for multiple transport mechanisms through the Golgi in the pancreatic beta-cell line, HIT15. *Biochemical Society Transactions*, **29**, 461-467.
- [75] Ladinsky MS, Mastronarde DN, McIntosh JR, Howell KE, Staehelin LA. (1999) Golgi structure in three dimensions: functional insights from the normal rat kidney cell. *Journal Cell Biology*, **144**, 1135-1149.
- [76] Ladinsky MS, Kremer JR, Furcinitti PS, McIntosh JR, Howell KE. (1994) HVEM tomography of the trans-Golgi network: structural insights and identification of a lace-like vesicle coat. *Journal Cell Biology*, **127**, 29-38.
- [77] Stinchcombe JC, Majorovits E, Bossi G, Fulle, S, Griffiths GM. (2006) Centrosome polarization delivers secretory granules to the immunological synapse. *Nature*, **443**, 462-465.
- [78] Gonzalez MA, Cope J, Rank KC, Chen CJ, Tittmann P, Rayment I, Gilbert SP, Hoenger A. (2013) Common mechanistic themes for the powerstroke of kinesin-14 motors. *Journal of Structural Biology*, **184**, 335-344.
- [79] Heuser T, Raytchev M, Krell J, Porter ME, Nicastro D. (2009) The dynein regulatory complex is the nexin link and a major regulatory node in cilia and flagella. *Journal Cell Biology*, **187**, 921-933.
- [80] He W, Ladinsky MS, Huey-Tubman KE, Jensen GJ, McIntosh JR, Björkman PJ. (2008) FcRn-mediated antibody transport across epithelial cells revealed by electron tomography. *Nature*, **455**, 542-546
- [81] Milosevic I, Giovedi S, Lou X, Raimondi A, Collesi C, Shen H, Paradise S, O'Toole E, Ferguson S, Cremona O, De Camilli P. (2011) Recruitment of endophilin to clathrin-coated pit necks is required for efficient vesicle uncoating after fission. *Neuron*, **72**, 587-601.
- [82] Fernández-Busnadiego R, Zuber B, Maurer E, Cyrklaff M, Baumeister W, Lucic V. (2010) Quantitative analysis of the native presynaptic cytomatrix by cryoelectron tomography. *Journal Cell Biology*, **188**, 145-156.

- [83] Bartesaghi A, Subramaniam S. (2009) Membrane protein structure determination using cryo-electron tomography and 3D image averaging. *Current Opinion in Structural Biology*, **19**, 402-407.
- [84] Chen X, Winters CA, Reese TS. (2008) Life inside a thin section: tomography. *Journal of Neuroscience*, **28**, 9321-9327.
- [85] Liu J, Hu B, Morado DR, Jani S, Manson MD, Margolin W. (2012) Molecular architecture of chemoreceptor arrays revealed by cryoelectron tomography of Escherichia coli minicells. *Proceedings of the National Academy of Sciences, USA*, **109**, E1481-E1488.
- [86] Kukulsk, W, Schorb M, Kaksonen M, Briggs JA. (2012) Plasma membrane reshaping during endocytosis is revealed by time-resolved electron tomography. *Cell*, **150**, 508-520.
- [87] Raimondi A, Ferguson SM, Lou X, Armbruster M, Paradise S, Giovedi S, Messa M, Kono N, Takasaki J, Cappello V, O'Toole, E, Ryan TA, De Camilli P. (2011) Overlapping role of dynamin isoforms in synaptic vesicle endocytosis. *Neuron*, **70**, 1100-1114.
- [88] Patla I, Volberg T, Elad N, Hirschfeld-Warneken V, Grashoff C, Fässler R, Spatz JP, Geiger B, Medalia O. (2010) Dissecting the molecular architecture of integrin adhesion sites by cryo-electron tomography. *Nature Cell Biology*, **12**, 909-915.
- [89] Chen X, Winters C, Azzam R, Li X, Galbraith JA, Leapman RD, Reese TS. (2008) Organization of the core structure of the postsynaptic density. *Proceedings of the National Academy of Sciences, USA*, **105**, 4453-4458.
- [90] Geerts WJ, Vocking K, Schoonen N, Haarbosch L, van Donselaar EG, Regan-Klapisz E, Post JA. (2011) Cobblestone HUVECs: a human model system for studying primary ciliogenesis. *Journal of Structural Biology*, **176**, 350-359.
- [91] Lacomble S, Vaughan S, Gadelha C, Morphew MK, Shaw MK, McIntosh JR, Gull K. (2009) Three-dimensional cellular architecture of the flagellar pocket and associated cytoskeleton in trypanosomes revealed by electron microscope tomography. *Journal of Cell Science*, **122**, 1081-1090.
- [92] Ylä-Anttila P, Vihinen H, Jokitalo E, Eskelinen EL. (2009) 3D tomography dimensional cellular architecture of the between the phagophore and endoplasmic reticulum. *Autophagy*, **5**, 1180-1185.
- [93] Lu L, Ladinsky MS, Kirchhause, T. (2009) Cisternal organization of the endoplasmic reticulum during mitosis. *Molecular Biology of the Cell*, **20**, 3471-3480.
- [94] Murk JL, Humbel BM, Ziese U, Griffith JM, Posthuma G, Slot JW, Koster AJ, Verkleij AJ, Geuze HJ, Kleijmeer MJ. (2003) Endosomal compartmentalization in three dimensions: implications for membrane fusion. *Proceedings of the National Academy of Sciences, USA*, **100**, 13332-13337.
- [95] Maimon T, Medalia O. (2010) Perspective nuclear pore tomography on the metazoan nuclear pore complex. *Nucleus*, **1**, 383-386.
- [96] Beck M, Lucic V, Förster F, Baumeister W, Medalia O. (2007) Snapshots of nuclear pore complexes in action captured by cryo-electron tomography. *Nature*, **449**, 611-615.
- [97] Beck M, Forster F, Ecke M, Plitzko JM, Melchior F, Gerisch G, Baumeister W, Medalia O. (2004) Nuclear pore complex structure and dynamics revealed by cryoelectron tomography. *Science*, **306**, 1387-1390.

- [98] Stoffler D, Feja B, Fahrenkrog B, Walz J, Typke D, Aebi U. (2003) Cryo-electron tomography provides novel insights into nuclear pore architecture: implications for nucleocytoplasmic transport. *Journal of Molecular Biology*, **328**, 119-130.
- [99] Winey M, Yarar D, Giddings TH, Mastronarde, D.N. (1997) Nuclear pore complex number and distribution throughout the *Saccharomyces cerevisiae* cell cycle by three-dimensional reconstruction from electron micrographs of nuclear envelopes. *Molecular Biology of the Cell*, **8**, 2119-2132.
- [100] Heymann JB, Winkler DC, Yim YI, Eisenberg E, Greene LE, Steven AC. (2013) Clathrin-coated vesicles from brain have small payloads: a cryo-electron tomographic study. *Journal of Structural Biology*, **184**, 43-51.
- [101] Heymann JB, Winkler DC, Yim Y, Eisenberg E, Greene LE, Steven AC. (2008) Cryo-electron tomography of coated vesicles and modeling the polyhedral clathrin network. *Microscopy and Microanalysis*, **14**(Suppl 2), 1064-1065.
- [102] Cheng Y, Boll W, Kirchhausen T, Harrison SC, Walz T. (2007) Cryo-electron tomography of clathrin-coated vesicles: structural implications for coat assembly. *Journal of Molecular Biology*, **365**, 892-899.
- [103] Zampighi GA, Zampighi L, Fain N, Wright EM, Cantele F, Lanzavecchia S. (2005) Conical tomography II: A method for the study of cellular organelles in thin sections. *Journal of Structural Biology*, **151**, 263-274.
- [104] Chrétien D, Buendia B, Fuller SD, Karsenti E (1997) Reconstruction of the centrosome cycle from cryoelectron micrographs. *Journal of Structural Biology*, **120**, 117-133.

Appendix VII: Animation List

7.0 Animations of Data Acquisition, Processing and Modelling

The interpretation of tomogram datasets and models derived from them is best achieved through direct visualisation. Included in this Appendix are a series of animations depicting the steps of the processes of data acquisition, processing, tomogram formation leading to the final staged of model construction. Movies are in Audio Video Interleave (AVI) format and supplied on the DVD attached.

7.1 Tilt Series Data Acquisition

A series of aligned tilt series are presented which form the imaging component of forming a tomogram. It is not until these tilt series are reconstructed that the quality of the information and structures contained within the tilt series can be established. Tilt series movies include <**TiltSeriesB4-3.avi**>, <**TiltSeriesK10.avi**> and <**TiltSeriesCulturedChondrocyte.avi**>

7.2 Fiducial Tracking

Tomogram generation requires the use of gold particle fiducial markers to enable tracking through the tilt series to form a final stack alignment. Tracking is an iterative process to accurately produce a high quality stack. Tracking errors frequently occur in automated tracking processes, requiring careful manual inspection and correction. See <**Fidtrackone.avi**> and <**Fidtracktwo.avi**>.

7.3 Stack Generation

Tomogram presentation is in the z-axis stack usually in nanometre increments of sequential two dimensional images traversing the section, as demonstrated in <**StackTomogramB4.avi**>, <**StackK10.avi**> and <**StackD2.avi**>.

7.31 Stack Image Series

Visualisation of areas of interest within the stack allows inspection of finer intricate features of the dataset. <**StackAxoneme.avi**> and <**StackCentrosomeB4.avi**>.

7.4 Stack and Model

Modelling occurs through manual tracing and volume rendering structures of interest as they are bisected by the z-axis image sets. <**StackandModel.avi**> demonstrates the derivation of the model from the stack, while <**StackandModelWithRotation.avi**> places the 3D makeup of the model in perspective with respect to the stack.

7.5 Model Construction

Basic hand tracing of contour arrays outlining vesicles contained within the section making up the Golgi apparatus <**BasicStackGolgiModel.avi**> which is visualised as a basic wireframe model <**BasicWireFrameGolgi.avi**>. Once traced, each contour is inspected for accuracy <**BasicModellingCilium.avi**>.

7.6 Model Interrogation

Interpretation of model features of matrix granules < **ModelofMatrixGranule.avi**>, the Axoneme < **ModelofAxoneme.avi**> and the Matrix-Cilium-Golgi Continuum <**ModelMCGContinuum.avi**>.

7.7 Alternative Visualisation Approaches

A virtual microtubule based ‘primary cilium’ was extruded in Solidworks as to represent the anatomical features of the cilium model <**SolidWorksModel.avi**>.

7.8 Science Learning Hub Documentary

A mini documentary made for the Science Learning Hub ©2007-2014 at The University of Waikato <**3DMODELOFTHEPRIMARYCILIUMMASTER.mp4**>.

Available online from: <http://www.sciencelearn.org.nz/Contexts/Exploring-with-Microscopes/Sci-Media/Video/A-3D-model-of-the-primary-cilium>

7.9 Animation Quality

The .avi movie format permits modest levels of video compression, without loss of image quality from the original image frames. The addition of introductory titles and labels resulted in larger files, while post editing resulted in unnecessary lossy compression of animations.

As such, videos are presented in their basic raw format, to achieve optimal viewing quality and translation between operating systems and video codecs. For the best performance, it is recommended that animation files are transferred to the computer hard drive for viewing.

Appendix VIII: Poster Presentations

Jennings M, Parker K, Eccles M, Poole CA, McGlashan SR, Jensen CG. (2008) Fibroblast primary cilia in a sheep model of ARPKD. *Queenstown Molecular Biology Meeting: Molecular mechanisms of kidney disease, Queenstown* August 31-September 3rd (Funded by a travel grant from the Maurice and Phyllis Paykel Trust).

Jennings M, Parker K, Eccles M, Poole CA. (2009) Tomography of primary cilia in connective tissue cells from an ovine model of autosomal recessive polycystic kidney disease. *Asian and Pacific Congress on Electron Tomography*, Brisbane, Australia.

Jennings M, Parker K, Eccles M, Poole CA. (2009) Tomography of primary cilia in connective tissue cells from an ovine model of autosomal recessive polycystic kidney disease. *Biennial meeting of Microscopy New Zealand*, Rotorua.

*Jennings M, Poole CA, Walker RJ, Mitchell A, Easingwood R, Harland D, Walls R. (2010) Electron tomographic model of the Matrix-Cilium-Golgi continuum in hyaline chondrocytes. (poster) *Triennial FASEB Summer Research Conference on the Biology of Cilia and Flagella*, Vermont, USA.

*Poole T, Jennings M, Walker R.J (2012) Modelling the Matrix-Cilium-Golgi continuum in hyaline chondrocytes by electron tomography. *Cilia*, **1**, P39.

*NB: These posters have been presented many times.

Images of Nanotechnology Competition 2012

An image was entered into the *Images of Nanotechnology Competition* held by The MacDiarmid Institute, for advanced Materials and Nanotechnology, titled 'The Primary Cilium - a Cellular Nanoswitch'. It was awarded first prize, and received media attention.



Television Three News, coverage at the Gus Fisher Gallery, Auckland New Zealand, 2013.

See Figure 3.41

Modelling the Matrix-Cilium-Golgi Continuum in Hyaline Chondrocytes by Electron Tomography

CAPoole, M Jennings, RJ Walker

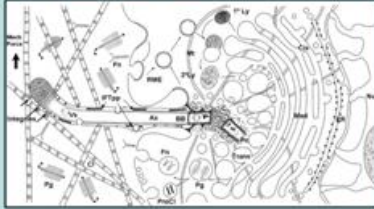
Department of Medicine, Dunedin School of Medicine, University of Otago, Dunedin, New Zealand

INTRODUCTION

The primary cilium is a single cytoplasmic organelle found in virtually all vertebrate cells^{1,2}. It consists of two parts (see figure below): a membrane-coated axeme (Ax) that projects from the cell surface into the extracellular microenvironment (ECM), and an intracellular basal body (BB) that comprises the most mature of the two centrosomes (CCs & NCI) located within the centrosome (CC).

The centrosome represents the Microtubule (MT) Organising Centre of the cell, and assembly of the microtubule network is essential for the differentiation of the Golgi apparatus into functional cis, medial and trans compartments. In connective tissue cells, the cilium interacts directly with the collagen fibres (CF), fibronectin (FN) and proteoglycans (PG) of the extracellular matrix via integrin receptors (IntR), introduced into the cilium membrane via vesicles (V) transported into the axeme on intracellular transport vesicles (IV) (Fig 1).

Vesicles formed by receptor mediated endocytosis (RME) at the base of the cilium fuse with primary lysosomes (PL) to form secondary lysosomes (SL), which are recycled into the Golgi network. Mechanical tensile forces (Mach For) transmitted via the collagen network result in bending of the cilium and initiation of signal transduction. (Nu, nucleus; ER, endoplasmic reticulum; Golgi, Golgi apparatus).



CONNECTIVE TISSUE PRIMARY CILIA

The ultrastructure of connective tissue primary cilia is well characterized and shows a physical continuum between the biomechanically functional extracellular matrix, the mechanosensory primary cilium, and the polarized Golgi secretory response required to create a mechanically effective connective tissue matrix. However, transmission electron microscopy essentially provides a two dimensional perspective of the cilium, and very few studies have attempted the precise 3D reconstructions required to re-create a three dimensional perspective of the primary cilium and its interaction with the extracellular matrix. Our objective was to create an ultrastructurally accurate, tomographic representation of the Matrix - Cilium - Golgi - Continuum in connective tissue cells.

METHODS

Chick embryo sternal chondrocytes have been developed as a model connective tissue to investigate the Matrix - Cilium - Golgi - Continuum. Slices were harvested at 15 days, and optimally fixed in glutaraldehyde and osmium tetroxide containing ruthenium hexamine tetroxide to stabilize matrix proteoglycans. Data in embedded samples were sectioned at 200nm, prepared for electron tomography and examined in a Techni G2 700 electron microscope. Tomographic models were prepared using IMOD. The model was composed of 300 axial slices containing 2211 voxels of 340 megapixels size.

RESULTS

Proteoglycan granules in the extracellular matrix consist of multiple minor proteoglycans traced three dimensionally to link up on the cilium membrane. These receptor mediated laterally connectors were matched by protein complexes connecting the cilium membrane to axemal microtubule doublets, each coated with multiple microtubule-associated proteins. Axemal doublets varied in position and length, and were limited relative to the microtubule triplets of the basal body. Transitional fibers link the distal end of the basal centrosome to the cilium membrane at the cilium junction, while basal feet proteins span three triplets of the basal centrosome but extend centripetally to anchor the microtubule tertiary network. The proximal end of the basal centrosome is linked to the proximal centrosome, which lacks appendages, but has protein linkages to nuclear pores in the nuclear membrane. The microtubule organizing centrosome is surrounded by polarized cis, medial and trans Golgi compartments involved in the post-translational modification of collagen, proteoglycans and glycosaminoglycans prior to translocation into the pericellular microenvironment at the cilium membrane.

CONCLUSION

We have developed an integrated, anatomically accurate, tomographic model of the matrix-cilium-golgi continuum in chondrocytes. It provides a new interactive tool to potentially examine the relationship between primary cilia ultrastructure and the cilium problems in connective tissue cells, and will be used in the future to investigate the functional relationship between the sensory cilium of connective tissue cells and the mechanically responsive extracellular matrix they produce.

REFERENCES

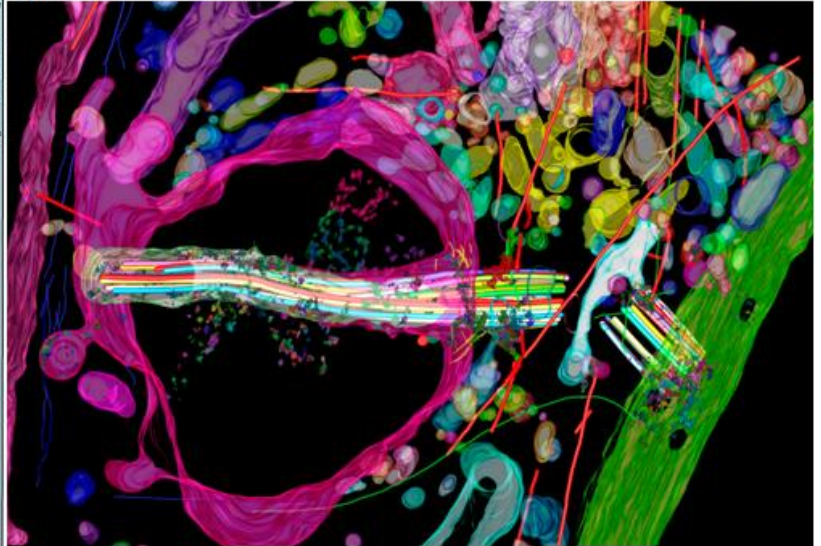
- 1) Patel CD, Rivlin AS, Bergman BL. Analysis of the morphology and function of primary cilia in mammalian tissues: a cellular systems approach. *Cell Mol Life Sci* 2002; 519:1-10.
- 2) Patel CD, Jensen CC, Ryan JJ, Day CC, Hernandez VL, Ulfelder DJ. Distal extension of primary cilia structure and relationship to the Golgi apparatus in mammalian tissues. *Cell Mol Life Sci* 2007; 519:10-20.
- 3) McCann BR, Jensen CC, Patel CD. Localization of extracellular matrix receptors on the mammalian primary cilium. *Int J Biochem Cell Biol* 2002; 34:101-110.
- 4) Jensen CC, Patel CD. The relationship of a golgi-derived microtubule network. *Biochem Biophys Res Commun* 2003; 303:103-112. <http://www.sciencedirect.com>.

ACKNOWLEDGEMENTS

Deep Centre for Biotech (Univ. of Otago) and Health Research, University of Otago
 CLF to James Cook Research Fellow at the Royal Society of New Zealand
 RESEARCH COORDINATOR: Sue Peeler, PhD - Otago Health Research Centre

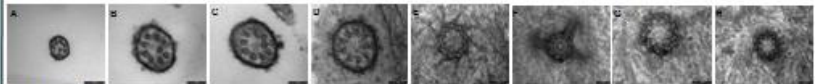
The Matrix-Cilium-Golgi-Continuum

An oblique view of the local cellular environment of the cilium and centrosome. The basal microtubule doublets of the cilium are oriented from the basal body. The centrosome is oriented from the basal body and the surrounding proximal centrosome. Note the centrosome of the cilium, the cilium, the Golgi apparatus, vesicles, cis, medial and trans compartments are oriented for the polarized and regulated secretion of matrix components. Note the centrosome of the cilium, the cilium, the Golgi apparatus, vesicles, cis, medial and trans compartments are oriented for the polarized and regulated secretion of matrix components. Note the centrosome of the cilium, the cilium, the Golgi apparatus, vesicles, cis, medial and trans compartments are oriented for the polarized and regulated secretion of matrix components.



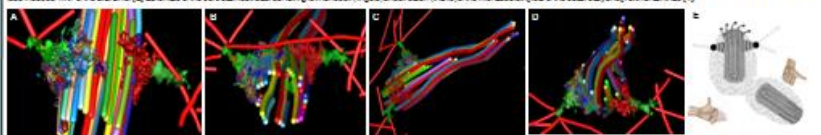
Ultrastructural details of a primary cilium in vitro

(A) Axial projection of the cilium and centrosome. (B) Local microtubule doublets reach the tip, and some localize axemally with the axeme. (C, D) Illustrate the vertical linkages between the microtubule doublets and the cilium membrane. (E) Individual basal body triplets are seen extending from the basal body, attaching to the cilium membrane. (F) Shows the basal body appendage, which anchors an axemal microtubule triplet, and axemally associated proteins that connect microtubule doublets (G) to the proximal centrosome and the basal body, and the A, B and C sub-fibrils of the triplets.



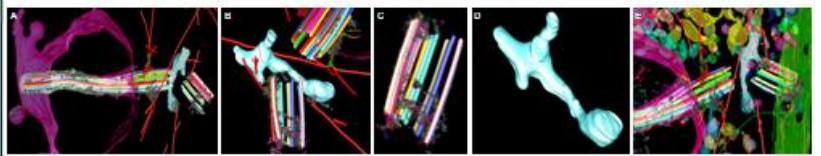
Cilium Projection

(A) Axial view of the basal appendages showing ultrafine structure and microtubule attachment points. (B) End on view of the basal body showing the microtubule doublets that meet and link to the microtubule triplets of the axeme. (C) Axemal view of the centrosome showing the microtubule triplets of the basal body and proximal centrosome. (D)



Centrosome Projection

(A) Axial view of the basal body showing the microtubule doublets. (B) Basal body, basal feet, proximal centrosome, and cytoplasmic microtubules. (C) Basal body and proximal centrosome showing linkages with the basal body and proximal centrosome. (D) The centrosome structure is a tubular annulus with high segments outside the junction between the microtubules. (E) Composite of centrosome, vesicles, Golgi apparatus, and nucleus membranes with nuclear pores.



Matrix - Cilium Membrane Interactions

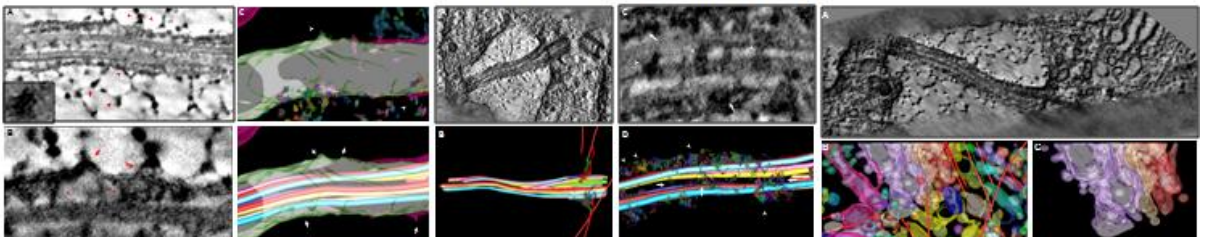
(A) An oblique reconstruction of a 1.0 nm slice of the axeme interacting with extracellular matrix granules of aggrecan. (A) Complete apical view of the axeme, basal body and proximal centrosome. Note all microtubule doublets (A) in optical slice of the cilium, proximal centrosome, and a segment of the Golgi network. Note assemblies of aggrecan which have been attached with ruthenium hexamine tetroxide to the cilium membrane. (B) Model of the cilium and basal body showing microtubule and membrane associated interactions. (C) Model of the cilium and basal body showing microtubule and membrane associated interactions. (D) Model of the cilium and basal body showing microtubule and membrane associated interactions. (E) Model of the cilium and basal body showing microtubule and membrane associated interactions. (F) Model of the cilium and basal body showing microtubule and membrane associated interactions. (G) Model of the cilium and basal body showing microtubule and membrane associated interactions. (H) Model of the cilium and basal body showing microtubule and membrane associated interactions. (I) Model of the cilium and basal body showing microtubule and membrane associated interactions. (J) Model of the cilium and basal body showing microtubule and membrane associated interactions. (K) Model of the cilium and basal body showing microtubule and membrane associated interactions. (L) Model of the cilium and basal body showing microtubule and membrane associated interactions. (M) Model of the cilium and basal body showing microtubule and membrane associated interactions. (N) Model of the cilium and basal body showing microtubule and membrane associated interactions. (O) Model of the cilium and basal body showing microtubule and membrane associated interactions. (P) Model of the cilium and basal body showing microtubule and membrane associated interactions. (Q) Model of the cilium and basal body showing microtubule and membrane associated interactions. (R) Model of the cilium and basal body showing microtubule and membrane associated interactions. (S) Model of the cilium and basal body showing microtubule and membrane associated interactions. (T) Model of the cilium and basal body showing microtubule and membrane associated interactions. (U) Model of the cilium and basal body showing microtubule and membrane associated interactions. (V) Model of the cilium and basal body showing microtubule and membrane associated interactions. (W) Model of the cilium and basal body showing microtubule and membrane associated interactions. (X) Model of the cilium and basal body showing microtubule and membrane associated interactions. (Y) Model of the cilium and basal body showing microtubule and membrane associated interactions. (Z) Model of the cilium and basal body showing microtubule and membrane associated interactions.

Cilium Membrane Membrane Interactions

(A) Complete apical view of the axeme, basal body and proximal centrosome. Note all microtubule doublets (A) in optical slice of the cilium, proximal centrosome, and a segment of the Golgi network. Note assemblies of aggrecan which have been attached with ruthenium hexamine tetroxide to the cilium membrane. (B) Model of the cilium and basal body showing microtubule and membrane associated interactions. (C) Model of the cilium and basal body showing microtubule and membrane associated interactions. (D) Model of the cilium and basal body showing microtubule and membrane associated interactions. (E) Model of the cilium and basal body showing microtubule and membrane associated interactions. (F) Model of the cilium and basal body showing microtubule and membrane associated interactions. (G) Model of the cilium and basal body showing microtubule and membrane associated interactions. (H) Model of the cilium and basal body showing microtubule and membrane associated interactions. (I) Model of the cilium and basal body showing microtubule and membrane associated interactions. (J) Model of the cilium and basal body showing microtubule and membrane associated interactions. (K) Model of the cilium and basal body showing microtubule and membrane associated interactions. (L) Model of the cilium and basal body showing microtubule and membrane associated interactions. (M) Model of the cilium and basal body showing microtubule and membrane associated interactions. (N) Model of the cilium and basal body showing microtubule and membrane associated interactions. (O) Model of the cilium and basal body showing microtubule and membrane associated interactions. (P) Model of the cilium and basal body showing microtubule and membrane associated interactions. (Q) Model of the cilium and basal body showing microtubule and membrane associated interactions. (R) Model of the cilium and basal body showing microtubule and membrane associated interactions. (S) Model of the cilium and basal body showing microtubule and membrane associated interactions. (T) Model of the cilium and basal body showing microtubule and membrane associated interactions. (U) Model of the cilium and basal body showing microtubule and membrane associated interactions. (V) Model of the cilium and basal body showing microtubule and membrane associated interactions. (W) Model of the cilium and basal body showing microtubule and membrane associated interactions. (X) Model of the cilium and basal body showing microtubule and membrane associated interactions. (Y) Model of the cilium and basal body showing microtubule and membrane associated interactions. (Z) Model of the cilium and basal body showing microtubule and membrane associated interactions.

Polarization of the Golgi apparatus

(A) Complete apical view of the axeme, basal body and proximal centrosome. Note all microtubule doublets (A) in optical slice of the cilium, proximal centrosome, and a segment of the Golgi network. Note assemblies of aggrecan which have been attached with ruthenium hexamine tetroxide to the cilium membrane. (B) Model of the cilium and basal body showing microtubule and membrane associated interactions. (C) Model of the cilium and basal body showing microtubule and membrane associated interactions. (D) Model of the cilium and basal body showing microtubule and membrane associated interactions. (E) Model of the cilium and basal body showing microtubule and membrane associated interactions. (F) Model of the cilium and basal body showing microtubule and membrane associated interactions. (G) Model of the cilium and basal body showing microtubule and membrane associated interactions. (H) Model of the cilium and basal body showing microtubule and membrane associated interactions. (I) Model of the cilium and basal body showing microtubule and membrane associated interactions. (J) Model of the cilium and basal body showing microtubule and membrane associated interactions. (K) Model of the cilium and basal body showing microtubule and membrane associated interactions. (L) Model of the cilium and basal body showing microtubule and membrane associated interactions. (M) Model of the cilium and basal body showing microtubule and membrane associated interactions. (N) Model of the cilium and basal body showing microtubule and membrane associated interactions. (O) Model of the cilium and basal body showing microtubule and membrane associated interactions. (P) Model of the cilium and basal body showing microtubule and membrane associated interactions. (Q) Model of the cilium and basal body showing microtubule and membrane associated interactions. (R) Model of the cilium and basal body showing microtubule and membrane associated interactions. (S) Model of the cilium and basal body showing microtubule and membrane associated interactions. (T) Model of the cilium and basal body showing microtubule and membrane associated interactions. (U) Model of the cilium and basal body showing microtubule and membrane associated interactions. (V) Model of the cilium and basal body showing microtubule and membrane associated interactions. (W) Model of the cilium and basal body showing microtubule and membrane associated interactions. (X) Model of the cilium and basal body showing microtubule and membrane associated interactions. (Y) Model of the cilium and basal body showing microtubule and membrane associated interactions. (Z) Model of the cilium and basal body showing microtubule and membrane associated interactions.



'Have a great idea, one great object, and follow it and never give in until you achieve it. You will win in the end though you may have to wait long for it.'

'It is the dreamers that move the world. Practical men are so busy being practical that they cannot see beyond their own lifetime. Dreamers and visionaries have made civilisations. It is trying to do the things that cannot be done that makes life worth while. The dream of today becomes the custom of tomorrow.'

CJR